Simultaneous carbon storage in marginal lands and anthropogenic products through biopump : potential to induce negative emission and environmental mitigation

Zhou Shen

Université Fédérale
Toulouse Midi-Pyrénées

THÈSE

En vue de l'obtention du

DOCTORAT DE L'UNIVERSITÉ DE TOULOUSE

Délivré par l'Institut National des Sciences Appliquées deToulouse

---

Présentée et soutenue par

Zhou SHEN

Le 18 mai 2022

Stockage simultané de carbone dans des terres marginales et des produits anthropiques grâce à la bio-pompe : potentiel d'induction d'émission négative et d'atténuation du changement climatique
Simultaneous carbon storage in marginal lands and anthropogenic products through biopump: potential to induce negative emission and environmental mitigation

---

Ecole doctorale : **MEGEP - Mécanique, Energétique, Génie civil, Procédés**

Spécialité : **Génie des Procédés et de l'Environnement**

Unité de recherche :

TBI - Toulouse Biotechnology Institute, Bio & Chemical Engineering

Thèse dirigée par

Ligia BARNA et Lorie HAMELIN

Jury

M. Bernard KUREK, Rapporteur
M. Hayo VAN DER WERF, Rapporteur
M. Thibaut LECOMPTE, Examinateur
M. Mathieu SPERANDIO, Président
Mme Ligia BARNA, Directrice de thèse
Mme Lorie HAMELIN, Co-directrice de thèse

ABSTRACT

The Paris Agreement implies human society to limit global temperature increase to 1.5°C or no more than 2°C, and this goal is confirmed in the 2021 United Nations Climate Change Conference. Many milestones have been set to reach this goal, for example France has announced that it will reduce its greenhouse gas (GHG) emissions by 40% before 2030 and that it will reach carbon neutrality before 2050. All of these climate goals are driving our society to develop methods to remove GHGs from the atmosphere and avoid the increased use of fossil carbon.

Plants utilize CO_2 through photosynthesis, which is considered a natural CO_2 capture. Inspired by this, this thesis proposes the concept of "biopump" to induce negative emissions and mitigate the global warming. The biopump is a plant that can convert some of the C captured by photosynthesis into soil organic carbon stocks (SOC). Once the plant matures, the harvestable parts are transformed into bio-based products, so that the carbon from this part of the biomass is conserved in the technosphere. These materials have a life span and end of life that will influence the carbon stock in the technosphere. Meanwhile, bio-based products replace fossil-based products with similar functions, which can contribute to climate change mitigation. Therefore, the biopump can capture carbon from the atmosphere in two sinks, the soil and the technosphere, while avoiding the production of fossil-based products, which can contribute to climate goals.

To remove more CO_2, biopumps should be planted in areas that are least disruptive to current agricultural and human activities, yet have high potential for additional carbon storage in the soil. These lands are referred to as "carbon vulnerable lands" (CV-lands). It is estimated that there are up to 24,000 km2 of CV lands in France. Planting biopump on these lands could increase by 0.23 to 0.49 Mt carbon stocked as SOC annually, which represents 0.19% to 0.41% from the 2015-2018 French annual carbon budget. If the carbon contained in the biomass is kept in anthropogenic products, it could represent up to 13.07% of the French annual carbon budget, proving the feasibility of the biopump strategy in general.

After the feasibility was confirmed, two specific case studies were conducted. Hemp and black locust were chosen as annual and perennial biopumps, respectively. Carbon fluxes were accounted for annually, consequential life cycle assessment (LCA) was conducted to assess the environmental effects of the biopump introduction in new value chains. Hemp and black locust were considered to be grown for 100 years without interruption. The change in SOC during cultivation was simulated based on the soil characteristics of the identified CV-lands, and the C inputs of the selected biopumps. The results were considered in the life cycle inventory from cultivation to disposal of the bio-based products, with different lifetimes. Since the systems under study have different temporalities and there are different climate milestones (e.g., 2030,

2050), it is necessary to estimate the effect on climate change with temporal parameters, using the dynamic LCA approach.

Compared to initial vegetation grown on CV-land, the results show that biopumps could not only induce more C stored in the soil, and mitigate the climate change, but also perform better in most environmental aspects (e.g., human health, eutrophication), partly due to the replacement of fossil products. In terms of timing, perennial wood biopumps allow higher carbon stock and reduce global warming more efficiently in the short-/ mid-term than annual herbaceous biopumps, while the duration of this benefit strongly depends on the lifetime of the bio-based products.

This work could be validated further by multiplying the case studies, or even by experimental approaches.

Key words: Biopump; life cycle assessment; climate change; dynamic life cycle assessment; soil organic carbon; carbon vulnerable land

RESUME

L'Accord de Paris exige que la société humaine limite l'augmentation de la température mondiale à 1,5°C ou maximum 2°C, et cet objectif est confirmé lors de la Conférence des Nations Unies sur le changement climatique de 2021. De nombreuses mesures ont été proposées pour atteindre cet objectif, par exemple la France a annoncé qu'elle réduirait ses émissions de gaz à effet de serre (GES) de 40 % avant 2030 et qu'elle atteindrait la neutralité carbone avant 2050. Tous ces objectifs climatiques sont le moteur pour développer des méthodes pour éliminer les GES de l'atmosphère et éviter l'utilisation accrue de carbone fossile.

Les plantes utilisent le CO_2 par la photosynthèse, qui est considérée comme une capture naturelle du CO_2. Inspirée par cela, cette thèse propose le concept de "bio-pompe" pour induire des émissions négatives et atténuer le réchauffement climatique. La bio-pompe est une plante capable de convertir une partie du carbone capté par la photosynthèse en stocks de carbone organique du sol(COS). Une fois la plante mature, les parties récoltables sont transformées en produits biosourcés, afin que le carbone de cette partie de la biomasse soit conservé dans la technosphère. Ces matériaux ont une durée de vie et une fin de vie qui vont influencer le stock de carbone dans la technosphère. En même temps, les produits biosourcés remplacent les produits fossiles avec des fonctions similaires, ce qui peut contribuer à l'atténuation du changement climatique. Ainsi, la bio-pompe peut capter le carbone de l'atmosphère dans deux puits, le sol et la technosphère, tout en évitant la production de produits à base de fossiles, qui peuvent contribuer aux objectifs climatiques.

Pour éliminer plus de CO_2, des bio-pompes devraient être plantées dans des zones qui perturbent le moins les activités agricoles et humaines actuelles, tout en ayant un potentiel élevé de stockage supplémentaire de carbone dans le sol. Ces terres sont appelées « terres vulnérables au carbone » (terres-CV). On estime qu'il existe jusqu'à 24 000 km^2 de terres-CV en France. La plantation de bio-pompes sur ces terres pourrait augmenter de 0,23 à 0,49 Mt de carbone stocké en COS annuellement, ce qui représente 0,19 % à 0,41 % par rapport au budget carbone annuel français 2015-2018. Si le carbone contenu dans la biomasse est conservé dans des produits anthropiques, il pourrait représenter jusqu'à 13,07 % du budget carbone annuel français, prouvant la faisabilité de cette stratégie en général.

Deux études de cas spécifiques ont été menées. Le chanvre et le robinier ont été choisis respectivement comme bio-pompes annuelles et pérennes. Les flux de carbone ont été comptabilisés annuellement, une analyse du cycle de vie (ACV) conséquentielle a été réalisée pour évaluer les effets environnementaux de l'introduction de la bio-pompe dans les nouvelles chaînes de valeurs. Le chanvre et le robinier étaient considérés comme cultivés pendant environ 100 ans sans interruption. Le changement de COS pendant la culture a été simulé sur la base

des caractéristiques des terres -CV et des apports de carbone des bio-pompes sélectionnées. Étant donné que les systèmes étudiés ont des temporalités différentes et qu'il existe différents objectifs climatiques (par exemple 2030, 2050), il est nécessaire d'estimer l'effet sur le changement climatique avec des paramètres temporels, en utilisant l'approche ACV dynamique.

Les résultats montrent que les bio-pompes pourraient non seulement induire plus de COS et atténuer le changement climatique, mais aussi être plus performantes dans la plupart des aspects environnementaux (par exemple, la santé humaine, l'eutrophisation), en partie du fait du remplacement des produits fossiles. En termes de calendrier, les biopompes à bois pérennes permettent un stock de carbone plus important et réduisent le réchauffement climatique plus efficacement à court/moyen terme que les biopompes herbacées annuelles. Cependant ce bénéfice dépend fortement de la durée de vie des produits biosourcés.

Mots-clés : Bio-pompe ; analyse du cycle de vie ; changement climatique ; analyse dynamique du cycle de vie ; carbone organique du sol ; terre vulnérable au carbone

摘要

巴黎协议提出了人类社会应当将全球温度控制在 1.5℃，最多 2℃。这一目标在 2021 年的联合国气候变化框架公约也被确认了。在实现这一目标的路上，有许多阶段性的目标，例如法国宣布了将在 2030 年前削减 40%的温室气体排放。所有这一系列的其后目标的设立，为的是推动人类社会发展温室科技以将温室气体从大气中去除，并避免化石源碳的使用增加。

植物能够通过光合作用吸收大气中的二氧化碳，因此被认为是一种天然的二氧化碳吸收池。受此启发，本文提出了“生物泵“的概念。生物泵是一种可以将光合作用捕获的部分碳转化为土壤有机碳储量 (SOC) 的植物。 一旦植物成熟，可收获部分将转化为生物基产品，因此这部分生物质中的碳在技术圈中得到保存。 这些材料的使用寿命和使用寿命将影响技术领域的碳储量。 同时，生物基产品取代具有相似功能的化石基产品，有助于减缓气候变化。因此，生物泵可以在土壤和技术圈这两个汇中从大气中捕获碳，同时避免生产化石产品，这有助于实现气候目标。

为了去除更多的二氧化碳，生物泵应该种植在对当前农业和人类活动破坏最小的地区，但在土壤中具有额外碳储存的潜力。 这些土地被称为“碳脆弱土地”（CV-lands）。 据估计，法国有多达 24,000 平方公里的 CV-lands。 在这些土地上种植生物泵每年可增加 0.23 至 0.49 吨碳储存量，即 2015-2018 年法国年度碳预算的 0.19% 至 0.41%。 如果生物质中所含的碳保留在人为产品中，它可能占法国年度碳预算的 13.07%，这证明了生物泵战略总体上的可行性。

在确认可行性后，进行了两个具体的案例研究。 大麻和刺槐分别被选为一年生和多年生生物泵。 每年计算碳通量，进行相应的生命周期评估 (LCA) 以评估在新价值链中引入生物泵对环境的影响。 大麻和刺槐被认为可以连续种植 100 年。 基于已识别的 CV 土地的土壤特征和所选生物泵的碳流动模拟了种植过程中 SOC 的变化。 结果被考虑在从种植到处置生物基产品的 LCA 中，具有不同的时间跨度。 由于所研究的系统具有不同的时间性和不同的气候目标（例如 2030 年、2050 年），因此有必要使用动态 LCA 方法利用时间参数估计对气候变化的影响。

与在 CV-lands 上生长的初始植被相比，结果表明，生物泵不仅可以诱导更多的碳储存在土壤中，缓解气候变化，而且在大多数环境方面（例如，人类健康、富营养化）表现更好，化石产品的替代是重要的贡献者之一。在时间方面，木本多年生生物泵可以比一年草本生物泵更有效的在中短期内减少全球变暖，而后者的在长期的碳储存上的效果更好。

通过增加案例研究，甚至通过实验方法，可以进一步验证这项工作。

关键词：生物泵，生命周期法，气候变化，动态生命周期法，土壤有机碳，碳脆弱土壤

ACKNOWLEDGMENT

It's the twilight of an ordinary day in the year 2022, I'm writing the acknowledgment, face to the view (a big tree!) outside of my windows. Four years ago, at a similar time, I arrived in INSA, installed my laptop against the window, I opened my laptop, faced the same tree, and began to write my life in France.

Before I came, I wondered what my PhD life would be, till now, I can say that it is much more fantastic than I have ever thought! First, I truly want to thank my two supervisors: Ligia Tirua-Barna and Lorie Hamelin. In the beginning, I was like an infant of the LCA, it was you who helped me to touch this subject step by step. I did not understand many terms of LCA even with the handbook (our bible!), thank you very much Ligia, for your patience to answer my very very simple questions. Every time I had questions, you responded quickly and with detailed answers, your answers were always longer than my questions, not simply giving me an answer but letting me know how to get the solutions. You also guided me on the way to gradually learning this project, the first half-year, every week you sent me several papers in different domains so I could understand what the meaning of my project is. Opposite to the stereotype, Lorie is the most diligent person I have ever seen, you give me a very good role model what is the right attitude to science, always should respect the truth and work hard enough to strike to our target. And you have a remarkable memory! Whatever the question was I went to your office to ask you directly, you could always give me a very instructive suggestions, and tell me where these suggestions came from and which papers I should check to confirm and explore the answers. I'm still impressed that once when we discussed, you told me this is in chapter A volume B table C, that is in the chapter X volume Y table Z of the IPCC report. I know I'm not a very careful person, sometimes made very stupid mistakes again and again, but both of you were never angry with me, always told me where I was wrong and what should I do to fix these mistakes with kindness and patience. Thank you very much my supervisors.

I would also express my acknowledgement to my thesis committee members : Bernard KUREK, Hayo VAN DER WERF, Thibaut LECOMPTE, and Mathieu SPERANDIO. Thanks for the time spent reviewing my work and the attention and dedication that you gave to this project. All contribution you have given was precious to improving the quality of this work.

It is my first time living in a foreign country for such a long time, I'd like to thank you my friends in the lab. Shivesh, Patrick, David, Concette, Dominica, Conrentin, Mondassa. I missed the time we hung out on the streets of Toulouse, whether in the daytime or at midnight, it was two years ago but every moment seems just like yesterday for me. Carlos, Camilo, Christhel, Ernesto, Marco, Nia and all my Spanish speaking friends, your passion fired the darkness of the night, you taught me how to dance, what is taxi, shark, cleaning the windows… you built me a dream to visit the South America Continent! Ugo, Pla, Seunghye, Glezza, Ryma, Vicent, I could not remember how many happy times we celebrated and how many tough times we experienced together, we are not only colleges but friends forever. Further, I'd like to say a

special thank you to Ariane, you're like my 'small supervisor', not only in the academic field. Three years ago, we met the first time in the bioeconomy meeting in Paris, my first time to communize with somebody known from a conference, thank you for always encouraging me to be brave to talk to people. To all my friends, no matter how many words I wrote, I could not express how much I love you.

Here are 10,000 kilometres to my home, but thanks to my Chinese friends, ZhangTianyi&Wangjin, Nanzibin&Lynn, ChenYifan couple, NiuYannan, Yangyan, MaoYao, BingQian, ChengGaoxing&XieXiner, ZhouTianbo, LuJingjing ChenFan, ChengMing, WuZhenhang, ShenBailin couple, ZouQilin couple, BieYiping couple, LiXiaoqian, LiAo, WuNao, MeiMei, MaQiuming, DengHui, ZouJin couple, HuangBaowen. I could only list your names here because even the whole thesis is not enough for writing the stories among us.

Finally and most essential, the Chinese Scholar Council provided the financial support to bring me here. I'm so excited to anticipate that I will be back to see may Dad, Mom, uncles, aunts, cousins, and all my friends in China, I chomp at the bit to hug you and tell you about my amazing life in France. 外婆你看到这句话的时候我就快到家了。

Scientific papers published in international and peer reviewed journals

Shen, Z., Tiruta-Barna, L., Karan, S.K., Hamelin, L., 2022b. Simultaneous carbon storage in arable land and anthropogenic products (CSAAP): Demonstrating an integrated concept towards well below 2° C. Resour. Conserv. Recycl. 182, 106293.

Shen, Z., Tiruta-Barna, L., Hamelin, L., 2022. From Hemp Grown on Carbon Vulnerable Lands to Long-Lasting Bio-Based Products: Uncovering Trade-Offs between Overall Environmental Impacts, Sequestration in Soils and Dynamic Influence on Global Temperature. Science of the Total Environment (under review)

Converting targeted land areas to wood plantations for use as building materials: a time-dependent assessment of carbon dioxide removals and overall environmental performance. (in preparation)

Conferences with abstract

Shen Zhou; Ligia Tiruta-Barna Shivesh Kishore Karan; Lorie Hamelin, 2021. Carbon Sequestration and Storage in the Soil and in Biobased. 29th European Biomass Conference & Exhibition (poster)

古人学问无遗力，少壮工夫老始成。

纸上得来终觉浅，绝知此事要躬行。

- (宋) 陆游《冬夜读书示子聿》

Context

Abstract III

Résumé V

摘要 VII

Acknowledgment VIII

Scientific papers published in international and peer reviewed journals X

Conferences with abstract X

List of Figures XVI

List of Tables XIX

Chapter I. Introduction- context of this work 1

List of abbreviations 2

1.1 Introduction 1

1.2 Involved project 2

Reference 2

Chapter II. Bibliography review: the role of biomass in climate change mitigation and the corresponding evaluation methods 3

List of abbreviations 4

2.1 Biomass in global warming mitigation 6

2.1.1 Carbon capture and greenhouse gas (GHG) release by biomass cultivation 6

2.1.2 Carbon involved in bioeconomy 7

2.2 Carbon in soil and biomass 8

2.2.1 C in the soil 8

2.2.2 Potential of the SOC in global warming mitigation 9

2.2.3 The role of biomass in SOC formation 10

2.2.4 The SOC simulation 12

2.3 Marginal lands 15

2.3.1 The importance of marginal lands 15

2.3.2 Marginal lands identification 16

2.4 Environmental impact evaluation 20

2.4.1 Principles of the LCA method 20

2.4.2 LCA of bio-based anthropogenic products 21

2.4.3 Dynamic LCA 22

2.5 Limitation of current evaluation about biomass 24
2.6 Research objectives and thesis structure 25
Reference 27
Chapter III. Biopump concept: definition and feasibility investigation 36
Context 37
1 Introduction 38
2 Materials and methods 39
2.1 Identification and ranking of biopump candidates 39
2.2 Scaling up the potential to a country: available and suitable lands for biopump cultivation 42
2.3 Carbon flow accounting 43
3 Result and discussion 43
3.1 Selected biopumps 43
3.2 Quantifying target areas – case of France 46
3.3 Dynamic carbon flows and climate mitigation potential – illustrative case 48
4 Perspective and limitations 51
5 Conclusions 51
References 53
Chapter IV. Biopump: annual plants 58
Context 59
1 Introduction 60
2 Methods 61
2.1 Overview of the step-wise approach used 61
2.2 Assessing SOC changes associated to converting CV-lands to hemp cultivation 61
2.3 Assessing environmental consequences of selected CSAAP scenarios: static LCA 62
2.4 Dynamic inventory for GHG flows and assessing related temperature changes 66
2.5 Sensitivity and uncertainty analysis 68
3 Results and discussion 68
3.1 SOC simulation by AMG 68
3.2 Environmental performance of the three hemp scenarios 69
3.3. Dynamic LCA 72
3.4 Sensitivity analysis 74

3.5. Uncertainty analysis 76
3.6. Overall implications, limitations and perspectives 78
Conclusion 78
Reference 80
Chapter V. Biopump: perennial plants 85
Context 86
1. Introduction 87
2. Methods 88
2.1. Scenarios description 88
2.2. Overview of the methodology used 92
2.3 Black locust growth rate 92
2.4 Simulating SOC on CV-lands for both scenarios, and wood residues decay 93
2.5 Environmental impact assessment through consequential LCA 93
2.6 Dynamic LCA for evaluating climate change impact 95
2.7 Sensitivity and uncertainty analysis 98
3 Result and discussion 99
3.1 Black locust growth and decay 99
3.2 SOC simulation results 99
3.3 Environmental impact results from the static LCA 101
3.4 Dynamic LCA results 105
3.5 Sensitivity analysis 107
3.6 Uncertainty analysis 108
3.7 Overall implications, limitations and perspectives 110
4 Conclusion 111
References 112
Chapter VI. Biopump: annual or perennial plants? 119
Context 120
List of abbreviations 121
1 Introduction 122
2 Methods 122
2.1 SOC simulation 122
2.1 Life cycle assessment (LCA) 123

2.3 Dynamic LCA 123
2.4 Uncertainty analysis 124
3 Results and discussion 124
3.1 SOC simulation results 124
3.2. C flows 131
3.3 Consequential LCA results 132
3.4 Dynamic LCA results 135
4 Conclusions 137
Reference 140
Chapter VII. Conclusion and perspective 142
Conclusion 143
Perspective 145

List of Figures

Fig. II-1 Carbon cycle and carbon pools. Data from (Lal, 2007). 9
Fig. II-2 Globally SOC distribution (a) in mass and (b) per 5° latitude, retrieved from~(Köchy et al., 2015). 10
Fig. II-3 The mechanism of the SOC change by biomass, retrieved from ~(Gross and Harrison, 2019). 12
Fig. II-4 C-TOOL model structure(Taghizadeh-Toosi et al., 2014). 16
Fig. II-5 Simplified structure of the thesis 26
Fig. III-1 Target areas identified as potentially suitable for biopumps implementation in France, without (left) and with (right) intensive grasslands. 47
Fig. III-2 Carbon flows analysis (a) fraction of biogenic carbon stored per year, (b) global mean temperature change 50
Fig. IV-1 Process flow diagram and system boundary considered for the three scenarios assessed. Box indicates processes. Solid lines: induced processes, dotted lines: avoided processes. *Landfilling without CH_4 recovery, **30% of car panel is disposed as incineration with power recovery, the rest is disposed as landfilling without CH_4 recovery. 65
Fig. IV-2 Timeline considered in dynamic LCA for the three scenarios. For Scenario SL, "residues" refer to the whole straw, while for Scenarios IB and CP, it refers to the un-harvestable above-ground portion only. 67
Fig. IV-3 100-year SOC stock evolution (a) under different C/N ratio for hemp cultivation on average CV-land, and (b) initial vegetation on CV-lands under C/N 17 69
Fig. IV-4 Life cycle impact assessment results for (a) climate change, (b) non-cancer human health effects, (c) freshwater- and (d) marine eutrophication impacts, with a breakdown per process contribution For tractability reasons, only the most significant processes are depicted. For this reason, the breakdown categories "others (+)" and "others (-)" are introduced, aggregating all remaining positive and negative contributions, respectively. 70
Fig. IV-5 Dynamic global mean temperature change in biogenic (bio) and non-biogenic (non-bio) flows for scenario SL, scenario IB and scenario CP, and the sensitivity CP sub-scenario where electric mobility is considered from 2040 case ELE with 42% photovoltaic in the electricity mix and case ELE-low with 12% (described in section 3.4.2). 74
Fig. IV-6 Sensitivity analysis portraying the relative changes observed, for all impact categories, from the baseline scenarios due to (a) no fertilizer use; and (b) electric car after 2040 (CP scenario only). The black line represents the initial baseline scenarios (i.e., no change). The positive value represents an improvement (%) of the net impact compared to the reference (bold line), and, *vice versa*. 75
Fig. IV-7 Uncertainty analysis of climate change, non-cancer human health, freshwater- and marine eutrophication impacts. The overall system uncertainty is presented on the left hand side, while the contribution of all identified sensitive parameters to this system uncertainty is represented on the right hand side. Red indicates overlap with impossibility to conclude. .. 77
Fig. V-1 Process flow diagram showing the key activities considered for (a) black locust cultivation, harvesting (green) and residual biomass management (orange), and (b) manufacture and disposal of cross-laminated timber (CLT; yellow) and medium density fiberboard (MDF; blue). 91
Fig. V-2 Calculation steps followed in this study 92
Fig. V-3 System diagrams showing the boundaries considered in consequential LCA of business as usual (REFc) and black locust (BLc) systems, built on REF and BL scenarios respectively. CV-land: carbon vulnerable land; iLUC: Indirect land use changes; CLT:

cross-laminated timber; MDF: medium density fiberboard. Full lines indicate induced processes while dotted lines represent avoided processes. 94
Fig. V-4 Timeline of processes for dynamic LCA. 97
Fig. V-5 System diagrams of business as usual (REFa) and black locust (BLa) systems, built on REF and BL scenarios respectively. 98
Fig. V-6 Simulated (a) biomass growth and decay for black locust during one rotation, and (b) SOC evolution for black locust and initial vegetation during the cultivation period. Harvestable biomass: stem, branch and bark. 100
Fig. V-7 Climate change impact for (a) BLc and (b) REFc. Processes with contributions lower than 1% of the total impact (in absolute) were attributed to categories others (+) or (-) (e.g., process A has a contribution of 1 and process B of -1, then the contribution of process A is 1/(abs(1)+abs(-1))=50%). 102
Fig. V-8 Characterized LCA results for BLc (left bar) and REFc (right bar) scenarios for all impact categories of the EF method, with the exception of climate change. 105
Fig. V-9 GMTC results for all GHG sources from REFc and BLc scenarios, and the consequence of replacing REFc with BLc. Total BLc = Bio BLc + Non bio BLc; Total REFc= Bio REFc + Non bio REFc; Net GMTC = Total BLc – Total REFc. 1st, 2nd, 3rd refer to the rotation number. 105
Fig. V-10 GMTC evolution in REFa (above) and BLa (bottom) scenario with time. 1st, 2nd, 3rd refer to the rotation number. Total BLa = Bio BLa + Non bio BLa; Net BLa = Total BLa+ Palm oil + Feed; Total VGa = Bio VGa + Non bio VGa; Net REFa = Total VGa + Heat + Plastic board + Brick. 107
Fig. V-11 Sensitivity analysis of: 100% CLT recycling, CLT avoids concrete, and MDF avoids plasterboard or PP board. The positive percentage means a scenario is better than the initial scenario in this impact. 108
Fig. V-12 Carbon captured over the culture period, and biogenic carbon stocks during the lifetime of the BL scenario. 110
Fig. VI-1 Timeline with important process points of scenarios SL, IB, CP, and BL. 1st, 2nd, 3rd mean the rotation 1, 2, 3. 124
Fig. VI-2 SOC evolution in CV-lands during the hemp and black locust cultivation, and for the initial vegetation. Simulations with C-tool for black locust and initial vegetation, and simulations with C-tool and AMG for hemp. 125
Fig. VI-3 Sankey diagram of C flows in scenario SL. The C flow of soil is a gain. Unit in t ha^{-1}. The flow with the red frame is C sink. 127
Fig. VI-4 Sankey diagram of C flows in scenario IB. The C flow of soil is a loss. Unit in t ha^{-1}. The flow with the red frame is C sink. 128
Fig. VI-5 Sankey diagram of C flows in scenario CP. The C flow of soil is a loss. Unit in t ha^{-1}. The flow with the red frame is C sink. 129
Fig. VI-6 Sankey diagram of C flows in scenario BL. 1st activities involved in the first thinning; 2nd: activities involved in the second thinning& pruning; H: activities involved in the harvesting; re: recycling; Unit in t ha-1. The flow with * is a C sink. The flow with the red frame is C sink. 130
Fig. VI-7 Annual C captured from the atmosphere by hemp and black locust. 132
Fig. VI-8 Environmental impacts for which the scenario BL is better than the others. 134
Fig. VI-9 Environmental impacts for which the scenario CP is better than the others. 134
Fig. VI-10 Mitigation effect from the avoided products and processes, in scenarios SL, IB, CP, and BL (normalized results) 135
Fig. VI-11 GMTC of scenarios SL, IB, CP, BL for bio and non-bio flows (consequential modeling) 136

Fig. VI-12 Total GMTC of scenarios SL, IB, CP, BL. 137

List of Tables

Table II-1 Review of marginal land selection criteria. 18
Table II-2 Review of marginal land type 19
Table III-1 Semi-quantitative criteria matrix used to score and select the biopumps potentially adapted for Francea. 41
Table III-2 Biopump ranking results[a] 45
Table III-3 Land cover types in France (2018) on C-poorer lands, detailed for 3 SOC range categories[a] 46
Table V-1 Uncertainty range of LCA results[a]. 109
Table VI-1 Carbon input of hemp for SOC simulation. 122
Table VI-2 SOC results obtained at 100 years of cultivation, with AMG and C-tool for hemp scenarios 125
Table VI-3 Results from dynamic LCA extrapolated to the total CV-land area in France, at three time horizon**s[a].** 139
Table VI-4 Selected results from static and dynamic LCA and biogenic flows modelling, for 1ha CV-land[a]. 139

Chapter I. Introduction- context of this work

List of abbreviations

C	Carbon
GHG	Greenhouse gas

1.1 Introduction

The well-mixed greenhouse gas (GHG) concentration in the atmosphere has been increasing for around 250 years. In 2019, CO_2, CH_4, and N_2O were three major GHGs in the atmosphere, with concentrations of 410 ppm, 1866 ppb, and 332 ppb, respectively (IPCC, 2021). These GHGs absorb the thermal radiation emitted by the earth's surface, raising the temperature of the earth, this effect is called global warming. The increasing concentration of GHG in the atmosphere leads to higher temperatures, the global mean surface temperature is 1.09 °C higher in these last ten years than 1850- 1900, especially over continents (1.59°C) (IPCC, 2021). The higher temperature has severe and wide-ranging impacts on the natural environment, which in turn affects the human society and the economy. For example the reduction of agricultural products (like rice) due to the sea level rise, resulted in annual welfare losses ranging up to US$10.59 billion, affecting people all over the world (Chen et al., 2012).

Reacting to global warming, 196 Parties adopted the Paris Agreement in 2015. The Paris Agreement is a bridge between today's policies and climate-neutrality before the end of the century. In short, it agrees(UNFCCC, 2015):

1) A long-term goal of keeping the increase of global mean temperature to well below 2°C with respect to the pre-industrial level;
2) To limit the GMT increase to 1.5°C;
3) To reach the peak of global emission as soon as possible (i.e., to decrease global emissions as soon as possible);
4) To achieve a balance between emissions and removals in the second half of the century

Although controlling the GMT rise under 2°C is one of the targets, limiting it to under 1.5°C would limit the risk of irreversible damages, like the disappearance of the Arctic continent and increasing the sea level rise, which could save US$ 1.4 trillion per year (Jevrejeva et al., 2018).

To achieve the objectives of the Paris Agreement, the French government fixed as objective to reach the carbon neutrality by 2050 and strive to limit the temperature increase to 1.5°C at the end of this century(Boudet et al., 2021), which required to reduce 40% of GHG emissions by 2030 compared to 1990 level. Several solutions were drafted to reduce the GHG emissions, such as no longer produce hydrocarbon energy by 2040, stopping sales of GHG-emitting vehicles by 2040, etc. Nevertheless, establishing approaches for lowering GHG emissions is necessary but far from sufficient to meet climate change targets on time. For instance, achieving carbon neutrality needs to reduce carbon emissions to one-sixth of what they are now and double the carbon (C) stock in 2050.

The Paris Agreement targets imply two key challenges. On the one hand, it implies to induce additional carbon dioxide removals or so-called negative emissions (Masson-Delmotte et al., 2018; Tanzer and Ramírez, 2019). The potential of soil carbon sequestration as a negative emission strategy has attracted increased attention because of its considerable potential, up to 13 Gt CO_2-eq $year^{-1}$, as reported in the literature (Shukla et al., 2019).

The second challenge is to transit towards a low fossil C economy. Fossil CO_2 represented more than 65% of global GHG emissions in 2016 (World Resources Institute, 2020). If efforts are deployed to decarbonize the energy sector, the total elimination of C form the economy is not possible because many sectors are dependent on like materials and chemicals. While some products and services can be supplied without any C (e.g., wind or solar electricity, which can in turn supply heat or transport services), other sectors of the economy (e.g., materials, chemicals) cannot be decarbonized and will require new C sources. For a low fossil C economy, biomass is the most abundant and accessible C source (Gautam et al., 2019; Office for National Statistics, 2019), at least until the large-scale deployment of technologies allowing to directly capture atmospheric carbon (so-called direct Direct Air Capture) and the use becomes a reality.

Therefore, this thesis focuses on strategies that use plants for C capture and storage in soil and in anthropogenic products and investigates the effectiveness of such solutions for global warming mitigation.

1.2 Involved project

This thesis is part of the project Cambiocop "Carbon Management & Bio-resources Strategies for Scoping the Transition towards low fossil Carbon" (https://cambioscop.cnrs.fr), financed by the French National Research Agency, Programme Investissement d'Avenir (Make Our Planet Great Again) and Region Occitanie, with a thesis grant from the Chinese Scholarship Council.

This project aims to build an approach for the establishment of geo-localized, dynamic and sustainable strategies for the development of the bioeconomy in France, aiming at optimizing the circularity of carbon. In the project frame, the possibilities of carbon storage in soils, and various biomass conversion chains are studied to produce a variety of innovative products (liquid hydrocarbons, proteins, biomaterials, etc.), with a time perspective by 2050, in France.

Reference

Boudet, F., Brunelle, T., Cazé, C., Mancebo, F., Mora, O., Paillard, S., Soussana, J.-F., Vandenbussche, A., 2021. En France, d'ici à 2030, renforcer la diversité des services rendus par les terres en préparant la neutralité carbone pour 2050.

Chen, C.C., McCarl, B., Chang, C.C., 2012. Climate change, sea level rise and rice: Global market implications. Clim. Change 110, 543–560. https://doi.org/10.1007/s10584-011-0074-0

Gautam, P., Kumar, S., Lokhandwala, S., 2019. Chapter 11 - Energy-Aware Intelligence in Megacities, in: Kumar, S., Kumar, R., Pandey, A.B.T.-C.D. in B. and B. (Eds.), . Elsevier, pp. 211–238. https://doi.org/https://doi.org/10.1016/B978-0-444-64083-3.00011-7

IPCC, 2021. Climate Change 2021: The Physical Science Basis. Contribution of Working Group I to the Sixth Assessment Report of the Intergovernmental Panel on Climate Change [Masson-Delmotte, V., P. Zhai, A. Pirani, S. L. Connors, C. Péan, S. Berger, N. Caud, Y. Chen,. Cambridge Univ. Press 3949.

Masson-Delmotte, V., Zhai, P., Pörtner, H.-O., Roberts, D., Skea, J., Shukla, P.R., Pirani, A., Moufouma-Okia, W., Péan, C., Pidcock, R., 2018. Global warming of 1.5 C. An IPCC Spec. Rep. impacts Glob. Warm. 1.

Office for National Statistics, 2019. A burning issue: biomass is the biggest source of renewable energy consumed in the UK [WWW Document]. Off. Natl. Stat. URL https://www.ons.gov.uk/economy/environmentalaccounts/articles/aburningissuebiomassisthebiggestsourceofrenewableenergyconsumedintheuk/2019-08-30

Shukla, P.R., Skea, J., Calvo Buendia, E., Masson-Delmotte, V., Pörtner, H.O., Roberts, D.C., Zhai, P., Slade, R., Connors, S., Van Diemen, R., 2019. IPCC, 2019: Climate Change and Land: an IPCC special report on climate change, desertification, land degradation, sustainable land management, food security, and greenhouse gas fluxes in terrestrial ecosystems.

Tanzer, S.E., Ramírez, A., 2019. When are negative emissions negative emissions? Energy Environ. Sci. 12, 1210–1218. https://doi.org/10.1039/c8ee03338b

UNFCCC, S., 2015. Report of the Conference of the Parties on its twenty-first session, held in Paris from 30 November to 13 December 2015. Addendum. Part two: Action taken by the Conference of the Parties at its twenty-first session. United Nations Framework Convention on Climate Change Bonn.

World Resources Institute, 2020. World Greenhouse Gas Emissions: 2016 [WWW Document]. URL https://www.wri.org/resources/data-visualizations/world-greenhouse-gas-emissions-2016

Chapter II. Bibliography review: the role of biomass in climate change mitigation and the corresponding evaluation methods

List of abbreviations

AGB	Aboveground biomass
ALCA	Attributional life cycle assessment
BCCS	Biomass with carbon capture and storage
BGB	Belowground biomass
C	Carbon
C_A	Active soil organic carbon
C_S	Stable soil organic carbon
CO_2	Carbon dioxide
CDR	Carbon dioxide removal
CLCA	Consequential life cycle assessment
CLT	Cross-laminated timber
CV-lands	Carbon vulnerable lands
DM	Dry mass
DOC	Dissolved organic carbon
Dy-LCA	Dynamic life cycle assessment
EF	Environmental Footprint initiative
FOC	Fresh organic carbon
FUM	Fresh organic matter
FU	Functional unit
HUM	Humified organic matter
IRF	Impulse response function
IPCC	Intergovernmental Panel on Climate Change
GHG	Greenhouse gas
GMT	Global mean temperature
LCA	Life cycle assessment
LU	Land use
LUC	Land use change
Methane	CH_4
MDF	Medium density board
N	Nitrogen
N-fertilizer	Nitrogen fertilizer

N_2O	Dinitrogen monoxide
GMTC	Global mean temperature change
GTP	Global Temperature Potential
GWP	Global Warming Potential
TH	Time horizon
RCP	Representative Concentration Pathway
RF	Radiative forcing
ROM	Resistant organic matter
SIC	Soil inorganic carbon
SOC	Soil organic carbon
SOM	Soil organic matter
SR	Shoot-to-root ratio
SRC	Short rotation coppice

2.1 Biomass in global warming mitigation

Removing CO_2 from the atmosphere by increasing terrestrial vegetation has become a global strategy to mitigate climate change(Barton et al., 2014; Meyer-Aurich et al., 2006; Patel et al., 2020). The first section of chapter 2 illustrated the potential CO_2 abatement capacity of biomass cultivation, and the influence of this extra cultivation on the bioeconomy.

2.1.1 Carbon capture and greenhouse gas (GHG) release by biomass cultivation

The scope of biomass herein refers to crops and forests. There are 286601 km^2 croplands in France, occupying 52% of the land area (Food and Agriculture Organization, 2018). These lands consist of 63% of cereal and forage crops, 34% grass, and 3% perennial crops (Minstère de l'agriculture et de l'alimentation, 2015). The cultivation of cereal and forage crops is a GHG intensive process, globally taking responsibility for 10% of N_2O, 7% of CH_4, and 12% of anthropogenic GHG emissions(World Resources Institute, 2020). Agricultural management plays a vital role in these emissions, especially soil management (fertilization) and enteric fermentation take the most responsibility for N_2O and CH_4 emission, respectively (Schahczenski and Hill, 2009). Fertilizers and pesticide (e.g., herbicide, insecticide, and fungicide) used to augment the yield also emit high amount of GHG. The production of 1 t N-fertilizer and fungicide would cause 814.08 kg C and 4825.68 kg carbon (C) emission respectively, not to mention the subsequent emission due to the application(West and Marland, 2002). According to the model of N_2O emission from the N-fertilizer adopted by IPCC, 1% of N from applied N-fertilizer is lost as N_2O (Hergoualc'h et al., 2019). Besides these direct emissions, a part of the N that is leached in the form of nitrate is converted to N_2O and ammonia, as indirect emissions. Although the application of fertilizers and pesticides could increase the yield, and the increased yield means more captured CO_2, this extra captured CO_2 will soon be released because of the fast consumption of downstream products (e.g., consuming food). Not to mention in some cases, the extra captured CO_2 could not even compensate the emission from fertilizers and chemicals (Benton et al., 2005). On the other hand, improving agricultural management could reduce GHG emissions. For example, using biochar amendments in the soil helps at decreasing the N_2O emissions by 54% and 53% during the rice and wheat seasons, respectively, without other effects on ecosystem respiration but increasing with around 15% the yield for both crops, attributing to this the nitrate retention in soils (Wang et al., 2012). In the actual agricultural work, the emissions need to be calculated comprehensively. West et al. compared the reduced tillage to the conventional tillage strategy in soybean cultivation. The reduced tillage strategy needs less water for irrigation and fossil fuel for machines, but more herbicide and fertilizer than traditional tillage. For instance in a soybean cultivation, if the soybean is fully irrigated, the reduced tillage could alleviate the C emission by 15.22 kg ha^{-1} compared to the conventional tillage since reduced tillage needs less water. Nevertheless, emit 5.78 kg C ha^{-1} more if there is no irrigation(West and Marland, 2002).

Another major kind of crop is the grass used for bioenergy. Typical bioenergy crops like the giant reed (*Arundo donax L.*), miscanthus (*Miscanthus x giganteus)*, and ryegrass (*Lolium perenne L.*), could capture 8.78, 12.11, 11.22 Mg C ha^{-1} $year^{-1}$ respectively, have relatively high yields and could be planted in poor land (Hamelin et al., 2012; Schmidt et al., 2015). They differ to annual crops which grow and are harvested in one year, and the yields are similar every year. The perennial biomass has less or even no yield in the first (several) years after seedling, while the yield increases after that and becomes stable till the end of the plant's lifespan (Hamelin, 2013).

The forest is known as a major component of the global C cycle, which stores 90% of the world's terrestrial carbon, namely 350 Pg of C (Patil and Kumar, 2017). Unlike crops with similar C absorption every year, forest sequestrates C increasingly over the time and age of trees until they are mature. For example pine plantations of 90 years could accumulate 2.5 Mg C ha^{-1} annually on average, the Mediterranean oak forests could absorb 340 t CO_2 ha^{-1} in a 120 years rotation (Cañellas et al., 2008; Heath et al., 1996). Studies also focused on woody species with fast growth rates to balance the harvested

biomass and harvesting frequency to accelerate providing harvested biomass to the market. Landgraf et al. measured the growth rate of 37 different poplar varieties, found they could yield from the lowest 0.8 to the highest dry mass(DM) 14.6 t ha^{-1} per year after a three-year rotation (Landgraf et al., 2020).

Part of the C captured is stored in soils mainly in form of organic matter. The soil organic carbon (SOC) is the result of residues decomposition belowground and aboveground. During the cultivation, tillage is an essential factor of SOC change, because it would disturb the soil, further oxidizing the SOC then emitting GHG. Thus reduced tillage, converting plowing to use disks or chisels, or even no-tillage strategy, is always adopted to protect the SOC (West and Marland, 2002). Less tillage would also leave more biomass residues covered after planting, increasing the C inputs to the soil. Converting conventional tillage to reduced tillage and no-tillage is estimated to gain the SOC in 300 and 500 kg ha^{-1} per year respectively in the Canadian prairie region (Follett, 2001). It should be noticed that which kind of tillage strategy is conducted needs to consider crop species and site specifically, extensive tillage means more fertilizer and chemicals demand, which might reduce the benefit from extra stored SOC or even emit more GHG.

2.1.2 Carbon involved in bioeconomy

Carbon is absorbed by biomass through photosynthesis, and, whatever crops or woods, the C content in the dry biomass ranges in 47- 59% DM (Lamlom and Savidge, 2003). Crops planted for food are not regarded as carbon store, since food would be consumed in a short time, resulting in C emitted to the atmosphere (for a mature organism). Thus, concerning the crops, the key action for climate mitigation is improving agricultural management (e.g., adding biochar amendments as mentioned above). Meanwhile, things are different if crops are converted into bioenergy or bio-based products. Though bioenergy would also be used in a short time, the difference is that it avoids using fossil fuel. There exists a vast potential for bioenergy crops in offsetting fossil fuel emission, 1 kg of C in biomass could offset 0.6 kg of C in fossil. Thus planting bioenergy crops in degraded soils is a promising option, with C sequestration rates ranging from 0.6 to 3.0 Mg C ha^{-1} yr^{-1}, further to 1631 Tg C yr^{-1} if expanding to the whole degraded soils in the world (Lemus and Lal, 2005). Crops like flax have high cellulose content, they have been widely used in textile since ancient(Rohit and Dixit, 2016), the textile could keep the C within it for several years (Manda et al., 2015). Due to the lightweight and good insulation characteristics, the fiber of these crops is extracted and processed in different products like panels or boards used in vehicles and structures, with C retention for decades(Andersson and Björhagen, 2018).

For woody biomass, short rotation copice (SRC) behaves similarly to the crops cultivated for bioenergy. The mitigation effect on climate change mainly comes from the avoided fossil energy rather than from the C stocked in the biomass itself: 36 g CO_2-eq could be avoided per 1 MJ bioenergy from SRC(Gerssen-Gondelach et al., 2014). In contrast, the trees planted in long rotations are considered as C stocks. The biomass is partitioned in aboveground and belowground. The aboveground biomass(AGB) referes to stem, branch, bark, while the belowground biomass(BGB) refers to all live roots except fine roots of sizes< 2mm diameter. During the long rotation, parts of biomass is lost due to the selective thinning or natural falling. Unlike grass crops, C contained in these woody residues would not emit back to the atmosphere in one or two years, but would slowly emit with a negative exponential tendency. According to the half-life decay value that depends on woody species and compartments, the emission could last for decades (Albers et al., 2019b).

For hundreds of years, logged roundwoods have been carpentered for buildings, in structures or in furniture, which could last fifty to hundred years (Dodoo et al., 2014). Combined with the long cultivating rotation, the life cycle of wood-building products could delay the C emission for around a hundred years, contributing to the mitigation target at 2100. In addition, at the end of the building's lifetime, landfilling and incineration are two critical options. Woody products decay slowly in the landfilling, the overall degradability of waste during 100 years is merely 1.5%, which means the C would be further kept out of the atmosphere for a long time (ecoinvent, 2020). However, landfilling demands

a lot of areas, and would cause other pollutants like leachate(Swati et al., 2019), thus incineration is the most common disposal way. Burning 1kg of wood could recover 3.5 MJ heat and 0.5 kWh electricity, with 0.164 kg CO_2-eq (ecoinvent, 2020) emissions.

the harvested biomass can be transformed into different kinds of bio-based anthropogenic products. These bio-based products broadly cover fuels, chemicals, materials, food, and feed, and replace fossil-based products, which could avoid C emission from fossil sources. Also, bio-based products could keep the biogenic C into the technosphere for a certain period, depending on the products' lifetime. For instance, the average impact of a building with 1 ton of wood instead of the same amount of concrete could reduce 2.1 t CO_2 over the whole life cycle, including use and disposal stages(Hurmekoski, 2017).

Industrial biotechnologyis one of the cornerstone of the bioeconomy, improving the conversion efficiency of these plant-derived resources into a wide range of anthropogenic products and maximizing the valorization of the biomass (Vanholme et al., 2013).

Besides biomass and bio-based products, the soil is another potential C tank. C stocked in soils could be assessed from soil organic carbon (SOC) changes. Kim et al. tracked the C flows of kenaf fiber-reinforced composite from cradle-to-grave, reported a 62 g C increase in the soil during the kenaf cultivation (Kim et al., 2008).

2.2 Carbon in soil and biomass

2.2.1 C in the soil

Soil carbon is the solid carbon stocked in the soil, including organic and inorganic carbon (SIC). The majority of carbon in most soils is stored in the form of soil organic matter(SOM) (Scharlemann et al., 2014). The SOM is the lifeblood of soil, generated from the decomposition of biomass residues, roots, soil organisms, whether living or dead. The SOM consists of humic, fulvic acids, and humin, containing functional groups such as R-COO-, R-C=O, R-COH, R-SH, and others, possessing cation exchange properties (Bianchi et al., 2008). This is similar to clay particles adsorbing metal cations on their surfaces, the difference is that the surface area and adsorptive capacity of SOM are much greater than those of clay. The clay percentage in the soil is critical in estimating the SOM. Clay particles and aggregates can reduce losses of SOM by physically protecting organic matter from decomposition. Particles of organic matter can become adsorbed to clay surfaces, coated with clay particles, or buried inside small pores or aggregates. These processes make it difficult for microorganisms to come in contact with organic matter. Therefore, the amount of SOM stored in soil tends to increase with increasing clay content. In contrast, in sand soil microorganisms can more easily access SOM. The SOM is evaluated by the determination of the SOC, the common practice in estimating the C change in the soil is directly estimating the situation of the SOC, the most cited indicator of soil quality in environmental assessment(Milà i Canals et al., 2007). The SOC could switch to the SOM by the van Bemmelen factor, which equals 1.724, based on the average C content of 58% in the organic matter(Pribyl, 2010). If this factor needs adjustment to fit a local case, it needs to measure the percentages of humic and non humic substances in the soil.

It is estimated that there is 950 Pg SIC in global soils (Fig. II-1), the form of SIC is carbonate minerals. It is the mineral form of C, predominately consisting of primary or lithogenic carbonates, and secondary or pedogenic carbonates. The SIC derives through two pathways (Lal, 2007):

1) Weathering of parent mineral ores;
2) Dissolution of CO_2 existing in the pores to form carbonic acid, then re-precipitating with Ca^{2+} or Mg^{2+} added into the soil as amendments or from other sources.

Fig. II-1 illustrates the C cycle between biomass, soil, and atmosphere, data were collected from (Lal, 2007). Biomass exchanges C with the atmosphere through photosynthesis and respiration. The term of soil C sequestration implies the transfer of atmospheric CO_2 into soil C pool through (i) humification of

crop residues and other bio-solids added to the soil, and (ii) formation of secondary carbonates or leaching of bicarbonates into the groundwater such that CO_2 thus captured is not immediately re-emitted (not shown in the figure). The pathway (ii) is not affected by biomass, it is not a strict soil C sequestration as the CO_2 could re-emit in a few weeks in the shortest situation (Lal, 2007). Pathway (ii) is not considered in this thesis. The relationship between land use (LU) and agricultural management is a two-way arrow since the C is sequestrated or emitted depending on different LU and management ways. Also, anthropogenic activities such as cultivation could accelerate the soil erosion and would break the C sequestration.

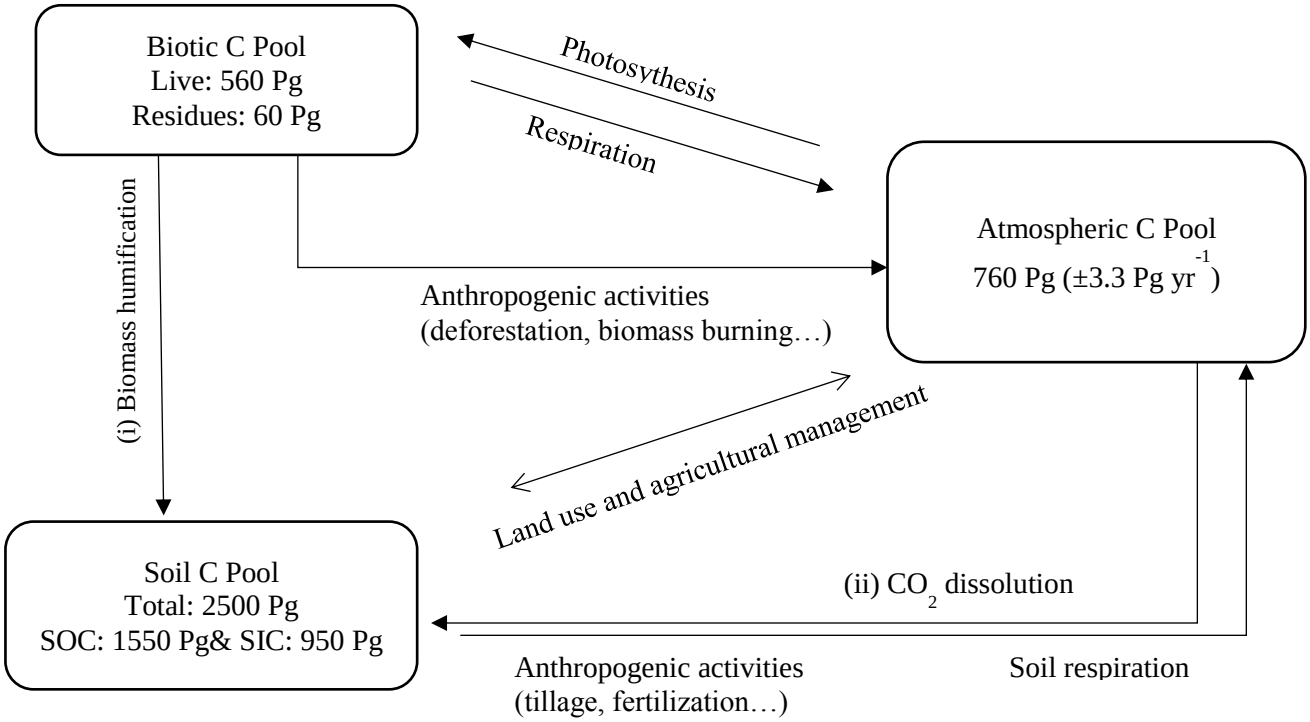

Fig. II-1 Carbon cycle and carbon pools. Data from (Lal, 2007).

2.2.2 Potential of the SOC in global warming mitigation

The SOC is recognized as the largest stock of terrestrial carbon. There is 125.8E8 ha soil in the world from 90° N to 60° S (Nachtergaele et al., 2012). The amount of the SOC varies among different estimations. For example, Scharlemann et al. counted recent 27 studies and determined a total average stock of 1500 Pg C, with a range from 504 to 3000 Pg, reflecting the disparity in sampling period, intensity and spatial resolution of the soil profile databases, and differences in calculation approaches (Scharlemann et al., 2014). According to the same database including the soil area, 1417 Pg SOC stock was counted in the upper 1 m of soils over the world (Nachtergaele et al., 2012). This amount of the SOC is twice the C in the atmosphere and three times those in the biomass, indicating a high potential of the soil C sink.

The worldwide SOC distribution is depicted in Fig. II-2. A large area fraction of deserts obviously reduces the continental average SOC stock, whereas a large fraction of frozen organic soil increases the continental average SOC stock, with the highest SOC deposit area in 50- 60° N, namely Canada, Eastern Europe, and Russia (Fig. II-2, b), because of the vast boreal climate lands.

Based on such a high potential of C sequestration by the soil, at the Paris Climate Summit in 2015, an initiative named '4 per 1000' was launched. The name of this initiative is based on the premise that if the SOC in global agricultural lands increases 0.4% per year(the first 30-40 cm), the soil could sequestrate 2.5 Gt C that can offset annual anthropogenic C emission from fossil sources(Minasny et al., 2017). This estimation is criticized because of intrinsic data and model uncertainty, but it represents a clear goal towards climate stabilization (Albers et al., 2021a).

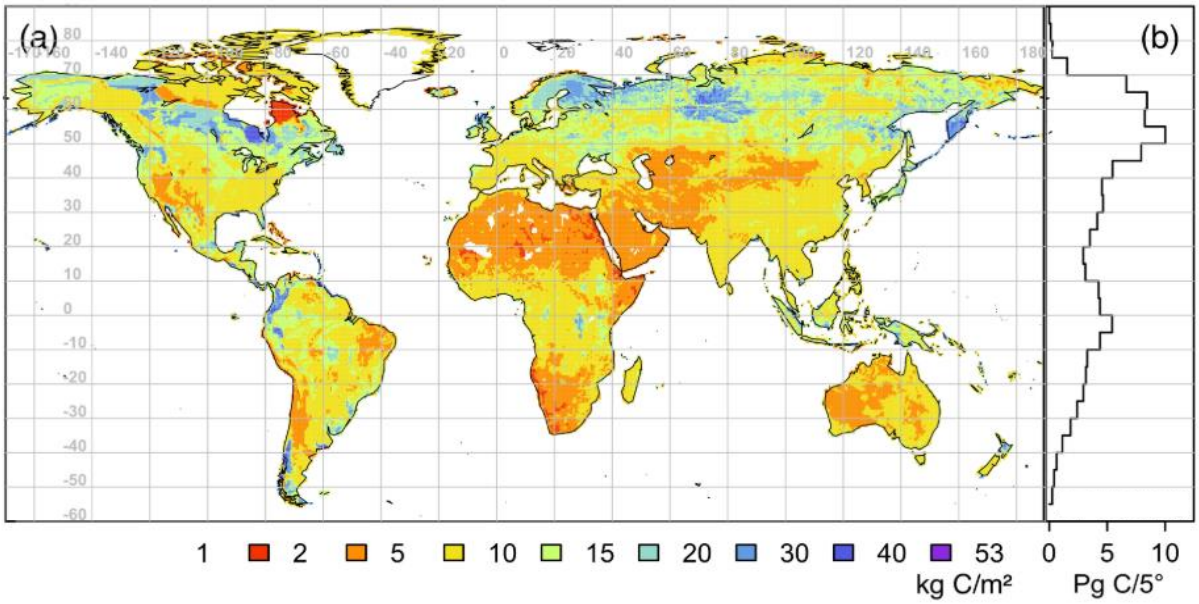

Fig. II-2 Globally SOC distribution (a) in mass and (b) per 5° latitude, retrieved from~(Köchy et al., 2015).

A particular drawback in current SOC studies is the lack of standardized carbon values to be reported. Ledo et al. counted 1605 ID entries in 180 studies, concluded that 70% of data use carbon stocks (Mg/ha), while 30% of studies use SOC concentration values (g/kg) (Ledo et al., 2019). SOC concentration values and stocks could be converted to each other through the equation (1)

$$SOC_{stock} = SOC_{con} * BD * depth * (1 - rock\ friction) * 10 \quad (1)$$

where SOC_{stock} is the SOC stock(Mg ha^{-1}), SOC_{con} is the SOC concentration in g/kg, BD is the soil bulk density in g/cm^3, $depth$ is the depth measured or simulated soil depth in cm, and $rock\ friction$ is the rock fragment percentage of the total soil. Though the SOC_{stock} and the SOC_{con} could be transformed each other, extra information is needed, which would induce uncertainty of the data. Further, not all researches would provide this additional information. From the statistics work of Ledo et al., only 43% and 51% of the studies provided the values of the soil texture and bulk density respectively (Ledo et al., 2019).

2.2.3 The role of biomass in SOC formation

The humification of the biomass is an important source of SOC (Fig. II-1). There is 560 Pg C in the live biotic pool and 60 Pg C in the residues (Lal, 2007). It is estimated that the average biomass of global

croplands could increase the SOC by 0.21-0.26 Mg ha^{-1} yr^{-1} in the future 50 years(Poeplau and Don, 2015).

The two main processes in the biomass-SOC relationship are mineralization and humification. Microorganisms help to decompose the biomass as organic matter, and emit back GHG (e.g., CO_2 and CH_4) to the atmosphere, which is called mineralization. In the humification process, the fraction that is not mineralized is transformed into concatenations of organic polymers which become the SOC. The humification is more efficient in cool and humid climates than warm and dry regions, thus the SOC stock in high altitudes is higher than in other areas (Fig. II-2,). The two major parameters of these two processes are microorganisms and C inputs (i.e., here from plant-based biomass but may also derive from external sources such as organic fertilizers). Fig. II-3 illustrates how microorganisms and C inputs influence the relationship between the SOC and biomass. First, plants fix/assimilate the inorganic C (mainly from CO_2) via photosynthesis and convert it into organic C which then goes into the soil as C-inputs from death organic matter of the plant. The soil is separated into AGB and BGB fractions (section 2.1.2). The AGB typically refers to the litter layer, where the organic matter is mineralized by earthworms and microbes, or oxidized partially via microbial extracellular enzymes. The BGB, on the other hand, is often assimilated by the microbes only, and undergoes biosynthesis, turns over prior to SOC incorporation. Around 25% of the BGB is released into the soil environment via the root rhizodeposition (Jones et al., 2009). The C deriving from BGB contributes approximately six times more C to the soil, as compared to the AGB, and may make up to 75% of total SOC (Jackson et al., 2017). There are several direct and indirect pathways responsible for the incorporation of C into the bulk of SOC. Direct mechanisms include exudate sorption to mineral surfaces and root litter protection in aggregate interiors, while indirect mechanisms include root-associated microorganisms or mycorrhizae (Pett-Ridge and Firestone, 2017; Sokol and Bradford, 2019).

The zoomed-out window in the upper right of Fig. II-3 represents the microbial activity and physical protections of SOC. The SOC mineralization process is fostered by certain root exudates of protective mineral associations. Microbial processes increase the solubility and potential for protecting the organic C compounds (Pett-Ridge and Firestone, 2017). Physical protection takes place in the fine pores of soil microaggregates (0.053 mm < diameter (Ø) < 0.25 mm) in which anoxic conditions prevail or which are inaccessible to, or spatially separated from, microbial decomposers (Rasse et al., 2005; Six et al., 2002). The creation of micrometer-scale pores and aggregates by mycorrhiza and root-hair activities enhances the physical protection of root-derived C from microorganisms (Stockmann et al., 2013). Microaggregates are often formed and stabilized within macroaggregates (Ø > 0.25 mm), the formation of which is fostered primarily by roots (Ge et al., 2018; Rasse et al., 2005). Both microbial and physical protections could reduce the probability of decomposition, slowing the decay rate, and creating the capacity of soil to sequester C (Lehmann and Kleber, 2015).

From the discussion above, the relationship between biomass and SOC is complex, plants could increase the SOC or not during the cultivation, depending on many factors. The same species might contribute to the SOC increase in one region but decreases it in another region (Shen et al., 2022b).

Understanding the mechanism of how biomass changes the SOC is essential. Based on a deep understanding of the mechanism, it is possible to build and simulate the SOC change in a future perspective.

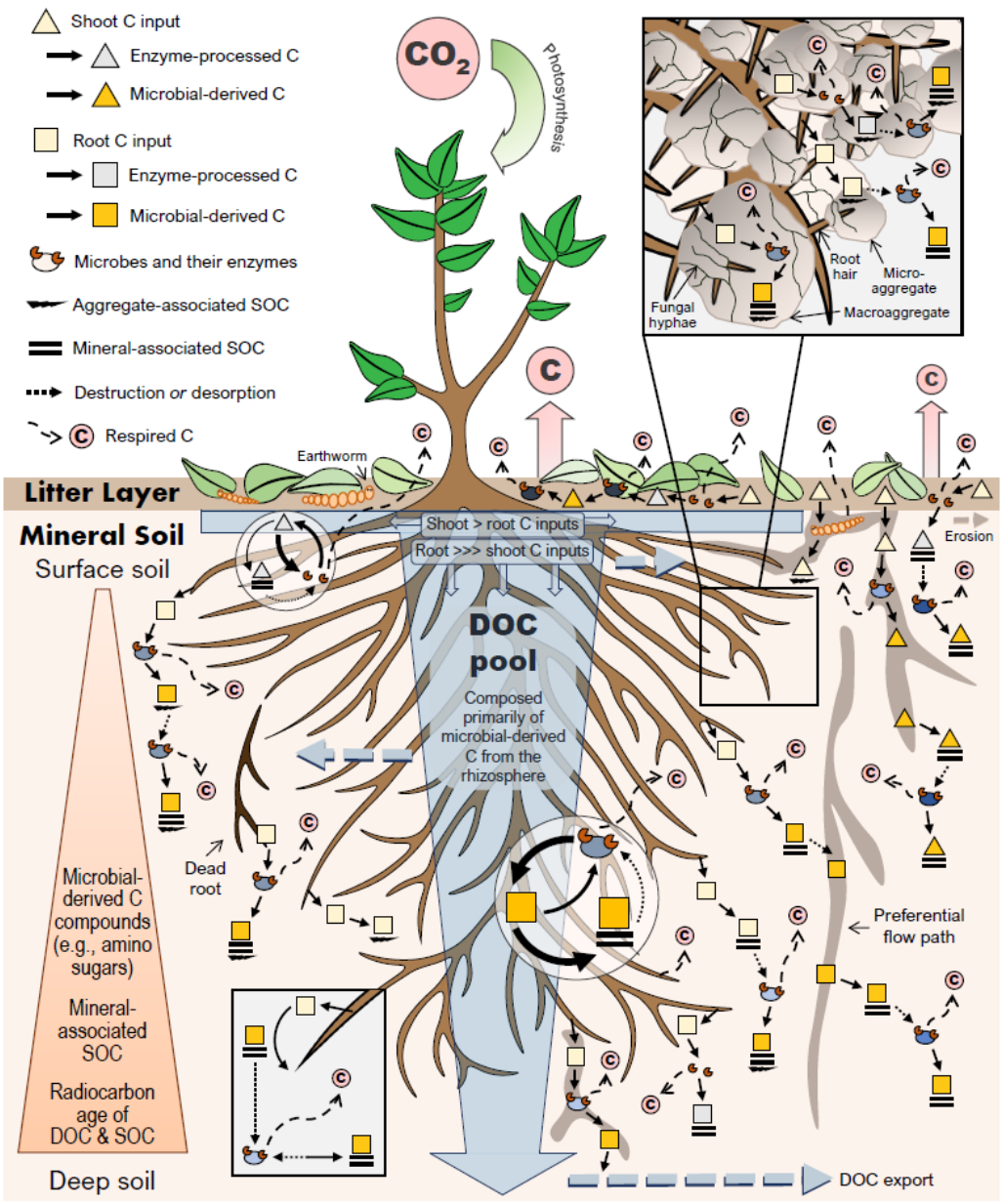

Fig. II-3 The mechanism of the SOC change by biomass, retrieved from ~(Gross and Harrison, 2019).

2.2.4 The SOC simulation

2.2.4.1 AMG model

Because of the complex relationship between biomass and SOC, the SOC change tendency under plants cultivation cannot be judged simply by the species. The measurement records are not always available, or even impossible when we want to know the future situation. Therefore, SOC simulation is a useful tool. The SOC simulation model provides a clear mathematical framework incorporating assumptions for soil processes, supporting hypothesis testing by predicting SOC dynamics in space and time. Because of the regional nature of the SOC simulation, researchers tend to propose and adjust the simulation tools by themselves based on their measurement data. There are more than seventy SOC simulation models published from 2000 to 2010 (Manzoni and Porporato, 2009). In this section, two models used in this thesis are introduced, AMG (Shen et al., 2022a) and C-Tool (Shen et al., 2022b, and chapter V).

AMG is a model simulating SOC at annual time steps, first proposed by Andriulo in 1999(Andriulo et al., 1999). It was proved to have satisfactory simulation results compared with measurement results, and was adopted to design innovative cropping systems (Autret et al., 2016; Saffih-Hdadi and Mary, 2008). AMG model is continuously updating, the version adopted in this thesis is AMGv2, which is calibrated for French users(Levavasseur et al., 2020). We use this version to illustrate how AMG simulates the SOC, based on the work of (Clivot et al., 2019).

AMG model considered three SOC components: the fresh SOC (FOC), active SOC (C_A), and stable SOC(C_S). The FOC comes from the biomass residues and organic amendments(e.g., biochar) that would experience mineralization or humification. The humified FOC might be mineralized and allocated to C_A, while C_S is resistant to mineralization. The SOC is described by formulas shown as below:

$$SOC = C_A + C_S \tag{2}$$

$$\frac{dSOC}{dt} = \sum_i m_i h_i - k\, C_A \tag{3}$$

where SOC is the SOC stock in Mg C ha^{-1}. C_A and C_S are C in active and stable SOC pool, respectively, both in Mg C ha^{-1}. m_i is the annual C inputs from source i (e.g., residues, manure), unit in t ha^{-1}, and h_i is the corresponding humification coefficient, which is dimensionless. k is the mineralization rate in the C_A, unit in yr^{-1}, calculated using environmental functions as follow:

$$k = k_0 * f(T) * f(H) * f(A) * f(CaCO_3) * f(pH) * f(C/N) \tag{4}$$

where k_0 is the potential mineralization rate in yr^{-1}, $f(T)$, $f(H)$, $f(A)$, $f(CaCO_3)$, $f(pH)$, and $f(C/N)$ are functions of temperature(°C), water input(mm)(including precipitation and irrigation), clay content, $CaCO_3$ content, soil pH, and C/N ratio, respectively. Among these factors, (T), $f(H)$, $f(A)$, $f(CaCO_3)$, $f(pH)$, and $f(C/N)$ come from soil texture and meteorological data of the aim region, the detail function could be found in appendix A of (Clivot et al., 2019), k_0 is calibrated according to the French environment and provided by AMG.

To use this model, besides the soil texture and meteorological data, C from biomass(or other sources) are entered the tool as aboveground C_{AG} and belowground C_{BG}.

$$C_{AG} = Y * C\% \tag{5}$$

where Y is the biomass DM left on the ground in t ha^{-1}, like stubble or residues, the harvestable part is not included here, and $C\%$ is the C content in the DM.

The calculation of C_{BG} is a little bit complex, it consists of C in the root (C_R) and C in the extra-root materials (C_E) that refer to the SOM due to root-turnover and root exudates. C_R could be measured directly, or calculated by the shoot-to-root ratio (SR) like below:

$$C_R = \left({}^{Y_t}/_{(SR * HI)}\right) * C\% \tag{6}$$

where here Y_t is the DM yield in t ha^{-1} of the whole crop (including the harvested part), HI is the grain to aerial biomass, called harvest index, $C\%$ is the C content in the DM.

$$C_E = 0.65 * C_R \tag{7}$$

The ratio between C_E and C_R is assumed by (Bolinder et al., 2007). After that, C_{BG} is calculated:

$$C_{BG} = BG_F * (C_R + C_E) \tag{8}$$

$$BG_{depth} = 1 - \beta^{depth} \quad (9)$$

Here BG_{depth} is the cumulative belowground input fraction from surface to the aim soil depth ($depth$ in cm), and β is the root distribution parameter, different for every plant but could be searched in the database.

After the user input C_{AG}, C_{BG}, and other soil texture and meteorological data, AMG would output the results in the aimed time period and soil depth range (from surface to the desired depth).

2.2.4.2 C-Tool model

Although AMG fits well for French soil cases, because it regards C_{BG} is the same every year, thus it does not support simulating the SOC change under perennial plants(Clivot et al., 2019). Therefore, to put the SOC change due to both annual and perennial plants under the same frame, C-TOOL is used. C-TOOL is proposed by (Taghizadeh-Toosi et al., 2014), and calibrated according to European situations. The illustration here of the mechanism of C-TOOL in simulating the SOC change is based on the work of (Taghizadeh-Toosi et al., 2014).

Similar to AMG, C-TOOL separates the soil in topsoil(0-25cm) and subsoil(25-100cm), accounting for 47% and 53% of the SOC of 1 m, respectively. Both topsoil and subsoil have three SOC pools: FOM, humified C(HUM), and C in the resistant organic matter(ROM) (Fig. II-4). In HUM pool, C experienced the microbial transformation and became stable in the soil, which is ascribed a decadal scale half-life. For organic amendments, like manure, part of it would undergo microbial activity, calculated by f_{HUM}(for biomass, f_{HUM} =0 since it begins at FOM). The recalcitrant C to the microbial mineralization is in the ROM pool, accounting for 25% of the initial SOC(Barré et al., 2010). The turnover of the C in this pool could be super slow, there is evidence that the SOC could survive 3300 years under aerobic conditions(Thomsen et al., 2008).

The C turnover in each pool is described in equation (10)

$$\frac{dC_i}{dt} = -k_i C_i F_T(T) \quad (10)$$

in the pool i, k_i is the mineralization coefficient(yr^{-1}), 1.44 yr^{-1} in the FOM pool, 0.0192 yr^{-1} in the HUM pool, and 4.63E-4 yr^{-1} in the ROM pool. C_i is the C amount in this pool (Mg ha^{-1}), $F_T(T)$ is the function of temperature(°C), which is the same for all three pools, default in 10°C but could be calibrated according to the local temperature as follow:

$$F_T(T) = 7.24exp\left[-3.432 + 0.168T\left(1 - \frac{0.5T}{36.9}\right)\right] \quad (11)$$

here T is the local temperature in °C.

The humification coefficient h is calculated according to the soil clay content,

$$h = \frac{1}{\left[1.67\left(1.85 + 1.6exp(-7.86clay)\right)\right] + 1} \quad (12)$$

$clay$ is the clay content in the soil in kg kg^{-1}.

Biomass first decomposes in the FOM pool, then a certain proportion of the C (t_f=0.03) is transported to the subsoil. The rest C (1-t_f) would be humified, the humified C (h) is allocated to the HUM pool, others (1-h) emits back to the air as CO_2(Fig. II-4). After that, f_{ROM} proportion (f_{ROM} =0.012) of the C is allocated to the ROM pool, part of C(f_{CO2}=0.628) turns over back as CO_2, the rest (1- f_{ROM}- f_{CO2}) is transported to the subsoil. In the ROM pool, undergoing the decomposition, a certain proportion of C(f_{CO2}) is emitted as CO_2, the rest (1-f_{CO2}) moves to the subsoil. Parameters like t_f are collected from the ^{14}C labeled experiments, and are exhibited in the (Taghizadeh-Toosi et al., 2014).

To use C-TOOL, besides soil texture and meteorological data, C are provided as C in topsoil $C_{top}$and in subsoil C_{sub}.

$$C_{top} = C_{AG} + \xi C_R \quad (12)$$

$$C_{sub} = (1 - \xi) C_R \quad (13)$$

where C_{AG} and C_R are same from equations (5) and (6) respectively, ξ is constant, equals to 0.7-0.9 depending on the land type.

As discussed in section 2.2.3, C inputs and microbes are two critical parameters in the SOC and biomass relation. However, the SOC models used now, such as CENTRUY, RothC, including two models introduced here, omit the function of microbial parameters, this shortage was also noticed by other users (Lehmann et al., 2020). Now, some researchers proposed potential ways to include that in the simulation (Woolf and Lehmann, 2019). However, these microbial included tools are not mature enough. The inputs of these novel models were not unified, leading to specific data requirements that are difficult to apply universally (Sulman et al., 2014; Wieder et al., 2014; Woolf and Lehmann, 2019). Therefore, since the AMG and C-TOOL have already been proved widely by the measurement data, here we still adopted these two in this thesis.

2.3 Marginal lands

Biomass has high potential in global mitigation, however, the land of intact and near intact ecosystems available for agricultural conversion is limited, even continues to shrink due to the increase of the population. Therefore, in global mitigation, effective land management for biomass must consider marginal landscapes.

2.3.1 The importance of marginal lands

With the growing demand for biomass, there is an increasing demand for corresponding lands. In the United States, biomass is the largest renewable energy source, coming from growing dedicated energy crops on agricultural lands (Langholtz et al., 2016). These increasing demands of energy crops squeezed the space of traditional agricultural products, causing the price surged in 2007 and 2008(Haberl et al., 2011). A common theme of why biomass is sustainable is that it should be cultivated in a sustainable way that is inextricably linked to its requirement for land for production. However, increasing demand for biomass inevitably leads to an increased demand for land on which energy crops could be grown. The extensive spatial footprint of bioenergy is problematic, and exploring areas where biomass can be planted and harvested sustainably has become the top priority (Thomas et al., 2021).

The land which might be converted, because its value under present usages are less than ideal, could have better values available in another context, is called marginal land (Richards et al., 2014). The context here means climate change mitigation. In cropland mineral soils, 30-50% of C has been lost due to degradation, which could be improved through converting land cover types(Albers et al., 2021b). Exploiting marginal lands could valorize their soil quality (e.g., soil fertility, soil structural stability) to a better C sequestration, because of the biodiversity conservation and eventual socio-economic development. Saha et al. estimated that 42130 t of biomass could be produced on marginal lands around Boston, the USA, further could yield 830 TJ bioenergy per year, equal to 8.1E7 kg CO_2-eq(ecoinvent, 2020; Saha and Eckelman, 2015).

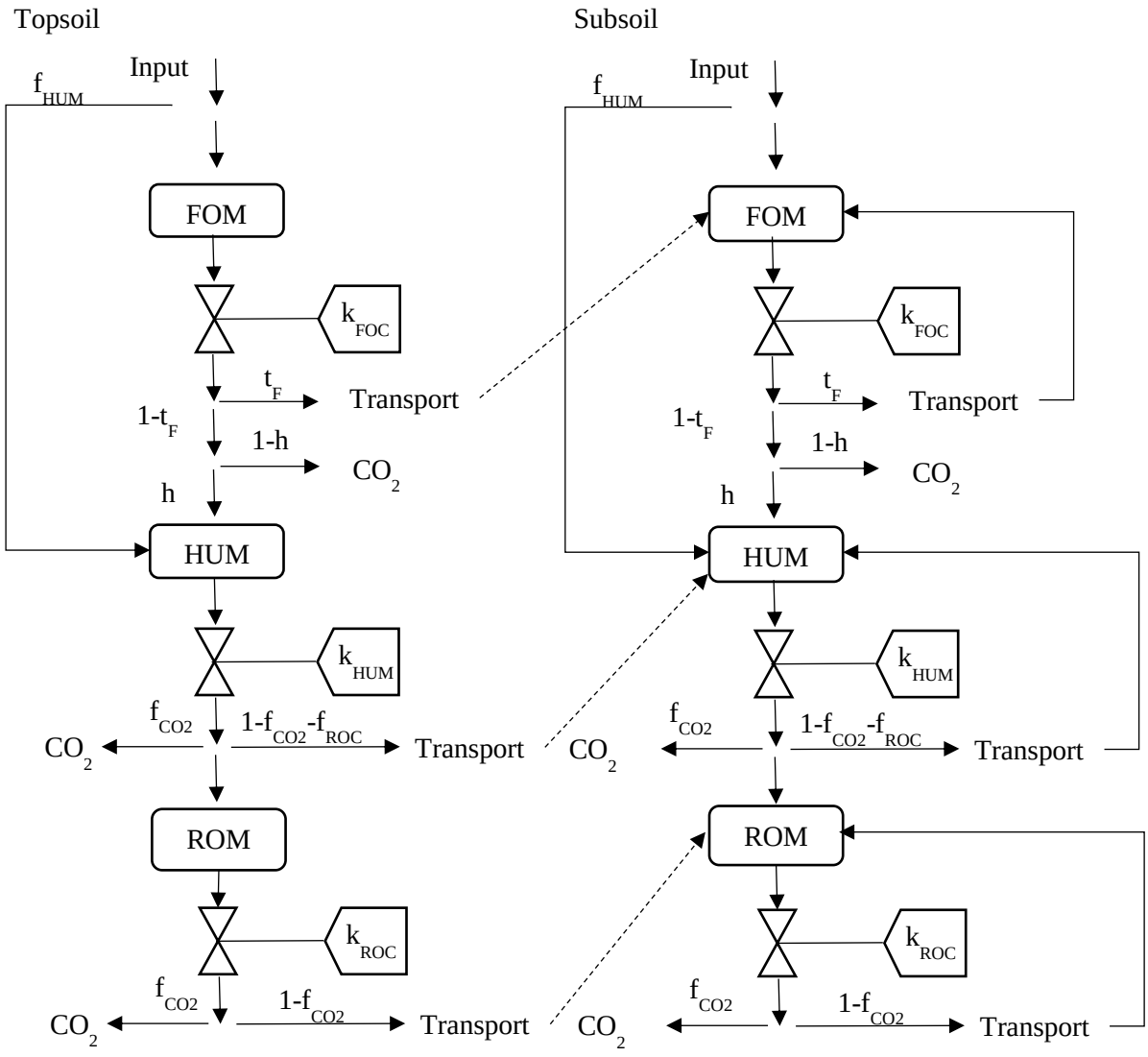

Fig. II-4 C-TOOL model structure(Taghizadeh-Toosi et al., 2014).

2.3.2 Marginal lands identification

The importance of marginal lands is widely admitted, but the land cover type range of 'marginal land' has been used loosely without a concrete definition. Thomas et al. proposed that marginal lands should benefit the carbon debt, not compete for food security, have no negative effects on ecosystem services and biodiversity quality (Thomas et al., 2021). Compared to agricultural crops (e.g., wheat, rice), bioenergy or biomaterial crops (e.g., miscanthus, willow) can adapt to various soil types, thus making them highly tolerant to multiple environmental conditions. In a general consensus, areas are marginal for conventional crops but not marginal for biofuel crops or other functions, based on economic, soil health, and environmental criteria, could be chosen as marginal lands. According to this rule, research has focused on identifying land that are unsuitable for food production but potentially suitable for non-food crops in the past decades.

Table II-1 reviews the principle of marginal land selection by different researchers. Some studies simplified the selection process but focused on the land type, which means all specific types of land would be regarded as marginal land (Niblick et al., 2013; Saha and Eckelman, 2015). Meanwhile, the criteria of most papers focus on three aspects, i.e., meteorology, geology, and soil characteristics. The temperature and precipitation could provide a suitable environment for plants, even for bioenergy/material plants that are adapted to various conditions, the extreme climate would cause less yield and decrease the amount of captured CO_2. Similar reasons for soil characteristics, if there is insufficient soil or the quality is not suitable for plants, it would be difficult to cultivate crops on these lands. In Table II-1, for example (Albers et al., 2021b) identified 2714 million ha marginal areas, but only 28 million ha could be used for growing plants for the C sequestration sake, because of the extreme climate and lousy soil conditions. The slope of the land is also frequently mentioned, because a gentle slope could minimize runoff and erosion, while the steep slope would lead to difficulty in agricultural management, commonly should not exceed 30% (Saha and Eckelman, 2015).

Table II-2 reviewed the main land cover types considered for marginal lands. Abandoned agricultural, degraded, and fallow lands are commonly selected since they have been proved for plants to live, though the yield of crops might not be satisfied. However, 'productivity' differs based on the land covers, these low 'productivity' lands might be well suited for bioenergy/biomaterial plants like sunflower (Saha and Eckelman, 2015). Converting low crop productivity lands to bioenergy/biomaterial plants fits the definition of marginal land from an economic point of view, which declares that certain lands have a comparably higher value if located in proximity to essential resources(Lewis and Kelly, 2014). Shrub, forest, and grassland are selected by many studies, while these studies also mentioned that the premise to choose these lands is excluding the natural reserve (Zhang et al., 2017). On behalf of shoal and bottomland, Wetland could not only be used for plants like giant reed, but also for cultivating algae (Saha and Eckelman, 2015). Idle and bare lands are considered widely are chosen since they are empty at present, while their availability needs to be further checked, especially in the economic aspect, since these lands could be part of the urban area, on commercial properties, thus the land values and labor costs could be high (Saha and Eckelman, 2015).

Table II-1 Review of marginal land selection criteria.

Ref	Meteorology		Geology		Soil characteristic										Applied location	Amount (M ha)	% total land
	Temperature	Precipitation	Slop	Flood risk	SOC	Type	pH	Salinity	Moisture	Coarse fragment	Groundwater	Fertility	Erosion	Depth			
(Zhang et al., 2017)	X	X	X		X	X	X								China	59.40	6.2%
(Albers et al., 2021b)	X	X	X	X	X		X	X	X	X		X	X	X	Global	2714	5.3%
(Milbrandt and Overend, 2009)			X				X		X	X					Asia-Pacific Economic Cooperation countries	4	6.5%
(Saha and Eckelman, 2015)			X			X									Boston, USA	2660 ha	24%
(Niblick et al., 2013)			X			X									Pittsburgh, USA	3500 ha	35%
(Kang et al., 2013)	X		X	X	X	X	X		X	X	X				Southwest Michigan, USA	0.56	40.03%
(Englund et al., 2019)				X	X							X	X		Europe		
(Shahid and Al-Shankiti, 2013)	X	X	X	X	X			X		X		X		X	Africa; Asia	1300;1100	42.8%; 24.67%

Table II-2 Review of marginal land type.

	Shrubs	Sparse forest	grassland	Bare area	Sparsely vegetated	Abandoned agricultural land	Urban land	Degraded land	Dump	Strip mines	Gullied land	Dry land	Saline land	Pastoralism	Desert	Fallow land	Wetland	Idle	Contaminated land
(Zhang et al., 2017)	X	X	X															X	
(Albers et al., 2021b)				X	X	X													
(Milbrandt and Overend, 2009)			X	X										X	X				
(Saha and Eckelman, 2015)			X					X											
(Niblick et al., 2013)							X		X	X	X								
(Shahid and Al-Shankiti, 2013)												X	X						
(Schubert et al., 2008)								X											
(Campbell et al., 2008)								X											
(Cai et al., 2011)						X		X										X	
(Wicke, 2011)						X		X								X		X	
(Dauber et al., 2012)						X		X								X			
(Fahd et al., 2012)						X		X										X	
(Liu et al., 2012)	X	X	X	X									X						
(Lu et al., 2012)	X	X	X	X									X				X		
(Rettenmaier et al., 2012)	X	X		X		X		X								X	X	X	
(Gopalakrishnan et al., 2009)			X													X	X	X	X
(Shortall, 2013)		X						X								X		X	
(Xue et al., 2016)	X	X		X	X								X		X		X		
(Blanco-Canqui, 2016)						X	X	X		X			X		X				X
(Milbrandt et al., 2014)						X	X		X	X								X	
(Elbersen et al., 2018)								X											X

2.4 Environmental impact evaluation

With the rising demand and use of biomass, regulating and controlling the environmental impacts of biomass utilizations has become a necessity. Life cycle assessment (LCA), including variants as social assessment or cost assessment, has continuously evolved and gained increasing recognition as an approach for evaluating the environmental impacts of anthropogenic activities.

2.4.1 Principles of the LCA method

LCA method accounts for all resources consumed and emissions associated with an anthropogenic product along its whole life cycle. These elementary flows form the life cycle inventory (LCI). LCI is further translated into several impact categories, like climate change, human toxicity, and eutrophication, credits to different life cycle impact assessment methods (LCIA).

A product's life cycle could be roughly divided into four phases: raw material extraction, product manufacturing, product use, and disposal. An LCA that includes all these four phases is called 'cradle-to-grave', while if a study considers only intermediate phases like manufacturing, it is called 'gate-to-grave'; similar, there are 'cradle-to-gate', or 'gate-to-gate' boundaries, depending on the assessment objective.

According to ISO standards 14040-14044 (International Organization for Standardization, 2006; International Standard Organization, 1997), there are four steps to conduct an LCA study: 1) goal and scope definition, including the definition of the system's function and functional unit, 2) LCI building, based on the knowledge of inputs and outputs related to each process in the life cycle system under study; 3) impact calculation by using appropriate LCIA methods; 4) result interpretation and conclusions.

Concerning impact calculation, different methods are available, based on either a mid-point (an environmental problem) or end-point (damages on the targets) evaluation. For example, CML and Environmental Footprint initiative (EF) are mid-point methods, while ReCiPe evaluates both. In this thesis, the EF method was chosen because it is recommended by the European Commission, for further standardization and homogenization of LCA in Europe (Albert, 2019).

Attributional and consequential are two main analytical approaches in LCA. Commonly, they are distinguished by different estimation targets: attributional LCA (ALCA) aims to describe all environmental flows within the designed life cycle, including flows from subsystems, answering 'what share of environmental impacts belong to a product system'; on the other hand, consequential LCA (CLCA) is a forward-looking approach, describing how flows will change in response to possible decisions in environmental impacts, aiming to answer 'what are potential environmental consequences of a product system'(Finnveden et al., 2009). The difference between ALCA and CLCA is not only to the goal of the study but also the dataset choices and the way to deal with multifunctionality.

In general, when a production system has more than one type of product, it is a multifunctional process. How to quantify the total functional outputs of the multi-productions system and then reflect the environmental burdens is a problem. The CLCA considers how the environmental burdens are affected by the multifunctional process, not only the outputs but also the flows of inputs, emissions, and wastes are included. Whenever these flows are affected, the system should be expanded to comprise the involved process. Therefore, the by-products production is affected by the change of the main product, which needs to be included in the CLCA. The by-product is typically assumed to substitute the product's manufacture with a competitive relationship in the market. The use of the by-product would not affect the main product production, but affect the marginal, alternative use of the by-production, which should be included in the CLCA (Ekvall, 2019). However, sometimes if the by-products are not utilized, like a residual material is disposed as waste, then the use of by-products does not affect the alternative service, just adding the disposal process in the CLCA. The system expansion is not endless, if ignoring an

involved process is not significant for the results and conclusions, the system expansion could be stopped. A cut-off criterion needs to be made to judge this situation.

Face to multifunctionality, ALCA allocates the share of inputs and outputs belonging to the investigated product, hence estimating the corresponding environmental burdens of the product. Price is commonly used as the allocation basis, because it can be consistent in the whole life cycle for products and functions (e.g., energy cannot be quantified in mass, *vice versa*). However, using price as the basis would bring uncertainty to LCA, because results would vary with the price over time and region.

Another major difference between ALCA and CLCA is the background dataset. For a substance used in the production system (e.g., resin in plastic production), the targeted product's environmental impact share comprises the production system of this substance with the same share (e.g., 80% flows belong to plastic, then 80% impact of resin should be included in the plastic investigation). As the goal of CLCA is to evaluate the environmental performance change of producing the target product, the product replaced must be chosen, these data are called marginal data.

Although ALCA and CLCA are different as discussed, the strict difference is ambiguous. In the ISO standard, there is no specific definition of these two approaches, thus there is no obvious way to recognize which approach is adopted by a LCA case (International Organization for Standardization, 2006; International Standard Organization, 1997). ALCA also adopts system expansion to deal with multifunctional systems, and in the system with only one output, there is no need to make an allocation (Douziech et al., 2021).

2.4.2 LCA of bio-based anthropogenic products

LCA has already been applied in assessing biomass and the corresponding bio-based anthropogenic products. Brassard et al. estimated pyrolyzing biomass from forest residues into biocrude oil, wood vinegar, biochar, and gas. Compared to the reference flow, pyrolyzing 1 t biomass could reduce 900 kg CO_2, and present trade-offs in cancer human effect and other five environmental impacts (Brassard et al., 2021). Tonini et al. evaluated cultivating 1 ha of willow (*Salix viminalis*) and *Miscanthus giganteus* to produce bioenergy, resulting in 82 and 45 t CO_2-eq reduction respectively, referring to the fossil energy. Bioenergy from ryegrass (*Lolium perenne*) would increase the GHG emission due to a 310 t CO_2-eq emission from 1 ha indirect land use change. At the same time, aquatic eutrophication of P and N should be noticed due to the fertilization (Tonini et al., 2012).

Once the bioenergy is used, the C within biomass would emit to the atmosphere immediately, without the C sequestration function. The major negative emission effect comes from the avoided fossil fuel. For biomass commonly grown in marginal lands, like vigorous herbaceous crops (e.g., flax, switchgrass) and SRC (e.g., willow, poplar), plant cell walls make up around 70% of the biomass. Further, 75% of cell walls are polysaccharides, and cellulose is the major polysaccharide of the cell wall, also considered as the world's most abundant biopolymer (Vanholme et al., 2013). Because of that, bio-based reinforcement materials have attracted lots of attention. Hottle et al. (2017) evaluated four bio-based plastics made from sugar cane, pointed out that bio-based plastic production emits roughly 50% CO_2-eq of fossil-based, and the disposal process is the main burden in climate change and fossil fuel depletion categories, recycling 1 kg of the bio-based plastic rather than landfilling or compositing would increase 0.81-1.09 CO_2-eq and 1-1.68 MJ surplus in climate change and fossil fuel depletion respectively, mainly because of the international shipping process. On the opposite, La Rosa et al. (2013) concluded during the disposal of hemp fiber composite, there was no significant change in resource depletion(including fossil fuel depletion impact) but recycling behaviors double better than landfilling in human health impact(including climate change). In addition, because hemp fiber is lighter than conventional glass fiber, when adopting hemp fiber in car panels, hemp fiber composites not only emit a quarter of GHG of conventional glass fiber composites during the production but also save 0.3-0.5 L $100km^{-1}$ $100kg^{-1}$ gasoline and sequester 91 g CO_2 per 820 g composite for 10 years in the use stage. While in Campos et

al.'s research, 1 m^2 of flax fiber textile could keep 1250 kg CO_2 for around 25 years but would emit overwhelming GHG because this biocomposite is heavier than the conventional aramid fiber panel, increasing the diesel consumption during the use phase (Gomez-Campos et al., 2021, 2020).

The long timespan trees are traditional raw materials for bio-based products , widely used in building for hundreds of years (Dodoo et al., 2014). In general, wood-based products have a longer lifespan than grass fiber composite, 1 m^3 properly installed wood board could keep around 800 kg CO_2 for 50 years in default, or even reach over 100 years in European service classes 1 and 2 (Stora Enso, 2020). Furthermore, erecting a building with wood boards instead of traditional materials like brick or concrete could save at least 30% energy consumption, and the same during the demolition (Jayalath et al., 2020).

In conclusion, there are many LCA on biomass and downstream anthropogenic products. A major part is about bioenergy, which could not keep C in the technosphere for a long time. For herbaceous crops and SRC, most studies before 2010 are attributional, allocated environmental impacts based on mass or economic values based on the old ISO standard (González-García et al., 2010; Norton et al., 2008), the different allocation rules from different studies induced subjectivity into the LCA results. Some studies adapted consequential analytical modeling but not on the whole life cycle, lacking the use and disposal stages (Chen et al., 2016; Zampori et al., 2013). Some studies included the entire product's life cycle, focusing on GHG emissions but not assessing all environmental impacts (Andersson and Björhagen, 2018; Chen et al., 2019). Two critical shortages of biomass- anthropogenic products studies yet are observed. The first is not considering the consequence of crops grown on expanded or substituted lands. The second is the lack of involving SOC change during the cultivation in the inventory. For studies object to long lifespan wood, the frontiers start with the biomass harvesting, namely gate-to-grave or even gate-to-gate (Corradini et al., 2019; Piekarski et al., 2017). If the growth period is skipped, it is impossible to know the C absorbed by year, since the growth is not constant and takes decades, and further also the C change in the soil is ignored. The disadvantage of not including the use phase is that some flows may be missed, like CO_2 absorption during the use of hemp concrete, or different energy consumption because of different thermal conductivity of the wood boards and bricks (Liu et al., 2016; Pretot et al., 2014). Different disposal ways might change the conclusion, incineration would emit biogenic C of products immediately while landfilling or recycling would delay the emission. Furthermore, lacking the disposal phase might overestimate the negative emission of biomass, since all biogenic C would back to the atmosphere eventually. A common way to avoid this mistake is taking neither C captured through photosynthesis nor C emission at the end of life in account to be balanced, ignoring the biogenic C but only considering the fossil-source C in estimating climate change. Nevertheless, the function of delaying C emission through keeping C in the technosphere is not assessed. To overtake this shortage, a dynamic method is expected.

2.4.3 Dynamic LCA

In static LCA, climate change is estimated by Global Warming Potential (GWP). GWP is the integrated radiative forcing(RF) of an impulse, unitary emission of a GHG, over a fixed time horizon, divided by the same parameter of CO_2. GWP provides a metric for comparing the global warming effects of different GHG, in CO_2-eq, widely used in the LCA method. However, it is calculated based on the pulse emission, while in the real world, GHG are emitted with various temporalities. Moreover the behavior of CO_2 is specific as it is the only GHG with infinite time residence in the atmosphere. Then, the lifetime of GHG in the atmosphere, whether long-lived or short-lived, is ignored, concealing the intrinsic behaviors and contributions of distinct types of GHGs. Last, calculating GWP needs to fix the time horizon(TH), commonly at 100 years, albeit other values are adopted like 20 or 500 years. These time horizons are arbitrarily chosen, without a scientific base (Smith, C., Z.R.J. Nicholls, K. Armour, W. Collins, P. Forster, M. Meinshausen, M.D. Palmer, 2021).

So far, there is no unified metric in dynamic climate change assessment. Similar to absolute GWP, some works proposed bio GWP for biogenic GHG, based on the integration of radiative efficiency of biogenic

GHG in a temporal period that integrates CO_2 radiative efficiency as the baseline(Cherubini et al., 2011). Cardellini et al. adapted the best-first graph traversal to calculate the inventory of a glued laminated timber product, developed software to assess the dynamic climate change, proving the climate change results differed a lot between static and dynamic approaches (Cardellini et al., 2018). All examples above evaluate climate change differently, they are still based on GWP, with fixed TH of 20, 100, or 500 years. Levasseur et al. proposed using absolute GWP value (or integrated radiative forcing of a impulse emission) in dynamic LCA, calculating the reminding gas amount after emission by a first-order decay equation, then multiplying the amount of reminding gas at time t with the initial emitted amount, as the climate change metric.

One of the physical parameters which measure the climate change effect is the change of the global mean surface temperature of the planet. The global mean temperature change(GMTC) can be used as an impact metric (in temperature units). The GMTC distinguishes systems with different temporalities, evaluates mitigation scenarios, as reported in previous studies(Negishi et al., 2019; Shimako et al., 2018a). Moreover, the method based on GMTC can include climate objectives and evaluate climate neutrality, in terms of temperature and time, as reference points for the analysis of a system's performance (Tiruta-Barna, 2021). This method is based on the modelling approach recommended by IPCC in 2013 (Thomas F. Stocker et al., 2013).

The first step of modeling GMTC is to know the amount of emission, for example, we refer to a GHG as s, and g_s means the amount of emission of s at a certain time (t), in kg year^{-1}. The concentration of s in the atmosphere in the function of time depends on the gas properties, i.e., its partitioning between the Earth compartments, chemical reactions and other bio-physical interactions. For example, in the case of CO_2, its behavior can be modeled by the Bern model (Den Elzen et al., 1999).

The complex behavior of gases can be represented by impulse response functions (IRF), obtained by simplified modeling, as taken from the IPCC report (Shimako, 2017; Thomas F. Stocker et al., 2013). IRF describes the concentration in the function of time of s emitted at the time t_0(impulse emission). Therefore, for any emission $g_s(t)$, the atmospheric burden (B_s) is calculated by the convolution of g_s and IRF_s.

$$B_s(t) = \int_{t_0}^{t} g_s(t')\, IRF_s(t - t')dt' \tag{14}$$

Then B_s is converted to RF by multiplying it with the radiative efficiency A_s (W m^{-2} kg^{-1}, the RF of 1 kg s, in W m^{-2}).

$$RF_s(t) = A_s(t)B_s(t) \tag{15}$$

If the burden is small, A_s could be regarded as time-invariant. Then summing up the RF of all involved GHG into one obtained the dynamic global RF(W m^{-2}).

$$RF(t) = \sum_{S} RF_s(t) \tag{16}$$

GMTC (in temperature units, K) is calculated similarly through the convolution of calculated RF and the temperature impulse response function ($IRFT$), which is also provided from IPCC report(Thomas F. Stocker et al., 2013).

$$GMTC_s(t) = \int_{t_0}^{t} RF_s(t')\, IRFT_s(t - t')dt' \tag{17}$$

Then summing up the GMTC of all GHG obtained in the function of time t.

$$GMTC(t) = \sum_{s} GMTC_s(t) \quad (17)$$

The cumulated GMTC, called here $iGMTC(TH)$ (K year), is defined by:

$$iGMTC(TH) = \int_{t_0}^{TH} GMTC(t)dt \quad (18)$$

where (t_0 – TH) represents the time interval of interest for the case under study.

Unlike the static LCA, there is no unified method for all impacts in dynamic LCA, thus in this work, only climate change is evaluate with a dynamic approach. The GHG included in this work are the GHG present in the ecoinvent database (ecoinvent, 2020).

Only few studies used the dynamic LCA as application for long-life bio-based products. In a recent work, a detailed model about perennial growth that included the SOC change, assessed the bioenergy production in the dynamic way, and highlighted the mitigation due to the C sequestration in the rhizome fraction (Albers et al., 2019a). Cherubini et al. estimated the dynamic emission for wood used for combustion, undertook a complete consideration of all C components and biogeochemical sinks, and proposed a method based on GWP to integrate the effect of biogenic CO_2 in static LCA (Cherubini et al., 2011). However, the CO_2 emissions from C pool other than aboveground vegetation (like SOC and residues) were not considered. Cardellini et al. did a cradle-to-grave for wood-glulam production, estimated 50-years lifetime glulam under the TH of 500 years GWP metric(Cardellini et al., 2018). Besides the fixed TH metric, in studies of both Cardellini and Cherubini, the biomass growth rate was not modeled, which would affect the absorbed C amount every year. Indeed the tree growth is not the same every year; the mature trees diminish their CO_2 absorption (Rédei et al., 2012). In addition, the residues of herbaceous biomass could be decomposed in a short period, while the decomposition of woody residues could take much more time. The half-time life of the woody residue decay varies from 10 years to 30 years, depending on the species (Albers et al., 2019b), delaying the C emission towards the atmosphere.

2.5 Limitation of current evaluation about biomass

From the bibliography survey, one can identify several shortages of current analyses of biomass-anthropogenic products.

In biomass evaluations, SOC was often ignored or assumed to be maintained, which does not suit the actual situation, missing a part of C stock or C emission that depends on crops typology.

Not all studies, a lot of which dealt with C footprint, evaluate all environmental impacts and identified the trade-offs between the impact results, with a view to respect all areas of protection.

Traditional biomass evaluation treats biogenic C as neutral, considering inputs and outputs of biogenic C are balanced thus do not need to be included in the inventory(da Costa et al., 2018). This is not a wrong way to handle biogenic C in the static situation but is suspected when considering a long time scale. Herein, because the milestones of achieving carbon neutrality and limiting the GMT are both in the future, it is necessary to be prospective and include temporal characteristics into the biomass evaluation.

There is no comprehensive research using dynamic LCA with temperature evaluation to investigate the C delay effect of bio-based anthropogenic products (compared to bioenergy), by assessing the whole life cycle including SOC change, biomass growth, and residue decomposition in the timeline.

Whether in static LCA or dynamic LCA, when assessing the plant-product process, plants are regarded to grow on existing lands, which means land use (LU) and land use change (LUC) are not properly included in the inventory and dynamic timeline.

To the best of authors' knowledge, this is the first work identifying French marginal lands, and assessing the whole life cycle of biomass-anthropogenic products with plants grown on identified marginal lands, through consequential and dynamic LCA, to investigate the biomass performance in global warming mitigation and other environmental impacts.

2.6 Research objectives and thesis structure

In this work we ambition to propose a strategy for climate mitigation based on a nexus "plant-land-product'. The difference with the current literature is that the product is not the goal *per se* but a mean to induce mitigation, and that the nexus must be regarded as a whole.

The thesis aims to answer three scientific questions:

1) Is it possible to select plants that could play the role of biopump ?

2) Which will be the environmental performances of such strategy ?

3) How effective will be the climate mitigation effect ?

Considering the shortages discussed from the literature review, the thesis aims to answer the three scientific questions and provide a framework to evaluate the environmental impacts of activities comprehensively involving biomass, especially for climate change that is assessed under a long timescale.

The thesis is composed of seven chapters and supplement information (chapter III, IV, and V) with detailed information and results. The report organization is schematically presented in Fig. II-5.

Chapter I: Introduction – the context of this research.

Chapter II: Literature review, about how biomass could help us mitigate global warming, the current evaluation methods, and the aim of this thesis.

Chapter III: The definition of biopump, identification of lands suitable for planting biopump, identifying potential biopump candidates, and demonstrating the feasibility of using biopump as negative emission.

Chapter IV: Application of the concept to annual plants, with hemp as example.

Chapter V: Application of the concept to perennial plants with black locust as example.

Chapter VI: Synthesis of the results and comparison of the different scenarios investigated in chapters IV and V.

Chapter VII: Final conclusions and perspectives.

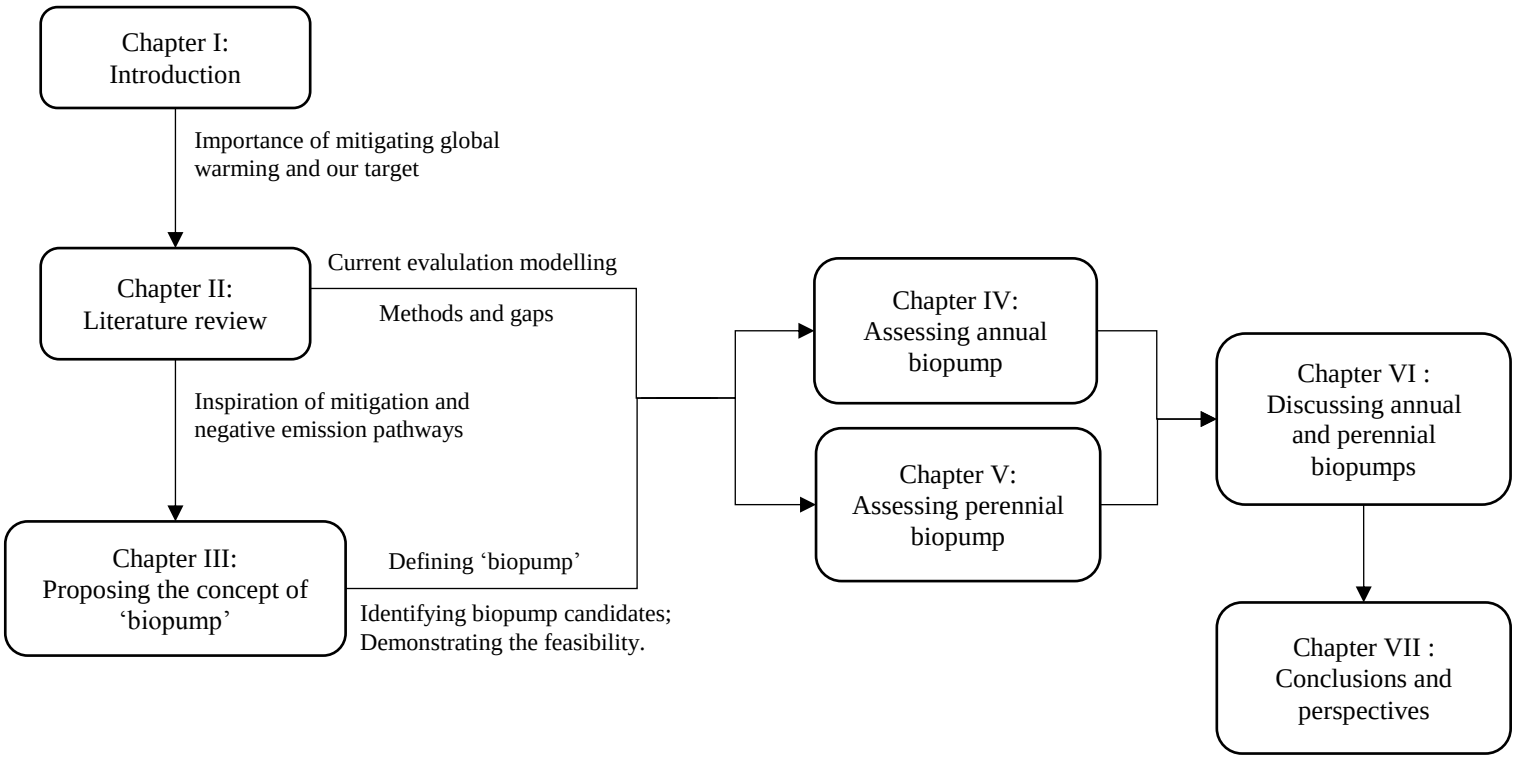

Fig. II-5 Simplified structure of the thesis

Publications :

Shen Z., Tiruta-Barna L., Hamelin L., Simultaneous Carbon Storage in Arable land and Anthropogenic Products (CSAAP): demonstrating an integrated concept towards well below 2°C, Resources, Conservation & Recycling, 182, 2022, 106293

Shen Z., Tiruta-Barna L., Hamelin L., From hemp grown on carbon vulnerable lands to long-lasting bio-based products: uncovering trade-offs between overall environmental impacts, sequestration in soils and dynamic influence on global temperature . submitted to Science of the total environmental

Reference

Albers, A., Avadí, A., Benoist, A., Collet, P., Hélias, A., 2019a. Modelling dynamic soil organic carbon flows of annual and perennial energy crops to inform energy-transport policy scenarios in France. Sci. Total Environ. 135278. https://doi.org/10.1016/j.scitotenv.2019.135278

Albers, A., Avadí, A., Hamelin, L., 2021a. SI-A generalizable framework for spatially explicit exploration of soil carbon sequestration on global marginal land. Sci. Rep. https://doi.org/10.21203/rs.3.rs-701807/v1

Albers, A., Avadí, A., Hamelin, L., 2021b. A generalizable framework for spatially explicit exploration of soil carbon sequestration on global marginal land. Sci. Rep. https://doi.org/10.21203/rs.3.rs-701807/v1

Albers, A., Collet, P., Lorne, D., Benoist, A., Hélias, A., 2019b. Coupling partial-equilibrium and dynamic biogenic carbon models to assess future transport scenarios in France. Appl. Energy 239, 316–330. https://doi.org/10.1016/j.apenergy.2019.01.186

Albert, A., 2019. The time dimension in the environmental assessment of biomass products: Dynamic carbon modelling.

Andersson, K., Björhagen, I., 2018. Material Choices for a Fossil-Free Preschool - An Interview Study on How Materials are Chosen, and a Life Cycle Assessment of Hemp Insulation. CHALMERS UNIVERSITY OF TECHNOLOGY.

Andriulo, A., Mary, B., Guerif, J., 1999. Modelling soil carbon dynamics with various cropping sequences on the rolling pampas. Agronomie 19, 365–377. https://doi.org/10.1051/agro:19990504

Autret, B., Mary, B., Chenu, C., Balabane, M., Girardin, C., Bertrand, M., Grandeau, G., Beaudoin, N., 2016. Alternative arable cropping systems: A key to increase soil organic carbon storage? Results from a 16 year field experiment. Agric. Ecosyst. Environ. 232, 150–164. https://doi.org/10.1016/j.agee.2016.07.008

Barré, P., Eglin, T., Christensen, B.T., Ciais, P., Houot, S., Kätterer, T., Van Oort, F., Peylin, P., Poulton, P.R., Romanenkov, V., Chenu, C., 2010. Quantifying and isolating stable soil organic carbon using long-term bare fallow experiments. Biogeosciences 7, 3839–3850. https://doi.org/10.5194/bg-7-3839-2010

Barton, L., Thamo, T., Engelbrecht, D., Biswas, W.K., 2014. Does growing grain legumes or applying lime cost effectively lower greenhouse gas emissions from wheat production in a semi-arid climate? J. Clean. Prod. 83, 194–203. https://doi.org/10.1016/j.jclepro.2014.07.020

Benton, J.R., Klopfenstein, T.J., Erickson, G.E., 2005. Effects of Corn Moisture and Length of Ensiling on Dry Matter Digestibility and Rumen Degradable Protein. Nebraska Beef Cattle Reports 31–33.

Bianchi, S.R., Miyazawa, M., De Oliveira, E.L., Pavan, M.A., 2008. Relationship between the mass of organic matter and carbon in soil. Brazilian Arch. Biol. Technol. 51, 263–269. https://doi.org/10.1590/S1516-89132008000200005

Blanco-Canqui, H., 2016. Growing Dedicated Energy Crops on Marginal Lands and Ecosystem Services. Soil Sci. Soc. Am. J. 80, 845–858. https://doi.org/10.2136/sssaj2016.03.0080

Bolinder, M.A., Janzen, H.H., Gregorich, E.G., Angers, D.A., VandenBygaart, A.J., 2007. An approach for estimating net primary productivity and annual carbon inputs to soil for common agricultural crops in Canada. Agric. Ecosyst. Environ. 118, 29–42. https://doi.org/10.1016/j.agee.2006.05.013

Brassard, P., Godbout, S., Hamelin, L., 2021. Framework for consequential life cycle assessment of

pyrolysis biorefineries: A case study for the conversion of primary forestry residues. Renew. Sustain. Energy Rev. 138, 110549. https://doi.org/10.1016/j.rser.2020.110549

Cai, X., Zhang, X., Wang, D., 2011. Land availability for biofuel production. Environ. Sci. Technol. 45, 334–339. https://doi.org/10.1021/es103338e

Campbell, J.E., Lobell, D.B., Genova, R.C., Field, C.B., 2008. The global potential of bioenergy on abandoned agriculture lands. Environ. Sci. Technol. 42, 5791–5794.

Cañellas, I., Sánchez-González, M., Bogino, S.M., Adame, P., Herrero, C., Roig, S., Tomé, M., Paulo, J.A., Bravo, F., 2008. Silviculture and carbon sequestration in Mediterranean oak forests, in: Managing Forest Ecosystems: The Challenge of Climate Change. pp. 317–338. https://doi.org/10.1007/978-1-4020-8343-3_18

Cardellini, G., Mutel, C.L., Vial, E., Muys, B., 2018. Temporalis, a generic method and tool for dynamic Life Cycle Assessment. Sci. Total Environ. 645, 585–595. https://doi.org/10.1016/j.scitotenv.2018.07.044

Chen, C.X., Pierobon, F., Ganguly, I., 2019. Life Cycle Assessment (LCA) of Cross-Laminated Timber (CLT) produced in Western Washington: The role of logistics and wood species mix. Sustain. 11. https://doi.org/10.3390/su11051278

Chen, L., Pelton, R.E.O., Smith, T.M., 2016. Comparative life cycle assessment of fossil and bio-based polyethylene terephthalate (PET) bottles. J. Clean. Prod. 137, 667–676. https://doi.org/10.1016/j.jclepro.2016.07.094

Cherubini, F., Peters, G.P., Berntsen, T., Strømman, A.H., Hertwich, E., 2011. CO2 emissions from biomass combustion for bioenergy: Atmospheric decay and contribution to global warming. GCB Bioenergy 3, 413–426. https://doi.org/10.1111/j.1757-1707.2011.01102.x

Clivot, H., Mouny, J.C., Duparque, A., Dinh, J.L., Denoroy, P., Houot, S., Vertès, F., Trochard, R., Bouthier, A., Sagot, S., Mary, B., 2019. Modeling soil organic carbon evolution in long-term arable experiments with AMG model. Environ. Model. Softw. 118, 99–113. https://doi.org/10.1016/j.envsoft.2019.04.004

Corradini, G., Pierobon, F., Zanetti, M., 2019. Product environmental footprint of a cross-laminated timber system: a case study in Italy. Int. J. Life Cycle Assess. 24, 975–988. https://doi.org/10.1007/s11367-018-1541-x

da Costa, T.P., Quinteiro, P., Tarelho, L.A. da C., Arroja, L., Dias, A.C., 2018. Environmental impacts of forest biomass-to-energy conversion technologies: Grate furnace vs. fluidised bed furnace. J. Clean. Prod. 171, 153–162. https://doi.org/10.1016/j.jclepro.2017.09.287

Dauber, J., Brown, C., Fernando, A.L., Finnan, J., Krasuska, E., Ponitka, J., Styles, D., Thrän, D., Van Groenigen, K.J., Weih, M., Zah, R., 2012. Bioenergy from "surplus" land: Environmental and socio-economic implications. BioRisk 50, 5–50. https://doi.org/10.3897/biorisk.7.3036

Den Elzen, M.G.J., Berk, M., Schaeffer, M., Olivier, J., Hendriks, C., Metz, B., 1999. The Brazilian proposal and other options for international burden sharing: an evaluation of methodological and policy aspects using the FAIR model. RIVM Rapp. 728001011, Glob. Chang. NOP-NRP Rep. 410200029.

Dodoo, A., Gustavsson, L., Sathre, R., 2014. Lifecycle carbon implications of conventional and low-energy multi-storey timber building systems. Energy Build. 82, 194–210. https://doi.org/10.1016/j.enbuild.2014.06.034

Douziech, M., Tosti, L., Ferrara, N., Parisi, M.L., Paula, P., Ravier, G., 2021. Guidelines to the Rittershoffen Geothermal Heat Plant.

ecoinvent, 2020. Ecoinvent 3.5 database [WWW Document]. URL

https://www.ecoinvent.org/database/ecoinvent-37/new-data-in-ecoinvent-37/new-data-in-ecoinvent-37.html

Ekvall, T., 2019. Attributional and Consequential Life Cycle Assessment, in: Sustainability Assessment at the 21st Century. p. 13.

Elbersen, B., van Eupen, M., Verzandvoort, S., Boogaard, H., Mucher, S., Cicarreli, T., Elbersen, W., Mantel, S., Bai, Z., Iqbal, Y., van Cossel, M., Mcallum, I., Carrasco, J., Ciria Ramos, C., Monti, A., Scordia, D., Eleftheriadis, I., 2018. Deliverable 2.6 Methodological approaches to identify and map marginal land suitable for industrial crops in Europe. EU Horiz. 2020; MAGIC; GA-No. 727698.

Englund, O., Scarlat, N., Grizzetti, B., Dimitriou, I., Mola-yudego, B., Fahl, F., Geolab, E., Engineering, S.B., Studies, E.S., 2019. Beneficial land use change : Strategic expansion of new biomass plantations can reduce environmental impacts from EU agriculture. Glob. Environ. Chang. 60, 101990. https://doi.org/10.1016/j.gloenvcha.2019.101990

Fahd, S., Fiorentino, G., Mellino, S., Ulgiati, S., 2012. Cropping bioenergy and biomaterials in marginal land: The added value of the biorefinery concept. Energy 37, 79–93. https://doi.org/10.1016/j.energy.2011.08.023

Finnveden, G., Hauschild, M.Z., Ekvall, T., Guinée, J., Heijungs, R., Hellweg, S., Koehler, A., Pennington, D., Suh, S., 2009. Recent developments in Life Cycle Assessment. J. Environ. Manage. 91, 1–21. https://doi.org/10.1016/j.jenvman.2009.06.018

Follett, R.F., 2001. Soil management concepts and carbon sequestration zin cropland soils. Soil Tillage Res. 61, 77–92. https://doi.org/10.1016/S0167-1987(01)00180-5

Food and Agriculture Organization, 2018. Agricultural land- France [WWW Document]. World Bank. URL https://data.worldbank.org/indicator/AG.LND.AGRI.ZS?locations=FR

Ge, Z., Fang, S., Chen, H.Y.H., Zhu, R., Peng, S., Ruan, H., 2018. Soil aggregation and organic carbon dynamics in poplar plantations. Forests 9, 1–15. https://doi.org/10.3390/f9090508

Gerssen-Gondelach, S.J., Saygin, D., Wicke, B., Patel, M.K., Faaij, A.P.C., 2014. Competing uses of biomass: Assessment and comparison of the performance of bio-based heat, power, fuels and materials. Renew. Sustain. Energy Rev. 40, 964–998. https://doi.org/10.1016/j.rser.2014.07.197

Gomez-Campos, A., Vialle, C., Rouilly, A., Hamelin, L., Rogeon, A., Hardy, D., Sablayrolles, C., 2021. Natural Fibre Polymer Composites - A game changer for the aviation sector? J. Clean. Prod. 286, 124986. https://doi.org/10.1016/j.jclepro.2020.124986

Gomez-Campos, A., Vialle, C., Rouilly, A., Sablayrolles, C., Hamelin, L., 2020. Flax Fiber for Technical textile: a life cycle inventory. J. Clean. Prod. 281, 125177. https://doi.org/10.1016/j.jclepro.2020.125177

González-García, S., Hospido, A., Feijoo, G., Moreira, M.T., 2010. Life cycle assessment of raw materials for non-wood pulp mills: Hemp and flax. Resour. Conserv. Recycl. 54, 923–930. https://doi.org/10.1016/j.resconrec.2010.01.011

Gopalakrishnan, G., Negri, M.C., Wang, M., Wu, M., Snyder, S.W., Lafreniere, L., 2009. Biofuels, land, and water: A systems approach to sustainability. Environ. Sci. Technol. 43, 6094–6100. https://doi.org/10.1021/es900801u

Gross, C.D., Harrison, R.B., 2019. The case for digging deeper: Soil organic carbon storage, dynamics, and controls in our changing world. Soil Syst. 3, 1–24. https://doi.org/10.3390/soilsystems3020028

Haberl, H., Erb, K.H., Krausmann, F., Bondeau, A., Lauk, C., Müller, C., Plutzar, C., Steinberger, J.K., 2011. Global bioenergy potentials from agricultural land in 2050: Sensitivity to climate

change, diets and yields. Biomass and Bioenergy 35, 4753–4769. https://doi.org/10.1016/j.biombioe.2011.04.035

Hamelin, L., 2013. Carbon management and environmental consequences of agricultural biomass in a Danish renewable energy strategy. University of Southern Denmark.

Hamelin, L., Jørgensen, U., Petersen, B.M., Olesen, J.E., Wenzel, H., 2012. Modelling the carbon and nitrogen balances of direct land use changes from energy crops in Denmark: A consequential life cycle inventory. GCB Bioenergy 4, 889–907. https://doi.org/10.1111/j.1757-1707.2012.01174.x

Heath, L.S., Birdsey, R.A., Row, C., Plantinga, A.J., 1996. Carbon pools and fluxes in US forest products, in: Forest Ecosystems, Forest Management and the Global Carbon Cycle. Springer, pp. 271–278.

Hergoualc'h, K., Akiyama, H., Bernoux, M., Chirinda, N., del Prado, A., Kasimir, Å., MacDonald, J.D., Ogle, S.M., Regina, K., Weerden, T.J. van der, 2019. N2O emissions from managed soils, and CO2 emissions from lime and urea application, in: 2019 Refinement to the 2006 IPCC Guidelines for National Greenhouse Gas Inventories. pp. 1–48.

Hottle, T.A., Bilec, M.M., Landis, A.E., 2017. Biopolymer production and end of life comparisons using life cycle assessment. Resour. Conserv. Recycl. 122, 295–306. https://doi.org/10.1016/j.resconrec.2017.03.002

Hurmekoski, E., 2017. How Can Wood Construction Reduce Environmental Degradation? Eur. For. Inst. 12.

International Organization for Standardization, 2006. Environmental management: life cycle assessment; requirements and guidelines. ISO Geneva.

International Standard Organization, 1997. ISO 14040: Environmental Management-Life Cycle Assessment-Principles and Framework.

Jackson, R.B., Lajtha, K., Crow, S.E., Hugelius, G., Kramer, M.G., Piñeiro, G., 2017. The Ecology of Soil Carbon: Pools, Vulnerabilities, and Biotic and Abiotic Controls. Annu. Rev. Ecol. Evol. Syst. 48, 419–445. https://doi.org/10.1146/annurev-ecolsys-112414-054234

Jayalath, A., Navaratnam, S., Ngo, T., Mendis, P., Hewson, N., Aye, L., 2020. Life cycle performance of Cross Laminated Timber mid-rise residential buildings in Australia. Energy Build. 223, 110091. https://doi.org/10.1016/j.enbuild.2020.110091

Jones, D.L., Nguyen, C., Finlay, R.D., 2009. Carbon flow in the rhizosphere: Carbon trading at the soil-root interface. Plant Soil 321, 5–33. https://doi.org/10.1007/s11104-009-9925-0

Kang, S., Post, W., Wang, D., Nichols, J., Bandaru, V., West, T., 2013. Hierarchical marginal land assessment for land use planning. Land use policy 30, 106–113. https://doi.org/10.1016/j.landusepol.2012.03.002

Kim, S., Dale, B.E., Drzal, L.T., Misra, M., 2008. Life cycle assessment of kenaf fiber reinforced biocomposite. J. Biobased Mater. Bioenergy 2, 85–93. https://doi.org/10.1166/jbmb.2008.207

Köchy, M., Hiederer, R., Freibauer, A., 2015. Global distribution of soil organic carbon – Part 1: Masses and frequency distributions of SOC stocks for the tropics, permafrost regions, wetlands, and the world. Soil 1, 351–365. https://doi.org/10.5194/soil-1-351-2015

La Rosa, A.D., Cozzo, G., Latteri, A., Mancini, G., Recca, A., Cicala, G., 2013. A comparative life cycle assessment of a composite component for automotive. Chem. Eng. Trans. 32, 1723–1728. https://doi.org/10.3303/CET1332288

Lal, R., 2007. Carbon management in agricultural soils. Mitig. Adapt. Strateg. Glob. Chang. 12, 303–322. https://doi.org/10.1007/s11027-006-9036-7

Lamlom, S.H., Savidge, R.A., 2003. A reassessment of carbon content in wood: Variation within and between 41 North American species. Biomass and Bioenergy 25, 381–388. https://doi.org/10.1016/S0961-9534(03)00033-3

Landgraf, D., Carl, C., Neupert, M., 2020. Biomass yield of 37 different src poplar varieties grown on a typical site in north eastern germany. Forests 11, 1–16. https://doi.org/10.3390/f11101048

Langholtz, M., Stokes, B., Eaton, L., 2016. 2016 Billion-Ton Report: Advancing Domestic Resources for a Thriving Bioeconomy (Executive Summary). Ind. Biotechnol. 12, 282–289. https://doi.org/10.1089/ind.2016.29051.doe

Ledo, A., Hillier, J., Smith, P., Aguilera, E., Blagodatskiy, S., Brearley, F.Q., Datta, A., Diaz-Pines, E., Don, A., Dondini, M., Dunn, J., Feliciano, D.M., Liebig, M.A., Lang, R., Llorente, M., Zinn, Y.L., McNamara, N., Ogle, S., Qin, Z., Rovira, P., Rowe, R., Vicente-Vicente, J.L., Whitaker, J., Yue, Q., Zerihun, A., 2019. A global, empirical, harmonised dataset of soil organic carbon changes under perennial crops. Sci. Data 6, 1–7. https://doi.org/10.1038/s41597-019-0062-1

Lehmann, J., Hansel, C.M., Kaiser, C., Kleber, M., Maher, K., Manzoni, S., Nunan, N., Reichstein, M., Schimel, J.P., Torn, M.S., Wieder, W.R., Kögel-Knabner, I., 2020. Persistence of soil organic carbon caused by functional complexity. Nat. Geosci. 13, 529–534. https://doi.org/10.1038/s41561-020-0612-3

Lehmann, J., Kleber, M., 2015. The contentious nature of soil organic matter. Nature 528, 60–68. https://doi.org/10.1038/nature16069

Lemus, R., Lal, R., 2005. Bioenergy crops and carbon sequestration. CRC. Crit. Rev. Plant Sci. 24, 1–21. https://doi.org/10.1080/07352680590910393

Levavasseur, F., Mary, B., Christensen, B.T., Duparque, A., Ferchaud, F., Kätterer, T., Lagrange, H., Montenach, D., Resseguier, C., Houot, S., 2020. The simple AMG model accurately simulates organic carbon storage in soils after repeated application of exogenous organic matter. Nutr. Cycl. Agroecosystems 117, 215–229. https://doi.org/10.1007/s10705-020-10065-x

Lewis, S.M., Kelly, M., 2014. Mapping the potential for biofuel production on marginal lands: Differences in definitions, data and models across scales. ISPRS Int. J. Geo-Information 3, 430–459. https://doi.org/10.3390/ijgi3020430

Liu, L., Zhuang, D., Jiang, D., Huang, Y., 2012. Assessing the potential of the cultivation area and greenhouse gas (GHG) emission reduction of cassava-based fuel ethanol on marginal land in Southwest China. African J. Agric. Res. 7, 5594–5603. https://doi.org/10.5897/AJAR12.1387

Liu, Y., Guo, H., Sun, C., Chang, W.S., 2016. Assessing cross laminated timber (CLT) as an alternative material for mid-rise residential buildings in cold regions in China-A life-cycle assessment approach. Sustain. 8. https://doi.org/10.3390/su8101047

Lu, L., Jiang, D., Zhuang, D., Huang, Y., 2012. Evaluating the marginal land resources suitable for developing Pistacia chinensis-based biodiesel in China. Energies 5, 2165–2177. https://doi.org/10.3390/en5072165

Manda, B.M.K., Worrell, E., Patel, M.K., 2015. Prospective life cycle assessment of an antibacterial T-shirt and supporting business decisions to create value. Resour. Conserv. Recycl. 103, 47–57. https://doi.org/10.1016/j.resconrec.2015.07.010

Manzoni, S., Porporato, A., 2009. Soil carbon and nitrogen mineralization: Theory and models across scales. Soil Biol. Biochem. 41, 1355–1379. https://doi.org/10.1016/j.soilbio.2009.02.031

Meyer-Aurich, A., Weersink, A., Janovicek, K., Deen, B., 2006. Cost efficient rotation and tillage options to sequester carbon and mitigate GHG emissions from agriculture in Eastern Canada. Agric. Ecosyst. Environ. 117, 119–127. https://doi.org/10.1016/j.agee.2006.03.023

Milà i Canals, L., Romanyà, J., Cowell, S.J., 2007. Method for assessing impacts on life support functions (LSF) related to the use of "fertile land" in Life Cycle Assessment (LCA). J. Clean. Prod. 15, 1426–1440. https://doi.org/10.1016/j.jclepro.2006.05.005

Milbrandt, A., Overend, R.P., 2009. Assessment of biomass resources from marginal lands in APEC economies. National Renewable Energy Lab.(NREL), Golden, CO (United States).

Milbrandt, A.R., Heimiller, D.M., Perry, A.D., Field, C.B., 2014. Renewable energy potential on marginal lands in the United States. Renew. Sustain. Energy Rev. 29, 473–481. https://doi.org/10.1016/j.rser.2013.08.079

Minasny, B., Malone, B.P., McBratney, A.B., Angers, D.A., Arrouays, D., Chambers, A., Chaplot, V., Chen, Z.S., Cheng, K., Das, B.S., Field, D.J., Gimona, A., Hedley, C.B., Hong, S.Y., Mandal, B., Marchant, B.P., Martin, M., McConkey, B.G., Mulder, V.L., O'Rourke, S., Richer-de-Forges, A.C., Odeh, I., Padarian, J., Paustian, K., Pan, G., Poggio, L., Savin, I., Stolbovoy, V., Stockmann, U., Sulaeman, Y., Tsui, C.C., Vågen, T.G., van Wesemael, B., Winowiecki, L., 2017. Soil carbon 4 per mille. Geoderma 292, 59–86. https://doi.org/10.1016/j.geoderma.2017.01.002

Minstère de l'agriculture et de l'alimentation, 2015. Overview of French Agricultural Diversity [WWW Document]. French governement. URL https://agriculture.gouv.fr/overview-french-agricultural-diversity

Nachtergaele, F., van Velthuizen, H., van Engelen, V., Fischer, G., Jones, A., Montanarella, L., Petri, M., Prieler, S., Teixeira, E., Shi, X., 2012. Harmonized World Soil Database (version 1.2). FAO, Rome, Italy IIASA, Laxenburg, Austria 1–50.

Negishi, K., Lebert, A., Almeida, D., Chevalier, J., Tiruta-Barna, L., 2019. Evaluating climate change pathways through a building's lifecycle based on Dynamic Life Cycle Assessment. Build. Environ. 164, 106377. https://doi.org/10.1016/j.buildenv.2019.106377

Niblick, B., Monnell, J.D., Zhao, X., Landis, A.E., 2013. Using geographic information systems to assess potential biofuel crop production on urban marginal lands. Appl. Energy 103, 234–242. https://doi.org/10.1016/j.apenergy.2012.09.036

Norton, A., Alexander, S., Building, F., 2008. Life Cycle Assessments of Natural Fibre Insulation Materials Final Report Study funded by Defra Life Cycle Assessments of Natural Fibre Insulation Materials. Building.

Patel, B., Patel, A., Gami, B., Patel, P., 2020. Energy balance, GHG emission and economy for cultivation of high biomass verities of bamboo, sorghum and pearl millet as energy crops at marginal ecologies of Gujarat state in India. Renew. Energy 148, 816–823. https://doi.org/10.1016/j.renene.2019.10.167

Patil, P., Kumar, A.K., 2017. Biological carbon sequestration through fruit crops (perennial crops-natural "sponges" for absorbing carbon dioxide from atmosphere). Plant Arch. 17, 1041–1046.

Pett-Ridge, J., Firestone, M.K., 2017. Using stable isotopes to explore root-microbe-mineral interactions in soil. Rhizosphere 3, 244–253. https://doi.org/10.1016/j.rhisph.2017.04.016

Piekarski, C.M., de Francisco, A.C., da Luz, L.M., Kovaleski, J.L., Silva, D.A.L., 2017. Life cycle assessment of medium-density fiberboard (MDF) manufacturing process in Brazil. Sci. Total Environ. 575, 103–111. https://doi.org/10.1016/j.scitotenv.2016.10.007

Poeplau, C., Don, A., 2015. Carbon sequestration in agricultural soils via cultivation of cover crops - A meta-analysis. Agric. Ecosyst. Environ. 200, 33–41. https://doi.org/10.1016/j.agee.2014.10.024

Pretot, S., Collet, F., Garnier, C., 2014. Life cycle assessment of a hemp concrete wall: Impact of thickness and coating. Build. Environ. 72, 223–231.

https://doi.org/10.1016/j.buildenv.2013.11.010

Pribyl, D.W., 2010. A critical review of the conventional SOC to SOM conversion factor. Geoderma 156, 75–83. https://doi.org/10.1016/j.geoderma.2010.02.003

Rasse, D.P., Rumpel, C., Dignac, M.F., 2005. Is soil carbon mostly root carbon? Mechanisms for a specific stabilisation. Plant Soil 269, 341–356. https://doi.org/10.1007/s11104-004-0907-y

Rédei, K., Csiha, I., KeserU, Z., Gál, J., 2012. Influence of regeneration method on the yield and stem quality of black locust (Robinia pseudoacacia L.) Stands: A case study. Acta Silv. Lignaria Hungarica 8, 103–112. https://doi.org/10.2478/v10303-012-0008-1

Rettenmaier, N., Schorb, A., Hienz, G., Diaz-Chavez, R.A., 2012. Report on sustainability impacts of the use of marginal areas and grassy biomass (D 5.4).

Rohit, K., Dixit, S., 2016. A review - future aspect of natural fiber reinforced composite. Polym. from Renew. Resour. 7, 43–60. https://doi.org/10.1177/204124791600700202

Saffih-Hdadi, K., Mary, B., 2008. Modeling consequences of straw residues export on soil organic carbon. Soil Biol. Biochem. 40, 594–607. https://doi.org/10.1016/j.soilbio.2007.08.022

Saha, M., Eckelman, M.J., 2015. Geospatial assessment of potential bioenergy crop production on urban marginal land. Appl. Energy 159, 540–547. https://doi.org/10.1016/j.apenergy.2015.09.021

Schahczenski, J., Hill, H., 2009. Agriculture, climate change and carbon sequestration. ATTRA Melbourne.

Scharlemann, J.P.W., Tanner, E.V.J., Hiederer, R., Kapos, V., 2014. Global soil carbon: Understanding and managing the largest terrestrial carbon pool. Carbon Manag. 5, 81–91. https://doi.org/10.4155/cmt.13.77

Schmidt, T., Fernando, A.L., Monti, A., Rettenmaier, N., 2015. Life Cycle Assessment of Bioenergy and Bio-Based Products from Perennial Grasses Cultivated on Marginal Land in the Mediterranean Region. Bioenergy Res. 8, 1548–1561. https://doi.org/10.1007/s12155-015-9691-1

Schubert, R., Schellnhuber, H.J., Buchmann, N., Epiney, A., Griesshammer, R., Kulessa, M.E., Messner, D., Rahmstorf, S., Schmid, J., 2008. World in Transition. Future Bioenergy and Sustainable Land Use: Summary for Policy-Makers. ETH Zurich.

Shahid, S.A., Al-Shankiti, A., 2013. Sustainable food production in marginal lands—Case of GDLA member countries. Int. Soil Water Conserv. Res. 1, 24–38. https://doi.org/10.1016/S2095-6339(15)30047-2

Shen, Z., Tiruta-Barna, L., Hamelin, L., 2022a. From Hemp Grown on Carbon Vulnerable Lands to Long-Lasting Bio-Based Products: Uncovering Trade-Offs between Overall Environmental Impacts, Sequestration in Soils and Dynamic Influence on Global Temperature. Sequestration Soils Dyn. Influ. Glob. Temp.

Shen, Z., Tiruta-Barna, L., Karan, S.K., Hamelin, L., 2022b. Simultaneous carbon storage in arable land and anthropogenic products (CSAAP): Demonstrating an integrated concept towards well below 2° C. Resour. Conserv. Recycl. 182, 106293.

Shimako, A.H., 2017. Contribution to the development of a dynamic Life Cycle Assessment method. Toulouse, INSA.

Shimako, A.H., Tiruta-Barna, L., Bisinella de Faria, A.B., Ahmadi, A., Spérandio, M., 2018. Sensitivity analysis of temporal parameters in a dynamic LCA framework. Sci. Total Environ. https://doi.org/10.1016/j.scitotenv.2017.12.220

Shortall, O.K., 2013. “Marginal land” for energy crops: Exploring definitions and embedded assumptions. Energy Policy 62, 19–27. https://doi.org/10.1016/j.enpol.2013.07.048

Six, J., Conant, R.T., Paul, E.A., Paustian, K., 2002. Stabilization mechanisms of soil organic matter: implications for C-saturation of soils. Plant Soil 241, 155–176.

Smith, C., Z.R.J. Nicholls, K. Armour, W. Collins, P. Forster, M. Meinshausen, M.D. Palmer, and M.W., 2021. The Earth’s Energy Budget, Climate Feedbacks, and Climate Sensitivity Supplementary Material., in: In Climate Change 2021: The Physical Science Basis. Contribution of Working Group I to the Sixth Assessment Report of the Intergovernmental Panel on Climate Change.

Sokol, N.W., Bradford, M.A., 2019. Microbial formation of stable soil carbon is more efficient from belowground than aboveground input. Nat. Geosci. 12, 46–53. https://doi.org/10.1038/s41561-018-0258-6

Stocker, T.F., Qin, D., Plattner, G.K., Tignor, M.M.B., Allen, S.K., Boschung, J., Nauels, A., Xia, Y., Bex, V., Midgley, P.M., 2013. Climate change 2013 the physical science basis: Working Group I contribution to the fifth assessment report of the intergovernmental panel on climate change. Clim. Chang. 2013 Phys. Sci. Basis Work. Gr. I Contrib. to Fifth Assess. Rep. Intergov. Panel Clim. Chang. 9781107057, 1–1535. https://doi.org/10.1017/CBO9781107415324

Stockmann, U., Adams, M.A., Crawford, J.W., Field, D.J., Henakaarchchi, N., Jenkins, M., Minasny, B., McBratney, A.B., Courcelles, V. de R. de, Singh, K., Wheeler, I., Abbott, L., Angers, D.A., Baldock, J., Bird, M., Brookes, P.C., Chenu, C., Jastrow, J.D., Lal, R., Lehmann, J., O’Donnell, A.G., Parton, W.J., Whitehead, D., Zimmermann, M., 2013. The knowns, known unknowns and unknowns of sequestration of soil organic carbon. Agric. Ecosyst. Environ. 164, 80–99. https://doi.org/10.1016/j.agee.2012.10.001

Stora Enso, 2020. Environmental Product Declaration CLT (Cross Laminated Timber), The International EPD System.

Sulman, B.N., Phillips, R.P., Oishi, A.C., Shevliakova, E., Pacala, S.W., 2014. Microbe-driven turnover offsets mineral-mediated storage of soil carbon under elevated CO 2. Nat. Clim. Chang. 4, 1099–1102. https://doi.org/10.1038/nclimate2436

Swati, Thakur, I.S., Vijay, V.K., Ghosh, P., 2019. Scenario of Landfilling in India: Problems, Challenges, and Recommendations. Handb. Environ. Mater. Manag. 321–336. https://doi.org/10.1007/978-3-319-73645-7_167

Taghizadeh-Toosi, A., Glendining, M., Vejlin, J., Hutchings, N.J., Olesen, J.E., Christensen, B.T., Kätterer, T., 2014. C-TOOL: A simple model for simulating whole-profile carbon storage in temperate agricultural soils. Ecol. Modell. 292, 11–25. https://doi.org/10.1016/j.ecolmodel.2014.08.016

Thomas, R., Hursthouse, A., Mellor, P., Lord, R.A., Jo, E., 2021. Identifying non-agricultural marginal lands as a route to sustainable bioenergy provision - A review and holistic definition 135. https://doi.org/10.1016/j.rser.2020.110220

Thomsen, I.K., Kruse, T., Bruun, S., Kristiansen, S.M., Knicker, H., Petersen, S.O., Jensen, L.S., Holst, M.K., Christensen, B.T., 2008. Characteristics of Soil Carbon Buried for 3300 Years in a Bronze Age Burial Mound. Soil Sci. Soc. Am. J. 72, 1292–1298. https://doi.org/10.2136/sssaj2007.0348

Tonini, D., Hamelin, L., Wenzel, H., Astrup, T., 2012. Bioenergy production from perennial energy crops: A consequential LCA of 12 bioenergy scenarios including land use changes. Environ. Sci. Technol. 46, 13521–13530. https://doi.org/10.1021/es3024435

Vanholme, B., Desmet, T., Ronsse, F., Rabaey, K., Van Breusegem, F., De Mey, M., Soetaert, W., Boerjan, W., 2013. Towards a carbon-negative sustainable bio-based economy. Front. Plant Sci.

4, 1–17. https://doi.org/10.3389/fpls.2013.00174

Wang, J., Pan, X., Liu, Y., Zhang, X., Xiong, Z., 2012. Effects of biochar amendment in two soils on greenhouse gas emissions and crop production. Plant Soil 360, 287–298. https://doi.org/10.1007/s11104-012-1250-3

West, T.O., Marland, G., 2002. A synthesis of carbon sequestration, carbon emissions, and net carbon flux in agriculture: Comparing tillage practices in the United States. Agric. Ecosyst. Environ. 91, 217–232. https://doi.org/10.1016/S0167-8809(01)00233-X

Wicke, B., 2011. Bioenergy Production on Degraded and Marginal Land.

Wieder, W.R., Grandy, A.S., Kallenbach, C.M., Bonan, G.B., 2014. Integrating microbial physiology and physio-chemical principles in soils with the MIcrobial-MIneral Carbon Stabilization (MIMICS) model. Biogeosciences 11, 3899–3917. https://doi.org/10.5194/bg-11-3899-2014

Woolf, D., Lehmann, J., 2019. Microbial models with minimal mineral protection can explain long-term soil organic carbon persistence. Sci. Rep. 9, 1–8. https://doi.org/10.1038/s41598-019-43026-8

World Resources Institute, 2020. World Greenhouse Gas Emissions: 2016 [WWW Document]. URL https://www.wri.org/resources/data-visualizations/world-greenhouse-gas-emissions-2016

Xue, S., Lewandowski, I., Wang, X., Yi, Z., 2016. Assessment of the production potentials of Miscanthus on marginal land in China. Renew. Sustain. Energy Rev. 54, 932–943. https://doi.org/10.1016/j.rser.2015.10.040

Zampori, L., Dotelli, G., Vernelli, V., 2013. Life cycle assessment of hemp cultivation and use of hemp-based thermal insulator materials in buildings. Environ. Sci. Technol. 47, 7413–7420. https://doi.org/10.1021/es401326a

Zhang, X., Fu, J., Lin, G., Jiang, D., Yan, X., 2017. Switchgrass-based bioethanol productivity and potential environmental impact from marginal lands in China. Energies 10. https://doi.org/10.3390/en10020260

Chapter III. Biopump concept: definition and feasibility investigation

Context

The target of the Paris Agreement is to limit the temperature rise at the end of this century within 1.5°C, or 2°C at most. There are two main challenges in the way of reaching this target. One is inducing additional CO_2 removal to lower the CO_2 concentration in the atmosphere, the other is reducing the fossil carbon (C) involved in our economy.

The plants capture CO_2 through photosynthesis, thus are regarded as natural CO_2 removals. Valuable parts are harvested for humans, while the rest is left as the residue. With the decomposition, a part of the C in the residues is emitted back to the atmosphere, while a part of C goes into the soil, is humified with the microbial activity, and is stored as SOC. When valuable biomass is transformed into bio-based products, the C in these products can be stored in the technosphere if the lifetime of these products is sufficiently long. Another part is lost during the manufacturing. The timespan of keeping C in the technosphere depends on the product lifetime, and on the end of life strategies.

Based on the two C sinks mentioned above (soil and anthropogenic products), the concept 'biopump' is defined: a plant that can to induce high C storage in soils (SOC) and, after harvesting and manufacturing, can keep another part of absorbed C in anthropogenic bio-based products.

In this chapter, we proposed and defined 'biopump' as the core concept of the thesis, and answer the scientific questions as follows:

1) What is biopump and how it works;
2) What kinds of plants have the potential to be biopump;
3) How many areas are suitable for planting biopump;
4) Does biopump contribute to global warming mitigation, if yes, how much could it help.

The following steps are conducted: (1) defining the function of biopump; (2) identifying plants that are potentially biopump; (3) identifying the land that is suitable for planting the biopump; (4) evaluating the mitigation effect based on identified biopump grown on identified lands. To quantify how much CO_2 might be removed, land that is suitable to be converted to plant biopump were identified in French territory, named 'carbon vulnerable lands' (CV-lands).

The content of this chapter was published in:

Shen Z., Tiruta-Barna L., Hamelin L., Simultaneous Carbon Storage in Arable land and Anthropogenic Products (CSAAP): demonstrating an integrated concept towards well below 2°C, Resources, Conservation & Recycling, 182, 2022, 106293

1 Introduction

The Paris Agreement calls for stabilizing the global mean surface temperature increase to well below 2°C above pre-industrial level(UNFCCC, 2015), a threshold that has endured in science to represent dangerous climate change(Sanderson et al., 2016). This target implies two key challenges. On the one hand, it implies to induce additional carbon dioxide removals (CDR, or so-called negative emissions)(Masson-Delmotte et al., 2018; Tanzer and Ramírez, 2019), at a rapid and large-, or more modest-, deployment scale, depending on the ambition with regards to the well below 2°C(Hilaire et al., 2019). The potential of soil carbon sequestration as a negative emission strategy has attracted increased attention because of its considerable potential, up to 13 Gt CO_2-eq $year^{-1}$, as reported by (Shukla et al., 2019). In comparison, China's net emission was 12 Gt CO_2-eq in 2018(Climate watch, 2021). Examples illustrating this potential include the study of Bastin(2019), where a total of 900 million ha of marginal land suited for re- and afforestation worldwide was reported, with a potential to store up to 42.5 Gt C in total (carbon in soils and biomes) (revised figure from the comment(Veldman et al., 2019)). Similarly, Poeplau and Don(2015) estimated, from their meta-analysis results, that through implementing cover crops on fallow land on just 25% of the global cropland area, a soil organic carbon (SOC) increase corresponding to 0.21-0.26 Mg ha^{-1} $year^{-1}$ (an accumulated sequestration corresponding to 11.77- 14.12 Mg in total) could be obtained after 50 years. This could compensate, according to the authors, ca. 8% of direct annual greenhouse gas (GHG) from agriculture. The review of Paustian et al. (2019) on the negative emission function of SOC highlights that a near complete adoption of 'best management practices' for building up SOC stocks on current agricultural lands could lead to an upper sequestration potential of 4-5 Gt CO_2-eq $year^{-1}$. Minasny et al. (2017) suggest, considering a global SOC stock estimate of 2,400 Gt (2m depth) (Batjes, 1996), an annual global SOC increase target of 4‰ per year in order to offset global fossil carbon (C) emissions, estimated to 8.9 Gt C $year^{-1}$ by the authors. Estimations performed for France revealed that as much as ca. 28,500 ha lands could be suitable for an increase of 4‰, corresponding to an upper limit of 2.9-5.7 Tg C stored per year in the future 30 years(Rodrigues et al., 2021).

SOC changes are mainly due to changes in the balance between the input and output of C to soils (Amundson, 2001). On vegetated soils, plants capture and store C from the atmosphere through photosynthesis, shed part of the accumulated biomass-C as above- and below-ground residues(Karan and Hamelin, 2021), and may be subjected to external C amendments (e.g., manure, compost, biochars)(Paustian et al., 2019). Part of the C in the above- and below-ground biomass residues undergoes microbial activity, humified to humic substances, allowing it to become part of the soil structure(Buscot and Varma, 2005). The other part, also the most important share is, through mineralization and then converted to inorganic C, essentially ending as carbon dioxide (CO_2) emissions to the atmosphere. Both humification and mineralization are highly governed by climatic factors (soil temperature and moisture). Any changes in this input-output balance induce a temporary perturbation to the long-term SOC stock that will result in either SOC losses or gains until a new equilibrium is reached.

The second challenge implied by the Paris Agreement target is to transit towards a low fossil C economy. Fossil CO_2 represented more than 65% of global GHG emissions in 2016 (World Resources Institute, 2020). While some products and services can be supplied without any C (e.g., wind or solar electricity, which can in turn supply heat or transport services), other sectors of the economy (e.g., materials, chemicals) cannot be decarbonized and will require new C sources. In the low fossil C economy, biomass is the most abundant and accessible C source (Gautam et al., 2019; Office for National Statistics, 2019), at least until the large-scale deployment of technologies allowing to directly capture atmospheric carbon (so-called direct Direct Air Capture) and the use becomes a reality.

With the emergence of bio-based materials (e.g., as new textiles, in the construction sector), the C contained in the biomass and subsequently in these anthropogenic products represents another potential C pool. Among the bio-based sectors, C storage in wood-based products is one of the most studied.

Despite this, several challenges remain to achieve consistent biogenic C accounting and ensure a proper inclusion of delayed emissions(Finkbeiner and Bach, 2021), which essentially depends on product durability and land management. In the study of Head et al. (2020), the potential for climate mitigation of wood-based products was assessed through dynamic life cycle assessment (DLCA), including C capture by trees, emissions from product manufacturing and end-of-life considerations, through different time horizons. The temporality of such scenarios (i.e. when the different processes emit and capture CO_2) is a key parameter: the benefit of C capture by trees could be lost sooner or later, depending on the product's lifetime.

This study aims to demonstrate an integrated concept simultaneously addressing these two challenges of negative emission (CDR) and emission mitigation (reduction), for climate change mitigation. We refer to this concept as CSAAP: Carbon Storage in Arable land and Anthropogenic Products. In a nutshell, it consists of *inducing* an additional net long-term biophysical removal of C from the atmosphere towards the soil, while using the produced biomass as a renewable C source to supply society's demands for hydrocarbons. The plant species allowed to meet (in a given geographical context) this double challenge are here referred to as biopumps. To qualify a CSAAP strategy as sustainable (i.e. a combination of biopump, bio-based product, and its use up to end-of-life), the vision is to ensure that (1) the cultivation of biopumps does enhance SOC stocks, while (2) not inducing competition for arable land nor adverse environmental trade-offs and (3) that biopumps are a source of C for anthropogenic products with a long lifetime, thus allowing for a net CDR for a time horizon as important and relevant as possible. To implement a CSAAP strategy on territory, we propose a methodology with several steps: (i) identification of suitable plants at the light of criteria (1) and selection of adapted biopumps for the studied territory; (ii) assessment of the lands with potential for SOC increase, and (iii) assessment of the climate mitigation potential of the whole chain, from CO_2 capture by biopumps to bio-based products in the technosphere and their end-of-life.

This concept proposes, thus, the implementation of specifically selected plants on specifically chosen carbon-poor lands, at large territorial scale (e.g., country), and their use in long-lived products, with a *primordial goal, to mitigate the climate change* by simultaneously inducing CDR (negative emissions) and GHG mitigation. A comprehensive methodology is proposed for systematic investigation and assessment of coupled C pools, from soil to biopumps and products in the technosphere, in order to quantify the effect on actual mean surface temperature. The novelty of the concept and methodology lies in the 'nexus biopump-land-product', combining the local natural potential to induce negative emissions with the product demands in the economy while creating temporal C sinks in bio-based products and reducing GHG emissions with the replacement of petrochemical products, over tailored periods (in line with the climate targets).

Further, it remains unclear to which extent and under which local conditions such concept could effectively lead to controlling temperature changes below 2°C. In an endeavor to understand the potential importance of CSAAP for climate mitigation and bioeconomy strategy, we here applied and scaled the concept to France. The case of *Miscanthus* (*Miscanthus x giganteus*) as biopump was considered for illustration, with a representation of the atmospheric C flow induced in soils and maintained in the technosphere and its evaluation in time, as well as the related effect on global mean temperature change as an indicator for climate change.

2 Materials and methods

2.1 Identification and ranking of biopump candidates

2.1.1. Assessing the specie-dependent potential to enhance SOC

The key determinant for labeling a plant as a biopump is its ability to induce net C sequestration in agricultural soils, reflected here by its ability to increase SOC over a long period, typically considered as 100 years in SOC-related studies(de Jong et al., 2019; Hamelin et al., 2012).

In order to pinpoint the plant species that could qualify as biopumps, the literature was screened in an endeavor to generate a database compiling the plants reported to increase SOC over time, the yield of these plants along with the key parameters upon which their sequestration performance depends on. The recent work of Ledo et al (Ledo et al., 2019) represents the most comprehensive attempt to collect a comparable dataset on SOC changes induced by the cultivation of perennial plants. The authors summarized SOC measurements (with standard deviations) before and after cultivation for 61 crop types on 709 sites all over the world, with harmonized documentation of site properties, including key parameters highlighted by Sanderman et al.(Sanderman et al., 2018) (climate, relief, lithology, and previous land use) as well as additional ones like soil depth, plantation lifetime, and agricultural management. For these reasons, the present work builds essentially upon the study of Ledo et al(Ledo et al., 2020, 2019). All the crops reported by Ledo et al (Ledo et al., 2019) were classified here as 'woody' or 'grass', and the average annual SOC change (ΔSOC) was calculated from the concentration (i.e. data in g C kg^{-1} soil) and/or stock data (i.e. data in t C ha^{-1}), considering the reported duration between the current and previous land use. This is summarized in table s1& s2 (supplement information I), along with additional parameters extracted from Ledo et al (Ledo et al., 2019) database, such as the soil depth for SOC measurements, or the location and number of plots. Among the 61 crop types presented in this database, 42 had a negative average annual ΔSOC. These were excluded from further consideration as candidates for biopumps. To this remaining list of crops, 10 additional plants were added, collected from a selection of 38 articles from recent literature (2005 - 2019).

2.1.2. Ranking the candidates

A semi-quantitative scoring framework adapted from(COWI A/S and Utrecht University, 2019) was built in order to rank the biopumps identified in the previous step, in the perspective of achieving the highest performance in terms of C sequestration, biomass yield, agricultural intensity, and risk of invasion, and to ensure suitability in a given geographic context (Table III-1). Accordingly, five specific criteria were defined. Each criterion was associated with a score ranging from 0 to 3, where each score corresponds to a quantitative or qualitative value. The SOC increase potential considered for the scoring is based on the screening work of section 2.1.1 potential can be addressed both in terms of concentration or stock (depending on data availability). When data were available both in SOC concentration and stock, the highest value was chosen for ranking. In order to supply quantitative data for all other criteria, an extensive literature review was made (supplement information I, table s5).

The rationale used for the yield criteria was to assign the top score to a threshold yield necessary to ensure SOC sequestration with a target of 4‰ increase annually ('4 per 1000' initiative), which roughly translates in a global average sequestration rate of 0.6 t C ha^{-1} annually(Minasny et al., 2017). On this basis, and considering plant's anabolism to 15% (the portion of the overall plant-C that is retained in soil) as well as an average plant-C content corresponding to 45% of the dry matter (DM) (Hamelin et al., 2012; Nguyen, 2003), the biopump yield must reach at least 9 t DM ha^{-1} $year^{-1}$ (score 3 set for yield >10 t DM ha^{-1} $year^{-1}$). It should be noticed that all the biopump candidates reported in tables S1-S2 englobe several sub-species, as further detailed in table s3 (supplement information I, for example, blueberry includes the following sub-species: *Vaccinium corymbosum, Vaccinium angustifolium L, Vaccinium darrowii Camp, Vaccinium virgatum Aiton, Vaccinium elliottii Chapm*).

The agricultural intensity criterion was divided into 3 sub-criteria to reflect the capability of the biopumps to grow with a minimal need for additional water, fertilizer, and pesticide input. For fertilizers, we only regarded nitrogen, due to its importance on global warming (N_2O emissions) and our concern for GHG neutrality. The average of the three sub-criteria was used as the final score for 'agricultural intensity'. The risk of invasiveness of the biopump candidates was also assessed based on qualitative scoring. It was determined based on databases like Invasive Species Compendium(CABI, 2021) and Global invasive species database in France(Invasive Species Specialist Group, 2020). Finally, the overall score by biopump was obtained by summing the five criterion scores.

Table III-1 Semi-quantitative criteria matrix used to score and select the biopumps potentially adapted for Francea.

Overall criteria	Sub-criteria	Score			
		0	1	2	3
Yield (harvestable)		<2 t DM ha^{-1} $year^{-1}$	2~5 t DM ha^{-1} $year^{-1}$	5~10 t DM ha^{-1} $year^{-1}$	>10 t DM ha^{-1} $year^{-1}$
SOC increase potential		<0 g kg^{-1} or <0 Mg ha^{-1}	0~0.1 g kg^{-1} or 0~0.35 Mg ha^{-1}	0.1~0.3 g kg^{-1} or 0.35~1 Mg ha^{-1}	>0.3 g kg^{-1} or >1 Mg ha^{-1}
Agricultural intensity	Water	Need irrigation regularly	Need irrigation in a certain period	Could grow without irrigation but water input would greatly enhance yield	Survives and grow with rainwater only in the region of origin, tolerant to drought
	Fertilizer	>180 kg N ha^{-1} $year^{-1}$	120-180 kg N ha^{-1} $year^{-1}$	60-120 kg N ha^{-1} $year^{-1}$	<60 kg N ha^{-1} $year^{-1}$
	Pesticides	Susceptible to pest/weed problem; Pesticides necessary.	There is at least one pest or weed problem that would cause a serious disease; Pesticides typically used.	There is at least one pest or weed problem but not serious; Pesticides sometimes used.	Great resistance against pest; Pesticides seldom used.
Suitability to grow in France		Not currently growing in France or countries with similar conditions.	Grows in other continents but with a similar environment to France (altitude, climate, latitude)	Grows in European countries with similar conditions	Already grows in France
Invasion risk		Invasive and difficult to control	Invasive but can be contained	Judged non-invasive, but no clear information.	Proved to be non-invasive

[a] The background data used for the quantification are presented in table s5 (supplement information I).

2.1.3. Possible utilization of biopumps

The aboveground biomass can be transformed into bioeconomy products depending on the plant key components, classified as cellulose, hemicellulose, lignin, proteins, sugars, and lipids, with various other specific molecules that can be extracted, separated, and further processed. The main product categories include materials, chemicals, energy, and food/dietary supplements. In the perspective of CSAAP, the lifetime of the final product (and eventual co-products) should be as long as possible, to keep a maximum of C out of the atmosphere for as long as possible. While materials may have a use phase greater than 10-20 years, energy, food, and most feedstock chemicals are produced and used rapidly, typically with a turnover of a year or less(Bataille, 2020). As an illustration, a non-exhaustive

inventory of 29 plant-to-bioeconomy products is presented in the supplement information I, table s6, including the main transformation process, product lifetime, and replaced conventional products.

2.2 Scaling up the potential to a country: available and suitable lands for biopump cultivation

The extent of available areas for biopump cultivation shapes both the negative emission and GHG mitigation potential at the scale of a territory. These areas will here be referred to as target areas (Albers et al., 2021b), and should be selected at the light of both environmental considerations and biophysical considerations (i.e. ensuring that the selected biopumps can grow on these lands). On the basis of (Guénon et al., 2016; Thomas et al., 2021; Zhang et al., 2020), two main guiding principles are considered, namely (i) minimizing disruption of existing activities and (ii) excluding unsuitable areas.

The vision of CSAAP is to grow biopumps exclusively on areas with low SOC content. Using Food and Agriculture Organization's Global SOC data (FAO, 2019), the soils were classified into five SOC classes, namely <40, 40-50, 50-60, 60-70, and >70 t C ha^{-1}. A threshold can then be selected as a cut-off for 'C-rich' and 'C-poor' soils. Here, on the basis of (Albers et al., 2021b), we propose the generic threshold of 50 t C ha^{-1} to distinguish between both. However, depending on the specific national context, a different threshold may be considered.

Besides this C-poor criteria, another key criteria is to prevent competition for arable land. As a general principle, this involves preventing biopumps are cultivated directly on arable land, where another crop is already grown. One exception to this, as further detailed in (Gylling et al., 2016; Hamelin et al., 2021; Larsen et al., 2017), is the case where the use of arable land would not translate to additional land demand as the result of specific agricultural intensification measures, or in the framework of a larger bioeconomy strategy where demand and supply are balanced. For example, (Larsen et al., 2017) describes the case of a grass biorefinery established on Danish rapeseed areas, producing both energy and a protein concentrate, the latter compensating for the rapeseed meal no longer produced in Denmark. In that specific case, it was also highlighted that only 60% of the rapeseed areas are currently connected to the food market, the remaining being used for the production of European biodiesel, a demand that may no longer exist in the future, as also highlighted by (Ekvall, 2019).

Plant species naturally growing on lands covered by shrubs or grasses (includes dense-, moderate, and spare grasslands) are often grazed. Yet, in many regions of Europe, North America, and Oceania, a significant surplus grass is available on these lands(Prochnow et al., 2009), among others due to a decline in the number of ruminants (in these regions), as well as to animal performances improvements. The tendency documented in Prochnow(2009) holds true today but has stabilized in the last five years (FAOSTAT, 2022; details in supplement information I, table s7). These areas of "surplus grass" could instead be used to grow biopumps with higher yields and SOC sequestration potential.

There is also the case of unused arable land, that is not put into production either because of economic reasons (land allowing better yields is available elsewhere; Richards et al., 2014) or because of organizational/societal reasons (e.g., abandoned land; Lewis and Kelly, 2014). Such lands are often referred to as marginal lands. These are the main target considered herein for biopump plantations.

It could be argued that other land types, such as urban areas or forests, could be converted for biopump implementation. Here, both options are disregarded, in the light of economic considerations for the former (Ackerman, 2012; Chin et al., 2013; Saha and Eckelman, 2015) and environmental considerations for the latter (Müller-Wenk and Brandão, 2010).

Finally, it must be ensured that the selected biopumps can grow on target areas, i.e. that the environment in which they are grown lies within their tolerances to a variety of abiotic factors (e.g., in terms of soil pH, slope, temperatures in can tolerate, etc.), as further detailed in (Albers et al., 2021b).

2.3 Carbon flow accounting

The CSAAP concept involves a strong time component of crucial effect on climate when emission and capture processes are combined. To investigate the viability of CSAAP, C flows are tracked from biopump cultivation through producing bio-based products, to the disposal. The potential benefit of biopump cultivation and utilization is ultimately determined by the net C capture and storage over time.

The CO_2 from the atmosphere is photosynthesized in biomass (plant), part of which is decomposed on/in the soil and stored as SOC accompanied by CO_2 release. The other part is harvested and enters the technosphere. From the technosphere, the biogenic C can be released into the atmosphere in different amounts depending on the anthropogenic products manufacturing and use. The global biogenic C balance can be written as:

$$dC_{air} + dC_{soil} + dC_{plant} + dC_{tech} = 0 \quad (1)$$

where dC_i is the variation of C quantity in compartment i. Finally, the biogenic C stored dC_{stock} is given by:

$$dC_{stock} = dC_{soil} + dC_{plant} + dC_{tech} \quad (2)$$

With:

$$dC_{soil} = \dot{C}_{tech,soil} + \dot{C}_{plant,soil} - \dot{C}_{soil,air} \quad (3)$$

$$dC_{plant} = \dot{C}_{air,plant} - \dot{C}_{plant,soil} - \dot{C}_{plant,tech} \quad (4)$$

$$dC_{tech} = \dot{C}_{plant,tech} - \dot{C}_{plant,air} - \dot{C}_{tech,soil} \quad (5)$$

The C released into the atmosphere: $dC_{air} = -dC_{stock}$

With:

$$dC_{air} = \dot{C}_{air,plant} - \dot{C}_{plant,air} - \dot{C}_{soil,air} \quad (6)$$

Where $\dot{C}_{i,j}$ are the C flows (t year^{-1}) from compartment i to compartment j. Compartments include technosphere (tech), the entire biopump (plant), atmosphere (air), soil and subsoil (soil), C captured from the atmosphere by photosynthesis (air, plant), C released by bio-based product at end-of-life (plant, air), C released from the soil (soil, air), the portion of the plant remaining on/in soil (plant, soil), biogenic C from the technosphere possibly added in the soil, e.g., waste biomass used as fertilizer (manure) (tech, soil), and the biogenic C harvested (fraction of the biopump), transformed and used in the technosphere (plant, tech).

3 Result and discussion

3.1 Selected biopumps

3.1.1. Identified candidates

Tables S1 and S2 report both the minimum, maximum, and average SOC changes observed for the inventoried biopump candidates, along with additional information such as the number of measurements reported, their duration, location, associated soil depth, as well as the expected plantation lifetime. Although SOC changes are intrinsically tight to site-specific physical and managerial conditions(Sanderman et al., 2018) (hence why some biopumps show indications of both SOC increases and decreases), tables S1 and S2 nevertheless provide indications of which biopumps may inherently lead to greater transfers of C from the atmosphere to the soil than others. For instance, it can be noticed from table s1 (supplement information I) that only acerola (*Malpighia glabra L.*), araucaria (*Acacia mangium*), and blueberry were not associated with dataset reporting SOC losses. Furthermore, olive (*Olea europaea L.*), blueberry, and araucaria can be highlighted as the woody species associated with the greatest SOC changes (supplement information I, table s1), while hemp (*Cannabis sativa L.*), ryegrass (*Lolium perenne L.*), and opuntia ficus-indica (*Opuntia ficus-indica (L.) Mill*) can be highlighted from the herbaceous species (supplement information I, table s2). Tables s1 and s2 also

highlight that some biopump candidates have been much more studied than others; *Miscanthus* (*Miscanthus x giganteus*), switchgrass (*Panicum virgatum L.*), and willow (*Salix spp.*) notably present much more measurements data than the other candidates.

3.1.2. Selected biopumps for France

The results of the semi-quantitative selection criteria matrix (Table III-1) applied to France and on the basis of biopumps presented in table s1& s2 (supplement information I), are presented in Table III-2. Accordingly, some species associated with high (or higher) SOC sequestration potential (tables S1-S2) do not figure on top of the list because of e.g., their low yield (e.g., opuntia ficus-indica, bungeana (*Stipa bungeana*)). As highlighted in Table III-2, the mean score for all woody and herbaceous candidates is similar, with 11.1 and 11.5 respectively (dimensionless, the maximum score being 15). The range of observed scores is greater for the woody candidates (8-14.3) than for herbaceous ones (6.3-13.3). For the woody candidates, there are eight species with scores above the mean, these are all already found in France, except microphylla (*Caragana microphylla*), which grows in Eastern Europe(POWO, 2021). For the herbaceous candidates, eight presented scores above the mean, and these are all currently found in the French ecosystem.

The yield of woody candidates (varying from 4.13 to 63 Mg DM ha^{-1} $year^{-1}$; supplement information I, table s5) is on average 38% higher than the yield of herbaceous candidates (varying from 1.6 to 40 Mg DM ha^{-1} $year^{-1}$; supplement information I, table s5), and this is reflected in the scoring (average of 2.6 vs 2.2 for this criteria) since the top score was attributed for yields above 10 Mg DM ha^{-1} $year^{-1}$. The potential to enhance SOC was inventoried both in terms of concentration and stock, and concentration data were available for most candidates. The mean SOC concentration of woody candidates is similar to herbaceous candidates, and there are some species with outstanding values in both wood and grass (acacia and olive for wood, ryegrass for herbaceous). Hence woody and herbaceous candidates obtained the same score for the SOC criteria (Table III-2). In terms of agricultural intensity, the average score for herbaceous candidates is slightly higher (14%) than their woody counterparts, with korshinsk peashrub (*Caragana korshinskii Kom*) standing out from the woody candidates while *Miscanthus* and bahiagrass (*Paspalum notatum Flüggé*) for the herbaceous ones. Most candidates are already grown in France, while acacia is suitable for warmer regions, mostly reported in Latin America(CABI, 2021). Ramie (*Boehmeria nivea L.*) and bungeana grow in East Asia but are reported to be able to grow in even harder environments, thus are judged to be suited for French conditions(Xu et al., 2019; Yu et al., 2009). Woody and herbaceous candidates are similar in terms of invasion risk; though this information was missing for some wood species. Poplar (*Populus spp*) and alder (*Alnus glutinosa*) grow in France, but korshinsk peashrub does not, and invasiveness risk is unclear.

In summary, among the fourteen woody and thirteen herbaceous candidates, eight were proposed in each group as potentially suitable biopumps in France. It should also be highlighted that, among the selected woody candidates, some species supply a third service on top of C sequestration and biomass production, namely the production of marketable fruits (i.e., blueberry).

3.1.3. Bio-based products

The composition of the selected biopump candidates is presented in table s4 (supplement information I). For the woody candidates, the cellulose content varies between 20% and 60% of the dry matter, while for the herbaceous selected candidates, it varies between 20 and 76% of the dry matter, highlighting suitability for possible uses as long-lived fiber products. Table s6 (supplement information I) outlines a documented inventory of twenty-nine biomass-to-bioproducts conversion pathways mainly focusing on building materials, vehicle panels, packaging, and textiles, where the product's lifetime varies between days (e.g., fast-moving consumer goods such as food and energy) to potentially 100 years (e.g., hemp-based plaster material for walls, often referred to as "hemp concrete"(de Bruijn et al., 2009; Ip and Miller, 2012)).

The identified biopumps could provide products with short lifetime e.g., fruits or energy materials (opuntia ficus-indica, poplar), or products with longer lifetime using extracted fiber or shives (e.g., transport pallet made from *Miscanthus*, panels for the automotive or construction sector made from hemp). Moreover, and despite not listed in table s6 (supplement information I), wood could be used in long-lived products as furniture or as chips included in particleboard, these potentially lasting for decades(Couret et al., 2017; Spitzley et al., 2006).

Table III-2 Biopump ranking results[a]

Biopump	Criteria								Total score
	1)Yield	2)SOC increase potential	3) Agricultural intensity				4)Suitability[b]	5)Invansion risk	
			Water	Fertilizer	Pesticides	Total			
Woody plants									
Black locust	3	3	3	2	2	2.3	3	3	14.3
Atriplex	3	3	1	3	3	2.3	3	3	14.3
Microphylla	3	2	3	3	0	2.0	2	3	14.0
Olive	3	3	2	1	1	1.3	3	3	13.3
Araucaria	3	2	1	3	2	2.0	3	3	13.0
Rhamnoides	2	3	2	2	0	1.3	3	3	12.3
Blueberry	3	3	0	0	1	0.3	3	3	12.3
Poplar	3	2	2	3	1	2.0	3	2	12.0
Alder	2	1	2	3	2	2.3	3	2	10.3
Willow	3	1	1	2	2	1.7	3	1	9.7
Acerola	2	2	3	3	2	2.7	1	2	9.7
Korshinsk peashrub	1	2	3	3	3	3.0	1	2	9.0
Acacia	3	3	3	3	0	2.0	0	1	9.0
Guava	3	1	0	0	0	0.0	1	3	8.0
Mean	2.6	2.2				1.8	2.3	2.4	11.5
Standard deviation	0.6	0.7				0.8	1.0	0.7	2.1
Herbaceous plants									
Switchgrass	3	2	3	2	2	2.3	3	3	13.3
Hemp	3	2	2	2	2	2.0	3	3	13.0
Miscanthus	3	1	2	2	2	2.0	3	3	12.0
Ryegrass	3	3	3	0	3	2.0	3	1	12.0
White clover	3	3	1	3	1	1.7	3	1	11.7
White mustard	1	3	1	1	3	1.7	3	3	11.7
Red clover	2	1	2	3	2	2.3	3	3	11.3
Giant reed	3	2	1	3	3	2.3	3	1	11.3
Opuntia ficus-indica	0	3	3	2	1	2.0	3	3	11.0
Ramie	3	3	1	3	1	1.7	0	3	10.7
Alfalfa	1	1	2	2	1	1.7	3	3	9.7
Bahiagrass	3	2	3	3	2	2.7	1	1	9.7
Bungeana	1	2	2	2	3	2.3	0	2	6.3
Mean	2.2	2.2				2.1	2.4	2.3	11.1
Standard deviation	1.0	0.8				0.32	1.1	0.91	1.1

a: Figures are presented with a maximum of 3 significant digits
b: Suitability to grow in France

The end-of-life management of bio-based products is similar to the traditional products they replaced, but have the advantage to be biodegradable, though not always if they were mixed with petrochemical additives (e.g.,(Rahman and Bhoi, 2021)). Recycling technologies are also in development(La Rosa et al., 2013). Short

lifetime implies short C stock turnover, but recycling being possible, one feasible compensation is to increase the number of use cycles. Notably, whether bio-based products are used in building or as fast-moving consumer goods, they often replace a fossil-based alternative (supplement information I, table s6), thereby preventing the extraction and refining of petrochemical resources, and associated GHG emissions.

3.2 Quantifying target areas – case of France

For illustrative purposes, the methodology proposed herein was applied to the national case study of France. To screen land types with low initial SOC stock, the global soil organic carbon (GSOC) map of the FAO (FAO, 2019) was cross-referenced with French high-resolution land cover maps (the year 2018)(Theia, 2021) to identify the areas potentially suitable for biopumps (target areas). SOC values were extracted by masking the global map with the French boundary data obtained from the GADM database(GDAM, 2018). Three SOC stock ranges were considered (t SOC ha^{-1}), namely <40, 40-50, and 50-60 (Table III-3).

After applying the selection rules (section 2.2), four out of twenty-three lands types of the French territory were identified as potential target areas, on the three SOC stock range categories. This includes lands currently used for rapeseed cultivation, natural grasslands, woody moorlands, and part of intensive grasslands (Table III-3). The case of rapeseed could be debated. Here, the rationale was, as detailed in section 2.2, that these can be considered, in part (here represented by the part grown on lands with <60 t SOC ha^{-1}), as supplying a market (European biodiesel) foreseen to decline (Staff, 2017). Of course, to respect the sustainability criteria detailed in 2.2, the portion of co-produced rapeseed meal no longer supplied must also be balanced, as detailed in e.g., (Hamelin et al., 2021; Larsen et al., 2017; Gylling 2016). Natural grasslands are often characterized by low productivity grass (e.g., briar and heather), and woody moorlands are lands covered by spontaneous woody or semi-woody vegetation(Inglada et al., 2017). The biomass productivity on these two lands is low and typically not market-driven, accordingly they were selected as target areas. Intensive grasslands, on the other hand, cover a vast share of areas with SOC stock< 60 t C ha^{-1}. They are covered by dense grasses that are not under a rotation system. The vision is to use part (0-100%) of these (shares on areas with lower SOC stocks), for instead growing biopump species that have the potential to induce additional SOC compared to current grass.

It can be seen from Table III-3 that the proportion of available target areas will differ significantly depending on the SOC threshold considered to define C-poor lands, passing from 14,600 km^2 (SOC < 40 tC ha^{-1}), to 98,108 km^2 (SOC< 50 tC ha^{-1}) and 98,191 km^2 (SOC< 60 tC ha^{-1}). There is, thus, little addition (barely 83 km^2) by considering the areas in the category 50-60 tC ha^{-1}. On this basis, a threshold of SOC < 50 tC ha^{-1} was selected. Accordingly, the target areas are dominated by natural grasslands (42.7% of the target areas), followed by rapeseed lands (41.8%) and woody moorlands (15.5%). Depending on the extent to which intensive grasslands are considered (0-100%), the overall target areas amount to either 11,187 km^2 (0% intensive grassland) to 24,007 km^2 (100% intensive grasslands), equal to 11.4%-24.5% of total areas with SOC< 50 t ha^{-1} in France. The spatial distribution of target areas over France is presented in Fig. III-1.

Table III-3 Land cover types in France (2018) on C-poorer lands, detailed for 3 SOC range categories[a]

Land cover type	SOC< 40 tha^{-1}		SOC in 40- 50 tha^{-1}		SOC in 50- 60 tha^{-1}	
	km^2	%	km^2	%	km^2	%
Continuous Urban Fabric	39.7	0.27%	47.1	0.06%	0.05	0.06%
Discontinuous Urban Fabric	1,470	10.1%	5,740	6.88%	13.8	16.70%

Industrial and Commercial Units	1,450	9.91%	5,290	6.34%	6.24	7.55%
Road Surfaces	64.1	0.44%	168	0.20%	0.29	0.35%
Rapeseed lands [b]	156	1.07%	4,620	5.53%	0.76	0.92%
Cereal Straw	1,170	8.04%	17,600	21.1%	8.59	10.4%
Legumes/Protein Crops	79.8	0.55%	1,070	1.29%	0.39	0.48%
Soybean	126	0.87%	658	0.79%	0	0.00%
Sunflower	586	4.01%	3,410	4.09%	0.07	0.09%
Corn/Maize	425	2.91%	5,120	6.14%	3.61	4.36%
Rice	6.06	0.04%	73.5	0.09%	0	0.00%
Roots and Tubers	29.4	0.2%	2,000	2.39%	3.01	3.64%
Intensive Grasslands [b]	1,020	7.01%	11,800	14.1%	12.7	15.3%
Orchards	373	2.55%	641	0.77%	0	0.00%
Vineyards	2,790	19.1%	3,110	3.73%	0.05	0.07%
Broad-leaved Forests	1,590	10.9%	11,800	14.1%	19.8	23.90%
Coniferous Forests	1,040	7.11%	4,750	5.68%	7.91	9.56%
Natural Grasslands [b]	1,510	10.3%	3,170	3.8%	0.88	1.07%
Woody Moorlands [b]	384	2.63%	1,350	1.62%	1.65	1.99%
Bare Rock	32.2	0.22%	46.2	0.06%	0.21	0.25%
Beaches, Dunes and Sand	22.6	0.15%	47.6	0.06%	0.69	0.83%
Glaciers and perpetual Snow	0.84	0.01%	0.46	0.00%	0	0.00%
Water Bodies	235	1.61%	969	1.16%	2.06	2.49%
Total	14,600	100%	83,500	100%	82.8	100%

[a] : Values are rounded to a maximum of 3 significant digits

[b] : chosen as target areas

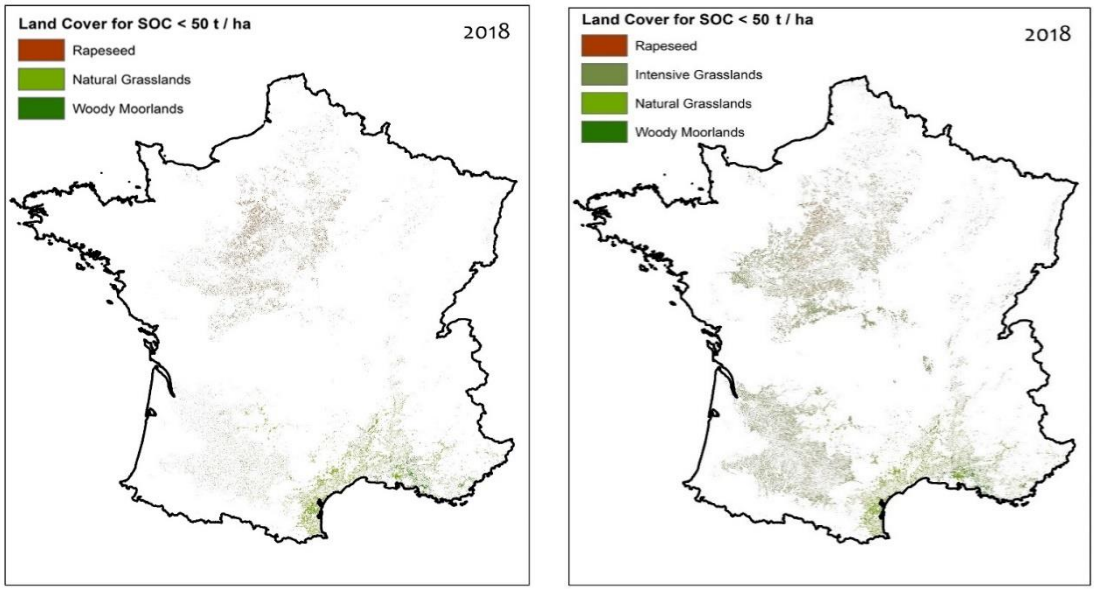

Fig. III-1 Target areas identified as potentially suitable for biopumps implementation in France, without (left) and with (right) intensive grasslands.

3.3 Dynamic carbon flows and climate mitigation potential – illustrative case

3.3.1. Case study of Miscanthus cultivation in French target areas

Miscanthus, one of the biopumps identified in Table III-2, is used as an illustrative biopump to illustrate the CSAAP concept, based on the available data on the above- and below-ground C flows for this plant. *Miscanthus* also has the interest that its rotation (ca. 20 years;Hamelin et al., 2012)) is in between those of herbaceous and woody plants. In France, *Miscanthus* is widely grown (6500 ha in 2019 with a growth rate of ca. 10% per year), leading the European *Miscanthus* cultivation (Ben Fradj et al., 2020; France Miscanthus, 2019).

3.3.2. SOC simulation and C sequestration

A continuous plantation from 2020 to 2100 was considered, with a rotation time of 20 years, the first year being dedicated to land preparation and second and third years being the establishment phase (no harvest the first two years, a harvest corresponding to 60% of yield the third year; Hamelin et al., 2012). This corresponds to four rotations. The evolution of SOC over the chosen time horizon was modeled with the C-TOOL software(Taghizadeh-Toosi et al., 2014). The SOC model used in this software considers two soil compartments, i.e. topsoil and subsoil, each of them with three C pools: fresh organic matter, humified organic matter, and resistant organic matter. Transformation and fate of C between these compartments and pools are endogenously modeled, including mineralization to gas, with calibrated first-order reaction kinetics, depending on temperature and clay content. The main output of C-TOOL is the yearly evolution of the soil stock. The key input includes: (i) the annual input of C to soil (farming practices dependant), (ii) soil clay content (retrieved from Harmonized World Soil Database for 1-m depth; Nachtergaele et al., 2012), (iii) soil C: N ratio (11) (Clivot et al., 2019; Launay et al., 2021), (iv) initial SOC stock (FAO, 2019), (v) year per year average monthly air temperature (SICLIMA data of DRIAS CERFACS, IPSL, last updated May 2013, for the RCP4.5 climate trajectory, downscaled by the model CNRM-CERFACS-CM5/CNRM-ALADIN63).

According to the C-TOOL simulation, after four rotations, the SOC increased from 42.35 (initial SOC) to 58.52 Mg ha^{-1}, which represents a 4.8‰ annual increase, slightly above the 4‰ objective advocated in Minasny et al. (2017). Scaling this to the target areas of Table III-3 and equally distributing the sequestration over the 100 years, there could be 0.23 (0% intensive grasslands) to 0.49 Mt C $year^{-1}$(100% intensive grasslands), translating to 0.83 to 1.78 Mt CO_2 $year^{-1}$ sequestered in France as a result of the *Miscanthus* cultivation. This figure covers only the Miscanthus production and disregards the sequestration that would have happened otherwise (e.g., as a result of rapeseed cultivation). These amounts nevertheless represent 0.19% to 0.41% of CO_2 emissions annually from the 2015-2018 French carbon budget (431 Mt CO_2-eq)(The High Council on Climate, 2019). This offsetting effect is here slightly overestimated (as foregone sequestration is disregarded), but would likely be more important when the whole biopump lifecycle is considered, as analyzed hereafter.

3.3.3. Dynamic C flows accounting

The case study aims at illustrating the partitioning of biogenic C between soil, technosphere, and atmosphere, considering 1 ha of the target area, and a 100-year time scope (2020-2120), encompassing the biopump cultivation and the anthropogenic products lifetime, with a 1-year time step. The biogenic fraction of the C from the harvested biopump (F) ending up stored in the anthropogenic products, as well as the anthropogenic products lifetime (L) are two key parameters. In this illustrative example, we consider three abstract narratives defining different F and L, namely:

- F100L100: the whole biogenic C harvested is stored in anthropogenic products with very long lifespan (e.g., a bio-based composite wall for buildings) and with multiple recycling loops, i.e. an overall storage time of more than 100 years. No biogenic C is lost as gas.

- F100L1: the whole harvested C is used as anthropogenic products with short lifespan (1 year), with incineration as end-of-life (e.g., a biofuel).
- FxLy/Fx'Ly': part of biogenic C harvested is lost during the manufacture, with C fractions Fx and Fx' in the product and lost, respectively. All biogenic C is emitted as CO_2 at the product end-of-life (e.g., incineration). Several combinations are considered for this example, with different lifetimes and carbon content (Fig. III-2; additional combinations in supplement information I, fig. s3). For tractability, manufacturing losses are considered to occur in year 1.

The year per year flows of biogenic C involved, from/to the atmosphere, were calculated through a mass balance. The actual year per year effect on global mean temperature change (GMTC) was calculated based on the impulse response function approach recommended by IPCC(Thomas F Stocker et al., 2013) and using the Python-based CCI-tool software(Tiruta-barna, 2021) developed in a previous study(Shimako et al., 2018b). For tractability reasons, it was considered that there are no differences in terms of CO_2 and other GHG emissions from the background activities (e.g., electricity, fertilizers) among the narratives illustrated herein. Therefore, the focus is maintained on the differences in biogenic C flows induced by different L and F only.

The evolution of the annual stocks is shown in Fig. III-2a as a fraction of the C absorbed i.e. $dC_{stock}/\dot{C}_{air,plant}$, for each couple of parameters (L, F). Positive values indicate the stock formed while negative values indicate stock consumed per year. The decrease in stock every 20 years corresponds to the land preparation phase between 2 rotations (bare soil). One should note the variety of behaviors and the difficulty of qualifying the mitigation potential of each case.

a

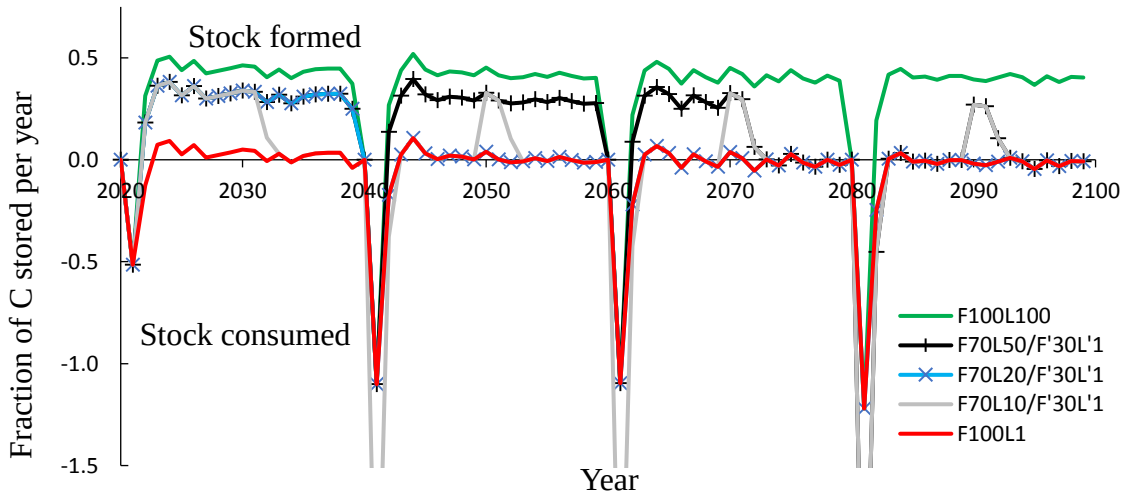

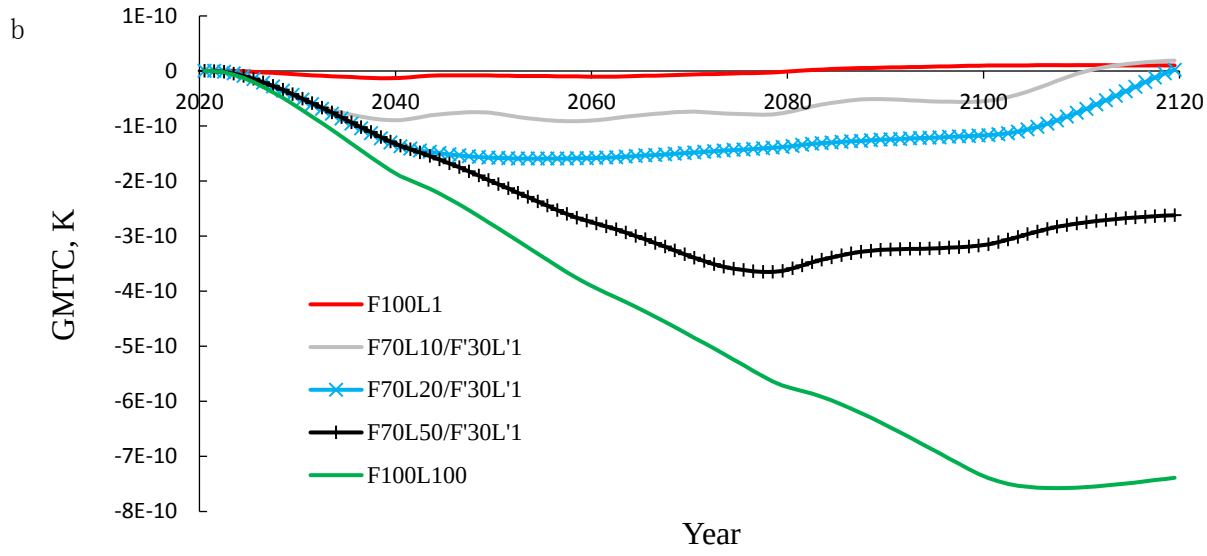

Fig. III-2 Carbon flows analysis (a) fraction of biogenic carbon stored per year, (b) global mean temperature change

The behaviors vary between two extreme situations: F100L100, i.e. all the harvested C is embedded in a product with a very long lifespan, and F100L1, i.e. all the harvested C is immediately released to the atmosphere due to the end-of-life of very short-lived products. While the former allows for significant stocks over the entire time horizon (except the inter-rotation periods), the latter, on the contrary, retains relatively little C and even offsets a part of the SOC stock formed after two rotations. For the other three intermediate situations, we observe a reduction of stock formation in time, highlighting the importance of the product lifetime. For example, F70L50/F'30L'1 creates stocks until about 2070, when end-of-life emissions start for the first products; at this time, the biogenic C embedded in the products is released as CO_2, and the process replicates each year for the subsequent products. The positive peaks (stocks) observed (especially in the case of F70L10/F'30L'1) correspond to years where no product reaches the end-of-life (no emissions). Then, the C fraction incorporated into the long-lived products affects the stock amount, visible on the plateau values for F100L100 and F70L50/F'30L'1. It can be concluded that the higher the fraction stored and the longer the lifetime, the longer the time horizon over which the stocks are effective, and the lower the overall CO_2 flow (supplement information I, fig. s2).

Fig. III-2b represents the effect of biogenic C balance (for 1 ha of land) on GMTC. Negative values indicate a beneficial effect (temperature decrease) and can be considered as targets. This representation clearly indicates that the short-lived products with end-of-life emissions occurring <1-year (e.g., F100L1) have little mitigation capacity, which vanishes after two rotations. On the contrary, the more the end-of-life emissions are postponed (or suppressed), the greater the beneficial effect. Here also a negative GMTC peak is observed, corresponding to the lifespan of the first products manufactured, and postponed by several years due to thermal inertia of Earth (e.g., in 2077 for F70L50/F'30L'1). After this time, the benefit diminishes until circa 80 years when the biopump culture and transformation into products are stopped. Till 2100, all scenarios except F100L1 are negative in GMTC, contributing to mitigating climate change. After 2100, the end-of-life effect is observed with a positive spread of GMTC over time until the last product disappears from the technosphere. Within the time boundary 2020-2120, C in F70L10/F'30L'1 is released to the atmosphere, causing GMTC to rise above 0 K; the same happens in F70L20/F'30L'1 but later. The benefit of suppressing the end-of-life emissions can be countered by a lower utilization fraction F in long-lived products, and trade-off situations between parameters L, L', F, and F' can occur (additional examples are given in supplement information I, fig. s3). Many other parameters influence the C stocks and their evolution in time, therefore detailed analyses are necessary before the practical implementation of a biopump. For example, the effect of initial SOC (100 Mg ha^{-1}

instead of 42 Mg ha^{-1}) and temperature (higher by 2℃) on GMTC results for F100L1 (all biogenic C is released within 1 year) are presented in supplement information I, Fig S4; in these conditions, there is no more mitigation potential.

4 Perspective and limitations

This study endeavored to propose and demonstrate the concept of CSAAP and biopump, further investigating the possible candidates and climate mitigation potential. Some limitations and perspectives can be highlighted:

- The list of potential biopumps obtained herein is based on available studies, mainly captured in Ledo et al.(2019)' meta-study on perennial plants, but more comparative data on both the species already documented and eventual additional ones (e.g., annual plants) would enhance the statistical robustness of this list. Moreover, the suitability for cultivating these on a studied territory was here determined based on a qualitative scoring matrix: this could be refined by cross-referencing spatially-explicit data on biopump tolerances and pedoclimatic data, among others.
- The equal weight given to the selection criteria could be challenged, and be considered in a more spatially-explicit manner, tailored to the specificities of each biopump-target area combination. One additional aspect that could be considered is the potential biodiversity impacts occurring as one land use is converted to biopump cultivation. These impacts will differ according to the type of initial land use being converted and could be considered according to different methodologies and metrics (Feest et al., 2014).
- Albeit the focus is here on CO_2 emissions, other greenhouse gases and emission flows need to be fully considered in order to fully address the trade-offs (if any) between negative emissions and overall environmental mitigation.
- The goal at this stage was not to determine the optimal biopump-anthropogenic product combination, but to present a methodology to do so, and to assess the magnitude of CSAAP as a strategy for controlling global warming. The real benefit of the implementation in the real world must be evaluated by integrating the entire anthropogenic system with associated technological GHG emissions and petrochemical product substitutions (e.g., fossil-based), by DLCA methodology for instance (e.g., Beloin-Saint-Pierre et al., 2020). Also, demonstration sites with actual biopump cultivation on relevant target areas would, as for most soil-based solutions for negative emissions(Romanenkov et al., 2019), be useful to validate the simulation results of this study.

5 Conclusions

In this study, the concept of storing carbon in both arable lands and anthropogenic products (CSAAP) has been demonstrated, in order to meet the challenges of inducing additional CDR (negative emissions) and CO_2 mitigating effect. It builds upon the biopump concept, i.e. plants able to induce a net transfer of C from the atmosphere to the soil that are grown on "low-impact" lands, and used as long-lived bio-based products in the technosphere. Here, we presented and demonstrated a 4-steps framework that can be applied to any region. The framework is composed of four steps and builds upon publicly available data and simulation tools: i) identification of biopump candidates, ii) selection and ranking of biopumps for the region of interest, iii) identification and selection of target areas suitable for sustainable biopump plantation, iv) assessment of the mitigation potential over time. The case study confirmed the relevance of CSAAP as a climate mitigation strategy, as it was shown to lead to net long-term reductions of GMTC after 100 years, under ideal conditions (100% conversion of biomass C to the bio-based product, having a 100-year lifetime). Less ideal conditions were also shown to lead to GMTC reductions in the shorter term, the extent of which was essentially shaped by the product lifetime. For greater flexibility towards climate mitigation, CSAAP strategies considering shorter/longer product lifetimes need to be assessed along with other mitigation strategies (e.g., methane emission reduction) themselves having different temporalities in terms of GMTC reductions achieved. In France alone, we identified 11,187-24,007 km^2 of potential target areas, expecting to stock the equivalent of 0.23-0.49 Mt SOC per year, over 100-year.

This represents 0.19- 0.41% of France's annual CO_2 emissions, and up to 13% if all produced biomass is stored in the technosphere over 100-years.

Supplement information

Supplement information I provided provides tables and figures related to this chapter.

References

Ackerman, K., 2012. The potential for urban agriculture in New York City: Growing capacity, food security, and green infrastructure, Columbia University, The Earth Institute, Urban Design.

Albers, A., Avadí, A., Hamelin, L., 2021. A generalizable framework for spatially explicit exploration of soil carbon sequestration on global marginal land. Sci. Rep. https://doi.org/10.21203/rs.3.rs-701807/v1

Amundson, R., 2001. The carbon budget in soils. Annu. Rev. Earth Planet. Sci. 29, 535–562.

Bastin, J.-F., Finegold, Y., Garcia, C., Mollicone, D., Rezende, M., Routh, D., Zohner, C.M., Crowther, T.W., 2019. The global tree restoration potential. Science (80-.). 366, 76–79. https://doi.org/10.1126/science.aay8060

Bataille, C., 2020. Physical and policy pathways to net-zero emissions industry. WIRES Wiley Interdiscip. Rev. Forthcomin, 1–20. https://doi.org/10.1002/wcc.633

Batjes, N.H., 1996. Total carbon and nitrogen in the soils of the world. Eur. J. Soil Sci. 47, 151–163.

Ben Fradj, N., Rozakis, S., Borzęcka, M., Matyka, M., 2020. Miscanthus in the European bio-economy: A network analysis. Ind. Crops Prod. 148. https://doi.org/10.1016/j.indcrop.2020.112281

Buscot, F., Varma, A., 2005. Microorganisms in soils: roles in genesis and functions.

CABI, 2021. Invasive Species Compendium. URL https://www.cabi.org/isc/

Chin, D., Infahsaeng, T., Jakus, I., Oorthuys, V., 2013. Urban farming in Boston: A survey of opportunities.

Climate watch, 2021. Historical GHG Emissions. World Resour. Inst. URL https://www.climatewatchdata.org/ghg-emissions?end_year=2018&start_year=1990

Clivot, H., Mouny, J.C., Duparque, A., Dinh, J.L., Denoroy, P., Houot, S., Vertès, F., Trochard, R., Bouthier, A., Sagot, S., Mary, B., 2019. Modeling soil organic carbon evolution in long-term arable experiments with AMG model. Environ. Model. Softw. 118, 99–113. https://doi.org/10.1016/j.envsoft.2019.04.004

Couret, L., Irle, M., Belloncle, C., Cathala, B., 2017. Extraction and characterization of cellulose nanocrystals from post-consumer wood fiberboard waste. Cellulose 24, 2125–2137. https://doi.org/10.1007/s10570-017-1252-7

COWI A/S and Utrecht University, 2019. Environmental impact assessments of innovative bio-based product - Publications Office of the EU, European Commission. https://doi.org/10.2777/251887

de Bruijn, P.B., Jeppsson, K.H., Sandin, K., Nilsson, C., 2009. Mechanical properties of lime-hemp concrete containing shives and fibres. Biosyst. Eng. 103, 474–479. https://doi.org/10.1016/j.biosystemseng.2009.02.005

de Jong, S., Staples, M., Grobler, C., Daioglou, V., Malina, R., Barrett, S., Hoefnagels, R., Faaij, A., Junginger, M., 2019. Using dynamic relative climate impact curves to quantify the climate impact of bioenergy production systems over time. GCB Bioenergy 11, 427–443. https://doi.org/10.1111/gcbb.12573

DRIAS CERFACS, IPSL, M.-F., 2013. CNRM-CERFACS-CM5/CNRM-ALADIN63-RCP4.5. DRIAS les Futur. du Clim.

Ekvall, T., 2019. Attributional and Consequential Life Cycle Assessment, in: Sustainability Assessment

at the 21st Century. p. 13.

FAO, 2019. GLOSIS - GSOCmap (v1.5.0). Glob. Soil Org. Carbon Map. URL http://54.229.242.119/GSOCmap/

FAOSTAT, 2022. Food and agriculture data. URL https://www.fao.org/faostat/en/#data/EK

Feest, A., Van Swaay, C., Van Hinsberg, A., 2014. Nitrogen deposition and the reduction of butterfly biodiversity quality in the Netherlands. Ecol. Indic. 39, 115–119. https://doi.org/10.1016/j.ecolind.2013.12.008

Finkbeiner, M., Bach, V., 2021. Life cycle assessment of decarbonization options—towards scientifically robust carbon neutrality. Int. J. Life Cycle Assess. 26, 635–639. https://doi.org/10.1007/s11367-021-01902-4

France Miscanthus, 2019. Les chiffres de la filière française. URL https://www.france-miscanthus.org/le-miscanthus-en-chiffres/

Gautam, P., Kumar, S., Lokhandwala, S., 2019. Chapter 11 - Energy-Aware Intelligence in Megacities, in: Kumar, S., Kumar, R., Pandey, A.B.T.-C.D. in B. and B. (Eds.), . Elsevier, pp. 211–238. https://doi.org/https://doi.org/10.1016/B978-0-444-64083-3.00011-7

GDAM, 2018. Database of Global Administrative Areas. URL https://gadm.org/data.html

Guénon, R., Bastien, J.C., Thiébeau, P., Bodineau, G., Bertrand, I., 2016. Carbon and nutrient dynamics in short-rotation coppice of poplar and willow in a converted marginal land, a case study in central France. Nutr. Cycl. Agroecosystems 106, 293–309. https://doi.org/10.1007/s10705-016-9805-y

Gylling, M., Jørgensen, U., Bentsen, N.S., Kristensen, I.T., Dalgaard, T., Felby, C., Larsen, S., Johannes, V.K., 2016. The + 10 million tonnes study increasing the sustainable production.

Hamelin, L., Jørgensen, U., Petersen, B.M., Olesen, J.E., Wenzel, H., 2012. Modelling the carbon and nitrogen balances of direct land use changes from energy crops in Denmark: A consequential life cycle inventory. GCB Bioenergy 4, 889–907. https://doi.org/10.1111/j.1757-1707.2012.01174.x

Hamelin, L., Møller, H.B., Jørgensen, U., 2021. Harnessing the full potential of biomethane towards tomorrow's bioeconomy: A national case study coupling sustainable agricultural intensification, emerging biogas technologies and energy system analysis. Renew. Sustain. Energy Rev. 138. https://doi.org/10.1016/j.rser.2020.110506

Head, M., Levasseur, A., Beauregard, R., Margni, M., 2020. Dynamic greenhouse gas life cycle inventory and impact profiles of wood used in Canadian buildings. Build. Environ. 173, 106751. https://doi.org/10.1016/j.buildenv.2020.106751

Hilaire, J., Minx, J.C., Callaghan, M.W., Edmonds, J., Luderer, G., Nemet, G.F., Rogelj, J., del Mar Zamora, M., 2019. Negative emissions and international climate goals—learning from and about mitigation scenarios. Clim. Change 157, 189–219. https://doi.org/10.1007/s10584-019-02516-4

Ingerson, A., 2011. Carbon storage potential of harvested wood: Summary and policy implications. Mitig. Adapt. Strateg. Glob. Chang. 16, 307–323. https://doi.org/10.1007/s11027-010-9267-5

Inglada, J., Vincent, A., Arias, M., Tardy, B., Morin, D., Rodes, I., 2017. Operational High Resolution Land Cover Map Production at the Country Scale Using Satellite Image Time Series. Remote Sens. 9, 95. https://doi.org/10.3390/rs9010095

Invasive Species Specialist Group, 2020. The Global Invasive Species Database. Glob. Invasive Species Program. URL

http://issg.org/database/species/search.asp?st=sss&sn=&rn=France&ri=18889&hci=-1&ei=-1&fr=1&sts=&lang=EN

Ip, K., Miller, A., 2012. Life cycle greenhouse gas emissions of hemp-lime wall constructions in the UK. Resour. Conserv. Recycl. 69, 1–9. https://doi.org/10.1016/j.resconrec.2012.09.001

Karan, S.K., Hamelin, L., 2021. Crop residues may be a key feedstock to bioeconomy but how reliable are current estimation methods? Resour. Conserv. Recycl. 164, 105211. https://doi.org/10.1016/j.resconrec.2020.105211

La Rosa, A.D., Cozzo, G., Latteri, A., Mancini, G., Recca, A., Cicala, G., 2013. A comparative life cycle assessment of a composite component for automotive. Chem. Eng. Trans. 32, 1723–1728. https://doi.org/10.3303/CET1332288

Larsen, S., Bentsen, N.S., Dalgaard, T., Jørgensen, U., Olesen, J.E., Felby, C., 2017. Possibilities for near-term bioenergy production and GHG-mitigation through sustainable intensification of agriculture and forestry in Denmark. Environ. Res. Lett. 12. https://doi.org/10.1088/1748-9326/aa9001

Launay, C., Constantin, J., Chlebowski, F., Houot, S., Graux, A.I., Klumpp, K., Martin, R., Mary, B., Pellerin, S., Therond, O., 2021. Estimating the carbon storage potential and greenhouse gas emissions of French arable cropland using high-resolution modeling. Glob. Chang. Biol. 27, 1645–1661. https://doi.org/10.1111/gcb.15512

Ledo, A., Hillier, J., Smith, P., Aguilera, E., Blagodatskiy, S., Brearley, F.Q., Datta, A., Diaz-Pines, E., Don, A., Dondini, M., Dunn, J., Feliciano, D.M., Liebig, M.A., Lang, R., Llorente, M., Zinn, Y.L., McNamara, N., Ogle, S., Qin, Z., Rovira, P., Rowe, R., Vicente-Vicente, J.L., Whitaker, J., Yue, Q., Zerihun, A., 2019. A global, empirical, harmonised dataset of soil organic carbon changes under perennial crops. Sci. Data 6, 1–7. https://doi.org/10.1038/s41597-019-0062-1

Ledo, A., Smith, P., Zerihun, A., Whitaker, J., Vicente-Vicente, J.L., Qin, Z., McNamara, N.P., Zinn, Y.L., Llorente, M., Liebig, M., Kuhnert, M., Dondini, M., Don, A., Diaz-Pines, E., Datta, A., Bakka, H., Aguilera, E., Hillier, J., 2020. Changes in soil organic carbon under perennial crops. Glob. Chang. Biol. 26, 4158–4168. https://doi.org/10.1111/gcb.15120

Lewis, S.M., Kelly, M., 2014. Mapping the potential for biofuel production on marginal lands: Differences in definitions, data and models across scales. ISPRS Int. J. Geo-Information 3, 430–459. https://doi.org/10.3390/ijgi3020430

Masson-Delmotte, V., Zhai, P., Pörtner, H.-O., Roberts, D., Skea, J., Shukla, P.R., Pirani, A., Moufouma-Okia, W., Péan, C., Pidcock, R., 2018. Global warming of 1.5 C. An IPCC Spec. Rep. impacts Glob. Warm. 1.

Minasny, B., Malone, B.P., McBratney, A.B., Angers, D.A., Arrouays, D., Chambers, A., Chaplot, V., Chen, Z.S., Cheng, K., Das, B.S., Field, D.J., Gimona, A., Hedley, C.B., Hong, S.Y., Mandal, B., Marchant, B.P., Martin, M., McConkey, B.G., Mulder, V.L., O'Rourke, S., Richer-de-Forges, A.C., Odeh, I., Padarian, J., Paustian, K., Pan, G., Poggio, L., Savin, I., Stolbovoy, V., Stockmann, U., Sulaeman, Y., Tsui, C.C., Vågen, T.G., van Wesemael, B., Winowiecki, L., 2017. Soil carbon 4 per mille. Geoderma 292, 59–86. https://doi.org/10.1016/j.geoderma.2017.01.002

Müller-Wenk, R., Brandão, M., 2010. Climatic impact of land use in LCA-carbon transfers between vegetation/soil and air. Int. J. Life Cycle Assess. 15, 172–182. https://doi.org/10.1007/s11367-009-0144-y

Nachtergaele, F., van Velthuizen, H., van Engelen, V., Fischer, G., Jones, A., Montanarella, L., Petri, M., Prieler, S., Teixeira, E., Shi, X., 2012. Harmonized World Soil Database (version 1.2). FAO,

Rome, Italy IIASA, Laxenburg, Austria 1–50.

Nguyen, C., 2003. Rhizodeposition of organic C by plants: mechanisms and controls. Agron. EDP Sci. 23, 375–396. https://doi.org/10.1051/agro:2003011

Office for National Statistics, 2019. A burning issue: biomass is the biggest source of renewable energy consumed in the UK. Off. Natl. Stat. URL https://www.ons.gov.uk/economy/environmentalaccounts/articles/aburningissuebiomassisthebiggestsourceofrenewableenergyconsumedintheuk/2019-08-30

Paustian, K., Larson, E., Kent, J., Marx, E., Swan, A., 2019. Soil C Sequestration as a Biological Negative Emission Strategy. Front. Clim. 1, 1–11. https://doi.org/10.3389/fclim.2019.00008

Poeplau, C., Don, A., 2015. Carbon sequestration in agricultural soils via cultivation of cover crops - A meta-analysis. Agric. Ecosyst. Environ. 200, 33–41. https://doi.org/10.1016/j.agee.2014.10.024

POWO, 2021. Plants of the World Online. Facil. by R. Bot. Gard. Kew. URL http://www.plantsoftheworldonline.org

Prochnow, A., Heiermann, M., Plöchl, M., Linke, B., Idler, C., Amon, T., Hobbs, P.J., 2009. Bioenergy from permanent grassland - A review: 1. Biogas. Bioresour. Technol. 100, 4931–4944. https://doi.org/10.1016/j.biortech.2009.05.070

Rahman, M.H., Bhoi, P.R., 2021. An overview of non-biodegradable bioplastics. J. Clean. Prod. 294, 126218.

Richards, B.K., Stoof, C.R., Cary, I.J., Woodbury, P.B., 2014. Reporting on marginal lands for bioenergy feedstock production: a modest proposal. BioEnergy Res. 7, 1060–1062.

Rodrigues, L., Hardy, B., Huyghebeart, B., Fohrafellner, J., Fornara, D., Barančíková, G., Bárcena, T.G., De Boever, M., Di Bene, C., Feizienė, D., Kätterer, T., Laszlo, P., O'Sullivan, L., Seitz, D., Leifeld, J., 2021. Achievable agricultural soil carbon sequestration across Europe from country-specific estimates. Glob. Chang. Biol. 27, 6363–6380. https://doi.org/10.1111/gcb.15897

Romanenkov, V., Belichenko, M., Petrova, A., Raskatova, T., Jahn, G., Krasilnikov, P., 2019. Soil organic carbon dynamics in long-term experiments with mineral and organic fertilizers in Russia. Geoderma Reg. 17, e00221.

Saha, M., Eckelman, M.J., 2015. Geospatial assessment of potential bioenergy crop production on urban marginal land. Appl. Energy 159, 540–547. https://doi.org/10.1016/j.apenergy.2015.09.021

Sanderman, J., Hengl, T., Fiske, G.J., 2018. Soil carbon debt of 12,000 years of human land use. Proc. Natl. Acad. Sci. 115, E1700–E1700. https://doi.org/10.1073/pnas.1800925115

Sanderson, B.M., O'Neill, B.C., Tebaldi, C., 2016. What would it take to achieve the Paris temperature targets? Geophys. Res. Lett. 43, 7133–7142. https://doi.org/doi.org/10.1002/2016GL069563

Shimako, A.H., Tiruta-Barna, L., Bisinella de Faria, A.B., Ahmadi, A., Spérandio, M., 2018. Sensitivity analysis of temporal parameters in a dynamic LCA framework. Sci. Total Environ. 624, 1250–1262. https://doi.org/10.1016/j.scitotenv.2017.12.220

Shukla, P.R., Skea, J., Calvo Buendia, E., Masson-Delmotte, V., Pörtner, H.O., Roberts, D.C., Zhai, P., Slade, R., Connors, S., Van Diemen, R., 2019. IPCC, 2019: Climate Change and Land: an IPCC special report on climate change, desertification, land degradation, sustainable land management, food security, and greenhouse gas fluxes in terrestrial ecosystems.

Spitzley, D. V, Dietz, B.A., Keoleian, G.A., 2006. Life cycle assessment of office furniture products,

Ann Arbor.

Staff, R., 2017. Rapeseed to decline in EU as biofuel wanes, exports to boost wheat: report. Reuters. URL https://www.reuters.com/article/us-eu-oilseeds-outlook-idUSKBN1EC1E0

Stocker, T.F., Qin, D., Plattner, G.-K., Alexander, L. V, Allen, S.K., Bindoff, N.L., Bréon, F.-M., Church, J.A., Cubasch, U., Emori, S., 2013. Technical summary, in: Climate Change 2013: The Physical Science Basis. Contribution of Working Group I to the Fifth Assessment Report of the Intergovernmental Panel on Climate Change. Cambridge University Press, pp. 33–115.

Taghizadeh-Toosi, A., Glendining, M., Vejlin, J., Hutchings, N.J., Olesen, J.E., Christensen, B.T., Kätterer, T., 2014. C-TOOL: A simple model for simulating whole-profile carbon storage in temperate agricultural soils. Ecol. Modell. 292, 11–25. https://doi.org/10.1016/j.ecolmodel.2014.08.016

Tanzer, S.E., Ramírez, A., 2019. When are negative emissions negative emissions? Energy Environ. Sci. 12, 1210–1218. https://doi.org/10.1039/c8ee03338b

The High Council on Climate team, 2019. FIRST ANNUAL REPORT OF THE HIGH COUNCIL ON CLIMATE OF FRANCE.

Theia, 2021. Map of land use in metropolitan France - THEIA-LAND. URL https://www.theia-land.fr/en/product/land-cover-map/

Thomas, R., Hursthouse, A., Mellor, P., Lord, R.A., Jo, E., 2021. Identifying non-agricultural marginal lands as a route to sustainable bioenergy provision - A review and holistic definition 135. https://doi.org/10.1016/j.rser.2020.110220

Tiruta-barna, L., 2021. Climate Change Impact tool. INSA. URL https://www.insa-toulouse.fr/fr/recherche/labo/lisbp/outil-de-calcul-changement-climatique.html

UNFCCC, S., 2015. Report of the Conference of the Parties on its twenty-first session, held in Paris from 30 November to 13 December 2015. Addendum. Part two: Action taken by the Conference of the Parties at its twenty-first session. United Nations Framework Convention on Climate Change Bonn.

Veldman, J.W., Aleman, J.C., Alvarado, S.T., Anderson, T.M., Archibald, S., Bond, W.J., Boutton, T.W., Buchmann, N., Buisson, E., Canadell, J.G., 2019. Comment on "The global tree restoration potential." Science (80-.). 366, 1–5. https://doi.org/10.1126/science.aaz0111

World Resources Institute, 2020. World Greenhouse Gas Emissions: 2016. URL https://www.wri.org/resources/data-visualizations/world-greenhouse-gas-emissions-2016

Xu, Y., Tang, Q., Dai, Z., Yang, Z., Cheng, C., Deng, C., Liu, C., Chen, J., Su, J., 2019. Yield components of forage ramie (Boehmeria nivea L.) and their effects on yield. Genet. Resour. Crop Evol. 66, 1601–1613. https://doi.org/10.1007/s10722-019-00800-x

Yu, Y.W., Nan, Z.B., Hou, F.J., Matthew, C., 2009. Response of stipa bungeana and pennisetum flaccidum to urine of sheep in steppe grassland of north-western China. Grass Forage Sci. 64, 395–400. https://doi.org/10.1111/j.1365-2494.2009.00704.x

Zhang, B., Hastings, A., Clifton-Brown, J.C., Jiang, D., Faaij, A.P.C., 2020. Modeled spatial assessment of biomass productivity and technical potential of Miscanthus × giganteus, Panicum virgatum L., and Jatropha on marginal land in China. GCB Bioenergy 12, 328–345. https://doi.org/10.1111/gcbb.12673

Chapter IV. Biopump: annual plants

Context

According to the research results from the previous chapter, hemp (*Cannabis sativa L.*) is selected as example for the annual biopumps. Hemp is already cultivated on French territory. After harvesting, we assumed three scenarios with different anthropogenic bio-based products:

i) Scenario SL: only hemp seeds are harvested to extract oil, while straws are left on the fields. Hemp oil would be consumed immediately (one year lifetime).
ii) Scenario IB: both hemp seeds and straws are harvested. Hemp seeds are used as the same as in scenario SL, and straws are manufactured into thermal insulations, with 40 years lifetime;
iii) Scenario CP: both hemp seeds and straw are harvested. Seeds are used as the same as in scenario SL. Here the straw is used to produce car panels, with a lifetime of 12 years.

Hemp will be cultivated on French CV-lands that are converted from identified lands in the previous chapter, therefore in all scenarios, land use change needs to be considered. Consequential LCA and dynamic LCA for climate change impact are used to evaluate the scenarios. Thus, this chapter aims to investigate the following issues:

1) How does the SOC change during hemp cultivation on French CV-lands;
2) How much cultivating hemp in 1 ha French CV-lands could mitigate the climate change;
3) Which are the environmental impacts of such scenarios;
4) How the temporality of these scenarios will affect the climate change;

The logic of exploring the answers are: simulating the SOC change during the cultivation by AMG model-> building the inventory of scenarios, including the results from SOC simulation-> estimating the climate change and other environmental impacts of three scenarios through consequential LCA-> building the inventory with temporal characteristics, based on the GHG emission results from consequential LCA and SOC simulation-> estimating the climate change dynamically in GMTC metric under the time boundary.

The content of this chapter is submitted for publication as:

Shen Z., Tiruta-Barna L., Hamelin L., From hemp grown on carbon vulnerable lands to long-lasting bio-based products: uncovering trade-offs between overall environmental impacts, sequestration in soils and dynamic influence on global temperature . submitted to Science of the total environmental

1 Introduction

In response to global warming, many governments, including France, signed the Paris Agreement, calling for limiting global warming to well below 2 °C above pre-industrial levels by 2100, and further committing to achieve carbon neutrality before 2050 (Boudet et al., 2021; UNFCCC, 2015). These climate targets imply to increase and safeguard carbon (C) sinks such as soils and plants. . This requirement inspired the concept of simultaneous Carbon Storage in Arable land and Anthropogenic Products (CSAAP), a strategy to use plants that could store additional C in the soil as soil organic carbon (SOC) during the growth phase, and in the technosphere as bio-based products obtained from the harvestable biomass (Shen et al., 2022). Accordingly, CSAAP implies inducing negative emissions and emission mitigation simultaneously. In order to avoid risks like hampering food security, plant (referred to as biopumps) cultivation needs to be conducted on lands not otherwise supplying products to the market, and where SOC can be increased. These are here referred to as carbon vulnerable lands (CV-lands). Carbon vulnerable lands are part of marginal lands that do not compete with crops or with other existing activities, and have low SOC stock, i.e. lower than 50 t ha^{-1}. The choice of land type in the French landscape was explained previously (Shen et al., 2022). This previous work identified up to 2,400,000 ha CV-lands potentially adapted for conducting CSAAP in France, with eight woody species and eight herbaceous plants. As a list-top, hemp (*Cannabis sativa L.*) is proposed in this work to apply and evaluate the CSAAP for France (Shen et al., 2022). France leads hemp cultivation in Europe, accounting for 40% of the European production, corresponding to 16,000 ha arable land (Carus and Sarmento, 2017; Moussa et al., 2018). However, hemp could also grow on CV-lands.

Unlike most fiber crops (e.g., flax), additional carbon storage in the SOC pool has been observed during hemp cultivation, .. Previous studies reported that 100 to 300 kg CO_2 ha^{-1} $year^{-1}$ is potentially stored into soils cultivated with hemp in France (Boutin et al.,2006). Similarly, annual SOC increases of 0.14 to 0.15 g/ kg have been reported in China (Li et al., 2012).

Hemp can be used in a variety of materials and products, the construction materials and the automotive industry being two sectors with the greatest growth potential (Hemp benchmarks, 2021). Using hemp instead of conventional materials could not only supply the same functions but also bring additional benefits like reducing the weight of composites. For instance, Audi has implemented hemp fiber to make side panels in one of its model(A3), instead of acrylonitrile butadiene styrene(ABS) plastic, which reduced the weight of vehicles and consequently the fuel consumption (Akampumuza et al., 2017). If 50% of glass fiber is replaced by natural fiber in the North American automobile market, then 3.07 million tonne CO_2 and 1.19 million m^3 crude oil could be saved (Pervaiz and Sain, 2003).

However, the relevance of cultivating and using hemp at large scale must be evaluated to demonstrate the mitigation potential for climate change and to anticipate potential adverse effects. Previous studies used the Life Cycle Assessment (LCA) method to assess the environmental impacts of hemp-based products. These studies used different allocation methods for the produced co-products, allocating the impacts by mass or economic value (Deng, 2014; Sinka et al., 2018), or excluded important co-products like shives (Andersson and Björhagen, 2018). Moreover, very few LCAs of hemp bio-products consider a detailed assessment of the emissions occurring at the cultivation stage, including those associated to SOC changes, being essentially focused on the manufacturing stage (e.g., Senga Kiessé et al., 2017).

To the best of authors' knowledge, no previous research has evaluated the climate mitigation potential and overall environmental impacts of a hemp-based CSAAP strategy for a country. To bridge this gap, the goal of this work is four-fold and aims to (i) quantify the long-term sequestration performance of hemp grown on French CV-lands; (ii) assess the overall environmental consequences of converting CV-lands for the cultivation of hemp and subsequently transforming the harvested hemp to long-lasting bio-based products, thereby replacing petrochemical counterparts; (iii) uncover the trade-offs of this hemp-to-bioeconomy products concept, both between the different environmental impacts, but also between

C sequestration in soils and climate change mitigation; and (iv) assess in time the effect of this CSAAP system on global temperature change.

To this end, the hemp cultivation on CV-lands and use in two different bio-based products with different lifetimes was investigated through three scenarios. Whereas all scenarios involve the cultivation of hemp and harvest of hemp seeds with subsequent production of hempseed oil, they differ with regards to the use of the straw (or hemp stem): scenario (i) incorporation of hemp straw to soils; scenario (ii) harvest of hemp straw to produce thermal insulation for buildings; scenario (iii) harvest of hemp straw to produce car panels.

2 Methods

2.1 Overview of the step-wise approach used

To determine the environmental performance of cultivating hemp on CV-lands, the SOC change in the soil was first simulated based on a state-of-the-art SOC model. The result was fed into consequential life cycle inventories, together with inputs and outputs from all other involved processes (Fig. IV-1), which was translated, through life cycle impact assessment(Fazio et al., 2018), to net environmental impacts, for all three scenarios. The effect of the temporality of the carbon emission and capture processes over the whole life cycle was evaluated, for the climate change impact, by a dynamic LCA approach. As required by the ISO standards for LCA (ISO 14040, 2006; ISO 14044; 2006), sensitivity and uncertainty analyses were conducted to explore the robustness of the results.

2.2 Assessing SOC changes associated to converting CV-lands to hemp cultivation

French CV-lands were identified (Shen et al., 2022) as areas currently under the following land covers (in % of the total CV-land area): (i) rapeseed cultivation (20%), (ii) intensive grasslands (53%), (iii) natural grasslands (20%) and (iv) woody moorlands (7%). This, thus, represents the reference management of the CV-lands prior to their conversion to hemp. Here, a few simplifications were made to ensure tractability. First, heather (*Calluna vulgaris*) was selected as a representative biomass specie for both natural grasslands and woody moorlands, based on the definitions provided in the literature (Inglada et al., 2017). Similarly, ryegrass (*Lolium perenne L.*) and rapeseed (*Brassica napus L.*) were chosen as representative species of intensive grassland and rapeseed cultivation, respectively (Kirwan et al., 2007). Accordingly, a representative hectare of 'French initial CV-land management' is here defined as 20% rapeseed cultivation, 53% perennial ryegrass cultivation and 27% heather natural growth.

The 100-year SOC changes associated with these three CV-land management, and with hemp cultivation (with and without harvest of the harvestable straw) was quantified with the AMG soil simulation model (detailed in Clivot et al., 2019), calibrated to estimate topsoil (<30 cm) SOC changes under French conditions. Inputs to AMG include meteorological data (mean yearly temperature, precipitation and evapotranspiration), soil characteristics (clay and rock percentage, C/N ratio, topsoil depth), agricultural management (tillage type and depth, amount of water supplied by irrigation), and carbon input from both biomass (above- and belowground) and eventual other sources (manure, compost, etc.). The model runs year by year, here from 2022 till 2122. For simplicity, the agricultural management parameters were considered not to vary through the 100 years studied. Similarly, the same starting point in terms of initial SOC stock (42.35 t ha^{-1}) and soil characteristics (supplement information II, table s1) were considered for all CV-lands. These figures represent weighted average for the four types of CV-lands and were derived from data extracted from the Harmonized World Soil Database (v1.2; FAO, 2021) (Nachtergaele et al., 2012). Because there is not such level of information for the C/N ratio, three C/N ratios were tested for the hemp scenarios (both with and without straw harvest), namely 11, 17, and 22, based on available French data (Clivot et al., 2019; Conen et al., 2008; Delmas et al., 2015). For the initial CV-land management, however, only a default C/N value of 17 was considered. All soil characteristics (except SOC) were considered to remain constant over the 100 years period. Future

yearly meteorological data averaged for the whole France were retrieved from SICLIMA(DRIAS CERFACS, IPSL, last updated May 2013), for the RCP4.5 climate trajectory (Representative Concentration Pathway(Chen et al., 2021)), downscaled by the model CNRM-CERFACS-CM5/CNRM-ALADIN63. These projections were not available beyond 2100. For the period from 2101 and 2122, average values from the last decade (i.e., from 2091 to 2100) were thus used.

The above- and belowground carbon inputs from hemp were calculated considering a harvest index of 0.9, a shoot/root ratio of 3.78 (Clivot et al., 2019) and a yield of 9.19 t ha^{-1} dry matter (DM). This value is the average of a compilation of yield data from hemp grown in France and neighboring countries, as further detailed in supplement information II, table s2. It should also be noted that AMG considers, for hemp straw, a technically harvestable rate of 100%. Yields of 8 and 2.2 t DM ha^{-1} $year^{-1}$ were considered for ryegrass and rapeseed, respectively, with shoot/root ratios of 1 and 3.26, and harvest indexes of 1 and 3.26, respectively (supplement information II, table s15). Unlike hemp, ryegrass and rapeseed, heather is not included within AMG, which was calibrated for cultivated plants. Therefore, SOC changes consisting of a 10% SOC increase in the topsoil after 100 years were considered (Pehme et al., 2017) to represent the system of "heather left as heather". This is to be seen as a conservative assumption for the system modelled herein, where hemp is to be cultivated instead of natural heather, for this specific case. As a result of this step, the 100-year SOC difference between hemp cultivation and each initial CV-land management could be calculated.

2.3 Assessing environmental consequences of selected CSAAP scenarios: static LCA

The environmental consequences of the CSAAP scenarios studied herein were assessed through LCA, a standardized (ISO 14040, 2006; ISO 14044; 2006) and leading environmental assessment methodology, recognized as a suitable tool to anticipate the consequences of long-term investment decisions (change-oriented study; Brandao et al., 2017; Sala et al., 2021; Weidema et al., 2013). The consequential assessment implies that multi-functionality is handled with system expansion, and marginal suppliers are considered (i.e. those reacting to a demand change). Moreover, full elasticity of supply was considered for product substitution (Weidema et al., 2013), involving 1:1 substitution ratios. This implies that short-term effects induced by price changes are not included.

The functional unit (FU) to which all input and output flows were related is the annual management of 1 ha of representative CV-land. The annualization technique was used for all processes involving releases happening over several years, i.e. these emissions were linearly distributed over the corresponding period to generate an annual emission. Because of this 1-year temporal scope, we refer to this assessment as "static LCA". Unless otherwise specified, inventory data were based upon a compilation of data retrieved from a comprehensive literature review; either averages or median of these compilations were used, as further detailed in the SI. The induced changes in SOC were retrieved from the AMG simulations (section 2.2). The amounts of all end-products generated in the three scenarios were linked to the FU through the yield of hemp, taken to 9.19 t DM ha^{-1} with 0.83 t DM seeds ha^{-1} and 8.37 t DM straw ha^{-1} (Ventura and Kiess, 2015), considering an annual fertilization rate of 107, 51, 90 kg N, P and K ha^{-1}, respectively (supplement information II, table s3). For all scenarios, hempseed meal is produced and used as a source of carbohydrate, protein and lipid, and accordingly prevents marginal proteins, carbohydrates and lipids to be produced. These were considered to be soybean meal, maize, and palm oil, respectively (Tonini et al., 2016).

Three scenarios of hemp use corresponding to different anthropogenic bio-based products are considered and assessed:

1) Scenario SL (straw left): only seeds are harvested, where 50 kg (fresh weight) of harvested seeds are used for being re-sown for the next rotation(Ventura and Kiess, 2015), and the remaining 925 kg seeds are used for extracting 296 kg hemp oil, avoiding the production of the same amount of palm oil. The seed meal after oil extraction is used for animal feed, thereby replacing marginal

feed ingredients. The corresponding substitution in terms of avoided soybean meal, maize and palm oil was calculated on the basis of the methodology presented in (Tonini et al., 2016). The hemp oil is assumed to be consumed in the year following its production, and all carbon in the oil was assumed, for tractability, to be emitted as CO_2 only. Straw is left to decay on the ground.

2) Scenario IB (insulation board): both seeds and straw are harvested. Harvested seeds go through the same pathway as the SL scenario. The harvested straw is then processed for fiber separation.. Besides fiber (circa 30% of straw DM), shives (65%) are obtained as a by-product with lower economic value, and the remaining 5% is lost as dust (Norton et al., 2009). Shives can be further mixed with lime blender and water to produce hemp concrete, which is considered in this scenario (in proportions of 17.9% shives, 32.9% lime and 49.3% water, , for 1 m^3 hemp concrete; supplement information II, table s9). Because of the lower strength of hemp concrete in comparison to traditional concrete, this product is assumed to replace gypsum board, based on their similar densities (Jiménez Rivero et al., 2016). During its use, hemp concrete absorbs CO_2 by a carbonation mechanism. Here, we considered 77 kg CO_2 absorbed per m^3 during the whole lifespan, based on (Pretot et al., 2014). The separated hemp fibers, on the other hand, are mixed with additives to ensure fire retardant and then undergo thermocompression, resulting in the production of the insulation boards; these processes were modeled based on data from (Andersson and Björhagen, 2018; Stapulionienė et al., 2016)(supplement information II, table s10). The thermal conductivity properties considered for the produced boards are detailed in the supplement information II, section 2.8. Moreover, a lifetime of 40 years was considered for the boards produced (Andersson and Björhagen, 2018). The produced hemp insulation boards aims to avoid the production of conventional insulation material like mineral wool (Uihlein et al., 2008). At the end-of-life, the boards are considered to be landfilled in installations without CH_4 recovery (Norton, 2008). This is a conservative assumption. We considered that all biogenic carbon will eventually degrade, with 19.98% degrading in the first 100 years (of which 87% as CO_2 and 13% as CH_4) according to (IPCC, 2019). On this basis, we considered, for the static LCA, that 2.6 % of the biogenic carbon contained in the board ends up emitted as CH_4, and the rest as CO_2.

3) Scenario CP (car panel): both seeds and straw are harvested and processed as in the IB scenario. The separated hemp fibers are used to produce lightweight structure car panel, as the main product of this scenario, with a lifetime of 12 years (La Rosa et al., 2013; Wötzel et al., 1999). During the use stage, the new lighter material allows for lower fuel consumption in vehicles in comparison to the conventional glass fiber panels (Deng, 2014). Here a consumption of 2.35 L gasoline per kg car panel over the panel lifetime was considered (supplement information II, section 2.11). It was considered that 30% of hemp car panels will be incinerated with power recovery at the end-of-life, while 70% will be landfilled (no CH_4 recovery), based on (Gueudet, 2016). Landfilling emissions are calculated as in scenario IB.

The conventional CV-land management was modelled distinctively for the three types of land cover chosen. For ryegrass, it was considered that it would have been used as cattle silage. This implies that the nutritional service no longer supplied has to be provided from elsewhere, thereby inducing an additional demand for animal feed ingredients. This was modelled with the method of (Tonini et al., 2016), as for hempseed meal. For rapeseed, it was considered that it would have been used to produce rapeseed oil and meal. Here, palm oil is considered to be the marginal vegetable oil reacting to the rapeseed oil no longer supplied (Schmidt and Weidema, 2008) and this was modelled by the use of the consequential Ecoinvent database (supplement information II, table s17; market for palm oil dataset, which already embeds interactions with the meal). The changed management from both rapeseed and ryegrass to hemp thus involves land use changes, and the emission flows related to these were modelled according to the method described in (Tonini et al., 2016, supplement information II, table s20). The heather from natural grasslands and woody moorlands are, on the other hand, considered to be left unharvested and simply decay on-site (supplement information II, table s18-s19).

The system boundaries considered for the three scenarios are summarized in (Fig. IV-1) while the corresponding inventory tables are available in the SI (SI 2.2- 2.14). Background data (e.g., electricity, fertilizer production, machines used in manufacture) were extracted mainly from the Ecoinvent v3.5 consequential life cycle inventory database. Foreground data were estimated based on published literature and simulations, as described above.

On the basis of a recent European Commission Recommendation (EC, 2021), the Environmental Footprint (EF) v2.0 life cycle impact assessment method (Fazio et al., 2018) was used to evaluate the environmental impacts of the scenarios, which assesses 16 impact categories (supplement information II, table s22). The LCA was facilitated with the SimaPro software, version 9.1.1.

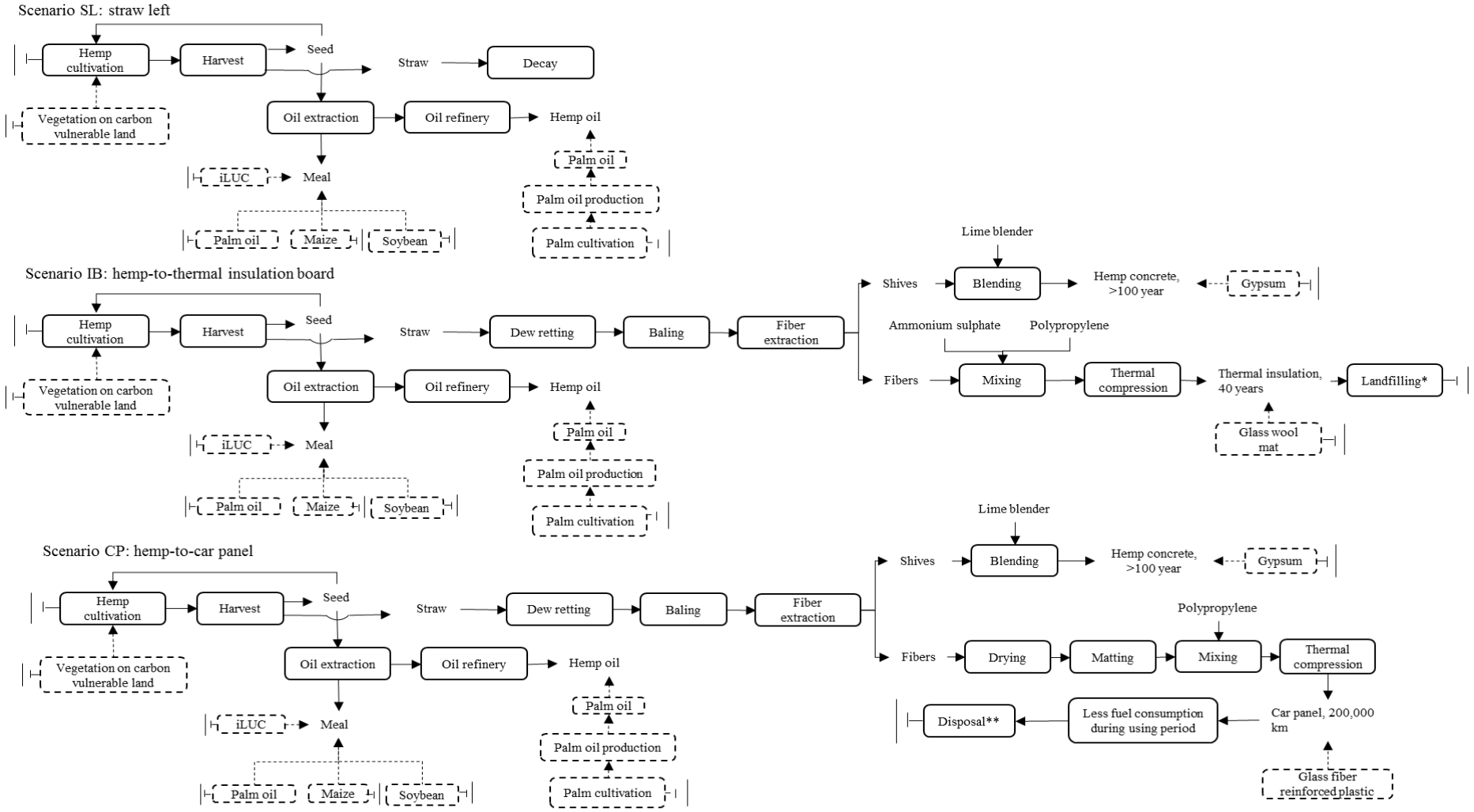

Fig. IV-1 Process flow diagram and system boundary considered for the three scenarios assessed. Box indicates processes. Solid lines: induced processes, dotted lines: avoided processes. *Landfilling without CH_4 recovery, **30% of car panel is disposed as incineration with power recovery, the rest is disposed as landfilling without CH_4 recovery.

2.4 Dynamic inventory for GHG flows and assessing related temperature changes

The analyzed systems are characterized, among others, by distinct temporalities of the processes it involve, which has significant effects on the climate change impact. In dynamic LCA, the extent of global warming is described in a metric called global mean temperature change (GMTC), based on the impulse response function approach recommended by IPCC (Thomas F. Stocker et al., 2013). This indicator is calculated in function of time and depends on the GHG nature and emission dynamics. Herein, GMTC is calculated with the CCI-tool (Tiruta-Barna, 2021; Shimako et al., 2016) available online (Tiruta-Barna, 2021).

The time scale of the functional unit (i.e. 1 ha of land) is set at 100 years of continuous hemp cultivation, starting in 2022. The time scale of the inventory is much larger because of the products' lifetimes (e.g., 40 years for thermal insulation) and because of the duration of end-of-life processes (e.g., emissions from sanitary landfilling). Notably, for bio-based products, natural degradation can take several decades (IPCC, 2019). For the temporal inventory and for GMTC calculation, a time step of 1 year is adopted, considered as sufficient.

Since hemp is an annual crop, cultivation (including plant' carbon uptake and agricultural processes) and harvesting happen in the same year. The SOC change simulated in section 2.2 was merged in the corresponding year annually, till the end of cultivation. The land use change might be changed again after the hemp cultivation, but as the functional unit is hemp cultivated on 1 ha CV-land, activities on CV-land after the 100-years hemp cultivation are out of the scope. Similarly, SOC changes after 100-years of hemp cultivation are not included. The manufacturing and above-ground residue decay is assumed to finish in the second year, thus the product's use stage begins in the third year (Fig. IV-2). The delay between consecutive manufacturing unit processes was assumed to be negligible. After the product's lifetime, disposal is considered. If products are incinerated, GHG are emitted to the atmosphere immediately. In case of landfilling, GHGs (mainly CH_4 and CO_2) are released gradually following the first-order decay kinetics (IPCC, 2019). For hemp concrete, landfilling is the most common practice, while there is no decomposition of the material at the end-of-life, which means no GHG emissions (Pretot et al., 2014). The timeline of the three scenarios is presented in Fig. IV-2. The temporal LCI was obtained from the consequential LCI by spreading the processes with their inventories on the timeline. The temporal LCI for each scenario was then used for time dependent GMTC calculation over a time horizon of 241 years, for all the GHGs existent in the Ecoinvent database (supplement information II, table s23).

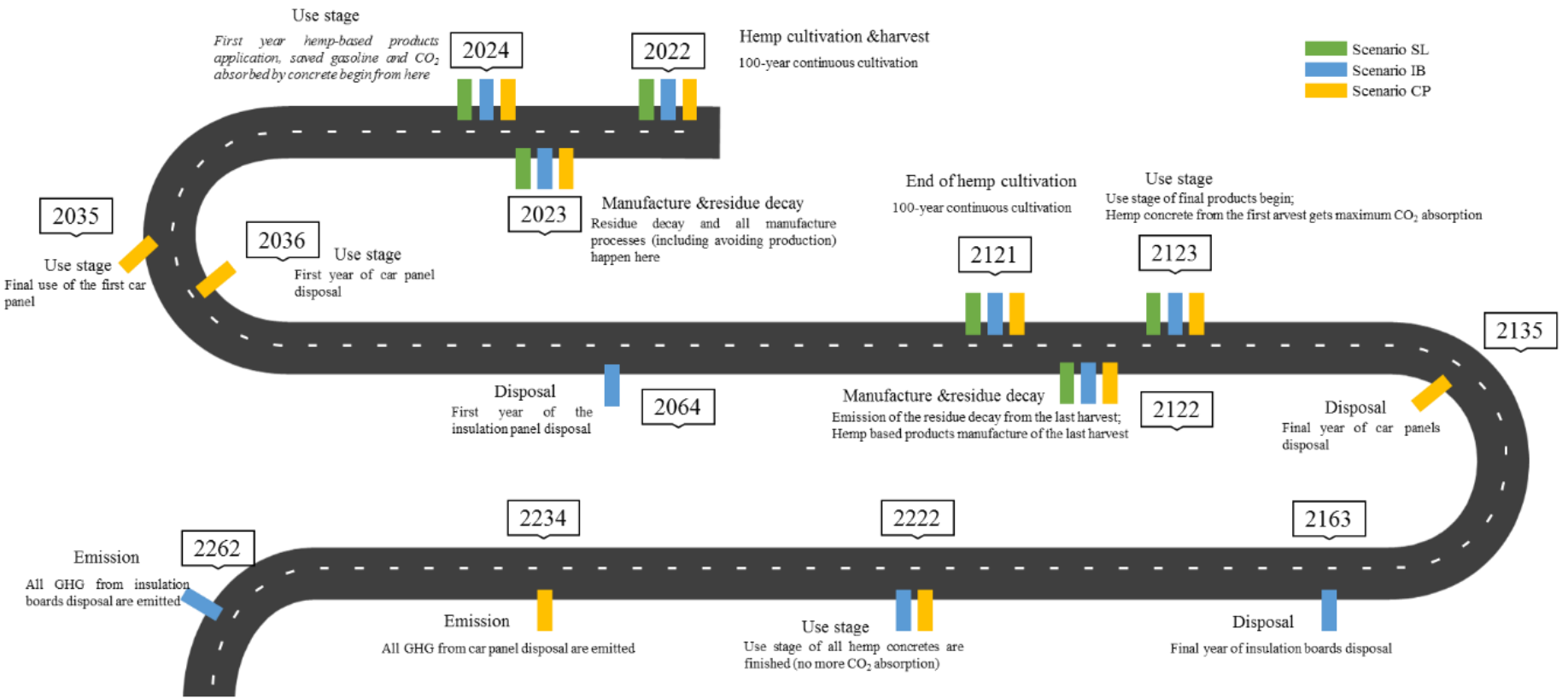

Fig. IV-2 Timeline considered in dynamic LCA for the three scenarios. For Scenario SL, “residues” refer to the whole straw, while for Scenarios IB and CP, it refers to the un-harvestable above-ground portion only.

2.5 Sensitivity and uncertainty analysis

Sensitivity analyses were performed to test the results sensitivity to two modeling hypotheses: (i) the use of fertilizers and (ii) the type of fuel being used for personal cars in the long-term. It could be argued that biopumps grown on CV lands (with the intention to increase SOC and mitigate overall environmental performance) belongs to a "low-input" type of agriculture. Here, this is considered with a zero fertilization sensitivity analysis. Fertilizers generate GHG not only from their production, but also during the use phase, e.g., extra N_2O emissions due to the extra available N through microbial nitrification and denitrification (Hergoualc'h et al., 2019). If fertilization is excluded in hemp cultivation, these GHG emissions could be avoided, however, the yield would be reduced as well, leading to less captured CO_2 and less amount of biomass for downstream manufacturing processes. The sensitivity analysis permits to investigate the relationship between fertilizers, yield, and environment. Here, a yield reduction of 60% compared to the default case (Aubin et al., 2015; Vera et al., 2010) was considered for this zero-fertilization sensitivity analysis.

The second sensitivity analysis is based on the French government announcement that thermal combustion engine cars will not be sold anymore after the year 2040, and will be replaced by cars using less GHG-intensive energy ("Climate Plan," 2017). Therefore, from year 2040, the saved gasoline consumption in the CP scenario is replaced by saved electricity consumption, in both static and dynamic LCAs.

The uncertainty analysis was conducted according to the Global sensitivity analysis (GSA) method proposed by Bisinella et al(Bisinella et al., 2016). GSA unifies the concepts of uncertainty and sensitivity (i.e. for small variations of parameters, 10%). In a first step, the parameters with high contribution on the environmental impacts were selected based on the contribution analysis results from the static LCA (supplement information II, fig. s4- s6). Then, a perturbation analysis was performed, in a one-at-the-time (OAT) fashion, considering how a variation of 10% of each of these parameters affects the normalized results (the approach is further described in supplement information II, section 5.1). A probability distribution (triangular, normal) was assigned to each parameters, which allowed using the analytical method proposed by Bisinella et al. (2016) to calculate the contribution each parameter has on the overall system uncertainty, impact per impact. The coefficient of variation was used to represent, for each impact, the overall system uncertainty.

3 Results and discussion

3.1 SOC simulation by AMG

Fig. IV-3a presents the 100-y SOC (<30 cm) simulated for hemp, with and without straw harvesting, and considering different C/N ratios of the soil. It can be contrasted with Fig. IV-3b, where the SOC evolution related to the conventional CV-land management is presented, both for individual and weighted average French CV-lands. As it can be observed in Fig. IV-3a, hemp does allow, in all but one case (straw harvest, C/N of 11) to increase long-term SOC stocks, in comparison to a given initial level of 42.35 Mg C ha^{-1}. These represent increases varying between 1.26 (straw left, C/N 11) and 53.68 Mg C ha^{-1} (straw left, C/N 22). If annualized, it corresponds to 0.0126 and 0.537 Mg C ha^{-1} $year^{-1}$, which corresponds to what was observed in previous studies (e.g., increases of 0.36 - 0.4 Mg ha^{-1} $year^{-1}$ reported in Li et al., 2012, where straw is left unharvested). Yet, a CSAAP strategy implies harvesting (and using) the hemp straw. Fig. IV-3a shows that when hemp is grown on CV-lands and fully harvested, a 100-y SOC increase of just 4.68 (straw harvest, C/N 17) – 11.56 Mg C ha^{-1} (straw harvest, C/N 22) is obtained. This is rather small, in comparison to the increase of 27.84 Mg C ha^{-1} (C/N 17) observed on average CV-land (Fig. IV-3b). In other words, when considering the SOC evolution that would have otherwise happened over the 100-y period, the hemp CSAAP strategy is rather uncompetitive on French CV-land, leading to a net SOC change of -27.68 Mg C ha^{-1} (i.e. no additional sequestration). This would be exacerbated with greater proportions of intensive grasslands and rapeseed lands in the CV-land mix.

This is, among others, explained by the important belowground carbon input of ryegrass, being three times higher than those of hemp (2.77 and 0.89 Mg ha^{-1} respectively, supplement information II, table s 2&s15), and by the very minor share (ca. 25%) of above-ground biomass harvested in the rapeseed system.

Whether hemp straw is harvested or not, the higher C/N ratio leads to higher SOC increases. This reflects that when C/N ratio increases, mineralization decreases (among others due to more immobilization by soil microbiota), leading to slower decomposition of soil organic matter (Clivot et al., 2019). This result is consistent with experimental measurements (Clivot et al., 2017). The C/N ratio is thus a sensitive parameter for which high data quality is important, with regards to assessing the sequestration performance of a CSAAP strategy.

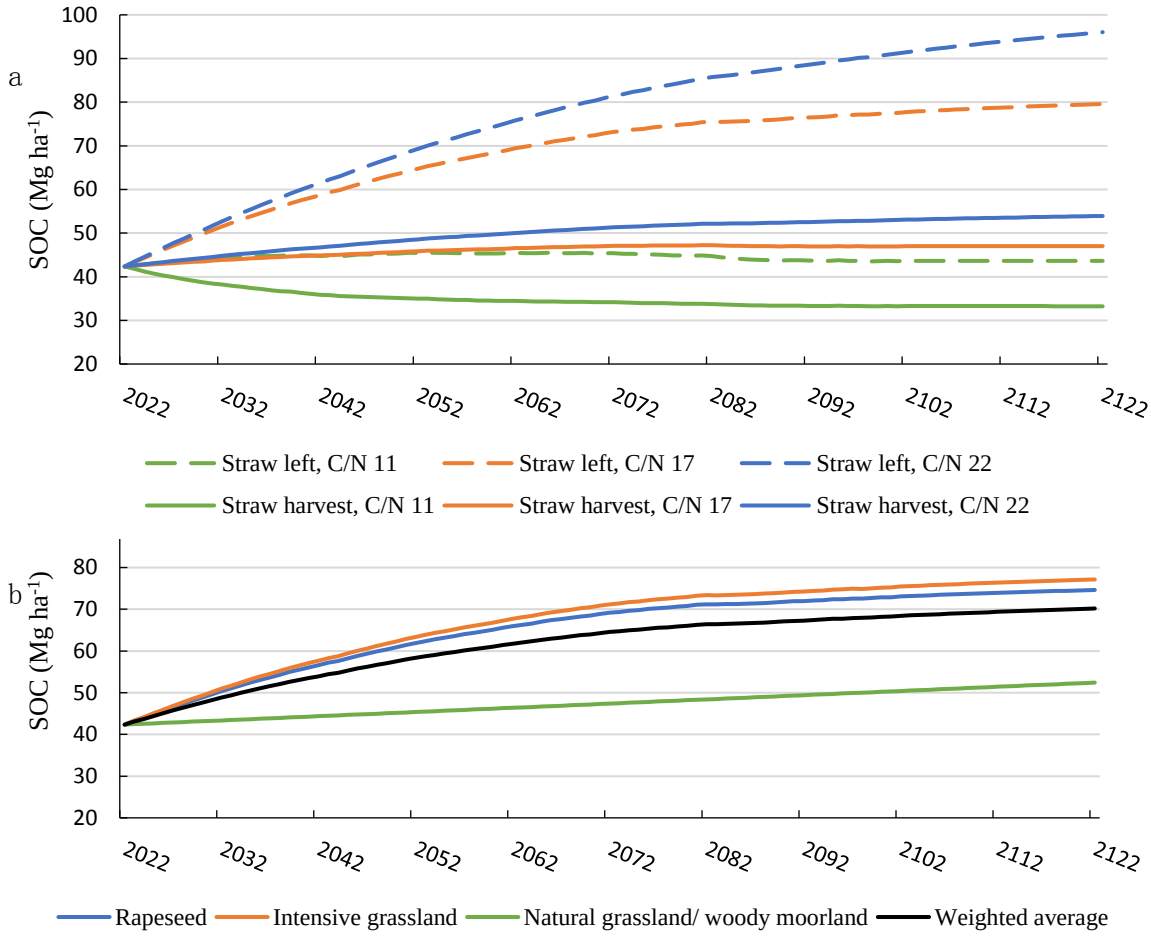

Fig. IV-3 100-year SOC stock evolution (a) under different C/N ratio for hemp cultivation on average CV-land, and (b) initial vegetation on CV-lands under C/N 17.

3.2 Environmental performance of the three hemp scenarios

The environmental performance of the three scenarios compared herein is presented in Fig. IV-4, with a breakdown per process, for four impact categories. The LCA results of all other impact categories are available in supplement information II, section 3.2), along with the contribution analysis. In Fig. IV-4, all processes above the abscissa represent contributions to the environmental impact studied, while those below abscissa (negative) are avoided impacts. The dots represent the net scenario performance. Fig. IV-4 illustrates that scenarios IB and CP allow, for all impacts presented in the figure, a net negative overall impact. This means that there are higher benefits to implement these scenarios as compared to leaving the system as it would have otherwise been (conventional CV-land management and production of petrochemical products). Fig. IV-4 also shows that this conclusion does not apply to the SL scenario

for the climate change (net 971.18 kg CO_2-eq ha^{-1}) and freshwater eutrophication impact (net 1.74 kg P-eq ha^{-1}).

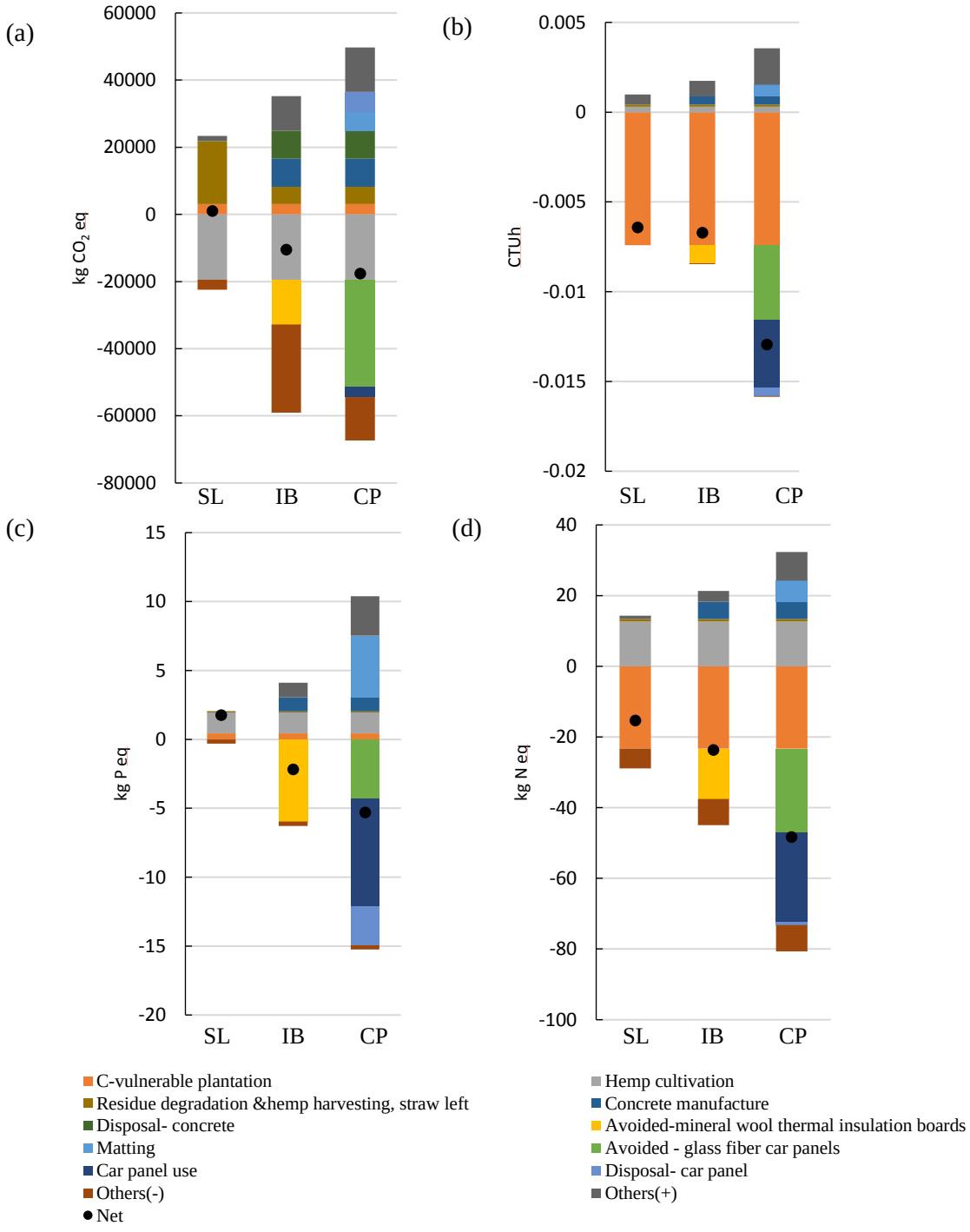

Fig. IV-4 Life cycle impact assessment results for (a) climate change, (b) non-cancer human health effects, (c) freshwater- and (d) marine eutrophication impacts, with a breakdown per process contribution For tractability reasons, only the most significant processes are depicted. For this reason, the breakdown categories "others (+)" and "others (-)" are introduced, aggregating all remaining positive and negative contributions, respectively.

In scenario SL, the 1 ha soil of CV-land could store carbon equal to 1.35 t CO_2 (Fig. IV-4), which is even higher than the net climate change result in this scenario. However, this SOC increase is at the expense of less carbon going into downstream processes, as well as higher CO_2 and N_2O emissions during residue decomposition (18.1 t CO_2 and 1.49 kg N_2O in scenario SL, and 4.81 t CO_2 and 0.46 kg N_2O in scenario IB&CP). In scenario IB&CP, because straw is harvested, there is more straw-C ending up in the technosphere than in the soil, therefore the benefit from SOC enhancement (-170 kg CO_2-eq) is not as important as in scenario SL.

Fig. IV-4 highlights the importance of the avoided petrochemical countered products in the IB (mineral wool insulation boards; in yellow) and CP (glass fiber car panels; light green) scenarios, for all impact categories. The avoided wool-based boards is beneficial to climate change, non-cancer human health, freshwater- and marine eutrophication (-13.32 t CO_2-eq, -0.001 CTUh, -5.97 kg P-eq, -14.17 kg N-eq respectively, per FU, which represents 29.12%, 11.84%, 94.9%, and 31.55% of the negative scores). The avoided car panels is also beneficial to the same impacts (-31.96 t CO_2-eq, -0.004 CTUh, -5.97 kg P-eq, -23.72 kg-N eq respectively, per FU, which represent 47.75%, 26.25%, 28.16%, 29.4% from the negative scores). The high contribution of the avoided products means that the manufacturing of hemp-based materials performs better than the conventional materials from the environmental point of view, which is in agreement with previous studies (Ardente et al., 2008; Kim et al., 2008; Norton, 2008; Tadele et al., 2020; Zampori et al., 2013). Of course, these benefits exist as long as the substitution of petrochemical counterparts is possible, which seems to be the case for the upcoming 10 years (Grand view research, 2021, 2019). Considering that the time scope of this study is 2022- 2262, it is hard to predict the development for the replaced products in such a long-term future, while it could be expected that with the development of new technologies, the emissions from producing insulation boards and car panels, whether based on new or conventional materials, could be significantly reduced (Jiménez Rivero et al., 2016; Schwarz et al., 2021).

Compared to avoided wool-based boards, the negative score in climate change of the avoided car panel is primarily due to the extraction and manufacture of materials (explaining 75% of the negative impact), rather than the direct use of energy (25% of the impact). Moreover, the fiber content in the car panel is half of that in insulation board (40% vs 88%), therefore more additive (polypropylene here) is required and results in higher climate change impact: 605 in scenario IB vs 6,752 kg CO_2-eq per FU in scenario CP. The lower fiber content and increased polypropylene demand also lead to more car panels produced than insulation boards, from 1 ha land, namely 5.33 t and 2.88 t respectively (supplement information II, table s10& s12). More products require more energy consumption in processing. Thus, though thermoforming is adopted in both insulation boards and car panels manufacturing, the emission from car panels production is triple that from insulation production (3,638 vs 1,092 kg CO_2-eq). Furthermore, fibers need to be spun into mats before mixing with polypropylene, which also emits 5,788 kg CO_2-eq per FU due to the energy consumption, and it is especially important in freshwater- and marine eutrophication due to the PO_4^{3-} and NO_x emissions from fossil fuel (e.g., coal and lignite) respectively (supplement information II, fig. s6).

Fig. IV-4 also illustrates, for the CP scenario, that the reduction of weight induced by the use of hemp fiber, which implies a decrease in gasoline use, translates into environmental benefits (in dark blue): 4.41, 23.71, 55.55, and 31.4% of negative scores, for climate change, non-cancer human health, freshwater- and marine eutrophication impacts, respectively. The energy consumption in the matting process is responsible for positive impacts in these four impacts. At the end-of-life, since one third of car panels are incinerated, the generated heat substituting marginal heat allows for benefits in all four impacts, and especially accounts for 18.19% of negative scores in freshwater eutrophication.

The use of lime binder for hemp concrete is responsible for a high amount of GHG (7,637 kg CO_2-eq per FU) due to the limestone decomposition and fuel use for binder production (e.g., coal and heavy fuel oil) (supplement information II, fig. s5). During the hemp concrete use phase, CO_2 is fixed by lime

permanently through carbonation, therefore hemp concrete could be considered as a real carbon sink. However, the emitted CO_2 in the production stage is not 100% compensated in the use stage, depending on the environmental conditions (Andersson et al., 2013). In IB and CP, CO_2 bound in the use stage is half of the GHG emission from binder production (-4,667 kg CO_2-eq per FU). Here, we considered a 100% return of the hemp concrete carbon at the end-of-life, hence its overall net positive score (6,598 kg CO_2-eq per FU, from manufacture till concrete disposal). Today, the most common disposal practice for concrete is landfilling (Pretot et al., 2014). Here, a slow biomass decay was assumed; if no decomposition is considered, hemp concrete could have a net negative score (Ip and Miller, 2012; Sinka et al., 2018), contributing to climate mitigation in the future (Lecompte et al., 2017).

Avoiding initial CV-land management brings positive emissions in climate change and freshwater eutrophication mainly from indirect sources like land use changes and extra crops needed to compensate for the reduction of ryegrass feed. On the other hand, transforming initial vegetation to hemp cultivation could avoid zinc accumulated in the soil due to the ryegrass silage, which explains the net negative results of non-cancer human health, for the three scenarios. Concerning marine eutrophication, maize and soybean cultivated for compensating the reduction of ryegrass feed need less nitrogen fertilizers than ryegrass; therefore avoiding ryegrass cultivation is shown to reduce emissions from nitrogen fertilizers in all three scenarios (Fig. IV-4 d).

3.3. Dynamic LCA

Fig. IV-5 shows the GMTC calculated for 250 years for the three scenarios, as a result from non-biogenic GHG emissions, biogenic GHG, and total result. Biogenic GHG are those of the foreground system and include CO_2 captured by plants, emitted CO_2 from the biomass during all the period considered (in manufacturing, decomposition, end-of-life), as well as CH_4 and N_2O emissions related to biomass (e.g., CH_4 during landfilling). All other GHG flows including replaced or induced production were attributed to non-biogenic sources (e.g., C from induced biomass used as feed to compensate for the loss of silage ryegrass). Negative values indicate a mitigation effect (temperature decrease).

Both scenarios IB and CP show a net negative trend, GMTCs from both biogenic and non-biogenic GHG decrease continuously during hemp cultivation and become almost flat for the next 150 years. The negative GMTC of non-biogenic flows is mainly due to the avoided productions, i.e. glass wool insulation boards and glass car panels, which is consistent with the static LCA results. At short-term, GMTC of non-biogenic CO_2 flow is positive in scenario CP, due to emissions from induced productions that correspond to intensive grasslands and rapeseed lands. Then, it decreases gradually with the hemp value chain implementation and perpetuation, becomes negative in the year 2038, and reaches the lowest value after the end-of-life of the final hemp car panel, owing to the avoided glass car panel and saved gasoline. GMTC of CH_4 reaches the lowest value in the year 2124, then increases because the CH_4 emission from the counter-flow ends at this time due to the end of cultivation; CH_4 from panel disposal (both incineration and landfilling) is continually released. The situation of captured CO_2 from avoided gasoline is opposite because part of avoided gasoline is made by bioethanol, thus the CO_2 absorbed by the bioethanol-related biomass is avoided, showing a negative CO_2 flow and resulting in a temperature rising. The captured CO_2 is one of the main contributors of the negative non-biogenic GMTC because of the important contribution of the induced biomass cultivation for forage production. Due to the long timespan of CO_2 in the atmosphere, after the final car panel is disposed of, the GMTC caused by the absorbed CO_2 remains negative. The main contributor to the non-biogenic negative GMTC is the carbonation of concrete in its use stage. In both scenarios IB and CP, non-biogenic CO_2 is the most critical GHG for climate mitigation, the negative GMTC decreases rapidly in the year hemp is growing, then slows down after all hemp is converted into insulation boards or car panels because it mainly benefits from avoided productions. In case of biogenic flows, CO_2 and CH_4 emissions lead to the GMTC increase, which mainly comes from above-ground residue decomposition and landfilling of products, respectively. The CO_2 captured during cultivation reduces GMTC drastically, leading to a decreasing trend of total biogenic flow. Noticeably, in biogenic flows, the quantity of CO_2 captured by hemp and

CO_2 emitted is not exactly matched, because of the actual disposal considered here (15.88% decomposition rate in landfilling in 100 years) (IPCC, 2019). For example, in scenario IB, for the hemp cultivated in the year 2022, 83.7% of carbon in harvested straw is stocked in the technosphere in the year 2024 as hemp concrete and insulation boards. Insulation boards would be landfilled in the year 2064 after 40 years of use, while there is no decomposition of hemp concrete. In the year 2163, the emission from landfilling is assumed to be over, and 78.4% of carbon from the initially harvested straw is stocked in the technosphere in IB scenario. Similarly, 70.8% of carbon from harvested straw is stored in the technosphere in scenario CP, and the small difference in negative emissions between IB and CP explain why the longer carbon delay effect of insulation boards (because of the longer lifespan) is not significant. Three major carbon pools exist in scenarios IB and CP, i.e. hemp insulation, car panel from fibers, and concrete from shives, while there is no such anthropogenic carbon pool in scenario SL. The negative values of both non-biogenic and biogenic lead to total negative GMTC in scenarios IB and CP, while the year with the lowest GMTC is slightly different due to the continuously avoided gasoline in CP and the difference between the products lifespans (hemp insulation versus car panel). According to the consequential LCA results, the avoided GHG emission is higher in avoided glass car panels (plus saved gasoline) than that in glass wool thermal insulation. Indeed, with the lower GMTC of non-biogenic flows (but similar for biogenic flows), scenario CP could mitigate global warming better than IB. If the results are extrapolated from 1 ha to the total area of CV-lands in France (i.e. 2,400,000 ha; (Shen et al., 2022)) cultivating hemp instead of initial vegetation in scenarios IB and CP leads to a potential decrease of global mean temperature with respect to the business as usual situation, in 2100, by 0.0022 and 0.0028 ℃ respectively. At the end of the system, around year 2262, the global mean temperature decrease is still of 0.0028 and 0.0035 ℃ for IB and CP, respectively.

In case of scenario SL (Fig. IV-5), the non-biogenic flows raise the temperature in the first 100 years, due to the agricultural management and hemp oil extraction, similarly to IB and CP, but here the avoided products, i.e. palm oil and meal, cannot compensate this rising. Another important source of non-biogenic flows is the induced products, the positive GTMC indicates that it is not wise to produce hemp oil rather than ryegrass feed and rapeseed oil in the future. When straw is left, carbon is released in short term after harvesting, and the lack of an anthropogenic carbon pool (in contrast with IB and CP) deprives this scenario of mitigation capacity. However, the GTMC due to the biogenic flows is still slightly negative, indicating that hemp has a better carbon capture capacity than initial vegetation, and the enhanced SOC stock also contributes to that. Because of SOC saturation, the SOC increases are modest with time (Fig. IV-3), affecting the biogenic flow which becomes stable before the end of the cultivation period. Scenario SL could not reach negative GMTC in the time boundary, and, when all French CV-lands are considered, this scenario would increase the temperature by 0.000168 ℃ in 2262.

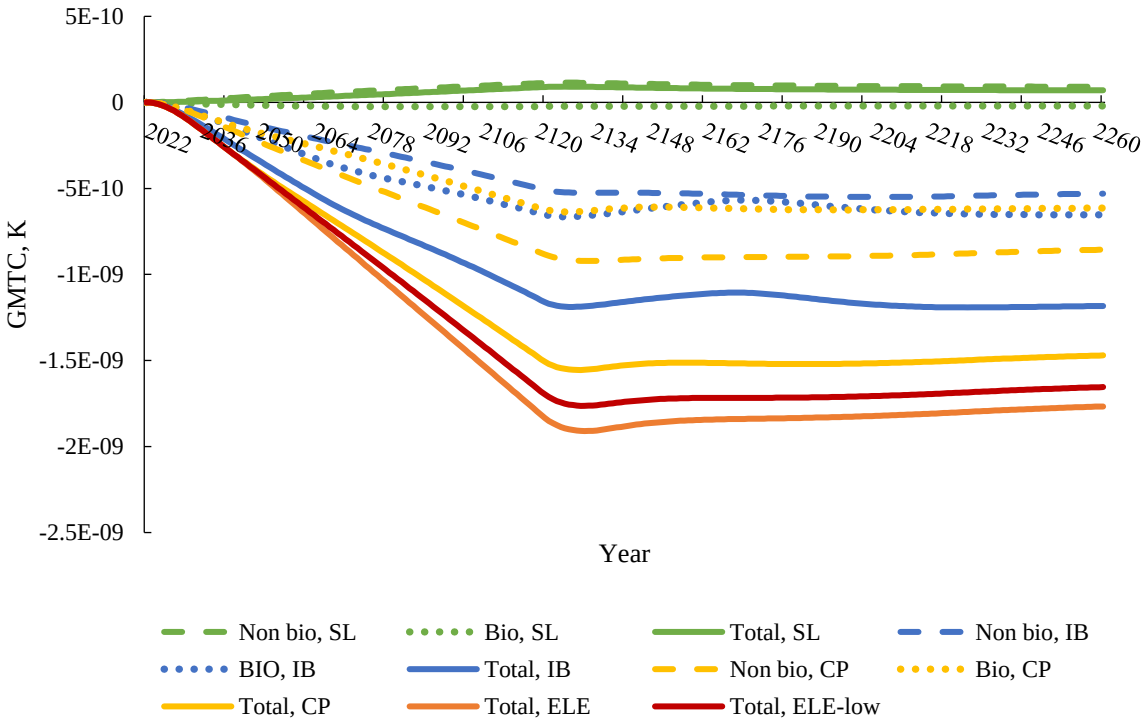

Fig. IV-5 Dynamic global mean temperature change in biogenic (bio) and non-biogenic (non-bio) flows for scenario SL, scenario IB and scenario CP, and the sensitivity CP sub-scenario where electric mobility is considered from 2040 case ELE with 42% photovoltaic in the electricity mix and case ELE-low with 12% (described in section 3.4.2).

3.4 Sensitivity analysis

3.4.1 Consequential LCA

Not using (nitrogen) fertilizers implies that all fertilization-related emissions do not occur: mainly N_2O, NO_x, NH_3 to air, nitrate and phosphate losses to water, emissions from fertilizer production having important contribution in most categories (according to the contribution analysis in supplement information II, fig. s4-6). The lack of fertilizers leads to lower yield, thus the energy and material consumption in manufacturing will decrease. However, the reduced yield will reduce the amount of bio-based products and petrochemical products replaced, shown as an important determinant of the environmental performance for most impact categories (Fig. IV-4). From Fig. IV-6a, the impact mineral and metal resources use (MU) is, for all scenarios, the one most affected by a change from conventional fertilization to zero-fertilizer. This is caused by sliver ore (Silver, Ag 1.5E-5%, Au 5.4E-4%) used in fertilizer lifecycle (all scenarios), titanium and strontium, due to the resulting lower share of avoided gypsum (IB&CP scenarios) and glass fiber consumption (CP), respectively. Due to its lower magnitude for most impact scores (case with fertilizers), the SL scenario is more sensitive to fertilizers than the two others. Fig. IV-6a shows that no fertilizers benefit, for this scenario, all impacts except ecotocixity freshwater and land use. For IB, no-fertilization benefits five (out of 16 impacts), and for CP, it benefits only two impacts. Scenario SL benefits from the lower emission of less fertilization, however in scenario IB&CP, this benefit cannot compensate for the reduction of advantages brought by the yield and the petrochemical products it substitutes. Therefore, no-fertilization could be a compelling alternative for straw left on the surface, but if the straw is intended to be used in the technosphere, the yield benefit tends to compensate for the trade-offs of the fertilizers.

a

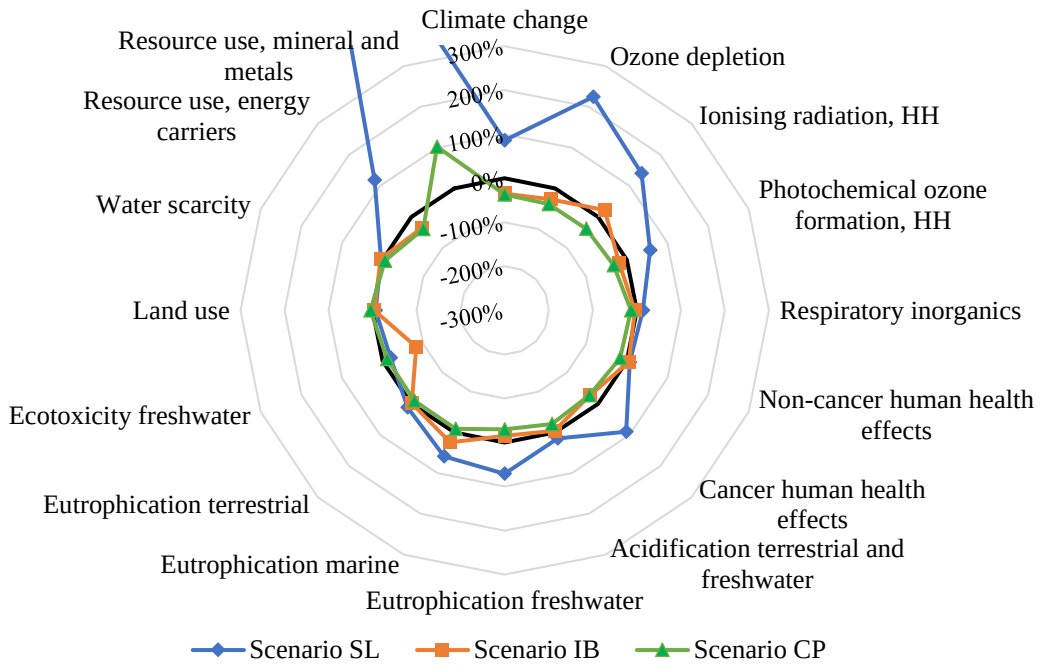

b

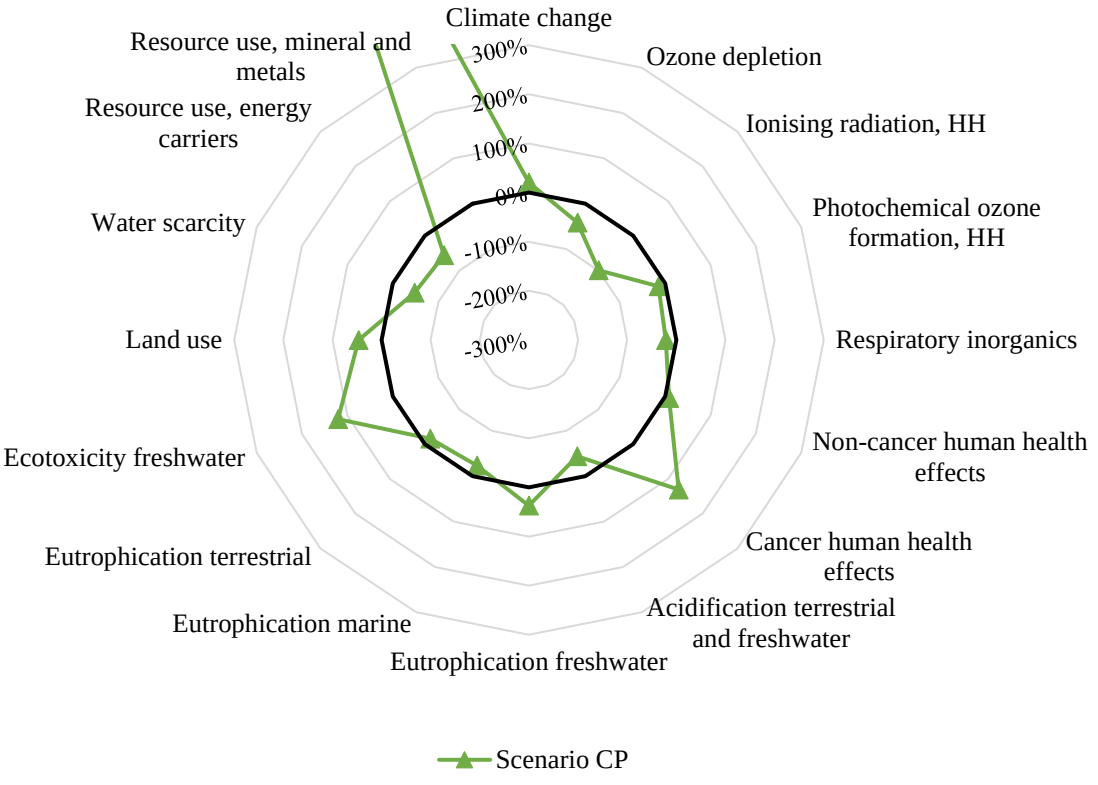

Fig. IV-6 Sensitivity analysis portraying the relative changes observed, for all impact categories, from the baseline scenarios due to (a) no fertilizer use; and (b) electric car after 2040 (CP scenario only). The black line represents the initial baseline scenarios (i.e., no change). The positive value represents an improvement (%) of the net impact compared to the reference (bold line), and, *vice versa*.

Similarly to the no-fertilization sensitivity analysis, MU and cancer are two of the most sensitive impacts to the replacement of thermic cars by electric cars because of the metal used in photovoltaic panel production for photovoltaic electricity. For most impacts but these two, along with climate change, freshwater eutrophication, freshwater ecotoxicity and land use, the sensitivity analysis indicates, as it could be expected, an overall reduction of the benefits as electricity is replaced instead of gasoline. For climate change, this shift leads, however, to a slight improvement of the impact.. This is in part due to the high GHG emissions occurring from photovoltaic panel production, and in part because the gasoline contains a share of bioethanol (based on the LCI dataset used). According to this situation, the performance of electric vehicles for global warming impact needs to be further investigated, not only at the light of revised inventories for photovoltaic electricity but also at the light of eventual different electricity mixes in the specific case of France (e.g., a mix of only wind- and hydropower after 2060; Kassara et al., 2019). Moreover, it should be noted that this sensitivity analysis was performed on the basis of a simple substitution of a certain amount of energy from gasoline to energy from electricity, without considering the differences in terms of performance between a thermic and electric car. This would likely render the analysis a little more in favor of avoiding 100% gasoline.

3.4.2 Dynamic LCA

Since electricity is predicted to determine the car market in the future, the influence of consuming electricity instead of gasoline is analyzed dynamically here. The generic trends are similar between scenarios with gasoline cars only and the scenario with electric cars after 2040 (Fig. IV-5, Total, ELE), but the GMTC is even more negative for ELE, indicating, as observed with the static LCA, that avoiding electricity is more beneficial than avoiding gasoline. Indeed, as discussed in section 3.4.1, this is due to the consequential modeling of the gasoline market and electricity mix in France in the future. Thus an electricity mix with a lower photovoltaic electricity proportion (11.92%;absolute value for 2050 based on European Commission, 2016; versus 42% in the baseline), was taken as an additional sensitivity to be analyzed (Fig. IV-5, Total, ELE-low). This scenario still has a more negative GMTC than gasoline due to the electricity derived from natural gas this time. The way electricity is produced is pivotal in scenario CP. These results show a promising performance of scenario CP for climate mitigation in the future. However, it is difficult to foresee the effect of replacing the energy source for cars in this timespan.

3.5. Uncertainty analysis

According to the contribution analysis shown in Fig. IV-4, 11, 12, and 14 parameters are selected for GSA, for scenario SL, IB, and CP, respectively (supplement information II, table s28- s30), The uncertainty in scenarios SL&IB concentrates on five parameters (not the same ones), and that in scenario CP on three parameters. These parameters together explain at least 90% of the system uncertainty for a given scenario. The hemp yield is the only parameter that is important in all three scenarios and impacts analyzed (Fig. IV-7). Further, parameters related to initial vegetation highly affect the SL scenario, including P2, P3, and P4. Consistent with the discussion that replacing petrochemical products plays a key role in the environmental performance of scenarios IB and SL, it is also crucial in the uncertainty (P12 and P14, in scenarios IB and CP, respectively). Within manufacture processes (Fig. IV-1b) of the scenario CP, the matting is more significant than mixing in the contribution analysis, while mixing represents more uncertainty than matting, for all impact categories represented in Fig. IV-7 (P14, the polypropylene amount used in the mixing process).

For climate change, freshwater- and marine eutrophication, the results show that scenario CP is unequivocally better than IB, and IB is better than SL (Fig. IV-7). For non-cancer human health impact, the results obtained do not allow differentiating between SL and IB. Similarly, it is hard to conclude on whether there are differences between scenarios for cancer human health impacts, ecotoxicity freshwater, water scarcity, mineral and metals resource use (supplement information II, fig. s7).

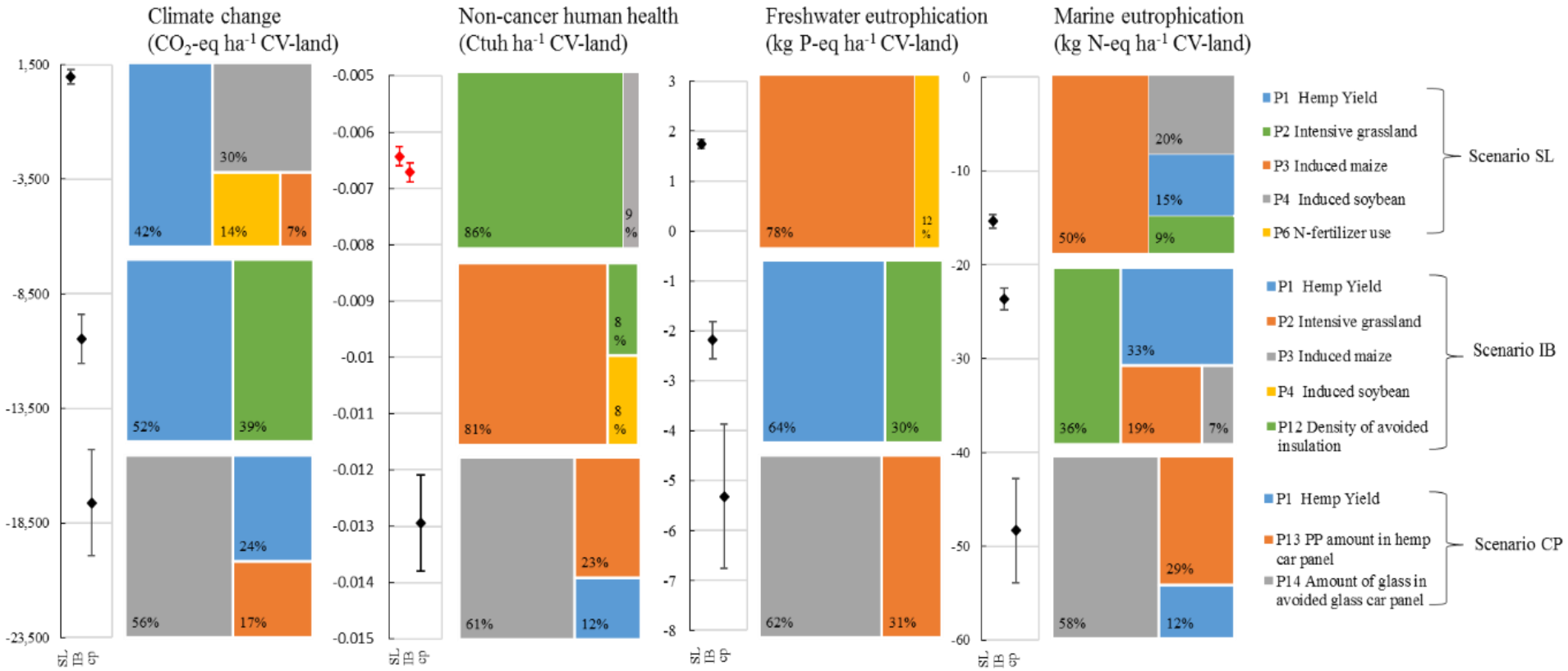

Fig. IV-7 Uncertainty analysis of climate change, non-cancer human health, freshwater- and marine eutrophication impacts. The overall system uncertainty is presented on the left hand side, while the contribution of all identified sensitive parameters to this system uncertainty is represented on the right hand side. Red indicates overlap with impossibility to conclude.

3.6. Overall implications, limitations and perspectives

According to the results of the consequential static LCA for climate change, the mitigation effectiveness of hemp product scenarios by replacing conventional materials is more important than the effect of negative emissions (carbon stored in anthropogenic products, as no additional C is stored as SOC in these scenarios). The increased SOC storage (negative emission) in scenario SL cannot compensate for the lack of mitigation (the climate benefit from SOC increase in scenario SL is equivalent to 10% and 4% of the climate benefit of avoided wool-insulation and avoided glass fiber car panel, respectively.). The carbon in hemp-based products was assumed to be totally emitted in consequential static LCA, thus the benefit of storing carbon in the technosphere is not reflected. In contrast, dynamic LCA allows identifying the time periods when carbon storage is effective and gives a temporal dimension to the negative emissions: negative emissions due to soil storage occur for the whole cultivation period (100 years) while negative emissions due to carbon storage in anthropogenic products last for a longer period, i.e. the cultivation period plus the lifetime of the products. Shares of 78.4% and 70.8% of carbon from the harvested hemp straw were showed to be stocked in IB and CP scenarios, respectively. Together with net SOC changes, this contributes to a temperature decrease (GMTC) 0.00157 and 0.00147 ℃ respectively, in 2262 (reductions due to the biogenic flows only, if all French CV-lands are cultivated with hemp). In the case of the IB scenario, the level of GMTC for biogenic flows (i.e. SOC and technosphere sinks) is similar to that caused by non-biogenic sources (determined by products replacement). The CP scenario shows a similar trend with a more important contribution to total GMTC of non-biogenic flows (60% versus 40% for biogenic flows). This result indicates that both the negative emissions and the GHG reductions from mitigation are important in controlling climate change, and their effects remain important for a long time afterward. Finally, both static and dynamic LCA result in the same scenario ranking for the climate change impact (CP better than IB better than SL)

As aforementioned and discussed, using hemp as CSAAP may not benefit climate change and other environmental impacts in scenario SL. One possible reason is the consideration of intensive grasslands among the CV-lands, as these could store higher amount of carbon in soils, and the replacement would induce additional forage production and land use changes which emit large quantities of GHG. Therefore, the type (land cover) of selected CV-lands could be reconsidered (i.e. lower share of intensive grasslands being mobilized). Yet, this did not impact the actual CSAAP scenarios (IB and CP).

The replacement of petrochemical products by hemp-based products contributes heavily to the overall environmental performance in both static and dynamic LCA. Yet, one may challenge to which extent these products are actually demanded, also in the light of higher penetration of advanced recycling technologies in the future, or re-use practices. For instance, using all CV-lands in France, 5,114,840 t hemp fibers could be produced in a year. Yet, only 80,000 t natural fibers (including wood and other plants) are actually used in the European car industry per year (Euorpean Commission, 2018). Similarly, the production of insulation boards from the total CV-lands in France could attain 230,102,600 m^3 $year^{-1}$, which represents as high as 85% of the European demand (269,300,000 m^3 in 2019; Pavel and Blagoeva, 2018), and 21% of the world demand foreseen for 2028 (1,098,600,000 m^3 $year^{-1}$,(Fortune Business Insights, 2022; Pavel and Blagoeva, 2018)).

This study focused on annual plants, but the performances associated with perennial species, because of their ability to stock carbon in the soil (Dobbratz et al., 2021), may be more interesting and should be investigated in future studies.

Conclusion

This study investigated various CSAAP strategies based on hemp cultivated on CV-lands in France. Three utilization scenarios were investigated, differentiated by the products lifetime in the technosphere, namely no carbon storage (SL), storage in two products one being considered as an infinite sink in the technosphere (hemp-cement) and the other with shorter lifetime (car panel in CP with 10 years, thermal

insulation in IB with 40 years). CV-land use change by cultivating hemp (replacing the current land cover type) with no utilization in long-lived products (SL) cannot mitigate climate change despite the negative emissions induced in the soil. In contrast, biomass utilization in long-lived products (CP and IB) acts as additional negative emissions by the technosphere, complemented by GHG mitigation through the displacement of conventional fossil-based products. Yet, no additional sequestration in the SOC pool could be obtained for these. The tendency is not the same for other impact categories, for example, water scarcity is increased in all scenarios indicating that at the light of this impact, it is better to keep CV-lands with initial vegetation rather than cultivating hemp.

This study considered that all C captured through photosynthesis is emitted at the end of life, thus the negative emission from storage in anthropogenic products is revealed by the delay of this release. While this could be captured in the dynamic calculation, it could not be reflected with the static LCA. In the long-term, the technosphere was shown to be a larger C sink than the soil for negative emissions. Climate mitigation was shown as slightly more important than negative emissions in the product scenarios, while the opposite conclusion is reached in scenario SL. If hemp is cultivated consecutively, till 2100, it could contribute to a temperature reduction of 0.0022 and 0.0028 ℃ in scenario IB and CP respectively, proved the feasibility of using hemp as CSAAP.

Supplement information

Supplement information III contains the inputs of all models, including AMG, LCA inventory, contribution analysis of LCA results, GHG in dynamic LCA, and uncertainty analysis.

Reference

Akampumuza, O., Wambua, P.M., Ahmed, A., Li, W., Qin, X.H., 2017. Review of the applications of biocomposites in the automotive industry. Polym. Compos. 38, 2553–2569. https://doi.org/10.1002/pc.23847

Andersson, K., Björhagen, I., 2018. Material Choices for a Fossil-Free Preschool - An Interview Study on How Materials are Chosen, and a Life Cycle Assessment of Hemp Insulation. CHALMERS UNIVERSITY OF TECHNOLOGY.

Andersson, R., Fridh, K., Stripple, H., Häglund, M., 2013. Calculating CO2 uptake for existing concrete structures during and after service life. Environ. Sci. Technol. 47, 11625–11633. https://doi.org/10.1021/es401775w

Ardente, F., Beccali, M., Cellura, M., Mistretta, M., 2008. Building energy performance: A LCA case study of kenaf-fibres insulation board. Energy Build. 40, 1–10. https://doi.org/10.1016/j.enbuild.2006.12.009

Aubin, M., Seguin, P., Vanasse, A., Tremblay, G.F., Mustafa, A.F., Charron, J., 2015. Industrial Hemp Response to Nitrogen, Phosphorus, and Potassium Fertilization. Crop. Forage Turfgrass Manag. 1, 1–10. https://doi.org/10.2134/cftm2015.0159

Barna, L.T., 2021. A climate goal – based , multicriteria method for system evaluation in life cycle assessment. Int. J. Life Cycle Assess. https://doi.org/10.1007/s11367-021-01991-1

Bisinella, V., Conradsen, K., Christensen, T.H., Astrup, T.F., 2016. A global approach for sparse representation of uncertainty in Life Cycle Assessments of waste management systems. Int. J. Life Cycle Assess. 21, 378–394. https://doi.org/10.1007/s11367-015-1014-4

Boudet, F., Brunelle, T., Cazé, C., Mancebo, F., Mora, O., Paillard, S., Soussana, J.-F., Vandenbussche, A., 2021. En France, d'ici à 2030, renforcer la diversité des services rendus par les terres en préparant la neutralité carbone pour 2050.

Boutin Marie-Pierre, Flamin Cyril, Quinton Samuel, G.G., 2006. Étude des caracteristiques environmentales du chanvre par l'analyse de son cycle de vie (Study of the environmental chracteristics of hemp using a life cycle analysis).

Brandao, M., Martin, M., Cowie, A., Hamelin, L., Zamagni, A., 2017. Consequential Life Cycle Assessment: What, How, and Why? Encycl. Sustain. Technol. 1, 277–284. https://doi.org/10.1016/B978-0-12-409548-9.10068-5

Carus, M., Sarmento, L., 2017. The European Hemp Industry: Cultivation, processing and applications for fibres, shivs, seeds and flowers. Eur. Ind. Hemp Assoc. 3, 1–9.

Chen, D., Rojas, M., Samset, B.H., Cobb, K., Diongue-Niang, A., Edwards, P., Emori, S., Faria, S.H., Hawkins, E., Hope, P., Huybrechts, P., Meinshausen, M., Mustafa, S.K., Plattner, G.-K., Treguier, A.M., 2021. Framing, Context, and Methods., in: Climate Change 2021: The Physical Science Basis. Contribution of Working Group I to the Sixth Assessment Report of the Intergovernmental Panel on Climate Change. IPCC.

Climate Plan [WWW Document], 2017. . French governement. URL https://www.gouvernement.fr/en/climate-plan

Clivot, H., Mary, B., Valé, M., Cohan, J.P., Champolivier, L., Piraux, F., Laurent, F., Justes, E., 2017. Quantifying in situ and modeling net nitrogen mineralization from soil organic matter in arable cropping systems. Soil Biol. Biochem. 111, 44–59. https://doi.org/10.1016/j.soilbio.2017.03.010

Clivot, H., Mouny, J.C., Duparque, A., Dinh, J.L., Denoroy, P., Houot, S., Vertès, F., Trochard, R., Bouthier, A., Sagot, S., Mary, B., 2019. Modeling soil organic carbon evolution in long-term arable experiments with AMG model. Environ. Model. Softw. 118, 99–113. https://doi.org/10.1016/j.envsoft.2019.04.004

Conen, F., Zimmermann, M., Leifeld, J., Seth, B., Alewell, C., 2008. Relative stability of soil carbon revealed by shifts in δ 15 N and C: N ratio. Biogeosciences 5, 123–128.

Delmas, M., Saby, N., Arrouays, D., Dupas, R., Lemercier, B., Pellerin, S., Gascuel-Odoux, C., 2015. Explaining and mapping total phosphorus content in French topsoils. Soil Use Manag. 31, 259–269. https://doi.org/10.1111/sum.12192

Deng, Y., 2014. Life cycle assessment of biobased fibre-reinforced polymer composites. World Scientific. https://doi.org/10.1142/9789814566469_0063

Dobbratz, M., Gutknecht, J., Wyse, D., Sheaffer, C.C., Jungers, J.M., 2021. Inconsistent effects of species diversity and N fertilization on soil microbes and carbon storage in perennial bioenergy cropping systems. Renew. Agric. Food Syst. https://doi.org/10.1017/S1742170521000302

DRIAS CERFACS, IPSL, M.-F., 2013. CNRM-CERFACS-CM5/CNRM-ALADIN63-RCP4.5. DRIAS les Futur. du Clim.

Euorpean Commission, 2018. Bio-composites for cars [WWW Document]. Cordis. URL https://cordis.europa.eu/article/id/124411-biocomposites-for-cars

European Commission, 2016. EU Reference Scenario 2016, EU Reference Scenario 2016.

Fazio, S., Biganzioli, F., De Laurentiis, V., Zampori, L., Sala, S., Diaconu, E., 2018. Supporting information to the characterisation factors of recommended EF Life Cycle Impact Assessment methods, version 2, from ILCD to EF 3.0, EUR 29600 EN, European Commission, Ispra, 2018, ISBN 978-92-79-98584-3, doi:10.2760/002447, PUBSY No. JRC114822., New Models and Differences with ILCD, EUR. https://doi.org/10.2760/002447

Fortune Business Insights, 2022. The global building thermal insulation market is projected to grow from $29.85 billion in 2021 to $40.34 billion in 2028 at a CAGR of 4.4% in forecast period... Read More at:- https://www.fortunebusinessinsights.com/building-thermal-insulation-market-1027.

Grand view research, 2021. Composites Market Size, Share & Trends Analysis Report By Product (Carbon, Glass), By Manufacturing Process (Layup, Filament, RTM), By End Use, By Region, And Segment Forecasts, 2021 - 2028.

Grand view research, 2019. Insulation Market Size, Share & Trends Analysis Report By Product (EPS, XPS, Glass Wool, Mineral Wool), By Application (Infrastructure, Industrial, HVAC & OEM), By Region, And Segment Forecasts, 2019 - 2025.

Gueudet, A., 2016. Analyse Du Cycle De Vie Comparative De Panneaux De Porte Automobiles Biosource (Pp / Fibres De Lin Et De Chanvre) Et Petrosource (Abs).

Hemp benchmarks, 2021. U.S. Hemp Market Landscape, Hemp business journal.

Hergoualc'h, K., Akiyama, H., Bernoux, M., Chirinda, N., del Prado, A., Kasimir, Å., MacDonald, J.D., Ogle, S.M., Regina, K., Weerden, T.J. van der, 2019. N2O emissions from managed soils, and CO2 emissions from lime and urea application, in: 2019 Refinement to the 2006 IPCC Guidelines for National Greenhouse Gas Inventories. pp. 1–48.

Inglada, J., Vincent, A., Arias, M., Tardy, B., Morin, D., Rodes, I., 2017. Operational High Resolution

Land Cover Map Production at the Country Scale Using Satellite Image Time Series. Remote Sens. 9, 95. https://doi.org/10.3390/rs9010095

Ip, K., Miller, A., 2012. Life cycle greenhouse gas emissions of hemp-lime wall constructions in the UK. Resour. Conserv. Recycl. 69, 1–9. https://doi.org/10.1016/j.resconrec.2012.09.001

IPCC, 2019. 2019 Refinement to the 2006 IPCC Guidelines for National Greenhouse Gas Inventories Volume 5 Waste, IPCC Good Practice Guidance and Uncertainty Management in National Greenhouse Gase Inventories.

Jiménez Rivero, A., Sathre, R., García Navarro, J., 2016. Life cycle energy and material flow implications of gypsum plasterboard recycling in the European Union. Resour. Conserv. Recycl. 108, 171–181. https://doi.org/10.1016/j.resconrec.2016.01.014

Kassara, G., Pena Verrier, G., Chammas, M., Fournie, L., Mainsant, A., Marchal, D., Parrouffe, J.-M., 2019. Trajectories of evolution of the electricity mix 2020-2060: Additional analyses, FAQs, Report on data.

Kim, S., Dale, B.E., Drzal, L.T., Misra, M., 2008. Life cycle assessment of kenaf fiber reinforced biocomposite. J. Biobased Mater. Bioenergy 2, 85–93. https://doi.org/10.1166/jbmb.2008.207

Kirwan, L., Lüscher, A., Sebastià, M.T., Finn, J.A., Collins, R.P., Porqueddu, C., Helgadottir, A., Baadshaug, O.H., Brophy, C., Coran, C., Dalmannsdóttir, S., Delgado, I., Elgersma, A., Fothergill, M., Frankow-Lindberg, B.E., Golinski, P., Grieu, P., Gustavsson, A.M., Höglind, M., Huguenin-Elie, O., Iliadis, C., Jørgensen, M., Kadziuliene, Z., Karyotis, T., Lunnan, T., Malengier, M., Maltoni, S., Meyer, V., Nyfeler, D., Nykanen-Kurki, P., Parente, J., Smit, H.J., Thumm, U., Connolly, J., 2007. Evenness drives consistent diversity effects in intensive grassland systems across 28 European sites. J. Ecol. 95, 530–539. https://doi.org/10.1111/j.1365-2745.2007.01225.x

La Rosa, A.D., Cozzo, G., Latteri, A., Mancini, G., Recca, A., Cicala, G., 2013. A comparative life cycle assessment of a composite component for automotive. Chem. Eng. Trans. 32, 1723–1728. https://doi.org/10.3303/CET1332288

Lecompte, T., Levasseur, A., Maxime, D., 2017. Lime and hemp concrete LCA: a dynamic approach of GHG emissions and capture. 2nd Int. Conf. Bio-based Build. Mater. 1st Conf. Ecol. Valoris. Granul. FIbrous Mater. 513–521.

Li, L.J., Zeng, D.H., Mao, R., Yu, Z.Y., 2012. Nitrogen and phosphorus resorption of Artemisia scoparia, Chenopodium acuminatum, Cannabis sativa, and Phragmites communis under nitrogen and phosphorus additions in a semiarid grassland, China. Plant, Soil Environ. 58, 446–451. https://doi.org/10.17221/6339-pse

Moussa, T., Maalouf, C., Ingrao, C., Scrucca, F., Costantine, G., Asdrubali, F., 2018. Bio-based and recycled-waste materials in buildings: A study of energy performance of hemp-lime concrete and recycled-polyethylene terephthalate façades for office facilities in France and Italy. Sci. Technol. Built Environ. 24, 492–501. https://doi.org/10.1080/23744731.2018.1438664

Nachtergaele, F., van Velthuizen, H., van Engelen, V., Fischer, G., Jones, A., Montanarella, L., Petri, M., Prieler, S., Teixeira, E., Shi, X., 2012. Harmonized World Soil Database (version 1.2). FAO, Rome, Italy IIASA, Laxenburg, Austria 1–50.

Norton, A.J., 2008. The Life Cycle Assessment and Moisture Sorption Characteristics of Natural Fibre Thermal Insulation Materials. University of Wales, Bangor.

Norton, A.J., Murphy, R., Hill, C.A.S., Newman, G., 2009. the Life Cycle Assessments of Natural

Fibre Insulation Materials. Mater. Technol. 6–9.

Pavel, C.C., Blagoeva, D.T., 2018. Competitive landscape of the EU's insulation materials industry for energy-efficient buildings. Publ. Off. Eur. Union 1–24. https://doi.org/10.2760/750646

Pehme, S., Veromann, E., Hamelin, L., 2017. Environmental performance of manure co-digestion with natural and cultivated grass – A consequential life cycle assessment. J. Clean. Prod. 162, 1135–1143. https://doi.org/10.1016/j.jclepro.2017.06.067

Pervaiz, M., Sain, M.M., 2003. Carbon storage potential in natural fiber composites. Resour. Conserv. Recycl. 39, 325–340. https://doi.org/10.1016/S0921-3449(02)00173-8

Pretot, S., Collet, F., Garnier, C., 2014. Life cycle assessment of a hemp concrete wall: Impact of thickness and coating. Build. Environ. 72, 223–231. https://doi.org/10.1016/j.buildenv.2013.11.010

Sala, S., Amadei, A.M., Beylot, A., Ardente, F., 2021. The evolution of life cycle assessment in European policies over three decades. Int. J. Life Cycle Assess. 26, 2295–2314. https://doi.org/10.1007/s11367-021-01893-2

Schmidt, J.H., Weidema, B.P., 2008. Shift in the marginal supply of vegetable oil. Int. J. Life Cycle Assess. 13, 235–239. https://doi.org/10.1065/lca2007.07.351

Schwarz, A.E., Ligthart, T.N., Godoi Bizarro, D., De Wild, P., Vreugdenhil, B., van Harmelen, T., 2021. Plastic recycling in a circular economy; determining environmental performance through an LCA matrix model approach. Waste Manag. 121, 331–342. https://doi.org/10.1016/j.wasman.2020.12.020

Senga Kiessé, T., Ventura, A., van der Werf, H.M.G., Cazacliu, B., Idir, R., Andrianandraina, 2017. Introducing economic actors and their possibilities for action in LCA using sensitivity analysis: Application to hemp-based insulation products for building applications. J. Clean. Prod. 142, 3905–3916. https://doi.org/10.1016/j.jclepro.2016.10.069

Shen, Z., Tiruta-Barna, L., Karan, S.K., Hamelin, L., 2022b. Simultaneous carbon storage in arable land and anthropogenic products (CSAAP): Demonstrating an integrated concept towards well below 2° C. Resour. Conserv. Recycl. 182, 106293.

Shimako, A.H., Tiruta-Barna, L., Pigné, Y., Benetto, E., Navarrete Gutiérrez, T., Guiraud, P., Ahmadi, A., 2016. Environmental assessment of bioenergy production from microalgae based systems. J. Clean. Prod. 139, 51–60. https://doi.org/10.1016/j.jclepro.2016.08.003

Sinka, M., Van den Heede, P., De Belie, N., Bajare, D., Sahmenko, G., Korjakins, A., 2018. Comparative life cycle assessment of magnesium binders as an alternative for hemp concrete. Resour. Conserv. Recycl. 133, 288–299. https://doi.org/10.1016/j.resconrec.2018.02.024

Stapulionienė, R., Tupčiauskas, R., Vaitkus, S., Vėjelis, S., 2016. Development and Investigation of Thermal Insulation From Hemp-Polylactide Fibres. Eng. Struct. Technol. 8, 23–30. https://doi.org/10.3846/2029882x.2016.1158127

Stocker, T.F., Qin, D., Plattner, G.K., Tignor, M.M.B., Allen, S.K., Boschung, J., Nauels, A., Xia, Y., Bex, V., Midgley, P.M., 2013. Climate change 2013 the physical science basis: Working Group I contribution to the fifth assessment report of the intergovernmental panel on climate change. Clim. Chang. 2013 Phys. Sci. Basis Work. Gr. I Contrib. to Fifth Assess. Rep. Intergov. Panel Clim. Chang. 9781107057, 1–1535. https://doi.org/10.1017/CBO9781107415324

Tadele, D., Roy, P., Defersha, F., Misra, M., Mohanty, A.K., 2020. A comparative life-cycle assessment of talc- and biochar-reinforced composites for lightweight automotive parts. Clean

Technol. Environ. Policy. https://doi.org/10.1007/s10098-019-01807-9

Tiruta-barna, L., 2021. Climate Change Impact tool [WWW Document]. INSA. URL https://www.insa-toulouse.fr/fr/recherche/labo/lisbp/outil-de-calcul-changement-climatique.html

Tonini, D., Hamelin, L., Astrup, T.F., 2016. Environmental implications of the use of agro-industrial residues for biorefineries: application of a deterministic model for indirect land-use changes. GCB Bioenergy 8, 690–706. https://doi.org/10.1111/gcbb.12290

Uihlein, A., Ehrenberger, S., Schebek, L., 2008. Utilisation options of renewable resources: a life cycle assessment of selected products. J. Clean. Prod. 16, 1306–1320. https://doi.org/10.1016/j.jclepro.2007.06.009

UNFCCC, S., 2015. Report of the Conference of the Parties on its twenty-first session, held in Paris from 30 November to 13 December 2015. Addendum. Part two: Action taken by the Conference of the Parties at its twenty-first session. United Nations Framework Convention on Climate Change Bonn.

Ventura, A., Kiess, T.S., 2015. Sensitivity Analysis of Environmental Process Modeling in a Life Cycle Context: A Case Study of Hemp Crop Production. J. Ind. Ecol. 19, 978–993. https://doi.org/10.1111/jiec.12228

Vera, C.L., Malhi, S.S., Phelps, S.M., May, W.E., Johnson, E.N., 2010. N, P, and S fertilization effects on industrial hemp in Saskatchewan. Can. J. Plant Sci. 90, 179–184. https://doi.org/10.4141/CJPS09101

Weidema, B.P., Bauer, C., Hischier, R., Mutel, C., Nemecek, T., Reinhard, J., Vadenbo, C.O., Wenet, G., 2013. Data quality guideline for the ecoinvent database version 3. Ecoinvent Report 1 (v3). Swiss Cent. Life Cycle Invent. 3, 169.

Wötzel, K., Wirth, R., Flake, M., 1999. Life cycle studies on hemp fibre reinforced components and ABS for automotive parts. Angew. Makromol. Chemie 272, 121–127. https://doi.org/10.1002/(SICI)1522-9505(19991201)272:1<121::AID-APMC121>3.0.CO;2-T

Zampori, L., Dotelli, G., Vernelli, V., 2013. Life cycle assessment of hemp cultivation and use of hemp-based thermal insulator materials in buildings. Environ. Sci. Technol. 47, 7413–7420. https://doi.org/10.1021/es401326a

Chapter V. Biopump: perennial plants

Context

At present, afforestation is considered as the only large-scale operational carbon capture and storage method (Terlouw et al., 2021). According to the potential biopumps ranked in chapter III, black locust (*Robinia pseudoacacia L.*) is selected on behalf of perennial plants which could be cultivated on French CV-lands. The whole life cycle of black locust, from seedling to products disposal, is investigated. Due to the specific quality of the different woody parts, different products are envisioned. Woody parts like branch have less strength than roundwood, and are suitable to be chipped to produce medium density board (MDF, 12 years lifetime), while bark is incinerated. The roundwood is widely used in the building industry, mainly as furniture or in structure. In this case study, roundwood is converted to be cross-laminated timber (CLT) for exterior walls, which could be used for 50 years. At the end of life, some products can be recycled, for example scraps from roundwood processing and part of CLT at the end of life are recycled to MDF, prolonging the C stocked in the technosphere. Also, incineration is another common approach in the disposal of wood-based products, generating heat to reuse.

The content of this chapter could answer the questions below:

1) to propose a value chain, from tree (black locust) plantation and harvesting, to wood-based product manufacturing and end of life, compatible with the biopump strategy,

2) to evaluate the C sinks and negative C emissions induced,

3) to investigate the environmental consequences of replacing current land cover and fossil-based products by the black locust and the related products, and particularly the global warming mitigation potential,

4) to investigate the effect on global mean temperature change

The main steps conducted are: modeling the black locust growth and the residue decay with time-> simulating the SOC change during cultivation on French CV-lands-> estimating environmental impacts of black locust from cradle-to-grave-> building the inventory with temporal characteristics based on the consequential LCA results-> estimating the GMTC change within time boundary.

1. Introduction

Achieving the climate objectives of the Paris Agreement and national policies in terms of emissions reduction and carbon neutrality by 2050 implies the implementation of drastic greenhouse gas (GHG) emission reductions and CO_2 capture and storage actions. To this end, the concept of Carbon Storage in Arable land and Anthropogenic Products (CSAAP) has recently been proposed (Shen et al., 2022a, 2022b), consisting in cultivating plants, also called biopumps, that can induce a net increase of soil organic carbon (SOC) stocks while providing biomass for long-lasting anthropogenic products.

Putting CSAAP into practice needs solving two issues, namely defining the type of suitable biopump species and areas to grow them. According to previous research (Shen et al., 2022b), there are up to 2,400,000 ha of suitable land in France alone that could be available for planting biopumps for climate mitigation purposes. These lands are called 'carbon vulnerable lands (CV-lands)' as they present a high potential for SOC sequestration due to their current SOC stock being <50 t C ha^{-1} (Minasny et al., 2017). They were also selected to respect a set of specific sustainability criteria defined in Shen et al., (2022b). Among the list of 14 suitable woody biopumps presented in (Shen et al., 2022b), black locust *(Robinia pseudoacacia L.*) was identified not only because it could capture 31.5 kg CO_2 per tree per year (supplement information III, section 2.1), but also for its capacity to convert part of the captured C in the soil as SOC (Wang et al., 2012). Furthermore, woody products have a relatively long lifetime, which could delay the C emission back to the atmosphere.

When analyzing how wood value chains affect climate change, the conventional theory considers biogenic C as neutral (balanced), thus neither C absorbed nor C emitted from biomass is included in the climate change impact calculation (Chen et al., 2019; da Costa et al., 2018). This approach is suitable for annual or short rotation coppice, while not proper in estimating forest mitigation potential because the effect of C storage and delayed emission is ignored. Guest et al. (2013) studied the relationship between the wood rotation and C storage in products on the biogenic global warming potential. They concluded in order to consider biogenic CO_2 as neutral, the lifespan of wood products should be at least half of the wood rotation. Another common accounting approach is considering the forest as a permanent C sink, where the C captured through photosynthesis is counted while the emission of biogenic C is not (González-García et al., 2011). This approach shows the effectiveness of biomass as a C sink on a limited time scale, however, it is not correct under time scales encompassing the life cycle of biomass from cradle-to-grave. Albers et al. modeled the trees' growth and residue decomposition, showing that the tree's lifetime highly influences the mitigation potential, the shorter the lifetime, the lower the mitigation effect of converting forests to biofuels (Albers et al., 2019b). However, since biofuels are used at once with almost all C emitted immediately, there is no technosphere C sink. Lan et al. (2020) tracked the carbon flows from one rotation of pine forest cultivation to the end of wood products on a 100-year scale, and highlighted the difference between using residue for wood products or energy. They treated biogenic C as neutral, only considering the influence of fossil C emissions. Zieger et al. (2020) countered both biogenic C absorption by timber and wheat, and degradation of biobased walls including incineration and compost, with temporal factor. However, the belowground part of plants and the SOC were not included in these studies. Soil is an important C sink, not taking it into account results in C flows that are not correctly balanced (Hamelin et al., 2012).

Because wood and wood-based products have a relatively long lifespan, and biomass residues decay at different rates, the temporal factor is essential in assessing the wood-product system. Recent studies demonstrated a considerable difference between static and dynamic LCA approaches for wood-based products (e.g., Cardellini et al., 2018; Göswein et al., 2020), especially for the quantification of biogenic C capture and release effects. Finally, most of the studies used CO_2-eq as an aggregation metric for all GHG, whatever the time scale, which misleads conclusions(Barna, 2021; Saez de Bikuña et al., 2018; Zieger et al., 2020).

This work explores the mitigation potential for global warming, and overall environmental impacts, of an application case of the CSAAP strategy with perennial plantations, selected in the light of earlier work (Shen et al., 2022b). The case is the implementation of a 35-y plantation of black locust on CV-lands in France, using the biomass for bio-based products intended for the construction. Objectives are to: 1) evaluate the C sinks induced over time, 2) investigate the overall environmental consequences of replacing current land covers and fossil-based products with the black locust and the related bio-based products, and particularly the global warming mitigation potential in order to contrast it with the sinks, and 3) investigate the effect on global mean temperature change in time. In the general endeavor to uncover environmentally-performant solutions towards both carbon dioxide removals and climate mitigation, this work proposes an original, comprehensive framework with adapted modeling tools to address all these questions.

2. Methods

2.1. Scenarios description

The point of departure of this analysis is one hectare of average French CV-land, to be either converted for black locust cultivation from the year 2022, over three rotations of 35-y each (BL Scenario), or maintained as CV-land for 105 y (reference scenario, from here onwards referred to as Scenario REF). For the static environmental assessment, only 35 years (the time of one rotation) is considered, as further detailed in section 2.5.

2.1.1 Initial vegetation scenario on CV-land (REF Scenario)

This scenario considers that CV-lands remain CV-lands throughout the time covered by the analysis. The vegetation considered on average French CV-land stem from the work of (Shen et al., 2022a, 2022b). Accordingly, four types of initial land cover are considered with different shares in terms of the area they cover, namely intensive grasslands (53%), natural grasslands (20%), rapeseed lands (20%), and woody moorlands (7%) (details in Shen et al., 2022b). Ryegrass (*Lolium perenne L.*) and rapeseed (*Brassica napus L.*) represent the initial vegetation on intensive grassland and rapeseed lands, respectively, while heather (*Calluna vulgaris*) is selected to represent both natural grasslands and woody moorlands vegetation. On CV-lands remaining CV-lands, ryegrass and rapeseed are harvested annually and used for animal feed and oil production respectively, while heather is considered to decay on-site (Pehme et al., 2017). The rapeseed cake co-produced with rapeseed oil is also considered to be used for animal feed.

2.1.2 Black locust scenario (BL)

In this scenario, CV-lands are ploughed prior to black locust planting. Black locust is a nitrogen-fixing species and tolerates droughts (Nicolescu et al., 2020; Seserman et al., 2018). For this reason, and also in accordance with the CSAAP vision to favor systems with minimal inputs (Shen et al., 2022), no fertilization or irrigation is considered. To remove defective trees, selective thinning is conducted twice, in the 10^{th} year and 20^{th} year of the plantation's lifetime, where whole trees are removed (Keresztesi, 1983; Nicolescu et al., 2020). After the second selective thinning, extra branches are pruned to provide enough space for stem growth. After harvesting, black locust is delimbed and debarked. Barks are incinerated to provide heat for downstream manufacture (Silva et al., 2013), while branches are chopped into wood chips (Fig. V-1a). Stumps are crushed and left on the ground as residues during thinning operations and when black locust is logged.

The processes after logging are depicted in Fig. V-1b. First, there is the processing of stems. After delimbing and debarking, the stems are dried on open fields to meet a moisture content of ca. 15% (Żelazna et al., 2019). The dried stems are trimmed and sawn into panels, then laminated into several layers (Sahoo et al., 2019). These high-value laminated panels, called 'cross-laminated timber' (CLT), are widely used in the building sector, as a more sustainable alternative than carbon-intensive materials

(Cadorel and Crawford, 2019; Cowie et al., 2021). Herein CLT is assumed to be used for exterior walls, with 50 years lifespan (Dodoo et al., 2014). After demolition, 45% of CLT is incinerated, 45% is recycled, while the remaining 10% is lost (regarded as open-landfills) (Jayalath et al., 2020). The recycled CLT is chopped into wood chips for further treatment.

Second, the branches from stem's trimming are cut into chips (to produce medium density fiberboard, MDF), then wood chips are washed to remove the dust. The clean chips are mixed with other wood chips obtained from branches, along with the woody material from 1st and 2nd thinning and recycled CLT. All these materials are softened in a steam-pressurized digester (the heat to generate steam commonly comes from burning barks), then mixed with urea-formaldehyde resin and additives in the resonating process, to improve the strength (Puettmann, 2016). The mixture is pressed into boards (MDF) under 170 °C for 5 minutes using a mechanically controlled oil-heated press (Yuan and Guo, 2017). The produced MDF has multiple usages, but having a lower mechanical strength than CLT, it is more suitable for furniture and interior architecture (Piekarski et al., 2017). After 12 years of use, most MDF in Europe is incinerated with heat recovery, while a minor part is landfilled (Couret et al., 2017; ecoinvent, 2020). The scraps occurring through the MDF production process are considered to end in open-landfills.

(a) Black locust- cultivation, harvesting and pretreatment

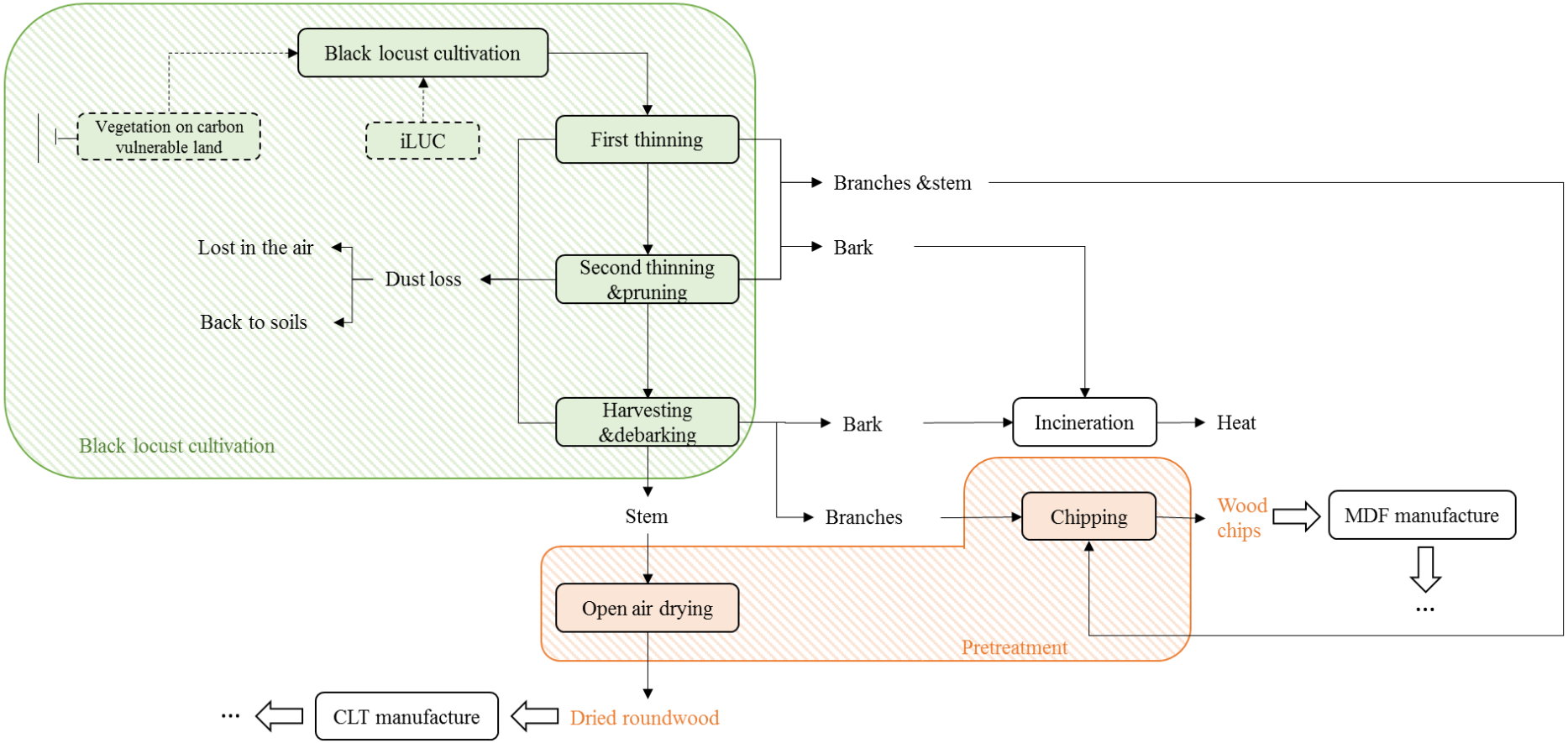

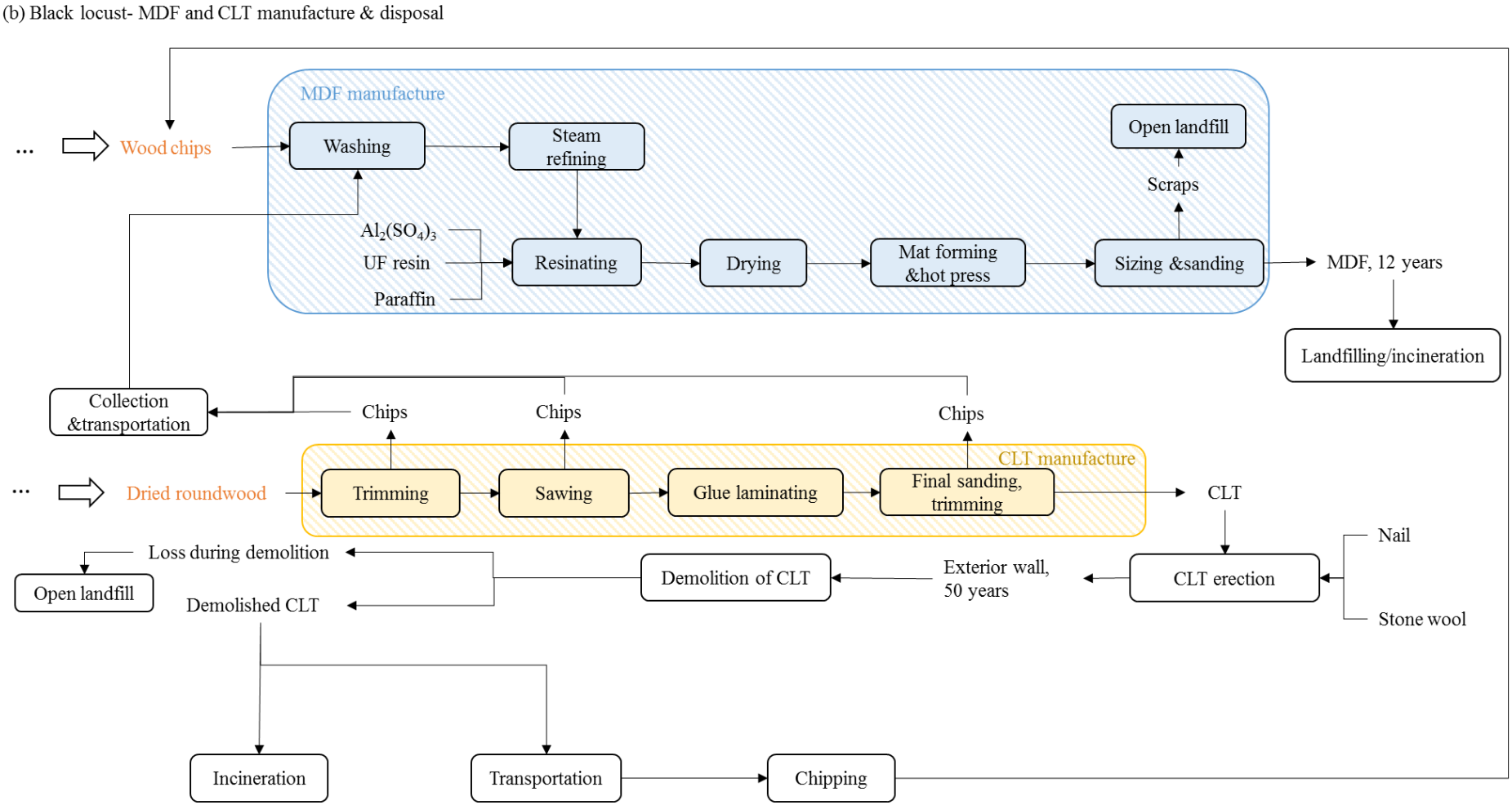

Fig. V-1 Process flow diagram showing the key activities considered for (a) black locust cultivation, harvesting (green) and residual biomass management (orange), and (b) manufacture and disposal of cross-laminated timber (CLT; yellow) and medium density fiberboard (MDF; blue).

2.2. Overview of the methodology used

The methodology used to achieve the objectives of this study builds on material and energy flow calculation, from plant cultivation, to anthropogenic production and products' end of life, to finally evaluate the carbon pools and environmental impacts.

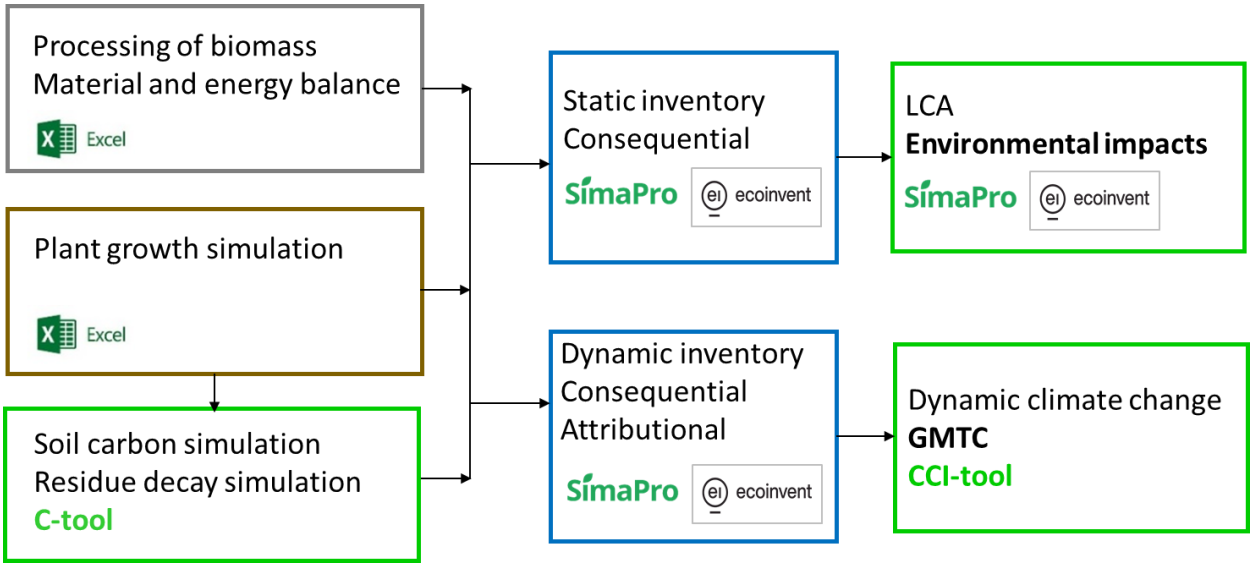

Fig. V-2 Calculation steps followed in this study

As shown in Fig. V-2, the first step calculates the growth of black locust to determine how much CO_2 is captured by photosynthesis, how much biomass is produced in the function of time in the different parts of the plant (e.g., belowground, aboveground), and the quantity of residues destined to decay above- and below ground. The carbon in the residues is an input to a SOC model, whose evolution is simulated over the rotation time span. In this way, the yearly content of SOC is estimated (over 105 years), along with the CO_2 releases from mineralization or native SOC losses, as detailed in section 2.4. The produced biomass determines the amount of products, associated by-products, and all related flows in the process chain, from harvesting to product manufacturing and end of life. These foreground flows are then used in three different LCA modeling approaches to respond to different questions as later detailed: static consequential LCA, dynamic LCA using the same consequential modeling of the inventory, and dynamic LCA using the attributional modelling of the background inventory with system expansion in the foreground part. Both dynamic approaches used temporal predictions for electricity mix based on either the absolute values or the rate of changes. In addition, sensitivity and uncertainty analyses were performed to explore the robustness of the results obtained.

2.3 Black locust growth rate

Black locust is a fast-growing tree species. After seedling planting, it reaches its fastest growth rate at year 20, then the growth rate slows down gradually till the end of the rotation (year 35) (Ciccarese et al., 2014; Nicolescu et al., 2018). The volume of biomass is estimated from the height and the diameter at breast height, all calculated in function of time(Rédei et al., 2014, 2012). Then the wood volume was converted to the biomass with the wood density of 785 kg m^{-3}, DM (Adamopoulos et al., 2007) (supplement information III, 2.2).

The whole stand is assumed to grow at the same rate, thus other parts were calculated based on a fixed shoot/ root ratio in time, here taken to 1.73 (Chen et al., 2020). In order to calculate the biomass amount

per ha in a specific year, a density varying between 560– 2240 trees per ha was considered, according to the growth stage (Keresztesi, 1983; Nicolescu et al., 2018). Details and results of simulated annual biomass partition (above- and below ground; in standing biomass and residues; as woody and non-woody portions) are presented in supplement information III, 2.2.

The foliage, pods, and seeds are considered jointly under the umbrella term 'aerial biomass', and are regarded as an annual input to soils from the 6th year of a rotation (Stone, 2009; Warne, 2016). Similar to the root part, the aerial biomass increase in time with the tree growth (Ciccarese et al., 2014), here aerial biomass was estimated based on a fixed ratio (1.2% of wood biomass, DM).

2.4 Simulating SOC on CV-lands for both scenarios, and wood residues decay

SOC in CV-lands cultivated with black locust or covered with initial vegetation was simulated with C-TOOL (Taghizadeh-Toosi et al., 2014). This model was adopted as one of the few models easily usable (i) with unconventional (non-agricultural) crops, (ii) for perennial systems, and (iii) calibrated for temperate areas (Andrade et al., 2022). Among others, it has the advantage that the proportion of C incorporated in the different (virtual) soil pools (each with a different turn-over rate affected by clay content and temperature; C-TOOL considers three pools) is easily customizable (e.g., Hansen et al., 2020). This ease of customization also applies to the allometric equations used to define the proportion of aboveground residual biomass input to the soil annually. Different applications of the model with perennial crops include (Hamelin et al., 2012) and (Keel et al., 2017).

The simulation was conducted with a one-year time step, for a timespan of 105 years from 2022 to 2126, corresponding to three consecutive rotations of black locust. Meteorological conditions in France were predicted by SICLIMA (DRIAS CERFACS, IPSL, last updated May 2013) for the RCP4.5 climate trajectory (Representative Concentration Pathway(Chen et al., 2021)), downscaled by the model CNRM-CERFACS-CM5/CNRM-ALADIN63. In C-TOOL, only the monthly average temperature is required in terms of meteorological data input (supplement information III, fig. s1). The required soil characteristics include the soil clay content and the C/N ratio. The former was retrieved from the same database used for identifying CV-lands (GSOC; Food and Agriculture Organization of the United Nations, 2020), the latter, not included in GSOC, was set to 11 based on literature (Clivot et al., 2019; Launay et al., 2021). The average initial SOC content for the CV-lands was evaluated as 42.35 Mg SOC ha^{-1} (Shen et al., 2022a).

Finally, one other key input required by the model is the monthly C input from residual above- and belowground biomass. The aboveground resides includes aerial biomass (foliage, seeds, and pods), which fall down annually (except for the first five years), and stumps, which are crushed and left on the ground as residues during thinning operations and when black locust is logged (year 10th, 20th, 35th of the rotation, respectively). Belowground residues consist of decaying roots and rhizodeposits. Decomposition rate coefficients of 0.12, 0.008, and 0.003 months^{-1} were set for aerial, aboveground- and belowground wood biomass, respectively (Taghizadeh-Toosi et al., 2014). To represent the slower decay of woody above- and below-ground residues, the simulation was conducted for an additional 100 years after the last rotation (the C not emitted after 100 years is considered as permanently stored).

For the initial vegetation, consisting of four different land types, the SOC of each land type was simulated individually, then aggregated together based on their respective shares in 1 ha CV-land (C input in supplement information III, table s19). A decomposition rate coefficient of 0.12 month^{-1} was used for the initial vegetation' residual biomass inputs to soil (above- and below-ground), as used for the foliage and as used in e.g., Hamelin et al. (2012) and Taghizadeh-Toosi et al. (2014) (both on the basis of Petersen et al., 2005).

2.5 Environmental impact assessment through consequential LCA

2.5.1 Goal, boundary, and functional unit

Consequential LCA is used to evaluate the environmental consequences of (i) cultivating black locust instead of the initial vegetation on the identified CV-lands in France and (ii) using the biomass in anthropogenic products while replacing conventional (fossil-based) products. This implies that multifunctionality was modeled with system expansion (Fig. V-3) and that the life cycle inventories for marginal suppliers were considered. The functional unit (FU) is defined as 'using 1 ha of CV-land in France for cultivating perennial crops over one full rotation, and using the biomass within the bioeconomy'. For the scenarios considered herein, this implies 35 years. The LCA framework follows the ISO 14040 and 14044 standards(Standardization, 2006a, 2006b). The system boundary considered for the consequential LCA is shown in Fig. V-3, both for the BL (here BLc) and REF (here REFc) scenarios.

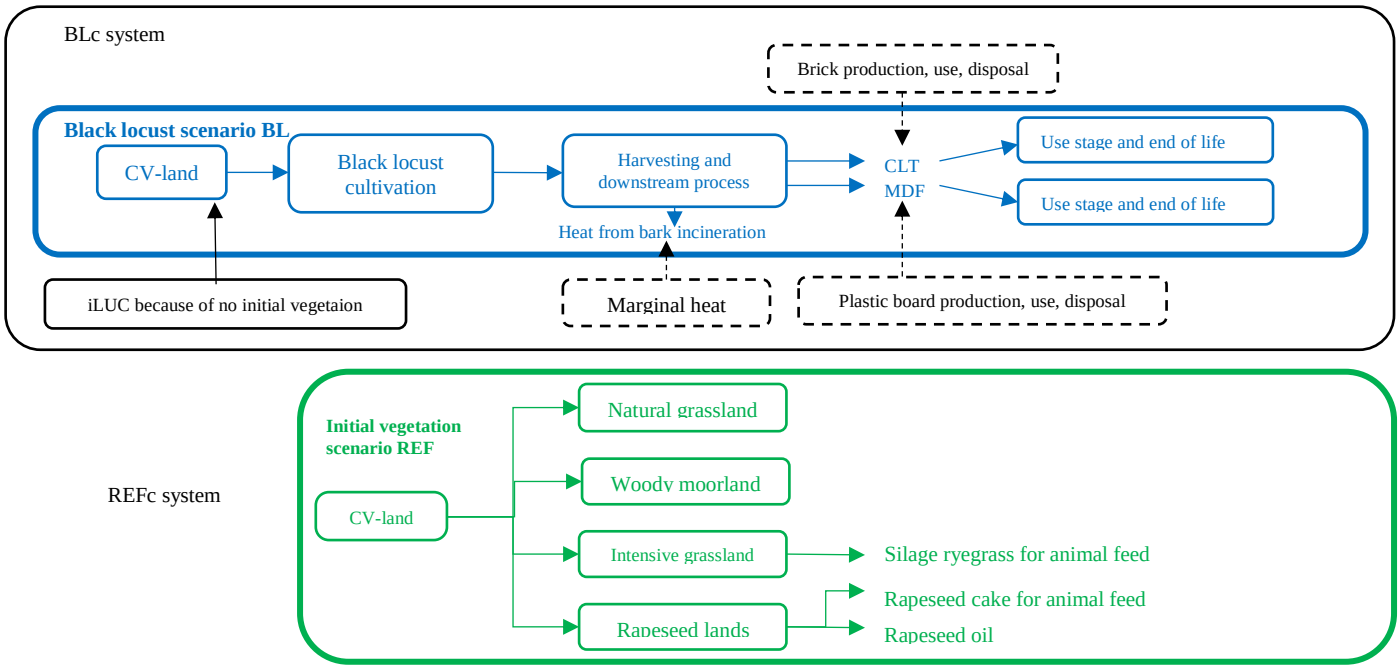

Fig. V-3 System diagrams showing the boundaries considered in consequential LCA of business as usual (REFc) and black locust (BLc) systems, built on REF and BL scenarios respectively. CV-land: carbon vulnerable land; iLUC: Indirect land use changes; CLT: cross-laminated timber; MDF: medium density fiberboard. Full lines indicate induced processes while dotted lines represent avoided processes.

System BLc involves a variety of substitutions. The replacement of the initial vegetation by black locust in the long-term, may happen through two main reactions, namely expansion of nature for agriculture (deforestation) or intensification of agricultural land (Tonini et al., 2016), both considered herein under the umbrella term of indirect land use changes (iLUC). According to market reports and literature review, the bio-based CLT and MDF will replace light-clay bricks and polyvinyl-chloride boards (herein referenced as plastic boards) respectively (Onyeaju et al., 2012; Takano et al., 2014). Incineration, at all stages where it happens, is considered with heat recovery, which implies that this heat will not need to be generated the way it would have otherwise been. As a result, corresponding heat generation is avoided. Finally, the use of CLT in buildings in comparison to brick (replaced material) is associated to a 52% reduction of electricity consumption because of the lighter mass(Corradini et al., 2019; Guo et al., 2017), which was considered within this system.

2.5.2 Life cycle inventory

Life cycle inventories for foreground processes (Fig. 1) were established on the basis of literature, models, and a variety of estimation proxies when necessary. These are comprehensively detailed in the supplement information (tables s3-s18). The displaced feed service (for the silage ryegrass and rapeseed cake of the initial vegetation) and its substitution by corresponding marginal carbohydrates, protein and lipid ingredients, along with the associated land use changes were modelled according to the methodology described in (Tonini et al., 2016). For landfilling processes (open-landfilling and landfilling of MDF at the end-of-life), 100% of the biogenic C was assumed to be emitted in the static LCA, while for the dynamic LCA (BLc and BLa), all emissions were estimated following the model provided in IPCC (2019) (around 14% C emitted as CH_4, and 86% as CO_2). All the background inventories were taken from Ecoinvent v3.5 (ecoinvent, 2020), with the consequential model.

2.5.3 Life cycle impact assessment and interpretation

The environmental impact assessment was performed with the Environmental Footprint method (EF) (Fazio et al., 2018a). The latest IPCC report (Masson-Delmotte, V., P. Zhai, A. Pirani et al., 2021) suggests updated factors for GHG to calculate the global warming potential, while these factors haven't yet been implemented in the EF method. Moreover, because all CO_2 releases and adsorption are accounted, biogenic CO_2 was considered with a global warming potential of 1 kg of CO_2-eq per kg biogenic CO_2 instead of the value of 0 used in (Fazio et al., 2018a).

For interpretation, a contribution analysis was performed for each impact category, where processes with negative and positive scores were analyzed separately in two groups. In each group, the processes contributing to at least 80% of the impact were selected for further in-depth analysis, e.g., identifying their sub-processes and substances contributing to the impact (Fazio et al., 2018b). The LCA was facilitated with the SimaPro software, version 9.1.

2.6 Dynamic LCA for evaluating climate change impact

Given the long lifetime of the studied system, a time-dependent method is necessary to address the temporal dimension of the climate change impact. Dynamic LCA with the global mean temperature change (GMTC) as an indicator was applied herein. The method and computational tool used were presented in previous works (Tiruta-Barna, 2021; CCI-tool, 2021). The GMTC calculation used the recommended method of IPCC for the emission timing over the whole life cycle of scenarios (Stocker et al., 2013), for all GHGs included in the ecoinvent v3.5 database (Supplement information III, table s21).

In scenario BL, trees are cultivated on 1 ha of land for three consecutive rotations, from 2022 to 2126. The same time span is considered for the initial vegetation lasting on the CV-lands in scenario REF. The temporal inventory (limited herein to GHGs) was obtained by placing each process on the timeline shown in Fig. 4. For long-lasting biogenic GHG emissions (e.g., disposal of CLT and MDF), the longest emission time was set as 100 years because the C released after 100 years could be considered permanently stored(European Commission-Joint Research Centre., 2010). Therefore, the temporal scope spans over the implantation of the first rotation in 2022, up to the end of the emissions from the last MDF disposal in 2290, 267 years in total. The manufacturing processes were considered to occur in the year of biomass harvesting. The time step for the inventory calculation was set to 1 year, regarded as sufficiently fine for climate change impact calculation.

Two perspectives were adopted for the dynamic modeling, here referred to 'consequential' and 'attributional', despite not fully embracing all features attributed to these two types of modeling approaches (Brandao et al., 2017; Schaubroeck et al., 2021). These two perspectives imply two main differences. One is the system boundary, as illustrated in Fig. 3 for the consequential perspective and Fig.5 for the attributional perspective. Both perspectives compare the black locust system to a reference

situation. In the consequential perspective, the system expansion reactions (associated with both the products generated in the BL system and the consequences of the foregone use of CV-land) are placed in the BL system (or here BLc). Even the foregone use of CV-land as CV-land itself (emissions associated with growing ryegrass, rapeseed, and heather) could have been placed in this system for an entirely relative perspective, but was left as a reference (here REFc) for comparison purposes. Two realities are compared in what is here referred to as "attributional perspective". In one (BLa), black locust is grown on CV-land and used to produce heat, CLT, MDF (the latter two being in use for a number of years and disposed of at their end-of-life, the same way as in the BLc system), while vegetable oil is supplied by palm oil and feed by marginal feed ingredients. In the other system (REFa), CV-land is used as CV-land, but to make it equivalent, the alternatives to products generated in the BLa system (heat, bricks, plastic boards) are considered here. Strictly speaking, these two system boundaries are equivalent (and would typically be both labelled as "consequential"). The major difference between the two perspectives lies in the type of background data being used. The consequential perspective considered marginal data, e.g., those foreseen to react to a demand change in the long-term (concretely translating in the use of the so-called consequential processes), while the attributional perspective used average background data (cut-off processes). Moreover, for the foreground data requiring heat and electricity, the attributional perspective considered the absolute predictions made for France for different periods (2020-2030, 2030-2040, 2040-2050), based on (ADEME, 2018) for electricity and Kassara et al. (2019) for heat. The heat and electricity mixes after 2050 were considered the same as in 2050 (Supplement information III, table s22-24).

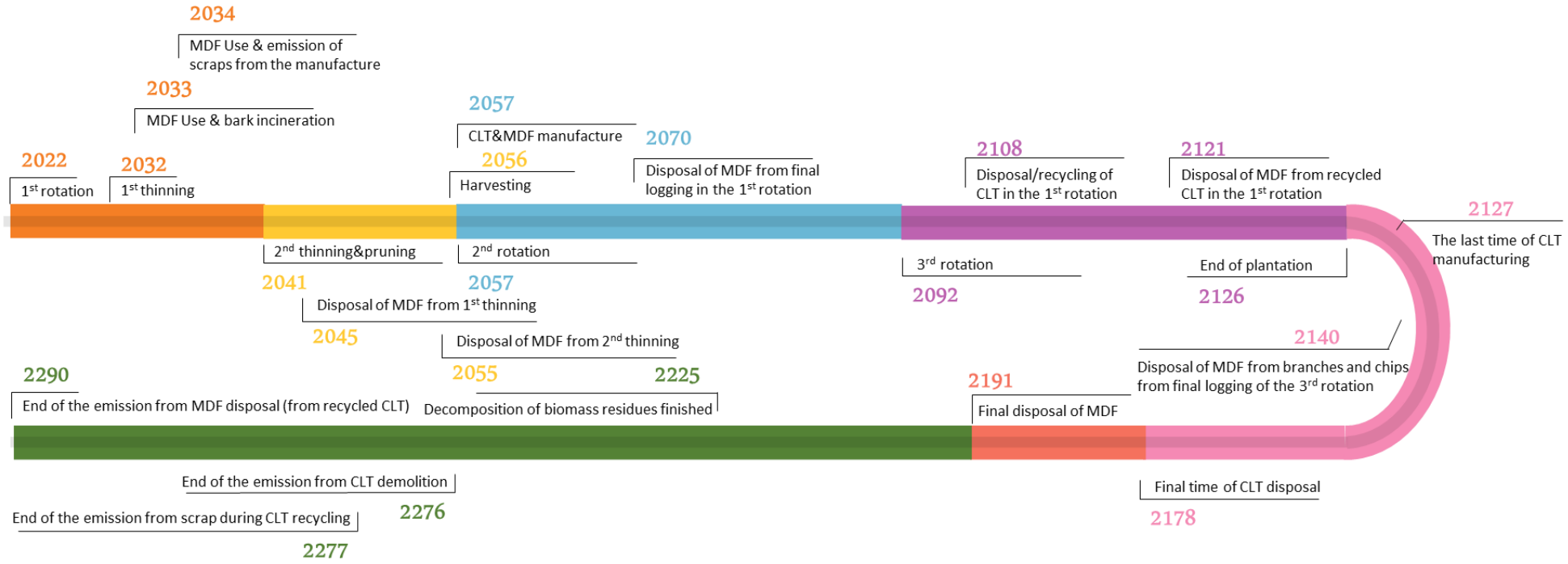

Fig. V-4 Timeline of processes for dynamic LCA.

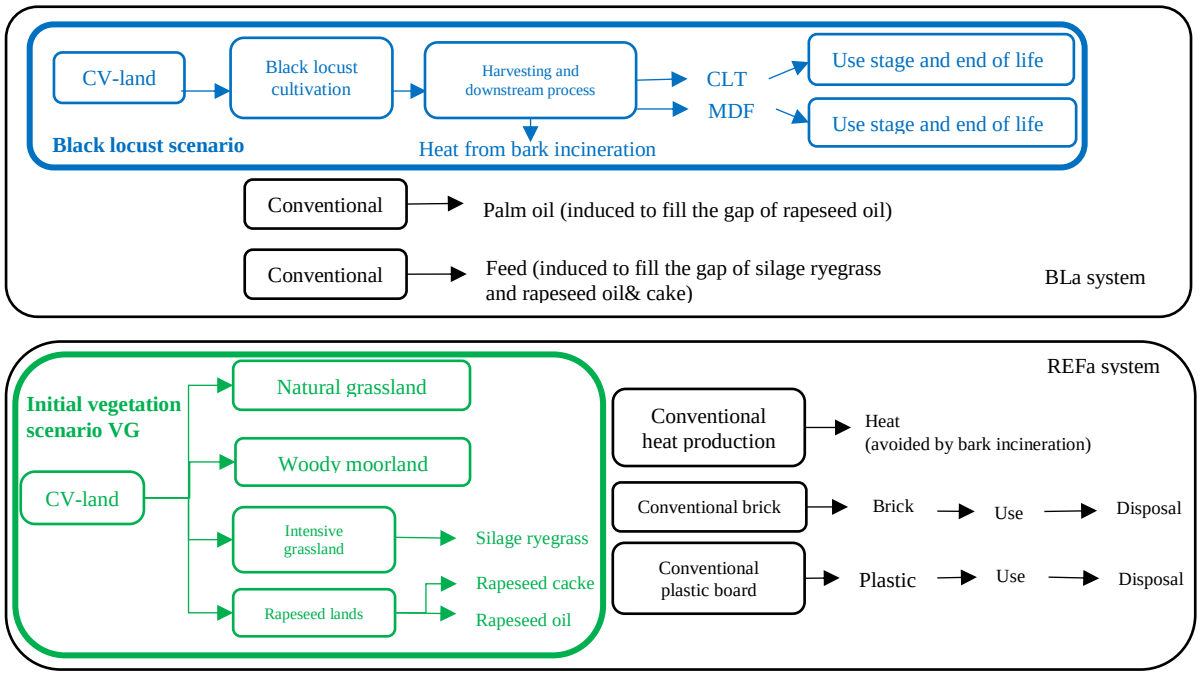

Fig. V-5 System diagrams of business as usual (REFa) and black locust (BLa) systems, built on REF and BL scenarios respectively.

2.7 Sensitivity and uncertainty analysis

2.7.1 Sensitivity analysis

In CLT disposal, the recycling rate is quite uncertain, and depends upon the country where it will be used (and disposed of). Since Europe is the largest current and future CLT consumer according to recent predictions, this study adopted a 45% recycling rate based on the European situation (Global Market Insights, 2021; Sahoo et al., 2019; Stora Enso, 2020). Yet, as this study covers a time period running until 2290, a higher recycling rate, e.g., 100%, is assumed from the year 2108 as a sensitivity analysis. Similarly, light-clay bricks and polyvinyl-chloride boards have been considered as fixed displaced products of CLT and MDF. As a sensitivity analysis, concrete and plasterboard are considered as avoided products of CLT and MDF, respectively, on the basis of previous studies (Brander, 2017; Liu et al., 2016). For MDF, an additional variant was taken into account by considering petrochemical polypropylene (PP) as the replaced product.

2.7.2 Uncertainty analysis

The uncertainty analysis was conducted according to the method proposed by Bisinella et al. (Bisinella et al., 2017, 2016). The parameters contributing the most to the impact results were identified in the contribution analysis (as described in section 2.5.3). Then, a one-at-the-time perturbation analysis was performed to evaluate how 10% of each parameter's variation affects the impact of normalization results. The parameters have been assigned a probability distribution (triangular or normal), allowing each impact category to calculate the uncertainty due to each parameter and the parameter’s contribution to the overall uncertainty. The calculated coefficient of variation represents the overall uncertainty of a given impact. The stepwise application of this method and result is described in section 5.1 of the supplement information III.

3 Result and discussion

3.1 Black locust growth and decay

Based on simulated height and diameter (supplement information III, fig. s5), the biomass amount on 1 ha CV-land is shown in Fig. V-6a, in different parts of black locust. During each thinning operation (year 10th and 20th), half of the tree (in terms of dry matter, DM) is logged, in year 10th and 20th, producing 26 and 110 t of woody DM respectively, being further chipped to produce MDF. The final harvesting at year 35 produces 368 t DM of the stem used to produce CLT, and 136 t DM of branches used for MDF. Based on the different turn-over rate simulated by C-tool, 10% and 27% of the DM in above- and belowground wood residues is still undegraded after 35 years. This falls to 1.5% and 2.8% after 100 years of decomposition.

3.2 SOC simulation results

The simulation results with C-TOOL (Fig. V-6b) show that SOC increased at the end of the rotation with black locust while slightly decreasing with the initial vegetation. The black locust induces a SOC increase periodically with each rotation, by 92.04 Mg ha^{-1} at the end of the third rotation (the year 2126), and mainly during the first rotation with 73.65 Mg ha^{-1}. The SOC increase rate declines sharply for the subsequent rotations, being only 15.54 and 2.84 Mg ha^{-1} for the second and third rotation respectively, since the SOC gradually reaches saturation in soils (Petersen et al., 2013). Existing organic matter is more mineralized than humified by soil microbes, thus SOC declines are observed following every biomass removal event (harvest, thinning).

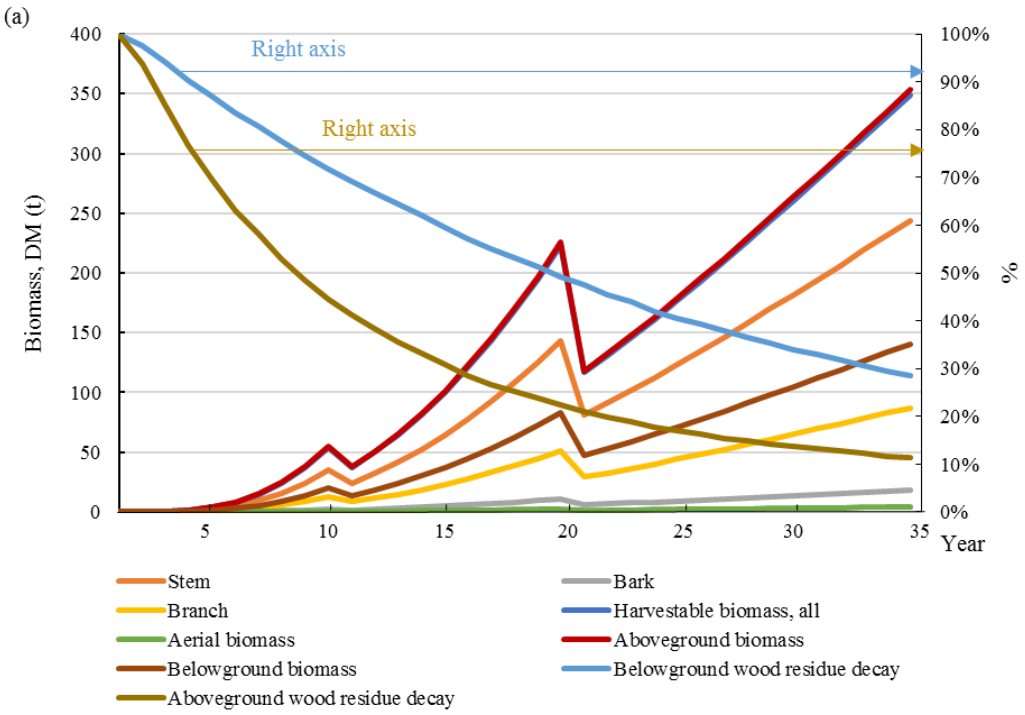

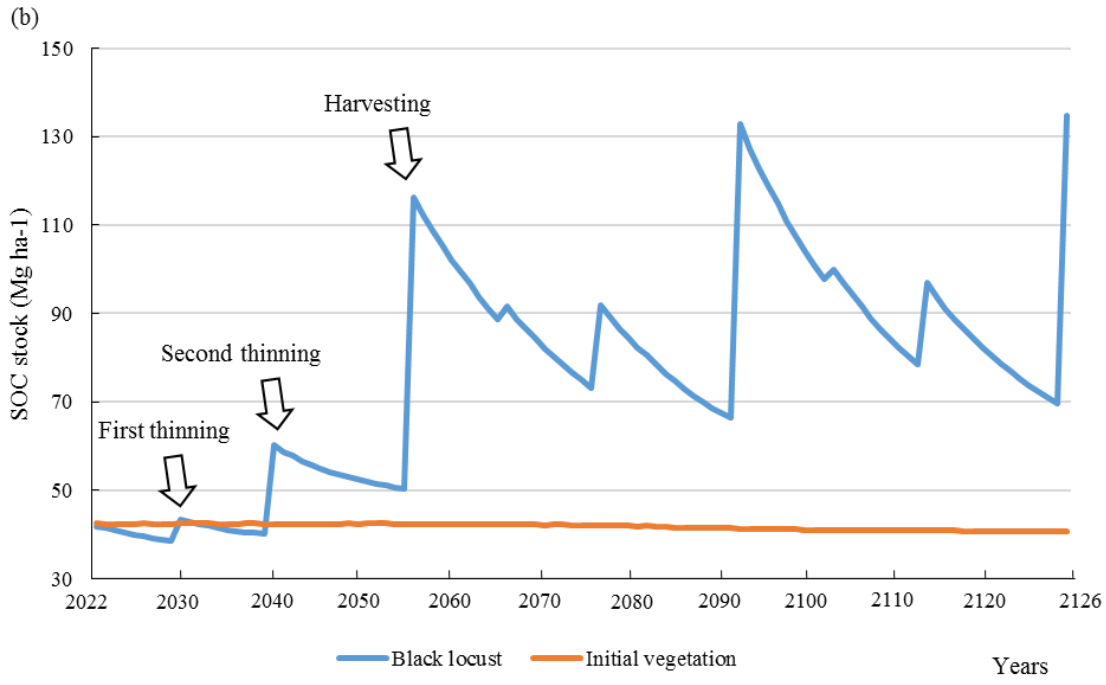

Fig. V-6 Simulated (a) biomass growth and decay for black locust during one rotation, and (b) SOC evolution for black locust and initial vegetation during the cultivation period. Harvestable biomass: stem, branch and bark.

Unlike the black locust system, the SOC in the initial vegetation system decreased from 42.35 to 40.68 Mg ha^{-1} during the cultivation. The main difference between black locust and initial vegetation is the C input. According to the literature data for vegetation yield and to the simulation results for black locust growth, the aboveground C inputs from initial vegetation is higher than that from black locust aerial biomass (foliage, seeds and pods) (1.27 and 0.91 t ha^{-1} $year^{-1}$ respectively). The higher C input means more amount of C is humified; as a result, the SOC of the initial vegetation is higher than black locust until the year 2031. But at years 10, 20, and 35 of the rotation, there are extra C inputs from logged stems, especially from the belowground root part (4.65, 19.23, 65.24 t ha^{-1} from the first-, second thinning, and harvesting respectively), making the SOC of the black locust system being higher than the one of the initial vegetation. Meanwhile, compared to the initial vegetation residues, the gradual decomposition of black locust residues keep the C in the soils for a longer time, leading to the SOC of black locust exceeding the SOC of the initial vegetation system by the year 2041 (second thinning).

Considering the 105 years studied herein, an annual SOC increase of 0.71 Mg ha^{-1} is observed for the black locust system, corresponding to an increase rate of 16 ‰ per year, which can be compared to the 4‰ target reported by Minasny et al. (2017) to offset the global annual GHG emissions. Looking at each rotation in isolation, this yearly increase rate is 50‰ during the first rotation and 30.09‰ during the second, indicating that short-term cultivation might be more efficient. Ciccarese et al. (2014) simulated one rotation of black locust with the Yasso model, and observed an annual SOC increase of 0.11 Mg ha^{-1} $year^{-1}$, which is half of our result (0.22 Mg ha^{-1} $year^{-1}$ for the first rotation). Wang et al. (2015) reported, based on field measurements, an average annual SOC increase of 0.93 Mg ha^{-1} (over 25 years). They measured this increase to 2.2 Mg ha^{-1} annually from year 5-10 but only 0.29 Mg ha^{-1} from year 10-25. Both studies also highlighted the contribution of dead wood incorporated in soils.

It should be noticed that the high SOC at the end of harvesting does not last for a long time. Fig. s2 (supplement information III) shows that following stem harvest, the SOC decreases gradually since there

is no extra C input anymore. After 51 years (2177), all increased SOC due to the black locust cultivation is lost, the SOC stock being equivalent to the initial level in 2022. In addition, the average annual SOC change of both black locust and the initial vegetation was used in building the inventory of scenario BLc and REFc for static LCA.

3.3 Environmental impact results from the static LCA

The LCA results are shown in Fig. V-7 (climate impact; global warming potential for a 100-y time horizon, GWP_{100}) & Fig. 8 (all other impacts); the negative contributions represent avoided processes or emissions while positive contributions represent the processed induced by implementing the studied scenario. The difference between these represents the net impact of a given category and scenario. Results are expressed per functional unit.

3.3.1 Climate change

Both scenarios lead to a negative characterization impact (hence climate mitigation), but in different magnitudes: 2202 t CO_2-eq mitigated for scenario BLc against 51 t CO_2-eq for scenario REFc (Fig. V-7).

In scenario BLc, the tree cultivation and the avoided plastic boards determine the net negative score, respectively contributing with -1283 and -2509 t CO_2-eq. The avoided plastic board category is an aggregation of several activities. About 61% of the impact is due to petrochemical plastic manufacture, while 24% stems from incineration at the end-of-life (supplement information III, fig. s6). The negative score of tree cultivation reflects the net 1305 t CO_2 captured by black locust in one rotation, offsetting the (positive) GHG emission due to the iLUC in the same process (21 t CO_2-eq).

The main processes with positive contributions are biomass harvesting and MDF disposal. The GHG emissions included in the harvesting process mainly (e.g., 93% of it) refer to the decomposition of residues composed of crushed stumps and roots. Here, CO_2 and CH_4 are respectively responsible for 68% and 26% of the CO_2-eq of this process. Besides the direct production of the MDF from biomass, 45% of CLT is recycled to produce MDF at the end of life, thus the disposal of MDF plays a role that is more critical than the one of CLT disposal (554 versus 139 t CO_2-eq respectively). Another critical process with positive impacts is resinating in MDF manufacture, emitting 129 t CO_2-eq because of the petrochemical resin used as an additive.

For scenario REFc (Fig. V-7b), natural grasslands and woody moorlands are shown as net contributors to the climate change impact. This reflects the emissions of CH_4 and N_2O due to the on-site decomposition of residues, and the fact that the GWP_{100} of these substances is respectively 34 and 298 times the one of CO_2. Intensive grasslands and rapeseed lands contribute to the total negative score with 68% and 32% respectively, reflecting the importance of avoiding palm oil and animal feed. However, these scores are less important than that in the scenario BLc because the palm oil and animal feed avoided come from plants that are no longer cultivated, and therefore, there is no more C absorbed in those plants. Based on the results in section 3.2, planting black locust increases, over the course of one rotation, the CV-lands SOC by an amount equivalent to 112 t CO_2-eq, while maintaining the initial vegetation leads to SOC decreases corresponding to 2 t CO_2–eq. Compared to the net results of the two scenarios, the effect of the C change in soils is relatively small, representing 5% and 4% of the net scores in scenario BLc and REFc respectively.

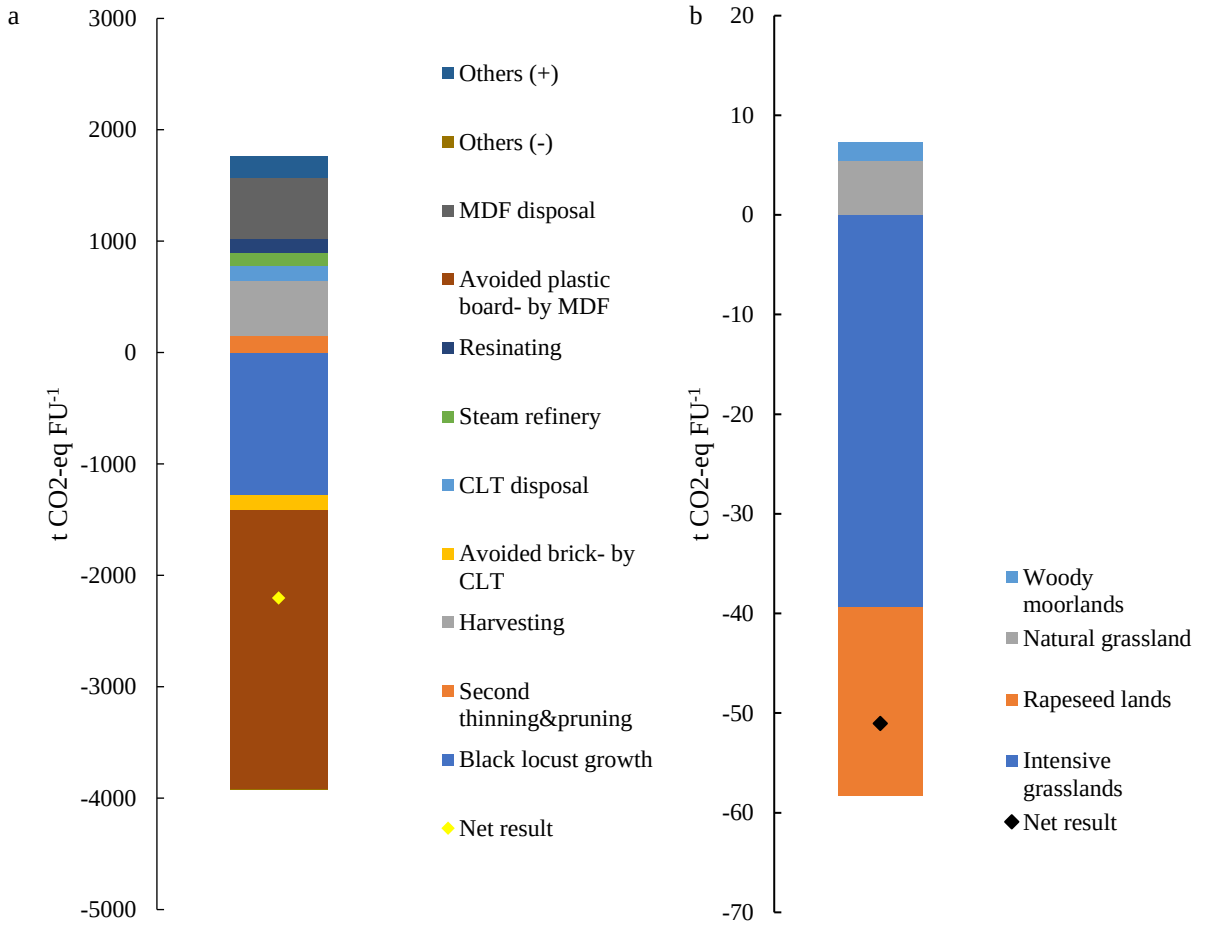

Fig. V-7 Climate change impact for (a) BLc and (b) REFc. Processes with contributions lower than 1% of the total impact (in absolute) were attributed to categories others (+) or (-) (e.g., process A has a contribution of 1 and process B of -1, then the contribution of process A is 1/(abs(1)+abs(-1))=50%).

3.3.2 Other environmental impacts

All impact results except climate change of scenario BLc and REFc are presented in Fig. V-8. Among fifteen impacts, scenario BLc shows four positive net impacts, while scenario REFc is positive in twelve impacts. Comparing scenario BLc to REFc, cultivating black locust instead of the initial vegetation benefits all environmental impacts except ionizing radiation, freshwater eutrophication, and land use.

In scenario BL, replacing conventional products is crucial, similar to climate change. The main negative contributor is the avoided raw materials production, especially due to the suspension polymerization operation in the plastic board production (supplement information III, fig. s6). However, the avoided use of plastic boards is not consistently scored in negative values. With their incineration at the end of life, heat and electricity are generated, inducing marginal heat and electricity production to compensate in the bio-based system. Hence, avoiding the disposal of plastic boards generates burdens in ionizing radiation, freshwater eutrophication, and land use, representing 13%, 81%, and 46% of the positive scores, respectively, because of the electricity produced from nuclear, plastic boards incineration, and induced heat from biomass. Because of this, BLc's net scores are positive in ionizing radiation and freshwater eutrophication. The replacement of brick brings fewer environmental benefits than the replacement of plastic boards. Most benefits come from the avoided straw (added for accelerating drying

and improving the mechanical stability, less prone to breakage and more durable in time(Snoeck and De Belie, 2015)) and energy use (heat in manufacturing and diesel in transportation). Similarly, the avoided energy consumption could be harmful to ionizing radiation. The heat generated in combined heat and power (CHP) plants would generate electricity at the same time, while the avoided bricks lower the heat demand, extra electricity needs to be generated, and electricity from nuclear would emit C-14 and radon-222, which explains 57% positive scores together. Unlike plastic boards, landfilling is more common for bricks at the end-of-life, which has few emission, hence the influence of brick disposal is not as important as that of plastic boards. Besides avoided products, the avoided energy by the energy recovered from CLT and MDF incineration also benefits the environment, especially in non-cancer human health and land use, together composing 31% and 70% of negative scores.

In the scenario BLc, positive scores in LCA mainly come from agricultural management and products manufacturing. Since there is no fertilizer and pesticide use, the influence of black locust cultivation is negligible except in land use. For scenario REFc, the land use score is lower than scenario BL, because rapeseed and silage ryegrass avoid palm oil and animal feed, further reducing the land needs to grow these. The major agricultural management activities are tree logging processes (first- and second thinning, harvesting). The diesel used in machines for logging and skidding trees to open-dry is the primary impact contribution source. The advantage of incinerating bark is similar to the CLT and MDF disposal, as a reasonable consequence of recovering heat. However, if the wood ash is left on the ground after incineration, the zinc contained in the ash would cause 36% of the total positive scores in non-cancer human health. Concerning products manufacturing, CLT is less environmentally intensive than MDF because of the urea-formaldehyde (UF) resin additive in resinating and the energy demand in matting and steaming. The production of UF resin brings 38% and 46% of the positive scores in ozone depletion and mineral resources use, respectively. Opposite to the reason why avoiding the heat generated in incineration would damage ionizing radiation, here using heat in matting is beneficial (42% of negative scores). On the other hand, this heat consumption leads to 18% positive ozone depletion scores.

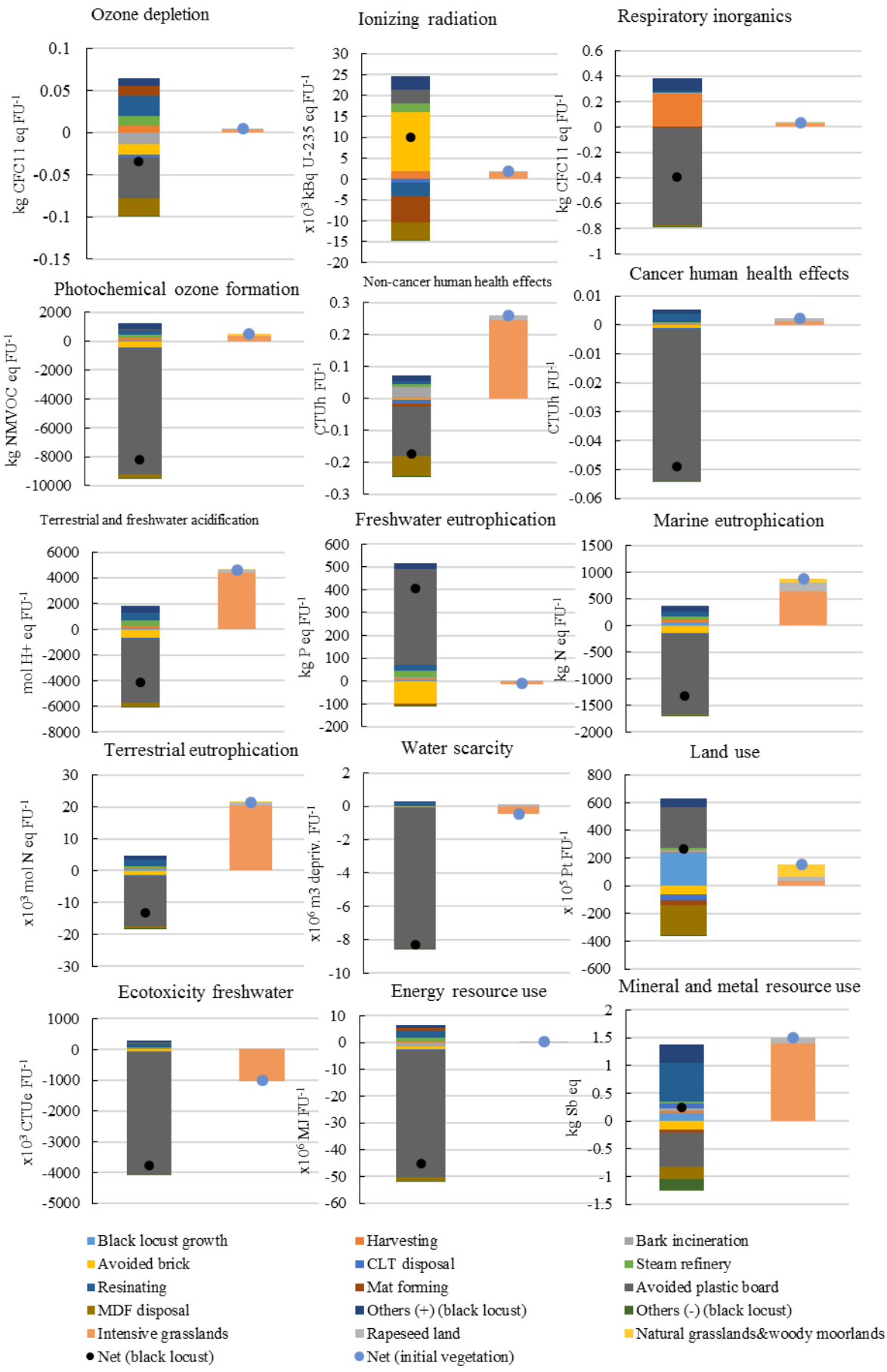
Ozone depletion
kg CFC11 eq FU-1
Ionizing radiation
x10³ kBq U-235 eq FU-1
Respiratory inorganics
kg CFC11 eq FU-1
Photochemical ozone formation
kg NMVOC eq FU-1
Non-cancer human health effects
CTUh FU-1
Cancer human health effects
CTUh FU-1
Terrestrial and freshwater acidification
mol H+ eq FU-1
Freshwater eutrophication
kg P eq FU-1
Marine eutrophication
kg N eq FU-1
Terrestrial eutrophication
x10³ mol N eq FU-1
Water scarcity
x10⁶ m3 depriv. FU-1
Land use
x 10⁵ Pt FU-1
Ecotoxicity freshwater
x10³ CTUe FU-1
Energy resource use
x10⁶ MJ FU-1
Mineral and metal resource use
kg Sb eq
Black locust growth
Harvesting
Bark incineration
Avoided brick
CLT disposal
Steam refinery
Resinating
Mat forming
Avoided plastic board
MDF disposal
Others (+) (black locust)
Others (-) (black locust)
Intensive grasslands
Rapeseed land
Natural grasslands&woody moorlands
Net (black locust)
Net (initial vegetation)

Fig. V-8 Characterized LCA results for BLc (left bar) and REFc (right bar) scenarios for all impact categories of the EF method, with the exception of climate change.

3.4 Dynamic LCA results

3.4.1 Dynamic LCA in consequential modelling

Since the consequential approach aims to evaluate the consequence of converting scenario REFc to BLc, the results for the two scenarios are compared in Fig. V-9. In the result analysis, distinction is made between the GHG (and related GMTC) stemming from the biomass (growth, decay, utilization, and end of life), noted as "bio", and the other GHG coming from anthropogenic processes referenced as "non-bio". The GMTC indicator has the property of additivity, thus the 'total' GMTC means the sum of GMTC from bio and non-bio contributors.

Concerning the REFc scenario, the GMTC (Total REFc) is positive during the cultivation period except the first five years due to the avoided products. During the cultivation, 76% of captured C is released in a short time from the residue decomposition. Moreover, the part of residues decomposed anaerobically emits CH_4 for 3% of the total C emission, in the first ten years (2022-2031); the CH_4 contribution in bio GMTC represents up to 25%, but decreases because of the short lifespan of CH_4 in the atmosphere (Masson-Delmotte et al., 2021). For the same reason, the CH_4 burden decreases sharply beyound the cultivation period, leading to the decrease of bio GMTC. Meanwhile, non-bio GMTC continuously decreases till the end of feedstock manufacturing, mainly because of the avoided CO_2 emission from the replaced feedstock by ryegrass. The short lifespan of biogenic CH_4 and the relatively long-term CO_2 emissions from non-bio sources lead the non-bio GHG to dominate the trend of scenario REFc after the year 2150.

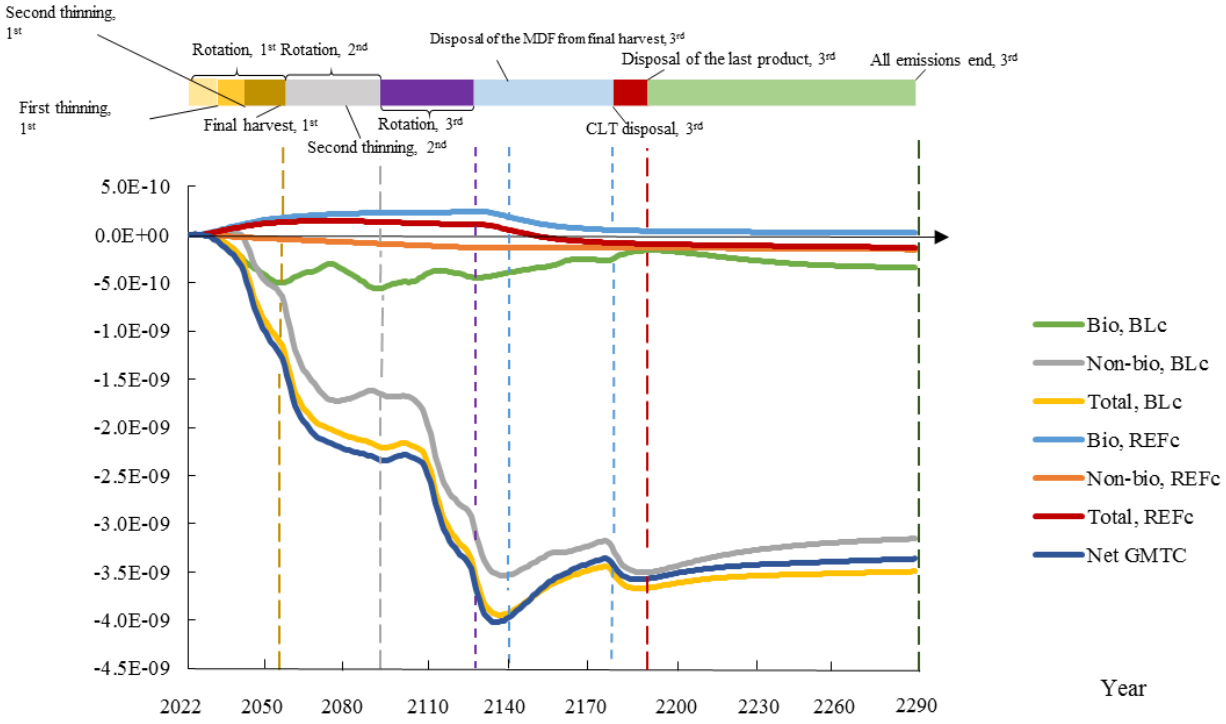

Fig. V-9 GMTC results for all GHG sources from REFc and BLc scenarios, and the consequence of replacing REFc with BLc. Total BLc = Bio BLc + Non bio BLc; Total REFc= Bio REFc + Non bio REFc; Net GMTC = Total BLc – Total REFc. 1st, 2nd, 3rd refer to the rotation number.

Concerning BLc scenario, in the first years of cultivation, the C captured is low and SOC mineralization is relatively high (Fig. V-6b), making the bio GMTC positive (Fig. V-9, Bio BLc). Along with black locust growth, the C capture and increased SOC lead the bio GMTC to be negative, and hence the scenario BL turns to negative GMTC in the year 2028 (Fig. V-9, Total BLc). The GMTC due to CH_4 emission represents a maximum of 9%, CO_2 being the most contributor to overall results. The increase of bio GMTC (Bio BLc) after the last rotation is explained by the stop of C capture, and the bio GHG emissions from the end of life incineration of MDF and CLT (the stored biogenic C is released back to the atmosphere).

The GMTC of non-bio sources (Non-bio BLc) is positive at the beginning, due to the emissions from tree plantation and iLUC. After the second thinning (the year 2041), non-bio GMTC becomes negative and more and more important due to the plastic boards and bricks replacement by the bio-based products (MDF and CLT), involving manufacturing, use, and end-of-life processes. The biggest contributor is the avoided CO_2 emission from the plastic board life cycle. The avoided plastic boards are counted at the time when MDF is produced, namely during first and second thinning and harvesting (the year 2032/2067/2102, 2042/2077/2112, 2057/2092/2127, 2108/2142/2178 respectively). The sharp decrease around 2057 is due to more plastic boards being avoided by more MDF being produced at the final harvest.

The non-bio GHG flows strongly determine the BL scenario result (Total BLc) after 2049 and finally, the net GMTC shows that replacing the scenario REFc by BLc can mitigate global warming. The mitigation effectiveness increases with the cultivation duration, and the negative peak on Net GMTC curve occurs several years later after the end of the cultivation, around 2135. The delay between the end of the cultivation and the GMTC peak is due to the thermal inertia of various environmental compartments(Shimako et al., 2016).

3.4.2 Dynamic LCA in attributional modeling

The GMTC results for the attributional (with average background processes) and system expansion modeling are presented in Fig. V-10, for REFa (top) and BLc (bottom) scenarios. The impact of each system is referenced as ‘net’ REFa and BLc, obtained by the aggregation of all system’s contributors. In this modeling approach, only the CO_2 capture processes result in negative GMTC, all other processes generate impacts, hence positive GMTC.

In REFa system, the bio REFa is the same as the bio REFc in 3.4.1 (it involves no background processes), and will not be detailed anymore. Non-bio GMTC remains at a higher level for long term due to the accumulation of CO_2 (long lived gas) emitted during the whole time span. In the first decades, the impacts of agricultural management and later activities (Non-bio REFa), involving oil mill operation and ryegrass silage, are negligible compared to the GMTC from biogenic GHG flows. In REFa system, the biggest contributor is the plastic board (production, use, and end-of-life incineration), dominating the net REFa after 2043. CO_2 and CH_4, emitted as pulse in the year of MDF manufacture and disposal, are the primary contributors to GMTC., while conventional brick and heat production contribute little to the net GMTC result. The REFa system, despite slightly negative net GMTC during the first years, is definitely inadequate for global warming mitigation.

The net GMTC of the BLa system presents zones with negative GMTC. The bio contributor of BL scenario is the same as in consequential modeling and was analyzed in section 3.4.1. The non-bio GHG emissions stem from iLUC, wood logging operation, MDF&CLT production, disposal processes, and all related background processes, and always lead to positive GMTC. The GMTC from non-biogenic sources increases continuously, with sharp slopes when impulse emissions occur from these processes. At the end of anthropogenic activities, non-bio GMTC decreases slowly due to the CO_2 accumulated during the activity period. Because the CO_2 capture vanishes with the harvesting of woods, the net GMTC increases and becomes positive in 2072, then decreases sharply with the tree growth during the

second rotation. Following the same trend, after the second rotation, the GMTC becomes positive for a while and continues to increase due to the non-bio contributors and additional processes. Concerning the additional products, feedstock affects the GMTC more than palm oil, CO_2 emission during the agricultural management being the major contributor.

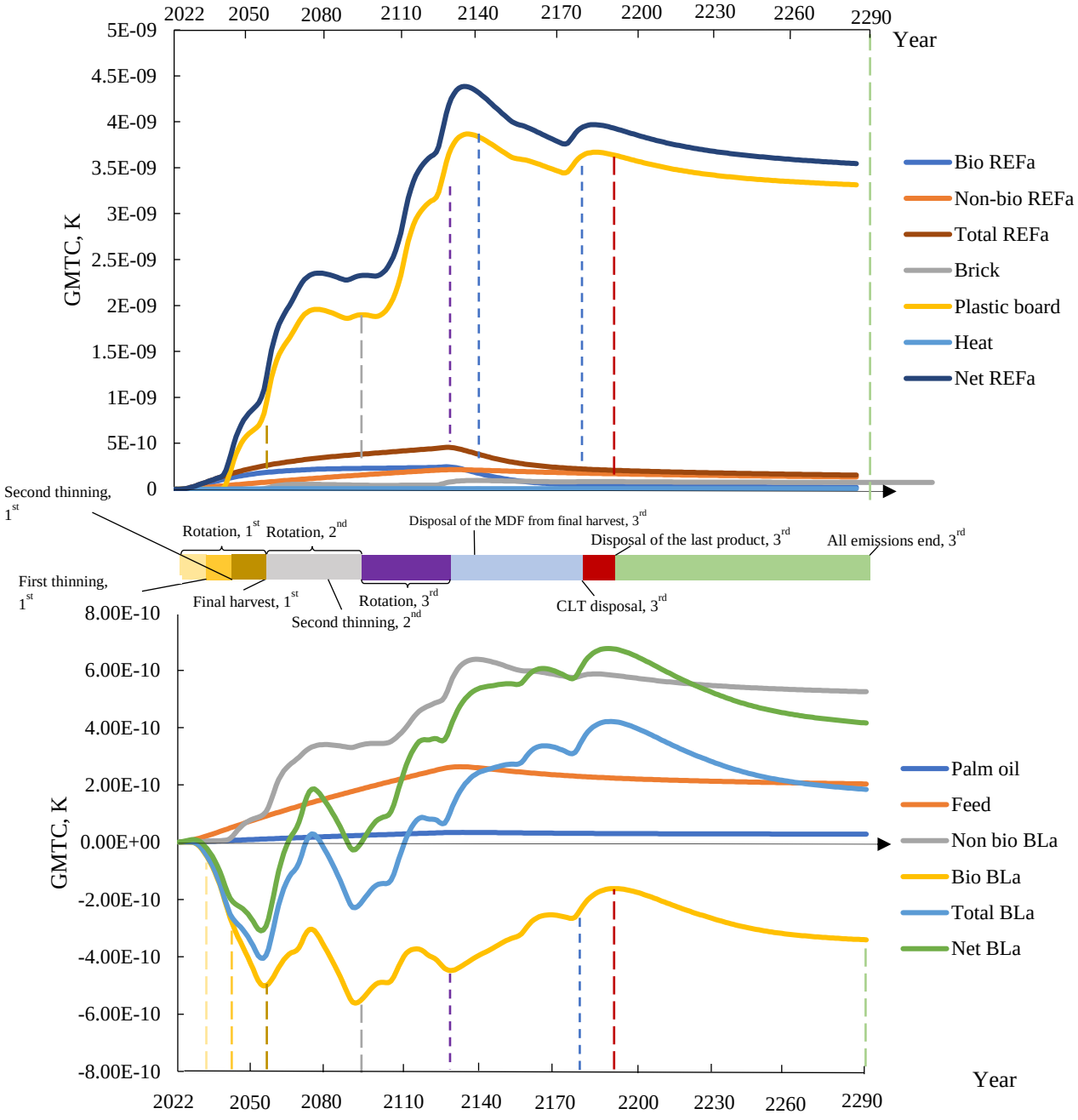

Fig. V-10 GMTC evolution in REFa (above) and BLa (bottom) scenario with time. 1st, 2nd, 3rd refer to the rotation number. Total BLa = Bio BLa + Non bio BLa; Net BLa = Total BLa+ Palm oil + Feed; Total VGa = Bio VGa + Non bio VGa; Net REFa = Total VGa + Heat + Plastic board + Brick.

3.5 Sensitivity analysis

Since the production and disposal of plasterboards and PP boards are less impacting than PVC boards, replacing plasterboards and PP boards instead of PVC boards would bring less environmental benefits, resulting in a negative percentage in most impacts (Fig. V-11, plasterboard, PP board), and mineral

resources is the most sensitive impact among them. In climate change, replacing plasterboards is more sensitive than replacing PP boards, since the plasterboard production is the least GHG intensive (especially for fossil CO_2). Interestingly, for impacts that the scenario BLc was worse than scenario REFc, plasterboards and PP boards would lead to better results in land use and freshwater eutrophication. At the end-of-life, the open burning of PP boards would emit a high amount of vanadium to soils, bringing more profits in ecotoxicity freshwater when it is avoided.

If CLT replaces concrete bricks rather than clay bricks, the ranking in most environmental impacts does not vary considerably except in ionizing radiation. Compared to clay bricks, concrete bricks demand less heat but more electricity. When CLT substitutes concrete bricks, this higher electricity consumption is avoided, leading to lesser C-14 and randon-222 emissions (from nuclear electricity).

When CLT is 100% recycled, more MDF are produced from recycled CLT, hence more plastic boards are avoided, this scenario performs better in most impacts, except in freshwater eutrophication (from avoided plastic board incineration) and mineral resources use (higher metal demand, e.g., cadmium and lead, for UF resin used in MDF manufacturing). Avoiding more plastic boards cannot compensate for this disadvantage. Among the four sensitivity scenarios, recycling 100% CLT could provide more benefits in most environmental impacts. Future studies could investigate the design of the recycling approach, the different approaches could cause more than double the difference in CO_2-eq (Cascione et al., 2022).

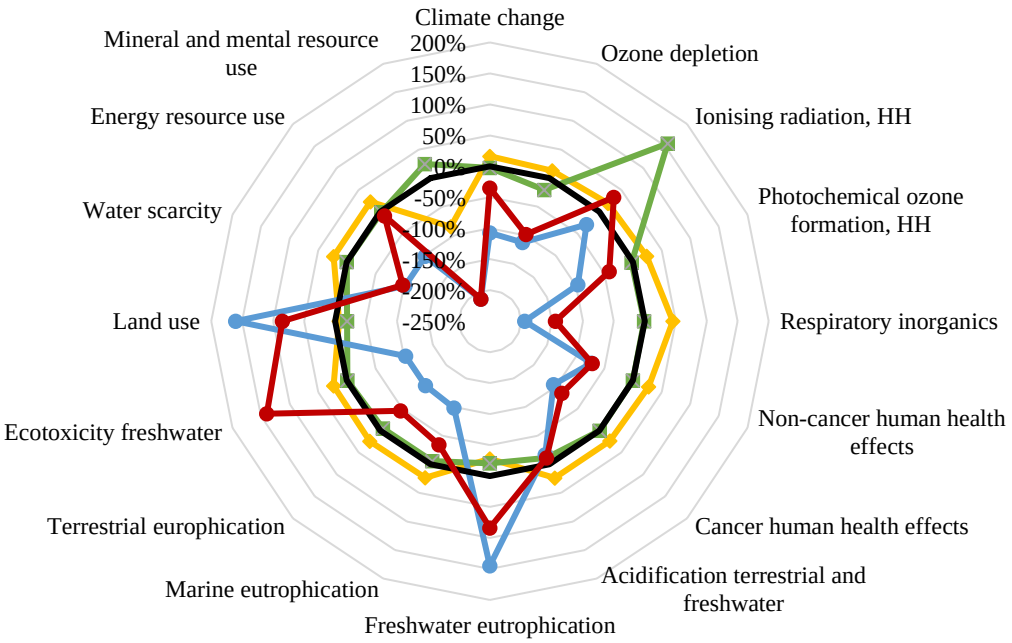

Fig. V-11 Sensitivity analysis of: 100% CLT recycling, CLT avoids concrete, and MDF avoids plasterboard or PP board. The positive percentage means a scenario is better than the initial scenario in this impact.

3.6 Uncertainty analysis

The contribution analysis and sensitivity analysis identified ten parameters in total that play key roles in environmental impacts (supplement information III, table s26). Based on their representative of the

uncertainty in all impacts, six of ten parameters are the most influential: quantity of avoided PVC; woody biomass yield; recycling/incineration ratio in CLT disposal; used UF resin amount; dust emitted during logging; fossil fuel for avoided heat generation.

In general, the uncertainty of all impacts for BLc is lower than 10% except for mineral resource use (12%) (supplement information III, table s27). Compared to BLc, the uncertainty of REFc is relatively higher, the freshwater eutrophication is the most uncertain impact (27%), due to the variance of the quantity of maize in the avoided feed (representative: 78%) (supplement information III, table s28). Considering the ranges of impact scores could vary based on the analyzed results, the orders of the two scenarios observed in Fig. V-7 and Fig. V-8 could be confirmed since they are the same as in Table V-1. There are significant differences between BLc and REFc in the sixteen environmental impacts, planting black locust on CV-lands is beneficial for thirteen environmental impacts.

Table V-1 Uncertainty range of LCA results[a].

Impact category		**Score range**			
		Scenario BLc		**Scenario REFc**	
	Unit	**Lower value**	**Higher value**	**Lower value**	**Higher value**
Climate change	t CO_2-eq	-2290	-2120	-58.9	-43.2
Ozone depletion	kg CFC11 eq	-0.0365	-0.0317	0.00459	0.00518
Ionizing radiation	kBq U-235 eq	9360	10500	1710	1980
Photochemical ozone formation, HH	kg NMVOC eq	-8710	-7730	449	507
Respiratory inorganics	disease inc.	-0.43	-0.358	0.0281	0.0324
Non-cancer human health effects	CTUh	-0.184	-0.163	0.242	0.278
Cancer human health effects	CTUh	-0.0517	-0.0459	0.0021	0.00231
Acidification terrestrial and freshwater	mol H+ eq	-4390	-3880	4300	4930
Freshwater eutrophication	kg P eq	382	432	-14.3	-8.14
Marine eutrophication	kg N eq	-1400	-1230	837	928
Terrestrial eutrophication	$x10^2$ mol N eq	-141	-124	199	229
Ecotoxicity freshwater	$x10^4$ CTUe	-399	-354	-109	-91.2
Land use	$x10^5$ Pt	261	277	147	165
Water scarcity	$x10^4$ m3 depriv.	-879	-780	-50.3	-41.7
Resource use, energy carriers	$x10^5$ MJ	-477	-423	2.34	2.93
Resource use, mineral and metals	kg Sb eq	0.217	0.278	1.39	1.60

[a] Impact with grey background means scenario REFc is better than BLc, otherwise, BLc is better.
Figures are presented with a maximum of 3 significant digits.

3.7 Overall implications, limitations and perspectives

The time horizon scrutinized herein encompasses this century, having in mind the climate goals of neutrality by 2050 and keeping the global mean temperature increase below 2°C. In the last report (IPCC, 2022), the IPCC stresses the importance of "near-term actions that limit global warming to close to 1.5°C would substantially reduce projected losses and damages related to climate change", near-term being 2021-2040, while mid-term and long-term refer to 2041-2060 and 2081-2100 respectively.

The average annual SOC increase in black locust cultivation is 0.72 Mg ha^{-1} higher than that of initial vegetation. Furthermore, the SOC level after three rotations (circa 134 Mg ha^{-1}) is higher than the average SOC in French lands covered by grass or forest(81- 85 Mg t ha^{-1}, Pellerin et al., 2021). SOC deserves more attention and experimental investigation in order to validate/fit the simulation results.

Gathering the simulation results for the SOC, biomass growth, decay, and amount of products, allows calculating the total C stock and comparing it to the C captured during the whole period (Fig. V-12), the difference between the two being the biogenic C released into the atmosphere. The C stock in products is higher than in soil. The net stock also represents the negative emissions that the BL scenario could induce (81%, 39%, 15% of total captured C, in the year 2050, 2100, 2290 respectively. Supplement information III, fig. s11).

Annualizing the CO_2 absorption to compare with annual grass, black locust could capture twice than the initial vegetation, similar to a vigorous energy grass (Hamelin et al., 2012). Compared to 14 wood species cultivated in France (Albers et al., 2019a), black locust could fix more C than the average of these species over the same period while attaining maturity well before the average maturity time of about 80 years.

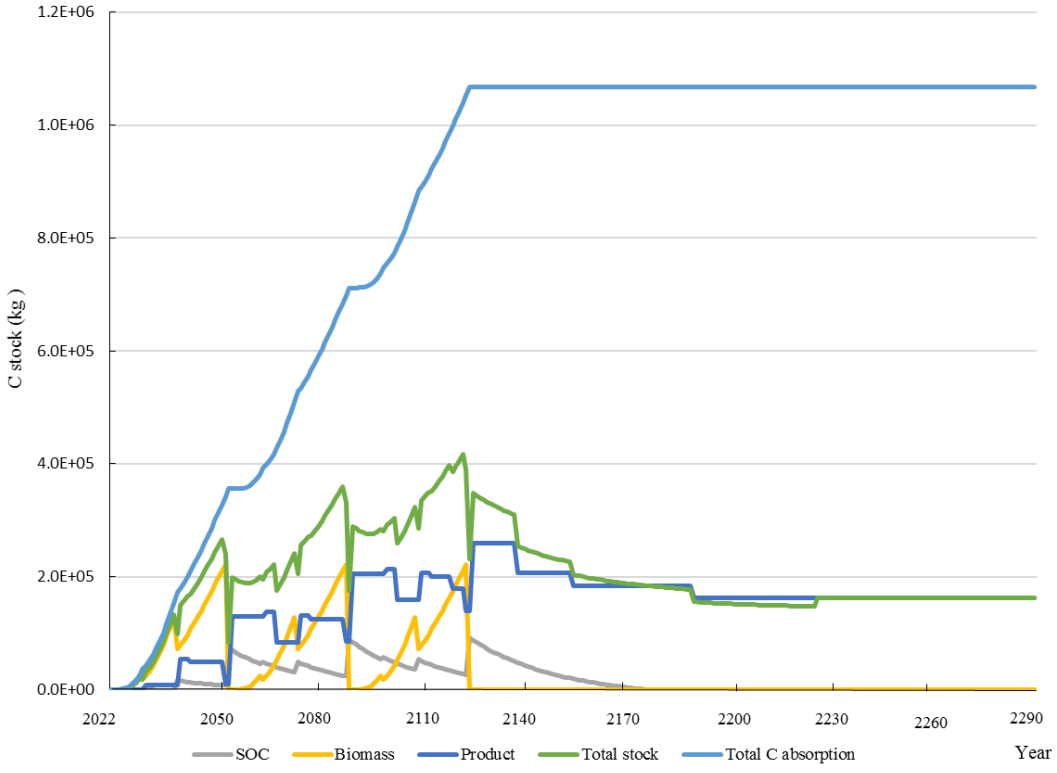

Fig. V-12 Carbon captured over the culture period, and biogenic carbon stocks during the lifetime of the BL scenario.

In the value chain proposed, bio-based products can replace fossil-based products with problematic environmental footprint at the level of their manufacturing and, significantly, of their end-of-life management.

The static LCA highlighted that replacing the initial vegetation with the black locust value chain is beneficial for the environment in 13 of 16 environmental impacts, mainly due to the fossil-based replacement. The use of resins/plastics in both bio-based and fossil-based products is critical in many impacts as figured out by LCA and confirmed by other studies (e.g., Nakano et al., 2018, Silva et al., 2013, etc.), therefore less or no resin additive is matter of investigation (Kouchaki-Penchah et al., 2016; Puettmann, 2016). The high environmental impacts of plastic production could be mitigated by other choices for the board material, as highlighted by the sensitivity analysis. Further, with the development of plastic recycling and replacement, lesser GHG emissions could be expected from production and incineration (Deng, 2014; Schwarz et al., 2021; Ye et al., 2017).

All conducted LCA modeling approaches indicate that black locust is better than the initial situation, either by measuring the consequence of this replacement as negative kg CO_2-eq and negative net GMTC, or by measuring/comparing the actual impact. BLa scenario could be a negative emission strategy in the near- and mid-term (2030-2063) when net GMTC is negative. It is certainly a mitigation solution from 2026- 2029, when the net GMTC is lower than that of REFa system but still positive (Fig. 10). The BL scenario alone satisfies the neutrality in this century (2027), but its implementation requires producing feedstock and oil elsewhere, hence attention must be paid to the net GMTC of the whole BLa system. Its increase in the second half of the century could be mitigated with appropriate solutions at the level of all manufacturing and end-of-life technologies, i.e. less fossil-based background processes and promoting wood material recycling instead of incineration. If the systems are scaled-up to the whole CV-lands in France, the REFa system increases the global mean temperature with 0.0020°C and 0.0056 °C by 2050 and 2100. BLa system decreases the temperature with 0.0006°C in the mid-term, but increases it by 2100 with 0.0002°C, with a peak in between which must be mitigated. Of course, these values are only orders of magnitude, to be relativized to the feasibility of using the whole CV-land potential.

4 Conclusion

This study investigated the relevance of using black locust as biopump to contribute to global warming mitigation following the CSAAP concept. A value chain was proposed from tree planting on CV-lands in France, to bio-based products manufacturing, use, and end-of-life, as an alternative to leaving the CV-lands as they are presently. This system runs from the first year of cultivation to the end of life of products, encompassing three rotations (in total 267 years).

Simulation results of biomass growth, decay, and SOC changes showed, throughout three rotations, that black locust induces more C stock in soils (considered as negative emission) and in the harvestable biomass (wood) than the initial vegetation, for an annual average SOC increase of 16‰.

Replacing the initial state with the black locust value chain could mitigate global warming and is beneficial to the environment for 13 of the 16 impact categories evaluated through consequential LCA. Hence, improving climate change impact does not worsen the other environmental issues.

Considering the climate goals, black locust value chain implementation results in climate cooling effect by net negative emissions, in the near and mid-term, but with a GMTC overshot in the second half of the century, which must be mitigated. Therefore, this study highlighted the importance of emissions stemmed from manufacturing and end-of-life (all background processes), which offset the benefit of C capture, and the need to act on every component of the system to achieve the goal of neutrality.

This study provided an integrated and comprehensive framework for proposing and analyzing mitigation solutions for global warming, which could be applied to other cases.

Supplement information

Supplementary information III contains : documented LCA inventory, details on modeling approaches, results.

References

Adamopoulos, S., Passialis, C., Voulgaridis, E., 2007. Strength properties of juvenile and mature wood in black locust (Robinia pseudoacacia L.). Wood Fiber Sci. 39, 241–249.

ADEME, 2018. ADEME 2035-2050 Updated Energy-Climate Scenario.

Albers, A., Collet, P., Benoist, A., Hélias, A., 2019a. Data and non-linear models for the estimation of biomass growth and carbon fixation in managed forests. Data Br. 23. https://doi.org/10.1016/j.dib.2019.103841

Albers, A., Collet, P., Lorne, D., Benoist, A., Hélias, A., 2019b. Coupling partial-equilibrium and dynamic biogenic carbon models to assess future transport scenarios in France. Appl. Energy 239, 316–330. https://doi.org/10.1016/j.apenergy.2019.01.186

Andrade, C., Rangueil, A. De, Zamora-ledezma, E., Hamelin, L., 2022. A review on the interplay between bioeconomy and soil organic carbon stocks maintenance .

Barna, L.T., 2021. A climate goal – based , multicriteria method for system evaluation in life cycle assessment. Int. J. Life Cycle Assess. https://doi.org/10.1007/s11367-021-01991-1

Bisinella, V., Conradsen, K., Christensen, T.H., Astrup, T.F., 2016. A global approach for sparse representation of uncertainty in Life Cycle Assessments of waste management systems. Int. J. Life Cycle Assess. 21, 378–394. https://doi.org/10.1007/s11367-015-1014-4

Bisinella, V., Götze, R., Conradsen, K., Damgaard, A., Christensen, T.H., Astrup, T.F., 2017. Importance of waste composition for Life Cycle Assessment of waste management solutions. J. Clean. Prod. 164, 1180–1191. https://doi.org/10.1016/j.jclepro.2017.07.013

Brandao, M., Martin, M., Cowie, A., Hamelin, L., Zamagni, A., 2017. Consequential Life Cycle Assessment: What, How, and Why? Encycl. Sustain. Technol. 1, 277–284. https://doi.org/10.1016/B978-0-12-409548-9.10068-5

Brander, M., 2017. Comparative analysis of attributional corporate greenhouse gas accounting, consequential life cycle assessment, and project/policy level accounting: A bioenergy case study. J. Clean. Prod. 167, 1401–1414. https://doi.org/10.1016/j.jclepro.2017.02.097

Cadorel, X., Crawford, R., 2019. Life cycle analysis of cross laminated timber in buildings: a review. Engag. Archit. Sci. Meet. Challenges High. Density 52nd Int. Conf. Archit. Sci. Assoc. 2018 15978, 107–114.

Cardellini, G., Mutel, C.L., Vial, E., Muys, B., 2018. Temporalis, a generic method and tool for dynamic Life Cycle Assessment. Sci. Total Environ. 645, 585–595. https://doi.org/10.1016/j.scitotenv.2018.07.044

Cascione, V., Roberts, M., Allen, S., Dams, B., Maskell, D., Shea, A., Walker, P., Emmitt, S., 2022.

Integration of life cycle assessments (LCA) in circular bio-based wall panel design. J. Clean. Prod. 344, 130938. https://doi.org/10.1016/j.jclepro.2022.130938

Chen, C.X., Pierobon, F., Ganguly, I., 2019. Life Cycle Assessment (LCA) of Cross-Laminated Timber (CLT) produced in Western Washington: The role of logistics and wood species mix. Sustain. 11. https://doi.org/10.3390/su11051278

Chen, D., Rojas, M., Samset, B.H., Cobb, K., Diongue-Niang, A., Edwards, P., Emori, S., Faria, S.H., Hawkins, E., Hope, P., Huybrechts, P., Meinshausen, M., Mustafa, S.K., Plattner, G.-K., Treguier, A.M., 2021. Framing, Context, and Methods., in: Climate Change 2021: The Physical Science Basis. Contribution of Working Group I to the Sixth Assessment Report of the Intergovernmental Panel on Climate Change. IPCC.

Chen, J., Zhang, H., Zhang, X., Tang, M., 2020. Arbuscular mycorrhizal symbiosis mitigates oxidative injury in black locust under salt stress through modulating antioxidant defence of the plant. Environ. Exp. Bot. 175, 104034. https://doi.org/10.1016/j.envexpbot.2020.104034

Ciccarese, L., Pellegrino, P., Silli, V., Zanchi, G., 2014. Short rotation forestry and methods for carbon accounting. A case study of black locust (Robinia pseudoacacia L.) plantation in central Italy. Rapporti 200, 5.

Clivot, H., Mouny, J.C., Duparque, A., Dinh, J.L., Denoroy, P., Houot, S., Vertès, F., Trochard, R., Bouthier, A., Sagot, S., Mary, B., 2019. Modeling soil organic carbon evolution in long-term arable experiments with AMG model. Environ. Model. Softw. 118, 99–113. https://doi.org/10.1016/j.envsoft.2019.04.004

Corradini, G., Pierobon, F., Zanetti, M., 2019. Product environmental footprint of a cross-laminated timber system: a case study in Italy. Int. J. Life Cycle Assess. 24, 975–988. https://doi.org/10.1007/s11367-018-1541-x

Couret, L., Irle, M., Belloncle, C., Cathala, B., 2017. Extraction and characterization of cellulose nanocrystals from post-consumer wood fiberboard waste. Cellulose 24, 2125–2137. https://doi.org/10.1007/s10570-017-1252-7

Cowie, A.L., Berndes, G., Bentsen, N.S., Brandão, M., Cherubini, F., Egnell, G., George, B., Gustavsson, L., Hanewinkel, M., Harris, Z.M., Johnsson, F., Junginger, M., Kline, K.L., Koponen, K., Koppejan, J., Kraxner, F., Lamers, P., Majer, S., Marland, E., Nabuurs, G.J., Pelkmans, L., Sathre, R., Schaub, M., Smith, C.T., Soimakallio, S., Van Der Hilst, F., Woods, J., Ximenes, F.A., 2021. Applying a science-based systems perspective to dispel misconceptions about climate effects of forest bioenergy. GCB Bioenergy 13, 1210–1231. https://doi.org/10.1111/gcbb.12844

da Costa, T.P., Quinteiro, P., Tarelho, L.A. da C., Arroja, L., Dias, A.C., 2018. Environmental impacts of forest biomass-to-energy conversion technologies: Grate furnace vs. fluidised bed furnace. J. Clean. Prod. 171, 153–162. https://doi.org/10.1016/j.jclepro.2017.09.287

Deng, Y., 2014. Life cycle assessment of biobased fibre-reinforced polymer composites. World Scientific. https://doi.org/10.1142/9789814566469_0063

Dodoo, A., Gustavsson, L., Sathre, R., 2014. Lifecycle primary energy analysis of low-energy timber building systems for multi-storey residential buildings. Energy Build. 81, 84–97. https://doi.org/10.1016/j.enbuild.2014.06.003

DRIAS CERFACS, IPSL, M.-F., 2013. CNRM-CERFACS-CM5/CNRM-ALADIN63-RCP4.5. DRIAS les Futur. du Clim.

ecoinvent, 2020. Ecoinvent 3.5 database [WWW Document]. URL https://www.ecoinvent.org/database/ecoinvent-37/new-data-in-ecoinvent-37/new-data-in-ecoinvent-37.html

European Commission-Joint Research Centre., 2010. General guide for life cycle assessment—detailed guidance. In: ILCD Handbook—International Reference Life Cycle Data System, first ed.

Fazio, S., Biganzioli, F., De Laurentiis, V., Zampori, L., Sala, S., Diaconu, E., 2018a. Supporting information to the characterisation factors of recommended EF Life Cycle Impact Assessment methods, version 2, from ILCD to EF 3.0, EUR 29600 EN, European Commission, Ispra, 2018, ISBN 978-92-79-98584-3, doi:10.2760/002447, PUBSY No. JRC114822., New Models and Differences with ILCD, EUR. https://doi.org/10.2760/002447

Fazio, S., Zampori, L., A, D.S., Kusche, O., 2018b. Guide on Life Cycle Inventory (LCI) data generation for the Environmental Footprint. https://doi.org/10.2760/745658

Food and Agriculture Organization of the United Nations, 2020. GSOCmap v1.5.0 [WWW Document]. URL http://54.229.242.119/GSOCmap/

Global Market Insights, 2021. Cross Laminated Timber (CLT) Market Size By Raw Materials (Spruce, Fir, Pine, Larch), By Press Type (Hydraulic, Vacuum, Pneumatic, Nails), By Application (Residential, Commercial, Industrial), Industry Analysis Report, Regional Outlook, Application Growth.

González-García, S., Gasol, C.M., Moreira, M.T., Gabarrell, X., Pons, J.R.I., Feijoo, G., 2011. Environmental assessment of black locust (Robinia pseudoacacia L.)-based ethanol as potential transport fuel. Int. J. Life Cycle Assess. 16, 465–477. https://doi.org/10.1007/s11367-011-0272-z

Göswein, V., Pittau, F., Silvestre, J.D., Freire, F., Habert, G., 2020. Dynamic life cycle assessment of straw-based renovation: A case study from a Portuguese neighbourhood. IOP Conf. Ser. Earth Environ. Sci. 588. https://doi.org/10.1088/1755-1315/588/4/042054

Guest, G., Cherubini, F., Strømman, A.H., 2013. Global Warming Potential of Carbon Dioxide Emissions from Biomass Stored in the Anthroposphere and Used for Bioenergy at End of Life. J. Ind. Ecol. 17, 20–30. https://doi.org/10.1111/j.1530-9290.2012.00507.x

Guo, H., Liu, Y., Meng, Y., Huang, H., Sun, C., Shao, Y., 2017. A Comparison of the energy saving and carbon reduction performance between reinforced concrete and cross-laminated timber structures in residential buildings in the severe cold region of China. Sustain. 9. https://doi.org/10.3390/su9081426

Hamelin, L., Jørgensen, U., Petersen, B.M., Olesen, J.E., Wenzel, H., 2012. Modelling the carbon and nitrogen balances of direct land use changes from energy crops in Denmark: A consequential life cycle inventory. GCB Bioenergy 4, 889–907. https://doi.org/10.1111/j.1757-1707.2012.01174.x

Hansen, J.H., Hamelin, L., Taghizadeh-Toosi, A., Olesen, J.E., Wenzel, H., 2020. Agricultural residues bioenergy potential that sustain soil carbon depends on energy conversion pathways. GCB Bioenergy 12, 1002–1013. https://doi.org/10.1111/gcbb.12733

IPCC, 2022. Climate Change: Impacts, Adaptation, and Vulnerability. Contribution of Working Group II to the Sixth Assessment Report of the Intergovernmental Panel on Climate Change; Pörtner, H, O., Roberts, DC, Tignor, ES, Poloczanska, M., Mintenbeck, K., Alegría, A., Craig, M., Langsdorf, S., Löschke, S., Möller, V., et al., Eds.

IPCC, 2019. Refinement to the 2006 IPCC Guidelines for National Greenhouse Gas Inventories

Volume 5 Waste, IPCC Good Practice Guidance and Uncertainty Management in National Greenhouse Gase Inventories.

Jayalath, A., Navaratnam, S., Ngo, T., Mendis, P., Hewson, N., Aye, L., 2020. Life cycle performance of Cross Laminated Timber mid-rise residential buildings in Australia. Energy Build. 223, 110091. https://doi.org/10.1016/j.enbuild.2020.110091

Kassara, G., Pena Verrier, G., Chammas, M., Fournie, L., Mainsant, A., Marchal, D., Parrouffe, J.-M., 2019. Trajectories of evolution of the electricity mix 2020-2060: Additional analyses, FAQs, Report on data.

Keel, S.G., Leifeld, J., Mayer, J., Taghizadeh-Toosi, A., Olesen, J.E., 2017. Large uncertainty in soil carbon modelling related to method of calculation of plant carbon input in agricultural systems. Eur. J. Soil Sci. 68, 953–963. https://doi.org/10.1111/ejss.12454

Keresztesi, B., 1983. Breeding and cultivation of black locust, Robinia pseudoacacia, in Hungary. For. Ecol. Manage. 6, 217–244. https://doi.org/10.1016/S0378-1127(83)80004-8

Kouchaki-Penchah, H., Sharifi, M., Mousazadeh, H., Zarea-Hosseinabadi, H., 2016. Life cycle assessment of medium-density fiberboard manufacturing process in Islamic Republic of Iran. J. Clean. Prod. 112, 351–358. https://doi.org/10.1016/j.jclepro.2015.07.049

Lan, K., Kelley, S.S., Nepal, P., Yao, Y., 2020. Dynamic life cycle carbon and energy analysis for cross-laminated timber in the Southeastern United States. Environ. Res. Lett. 15, 124036. https://doi.org/10.1088/1748-9326/abc5e6

Launay, C., Constantin, J., Chlebowski, F., Houot, S., Graux, A.I., Klumpp, K., Martin, R., Mary, B., Pellerin, S., Therond, O., 2021. Estimating the carbon storage potential and greenhouse gas emissions of French arable cropland using high-resolution modeling. Glob. Chang. Biol. 27, 1645–1661. https://doi.org/10.1111/gcb.15512

Liu, Y., Guo, H., Sun, C., Chang, W.S., 2016. Assessing cross laminated timber (CLT) as an alternative material for mid-rise residential buildings in cold regions in China-A life-cycle assessment approach. Sustain. 8. https://doi.org/10.3390/su8101047

Masson-Delmotte, V., P. Zhai, A. Pirani, S.L., Connors, C. Péan, S. Berger, N. Caud, Y. Chen, L. Goldfarb, M.I. Gomis, M. Huang, K. Leitzell, E. Lonnoy, J.B.R., Matthews, T.K. Maycock, T. Waterfield, O. Yelekçi, R. Yu, and B.Z. (eds. ., 2021. IPCC, 2021: Climate Change 2021-the Physical Science basis, Cambridge University Press.

Minasny, B., Malone, B.P., McBratney, A.B., Angers, D.A., Arrouays, D., Chambers, A., Chaplot, V., Chen, Z.S., Cheng, K., Das, B.S., Field, D.J., Gimona, A., Hedley, C.B., Hong, S.Y., Mandal, B., Marchant, B.P., Martin, M., McConkey, B.G., Mulder, V.L., O'Rourke, S., Richer-de-Forges, A.C., Odeh, I., Padarian, J., Paustian, K., Pan, G., Poggio, L., Savin, I., Stolbovoy, V., Stockmann, U., Sulaeman, Y., Tsui, C.C., Vågen, T.G., van Wesemael, B., Winowiecki, L., 2017. Soil carbon 4 per mille. Geoderma 292, 59–86. https://doi.org/10.1016/j.geoderma.2017.01.002

Nakano, K., Ando, K., Takigawa, M., Hattori, N., 2018. Life cycle assessment of wood-based boards produced in Japan and impact of formaldehyde emissions during the use stage. Int. J. Life Cycle Assess. 23, 957–969. https://doi.org/10.1007/s11367-017-1343-6

Nicolescu, V.N., Hernea, C., Bakti, B., Keserű, Z., Antal, B., Rédei, K., 2018. Black locust (Robinia pseudoacacia L.) as a multi-purpose tree species in Hungary and Romania: a review. J. For. Res. 29, 1449–1463. https://doi.org/10.1007/s11676-018-0626-5

Nicolescu, V.N., Rédei, K., Mason, W.L., Vor, T., Pöetzelsberger, E., Bastien, J.C., Brus, R., Benčať, T., Đodan, M., Cvjetkovic, B., Andrašev, S., La Porta, N., Lavnyy, V., Mandžukovski, D., Petkova, K., Roženbergar, D., Wąsik, R., Mohren, G.M.J., Monteverdi, M.C., Musch, B., Klisz, M., Perić, S., Keça, L., Bartlett, D., Hernea, C., Pástor, M., 2020. Ecology, growth and management of black locust (Robinia pseudoacacia L.), a non-native species integrated into European forests. J. For. Res. 31, 1081–1101. https://doi.org/10.1007/s11676-020-01116-8

Onyeaju, M.C., Osarolube, E., Chukwuocha, E.O., Ekuma, C.E., Omasheye, G.A.J., 2012. Comparison of the Thermal Properties of Asbestos and Polyvinylchloride (PVC) Ceiling Sheets. Mater. Sci. Appl. 03, 240–244. https://doi.org/10.4236/msa.2012.34035

Pehme, S., Veromann, E., Hamelin, L., 2017. Environmental performance of manure co-digestion with natural and cultivated grass – A consequential life cycle assessment. J. Clean. Prod. 162, 1135–1143. https://doi.org/10.1016/j.jclepro.2017.06.067

Pellerin, S., Bamière, L., Savini, I., Réchauchère, O., 2021. Stocker du carbone dans les sols français. Quel potentiel au regard de l'objectif 4 pour 1000 et à quel coût? Stock. du carbone dans les sols français. https://doi.org/10.35690/978-2-7592-3149-2

Petersen, B.M., Berntsen, J., Hansen, S., Jensen, L.S., 2005. CN-SIM - A model for the turnover of soil organic matter. I. Long-term carbon and radiocarbon development. Soil Biol. Biochem. 37, 359–374. https://doi.org/10.1016/j.soilbio.2004.08.006

Petersen, B.M., Knudsen, M.T., Hermansen, J.E., Halberg, N., 2013. An approach to include soil carbon changes in life cycle assessments. J. Clean. Prod. 52, 217–224. https://doi.org/10.1016/j.jclepro.2013.03.007

Piekarski, C.M., de Francisco, A.C., da Luz, L.M., Kovaleski, J.L., Silva, D.A.L., 2017. Life cycle assessment of medium-density fiberboard (MDF) manufacturing process in Brazil. Sci. Total Environ. 575, 103–111. https://doi.org/10.1016/j.scitotenv.2016.10.007

Puettmann, M., 2016. Cradle to Gate Life Cycle Assessment of North American Cellulosic Fiberboard Production 1–66.

Rédei, K., Csiha, I., KeserU, Z., Gál, J., 2012. Influence of regeneration method on the yield and stem quality of black locust (Robinia pseudoacacia L.) Stands: A case study. Acta Silv. Lignaria Hungarica 8, 103–112. https://doi.org/10.2478/v10303-012-0008-1

Rédei, K., Csiha, I., Keseru, Z., Rásó, J., Kamandiné Végh, Á., Antal, B., 2014. Growth and Yield of Black Locust (Robinia pseudoacacia L.) Stands in Nyírség Growing Region (North-East Hungary). South-east Eur. For. 5, 13–22. https://doi.org/10.15177/seefor.14-04

Saez de Bikuña, K., Hamelin, L., Hauschild, M.Z., Pilegaard, K., Ibrom, A., 2018. A comparison of land use change accounting methods: seeking common grounds for key modeling choices in biofuel assessments. J. Clean. Prod. 177, 52–61. https://doi.org/10.1016/j.jclepro.2017.12.180

Sahoo, K., Bergman, R., Alanya-Rosenbaum, S., Gu, H., Liang, S., 2019. Life cycle assessment of forest-based products: A review. Sustain. 11, 1–30. https://doi.org/10.3390/su11174722

Schaubroeck, T., Schaubroeck, S., Heijungs, R., Zamagni, A., Brandão, M., Benetto, E., 2021. Attributional & consequential life cycle assessment: Definitions, conceptual characteristics and modelling restrictions. Sustain. 13. https://doi.org/10.3390/su13137386

Schwarz, A.E., Ligthart, T.N., Godoi Bizarro, D., De Wild, P., Vreugdenhil, B., van Harmelen, T., 2021. Plastic recycling in a circular economy; determining environmental performance through an LCA matrix model approach. Waste Manag. 121, 331–342.

https://doi.org/10.1016/j.wasman.2020.12.020

Seserman, D.M., Pohle, I., Veste, M., Freese, D., 2018. Simulating climate change impacts on hybrid-poplar and black locust short rotation coppices. Forests 9, 1–25. https://doi.org/10.3390/f9070419

Shen, Z., Tiruta-Barna, L., Hamelin, L., 2022a. From Hemp Grown on Carbon Vulnerable Lands to Long-Lasting Bio-Based Products: Uncovering Trade-Offs between Overall Environmental Impacts, Sequestration in Soils and Dynamic Influence on Global Temperature. Sequestration Soils Dyn. Influ. Glob. Temp.

Shen, Z., Tiruta-Barna, L., Karan, S.K., Hamelin, L., 2022b. Simultaneous carbon storage in arable land and anthropogenic products (CSAAP): Demonstrating an integrated concept towards well below 2° C. Resour. Conserv. Recycl. 182, 106293.

Shimako, A.H., Tiruta-Barna, L., Pigné, Y., Benetto, E., Navarrete Gutiérrez, T., Guiraud, P., Ahmadi, A., 2016. Environmental assessment of bioenergy production from microalgae based systems. J. Clean. Prod. 139, 51–60. https://doi.org/10.1016/j.jclepro.2016.08.003

Silva, D.A.L., Lahr, F.A.R., Garcia, R.P., Freire, F.M.C.S., Ometto, A.R., 2013. Life cycle assessment of medium density particleboard (MDP) produced in Brazil. Int. J. Life Cycle Assess. 18, 1404–1411. https://doi.org/10.1007/s11367-013-0583-3

Snoeck, D., De Belie, N., 2015. From straw in bricks to modern use of microfibers in cementitious composites for improved autogenous healing - A review. Constr. Build. Mater. 95, 774–787. https://doi.org/10.1016/j.conbuildmat.2015.07.018

Standardization, I.O. for, 2006a. Environmental management: life cycle assessment; Principles and Framework. ISO.

Standardization, I.O. for, 2006b. Environmental management: life cycle assessment; requirements and guidelines. ISO Geneva, Switzerland.

Stocker, T.F., Qin, D., Plattner, G.K., Tignor, M.M.B., Allen, S.K., Boschung, J., Nauels, A., Xia, Y., Bex, V., Midgley, P.M., 2013. Climate change 2013 the physical science basis: Working Group I contribution to the fifth assessment report of the intergovernmental panel on climate change. Clim. Chang. 2013 Phys. Sci. Basis Work. Gr. I Contrib. to Fifth Assess. Rep. Intergov. Panel Clim. Chang. 9781107057, 1–1535. https://doi.org/10.1017/CBO9781107415324

Stone, K.R., 2009. Robinia pseudoacacia. In: Fire Effects Information System [WWW Document]. U.S. Dep. Agric. For. Serv. Rocky Mt. Res. Station. Fire Sci. Lab. URL https://www.fs.fed.us/database/feis/plants/tree/robpse/all.html

Stora Enso, 2020. Environmental Product Declaration CLT (Cross Laminated Timber), The International EPD System.

Taghizadeh-Toosi, A., Glendining, M., Vejlin, J., Hutchings, N.J., Olesen, J.E., Christensen, B.T., Kätterer, T., 2014. C-TOOL: A simple model for simulating whole-profile carbon storage in temperate agricultural soils. Ecol. Modell. 292, 11–25. https://doi.org/10.1016/j.ecolmodel.2014.08.016

Takano, A., Hughes, M., Winter, S., 2014. A multidisciplinary approach to sustainable building material selection: A case study in a Finnish context. Build. Environ. 82, 526–535. https://doi.org/10.1016/j.buildenv.2014.09.026

Tonini, D., Hamelin, L., Astrup, T.F., 2016. Environmental implications of the use of agro-industrial residues for biorefineries: application of a deterministic model for indirect land-use changes.

GCB Bioenergy 8, 690–706. https://doi.org/10.1111/gcbb.12290

Wang, B., Liu, G., Xue, S., 2012. Effect of black locust (Robinia pseudoacacia) on soil chemical and microbiological properties in the eroded hilly area of China's loess plateau. Environ. Earth Sci. 65, 597–607. https://doi.org/10.1007/s12665-011-1107-8

Wang, J.J., Hu, C.X., Bai, J., Gong, C.M., 2015. Carbon sequestration of mature black locust standson the loess plateau, China. Plant, Soil Environ. 61, 116–121. https://doi.org/10.17221/931/2014-PSE

Warne, A., 2016. Black locust (Robinia pseudoacacia L.). Best management practices in Ontario, Ontario invasive plant council, Peterborough.

Ye, L., Qi, C., Hong, J., Ma, X., 2017. Life cycle assessment of polyvinyl chloride production and its recyclability in China. J. Clean. Prod. 142, 2965–2972. https://doi.org/10.1016/j.jclepro.2016.10.171

Yuan, Y., Guo, M., 2017. Do green wooden composites using lignin-based binder have environmentally benign alternatives? A preliminary LCA case study in China. Int. J. Life Cycle Assess. 22, 1318–1326. https://doi.org/10.1007/s11367-016-1235-1

Żelazna, A., Kraszkiewicz, A., Przywara, A., Łagód, G., Suchorab, Z., Werle, S., Ballester, J., Nosek, R., 2019. Life cycle assessment of production of black locust logs and straw pellets for energy purposes. Environ. Prog. Sustain. Energy 38, 163–170. https://doi.org/10.1002/ep.13043

Zieger, V., Lecompte, T., Hellouin de Menibus, A., 2020. Impact of GHGs temporal dynamics on the GWP assessment of building materials: A case study on bio-based and non-bio-based walls. Build. Environ. 185, 107210. https://doi.org/10.1016/j.buildenv.2020.107210

Chapter VI. Biopump: annual or perennial plants?

Context

Based on the conclusion in chapter III, the biopump strategy could simultaneously contribute to stock carbon in arable lands and anthropogenic products (CSAAP). A list of potential biopumps suitable for growing in French carbon vulnerable lands (CV-lands), was recommended and ranked in chapter III. Case studies were developed in chapters IV and V for hemp and black locust respectively, as these two plants ranked at the top of herbaceous and woody biopump recommendations. This chapter presents a comparison of the two systems: hemp and black locust, based on the results obtained in the previous chapters and their adaptation for this comparison. Although both chapters IV and V used the same methodology, based on SOC calculation, on life cycle assessment of the biopump system, and the dynamic climate change evaluation, the framework of these two cases are slightly different due to the particularities of the plants, for example, different rotations lead to different time scales.

To summarize, the scenarios studied are:

1) scenario SL: cultivating hemp but only seeds are harvested, same process diagram as the scenario SL in chapter IV;

2) scenario IB: cultivating hemp, harvesting both seeds and straw, the harvested straw is converted into thermal insulation boards and hemp-cement as co-product, same process diagram as the scenario IB in chapter IV;

3) scenario CP: cultivating hemp, harvesting both seeds and straw, the harvested straw is produced to be car panels and hemp-cement as co-product, same process diagram as the scenario CP in chapter IV;

4) scenario BL: cultivating black locust, the logged woody is manufactured as medium density fiberboards and cross-laminated timbers. Because the benefits of planting black locust in CV-lands have been confirmed in chapter V, and chapter VI aims to compare hemp and black locust, the initial vegetation system was merged with the black locust system as a negative input. The cultivation, manufacturing, and product disposal processes are the same as in scenario BL in chapter V.

As discussed in chapters IV and V, the biopump provides two functions in climate change abatement: negative emission (in soils and technosphere) and mitigation effect (by replacing the production and use of petrochemical products). This chapter focuses on these two functions for the four scenarios, in both static and dynamic ways. The trade-off for the other sixteen environmental impacts was also discussed, with corresponding uncertainties.

List of abbreviations

BL	Scenario black locust
C	Carbon
CSAAP	Carbon storage in arable land and anthropogenic products
CP	Scenario hemp straw is produced to be car panel
CV-land	Carbon vulnerable land
DM	Dry matter
GMTC	Global mean temperature change
HI	Harvest index
IB	Scenario hemp straw is produced to be insulation boards
LCA	Life cycle assessment
SOC	Soil organic carbon
SL	Scenario hemp straw left on the ground

1 Introduction

The concept of using biopump to store carbon (C) in both arable lands and anthropogenic products (CSAAP) for global warming mitigation is proposed in chapter III. Based on the evaluation of potential biopump for French on carbon vulnerable lands (CV-lands), chapters IV and V present climate change and other environmental impacts for hemp and black locust scenarios, respectively. The function of global warming mitigation is attributed to GHG reduction and to CO_2 negative emissions, which include soils and technosphere as two C pools. The global mean temperature change (GMTC) affected by different biopump strategies was estimated on different scales. Thus, this chapter aims to harmonize the obtained results in the same framework, analyzing the pros and cons of hemp and black locust.

2 Methods

To compare the performance of annual and perennial biopumps (represented by hemp and black locust, respectively), the results from chapters IV and V were harmonized into the same framework, following the route: soil organic carbon (SOC) simulation--> static LCA--> dynamic LCA, with proper uncertainty analysis.

2.1 SOC simulation

Because black locust has a lifespan of 35 years, the SOC simulation span is 105 years. To match the lifespan of black locust, the hemp cultivation, as well as the initial vegetation timespan, was set as 105 years too.

Different SOC simulation models were used for hemp and black locust, i.e., AMG and C-tool respectively. The AMG model was used because it was specially calibrated for the France conditions, and focuses on annual plants. Black locust needs various C inputs every year following the various growth rate. Though C-tool is not specially calibrated for France (but for Europe), it could handle these various inputs, and its reliability has been proven and admitted by many applications (Hansen et al., 2020; Keel et al., 2017; Taghizadeh-Toosi and Christensen, 2021). Herein, to harmonize the result in the same framework, the SOC evolution of CV-lands under hemp growth was simulated by C-tool, while that of black locust and initial vegetation were obtained from chapter V (C-tool).

There are two cases for hemp, one is only harvesting seeds thus straw is left on the ground, and the other is harvesting both seeds and straw. Carbon inputs for SOC simulation with C-tool are listed in Table VI-1, while the input data for black locust and initial vegetation are available in supplement information III, table s2& s19 of chapter V.

Table VI-1 Carbon input of hemp for SOC simulation.

	Yield* (DM t/ha)	Aboveground biomass left (DM t/ha)	Belowground biomass left (DM t/ha)	Input to topsoil (t/ha)	Input to subsoil (t/ha)
Straw left	0.83	4.41	0.89	4.64	0.66
Straw harvested	9.19	0.47	0.89	0.69	0.66

*DM : dry matter

Other inputs include soil characteristics and meteorological data which are the same for hemp, black locust, and initial vegetation since they grow in the same area, the French CV-land identified in chapter III. Again, soil data were extracted from the same database where CV-lands were defined, the Harmonized World Soil Database (v1.2; FAO, 2021) (Nachtergaele et al., 2012) (supplement information III, table s1). A variable parameter is N content in soils. In chapter IV, three C/N ratios have

been tested (11, 17, 22) and the second (17) was used in simulations. Here, in order to use homogenous conditions for all scenarios, the C/N ratio was set as 11 based on the literature on the France condition since this parameter is not available in the database (Clivot et al., 2019; Launay et al., 2021). Future monthly meteorological data were averaged for France and predicted from 2020-2100, by SICLIMA(DRIAS CERFACS, IPSL, last updated May 2013), for the RCP4.5 climate trajectory (Representative Concentration Pathway (Chen et al., 2021)), downscaled by the model CNRM-CERFACS-CM5/CNRM-ALADIN63. These projections were not available beyond 2100. For the period after 2100, average temperatures from the last decade (i.e., from 2091 to 2100) were thus used (chapter IV, supplement information II, fig. s1, chapter V, supplement information III, fig. s1). The rate constant of the decomposition of hemp in the C-Tool is set as 0.12 $month^{-1}$ (or 1.44 $year^{-1}$) as default, since hemp is a herbaceous plant (Hamelin et al., 2012). The decomposition constant of black locust aerial biomass (foliage+seeds+pods) and the initial vegetation residues were 0.12 $month^{-1}$ too, but for above- and belowground wood residue, it was set as 0.008 $month^{-1}$ and 0.003 $month^{-1}$ respectively due to the different rates as stated in chapter V (section 2.4).

2.1 Life cycle assessment (LCA)

In order to homogenize the LCA results analysis, the functional unit was adapted to match all studied scenarios as 'biopump cultivation on 1 ha of CV-land for 35 years, use and end of life of the bio-based products'. The time corresponds to one rotation of black locust, and 35 rotations of hemp.

Similar to chapter IV, hemp is objected to producing insulation boards (IB) and car panels (CP) when the straw is harvested, while just hemp oil if the straw is left and only seeds are harvested (SL), referring to scenario IB, CP, and SL respectively. The black locust is used to produce two main products, i.e., medium density fiberboards and cross-laminated timber, named scenario BL. The process diagrams of hemp (scenario SL, IB, and CP) and black locust (scenario BL) are the same as Fig. IV-1 and Fig. V-1 in chapters IV and V respectively, they were not shown here to avoid repetition. Since this LCA study aims to compare the environmental consequences of using hemp and black locust, the initial vegetation scenario is considered a negative input. The inventory of initial vegetation and scenario BL is the same as the inventory calculated in chapter V (supplement information III, table s3- s13), while the inventory of hemp case (scenario SL, IB, and CP) was modified in order to match the longer cultivation time in the functional unit (chapter IV, supplement information II, table s3- s14).

The LCA framework follows the ISO standard (International Organization for Standardization, 2006; International Standard Organization, 1997), and is conducted through the SimaPro software, version 9.1.1. Foreground data were collected from the literature and shown in the inventory tables, and the background data came from the Ecoievent consequential modeling (ecoinvent, 2020). The assessment method is the Environmental Footprint v2.0 based on the European Commission Recommendation (Fazio et al., 2018). The LCA result of scenario BL was taken from chapter V, while for scenario SL, IB, and CP, LCA was conducted according to the new functional unit and expanded inventory.

2.3 Dynamic LCA

The comparison of the annual and perennial biopumps on CV-lands also includes the performance of different scenarios on GMTC. Because the temporal boundaries in chapters IV and V are not the same, the time boundary for scenarios SL, IB, CP, and BL was harmonized to begin in the year 2022 and end in the year 2290, i.e., 269 years in total. Fig. VI-1 shows the essential points in the studied time axis. All the methods and assumptions in chapters IV and V were adopted here also.

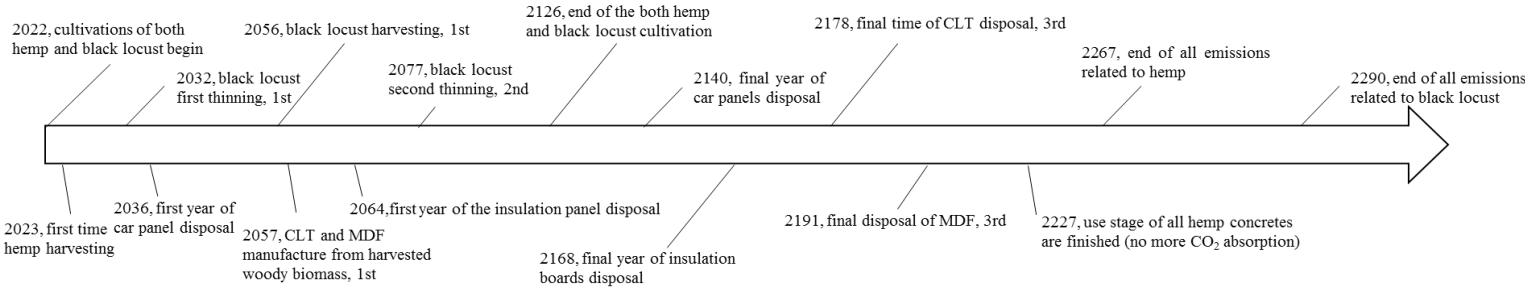

Fig. VI-1 Timeline with important process points of scenarios SL, IB, CP, and BL. 1st, 2nd, 3rd mean the rotation 1, 2, 3.

2.4 Uncertainty analysis

The uncertainty analysis of scenarios SL, IB, CP, and BL follows the global sensitivity analysis based on (Bisinella et al., 2016). For scenarios SL, IB, CP, the functional unit is extended from 1 year to 35 years, the inventory was generically expanded accordingly (e.g., N-fertilizer use for 1 year is 107 kg in chapter IV, then it is 3745 kg here). Since the uncertainty results are in percentage, and there is no significant change in the composition of processes, the uncertainty results in chapter IV are inherited. For black locust, the functional unit is the same as in chapter V, but the initial vegetation aggregated as a negative input herein. Based on the LCA result in chapter V (Fig. V-7& Fig. V-8), the magnitude of black locust is much larger than the initial vegetation, thus the uncertainty results from chapter V are also regarded to fit this chapter.

3 Results and discussion

3.1 SOC simulation results

The following sets of simulations were performed – results are presented in Fig. VI-2.

- For hemp: AMG with C/N=17 (as in chapter IV)
- For hemp: AMG with C/N=11 (as in chapter IV)
- For all scenarios in this chapter: C-tool with C/N=11

The comparison between the SOC results obtained for hemp with both software shows differences (Table VI-2) which are explained here below.

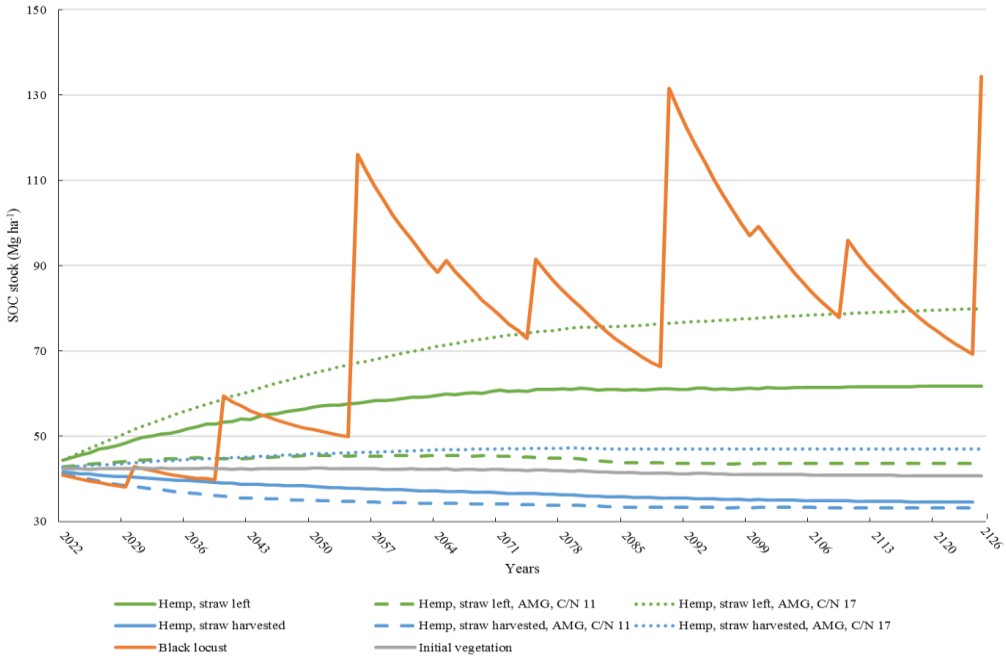

Fig. VI-2 SOC evolution in CV-lands during the hemp and black locust cultivation, and for the initial vegetation. Simulations with C-tool for black locust and initial vegetation, and simulations with C-tool and AMG for hemp.

Table VI-2 SOC results obtained at 100 years of cultivation, with AMG and C-tool for hemp scenarios

Model	SOC, Mg ha^{-1} Hemp, straw left	SOC, Mg ha^{-1} Hemp, straw harvested
AMG, C/N=17	79.58	33.26
AMG, C/N=11	43.61	33.25
C-tool, C/N=11	61.68	34.58

The simulation results of the case ‘hemp, straw harvested’ are close and show the same tendency, the differences observed with respect to the C-tool results are in the order of a maximum of 10%. At the end of simulation years, and for C/N=11, the difference between the two software results, with respect to C-tool results, represents 30% for straw left (Fig. VI-2). The difference in SOC stock could come from the different values of parameters used and simulation approaches (e.g., the consideration of bulk density) (Ledo et al., 2020), which determines the different levels of SOC even with the same input parameters in the software. This explains why when the straw is left on the field, both models show the SOC stabilize the value, but the limits differ significantly. The difference between AMG and C-TOOL shows the potential uncertainty induced by the choice of different SOC models.

The difference between AMG and C-TOOL results (in the same conditions, C/N=11) does not change the rank of the scenarios of interest, i.e., black locust, hemp straw left, initial vegetation, and hemp straw harvested (Fig. VI-2). Concerning the SOC evolution in the function of time, black locust curve presents peaks due to the pulse C inputs in soil from the dead wood during the first and second thinning and harvesting. At the beginning of the first rotation (2022-2031), the growth rate of black locust is low, there is few C inputs into the soil from the biomass, resulting in the decrease of SOC stock, under the level of hemp straw harvested and initial vegetation scenarios. With pulse wood input and a slower

decay rate (chapter V, Fig. V-6a), the SOC stock increases rapidly in the year that logging happens, and decreases gradually after that. In the year 2031, after the first thinning, the SOC stock exceeds the SOC stock of hemp straw harvested and the initial vegetation. But the SOC decreases to lower than the initial vegetation after that, and would not exceed till the second thinning (the year 2041, exceed the SOC of hemp straw harvested at the same time). Therefore, when discussing the negative emission of SOC by cultivating biopumps, the studied time period (black locust) and agricultural management (straw left/harvested) should be mentioned.

One of the barriers to expanding the soil stock is SOC saturation. Even with massive C inputs, the soil could not contain infinite SOC, it has a saturation level that depends on soil chemical, physical, and biochemical conditions (Six et al., 2002). Because of the effect of SOC saturation, there is less SOC increase with the same quantity of C input. It is a common issue of considering the soil as a C sink to control global warming. It was estimated that the potential of SOC stock in global agricultural lands would reach saturation in 50-100 years (Stockmann et al., 2013). In hemp straw left and black locust cases, after 35 years (one black locust rotation), the SOC has increased by 79.31% and 80.03% of the total SOC augmentation. When a relatively close target (e.g., reaching climate neutrality in 2050) is considered, inducing C from the atmosphere into the soil through the biopump could be an efficient method. If a relatively long target is considered (e.g., limiting temperature increase by 2100), the C storage result is uncertain and even reversible (C emission). Another important issue is the duration of increased SOC, though the stable SOC could last for thousands years (Thomsen et al., 2008), a large portion of initial and high SOC is in the active pool, which would decrease in decades. For instance, fig. s2 in chapter V (supplement information III) shows the SOC stock goes back to the initial level in the 51st year after the black locust cultivation.

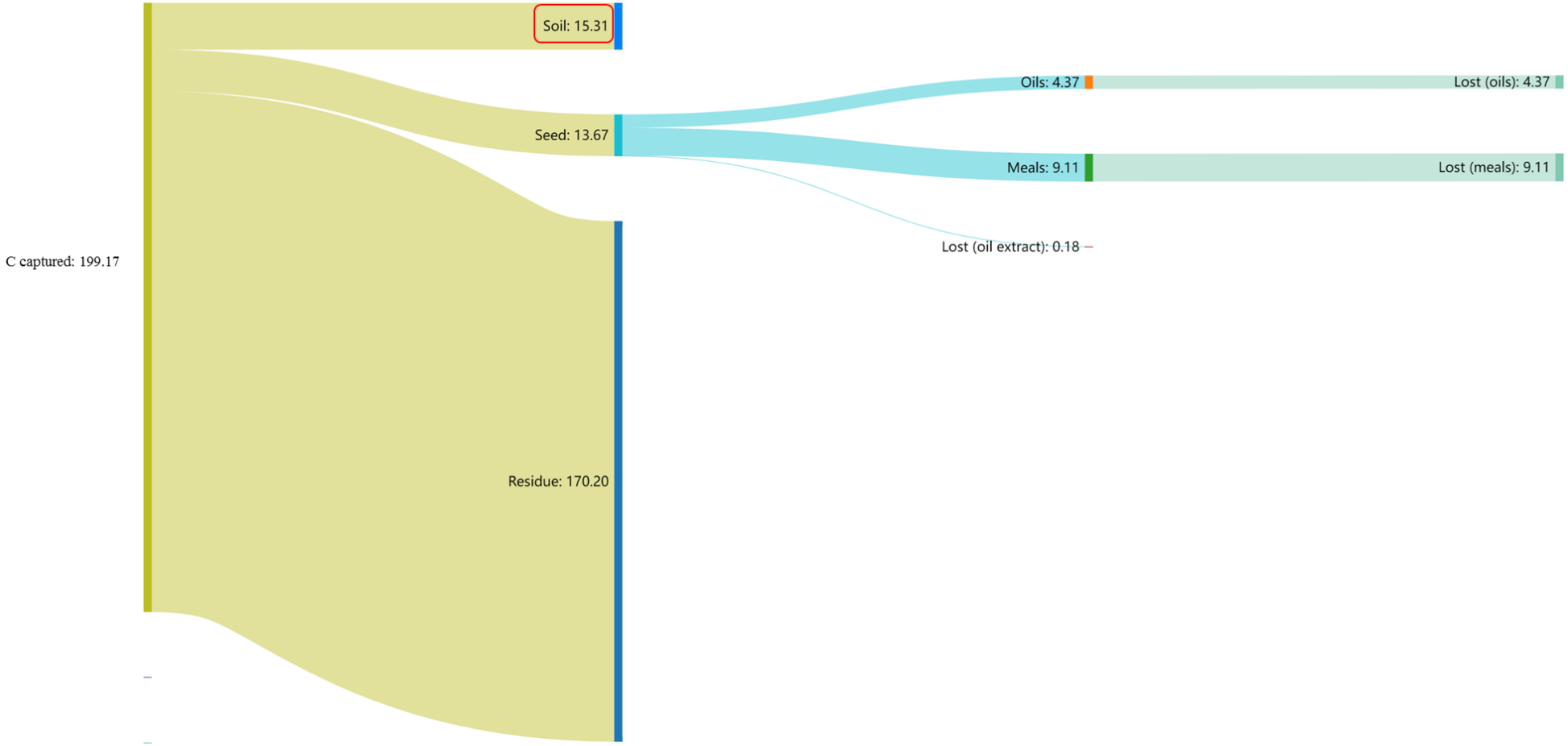

Fig. VI-3 Sankey diagram of C flows in scenario SL. The C flow of soil is a gain. Unit in t ha^{-1}. The flow with the red frame is C sink.

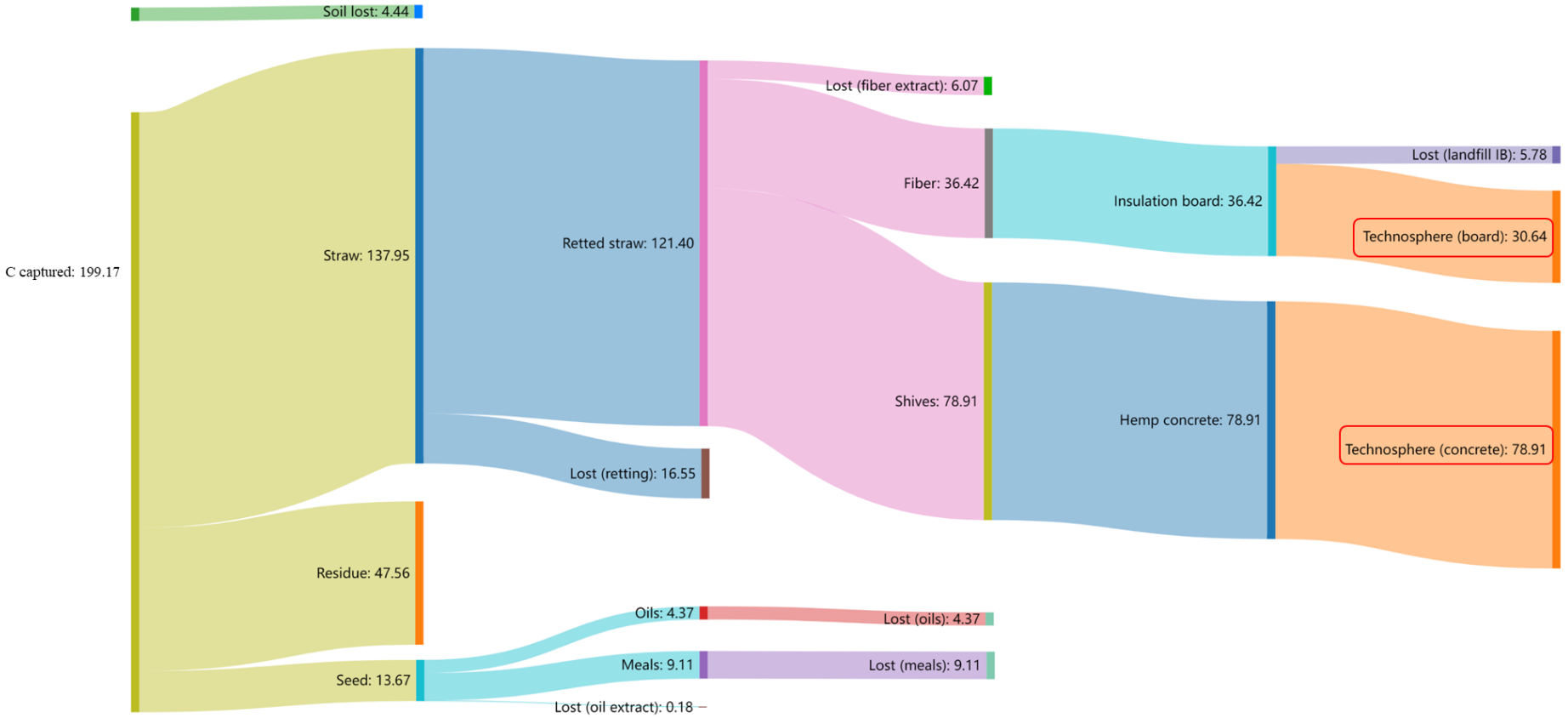

Fig. VI-4 Sankey diagram of C flows in scenario IB. The C flow of soil is a loss. Unit in t ha^{-1}. The flow with the red frame is C sink.

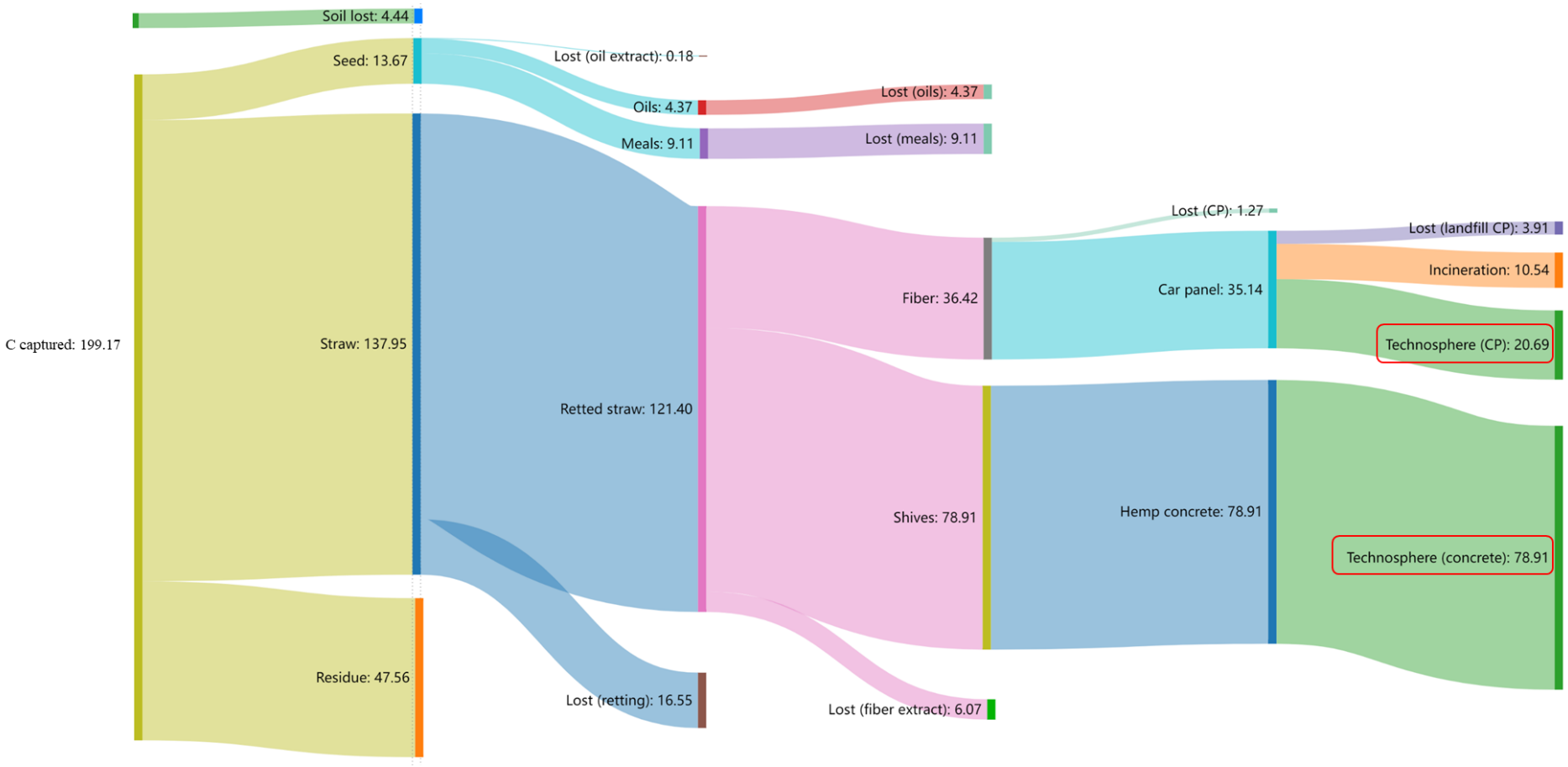

Fig. VI-5 Sankey diagram of C flows in scenario CP. The C flow of soil is a loss. Unit in t ha^{-1}. The flow with the red frame is C sink.

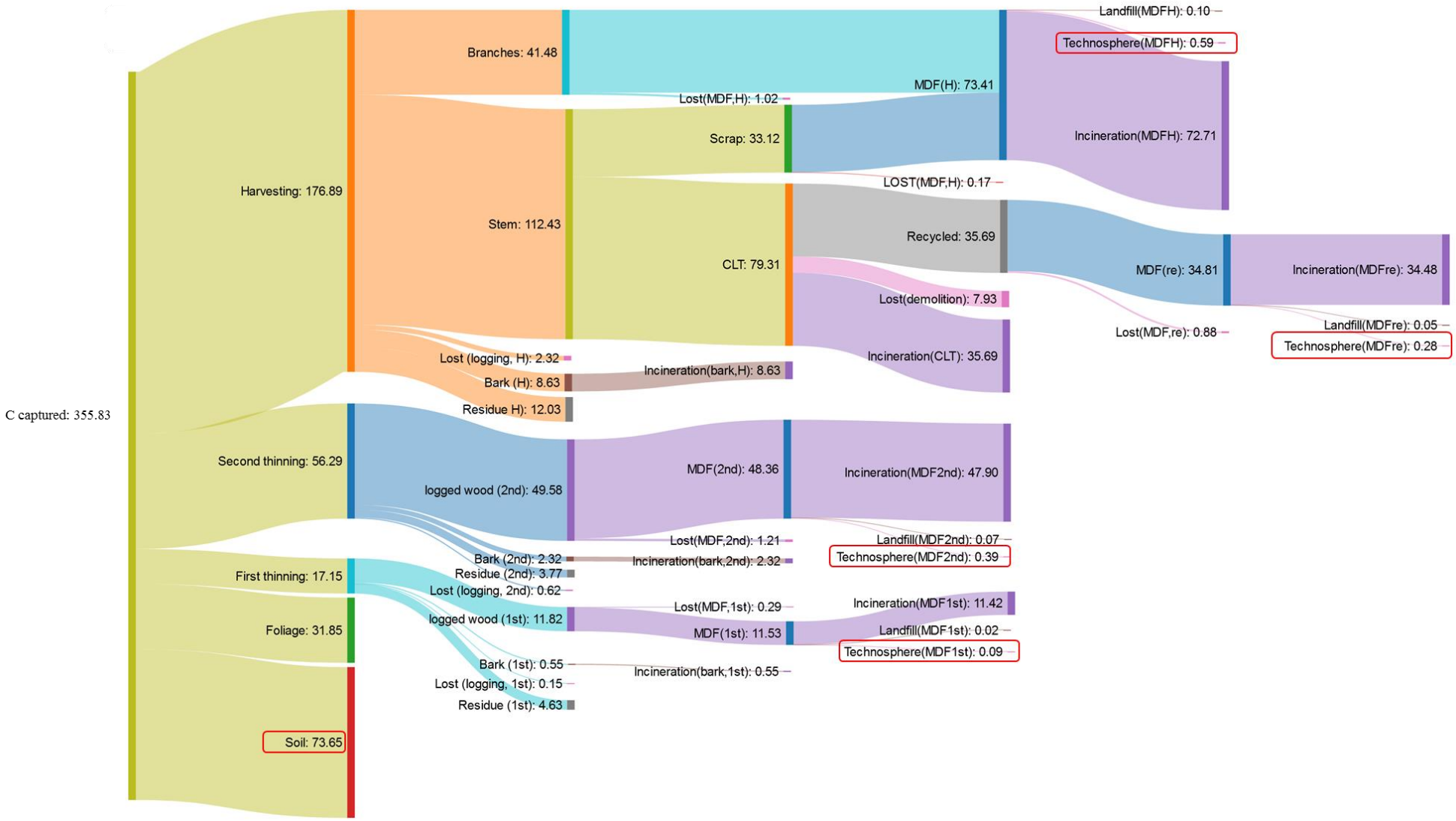

Fig. VI-6 Sankey diagram of C flows in scenario BL. 1st activities involved in the first thinning; 2nd: activities involved in the second thinning& pruning; H: activities involved in the harvesting; re: recycling; Unit in t ha-1. The flow with * is a C sink. The flow with the red frame is C sink.

3.2. C flows

The atmospheric C captured by biopumps (named biogenic here) is further split into several flows (stocks and emissions) according to the processes in scenarios SL, IB, CP, and BL (Fig. VI-3, Fig. VI-4, Fig. VI-5, Fig. VI-6, respectively). These Sankey representations show the static repartition of the biogenic C as mass balance aver 35 years of cultivation. Hemp is an annual plant, thus the C captured is assumed to be the same every year, while the capture ability of black locust changes every year (Fig. VI-7). With the tree's growth, the annual C capture per tree increases and exceeds the C captured by hemp after seven years of cultivation.

In 35 years of cultivation, hemp could absorb 199.17 t C, while black locust could absorb 355.83t C, which is 1.8 times hemp. From Fig. VI-7, it could be found that aboveground biomass contains most part of the absorbed C, in both hemp and black locust. The share of C captured by belowground biomass of black locust is slightly higher than that of hemp, at around 26% and 16% respectively, since black locust shoot/root ratio is also higher than for hemp. The harvest index (HI) indicates, for the aboveground biomass, the ratio between harvested biomass and left as residues. The scenario SL has the least HI because only 8.127% of aboveground is harvested, while 82.04% in scenario IB and CP, and more than 99% for black locust (only the stump is left, its proportion varies among the first thinning, second thinning, and the harvesting; the lost during logging is no counted here). As the harvested biomass is transformed into products to replace petrochemical products, a higher HI contributes to both storing more biogenic C in the products (negative emission), and replacing more petrochemical products (mitigation). This is one of the reasons why the mitigation potential of scenario IB&CP is higher than that of scenario SL, and that of scenario BL is the highest.

In scenario SL (Fig. VI-3), 85.45% of captured C goes into the residues, and back to the atmosphere in a short time through the decomposition. 6.86% of C contained in the harvested part is used as oil and feed, but all this C would go back to the atmosphere through the loss in manufacturing and product consumption. Therefore, in scenario SL, only 7.7% of captured C is stocked in the form of SOC.

When straw is harvested and used downstream (Fig. VI-4, Fig. VI-5), the residues are not the most prominent part, the most C is found in the straw. The biogenic C loss during manufacturing is not significant, but the biomass loss by disposal is. If a product is landfilled, then only part of C would be emitted back to the atmosphere (insulation board, car panel) or even no emission if there is assumed no decomposition (hemp concrete (Pretot et al., 2014)). The biogenic C that is not emitted in 100 years is considered as left in the technosphere as a C sink, therefore, 55.00% and 50.01% of captured C remain in scenarios IB and CP respectively. The C fraction remaining in technosphere in scenario IB is slightly higher than that in scenario CP because 1/3 of car panels are incinerated at the end of life.

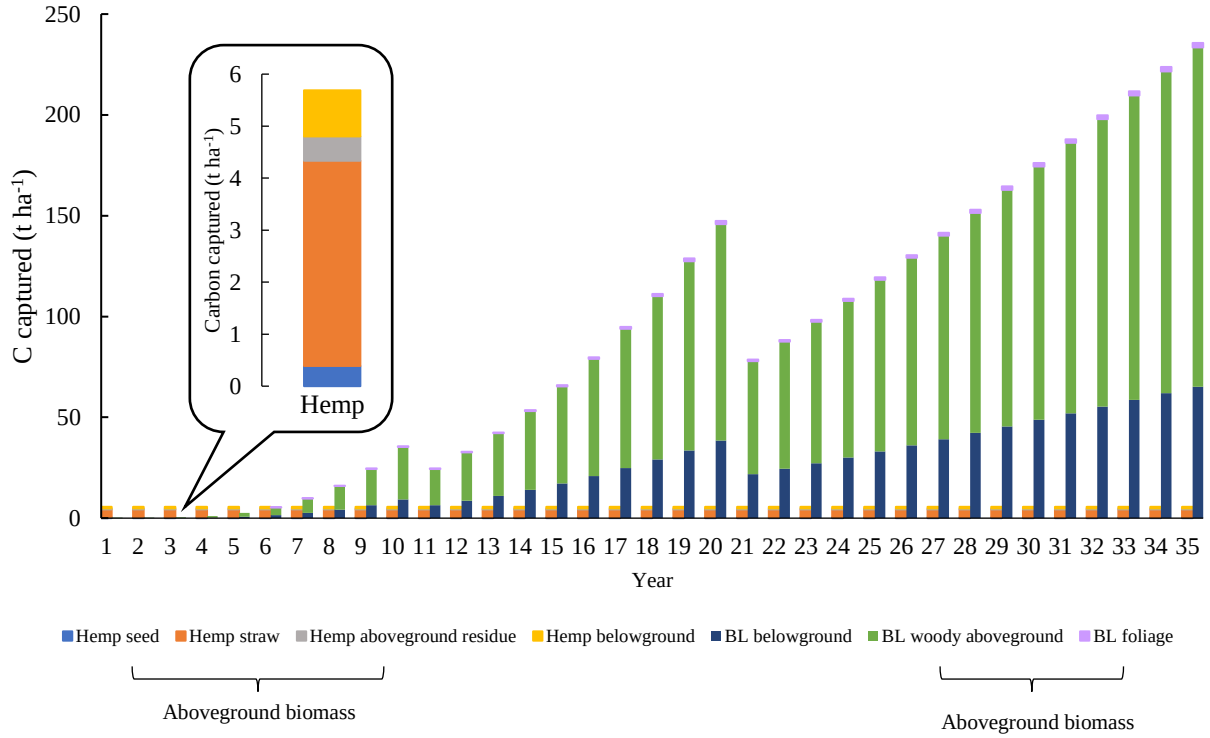

Fig. VI-7 Annual C captured from the atmosphere by hemp and black locust.

In scenario BL (Fig. VI-6), the captured C is mostly contained in the harvested woody biomass (49.71%), then in the second thinned biomass (15.82%), in the foliage (8.95%), in the first thinned woody biomass (4.82%), and the least stored in the soil (20.7%). Besides the C lost during processing, C in the foliage and bark would go back to the atmosphere in a short time through decomposition and incineration respectively. For C in the woody residues, though it decays slowly, the residues are not regarded as a permanent C sink because the decomposition rates after 100 years are 98.56% and 97.25% (chapter V, Fig. V-6a) for above- and belowground residue respectively, and as a comparison, around 20% of biogenic C is decayed after 100 years landfilling (chapter section 2.3). Unlike hemp-based products, incineration is more common than landfilling for woody-based products at the end of life because of the recovered heat. As the biogenic C in the burned woody part is considered all emitted back to the atmosphere immediately, the C remaining fraction in scenario BL is 21.08% (stocked as SOC and tiny part stocked in the landfilling), which is much lower than scenario IB and CP but higher than scenario SL since the SOC due to the higher SOC stock.

We compare the studied scenarios with similar climate change mitigation methods, for example, those of Bastin et al. These authors estimated there are 900 million ha of lands suitable in the world for afforestation and reforestation, which could store 42 Gt C in total (Bastin et al., 2019, with the revised figure from (Veldman et al., 2019)). This amount of C storage requires 2744, 383, 422, and 560 million ha lands under the scenarios SL, IB, CP, and BL, respectively. One concludes that IB, CP, and BL scenarios are the most efficient for inducing negative emissions.

3.3 Consequential LCA results

The environmental impacts of scenarios SL, IB, CP, and BL are compared on the base of the normalized results in Fig. VI-8 and Fig. VI-9. A positive score represents damage, while a negative result means a benefit. Here we only discussed the net values of impacts since the detailed contribution analysis has

been done in the corresponding chapters. Although the inventory of hemp scenarios changed, the contribution of each process to environmental impacts remains similar.

Among sixteen environmental impacts in Fig. VI-8 and Fig. VI-9, scenario SL shows a positive value in seven impacts, scenarios IB and CP are positive in three, scenario BL is positive in three impacts. Scenario BL is positive in ionizing radiation and freshwater eutrophication, both relate to induced energy, compensating for the less energy generation because of the avoided plastic boards incineration. All three hemp scenarios are positive in ecotoxicity freshwater, land use, and water scarcity due to the emission from the induced feed to compensate for the replacement of silage ryegrass. The induced feed brings the scores in the same size as scenario BL, while the negative scores from the avoided plastic boards cover the positive scores, leading to negative net values in ecotoxicity freshwater and water scarcity and a positive but smaller value in land use. Similarly, within three hemp scenarios, scenario IB&CP has more minor impacts in positive net value than scenario SL because of the higher mitigation effect from avoided conventional insulation boards and car panels.

Fig. VI-10 shows the mitigation effect due to the replacement of fossil-based products, in the four scenarios. It could be noted that the mitigation effect of three hemp scenarios in ecotoxicity freshwater and water scarcity is far less than that of scenario BL, which could not offset the influence from the induced feed.

Concerning climate change, planting black locust is better than planting hemp on CV-lands. The BL scenario could mitigate about twice as much kg CO_2-eq as the CP scenario, which also mitigates twice as much kg CO_2-eq as the IB scenario. The net scores of scenario SL are even positive. Comparing the four scenarios in all impacts, scenario BL is better than the other three in eleven impacts (Fig. VI-8), while scenario CP is the best in the remaining five impacts (Fig. VI-9). The order of results is confirmed by the uncertainty analysis conducted in chapter IV and chapter V. Except in non-cancer human health and terrestrial eutrophication, where the ranking of CP and BL can not be concluded. Therefore, considering all environmental impacts, it is hard to judge which biopump is better since black locust performs better in around 2/3 impacts and hemp is better in the rest 1/3.

The mitigation effects that come from the replacement of petrochemical products substantially contribute to the impact scores, especially in scenarios CP and BL. For example, climate mitigation is 246% and 122% of the net value of climate change, in CP and BL respectively. From Fig. VI-10, it could be noticed that the mitigation has a good correlation with the impact scores.

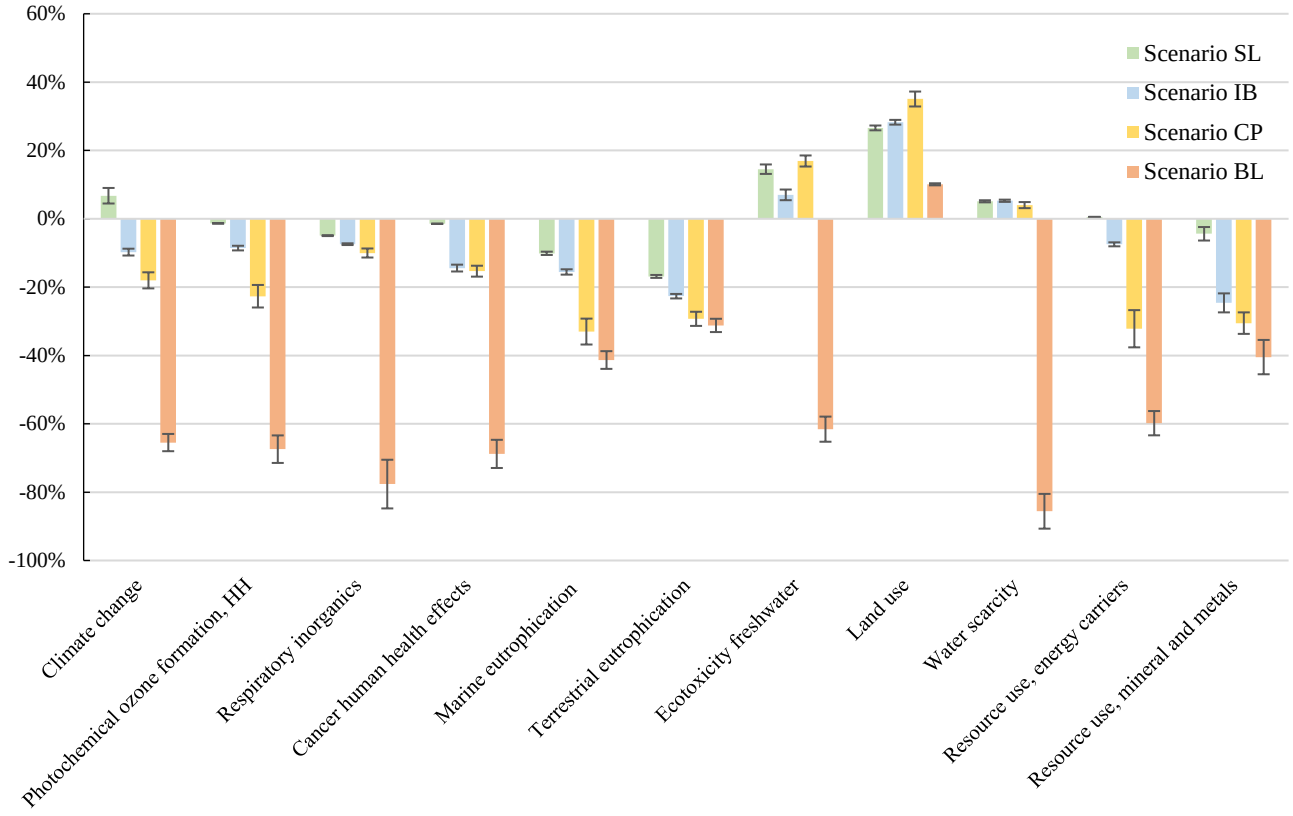

Fig. VI-8 Environmental impacts for which the scenario BL is better than the others.

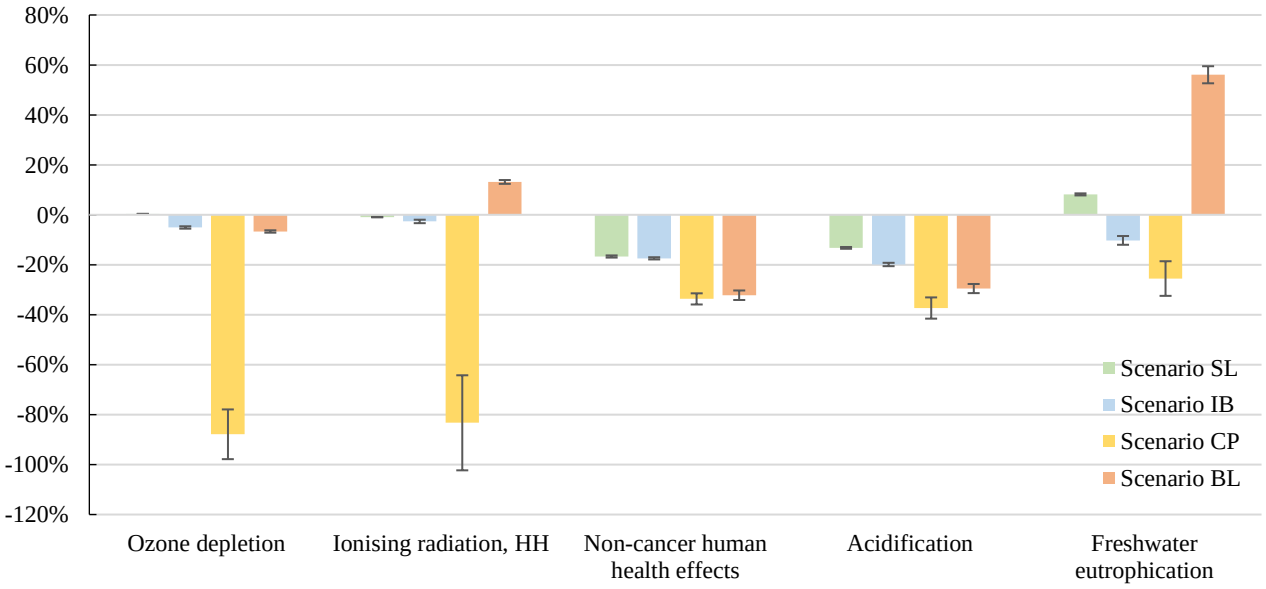

Fig. VI-9 Environmental impacts for which the scenario CP is better than the others.

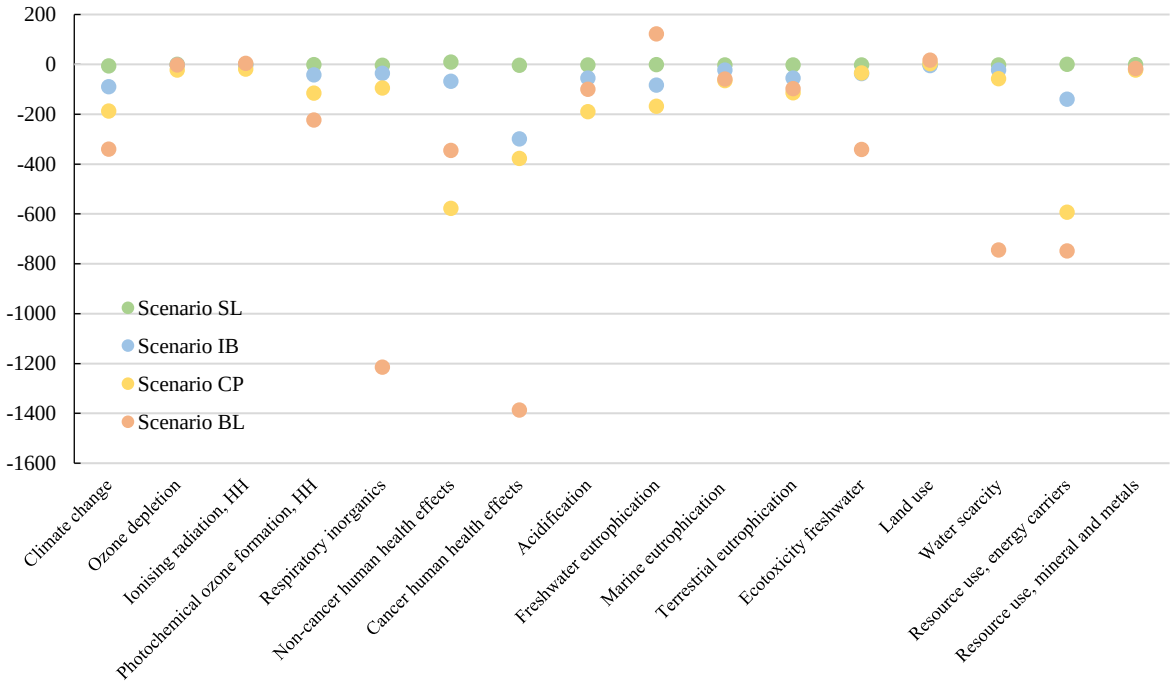

Fig. VI-10 Mitigation effect from the avoided products and processes, in scenarios SL, IB, CP, and BL (normalized results)

3.4 Dynamic LCA results

The negative emissions come from the captured C during photosynthesis, as biogenic C flows in the soil and technosphere, marked as 'bio' in Fig. VI-11. We recall here that the bio flows are related to the actual flows from biopump life cycle, while the non-bio flows are the result of emissions from the manufacturing and avoided emissions from avoided processes.

The biogenic flow of the scenario SL is positive during the cultivation time because a considerable part of captured C is emitted back from residue decomposition, as also shown in Fig. VI-3. The methane emission from the residue decomposition plays a crucial role at the beginning due to its high effect on global warming, but its proportion decreases fast as the lifespan of methane in the air is short. Therefore, after the year 2225, the biogenic flow of the scenario SL becomes negative due to the end of emissions from cultivation, and to the persistent SOC as negative emission.

The biogenic flows of scenario IB and CP are similar since they have similar agricultural management (straw harvested), but slightly different because of the loss during the manufacturing and the ways of disposal. The biogenic flows of both scenarios IB and CP are constantly negative, indicating the negative emission in the two scenarios, as also shown in Fig. VI-4, Fig. VI-5. The insulation boards have a longer lifespan than car panels; this delayed emission leads to slightly lower GMTC for IB than for CP. On the other hand, the biogenic GMTC of BL waves along with the tree growth rate. This particular shape is explained by the thinning or harvesting operations which reduce the tree density and thus the amount of C captured, and the increased emissions from residues, periodically. Further, as most wood products are incinerated in the disposal phase, the C storage level is lower and GMTC increases, and becomes higher than GMTC of bio- IB and CP. Bio GMTC of CP and IB remains negative, constant and more negative than those of BL because of the hemp-cement products with a very long lifetime and no decomposition, representing a permanent C sink.

Since there is consumption during the cultivation and product manufacture, the emission from that should cause positive GMTC results. However, in Fig. VI-11, the non-biogenic GMTC of all scenarios are negative except for the scenario SL, indicating the mitigation effect of non-biogenic flows. The non-bio GMTC of the scenario SL is positive, and corroborates the static LCA result (Fig. VI-10). For the other three scenarios, the GMTC performance of the non-biogenic flows fits the ranking observed for climate change in Fig. VI-10. The non-biogenic flow of the scenario BL also waves along with the black locust logging activities, but in the reverse direction than the biogenic flow, as the logged biomass is produced into wood products to avoid the use of conventional materials. As hemp is an annual plant, the biomass could be harvested every year. Then hemp-based products could provide climate mitigation rapidly, by replacing conventional materials. In contrast, the woody biomass can not be harvested until the first thinning (it is only harvested in the 20 and 35 years after plantation). Therefore, the non-biogenic flow in scenario BL is positive before 2042. Though the mitigation of scenario BL is the highest, it will not exceed those of IB and CP until the years 2044 and 2045, respectively. After this first period, IB, CP and BL scenarios show the same ranking of non-bio GMTC till the end of the time boundary, with the same ranking of climate mitigation.

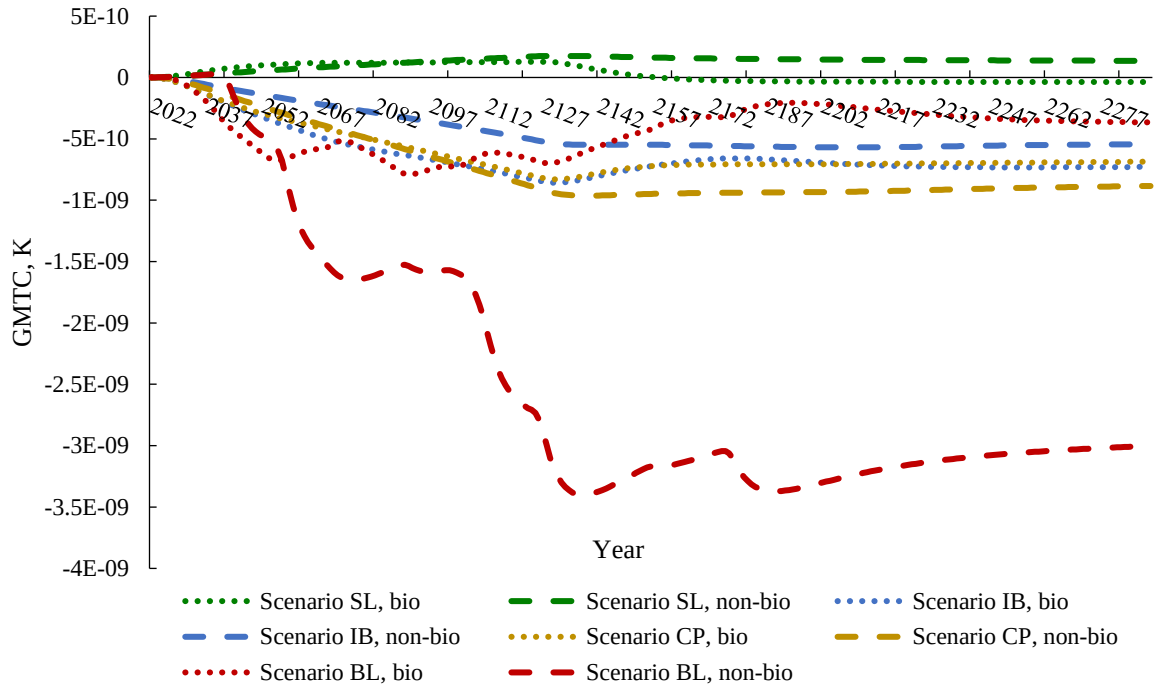

Fig. VI-11 GMTC of scenarios SL, IB, CP, BL for bio and non-bio flows (consequential modeling).

Combining the mitigation (non-biogenic flow) and negative emission (biogenic flow) together, Fig. VI-12 shows the total GMTC for the four scenarios. Though the negative emission of scenario BL is smaller than that of scenario IB and CP after the year 2108, due to the highest mitigation effect, scenario BL still contributes to the largest temperature reduction in general. At the very beginning, the negative emissions (bio GMTC) determine the GMTC of scenario BL since manufacturing of harvested biomass starts later. With the increasing C capture capacity of black locust, the negative emission leads the total GMTC to turn negative in the year 2027. It further exceeds (in negative) the scenario IB and CP in the year 2039 and 2042. Since scenarios IB and CP have a similar negative emission effect but CP has a larger mitigation effect, its total GMTC is more negative. The generic trends of the three scenarios are similar, they decrease fast during the cultivation phase since both negative emission and mitigation effects relate to the biomass. In contrast to the steady GMTC of scenario IB and CP, the GMTC of BL

increases at the end of cultivation, because there is no more C capture, but more delayed residue emission. It further decreases a bit in the year 2178 as part of cross-laminated timber (produced from black locust roundwood) is recycled and replaces the production of conventional material. Opposite to the trend of the other three, the GMTC of scenario SL decreases after the cultivation is finished, determined by its negative emission.

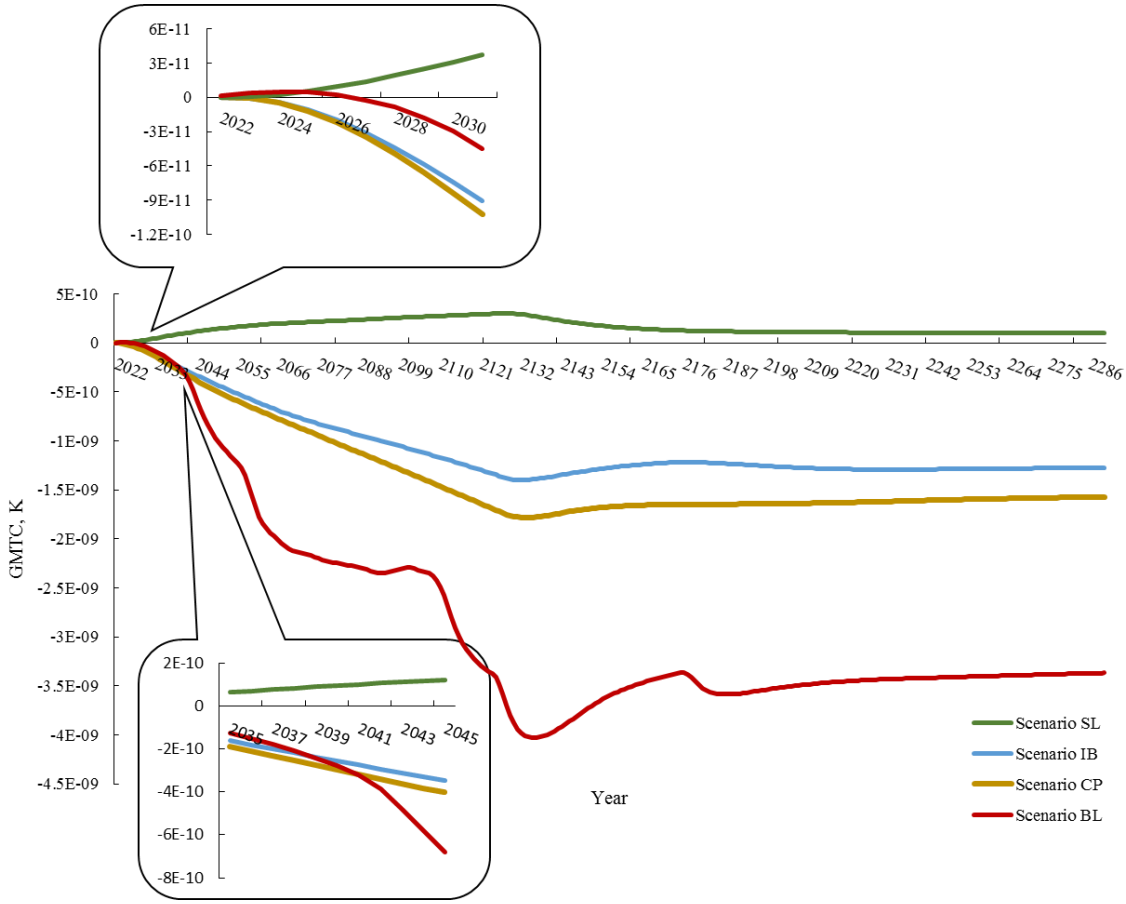

Fig. VI-12 Total GMTC of scenarios SL, IB, CP, BL.

4 Conclusions

In order to summarize the outcomes from the static and dynamic analyses (Fig. VI-11, Fig. VI-12), the results for scenarios SL, IB, CP, and BL are gathered in

Table VI-4 with 2050, 2100, and 2290 as three milestones. The comparison focuses on climate mitigation, and C sinks in soil and technosphere.

Concerning the CO_2 captured, black locust culture captures practically twice than hemp, for the same time horizon. However, only a limited part of the C captured is stored in the technosphere in scenario BL, C in the wood products shows a delayed emission rather than storage. Therefore, the C stock rate of scenario BL decreases with the end of the rotation, from 80.92% in 2050 (no harvesting yet), to 51.4% in 2100 (all biomass in the first rotation is harvested), till 15.21% (all cultivated biomass is harvested, residues are decayed, and biogenic C in the products is emitted). It is higher than the C stock rate of scenario IB and CP in the year 2050, similar in the year 2100, but lower at the end, indicating the importance of involving a temporal factor in selecting biopump. It should be noted that the final C stock rate is different from the estimation in Fig. VI-3, Fig. VI-4, Fig. VI-5, Fig. VI-6, for scenario IB and CP,

the C storage rate in the dynamic analysis is higher, because some C loss (e.g., scraps during the manufacturing) is not regarded as C stock, thus is not counted in the C storage rate estimation in Sankey diagram, while in fact this part of biogenic C does not go back to the atmosphere immediately (treated as landfilled in the dynamic analysis). The SOC of scenario BL has a high increase at the end of cultivation because there is a pulse dead wood input in the soil. However, the SOC would gradually decrease with time later, along with the wood residue decomposition, causing the decrease of C stock. This is not considered in hemp scenarios, because the hemp residues were regarded to be decayed in one year, thus after cultivation, the influence of the hemp on soils stops.

Total SOC increase (with respect to the initial value in CV-land) for the 105 years of cultivation is the highest for scenario BL, followed by scenario SL. For scenario SL, besides the soil, there is practically no other carbon stock (see net C stock at different time horizons in

Table VI-4). Other scenarios (IB and CP) would decrease the SOC since the straw is harvested. For hemp scenarios (SL, IB, and CP), SOC variation (either positive or negative) represents a very small fraction of the total C captured in the same period but is crucial in scenario BL.

Limitations: The SOC modeling is a challenging task, due to the simplified models implemented in the existent, used software. We are aware of these limitations and consider that our SOC results are rather orders of magnitude and show the tendencies of increasing or decreasing but not precise results. Moreover, the initial SOC for CV-lands was taken as an average value, and not specific to a given land. To validate those results, experimental data are needed, which is out of the scope of this thesis.

However, the stock should be analyzed for the different time horizons, in a more realistic way, and in relation to the climate goals. The total C stock (SOC+ technosphere) is variable in time and will decrease in the long term tending towards zero. This total stock is the highest for BL in the long term and beyond, but the net stock decreases faster than that of IB and CP in the very long term. IB and CP stock represents about 60% of the CO_2 captured in the case of hemp harvested and this stock lasts for longer than in scenario BL since it is the C in the products. According to the accounting principles in static LCA, the net C stock is practically limited to the SOC for BL scenario, there is hardly any C storage in the technosphere. The C stock for IB and CP scenarios comes from the hemp-concrete co-product with 100 years lifetime, and insulation boards and car panels, because the common disposal of these products is landfilling instead of incineration for wood products, preventing the massive C emission in a short time.

Limitation: This study does not analyze all possible bio-based products, nor their combinations or possible share of biomass in various products.

If the range is extrapolated to the whole CV-land in France (Shen et al., 2022), the C stock and GMTC of four scenarios are shown in Table VI-3. The annualized C stock capacity for scenario IB and CP is similar in the short-/ mid-term, while scenario BL is more efficient in the short-term. In the long-term, because there is no more C captured after three rotations, the stock capacity decreases in the order: IB≈CP> BL> SL.

For the GMTC change, the levels of temperature variation seem very important with respect to the targets of 1.5°C or 2°C. But this comparison is not reasonable as the results obtained reflect the difference between the two states (product replacements in the background and foreground) and not the actual absolute impact. What could be concluded from these consequences is that (except for the scenario SL the less favorable in climate change) the selection of biopump needs to involve the target period. Black locust is more efficient for shorts and mid-term, while hemp is a better choice for achieving a long-term aim.

Table VI-4 Selected results from static and dynamic LCA and biogenic flows modelling, for 1ha CV-land[a].

Parameter for 1 ha[b]	**Scenario SL**	**Scenario IB**	**Scenario CP**	**Scenario BL**
SOC change* in 2127, C-tool, Mg ha^{-1} (t ha^{-1})	19.43	-7.85	-7.85	92.03
Static LCA (one rotation)				
CO_2 captured in 35 y, t ha^{-1}	730	730	730	1305
Net C stock, at 35 y, t ha^{-1}	15.31	109.55	99.6	75.0
Climate change: Net t CO_2-eq	222	-320	-592	-2202
Climate change: t CO_2-eq, mitigation	-47	-700	-1457	-2643
Dynamic LCA (three rotations)				
Net GMTC 2050, K	2.63E-10	-3.18E-10	-3.83E-10	-1.02E-09
Net GMTC 2100, K	3.92E-10	-9.28E-10	-1.17E-09	-2.30E-09
Net GMTC 2290, K	-2.85E-11	-1.40E-09	-1.70E-09	-3.37E-09
Bio GMTC 2050, K	2.50E-10	-1.49E-10	-1.24E-10	-5.76E-10
Bio GMTC 2100, K	3.58E-10	-4.50E-10	-3.98E-10	-7.26E-10
Bio GMTC 2290, K	-1.14E-11	-7.03E-10	-6.61E-10	-3.66E-10
Total CO_2 captured until 2127 y, t ha^{-1}	2191	2191	2191	3914
Net C stock 2050, t ha^{-1}	18.5	106	101	221
% of stock from the captured at this time	11.20%	64.11%	61.04%	80.92%
Net C stock 2100, t ha^{-1}	23.4	284	263	285
% of stock from the captured at this time	5.20%	63.10%	58.50%	51.40%
Net C stock 2290, t ha^{-1}	19.4	361	338	162
% of stock from the captured at this time	3.25%	60.38%	56.65%	15.21%

[a]: The ranking of scenarios is visible with colours: from green for the best, to red for the worst.
[b]: The difference with respect to the initial SOC in CV-land

Table VI-3 Results from dynamic LCA extrapolated to the total CV-land area in France, at three time horizons[a].

Parameter	**Scenario SL**	**Scenario IB**	**Scenario CP**	**Scenario BL**
2050				
Total C captured, 2050, Mt	396	396	396	655.2
Net C storage 2050, Mt	44.4	254.4	242.4	530.4
Annualized C stock of French carbon budget[b] %	0.24%	1.37%	1.31%	2.86%
Bio GMTC 2050, °C	2.30E-04	-7.28E-04	-6.68E-04	-1.38E-03
Non-bio GMTC 2050, °C	1.22E-04	-3.15E-04	-5.31E-04	-1.06E-03
Net GMTC 2050, °C	3.52E-04	-1.04E-03	-1.20E-03	-2.44E-03
2100				
Total C captured, 2100, Mt	396	396	396	1768.8
Net C storage 2100, Mt	56.16	681.6	631.2	684
Annualized C stock of French carbon budget %	0.11%	1.35%	1.25%	1.35%
Bio GMTC 2100, °C	2.97E-04	-1.64E-03	-1.52E-03	-1.74E-03
Non-bio GMTC 2100, °C	3.26E-04	-9.02E-04	-1.61E-03	-3.77E-03
Net GMTC, °C	6.23E-04	-2.54E-03	-3.13E-03	-5.52E-03
2290				
Total C captured, 2290, Mt	1435.2	1435.2	1435.2	2560.8
Net C storage 2290, Mt	46.56	866.4	811.2	388.8
Annualized C stock of French carbon budget %	0.03%	0.50%	0.47%	0.23%
Bio GMTC 2290, °C	-8.87E-05	-1.75E-03	-1.65E-03	-8.78E-04
Non-bio GMTC, °C	3.25E-04	-1.30E-03	-2.12E-03	-7.21E-03
Net GMTC 2290, °C	2.36E-04	-3.05E-03	-3.77E-03	-8.08E-03

[a]: The ranking of scenarios is visible with colours: from green for the best, to red for the worst.
[b]: (The High Council on Climate, 2019)

Reference

Bastin, J.-F., Finegold, Y., Garcia, C., Mollicone, D., Rezende, M., Routh, D., Zohner, C.M., Crowther, T.W., 2019. The global tree restoration potential. Science (80-.). 366, 76–79. https://doi.org/10.1126/science.aay8060

Bisinella, V., Conradsen, K., Christensen, T.H., Astrup, T.F., 2016. A global approach for sparse representation of uncertainty in Life Cycle Assessments of waste management systems. Int. J. Life Cycle Assess. 21, 378–394. https://doi.org/10.1007/s11367-015-1014-4

Chen, D., Rojas, M., Samset, B.H., Cobb, K., Diongue-Niang, A., Edwards, P., Emori, S., Faria, S.H., Hawkins, E., Hope, P., Huybrechts, P., Meinshausen, M., Mustafa, S.K., Plattner, G.-K., Treguier, A.M., 2021. Framing, Context, and Methods., in: Climate Change 2021: The Physical Science Basis. Contribution of Working Group I to the Sixth Assessment Report of the Intergovernmental Panel on Climate Change. IPCC.

Clivot, H., Mouny, J.C., Duparque, A., Dinh, J.L., Denoroy, P., Houot, S., Vertès, F., Trochard, R., Bouthier, A., Sagot, S., Mary, B., 2019. Modeling soil organic carbon evolution in long-term arable experiments with AMG model. Environ. Model. Softw. 118, 99–113. https://doi.org/10.1016/j.envsoft.2019.04.004

DRIAS CERFACS, IPSL, M.-F., 2013. CNRM-CERFACS-CM5/CNRM-ALADIN63-RCP4.5. DRIAS les Futur. du Climat.

ecoinvent, 2020. Ecoinvent 3.5 database [WWW Document]. URL https://www.ecoinvent.org/database/ecoinvent-37/new-data-in-ecoinvent-37/new-data-in-ecoinvent-37.html

Fazio, S., Biganzioli, F., De Laurentiis, V., Zampori, L., Sala, S., Diaconu, E., 2018. Supporting information to the characterisation factors of recommended EF Life Cycle Impact Assessment methods, version 2, from ILCD to EF 3.0, EUR 29600 EN, European Commission, Ispra, 2018, ISBN 978-92-79-98584-3, doi:10.2760/002447, PUBSY No. JRC114822., New Models and Differences with ILCD, EUR. https://doi.org/10.2760/002447

Hamelin, L., Jørgensen, U., Petersen, B.M., Olesen, J.E., Wenzel, H., 2012. Modelling the carbon and nitrogen balances of direct land use changes from energy crops in Denmark: A consequential life cycle inventory. GCB Bioenergy 4, 889–907. https://doi.org/10.1111/j.1757-1707.2012.01174.x

Hansen, J.H., Hamelin, L., Taghizadeh-Toosi, A., Olesen, J.E., Wenzel, H., 2020. Agricultural residues bioenergy potential that sustain soil carbon depends on energy conversion pathways. GCB Bioenergy 12, 1002–1013. https://doi.org/10.1111/gcbb.12733

International Organization for Standardization, 2006. Environmental management: life cycle assessment; requirements and guidelines. ISO Geneva.

International Standard Organization, 1997. ISO 14040: Environmental Management-Life Cycle Assessment-Principles and Framework.

Keel, S.G., Leifeld, J., Mayer, J., Taghizadeh-Toosi, A., Olesen, J.E., 2017. Large uncertainty in soil carbon modelling related to method of calculation of plant carbon input in agricultural systems. Eur. J. Soil Sci. 68, 953–963. https://doi.org/10.1111/ejss.12454

Launay, C., Constantin, J., Chlebowski, F., Houot, S., Graux, A.I., Klumpp, K., Martin, R., Mary, B., Pellerin, S., Therond, O., 2021. Estimating the carbon storage potential and greenhouse gas emissions of French arable cropland using high-resolution modeling. Glob. Chang. Biol. 27, 1645–1661. https://doi.org/10.1111/gcb.15512

Ledo, A., Smith, P., Zerihun, A., Whitaker, J., Vicente-Vicente, J.L., Qin, Z., McNamara, N.P., Zinn, Y.L., Llorente, M., Liebig, M., Kuhnert, M., Dondini, M., Don, A., Diaz-Pines, E., Datta, A., Bakka, H., Aguilera, E., Hillier, J., 2020. Changes in soil organic carbon under perennial crops. Glob. Chang. Biol. 26, 4158–4168. https://doi.org/10.1111/gcb.15120

Nachtergaele, F., van Velthuizen, H., van Engelen, V., Fischer, G., Jones, A., Montanarella, L., Petri, M., Prieler, S., Teixeira, E., Shi, X., 2012. Harmonized World Soil Database (version 1.2). FAO, Rome, Italy IIASA, Laxenburg, Austria 1–50.

Pretot, S., Collet, F., Garnier, C., 2014. Life cycle assessment of a hemp concrete wall: Impact of thickness and coating. Build. Environ. 72, 223–231. https://doi.org/10.1016/j.buildenv.2013.11.010

Shen, Z., Tiruta-Barna, L., Karan, S.K., Hamelin, L., 2022. Simultaneous carbon storage in arable land and anthropogenic products (CSAAP): Demonstrating an integrated concept towards well below 2° C. Resour. Conserv. Recycl. 182, 106293.

Six, J., Conant, R.T., Paul, E.A., Paustian, K., 2002. Stabilization mechanisms of soil organic matter: implications for C-saturation of soils. Plant Soil 241, 155–176.

Stockmann, U., Adams, M.A., Crawford, J.W., Field, D.J., Henakaarchchi, N., Jenkins, M., Minasny, B., McBratney, A.B., Courcelles, V. de R. de, Singh, K., Wheeler, I., Abbott, L., Angers, D.A., Baldock, J., Bird, M., Brookes, P.C., Chenu, C., Jastrow, J.D., Lal, R., Lehmann, J., O'Donnell, A.G., Parton, W.J., Whitehead, D., Zimmermann, M., 2013. The knowns, known unknowns and unknowns of sequestration of soil organic carbon. Agric. Ecosyst. Environ. 164, 80–99. https://doi.org/10.1016/j.agee.2012.10.001

Taghizadeh-Toosi, A., Christensen, B.T., 2021. Filling gaps in models simulating carbon storage in agricultural soils: the role of cereal stubbles. Sci. Rep. 11, 1–8. https://doi.org/10.1038/s41598-021-97744-z

The High Council on Climate team, 2019. FIRST ANNUAL REPORT OF THE HIGH COUNCIL ON CLIMATE OF FRANCE.

Thomsen, I.K., Kruse, T., Bruun, S., Kristiansen, S.M., Knicker, H., Petersen, S.O., Jensen, L.S., Holst, M.K., Christensen, B.T., 2008. Characteristics of Soil Carbon Buried for 3300 Years in a Bronze Age Burial Mound. Soil Sci. Soc. Am. J. 72, 1292–1298. https://doi.org/10.2136/sssaj2007.0348

Veldman, J.W., Aleman, J.C., Alvarado, S.T., Anderson, T.M., Archibald, S., Bond, W.J., Boutton, T.W., Buchmann, N., Buisson, E., Canadell, J.G., 2019. Comment on "The global tree restoration potential." Science (80-.). 366, 1–5. https://doi.org/10.1126/science.aaz0111

CHAPTER VII. Conclusion and perspective

Conclusion

In the context of the urgent need to reduce the pressure on the climate, France has announced the objective to reach climate neutrality in 2050 and will endeavor to contribute at limiting global temperature increase to well below 2°C (with respect to pre-industrial level). To achieve these targets, the GHG emission should be 25%-45% less by 2030 than 2010 level. The reduction of CO_2 in the atmosphere implies to induce carbon dioxide removals (CDR). Due to the lack of mature technologies, CDR from the atmosphere is less accessible yet than by the biomass through the photosynthesis way. Furthermore, the harvested biomass is a useful raw material and source of C to feed the technosphere for energy and material production. Energy and material demand is thus pivotal to mitigate climate change, since the biogenic C replaces the fossil C. Besides, the territory for planting biomass is a key parameter since soil could be a C sink.

Inspired by the importance of biomass, this study proposes a strategy for global warming alleviation, consisting in CO_2 capture by plants able to induce important C stock in soils (arable lands), then stock the C in anthropogenic products (carbon storage in arable lands and anthropogenic products, CSAAP). The plants that have these two functions are called 'biopump', as they pump the C from the atmosphere into soils and then technosphere. Besides the C removals and storage, the bio-based product reduce the production of petrochemical-based products, therefore lowering the use of fossil C in the economy. For a successful CSAAP roadmap, the area used for biopump growth does not cross the boundary of over-exploitation with consequences such as additional degradation and greater food insecurity. Because of the SOC saturation in soils, the initial SOC in the lands should be low enough to store extra induced C. Lands that do not interfere with food security or other activities, and have a low initial SOC, are called 'carbon vulnerable lands' (CV-lands).

A 4-steps framework was proposed to implement CSAAP in a particular region: i) identification of biopump candidates, ii) selection and ranking of biopumps for the region of interest, iii) identification and selection of target areas suitable for sustainable biopump plantation, iv) assessment of the mitigation potential over time.

According to the French context, the biopump candidates were identified and ranked following five criteria: yield, SOC increase capacity, agricultural management intensity, suitability, and risk of invasion. Among potential candidates, hemp (*Cannabis sativa* L.) and black locust (*Robinia pseudoacacia L.*) ranked on the top in herbaceous and woody plants, respectively.

Further, three to four types of land-covers where identified as CV-lands in France, arable and marginal and based on their C content. Based on the characteristics of CV-lands, a case study based on Miscanthus confirmed the relevance of CSAAP as a climate mitigation strategy, with a negative global temperature change (GMTC) during the cultivation plus the time the products are in use. The case study further highlighted the importance of C loss with the biomass residues, either on land, or in technosphere. Moreover, the lifetime of products is of major importance for how long the mitigation is effective.

The two top selected biopumps, i.e., hemp and black locust, were investigated as case studies.

In the hemp study, the difference in agricultural management would determine the SOC change, leaving the straw on the ground could increase more SOC substantially than harvesting it. However, this substantial SOC augmentation cannot compensate for the lower mitigation effect in the technosphere, resulting in a higher temperature in the future, compared to the initial vegetation on CV-lands. With the relatively high and similar C storage rate in the technosphere, hemp-based products with different lifespans do not show a significant difference in future temperature change, but both contribute to a temperature reduction in the studied timespan. For the environmental impacts other than climate change, the mitigation effect from hemp straw-based products is able to offset the emission from manufacturing and disposal, leading the straw harvested scenarios to perform better than the straw left scenario. The results highlight the hemp function as a biopump, and raise the potential problems in ecotoxicity

freshwater, land use, water scarcity, when the cultivation is converted from the initial vegetation on the French CV-lands.

When black locust is planted in CV-lands, it increases the SOC efficiently in the first rotation but not in the later rotations due to the saturation of SOC. Because of the high mitigation effect from replacing plastic boards production and incineration, black locust performs better than initial vegetation in all environmental impacts, except in freshwater eutrophication and ionizing radiation. Compared to the initial vegetation, planting black locust contribute to the temperature reduction after six years and forward. However, the mitigation effect is limited in time, after cultivation is stopped and the products are disposed by incineration.

From a dynamic point of view, the captured C is stored in the biomass during the cultivation, and in the bio-based products during the lifetime, which also refers to delayed emission. Black locust shows a higher negative emission than hemp during the cultivation period, while it becomes smaller after that because of the end of life management of products in the two systems. Also, the hemp-based products with a longer lifespan show a larger negative emission than products with a shorter lifespan during the product use phase, indicating the effect of delayed emissions. In the hemp scenario, the mitigation potential of the negative emissions and of the GHG reduction is similar, while GHG mitigation is more important in the black locust scenario. Finally, the carbon flow calculation shown that the SOC stock is much lower than the C stock in products and standing biomass, the climate mitigation effect from SOC (negative emission toward soil) is negligible with respect to the potential of technosphere to store C and mitigate GHG.

The results for climate change show that black locust scenario performs better than hemp in the timespan of the climate goals (during 100 years). The results of other static environmental impacts are highly correlated to the mitigation effect. With the higher mitigation, black locust performs better than hemp in around two-thirds of impacts, while hemp is better in the remaining. Therefore, the selection of biopump cultivation between hemp and black locust in French CV-lands should be based on the trade-offs among all environmental impacts, and time scale in climate change.

Perspective

When simulating the SOC change during the cultivation, AMG and C-tool were adopted as recognized models by the research community. However these models have limitations (for example it is impossible to simulate simultaneously the degradation of 2 or more kinds of residues into the same SOC stock). The choice of model would induce uncertainty in SOC results, further increasing the uncertainty of the whole analysis. To reduce this uncertainty, a model that could suit the more general scope of biopump needs to be investigated, or drawing a wide-accepted principle in selecting SOC simulation model. Meanwhile, because CV-lands are not supposed to be heavily exploited arable land, this study focused on monoculture. However, in the aspect of SOC, including cover-crop could raise the SOC increase, and more realistic in the factor.

In addition, the consequential LCA provides a perspective system to answer the consequence of planting biopump instead of the initial vegetation in CV-lands. Because of the complex consequential chains in the background data, it is hard to calculate the uncertainty of the whole biopump system in a mathematical way or a numerical simulation approach (e.g., Monte Carlo method) in the SimaPro, which is the software used in this thesis. This thesis adopted the global sensitivity analysis approach to calculate the uncertainty, the method being a proxy for a complete uncertainty analysis, and requires important time to be spent. Implementation of a sensitivity and uncertainty numerical method in LCA software will be of great help for the LCA practitioners.

In both hemp and black locust LCA studies, the functional units were set as the biomass grown in 1 ha CV-land, thus the product markets were regarded as elastic. However, when extrapolating results from 1 ha to all CV-lands in France, or even the whole world, the vast amount of harvested biomass would shock the markets, making them lose the elasticity. LCA method is not applicable to important changes in the economy, in this case a coupled Integrated Modelling Approach model would be useful. On the other hand, in this work, only several bio-based products have been considered, while in reality, biomass has diverse uses, used for producing only one or two products is impossible in the market perspective. A more detailed investigation could include the share of the biomass between many other possible products.

Concerning climate change evaluation, the gap between different metrics leads it hard to compare the results and conclusions from different studies. Therefore, more studies using GMTC need to be conducted to build the foundation and provide more information for the decision-makers. Furthermore, since the dynamic estimation methods are still developing, there is no a widely accepted approach for all impacts like in the static LCA. Applying a mature dynamic LCA would help us to comprehensively know the trade-off of biopump strategy for the environment. Having such comprehensive dynamic methods and temporal thresholds for impacts, would be very useful to the LCA community in the long-term.

Finally, as a very important step, experiments on field are necessary in order to validate the biopump capability to stock C in specific sites.

Supplement Information

Table of content

Supplyment Information I. for Chapter III 148

1 Biopump candidates and their properties 149

2 Methodology for biopump selection for France 156

3 Suitable anthropogenic products 158

4 Carbon vulnerable arable land in France 164

5 Results for application case – sensitive analysis on miscanthus chosen as biopump 164

References 167

Supplyment Information II. for Chapter IV 177

1 AMG model 178

2 Life cycle inventory 180

2.1 Cultivation 180

2.2 Harvesting 180

2.3 Hemp oil and avoided products 182

2.4 Retting 185

2.5 Baling 185

2.6 Fiber extraction 186

2.7 Hemp concrete 186

2.8 Thermal insulation manufacture 188

2.9 Thermal insulation disposal 189

2.10 Car panel manufacture 190

2.11 Car panel use stage 192

2.12 Disposal 192

2.13 Images of hemp-based products 193

2.14 Planting in the carbon vulnerable land 194

3 Environmental impact in consequential LCA 200

3.1 Environmental impact categories in consequential LCA 200

3.2 Environmental impact results 200

4 GHG considered in dynamic LCA 219

5 Uncertainty analysis 220

5.1 Method 220

5.2 Parameters in uncertainty analysis....220
5.3 Uncertainty analysis results....223
Reference....228
Supplyment Information III. for Chapter V....234
1 SOC simulation....235
2 Life cycle inventory....238
2.1 Black locust cultivation....238
2.2 Black locust growth....238
2.3 Logging....241
2.4 CLT manufacture....247
2.5 MDF manufacture....252
2.6 Carbon vulnerable lands....257
3 Consequential LCA....265
3.1 Environmental impact categories in consequential LCA....265
3.2 Consequential LCA results : Contribution analysis....266
4 Dynamic LCA....269
4.1 GHG considered in dynamic LCA....269
4.2 Electricity and heat mix in the future....271
4.3 Dynamic LCA results....272
5 Uncertainty analysis....277
5.1 Method....277
5.2 Parameters in uncertainty analysis....278
5.3 Uncertainty analysis results....279
Reference....283

Supplyment Information I. for Chapter III

1 Biopump candidates and their properties

Table S I-1 SOC changes induced by woody biopump candidates. (unless otherwise indicated, SOC data are extracted from the meta-study by Ledo et al.[a])

No.	Name	ΔSOC concentration [g kg^{-1} y^{-1}]			ΔSOC stock [Mg ha^{-1} y^{-1}]			Number of measurements	Years since LUC[b] [year]	Expected plantation duration [year]	Country	Soil depth (cm)
		Average	Min	Max	Average	Min	Max					
Current land use: fruit												
1	Acerola	0.21	0.21	0.21				1	9	15-40 [1]	Brazil	0-20
2	Blueberry*				1.41	0.43	2.26	5		12-50[2,3]	USA	0-30
3	Guava				0.01	-0.88	0.26	11	22.4	15-40[4,5]	Brazil, India	0-20, 20-40, 40-60, 60-80, 80-100, 100-150, 150-200
4	Olive	1.06	-0.17	1.91				81	9.4	150-600[6,7]	Spain, Italy, Portugal	0-5, 0-20, 0-24
Current land use: short rotation coppice												
5	Acacia				1.07	-0.26	2.40	10	5	15-50 [8,9]	Tanzania	0-15
6	Alder*	0.08	-0.01	0.15				5		40-160[10,11]	Germany	0-20
7	Araucaria				1.15	0.68	1.62	2	30	150-1000[12,13]	Brazil	0-20, 20-40
8	Black locust	0.247	-0.07	0.65	0.003	-0.01	0.02	18	12.4	60-100[14,15]	Germany, Italy	0-3, 3-10, 0-10, 10-30, 30-60, 60-100
9	Poplar	0.20	-0.70	1.06				78	13.8	40-150[16,17]	Canada, Italy, Germany, USA	0-10, 0-3, 0-5, 0-15, 3-10, 10-30, 20-25,30-60, 30-80, 60-100
10	Willow	0.10	-0.11	0.57				117	8.6	20-30[18,19]	Italy, Germany, Canada, UK, Sweden	0-10, 0-20, 0-30, 0-100, 10-20, 10-30, 20-30, 20-40, 30-50, 30-60, 30-80, 50-80, 60-90, 60-100
Current land use: animal feed												
11	Atriplex				0.46	-0.18	1.26	7	6.7	Annual or 12-27[20,21]	Australia	0-30, 30-200, 0-100
Current land use: no definition												

12	Korshinsk pea shrub	0.16	0.38	12	4	10-50[22,23]	China	0-20, 20-40, 40-60, 60-80, 80-100
13	Rhamnoides	0.25	0.58	5	27	30-40[24]	China	0-10, 10-20, 20-40
14	Microphylla	0.22	0.50	5	27	50-150[25,26]	China	0-10, 10-20, 20-40

a: SOC data taken from Ledo et al.[27], except for korshinsk pea shrub[28], bungeana, rhamnoides and microphylla[29].
b: LUC- land use changes

Table S I-2. SOC changes induced by grassy biopump candidates. (unless otherwise indicated, SOC data are extracted from the meta-study by Ledo et al.[a])

No.	Name	ΔSOC concentration [g kg^{-1} y^{-1}]			ΔSOC stock [Mg ha^{-1} y^{-1}]			Number of measurements	Years since LUC[b] [year]	Expected plantation duration [year]	Country	Soil depth (cm)
		Average	Min	Max	Average	Min	Max					
Current land use: food												
1	Bahiagrass	0.23						1	6	2-5[30]	Germany	0-20
Current land use: bioenergy												
2	Giant reed	0.19	-0.15	0.58				6	8	12-25[31,32]	Italy	0-15, 10-30, 15-30, 30-60, 60-100
3	Miscanthus	0.09	-1.15	1.46	0.25	-10.27	9.08	198	6.7	15-30[33,34]	Italy, Germany, Ireland, France, USA, UK	0-10, 0-15, 0-20, 0-30, 0-40, 0-100, 10-20, 10-30, 10-100, 15-30, 20-30, 20-50, 30-45, 30-50, 50-100, 60-90, 90-120, 120-150
4	Switchgrass	0.08	-0.06	0.53	0.40	-6.75	8.83	186	7.27	>10[35,36]	USA, Italy, Germany, Canada,	0-10, 0-15, 0-30, 10-20, 10-30, 15-30, 20-30, 30-45, 30-60, 30-100, 45-60, 60-90, 60-100
Current land use: bioproduct												
5	Ramie	0.45	0.39	0.55				7	9	6-40 [37,38]	Italy	0-30
Current land use: crop												
6	Ryegrass	1.22	-2.00	4.00				9	1	Annual[39]/ 6-10[40]	Germany	0-30
7	Hemp	0.15	0.14	0.15				6	5	Annual	China	0-15
8	Alfalfa				0.28			20	6-8	3-20[41,42]	USA	0-5
9	Opuntia ficus-indica				2.18	0.97	3.38	5	9	10-200[43]	Mexico	0-25
10	Red clover	0.05							2	3-4[44] annual[41,45]	Lithuanian	0-25
11	White mustard	0.40							2	Annual	Lithuanian	0-25
Current land use: crop &forest												
12	White clover	0.6	0.55	0.65				30	4	Annual/	Zimbabwe	0-15

						2-4[46,47]		
Current land use: no definition								
13	Bungeana	0.16	0.40	5	27	>150[48]	China	0-10, 10-20, 20-40

a: SOC data taken from Ledo et al.[27], except for hemp[49], alfalfa[50], opuntia ficus-indica [51], red clover, white mustard[52], white clover[53], bungeana[29].
b: LUC: land use changes

Table S I-3 shows binomial names of biopump candidates in Latin, it should be noticed that not only the plants as binomial names recorded in Table S I-3 but subspecies and varieties were also considered in data collection. For example, blueberry was recorded as *Vaccinium corymbosum*, while *Vaccinium angustifolium L, Vaccinium darrowii Camp, Vaccinium virgatum Aiton, Vaccinium elliottii Chapm* were also adopted as varieties[54].

Table S I-3 Binomial name of biopump candidates.

Candidate	Binomial name in Latin
Woody	
Acacia	Acacia mangium
Acerola	Malpighia glabra L.
Alder	Alnus glutinosa
Araucaria	Araucaria angustifolia
Atriplex	Atriplex nummularia
Black locust	Robinia pseudoacacia
Blueberry	Vaccinium corymbosum L.
Guava	Psidium guajava L
Olive	*Olea europaea L.*
Poplar	Populus spp
Willow	Salix spp.
Korshinsk peashrub	Caragana korshinskii Kom
Rhamnoides	Hippophae rhamnoides L
Microphylla	Caragana microphylla
Grassy	
Opuntia ficus-indica	Opuntia ficus-indica (L.) Mill
Alfalfa	Medicago sativa
Red clover	Trifolium pratense L.
Hemp	Cannabis sativa L.
Switchgrass	Panicum virgatum L.
White clover	Trifolium repens L.
Miscanthus	Miscanthus x giganteus
Ryegrass	Lolium perenne L.
Giant reed	Arundo donax L.
White mustard	Sinapis alba L.
Bahiagrass	Paspalum notatum Flüggé
Ramie	Boehmeria nivea L.
Bungeana	Stipa bungeana

Table S I-4 Biopump composition (in g/100g dry mass, unless otherwise specified). The biopumps in bold are those identified as suitable for a CSAAP strategy in France

No.	Name	Expected composition of the harvested biomass								
		Lignocellulosic				Crude protein	Sugar	Ash	Others	Ref
		Lignin	Cellulose	Hemicellulose	Total					
Woody										
1	Acacia	19.3-26.0	42.0	19.0		1.6	59.1	0.5		[55,56]
2	Acerola*				12.8-34.5	2.4-9.2			Lipid: 2.64-9.20	[57,58]
3	Alder	21.2-24.8	32.3-32.4	23.5-34.6				0.3-0.6		[59,60]
4	Araucaria	27.2-28.5	58.3							[61,62]
5	Atriplex				14.0-34.0	9.0-26.9			Sodium: 5- 6.05; potassium: 2-4.95; calcium: 0.41 gross energy: 15 MJ/kg.	[63,64]
6	Black locust	7.0-27.1	46.5	13.3		7.0-16.0		0.2-13.2	Acetate: 1.30;	[65,66]
7	Blueberry*	0.8	0.5			3.6-3.8	90.4	>0.1	Lipid 2.5-3.61; Vitamin B1: 0.02; Vitamin B2: 0.02; Vitamin C: 16 [mg/100g]	[54,67]
8	Guava*	16.2-22.1	33.2	14.4	63.8-69.6	7.7-11.7	11.5	1.0-6.3	Iron: 3.32; calcium: 60.07; phosphorus: 160.55; vitamin A: 50.13; vitamin C: 0.2; vitamin B3: 0.16; vitamin B6: 0.42; [mg/100g DM] gross energy: 18 MJ/kg.	[68,69]
9	Olive	17.9-27.7	26.1-36.6	17.9-25.0						[70,71]
10	Poplar	22.3	22.0-46.7	16.6				2.1		[72,73]
11	Willow		43.8	31.2	18.0-74.9	16.7		10.2	Pentosans: 20.98 calcium : 1.60; phosphorus : 0.26; gorss energy: 17.8 MJ/kg	[74,75]

12	Korshinsk pea shrub	11.2	16.6	26.4						[76]
13	Rhamnoides*	6.8	12.0	6.5		14.9	43.4	4.1	Quinic: 26.5; malic: 13.8 ; citric: 2.21; oxalic: 0.26; tartaric: 0.81; Lipid: 5.44;	[77,78]
14	Microphylla*				34.1	11.4		8.8	Gross energy: 18.6 MJ/kg; **calcium: 0.91;** **phosphorus: 0.62.**	[79]
Grass										
1	Bahiagrass	4.7			31.5-33.5	9.7-14.2		10.7	Gross energy: 18.3 MJ/kg DM	[69,80]
2	Giant reed	8.0-34.0	21.0-42.0	7.0-23.0		4.0-8.0		3.0-8.0		[81,82]
3	Miscanthus	10.5-16.5	30.2.-57.6	15.9-19.2		3.4-6.8		2.0		[83,84]
4	Ryegrass				43.3	20.8	54.0	9.20	Lipid: 3.4	[85,86]
5	Switchgrass	10.8	45.0	27.0		7.3	46.3		Lipid: 7.3	[87,88]
6	Ramie	0.6-0.7	68.6-76.2	13.1-16.7					Pectin: 1.9; wax: 0.3.	[89,90]
7	Hemp	4.0-19.0	40.0-67.0	13.0-26.0						[88,91]
8	Alfalfa	7.0-21.3	20.0-67.2	11.0-23.5		21.0				[92,93]
9	Opuntia ficus-indica				13.8	12.0-15.8			Lipid: 2.2-2.7	[94,95]
10	Red clover	13-15.5	36.7	20.6						[96,97]
11	White mustard*				7.1-8.6	23.4-36.9		5.10-8.3	Calcium : 0.05; Phosphorus : 1.11; Gross energy: 20.3 MJ/kg.	[98,99]
12	White clover	3.5-15.2			23.4	22.7		12.3	Gross energy: 17.4MJ/kg	[96,100–102]
13	Bungeana	15.4	45.2	26.8				2.7		[103]

Plant compositions are given in g/100g DM, otherwise specified.
*: Composition of fruit or seed.

2 Methodology for biopump selection for France

Table S I-5 The yield, SOC change, agricultural intensity, suitability in France, and invasion risk of biopump candidates.

Biopump candidates	Criteria							
	1)Yield	2)SOC increase capacity		3)Agricultural intensity			4)Suitability[c]	5)Invasion risk[d]
		SOC concentration (g kg-1 y-1)	SOC stock (Mg ha-1 y-1)	Water[a]	Annual N input (kg ha^{-1})	Pesticides [b]		
Woody								
Acacia	12-22.3[104]	1.07		W3[105,106]	0[107]	I0[108]	S0[109]	R1
Acerola	6.7-10.5[110]	0.21		W3[111]	40[112]	I2[113]	S1[114,115]	R2
Alder	5.9 [114,116]	0.08		W2[117]	0[117]	I2[105,118]	S3[114]	R2
Araucaria	34.6 [114,119]		1.15	W1[120]	0[121]	I2[2]	S3[122]	R3
Atriplex	25[123]	0.46		W1[124]	37[125]	I3[115]	S3[122]	R3
Black locust	62.6[114,126]	0.65	0.003	W3[127]	92[127]	I2[128]	S3[129]	R3
Blueberry	14.8[2]		1.41	W0[130]	100-300[131]	I1[2]	S3[132]	R3
Guava	11.2-16.8[133]	0.01		W0[134]	143-571[135]	I0[115]	S1[115,136]	R3
Olive	37[114,137]	1.06		W2[138]	120-150[139]	I1[139]	S3[138]	R3
Poplar	4.3-10.7[140,141]	0.2		W2[142]	0[143]	I1[144]	S3[129]	R2
Willow	20[145]	0.1		W1[146]	80-120[146]	I2[18,146]	S3[129]	R1
Korshinsk peashrub	4.13[22,147]	0.16	0.38	W3[22,28]	0[28]	I3[28]	S1[148]	R2
Rhamnoides	5-6[149]	0.25	0.58	W2[24,150]	0-238[150,151]	I0[150]	S3[152]	R3
Microphylla	16.53[153]	0.22	0.5	W3[154,155]	0[154]	I0[156]	S2[115,152]	R3
Grassy								
Opuntia ficus-indica	1.56[157]		8.7	W3[157]	100[157]	I1[158]	S3[115]	R3
Alfalfa	3-8.3[159]		0.28	W2[123]	0[160]	I1[161]	S3[115]	R3
Red clover	3[52]	0.05		W2[162]	0[161,163]	I2[164]	S3[115,152]	R3
Hemp	6.7[165]	0.15		W2[166–168]	60-200[165]	I2[167,169]	S3[165]	R3
Switchgrass	15[145]	0.08	0.4	W3[170]	50-100[145]	I2[170]	S3[115]	R3
White clover	7-13.6[171]	0.6		W1[172]	0[161]	I1[161]	S3[115,152]	R1[115]
Miscanthus	12.15-40[145,173]	0.09	0.25	W2[173–175]	40-107.1[145,173,174]	I2[175]	S3[176]	R3[174]
Ryegrass	9.4[173]	1.22		W3[177,178]	386.9-407.1[173]	I3[40]	S3[177]	R1
Giant reed	30[145]	0.19		W1[174]	40[174]	I3[174]	S3[115]	R1[174]
White mustard	3.42[52]	0.4		W1[179]	80-160[180]	I3[181]	S3[115]	R3
Bahiagrass	13.49[182]	0.23		W3[183]	0[183]	I2[183]	S1[69]	R1[183]
Ramie	13[184]	0.45		W1[184,185]	30-72[184,185]	I1[184,185]	S0[185]	R3
Bungeana	3[186]	0.16	0.4	W2[187]	0-138[188]	I3[187,188]	S0[105]	R2

a: W0: Need irrigation regularly; W1: Need irrigation in certain period; W2: Could live without irrigation but water would prompt the yield; W3: Survives with rain water only in region of origin, tolerant to drought.
b: P0: Susceptible to get pest/weed problem. Pesticides necessary; P1: There is at least one pest or weed problem would cause a serious disease. Pesticides typically used; P2: There is at least one pest or weed problem but not serious. Pesticides sometimes used; P3: Great resistance against the pest. Pesticides seldom used.
c: S0: Not currently growing in France or countries with similar conditions; S1: Grows in countries in other continents but have similar environment to France; S2: Grows in European countries with similar conditions; S3: Already grows in France.
d: R0: Invasive and difficult to control; R1: Invasive but can be contained; R2: No information about invasion, judged to be non-invasive /the species in table s3 is not invasive but subspecies or varieties would be. R3: Proved to be non-invasive

3 Suitable anthropogenic products

Table S I-6 Non-exhaustive list of studies with examples of bio-based materials and chemicals produced from plant biomass (not only biopumps), with a focus on the parameters affecting the conceptual biomass-to-bioeconomy performance. Biopump species identified in this study are marked with a *. Lifetime are as reported by the studies, unless otherwise specified.

Biomass	Key Processes involved	Plant used parts	Potential Final Products	Intermediate to finial product	Life time (years)	End-of-life	Type of use / sector of activity	Likely Replaced product†	Ref
Maize	Starch extraction, film production	Fruit	Packaging film		Few days[a]	Landfill/ composting/ digestion	Packaging	Petrochemical Polypropylene/ polyethylene	[189]
Opuntia ficus-indica*	Mucilage extraction, mixing with plasticizer, drying.	Stem	Food packaging films and coatings.		Few days[a]	Landfill/ composting/ digestion	Packaging	Petrochemical Polypropylene/ polyethylene	[190]
Maize	Wet milling, fermentation, recovery, blown film extrusion	Fruit	Carrier bag	Polyhydroxyal kanoates	Few days[a]	Landfill/ incineration/ composting	Plastic	Petrochemical Polypropylene	[191]
Residues from maize & rice harvest.	Furfural extraction, oxidation, dehydration, Diels-Alder with furan, polymerization	Cob, stock, hull.	Bottle	Terephthalic acid	Few days[b]	Gasification/ recycling/ pyrolysis/ incineration	Packaging	Polyethylene terephthalate	[192]

Beech	Viscose process[193], spinning, kitting, dyeing, confection	Bark, stick, stem, branch	T-shirt		<5[a]	Incineration/ landfill/ recycling[194]	Textile	Petrochemical-based textile (PET)†	[195]
Sorghum	Fermentation, salt separation, evaporation and crystallization	Grain	Food supplement (for Soups, salads)	Succinic acid	Few days[a]		Food & Beverage	Fresh meat extracts	[196]
Giant reed*	Crushing, drying, pelletising, hydrolysis, fermentation		Bottle	Biopolymer (1,3-propanediol)	Few days[b]	Gasification/ recycling/ pyrolysis/ incineration	Packaging	Petrochemical Polyethylene terephthalate (PET)[a]	[197]
Eucalyptus	Dissolution, mixing with additives	Pulp	Oriented strand board/ plywood/ particleboard/ fiberboard	Wood adhesives	50	Recycling/ incineration	Nanocomposites(adhesives)	Urea-formaldehyde, phenol-formaldehyde/ melamine formaldehyde	[198]
Eucalyptus	Alkalisation, preageing, xanthation, dissolving, ageing, viscose, spinning, desulf, drying	Stem, branch	Silk, velvet	Viscose/ tencel for biopolymer	2	Recycling/ compost /incineration	Textile	Petrochemical-based textile (PET)[a]	[193]
Eucalyptus/ maple wood/ pine*/ poplar*	Hydrolysis, isomerization, dehydration	Stem	Bottle	Furfural	Few days[b]	Gasification/ recycling/ pyrolysis/ incineration	Packaging	Polyethylene terephthalate[a]	[199]
Sweet chestnut	Drying, grinding, suspend in solvent, filtration, evaporation	Sawdust	Flame retardants		Few days[a]		Chemical	Triphenyl phosphate (TPP)[a]	[200]

Pine*	Mill, sieve, water extraction.	Branch, stump	T shirt	Lignin, cellulose, hemicellulose	<5[a]	Incineration/ recycle	Textile	Petrochemical-based textile (PET)	[201]
Poplar*	Fe^{3+}-assisted acetic acid pretreatment, enzymatic hydrolysis.	Sawdust	Ethanol	Xylose, lignin	Few days[a]		Chemicals	Fossil	[202]
Birch	Polyesterification, molding.	Bark	Mattress, car parts,	Polyester thermoset	10[a]	Incineration/ landfill/ recycling	Plastic	Polyurethane[a]	[203]
Sugarcane	Soaking, chemical impregnation, steaming, defibration, screening& refining.	Bagasse	Paper		Few days[a]	Incineration/ recycle	Textile	Soda,kraft, sulphite[a]	[204]
Bamboo	Fiber extraction, dissolution with polylactic acid, casting, evaporation.	Stem	Membrane for desalination, food processing.	Fiber	10	Landfill	Plastic	Petroleum-based polymer†	[205]
Palm	Maleinization, epoxy-carboxyl reaction, copolymerization	Fruit	Pipe	Unsaturated resin	100	Recycling/ landfill	Plastic	Fossil glycerol	[206]
Cardoon/ miscanthus*/ switchgrass*	Drying, pelletising, hydrolysis, fermentation	Above ground	Bottle	Biopolymer (1,3-propanediol	Few days[b]	Gasification/ recycling/ pyrolysis/ incineration	Packaging	Polyethylene terephthalate[a]	[197]
Miscanthus*		Stalk	Transport pallet	Fiber	5	Landfill/ Incineration/ recycle	Building	Wood†	[207]
Flax	Fiber extraction, preliminary	Stalk	Beam	Fiber	50	Recycle	Building	Epoxy, polyester,	[208,209]

	molding, wrapping with fax mat, reinforcement.							phenolic, vinyl-ester[a]	
Flax	Fiber extrusion, injection, molding.	Stalk	Under-engine panels	Fiber	7.5	Incineration	Automotive	Plastic[a]	210
Kenaf	Cleaning, binder addition, molding.	Stalk	Thermal insulation board	Fiber	30	Incineration	Building	Polystyrene (EPS), extruded polystyrene (XPS), polyurethane (PUR)[a]	211
Kenaf	Grinding, mixing, foaming in mold, curing.	Stalk	Thermal insulated panels	Fiber	10	Landfill	Building	Mineral, chemical[a]	212
Hemp*/ cotton	Fiber extraction, mattress manufacture	Stalk/fruit	Pocket spring mattress	Fiber	10	Landfill/ incineration/ recycling /conversion to ethanol	Textile	Petrochemical textile (PET)[a]	213
Hemp*	Process chain not detailed.	Stalk	Side panel	Fiber	14	Landfill	Automotive	Plastic[a]	214
Hemp*	Fiber extraction, wrapping fiber fabric onto a steel mandrel, curing.	Stalk	Elbow fitting	Fiber	20	Landfill	Building	Glass fabrics[a]	215
Hemp*	Blending with epoxy resin.	Stalk	Composite component for automotive	Fiber	10	Recycle	Automotive	Plastic[a]	216
Hemp*	Process chain not detailed.	Stalk	Reinforced component in car	Fiber	7.5	Incineration/ landfill	Automotive	Plastic[a]	217

Hemp*	Defibering, sieving, mixing with binder	Stalk	Wall	Shives	100	Recycle/ landfill	Building	Brick	[218]

a: Own evaluation
b: Plastic could keep in use with a proper recycling pathway, like adding plasticizer[219].
* Biopumps

Table S I-7 Trends of grassland area and ruminant production for different regions[220]

	Runminant[a]	Grass land[b]
World		
2005	73.86	3009449.62
2010	72.32	3019698.47
2015	71.86	3006498.91
2019	72.35	3008311.60
Northern America		
2005	74.6	478999.55
2010	74.14	480902.05
2015	72.37	477310.28
2019	72.22	473703.14
Europe		
2005	65.13	304379.19
2010	63.26	307475.52
2015	62.5	304689.05
2019	62.33	304017.76
Oceania		
2005	95.51	195907.55
2010	94.99	202221.67
2015	94.87	183263.87
2019	93.84	185794.23

[a] Cattle, sheep, goats, horses, buffaloes; unit in % of total live stock unit.
[b] Unit in 1000 ha.

Table S I-8 Examples of carbon distribution during biomass processing (% in the final product, the rest being a residue), and lifetime of the carbon-based products

Product	Plant	Carbon in product [%]	Product lifetime [year]	Reference
Transport pallet	Miscanthus	70	5	[214]
Elbow fitting	Hemp	87.8	20	[215]
Under-engine panels	Flax	70	7.5	[210,216]
Insulated panels	Kenaf	80	10	[212,216]
Composite component for Automotive	Hemp	100	10	[216]
Reinforced component in Ford car	Hemp	100	7.5	[216,217]
Wall	Hemp	60	100	[218]
Bioenergy	Miscanthus	65	short	[221]
Heat	Willow	100	short	[222]

4 Carbon vulnerable arable land in France

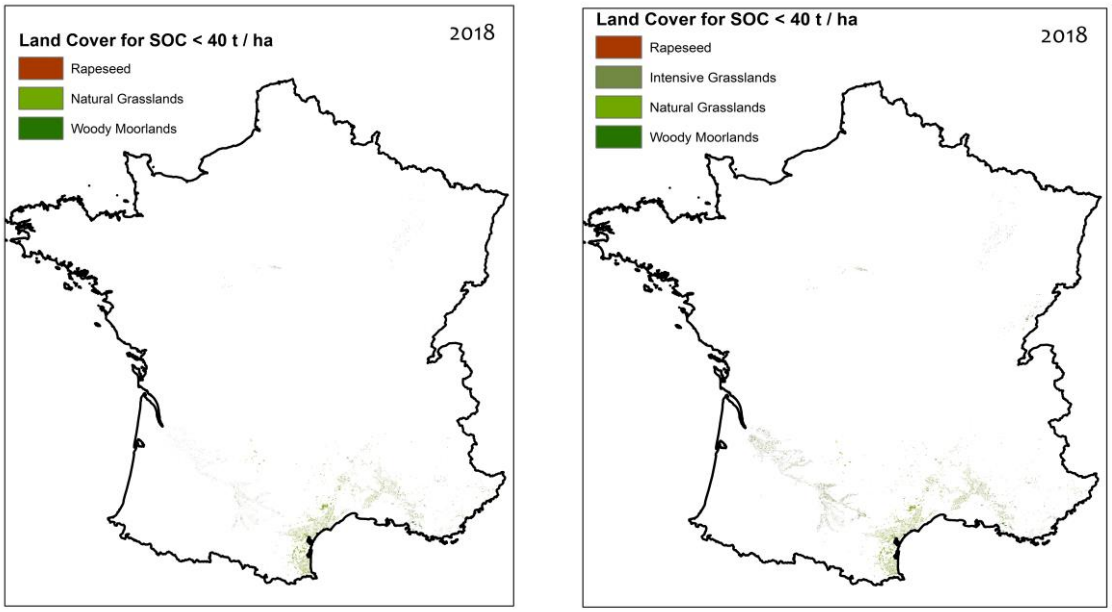

Fig. s I-1 Area with SOC < 40 t/ha in France, without (left) and with (right) Intensive Grasslands.

5 Results for application case – sensitive analysis on miscanthus chosen as biopump

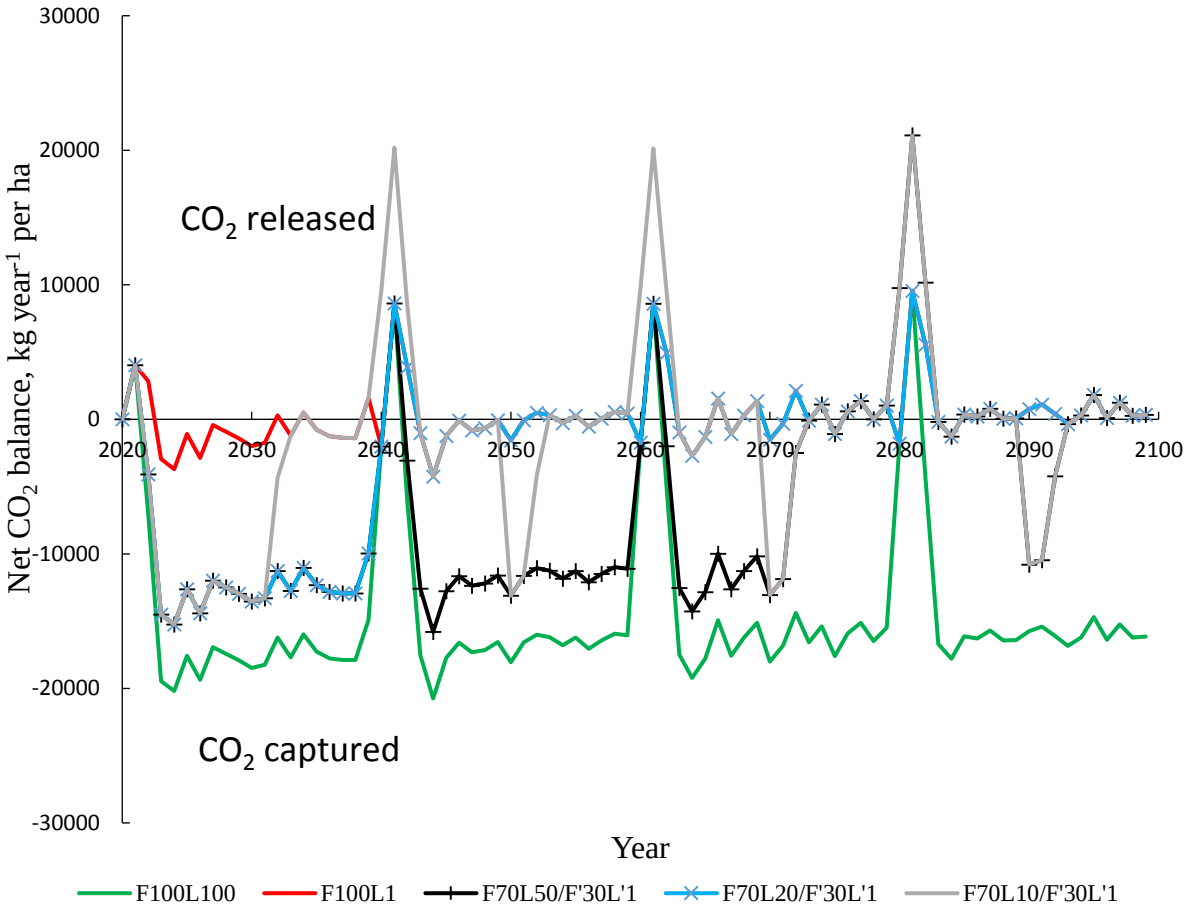

Fig. s I-2 Net biogenic carbon flows.

F =fraction of biogenic carbon used in the main product (100%, 100%, 70%, 70%, 70%), L = lifetime of the main product (100, 1, 50, 20, 10 years); F'=fraction of biogenic carbon in the by-product (0, 0, 30%, 30%, 30%), L'=lifetime of by-product (no, no, 1, 1, 1 years).

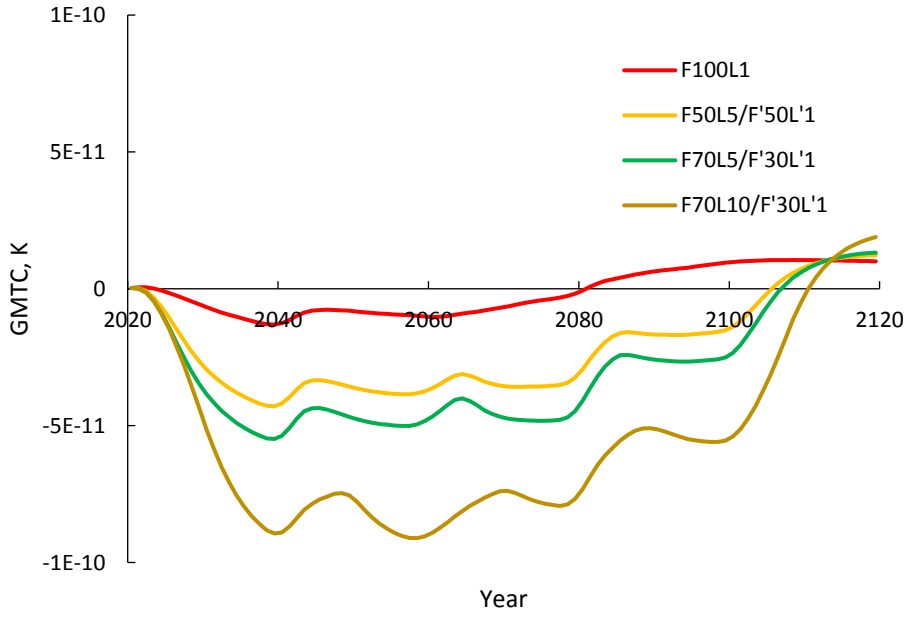

Fig. s I-3 Sensitivity analysis on global mean temperature change (GMTC) following the life time of bio-based products.

F =fraction of biogenic carbon used in the main product (100%, 50%, 70%, 70%), L = lifetime of the main product (1, 5, 5, 10 years); F'=fraction of biogenic carbon in the by-product (0%, 50%, 30%, 30%), L'=lifetime of by-product (no, 1, 1, 1 years).

Lifetimes lesser than 5 years could potentially increase the net carbon flow towards atmosphere and determine an increase in global mean temperature as global warming indicator. Two cases are shown in Fig. s I-3 with 2 different fractions of biogenic carbon incorporated in the main product (lifetime of 5 years): 50% and 70%, the rest being transformed in GHG within 1 year. More this fraction is important, more the effect on global warming is benefic (case of F70L5/F'30L'1 versus F50L5/F'50L'1).

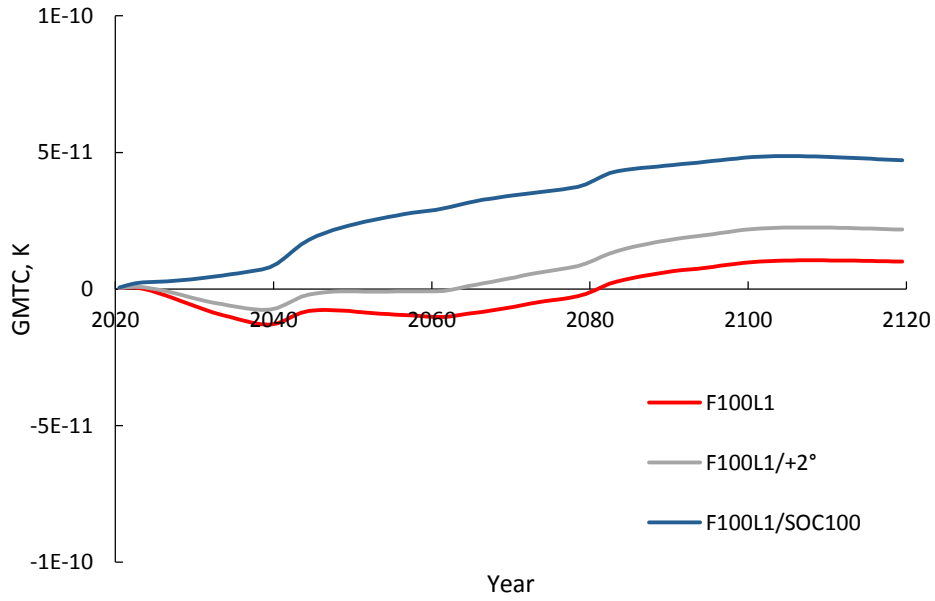

Fig. s I-4 Sensitivity analysis on global mean temperature change (GMTC) for different initial SOC and temperature conditions.

F100L1; initial SOC of 100 Mg ha^{-1} noted F100L1/SOC100; temperatures higher by 2° noted F100L1/+2 °C .

The case of F100L1 is considered here because for this scenario with rapid emission of all biogenic carbon, the mitigation potential is uncertain. The simulations for higher initial SOC (100 instead of 42.35 Mg ha^{-1}) or for higher temperatures by 2 °C, show that the mitigation potential completely vanishes.

References

(1) Gardening in Tucson, P.; California, A. and. Growing Barbados Cherry / Acerola: Malpighia https://gardenoracle.com/images/malpighia.html.
(2) Wilk, P.; Simpson, M.; Blueberry, I. D. Blueberry Establishment and Production Costs. **2015**, No. September.
(3) Life Cycle of a Blueberry Bush https://www.hunker.com/12531865/life-cycle-of-a-blueberry-bush.
(4) Morton, J. F.; Dowling, C. F. *Fruits of Warm Climates*; JF Morton Miami, FL, 1987; Vol. 20534.
(5) Guava lifespan http://www.iucngisd.org/gisd/species.php?sc=211.
(6) Urban Forest Ecosystems Institute. Oliver https://selectree.calpoly.edu/tree-detail/olea-europaea.
(7) Growing Olives: Olea europaea https://gardenoracle.com/images/olea-europaea.html.
(8) Urban Forest Ecosystems Institute. ACACIA https://selectree.calpoly.edu/tree-detail/acacia-abyssinica.
(9) Lisan, B. *Fiche Présentation Arbre : Acacia Mangium*. https://m.20-bal.com/law/1895/index.html
(10) Urban Forest Ecosystems Institute. Alder https://selectree.calpoly.edu/tree-detail/alnus-cordata.
(11) European black alder lifespan http://www.iucngisd.org/gisd/speciesname/Alnus+glutinosa.
(12) Institute, Urban Forest Ecosystems, C. P. S. U. Araucaria https://selectree.calpoly.edu/tree-detail/araucaria-araucana.
(13) Araucarias lifespan https://www.edenproject.com/learn/for-everyone/plant-profiles/monkey-puzzle.
(14) Warne, A. Black Locust (Robinia Pseudoacacia L.). Best Management Practices in Ontario. *Ontario invasive plant Counc. Peterbrgh.* **2016**.
(15) Sitzia, T.; Cierjacks, A.; Rigo, D. De; Caudullo, G. Robinia Pseudoacacia Linn. *SpringerReference* **2011**, 166–167. https://doi.org/10.1007/springerreference_69293.
(16) poplar lifespan https://www.hunker.com/12286306/the-lifespan-of-a-poplar-tree.
(17) Populus alba lifespan https://selectree.calpoly.edu/tree-detail/populus-alba.
(18) sciencing. What Is the Lifespan of a Weeping Willow? https://sciencing.com/lifespan-weeping-willow-6497094.html.
(19) Gustafsson, J.; Larsson, S.; Nordh, N. E. Manual for SRC Willow Growers. Lantmännen Agroenergi, Sweden. 18 P. 2009.
(20) Cibils, A. F. *Plant-Herbivore Interactions in Atriplex: Current State of Knowledge*; US Department of Agriculture, Forest Service, Rocky Mountain Research Station, 1998.
(21) Oxford University Press. In: Flora of North America Editorial Committee (ed.): Magnoliophyta:Caryophyllidae, part 1.
(22) Xiao, S.; Xiao, H.; Peng, X.; Wang, W.; Chen, X.; Tian, Q. Dendroecological Assessment of Korshinsk Peashrub (Caragana Korshinskii Kom.) from the Perspective of Interactions among Growth, Climate, and Topography in the Western Loess Plateau, China. *Dendrochronologia* **2015**, *33*, 61–68. https://doi.org/10.1016/j.dendro.2015.01.001.
(23) Fang, X. W.; Turner, N. C.; Xu, D. H.; Jin, Y.; He, J.; Li, F. M. Limits to the Height Growth of Caragana Korshinskii Resprouts. *Tree Physiol.* **2013**, *33* (3), 275–284. https://doi.org/10.1093/treephys/tpt006.
(24) Interactive Agricultural Ecological Atlas of Russia and Neighboring Countries. Hippophae rhamnoides L.- Sea Buckthorn http://www.agroatlas.ru/en/content/cultural/Hippophae_rhamnoides_K/index.html.
(25) Urban Forest Ecosystems Institute. Bursera microphylla https://selectree.calpoly.edu/tree-detail/bursera-microphylla.
(26) AUB Landscape database https://landscapeplants.aub.edu.lb/Plants/PlantProfile/a641773d-0adb-4bad-b931-9121612e079e.
(27) Ledo, A.; Hillier, J.; Smith, P.; Aguilera, E.; Blagodatskiy, S.; Brearley, F. Q.; Datta, A.; Diaz-Pines, E.; Don, A.; Dondini, M.; et al. A Global, Empirical, Harmonised Dataset of Soil Organic Carbon Changes under Perennial Crops. *Sci. Data* **2019**, *6* (1), 1–7. https://doi.org/10.1038/s41597-019-0062-1.

(28) Fu, X.; Shao, M.; Wei, X.; Horton, R. Soil Organic Carbon and Total Nitrogen as Affected by Vegetation Types in Northern Loess Plateau of China. *Geoderma* **2010**, *155* (1–2), 31–35. https://doi.org/10.1016/j.geoderma.2009.11.020.
(29) Chen, L.; Gong, J.; Fu, B.; Huang, Z.; Huang, Y.; Gui, L. Effect of Land Use Conversion on Soil Organic Carbon Sequestration in the Loess Hilly Area, Loess Plateau of China. *Ecol. Res.* **2007**, *22* (4), 641–648. https://doi.org/10.1007/s11284-006-0065-1.
(30) Burgess, J. L.; Worthen, E. L. *Soil Survey of Lancaster County, Nebraska*; US Government Printing Office, 1908.
(31) Amarasekara, A. S. *Handbook of Cellulosic Ethanol*; John Wiley & Sons, 2013.
(32) El-ramady, H. R.; Abdalla, N.; Alshaal, T.; Fári, M.; Prokisch, J.; Pilon-smits, E. A. H.; Domokos-szabolcsy, É. *Selenium Phytoremediation by Giant Reed*; 2015. https://doi.org/10.1007/978-3-319-19375-5.
(33) Heaton, E.; Taske, T. Department of Agronomy Giant Miscanthus for Biomass Production Comparison of Dry Matter Yields. *Iowa State Univ. Univ. Ext.* **2010**, No. January, 201–202.
(34) Peri, M.; Komatina, M.; Antonijevi, D. Life Cycle Impact Assessment of Miscanthus Crop for Sustainable Household Heating in Serbia. 1–26. https://doi.org/10.3390/f9100654.
(35) Duffy, M. D.; Nanhou, V. Y. Costs of Producing Switchgrass for Biomass in Southern Iowa. *Trends new Crop. new uses* **2002**, *1998* (November 1998), 267–275.
(36) Lerkkasemsan, N.; Achenie, L. E. K. Life Cycle Costs and Life Cycle Assessment for the Harvesting, Conversion, and the Use of Switchgrass to Produce Electricity. *Int. J. Chem. Eng.* **2013**, *2013*, 1–16. https://doi.org/10.1155/2013/492058.
(37) Ramie https://www.swicofil.com/commerce/products/ramie/145/introduction.
(38) Sen, T.; Reddy, H. N. J. Various Industrial Applications of Hemp , Kinaf , Flax and Ramie Natural Fibres. *Int. J. Innov. Manag. Technol.* **2011**, *2* (3), 192–198. https://doi.org/http://dx.doi.org/10.7763/IJIMT.2011.V2.130.
(39) U.S. DEPARTMENT OF AGRICULTURE. Lolium perenne L. Show All perennial ryegrass https://plants.sc.egov.usda.gov/core/profile?symbol=LOPE.
(40) Dodd, M. B.; Chapman, D. F.; Ludemann, C. I.; Griffiths, W.; Tozer, K. N.; Donnelly, L. The Measurement of Perennial Ryegrass Persistence. *J. New Zeal. Grasslands* **2018**, *80*, 161–168.
(41) Saskatchewan Forage Council. *Forage Factsheet – Alfalfa*; 2007. https://trawinseeds.ca/wp-content/uploads/2018/09/Forage-Factsheet-%E2%80%93-Alfalfa.pdf
(42) AlphaAlfa. Production and Procurement of Alfalfa in South Africa. **2016**, No. February, 1–10.
(43) Urban Forest Ecosystems Institute. SAGUARO CACTUS https://selectree.calpoly.edu/tree-detail/carnegiea-gigantea.
(44) Rural Economy & Development Programme. *ORGANIC FARMING A Guide to Red Clover*.
(45) Sustainable Agriculture Research & Education. Red Clover https://www.sare.org/Learning-Center/Books/Managing-Cover-Crops-Profitably-3rd-Edition/Text-Version/Legume-Cover-Crops/Red-Clover.
(46) Sustainable Agriculture Research & Education. WHITE CLOVER https://www.sare.org/Learning-Center/Books/Managing-Cover-Crops-Profitably-3rd-Edition/Text-Version/Legume-Cover-Crops/White-Clover.
(47) Department of Health and Ageing Office of the Gene Technology Regulator, A. environment. *The Biology of Trifolium Repens L. (White Clover)*; 2008.
(48) Urban Forest Ecosystems Institute. Pinus bungeana https://selectree.calpoly.edu/tree-detail/pinus-bungeana.
(49) Li, L. J.; Zeng, D. H.; Mao, R.; Yu, Z. Y. Nitrogen and Phosphorus Resorption of Artemisia Scoparia, Chenopodium Acuminatum, Cannabis Sativa, and Phragmites Communis under Nitrogen and Phosphorus Additions in a Semiarid Grassland, China. *Plant, Soil Environ.* **2012**, *58* (10), 446–451. https://doi.org/10.17221/6339-pse.
(50) Grandy, A. S.; Robertson, G. P. Land-Use Intensity Effects on Soil Organic Carbon Accumulation Rates and Mechanisms. *Ecosystems* **2007**, *10* (1), 58–73. https://doi.org/10.1007/s10021-006-9010-y.
(51) Bautista-Cruz, A.; Leyva-Pablo, T.; de Leon-Gonzalez, F.; Zornoza, R.; Martinez-Gallegos, V.; Fuentes-Ponce, M.; Rodriguez-Sanchez, L. Cultivation of Opuntia Ficus-Indica under Different Soil Management Practices: A Possible Sustainable Agricultural System to Promote Soil Carbon

Sequestration and Increase Soil Microbial Biomass and Activity. *L. Degrad. Dev.* **2018**, *29* (1), 38–46. https://doi.org/10.1002/ldr.2834.
(52) Arlauskienė, A.; Maikštėnienė, S.; Šlepetienė, A. APPLICATION OF ENVIRONMENTAL PROTECTION MEASURES FOR CLAY LOAM CAMBISOL USED FOR AGRICULTURAL PURPOSES. *J. Environ. Eng. Landsc. Manag.* **2011**, *19* (1), 71–80. https://doi.org/10.3846/16486897.2011.557266.
(53) Abbasi, M. K.; Khizar, A.; Tahir, M. M. Forage Production, Nitrogen Fixation, and Soil N Accumulation of White Clover in the Hill Farming System of Azad Jammu and Kashmir. *Commun. Soil Sci. Plant Anal.* **2009**, *40* (9–10), 1546–1565. https://doi.org/10.1080/00103620902831545.
(54) Michalska, A.; Łysiak, G. Bioactive Compounds of Blueberries: Post-Harvest Factors Influencing the Nutritional Value of Products. *Int. J. Mol. Sci.* **2015**, *16* (8), 18642–18663.
(55) Yáñez, R.; Romaní, A.; Garrote, G.; Luis Alonso, J.; Parajó, J. C. Processing of Acacia Dealbata in Aqueous Media: First Step of a Wood Biorefinery. *Ind. Eng. Chem. Res.* **2009**, *48* (14), 6618–6626. https://doi.org/10.1021/ie900233x.
(56) Han, J. S. Properties of Nonwood Fibers. In *Proceedings of the Korean society of wood science and technology annual meeting*; The Korean Society of Science and Technology Seoul, Korea, 1998; pp 3–12.
(57) Mezadri, T.; Villan, D. Journal of Food Composition and Analysis Antioxidant Compounds and Antioxidant Activity in Acerola (Malpighia Emarginata DC .) Fruits and Derivatives. **2008**, *21*, 282–290. https://doi.org/10.1016/j.jfca.2008.02.002.
(58) Prakash, A.; Baskaran, R. Acerola , an Untapped Functional Superfruit : A Review on Latest Frontiers. *J. Food Sci. Technol.* **2018**, *55* (9), 3373–3384. https://doi.org/10.1007/s13197-018-3309-5.
(59) Thomsen, T. P.; Ahrenfeldt, J.; Thomsen, S. T. Assessment of a Novel Alder Biorefinery Concept to Meet Demands of Economic Feasibility, Energy Production and Long Term Environmental Sustainability. *Biomass and Bioenergy* **2013**, *53*, 81–94. https://doi.org/10.1016/j.biombioe.2013.02.022.
(60) Antal Jr, M. J.; Allen, S. G.; Dai, X.; Shimizu, B.; Tam, M. S.; Grønli, M. Attainment of the Theoretical Yield of Carbon from Biomass. *Ind. Eng. Chem. Res.* **2000**, *39* (11), 4024–4031.
(61) Guerra, M. P.; Silveira, V.; dos Santos, A. L. W.; Astarita, L. V; Nodari, R. O. Somatic Embryogenesis in Araucaria Angustifolia (Bert) O. Ktze. In *Somatic Embryogenesis in Woody Plants: Volume 6*; Jain, S. M., Gupta, P. K., Newton, R. J., Eds.; Springer Netherlands: Dordrecht, 2000; pp 457–478. https://doi.org/10.1007/978-94-017-3030-3_15.
(62) Bengt Leopold, I. M. Investigation on the Nitrobenzene Oxidation Products of Lignin from Different Woods by Paper Partition Chromatography. *Acta Chem. Scand.* **1952**, *6*, 49–54.
(63) Fernández, S. S.; Padilla, A. P.; Mucciarelli, S. Protein Extraction from Atriplex Lampa Leaves: Potential Use as Forage for Animals Used for Human Diets. *Plant Foods Hum. Nutr.* **1999**, *54* (3), 251–259. https://doi.org/10.1023/A:1008148803544.
(64) Feedipedia, Inra, F. and A. O. of the U. N. Atriplex nummularia https://www.feedipedia.org/node/184.
(65) González-García, S.; Moreira, M. T.; Feijoo, G.; Murphy, R. J. Comparative Life Cycle Assessment of Ethanol Production from Fast-Growing Wood Crops (Black Locust, Eucalyptus and Poplar). *Biomass and Bioenergy* **2012**, *39*, 378–388. https://doi.org/10.1016/j.biombioe.2012.01.028.
(66) Yang, B.; Abula, R.; Xu, X.-L.; Aniwaer, A. Chemical Composition and in Vitro Ruminal Fermentation Characteristics of Tetraploid Black Locust (Robinia Pseudoacacia L.). *Asian J. Anim. Vet. Adv.* **2011**, *6* (7), 706–714.
(67) Skupień, K. Chemical Composition of Selected Cultivars of Highbush Blueberry Fruit (Vaccinium Corymbosum L.). *Folia Hortic* **2006**, *18* (2), 47–56.
(68) SERNA COCK, L.; MERA AYALA, J. D.; ANGULO LÓPEZ, J. E.; GÓMEZ SCHOUBEN, A. N. A. L. Kinetics of Alcoholic Fermentation Using Guava (Psidium Guajava) Seed Flour and Dry Mycelium of Aspergillus Niger as Nitrogen Sources. *Dyna* **2013**, *80* (180), 113–121.
(69) INRAE CIRAD AFZ and FAO. Feedipedia - Animal Feed Resources Information System https://www.feedipedia.org/.
(70) Romero-García, J. M.; Niño, L.; Martínez-Patiño, C.; Álvarez, C.; Castro, E.; Negro, M. J. Biorefinery Based on Olive Biomass. State of the Art and Future Trends. *Bioresour. Technol.* **2014**, *159*, 421–432. https://doi.org/10.1016/j.biortech.2014.03.062.

(71) Cuevas, M.; Sánchez, S.; Bravo, V.; García, J. F.; Baeza, J.; Parra, C.; Freer, J. Determination of Optimal Pre-Treatment Conditions for Ethanol Production from Olive-Pruning Debris by Simultaneous Saccharification and Fermentation. *Fuel* **2010**, *89* (10), 2891–2896.
(72) Devappa, R. K.; Rakshit, S. K.; Dekker, R. F. H. Forest Biorefinery: Potential of Poplar Phytochemicals as Value-Added Co-Products. *Biotechnol. Adv.* **2015**, *33* (6), 681–716. https://doi.org/10.1016/j.biotechadv.2015.02.012.
(73) Phyllis2. Poplar RMP (#2518) https://phyllis.nl/Browse/Standard/ECN-Phyllis#poplar.
(74) Krzyzaniak, M.; Stolarski, M. J.; Waliszewska, B.; Szczukowski, S.; Tworkowski, J.; Załuski, D.; Śnieg, M. Willow Biomass as Feedstock for an Integrated Multi-Product Biorefinery. *Ind. Crops Prod.* **2014**, *58*, 230–237. https://doi.org/10.1016/j.indcrop.2014.04.033.
(75) Anonymous. Analyses of Rhodesian Foodstuffs. *Rhod. Agric. J* **1934**, *31*, 651–658.
(76) Zou, Y.; Du, F.; Zhang, H.; Hu, Q. Evaluation of Korshinsk Peashrub (Caragana Korshinskii Kom.) as a Substrate for the Cultivation of Pleurotus Eryngii. *Waste and Biomass Valorization* **2019**, *10* (10), 2879–2885. https://doi.org/10.1007/s12649-018-0301-2.
(77) Beveridge, T.; Harrison, J. E.; Drover, J. Processing Effects on the Composition of Sea Buckthorn Juice from Hippophae Rhamnoides L. Cv. Indian Summer. *J. Agric. Food Chem.* **2002**, *50* (1), 113–116. https://doi.org/10.1021/jf010369n.
(78) Jaroszewska, A.; Biel, W. Chemical Composition and Antioxidant Activity of Leaves of Mycorrhized Sea-Buckthorn (Hippophae Rhamnoides L.). *Chil. J. Agric. Res.* **2017**, *77* (2), 155–162.
(79) Dougall, H. W.; Bogdan, A. V. Browse Plants of Kenya: With Special Reference to Those Occurring in South Baringo. *East African Agric. J.* **1958**, *23* (4), 236–245.
(80) Arthington, J. D.; Brown, W. F. Estimation of Feeding Value of Four Tropical Forage Species at Two Stages of Maturity. *J. Anim. Sci.* **2005**, *83* (7), 1726–1731.
(81) Vamvuka, D.; Sfakiotakis, S. Effects of Heating Rate and Water Leaching of Perennial Energy Crops on Pyrolysis Characteristics and Kinetics. *Renew. Energy* **2011**, *36* (9), 2433–2439.
(82) Yang, L.; Li, Y. Anaerobic Digestion of Giant Reed for Methane Production. *Bioresour. Technol.* **2014**, *171*, 233–239.
(83) Vasco-Correa, J.; Li, Y. Solid-State Anaerobic Digestion of Fungal Pretreated Miscanthus Sinensis Harvested in Two Different Seasons. *Bioresour. Technol.* **2015**, *185*, 211–217.
(84) Karp, A.; Shield, I. Bioenergy from Plants and the Sustainable Yield Challenge. *New Phytol.* **2008**, *179* (1), 15–32.
(85) Zhang, H.; Lopez, P. C.; Holland, C.; Lunde, A.; Ambye-Jensen, M.; Felby, C.; Thomsen, S. T. The Multi-Feedstock Biorefinery – Assessing the Compatibility of Alternative Feedstocks in a 2G Wheat Straw Biorefinery Process. *GCB Bioenergy* **2018**, *10* (12), 946–959. https://doi.org/10.1111/gcbb.12557.
(86) Cosgrove, G. P.; Koolaard, J.; Luo, D.; Burke, J. L.; Pacheco, D. The Composition of High Sugar Ryegrasses. In *Proceedings of the New Zealand Grassland Association*; New Zealand Grassland Association, 2009; Vol. 71, pp 187–193.
(87) Bals, B.; Teachworth, L.; Dale, B.; Balan, V. Extraction of Proteins from Switchgrass Using Aqueous Ammonia within an Integrated Biorefinery. *Appl. Biochem. Biotechnol.* **2007**, *143* (2), 187–198. https://doi.org/10.1007/s12010-007-0045-0.
(88) Leemhuis, R. J.; Jong, R. M. Biomassa: Biochemische Samenstelling En Conversiemethoden. *Petten, ECN* **1997**.
(89) Mohanty, A. K.; Misra, M. and; Hinrichsen, G. I. Biofibres, Biodegradable Polymers and Biocomposites: An Overview. *Macromol. Mater. Eng.* **2000**, *276* (1), 1–24.
(90) Gaur, S.; Reed, T. B. *An Atlas of Thermal Data for Biomass and Other Fuels*; National Renewable Energy Lab., Golden, CO (United States), 1995.
(91) Lavoie, J. M.; Beauchet, R. Biorefinery of Cannabis Sativa Using One- and Two-Step Steam Treatments for the Production of High Quality Fibres. *Ind. Crops Prod.* **2012**, *37* (1), 275–283. https://doi.org/10.1016/j.indcrop.2011.11.016.
(92) Dien, B. S.; Jung, H. J. G.; Vogel, K. P.; Casler, M. D.; Lamb, J. A. F. S.; Iten, L.; Mitchell, R. B.; Sarath, G. Chemical Composition and Response to Dilute-Acid Pretreatment and Enzymatic Saccharification of Alfalfa, Reed Canarygrass, and Switchgrass. *Biomass and Bioenergy* **2006**, *30* (10), 880–891. https://doi.org/10.1016/j.biombioe.2006.02.004.

(93) Cherney, J. H.; Lowenberg-DeBoer, J.; Johnson, K. D.; Volenec, J. J. Evaluation of Grasses and Legumes as Energy Resources. *Eval. grasses Legum. as energy Resour.* **1989**, 289–323.
(94) Rodriguez-Felix, A.; Cantwell, M. Developmental Changes in Composition and Quality of Prickly Pear Cactus Cladodes (Nopalitos). *Plant Foods Hum. Nutr.* **1988**, *38* (1), 83–93. https://doi.org/10.1007/BF01092314.
(95) Makkar, H. P. S. *Cactus as a Fodder and Beyond*; 2017. www.feedipedia.org Broaden.
(96) Wilman, D.; Altimimi, M. A. K. The In-vitro Digestibility and Chemical Composition of Plant Parts in White Clover, Red Clover and Lucerne during Primary Growth. *J. Sci. Food Agric.* **1984**, *35* (2), 133–138. https://doi.org/10.1002/jsfa.2740350203.
(97) M.D.Ackerson, E.C. Clausen, J. L. G. Production of Ethanol from the Lignocellulosic Fraction of MSW. In *7th E.C. Conference Biomass for Energy and Industry*; 1992; pp 876–890.
(98) Ildikó, S. G.; Klára, K. A.; Marianna, T. M.; Ágnes, B.; Zsuzsanna, M. B.; Bálint, C. The Effect of Radio Frequency Heat Treatment on Nutritional and Colloid-Chemical Properties of Different White Mustard (Sinapis Alba L.) Varieties. *Innov. Food Sci. Emerg. Technol.* **2006**, *7* (1–2), 74–79. https://doi.org/10.1016/j.ifset.2005.06.001.
(99) Lim, H. K. Animal Feeding Stuffs. 3. Compositional Data of Feeds and Concentrates. *Malaysian Agric. J.* **1967**, *46*, 63–79.
(100) Giovanni, R. Feeding Value of Grass-with Clover Swards. *Prod. Anim.* **1988**.
(101) Alibes, X.; Tisserand, J. L. Tables of the Nutritive Value for Ruminants of Mediterranean Forages and By-Products. *Options Mediterr. Ser. B Etudes Rech.* **1990**.
(102) Aitchison, E. M.; Gill, M.; Dhanoa, M. S.; Osbourn, D. F. The Effect of Digestibility and Forage Species on the Removal of Digesta from the Rumen and the Voluntary Intake of Hay by Sheep. *Br. J. Nutr.* **1986**, *56* (2), 463–476.
(103) Belkhir, S.; Koubaa, A.; Khadhri, A.; Ksontini, M.; Nadji, H.; Smiti, S.; Stevanovic, T. Seasonal Effect on the Chemical Composition of the Leaves of Stipa Tenacissima L. and Implications for Pulp Properties. *Ind. Crops Prod.* **2013**, *44*, 56–61. https://doi.org/10.1016/j.indcrop.2012.09.023.
(104) Torres Vélez, D. A.; Del Valle, J. I. Growth and Yield Modelling of Acacia Mangium in Colombia. *New For.* **2007**, *34* (3), 293–305. https://doi.org/10.1007/s11056-007-9056-5.
(105) Urban Forest Ecosystems Institute https://ufei.calpoly.edu/.
(106) Getahun, A.; Muleta, D.; Assefa, F.; Kiros, S. Plant Growth-Promoting Rhizobacteria Isolated from Degraded Habitat Enhance Drought Tolerance of Acacia (Acacia Abyssinica Hochst. Ex Benth.) Seedlings. *Int. J. Microbiol.* **2020**, *2020*. https://doi.org/10.1155/2020/8897998.
(107) Forrester, D. I.; Pares, A.; O'Hara, C.; Khanna, P. K.; Bauhus, J. Soil Organic Carbon Is Increased in Mixed-Species Plantations of Eucalyptus and Nitrogen-Fixing Acacia. *Ecosystems* **2013**, *16* (1), 123–132. https://doi.org/10.1007/s10021-012-9600-9.
(108) Chauhan, J.; Saini, I.; Kumar, T.; Kaushik, P. Integrated Pest Management for Acacia: Prospects and Challenges. *Preprints* **2020**, No. June. https://doi.org/10.20944/preprints202006.0164.v1.
(109) CABI. Invasive Species Compendium https://www.cabi.org/isc/.
(110) Plant Production and Protection Division of FAO (AGPC). Malpighia glabra http://ecocrop.fao.org/ecocrop/srv/en/cropView?id=1406.
(111) wikipedia. Malpighia emarginata https://en.wikipedia.org/wiki/Malpighia_emarginata.
(112) Cardoso, P. C.; Tomazini, A. P. B.; Stringheta, P. C.; Ribeiro, S. M. R.; Pinheiro-Sant'Ana, H. M. Vitamin C and Carotenoids in Organic and Conventional Fruits Grown in Brazil. *Food Chem.* **2011**, *126* (2), 411–416. https://doi.org/10.1016/j.foodchem.2010.10.109.
(113) How to Grow Acerola Cherries https://www.madaboutberries.com/acerola.html.
(114) The wood database https://www.wood-database.com/.
(115) Plants For A Future. Plants For A Future https://pfaf.org/user/Default.aspx.
(116) Fennessy, J. Common Alder (Alnus Glutinosa) as a Forest Tree in Ireland. *Coford Connect* **2004**, *8* (8), 1–4.
(117) Woodland trust. Alder https://www.woodlandtrust.org.uk/trees-woods-and-wildlife/british-trees/a-z-of-british-trees/alder/.
(118) Cardoso, A.; Gómez-Zurita, J. Food Resource Sharing of Alder Leaf Beetle Specialists (Coleoptera: Chrysomelidae) as Potential Insect–Plant Interface for Horizontal Transmission of Endosymbionts. *Environ. Entomol.* **2020**, No. Xx, 1–13. https://doi.org/10.1093/ee/nvaa111.

(119) Zamorano-Elgueta, C.; Cayuela, L.; González-Espinosa, M.; Lara, A.; Parra-Vázquez, M. R. Impacts of Cattle on the South American Temperate Forests: Challenges for the Conservation of the Endangered Monkey Puzzle Tree (Araucaria Araucana) in Chile. *Biol. Conserv.* **2012**, *152* (August 2012), 110–118. https://doi.org/10.1016/j.biocon.2012.03.037.
(120) Vennel, R. Invasive Species Report : Araucaria Heterophylla (Salisb .) Franco. **2015**, 4–5.
(121) Ecology, S.; Jan, N. Nitrogen in the Growth of Araucaria Cunninghamii Ait . Underplanted in Pinus Stands Author (s): D . I . Bevege and B . N . Richards Published by : Wiley Stable URL : Http://Www.Jstor.Org/Stable/1933607 Accessed : 25-06-2016 04 : 48 UTC Your Use of the J. **2016**, *51* (1), 134–142.
(122) Plantes Bontanique https://www.plantes-botanique.org/espece_atriplex_nummularia.
(123) Guevara, J. C.; Allegretti, L. I.; Paez, J. A.; Estevez, O. R.; Le Houérou, H. N.; Silva Colomer, J. H. Yield, Nutritional Value, and Economic Benefits of Atriplex Nummularia Lindl. Plantation in Marginal Dryland Areas for Conventional Forage Crops. *Arid L. Res. Manag.* **2005**, *19* (4), 327–340. https://doi.org/10.1080/15324980500299672.
(124) Jardinage Ooreka https://jardinage.ooreka.fr/.
(125) Eissa, M. A.; Ahmed, E. M. Nitrogen and Phosphorus Fertilization for Some Atriplex Plants Grown on Metal-Contaminated Soils. *Soil Sediment Contam.* **2016**, *25* (4), 431–442. https://doi.org/10.1080/15320383.2016.1158693.
(126) Vítková, M.; Müllerová, J.; Sádlo, J.; Pergl, J.; Pyšek, P. Black Locust (Robinia Pseudoacacia) Beloved and Despised: A Story of an Invasive Tree in Central Europe. *For. Ecol. Manage.* **2017**, *384* (November 2016), 287–302. https://doi.org/10.1016/j.foreco.2016.10.057.
(127) Żelazna, A.; Kraszkiewicz, A.; Przywara, A.; Łagód, G.; Suchorab, Z.; Werle, S.; Ballester, J.; Nosek, R. Life Cycle Assessment of Production of Black Locust Logs and Straw Pellets for Energy Purposes. *Environ. Prog. Sustain. Energy* **2019**, *38* (1), 163–170. https://doi.org/10.1002/ep.13043.
(128) University of Kentucky College of Agriculture. Guide to Insect Pests of Woody Plants http://www.uky.edu.
(129) Monumental Trees https://www.monumentaltrees.com/en/fra-blacklocust/.
(130) University of California, A. and N. R. Irrigating Coastal Blueberries While. http://cesanluisobispo.ucanr.edu/files/185732.pdf.
(131) Bryla, D. R.; Strik, B. C.; Pilar Bañados, M.; Righetti, T. L. Response of Highbush Blueberry to Nitrogen Fertilizer during Field Establishment-II. Plant Nutrient Requirements in Relation to Nitrogen Fertilizer Supply. *HortScience* **2012**, *47* (7), 917–926. https://doi.org/10.21273/hortsci.47.7.917.
(132) Fruits rouges & co. Blueberry production https://www.fruitsrougesandco.com/en/fruits-frais-myrtilles/.
(133) GUAVA http://nhb.gov.in/model-project-reports/Horticulture Crops/Guava/Guava1.htm.
(134) BaKhabar Kissan. Guava Production Technology https://www.bakhabarkissan.com/guava/.
(135) Montes, R. M.; Parent, L. É.; de Amorim, D. A.; Rozane, D. E.; Parent, S. É.; Natale, W.; Modesto, V. C. Nitrogen and Potassium Fertilization in a Guava Orchard Evaluated for Five Cycles: Effects on the Plant and on Production. *Rev. Bras. Cienc. do Solo* **2016**, *40*. https://doi.org/10.1590/18069657rbcs20140532.
(136) Déco. fr. Comment planter et entretenir le goyavier ? https://www.deco.fr/jardin-jardinage/arbre-a-fruits/goyavier.
(137) R., F. E.; R., de la R.; L., L.; J.A., G.; F., T.; M., O.; J.A., G.-R.; E., Q.-M.; A., T. Evolution and Sustainability of the Olive Production Systems. *Options Méditerranéennes. Séries A Mediterr. Semin.* **2013**, *106* (106), 11–41.
(138) European Commission, D.-G. for A. and R. D. *Olive Oil Market*; 2012.
(139) Haifa. A complete fertilization program for olive trees https://www.haifa-group.com/complete-fertilization-program-olive-trees.
(140) Aylott, M. J.; Casella, E.; Tubby, I.; Street, N. R.; Smith, P.; Taylor, G. Yield and Spatial Supply of Bioenergy Poplar and Willow Short-Rotation Coppice in the UK. *New Phytol.* **2008**, *178* (4), 897. https://doi.org/10.1111/j.1469-8137.2008.02469.x.
(141) Dillen, S. Y.; Djomo, S. N.; Al Afas, N.; Vanbeveren, S.; Ceulemans, R. Biomass Yield and Energy Balance of a Short-Rotation Poplar Coppice with Multiple Clones on Degraded Land during 16 Years. *Biomass and Bioenergy* **2013**, *56*, 157–165. https://doi.org/10.1016/j.biombioe.2013.04.019.

(142) Shock, C. C.; Flock, R.; Feibert, E.; Pereira, A. Drip Irrigation Guide for Growers of Hybrid Poplar. *Soil Sci.* **2005**, No. December, 1–7.
(143) Forest Science Database. Nitrogen fixation discovered in wild poplar https://www.cabi.org/forestscience/news/25012.
(144) University of Kentucky College of Agriculture. Guide to Insect Pests of Woody Plants.
(145) Magic. Industrial Crops https://iiasa.shinyapps.io/magic/.
(146) Ericsson, K.; Rosenqvist, H.; Ganko, E.; Pisarek, M.; Nilsson, L. An Agro-Economic Analysis of Willow Cultivation in Poland. *Biomass and Bioenergy* **2006**, *30* (1), 16–27. https://doi.org/10.1016/j.biombioe.2005.09.002.
(147) Dou, Y.; Yang, Y.; An, S. Above-Ground Biomass Models of Caragana Korshinskii and Sophora Viciifolia in the Loess Plateau, China. *Sustain.* **2019**, *11* (6). https://doi.org/10.3390/su11061674.
(148) Kew science. Plants of the World Online http://plantsoftheworldonline.org/taxon/urn:lsid:ipni.org:names:483847-1.
(149) Bernáth, J.; Földesi, D. Journal of Herbs , Spices & Sea Buckthorn (Hippophae Rhamnoides L .): **2011**, *6475* (April 2015), 37–41. https://doi.org/10.1300/J044v01n01.
(150) Mozūraitis, R.; Aleknavičius, D.; Vepštaitė-Monstavičė, I.; Stanevičienė, R.; Emami, S. N.; Apšegaitė, V.; Radžiutė, S.; Blažytė-Čereškienė, L.; Servienė, E.; Būda, V. Hippophae Rhamnoides Berry Related Pichia Kudriavzevii Yeast Volatiles Modify Behaviour of Rhagoletis Batava Flies. *J. Adv. Res.* **2020**, *21*, 71–77. https://doi.org/10.1016/j.jare.2019.08.001.
(151) Heinäaho, M.; Pusenius, J.; Julkunen-Tiitto, R. Effects of Different Organic Farming Methods on the Concentration of Phenolic Compounds in Sea Buckthorn Leaves. *J. Agric. Food Chem.* **2006**, *54* (20), 7678–7685. https://doi.org/10.1021/jf061018h.
(152) POWO. Plants of the World Online http://www.plantsoftheworldonline.org.
(153) Kannaiyan, S. *Biotechnology of Biofertilizers*; Springer Science & Business Media, 2002.
(154) Zhang, T. H.; Su, Y. Z.; Cui, J. Y.; Zhang, Z. H.; Chang, X. X. A Leguminous Shrub (Caragana Microphylla) in Semiarid Sandy Soils of North China. *Pedosphere* **2006**, *16* (3), 319–325. https://doi.org/10.1016/S1002-0160(06)60058-1.
(155) Yue, G.; Zhao, H.; Zhang, T.; Zhao, X.; Niu, L.; Drake, S. Evaluation of Water Use of Caragana Microphylla with the Stem Heat-Balance Method in Horqin Sandy Land, Inner Mongolia, China. *Agric. For. Meteorol.* **2008**, *148* (11), 1668–1678. https://doi.org/10.1016/j.agrformet.2008.05.019.
(156) The Royal Horticultural Society. Box: problems https://www.rhs.org.uk/advice/profile?PID=851.
(157) Galizzi, F. A.; Felker, P.; González, C.; Gardiner, D. Correlations between Soil and Cladode Nutrient Concentrations and Fruit Yield and Quality in Cactus Pears, Opuntia Ficus Indica in a Traditional Farm Setting in Argentina. *J. Arid Environ.* **2004**, *59* (1), 115–132. https://doi.org/10.1016/j.jaridenv.2004.01.015.
(158) Moussa, Z.; Yammouni, D.; Azar, D. Dactylopius Opuntiae (Cockerell, 1896), a New Invasive Pest of the Cactus Plants Opuntia Ficus-Indica in the South of Lebanon (Hemiptera, Coccoidea, Dactylopiidae). **2017**, *122* (2), 173–178.
(159) Hoy, M. D.; Moore, K. J.; George, J. R.; Brummer, E. C. Alfalfa Yield and Quality as Influenced by Establishment Method. *Agron. J.* **2002**, *94* (1), 65–71. https://doi.org/10.2134/agronj2002.0065.
(160) Barsotti, J. L.; Sainju, U. M.; Lenssen, A. W.; Montagne, C.; Hatfield, P. G. Crop Yields and Soil Organic Matter Responses to Sheep Grazing in US Northern Great Plains. *Soil Tillage Res.* **2013**, *134*, 133–141. https://doi.org/10.1016/j.still.2013.07.015.
(161) Institute of Agriculture and Natural Resources. CropWatch https://cropwatch.unl.edu/.
(162) Anderson, N. P.; Chastain, T. G.; Garbacik, C. J. Irrigation and Trinexapac-Ethyl Effects on Seed Yield in First- and Second-Year Red Clover Stands. *Agron. J.* **2016**, *108* (3), 1116–1123. https://doi.org/10.2134/agronj2015.0513.
(163) Programme, R. E. & D. *ORGANIC FARMING A Guide to Red Clover*. https://www.teagasc.ie/media/website/rural-economy/organics/Red-Clover-leaflet-update.pdf.
(164) Conaghan, P.; Clavin, D. Red Clover – Agronomy and Management. https://www.teagasc.ie/media/website/publications/2017/6-Red-clover-agronomy-and-management.pdf

(165) Ip, K.; Miller, A. Life Cycle Greenhouse Gas Emissions of Hemp-Lime Wall Constructions in the UK. *Resour. Conserv. Recycl.* **2012**, *69*, 1–9. https://doi.org/10.1016/j.resconrec.2012.09.001.
(166) Zampori, L.; Dotelli, G.; Vernelli, V. Life Cycle Assessment of Hemp Cultivation and Use of Hemp-Based Thermal Insulator Materials in Buildings. *Environ. Sci. Technol.* **2013**, *47* (13), 7413–7420. https://doi.org/10.1021/es401326a.
(167) Interchanvre. La Culture Écologique, Agronomique et Éco-Responsable; 2018.
(168) Andersson, K.; Björhagen, I. Material Choices for a Fossil-Free Preschool - An Interview Study on How Materials Are Chosen, and a Life Cycle Assessment of Hemp Insulation, CHALMERS UNIVERSITY OF TECHNOLOGY, 2018.
(169) Amaducci, S.; Scordia, D.; Liu, F. H.; Zhang, Q.; Guo, H.; Testa, G.; Cosentino, S. L. Key Cultivation Techniques for Hemp in Europe and China. *Ind. Crops Prod.* **2015**, *68*, 2–16. https://doi.org/10.1016/j.indcrop.2014.06.041.
(170) Kalita, B. Life Cycle Assesment of Switchgrass (Panicum Virgatum L.) Biomass Production in Ontario. **2012**, 115.
(171) Campillo, R.; Urquiaga, S.; Undurraga, P.; Pino, I.; Boddey, R. M. Strategies to Optimise Biological Nitrogen Fixation in Legume/Grass Pastures in the Southern Region of Chile. *Plant Soil* **2005**, *273* (1–2), 57–67. https://doi.org/10.1007/s11104-004-6717-4.
(172) Lay, J. K. White Clover Seed Production with Irrigation. *Herb. Seed Prod. New Zeal. New Zeal. Grassl. Assoc.* **1979**, 70–73.
(173) Hamelin, L.; Jørgensen, U.; Petersen, B. M.; Olesen, J. E.; Wenzel, H. Modelling the Carbon and Nitrogen Balances of Direct Land Use Changes from Energy Crops in Denmark: A Consequential Life Cycle Inventory. *GCB Bioenergy* **2012**, *4* (6), 889–907. https://doi.org/10.1111/j.1757-1707.2012.01174.x.
(174) Ge, X.; Xu, F.; Vasco-Correa, J.; Li, Y. Giant Reed: A Competitive Energy Crop in Comparison with Miscanthus. *Renew. Sustain. Energy Rev.* **2016**, *54*, 350–362. https://doi.org/10.1016/j.rser.2015.10.010.
(175) University of Hertfordshire. Planting and Growing Miscanthus http://adlib.everysite.co.uk/adlib/defra/content.aspx?id=000IL3890W.18LWTVKBSSG3EF.
(176) Martin, L.; Wohlfahrt, J.; Le Ber, F.; Benoît, M. Perennial Biomass Crops and Their Territorial Patterns: A Case Study of Miscanthus in the Côte-d'Or Département of France. *Lesp. Geogr.* **2012**, *41* (2), 138–153.
(177) Charmet, G.; Balfourier, F.; Bion, A. Agronomic Evaluation of a Collection of French Perennial Ryegrass Populations: Multivariate Classification Using Gentotype × Environment Interactions. *Agronomie* **1990**, *10* (10), 807–823. https://doi.org/10.1051/agro:19901004.
(178) U.S. DEPARTMENT OF AGRICULTURE. USDA https://www.usda.gov/.
(179) Groww. White mustard https://www.groww.fr/en/plants/white-mustard.
(180) Jankowski, K. J.; Załuski, D.; Sokólski, M. Canola-Quality White Mustard: Agronomic Management and Seed Yield. *Ind. Crops Prod.* **2020**, *145* (January). https://doi.org/10.1016/j.indcrop.2020.112138.
(181) Berlanas, C.; Andrés-sodupe, M.; López-manzanares, B.; Maldonado-gonzález, M.; Gramaje, D. Effect of White Mustard Cover Crop Residue, Soil Chemical Fumigation And.
(182) Twidwell, E.; Pitman, W. D.; Cuomo, G. J. Bahiagrass Production and Management. **1998**, 6.
(183) U.S. DEPARTMENT OF AGRICULTURE. USDA. https://www.usda.gov/
(184) Xu, Y.; Tang, Q.; Dai, Z.; Yang, Z.; Cheng, C.; Deng, C.; Liu, C.; Chen, J.; Su, J. Yield Components of Forage Ramie (Boehmeria Nivea L.) and Their Effects on Yield. *Genet. Resour. Crop Evol.* **2019**, *66* (7), 1601–1613. https://doi.org/10.1007/s10722-019-00800-x.
(185) Mitra, S.; Saha, S.; Guha, B.; Chakrabarti, K.; Satya, P.; Sharma, A. K.; Gawande, S. p.; Kumar, M.; Saha, M. Ramie : The Strongest Bast Fibre of Nature. *Tech. Bull. No. 8, Cent. Res. Inst. Jute Allied Fibres* **2013**, No. May, 1–38. https://doi.org/10.13140/2.1.3519.5842.
(186) Yu, Y. W.; Nan, Z. B.; Hou, F. J.; Matthew, C. Response of Stipa Bungeana and Pennisetum Flaccidum to Urine of Sheep in Steppe Grassland of North-Western China. *Grass Forage Sci.* **2009**, *64* (4), 395–400. https://doi.org/10.1111/j.1365-2494.2009.00704.x.
(187) Jie, C.; Tian-Ming, H.; Ji-Min, C.; Gao-Lin, W. Distribution of Biomass and Diversity of Stipa Bungeana Community to Climatic Factors in the Loess Plateau of Northwestern China. *African J. Biotechnol.* **2010**, *9* (40), 6733–6739. https://doi.org/10.5897/AJB10.910.

(188) AN, Z.; NIU, D.-C.; WEN, H.-Y.; YANG, Y.; ZHANG, H.-R.; FU, H. Effects of N Addition on Nutrient Resorption Efficiency and C:N:P Stoichiometric Characteris-Tics in Stipa Bungeana of Steppe Grasslands in the Loess Plateau, China. *Chinese J. Plant Ecol.* **2011**, *35* (8), 801–807. https://doi.org/10.3724/sp.j.1258.2011.00801.
(189) Hermann, B. G.; Blok, K.; Patel, M. K. Twisting Biomaterials around Your Little Finger: Environmental Impacts of Bio-Based Wrappings. *Int. J. Life Cycle Assess.* **2010**, *15* (4), 346–358. https://doi.org/10.1007/s11367-010-0155-8.
(190) Gheribi, R.; Puchot, L.; Verge, P.; Jaoued-grayaa, N.; Mezni, M. Development of Plasticized Edible Fi Lms from Opuntia Fi Cus-Indica Mucilage : A Comparative Study of Various Polyol Plasticizers. *Carbohydr. Polym.* **2020**, *190* (Feb 2018), 204–211. https://doi.org/10.1016/j.carbpol.2018.02.085.
(191) Khoo, H. H.; Tan, R. B. H.; Chng, K. W. L. Environmental Impacts of Conventional Plastic and Bio-Based Carrier Bags. *Int. J. Life Cycle Assess.* **2010**, *15* (3), 284–293. https://doi.org/10.1007/s11367-010-0162-9.
(192) Tachibana, Y.; Kimura, S.; Kasuya, K. I. Synthesis and Verification of Biobased Terephthalic Acid from Furfural. *Sci. Rep.* **2015**, *5*, 1–5. https://doi.org/10.1038/srep08249.
(193) Shen, L.; Worrell, E.; Patel, M. K. Environmental Impact Assessment of Man-Made Cellulose Fibres. *Resour. Conserv. Recycl.* **2010**, *55* (2), 260–274. https://doi.org/10.1016/j.resconrec.2010.10.001.
(194) Beton, A.; Dias, D.; Farrant, L.; Gibon, T.; Le Guern, Y.; Desaxce, M.; Perwueltz, A.; Boufateh, I.; Wolf, O.; Kougoulis, J.; et al. *Environmental Improvement Potential of Textiles (IMPRO Textiles)*; 2014. https://doi.org/10.2791/52624.
(195) Manda, B. M. K.; Worrell, E.; Patel, M. K. Prospective Life Cycle Assessment of an Antibacterial T-Shirt and Supporting Business Decisions to Create Value. *Resour. Conserv. Recycl.* **2015**, *103*, 47–57. https://doi.org/10.1016/j.resconrec.2015.07.010.
(196) Moussa, H. I.; Elkamel, A.; Young, S. B. Assessing Energy Performance of Bio-Based Succinic Acid Production Using LCA. *J. Clean. Prod.* **2016**, *139*, 761–769. https://doi.org/10.1016/j.jclepro.2016.08.104.
(197) Fernando, A. L.; Boléo, S.; Barbosa, B.; Costa, J.; Duarte, M. P.; Monti, A. Perennial Grass Production Opportunities on Marginal Mediterranean Land. *Bioenergy Res.* **2015**, *8* (4), 1523–1537. https://doi.org/10.1007/s12155-015-9692-0.
(198) Oh, M.; Ma, Q.; Simsek, S.; Bajwa, D.; Jiang, L. Comparative Study of Zein- and Gluten-Based Wood Adhesives Containing Cellulose Nanofibers and Crosslinking Agent for Improved Bond Strength. *Int. J. Adhes. Adhes.* **2019**, *92* (April), 44–57. https://doi.org/10.1016/j.ijadhadh.2019.04.004.
(199) Yu, I. K. M.; Tsang, D. C. W. Conversion of Biomass to Hydroxymethylfurfural: A Review of Catalytic Systems and Underlying Mechanisms. *Bioresour. Technol.* **2017**, *238*, 716–732. https://doi.org/10.1016/j.biortech.2017.04.026.
(200) Karaseva, V.; Bergeret, A.; Lacoste, C.; Ferry, L.; Fulcrand, H. Influence of Extraction Conditions on Chemical Composition and Thermal Properties of Chestnut Wood Extracts as Tannin Feedstock. *ACS Sustain. Chem. Eng.* **2019**, *7* (20), 17047–17054. https://doi.org/10.1021/acssuschemeng.9b03000.
(201) Gaspar, M. C.; Mendes, C. V. T.; Pinela, S. R.; Moreira, R.; Carvalho, M. G. V. S.; Quina, M. J.; Braga, M. E. M.; Portugal, A. T. Assessment of Agroforestry Residues: Their Potential within the Biorefinery Context. *ACS Sustain. Chem. Eng.* **2019**, *7* (20), 17154–17165. https://doi.org/10.1021/acssuschemeng.9b03532.
(202) Huang, K.; Das, L.; Guo, J.; Xu, Y. Catalytic Valorization of Hardwood for Enhanced Xylose-Hydrolysate Recovery and Cellulose Enzymatic Efficiency via Synergistic Effect of Fe3+ and Acetic Acid. *Biotechnol. Biofuels* **2019**, *12* (1), 1–11. https://doi.org/10.1186/s13068-019-1587-4.
(203) Curia, S.; Dautle, S.; Satterfield, B.; Yorke, K.; Cranley, C. E.; Dobson, B. E.; La Scala, J. J.; Soh, L.; Gordon, M. B.; Stanzione, J. F. Betulin-Based Thermoplastics and Thermosets through Sustainable and Industrially Viable Approaches: New Insights for the Valorization of an Underutilized Resource. *ACS Sustain. Chem. Eng.* **2019**, *7* (19), 16371–16381. https://doi.org/10.1021/acssuschemeng.9b03471.

(204) Pathak, S.; Saxena, P.; Ray, A. K.; Großmann, H.; Kleinert, R. Irradiation Based Clean and Energy Efficient Thermochemical Conversion of Biowaste into Paper. *J. Clean. Prod.* **2019**, *233*, 893–902. https://doi.org/10.1016/j.jclepro.2019.06.042.
(205) Le Phuong, H. A.; Izzati Ayob, N. A.; Blanford, C. F.; Mohammad Rawi, N. F.; Szekely, G. Nonwoven Membrane Supports from Renewable Resources: Bamboo Fiber Reinforced Poly(Lactic Acid) Composites. *ACS Sustain. Chem. Eng.* **2019**, *7* (13), 11885–11893. https://doi.org/10.1021/acssuschemeng.9b02516.
(206) Gómez, C. L.; Echeverri, D. A.; Inciarte, H. C.; Rios, L. A. Efficient Processing of Bioglycerol to a Novel Biobased Polyunsaturated Monomer. *J. Chem. Technol. Biotechnol.* **2019**, *94* (2), 634–640. https://doi.org/10.1002/jctb.5818.
(207) Corbière-Nicollier, T.; Gfeller Laban, B.; Lundquist, L.; Leterrier, Y.; Månson, J. A. E.; Jolliet, O. Life Cycle Assessment of Biofibres Replacing Glass Fibres as Reinforcement in Plastics. *Resour. Conserv. Recycl.* **2001**, *33* (4), 267–287. https://doi.org/10.1016/S0921-3449(01)00089-1.
(208) Hu, B.; Dweib, M.; Wool, R. P.; Shenton, H. W. Bio-Based Composite Roof for Residential Construction. *J. Archit. Eng.* **2007**, *13* (3), 136–143. https://doi.org/10.1061/(ASCE)1076-0431(2007)13:3(136).
(209) Parthasarathy, P.; Narayanan, S. K. Effect of Hydrothermal Carbonization Reaction Parameters On. *Environ. Prog. Sustain. Energy* **2014**, *33* (3), 676–680. https://doi.org/10.1002/ep.
(210) Le Duigou, A.; Baley, C. Coupled Micromechanical Analysis and Life Cycle Assessment as an Integrated Tool for Natural Fibre Composites Development. *J. Clean. Prod.* **2014**, *83*, 61–69. https://doi.org/10.1016/j.jclepro.2014.07.027.
(211) Ardente, F.; Beccali, M.; Cellura, M.; Mistretta, M. Building Energy Performance: A LCA Case Study of Kenaf-Fibres Insulation Board. *Energy Build.* **2008**, *40* (1), 1–10. https://doi.org/10.1016/j.enbuild.2006.12.009.
(212) Batouli, S. M.; Zhu, Y.; Nar, M.; D'Souza, N. A. Environmental Performance of Kenaf-Fiber Reinforced Polyurethane: A Life Cycle Assessment Approach. *J. Clean. Prod.* **2014**, *66*, 164–173. https://doi.org/10.1016/j.jclepro.2013.11.064.
(213) Glew, D.; Stringer, L. C.; Acquaye, A. A.; McQueen-Mason, S. How Do End of Life Scenarios Influence the Environmental Impact of Product Supply Chains? Comparing Biomaterial and Petrochemical Products. *J. Clean. Prod.* **2012**, *29–30*, 122–131. https://doi.org/10.1016/j.jclepro.2012.02.005.
(214) Wötzel, K.; Wirth, R.; Flake, M. Life Cycle Studies on Hemp Fibre Reinforced Components and ABS for Automotive Parts. *Angew. Makromol. Chemie* **1999**, *272* (4763), 121–127. https://doi.org/10.1002/(SICI)1522-9505(19991201)272:1<121::AID-APMC121>3.0.CO;2-T.
(215) La Rosa, A. D.; Cozzo, G.; Latteri, A.; Recca, A.; Björklund, A.; Parrinello, E.; Cicala, G. Life Cycle Assessment of a Novel Hybrid Glass-Hemp/Thermoset Composite. *J. Clean. Prod.* **2013**, *44*, 69–76. https://doi.org/10.1016/j.jclepro.2012.11.038.
(216) La Rosa, A. D.; Cozzo, G.; Latteri, A.; Mancini, G.; Recca, A.; Cicala, G. A Comparative Life Cycle Assessment of a Composite Component for Automotive. *Chem. Eng. Trans.* **2013**, *32*, 1723–1728. https://doi.org/10.3303/CET1332288.
(217) Schmidt, W. P.; Beyer, H. M. Life Cycle Study on a Natural Fibre Reinforced Component. *SAE Tech. Pap.* **1998**, No. 724. https://doi.org/10.4271/982195.
(218) Pretot, S.; Collet, F.; Garnier, C. Life Cycle Assessment of a Hemp Concrete Wall: Impact of Thickness and Coating. *Build. Environ.* **2014**, *72*, 223–231. https://doi.org/10.1016/j.buildenv.2013.11.010.
(219) Kilinc, S.; Emik, S.; S. O ¨mu¸; Emik, S.; Kilinç, S.; T. B. İyim; S. Özgümüş; I, T. B. I. Polymer-Plastics Technology and Engineering Recycling of Waste PET : Usage as Secondary Plasticizer For. *Polym. Plast. Technol. Eng.* **2005**, *44* (8–9), 1379–1388.
(220) FAOSTAT. Food and agriculture data https://www.fao.org/faostat/en/#data/EK.
(221) Zhuang, Q.; Qin, Z.; Chen, M. Biofuel, Land and Water: Maize, Switchgrass or Miscanthus? *Environ. Res. Lett.* **2013**, *8* (1). https://doi.org/10.1088/1748-9326/8/1/015020.
(222) Ericsson, N.; Porsö, C.; Åhlgren, S.; Nordberg, Å.; Sundberg, C.; Hansson, P. A. Time-Dependent Climate Impact of a Bioenergy System - Methodology Development and Application to Swedish Conditions. *GCB Bioenergy* **2013**, *5* (5), 580–590. https://doi.org/10.1111/gcbb.12031.

Supplyment Information II. for Chapter IV

1 AMG model

All the inputs of AMG model demands are meteorology, soil, cultivation management, and biomass C input parameters. (Clivot et al., 2019). Meteorology data are provided by Drias in (DRIAS les futurs du climat, 2014), which predicts climate for the whole of France from 2020 to 2100, average values of temperature and potential evapotranspiration (the difference of precipitation and evaporation, for describing the effects of soil moisture) are calculated then to use during 2020 to 2100. For years later than 2100, the average temperature and net precipitation in the last 10 years (2091- 2100) are chosen as inputs, shown in fig. 1. The initial SOC and other soil parameters are extracted from Harmonized World Soil Database(Nachtergaele et al., 2012), which are calculated as the arithmetic mean proportionally according to different hectares of each carbon vulnerable land, consisting with group's former study(Shen et al., 2021). SOC simulation is sensitive to the C/N ratio due to its impact on humification(Nicolardot et al., 2001), while soil C/N ratio does not exist in the same edaphic database. Thus three C/N ratios are conducted in the AMG(11, 17, and 22), which are determined by previous references considering the previous land use and situations in France(Clivot et al., 2019; Conen et al., 2008; Delmas et al., 2015; Yang et al., 2017). Soil inputs can be found in table S1.

Hemp (*Cannabis sativa L.*) is an annual plant, which means it's planted and harvested every year. To match the time scale in dynamic, SOC is simulated for 100 years in 1-year time step, from 2020 to 2120. In the scenario that straw is harvested, only the button of the straw, also called non-harvestable part. This part is the residue of hemp, providing the aboveground C input. In the scenario that straw is left on the surface, the straw that includes the non-harvestable part, is regarded as residue thus C in the straw is the aboveground input. The belowground C inputs are the same in both scenarios, consisting of C in roots and C in extra-root materials. Biomass inputs are shown in table S2.

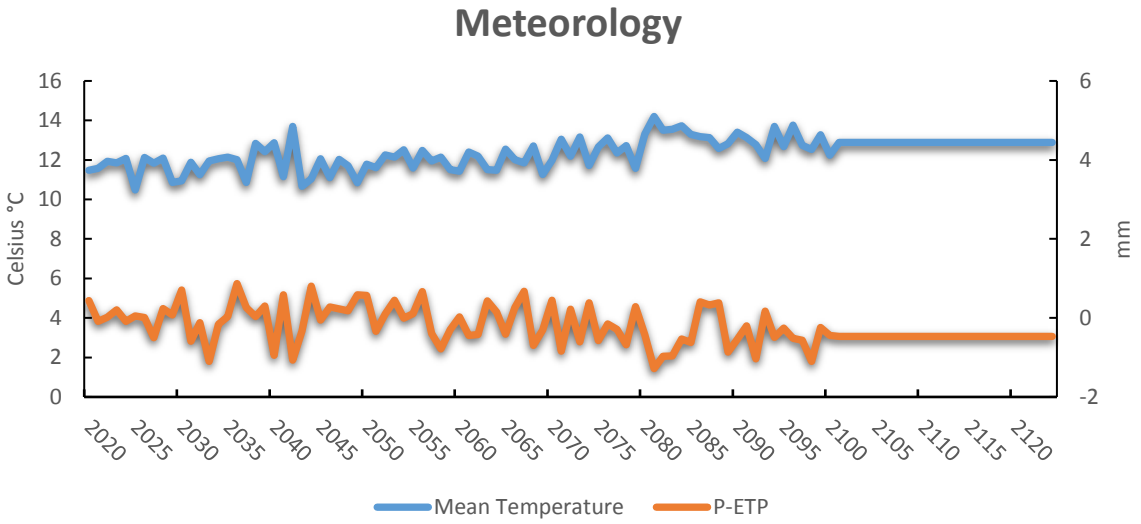

Fig. S1 Temperature and P-ETP inputs for AMG model, P-ETP is the difference of precipitation P and potential evapotranspiration ETP. Data from Drias(DRIAS les futurs du climat, 2014).

Table S1 Input of AMG, soil characteristics(Nachtergaele et al., 2012).

	Measured depth	Clay	CaCO3	pH	Bulk density	Coarse fragment %	SOC concentration g/kg	SOC stock Mg/ ha	C/N
Carbon vulnerable land	30	215.97	26.36	6.6	1.4	6.63	10.79	42.35	11/17/22

Table S2 Input of AMG, biomass.

	Irrigation	Tillage cm [a]	Proportion of harvestable part(RP), residue(RS), root(RR), extra-root(RE)[b]				Root contribution[b]	Aboveground carbon input Mg/ ha	Belowground carbon input Mg/ ha
			RP	RS	RR	RE			
Straw harvested	0	0	0.713	0.078	0.127	0.082	0.961	0.47	0.89
Straw left	0	0	0.064	0.726	0.127	0.082	0.961	4.41	0.89

[a]: (González-García et al., 2007; Nicolescu et al., 2018)
[b]: (Clivot et al., 2019)

2 Life cycle inventory

Inventories of hemp cases are presented here, and all data correspond to the functional unit, which is 1 ha carbon vulnerable land. Data are collected from several sources to be reliable, then the average or median is used. Here the primary references are listed in the table due to the space limitation.

2.1 Cultivation

Since biopumps aim to grow in carbon vulnerable land and hemp is a rather easy plant to cultivate, the agricultural management would be less intensive, and try best to protect SOC and emit less greenhouse gas. Therefore, irrigation is avoided and a no-tillage strategy is adopted (Andersson and Björhagen, 2018; González-García et al., 2007). However, fertilization is necessary to get a good quantity of captured CO_2, phosphorus pentoxide, ammonium nitrate, and potassium oxide are used as P, N, and K fertilization, respectively.

2.2 Harvesting

After cultivation, hemp is harvested to produce biobased products by combine harvesters. Whether straw is harvested or not, only seed would be harvested in the process, straw would be cut down and left on the surface. In the scenario that straws are harvested, they would spend around 14 days on the field as dew retting, then be baled to the downstream process. In the scenario that straws are left, they are regarded as residues, thus emissions in harvesting are different in two scenarios due to the different amount of residues, table S4 shows the emission when the straw is harvested or left.

Table S3 Inventory sheet of hemp cultivation				
Cultivation				
Input	Quantity	Unit	Source	Process
Seed for sowing	50	kg	(Ventura and Kiess, 2015)	From hemp yield in table s4
Sowing	1	ha	(ecoinvent, 2020)	Sowing {GLO}| market for | Conseq, U
Fertilizer				
P input	50.9	kg	(Ventura and Kiess, 2015)	Phosphate fertiliser, as P2O5 {GLO}| market for | Conseq, U
N input	106.73	kg	(Ventura and Kiess, 2015)	Nitrogen fertiliser, as N {GLO}| market for | Conseq, U
K input	89.87	kg	(Ventura and Kiess, 2015)	Potassium fertiliser, as K2O {GLO}| market for | Conseq, U
Fertilizing	1	ha	(ecoinvent, 2020)	Fertilising, by broadcaster {GLO}| market for | Conseq, U
CO_2 total captured from air	20.87	t	(TNO innovation for life, 2020)	
Land occupation	1	ha a	(ecoinvent, 2020)	Occupation, annual crop, non-irrigated
Output				
Emission to air				
N_2O direct, from fertilization	1.68	kg	(Hergoualc'h et al., 2019)	
N_2O indirect Volatilization	0.18	kg	(Hergoualc'h et al., 2019)	
NO_x-N (NO_2)	0.74	kg	(Nemecek and Kägi, 2007)	
NH_3	2.59	kg	(Nemecek and Kägi, 2007)	
NMVOC	0.46	kg	(European Environment Agency, 2019)	
Discharge to water				
NO_3^-	40	kg	(Nemecek and Kägi, 2007)	
PO_4^{3-}	1.56	kg	(Nemecek and Kägi, 2007)	
N_2O indirect, leaching from fertilization	0.39	kg	(Hergoualc'h et al., 2019)	

Table S4 Inventory sheet of hemp harvesting				
Hemp harvesting, straw harvested				
Input	Quantity	Unit	Source	Process
Harvesting	1	ha	(ecoinvent, 2020)	Combine harvesting {GLO}| market for | Conseq, U
Output				
Straw	11.69	t	(Ventura and Kiess, 2015)	
Seed	0.98	t	(Ventura and Kiess, 2015)	
Emission to air				
CO_2 from degradation	4.81	t	(TNO innovation for life, 2020)	
N_2O direct, from residue &root, straw harvested	0.37	kg	(Hergoualc'h et al., 2019)	
N_2O indirect, from the nitrogen leaching	0.09	kg	(Hergoualc'h et al., 2019)	
Emission to soil				
SOC change	0.17	t	(Clivot et al., 2019)	Carbon dioxide, to soil or biomass stock
Hemp harvesting, straw left				
Input	Quantity	Unit	Source	Process
Harvesting	1	ha	(ecoinvent, 2020)	Combine harvesting {GLO}| market for | Conseq, U
Output				
Seed	0.98	t	(Ventura and Kiess, 2015)	
Emission to air				
CO_2 from degradation	18.08	t	(TNO innovation for life, 2020)	
N_2O direct, from residue &root, straw harvested	1.21	kg	(Hergoualc'h et al., 2019)	
N_2O indirect, from the niteogen leaching	0.28	kg	(Hergoualc'h et al., 2019)	
Emission to soil				
SOC change	1.35	t	(Clivot et al., 2019)	Carbon dioxide, to soil or biomass stock

2.3 Hemp oil and avoided products

Hemp seed is the first co-product in the straw harvested scenario, while it is the main product if it is the only yield harvested. Animal nutrition for non-food producing birds and food are major markets of hemp seed(Opinion, 2011). Although 95% of hemp seeds are used for birds, the market for hemp seed oil is increasing more dramatically, at a 35.8% compound annual growth rate (CAGR) from 2018 to

2026(RESEARCH AND MARKET, 2018). In contrast, the CAGR of hemp seed in bird feed is less competitive, at a CAGR of 3.8%(MARKET STUDY REPORT, 2020). Thus, following the rule of consequential LCA, 50 kg harvested seeds would back to sow for the next rotation, and the rest would be processed as oil for all three scenarios.

Because hemp contains δ-9-tetrahydrocannabinol (THC) lower than 0.2%, hemp seed could extract oil for the market legally(Aladić et al., 2015). From the processing, the meal is derived as a co-product. Hemp meal is nutritious for ruminants as fodder due to the high protein content (Mustafa et al., 1999). In this process, oil is extracted as 34% of the seed dry mass(Da Porto et al., 2015; Rapa et al., 2019), the left part is the meal. Because of the lack of information about the hemp meal proportion, it refers to the meal proportion of flax since these two plants have similar content in seed and similar usage(Deng et al., 2011). The protein, carbohydrate, and oil from the meal replace corresponding marginal sources in animal feed(Gomez-Campos et al., 2020). After extracting and refinery, hemp oil could be used as body care products and industrial detergents(Garcia, 2017). At the same time that hemp oil and meal replace corresponding marginal products, the land demand is reduced too, thus the indirect land use change (iLUC) is considered here, detail could be found in the later part (section 2.14). Table S5 depicts the hemp seed processing.

Table S5 Inventory sheet of hemp oil extracting				
Seeds after harvesting				
Input	Quantity	Unit	Source	Process
Harvested seeds	975	kg		
Output				
Seeds for resowing	50	kg	(Ventura and Kiess, 2015)	
Seeds for oil extraction	925	kg		
Oil extraction				
Input	Quantity	Unit	Source	Process
Oil extraction, input-seeds	925	kg	(ecoinvent, 2020)	"Rape oil, crude {CH}| rape oil mill operation | Conseq, U"
Output				
Hemp oil, crude	308.33	kg	(Rapa et al., 2019)	
Hemp meal	616.67	kg	(Deng et al., 2011)	
Oil refinery, operation				
Input	Quantity	Unit	Source	Process
Oil refinery operation, input- hemp oil, crude	308.33	kg	(ecoinvent, 2020)	Palm oil, refined {GLO}| palm oil refinery operation | Conseq, U
Output				
Hemp oil, refined	296	kg		
Hemp seed oil market				
Input	Quantity	Unit	Source	Process
Oil refinery market, input- hemp oil, refined	296	kg	(ecoinvent, 2020)	Palm oil, refined {GLO}| market for | Conseq, U
Output				
Hemp oil, refined	296	kg		
Hemp seed oil market				
Input	Quantity	Unit	Source	Process
Hemp oil, refined	296	kg		
Output				
CO_2, biogenic	1431.72	kg		All C in within the oil would emit back to the atmosphere
Co-products fate[a]				
Co-product	Quantity	Unit	Source	Process
Hemp meal	616.67	kg		
Marginal products				
Carbohydrate	-159.41	kg	(Tonini et al., 2016)	Maize grain {GLO}| market for | Conseq, U
Protein	-97.87	kg	(Tonini et al., 2016)	Soybean meal {GLO}| market for | Conseq, U

Fats	-16.84	kg	(Tonini et al., 2016)	Palm oil, refined {GLO}| market for | Conseq, U
Co-product[b]	Quantity	Unit	Source	Process
Hemp oil, refined	298	kg		
Marginal products				
Palm oil	-298	kg	(Gomez-Campos et al., 2020)	Palm oil, refined {GLO}| market for | Conseq, U
iLUC	572	m^2	(COWI A/S and Utrecht University, 2019)	

[a]: the value of avoided product is marked as negative.
[b]: not co-product when straw is left, but the quantity is the same.

2.4 Retting

The harvested straw need retting to be soft and loose, fiber would partially dissociate from the straw by the degradation of the pectin-rich middle lamella(Bleuze et al., 2018). Here the harvested hemp straws are laid over the field, rotting by dew, which is a traditional and dominant procedure. This process could last around two weeks, and straws would lose 12% of dry mass(Bleuze et al., 2020; Turunen and van der Werf, 2006). Possible dust and small shives produced from the retting process and their contribution to adverse health or as an input of carbon and macronutrients to soil are considered negligible(Gomez-Campos et al., 2020). Therefore, the mass loss is assumed to be emissions to the air. Consequently, carbon (CO_2, CO, CH_4) and nitrogen (N_2O, NO_x, NH_3) emission flow from the decomposition of biomass were estimated in order to model the overall environmental impact of the retting process. Table S6 shows the retting process.

Table S6 Inventory sheet of hemp retting				
Retting				
Input	Quantity	Unit	Source	Process
Straw	11.69	t		
Output				
Retted straw	8.44	t		
Emission to air				
CO_2	788.88	kg	(Gomez-Campos et al., 2020)	
CO	1.75	kg	(Gomez-Campos et al., 2020)	
CH_4	6.6	kg	(Gomez-Campos et al., 2020)	
N_2O	0.14	kg	(Gomez-Campos et al., 2020)	
NH_3	0.61	kg	(Gomez-Campos et al., 2020)	
H_2O	2250.18	kg	(Bleuze et al., 2020)	

2.5 Baling

During the dew retting, straws scattered on the ground, need to be collected and transported to the factory then. In this process, straws are baled and then loaded onto the trailer by the gripper, this step is shown in table S7.

Table S7 Inventory sheet of hemp baling				
Retting				
Input	Quantity	Unit	Source	Process
Baling	12.06	P[a]	(ecoinvent, 2020)	Baling {RoW}| processing | Conseq, U
Bale loading	12.06	P	(ecoinvent, 2020)	Bale loading {RoW}| processing | Conseq, U
Output				
Baled straw	8.44	t		

[a]: 700kg /P

2.6 Fiber extraction

After the retted straw is transported to the plant, fiber and shives will be separated. Commonly fiber and shives represent 30% and 65% of the straw, the rest is dust emitted into the air(de Bruijn et al., 2009; Zampori et al., 2013). In this study, fiber is the main product and would be used to make thermal insulation or car panel in the later processes, while shives are regarded as a co-product. Fiber separation is conducted by a schutcher type decorticator and separator, from this, the fiber is air cleaned to remove any further dust(Norton et al., 2008).

Table S8 Inventory sheet of hemp fiber extraction				
Fiber extraction				
Input	Quantity	Unit	Source	Process
Retted straw	8.44	t		
Electricity	1816.43	kwh	(Norton et al., 2008)	
Output				
Fiber	2.53	t	(Norton et al., 2009)	
Shives	5.48	t	(Norton et al., 2009)	
Emission to air				
Dust	0.42	t	(Norton et al., 2009)	

2.7 Hemp concrete

Shives extracted from straw are the main co-product during the fiber extraction, and would be used as so-called hemp concrete to increase economic value(Senga Kiessé et al., 2017). Hemp concrete is made by shives mixing with a lime binder, which consists of 75% hydrated binder, 15% hydraulic binder, and 10% pozzolanic binder(Lecompte et al., 2017). Hemp concrete is attractive by its mechanical, thermal, and acoustic properties, thus it is multifunction in construction. Consider the compressive and shear strength of hemp concrete ranging in 0.29 to 1.13MPa and 0.05 to 0.24 MPa, respectively(Brzyski et al., 2017; Novakova and Sal, 2019), cannot meet the standard of the normal concrete (>5MPa). Therefore, it's not appropriate to say the hemp concrete would replace the normal concrete, especially when used to be loading-bearing. Thus hemp concrete aims to apply and replace the material in structure parts that demand less loading-bearing, e.g. gypsum(Pretot et al., 2014). Hereby, gypsum plasterboard is assumed to be replaced because of the similar density(Jiménez Rivero et al., 2016). The end-of-life is not included because there is little emission during the gypsum plasterboards landfilling(ecoinvent, 2020).

During the use stage, which lasts over 100 years, hemp concrete would absorb CO_2 through the blinder carbonation. Hydrated binder and hydraulic binder take up 594 and 106.9 g CO_2/ kg binder, respectively(Pretot et al., 2014), and release the same amount of H_2O. Because the lifespan of hemp concrete is long enough, carbonation could be achieved over the hemp concrete using phase. The marginal product, which is gypsum here, would not absorb CO_2 as hemp concrete during the use. At the end of life, the practicable disposal way is landfilling, through this way, hemp concrete is considered that there is no decomposition of the material(Pretot et al., 2014). At the end of life, because of the long lifetime, similar to the time scale set in this study. Plus, landfilling is the most common for architecture materials, while there is no decomposition of the hemp concrete(Pretot et al., 2014), which means there is no emission before the year 2135. Therefore, the disposal of hemp concrete is not considered. Thus, there are no greenhouse gas emissions in fact. The CO_2 emission from concrete disposal in table S9 is the C from the shives, originally from hemp. In order to involve the SOC change in the assessment, carbon captured by hemp during cultivation is accounted for in the inventory. After deducting the carbon in the soil, this captured carbon would go to downstream processes, some of them are lost during manufacturing, the rest are kept in corresponding products. At the end of life, C in these products would finally back to the atmosphere, and the consequential LCA is static, the time is not considered, therefore, the C input and output in the system need to be balanced, thus we assume all C in the product, in this section, which is in the concrete, would back to the atmosphere as CO_2. Similar actions are conducted in the disposal of the thermal insulation and car panel. All information about hemp concrete is included in table S9.

Table S9 Inventory sheet of hemp concrete manufacture				
Hemp concrete manufacture				
Input	Quantity	Unit	Source	Process
Water	15.15	t	(Ip and Miller, 2012)	Tap water {Europe without Switzerland}| market for | Conseq, U
Lime binder				
Hydrated binder	7.58	t	(Ip and Miller, 2012)	Lime, hydrated, packed {RER}| market for lime, hydrated, packed | Conseq, U
Hydraulic binder	1.52	t	(Ip and Miller, 2012)	Lime, hydraulic {RER}| market for lime, hydraulic | Conseq, U
Pozzolanic binder	1.01	t	(Ip and Miller, 2012)	Cement, pozzolana and fly ash 36-55%,non-US {Europe without Switzerland}| market for cement, pozzolana and fly ash 36-55% | Conseq, U
Shivs	5.48	t		
Electricity	336.63	kwh	(Ip and Miller, 2012)	Electricity, low voltage {FR}| market for | Conseq, U
Output				
Hemp concrete	60.61	m^3		
Hemp concrete use				
Input	Quantity	Unit	Source	Process
Hemp concrete	60.61	m^3		
Output				
CO_2 absorbtion	-4.67	t	(Pretot et al., 2014)	
H_2O replaced	1.91	kg	(Pretot et al., 2014)	
Hemp concrete end of life				
Input	Quantity	Unit	Source	Process
Hemp concrete	60.61	m^3		
Output				
CO_2 from hemp concrete	8.2	t		
Co-products fate				
Co-product	Quantity	Unit	Source	Process
Hemp concrete	60.61	m^3		
Marginal product				
Gypsum plasterboard	-48.59	t	(ecoinvent, 2020)	Gypsum plaster (CaSO4 beta hemihydrates) DE S

2.8 Thermal insulation manufacture

The extracted fibers are used to be thermal insulation panels in the first case. Fiber is going to mix with the polypropylene(PP) to form a mat, and ammonium sulfate ($(NH_4)_2SO_4$) is added to increase the fire retardant(Andersson and Björhagen, 2018; Zhang, 2016). Similar to the insulation manufacture of traditional materials, the mixed mat is formed into a fleece material with several layers put on top of each other and finally pressed with heat to get the insulation(Stapulionienė et al., 2016). In comparison, the traditional insulation made by mineral wool is assumed to be avoided(Uihlein et al., 2008), to achieve the same insulation function (λ=0.038 W $m^{-1}K^{-1}$), wool insulation would be 33% heavier than hemp insulation due to its higher density (40 kg m^{-3})(ecoinvent, 2020). As landfilling is the most common way for mineral wool mat disposal, it is not included because of few emission The end-of-life is not included

because there is little emission during the gypsum plasterboards landfilling(ecoinvent, 2020). The whole process from fiber to thermal insulation is displayed in table S10.

Table S10 Inventory sheet of hemp thermal insulation manufacture				
Mixing				
Input	Quantity	Unit	Source	Process
Fiber	2.53	t		
Ammonium sulphate	0.09	t	(Andersson and Björhagen, 2018)	Ammonium sulfate, as 100% (NH4)2SO4 (NPK 21-0-0), at plant/RER Economic
Polypropylene	0.26	t	(Andersson and Björhagen, 2018)	Polypropylene, granulate {RER}| production | Conseq, U
Output				
Mixed mat	2.88	t		
Insulation Manufacture				
Input	Quantity	Unit	Source	Process
Thermocompression, input- mixed mat	2.88	t	(Stapulionienė et al., 2016)	Thermoforming, with calendering {RoW}| thermoforming, with calendering | Conseq, U
Output				
Thermal insulation	2.88	t		
Marginal product				
Wool mat	-3.83	t	(Uihlein et al., 2008)	Glass wool mat {GLO}| market for | Conseq, U

2.9 Thermal insulation disposal

To this day and recent future, compared to innovative methods like composting and recycling, landfilling is still the most common and commercial way for disposing of insulation removed from refurbishment or demolition(Norton et al., 2008). Table S11 describes the end life of hemp insulation, because there is no hemp fiber disposal way in the database yet, here using the wood disposal process for fiber as a proxy(Gueudet, 2016a).

CH_4 and CO_2 are the major emissions due to the landfilling, which vary on factors like landfill management and depth, IPCC described a First Order Decay (FOD) method to estimate the CH_4 in the landfilling, and then CO_2 is computed according to the CH_4/ CO_2 ratio(IPCC, 2019). Based on the FOD method, 15.88% of C in the fiber in the insulation would be emitted, including 12.9% CH_4 and 87.1% CO_2(appendix C). However, as the reason we put CO_2 emission in the hemp concrete inventory sheet

(table S9), we deem all C would back to the atmosphere anyhow, thus in the inventory list, we regard the C in the fiber of insulation other than 15.88% is all emitted as CO_2.

Table S11 Inventory sheet of hemp thermal insulation disposal				
Disposal				
Input	Quantity	Unit	Source	Process
Thermal insulation	2.88	t		
Output				
Landfilling PP	0.26	t	(ecoinvent, 2020)	Waste polypropylene {RoW}| treatment of waste polypropylene, sanitary landfill | Conseq, U
Landfilling fiber	2.21	t	(ecoinvent, 2020)	Waste wood, untreated {CH}| treatment of, sanitary landfill | Conseq, U
Emission to air				
CO_2 from fiber in the insulation	3.21	t		Compensated CO_2 emission

2.10 Car panel manufacture

Compared with traditional materials like wool or glass fiber, grass fiber has similar characteristics in insulation and strength but is lighter in weight. Thus, grass fiber is commonly used in the vehicle industry now to reduce the vehicle weight, to achieve less fuel consumption, both economically and environmentally friendly. Here, hemp fiber is one of the novel grass fibers that aims to produce the side panel in the car.

The first step is drying, the extracted fiber contains 12.75% moisture, would be dried under 80°C for 24h (Islam, 2008; Walker et al., 2014). The energy consumption is evaluated by the formula below:

$$Q = m*cv(Tf-Ti) + m*Hv \quad (1)$$

Here, Q is the energy consumption in MJ, m is the water mass in kg, cv is the heat capacity in 4.18 kJ/(kg/K), Tf is the final temperature in °C, Ti is the initial temperature in °C, equal to the ambient temperature 25 °C, Hv is the latent heat of vaporization, 2256 kJ/kg.

After drying, the fiber should be fabricated into a randomly oriented mat according to the mold shape, here the energy consumption of making a hemp mat is not found, so use the consumption of similar grass flax instead(Deng, 2014). Then polypropylene (PP) resin is added to reinforce the fiber(Boland et al., 2016). Finally, the reinforced mat is heated at 205°C at 10 min, compressed in 1.4 mPa(Pervaiz and Sain, 2003). The hemp car panel is designed to replace the car panel made by glass fiber(Lee et al., 2016; Sepe et al., 2018), to reduce the weight of automobiles, thereby benefiting the fuel economy. For two panels with the same function, the panel made by hemp fiber could be 20% lighter than that made by glass fiber(Gueudet, 2016a), in other words, the marginal glass panel would be 20% heavier than hemp panel. Then the quantity of fuel reduction is shown in the next section (Table S13), and the inventory of car panel manufacture is 3shown below (table S12). Similar to gypsum plasterboards and wool mineral boards, the disposal of glass fiber panels is ignored since there is few emission.

Table S12 Inventory sheet of hemp car panel manufacture				
Drying				
Input	Quantity	Unit	Source	Process
Fiber	2.53	t		
Natural gas	20.73	m^3	(Islam, 2008)	Drying, natural gas {GLO}| market for | Conseq, U
Output				
Dry fiber	2.21	t		
Water evaporated	0.32	t		
Matting				
Input	Quantity	Unit	Source	Process
Matting, input- dry fiber	2.21	t	(Deng, 2014)	Spinning, bast fibre {GLO}| market for | Conseq, U
Output				
Fiber mat	2.21	t		
Mixing				
Input	Quantity	Unit	Source	Process
Fiber mat	2.21	t		
Polypropylene (PP) resin	3.35	t	(Boland et al., 2016)	Polypropylene resin, at plant/RNA
Output				
Reinforced mat	5.56	t		
Thermal compression molding				
Input	Quantity	Unit	Source	Process
Thermoforming, input- mixed mat	5.56	t	(Pervaiz and Sain, 2003)	Thermoforming, with calendering {GLO}| market for | Conseq, U
Output				
Car panel	5,33	t		
Fiber waste	0.08	t	(Boland et al., 2016)	Waste wood, untreated {FR}| market for waste wood, untreated | Conseq, U
PP resin waste	0.15	t	(Boland et al., 2016)	Waste polypropylene {FR}| market for waste polypropylene | Conseq, U
Marginal product				
Glass fiber car panel[a]	-6.61	t	(Sepe et al., 2018)	Glass fibre reinforced plastic, polyamide, injection moulded {RER}| production | Conseq, U

a: Because hemp fiber aims to replace the glass fiber. 'Glass fibre {RER}| production | Conseq, U' is used instead of 'Nylon 6-6, glass-filled {RER}| market for nylon 6-6, glass-filled | Conseq, U' in the original process.

2.11 Car panel use stage

Compared to the traditional panel, using hemp fiber could reduce around 20% mass(Akampumuza et al., 2017). Thus, during the driving, less fuel would be consumed, the saved fuel could be calculated as follow:

$$\text{Fuel reduction} = f^{*}\Delta m^{*}\text{distance} \quad (2)$$

Where Fuel reduction is the amount of saved fuel in L. f is the fuel reduction coefficient, equal to 0.5 here, in $L\cdot(100km^{-1})\cdot(100kg^{-1})$ for the gasoline vehicle, Δm is the mass reduction between the traditional panel and hemp fiber panel in kg. distance is the lifetime of a vehicle, regarded as 20,000 km(La Rosa et al., 2013).

Table S13 Inventory sheet of hemp car panel use stage				
Drying				
Input	Quantity	Unit	Source	Process
Car panel	5.33	t		
Output[a]				
Fuel reduction (gasoline)	-12530.38	L	(La Rosa et al., 2013)	Petrol, 5% ethanol by volume from biomass {GLO}| market for | Conseq, U

[a]: negative value means avoided

2.12 Disposal

At the end of life, an automobile would be transported to the crusher, where it undergoes compaction, pre-crushing, and crushing operations. After grinding, the fractions of the different materials are sorted and managed according to the fraction. Door panels are not affected by operations taking place at the crushing center (pollution control and dismantling of certain parts), this step is therefore excluded from the scope of the study: no consumption or emission is considered, only the electricity consumption of this step is taken into account. In the same way as the assembly phase, it is considered that the grinding consumptions and emissions do not change significantly if the door panel is bio-based (lighter) or not(Gueudet, 2016a). Nowadays, there is no proper way to recycle the hemp fiber car panel, landfilling and incineration are still the most possible ways at the end of life(Norton, 2008; Zah et al., 2007). According to the France situation, 70% of car panels are disposed of through landfilling while the rest 30% would be incinerated(Gueudet, 2016a). Similar to the hemp insulation disposal, 15.32% of C in the fiber of car panel is emitted as CH_4 and CO_2, 1.97% and 13.34% respectively, according to the FOD method(IPCC, 2019). Then, CO_2 emission from the fiber other than 15.32% during the landfilling is listed to complete the C cycle, detail about hemp car panel disposal is depicted in Table S14.

Table S14 Inventory sheet of hemp car panel disposal				
Disposal				
Input	Quantity	Unit	Source	Process
Car panel	5.33	t		
Electricity for compaction	10.66	kwh	(Gueudet, 2016a)	Electricity, medium voltage {FR}| market for | Conseq, U
Electricity for pre-grinding	8	kwh	(Gueudet, 2016a)	Electricity, medium voltage {FR}| market for | Conseq, U

Electricity for grinding	354.45	kwh	(Gueudet, 2016a)	Electricity, medium voltage {FR}| market for | Conseq, U
Output				
Landfilling	3.55	t	(Gueudet, 2016a)	
Incineration	1.78	t	(Gueudet, 2016a)	
Landfilling				
Input	Quantity	Unit	Source	Process
Car panel	3.55	t		
Output				
Landfilling, car panel	3.57	t		Waste fibreboard {CH}| market for waste fibreboard | Conseq, U
Emission to air				
CO_2 from fiber in the car panel	2.08	t		Compensated CO_2 emission
Incineration				
Input	Quantity	Unit	Source	Process
Car panel	1.78	t		
Output				
Incineration fiber in the car panel	0.7	t		Waste wood, untreated {FR}| market for waste wood, untreated | Conseq, U
Incineration PP in the car panel	1.06	t		Waste polypropylene {FR}| market for waste polypropylene | Conseq, U

2.13 Images of hemp-based products

The images of hemp-based products studied in the LCA are collected from literature, shown in Fig. S2.

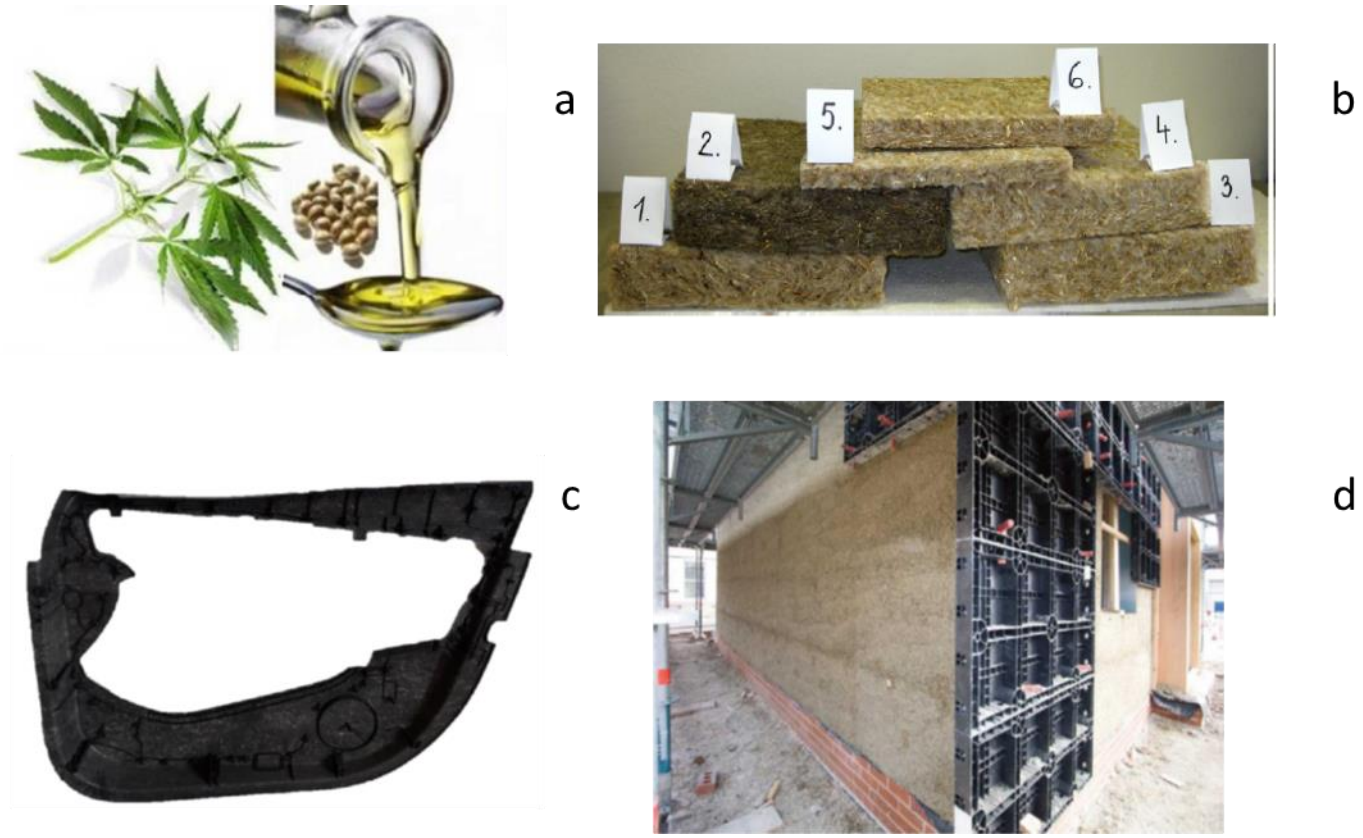

Fig. S2 Images of hemp based products in this study. Hemp seed oil (a), thermal insulation (b), car panel (c), concrete (d) (Gueudet, 2016b; Ip and Miller, 2012; Korjenic et al., 2011; Montserrat-De La Paz et al., 2014).

2.14 Planting in the carbon vulnerable land

Marginal lands are separated into four land cover types, namely rapeseed, natural grassland, intensive grassland, and woody moorland, there are 0.2, 0.53, 0.2, and 0.07 ha for these four land cover types in 1 ha carbon vulnerable land respectively, referring to their proportions(Shen et al., 2021). These four types of land cover are considered separately to estimate the avoided emission or sequestration.

For intensive grassland, according to the determined species, perennial ryegrass (*Lolium perenne L.*) is used for representing the plant in the intensive grassland(Kirwan et al., 2007; PLANTUREUX et al., 2005). Then harvested ryegrass would go silage and use as forage later. The SOC change during the cultivation is estimated by AMG (described in section 1), conditions like soil characteristics and temperature are the same as that in hemp simulation, while carbon inputs are different, which could be found in Table S15. The inventory of intensive grassland is shown in Table S16. For rapeseed (*Brassica napus L.*), the harvested seeds aim to extract oil, the seed meal produced as a by-product would further feed the livestock. Also, SOC change is estimated by AMG, input is shown in Table S15. If the products from intensive grassland and rapeseed are replaced by hemp, other products would be induced to fill this vacancy (like more soybean would be cultivated to provide protein to compensate the missed protein from ryegrass). This kind of induced demand would raise indirect land use change, consisting of land expansion (which means more land demand) and intensification (which means additional fertilizers due to demand for higher yield)(COWI A/S and Utrecht University, 2019; Tonini et al., 2016).

For natural grassland, heathland (*Calluna vulgaris*) is the representative(Inglada et al., 2017). The biomass grown in the natural grassland is regarded as no specific usage, in other words, it would decay on-site except 10% of C in the biomass would be sequestered(Pehme et al., 2017) (AMG model cannot

be applied here because heathland doesn't exist in the AMG database), detail inventory is described in Table S18. According to the definition of land cover, the determined species in woody moorland are similar to natural grassland (heathland, briars), plus the proportion of woody moorland is the least among carbon vulnerable lands, thus the situation is considered as same as that in natural grassland (Table S19), except the NMVOC emission(European Environment Agency, 2019). Figure S3 depicts the situation of carbon vulnerable lands, while table S14-19 detail in math. The 'avoided carbon sequestration or emission' means the carbon change due to the avoided activities (e.g. silage for ryegrass), it's hard to predict the carbon change is negative or positive before analyzing, both sequestration and emission could be possible, results could be found in the result part in the main paper or detail in appendix B ('C-vulnerable vegetation' in stack graph, sunburst figure and contribution table). Inventory data in table S16-19 are based on 1 ha of carbon vulnerable land, in fact, what happened in these tables would be avoided, that's why the value in table S21 is negative, which means values in table S16-19 would be reversed in the LCA calculation.

After the conversion, all biomass is lost immediately from the carbon vulnerable land(Verchot et al., 2006). Tillage is applied to cleaning the field before the first time hemp cultivation, while in propose to less disturb the SOC storage, no-tillage strategy is adopted in the following cultivation till the end of time scale(Amaducci et al., 2015), thus tillage in the first year is negligible in the inventory building because it only happens once.

Table S15 Input of AMG, ryegrass and rapeseed (Clivot et al., 2019).

	Irrigation	Tillage cm	Proportion of harvestable part(RP), residue(RS), root(RR), extra-root(RE)				Root contribution	Aboveground carbon input Mg/ ha	Belowground carbon input Mg/ ha
			RP	RS	RR	RE			
Ryegrass	0	30	0.417	0.083	0.303	0.197	0.953	0.68	2.77
Rapeseed	0	27	0.191	0.574	0.142	0.093	0.920	3.12	1.17

Table S16 Inventory sheet of intensive grassland.				
Silage				
Input	Quantity	Unit	Source	Process
Silage process[a, b]	8	t	(ecoinvent, 2020)	Ryegrass silage {CH}| catch crop growing, ryegrass, August-April, organic fertiliser 80 kg N, three cuts | Conseq, U; 8 t/ha is the amount of ryegrass that would go through the silage.
N fertilizer	222	kg	(Hamelin et al., 2012)	Nitrogen fertiliser, as N {GLO}| market for | Conseq, U
P fertilizer	53.47	kg	(Hamelin et al., 2012)	Phosphate fertiliser, as P2O5 {GLO}| market for | Conseq, U
K fertilizer	18.69	kg	(Hamelin et al., 2012)	Potassium sulfate, as K2O {GLO}| market for | Conseq, U
Lime	542.05	kg	(Hamelin et al., 2012)	Lime, packed {CH}| lime production, milled, packed | Conseq, U
CO_2 in air	12.32	t		CO_2 captured from harvestable part
CO_2 in air	12.58	t		CO_2 captured from above+ belowground residue

Output				
Ryegrass silage	20.6	t	(ecoinvent, 2020)	65% water content
iLUC	-1	ha	(COWI A/S and Utrecht University, 2019)	
Emission to air				
NH_3	69.92	kg	(Hamelin et al., 2012)	From urea
NH_3	4.97	kg	(Hamelin et al., 2012)	From mineral fertilizer like $(NH_4)_2HPO_4$ or $5Ca(NO_3)_2$ $NH_4{\cdot}NO_3$
NO	7.64	kg	(Hamelin et al., 2012)	From fertilizer
NO	1.51	kg	(Hamelin et al., 2012)	From residue
NO_x	14	kg	(Hamelin et al., 2012)	
N_2	74.96	kg	(Hamelin et al., 2012)	
N_2O	4.31	kg	(Hamelin et al., 2012)	From fertilizer &residue
N_2O	1.58	kg	(Hamelin et al., 2012)	From N mineralized because of soil carbon loss
CO_2	11.28	t	(Hamelin et al., 2012)	From residue, considered the SOC increased.
CO_2	0.43	t	(Hamelin et al., 2012)	From urea
CO_2	1.23	t	(ecoinvent, 2020)	From carbon loss during the silage
NMVOC	0.36	kg	(Hamelin et al., 2012)	
Emission to water				
Nitrate	149.5	kg	(Hamelin et al., 2012)	N-leaching
Phosphorus	0.032	kg	(Hamelin et al., 2012)	P-leaching
Use of ryegrass silage				
Input	Quantity	Unit	Source	Process
Ryegrass silage	20.6	t		
Output				
CO_2, biogenic	11	t		All carbon in the silage would emit back to the atmosphere
Marginal products				
Carbohydrate	-2.4	t	(Tonini et al., 2016)	Maize grain {GLO}| market for | Conseq, U
Protein	-0.49	t	(Tonini et al., 2016)	Soybean meal {GLO}| market for | Conseq, U
Fats	-34.53	kg	(Tonini et al., 2016)	Palm oil, refined {GLO}| market for | Conseq, U

a: plant cultivation and land occupation are included in the process;

b: silage process is modified by using mineral fertilizer, consequential inputs and emissions are shown in the inventory;

Table S17 Inventory sheet of rapeseed.				
Input	Quantity	Unit	Source	Process
Oil extraction[a,b]	822	kg	(ecoinvent, 2020)	Rape oil, crude {Europe without Switzerland}| rape oil mill operation | Conseq, U
Output				
Crude rapeseed oil	822	kg	(ecoinvent, 2020)	
SOC change	1.18	t	(Clivot et al., 2019)	Carbon dioxide, to soil or biomass stock
iLUC	-1	ha	(COWI A/S and Utrecht University, 2019)	Indirect land use change
Marginal product				
Crude palm oil	822	kg	(ecoinvent, 2020)	Palm oil, crude {RoW}| palm oil mill operation | Conseq, U
Use of rapeseed				
Input	Quantity	Unit	Source	Process
Crude rapeseed oil	822	kg		
Output				
CO2, biogenic	3814.93	kg		All C in rapeseed oil would emit back to the atmosphere.

a: plant cultivation and land occupation are included in the process;
b: the avoided protein because of the rapeseed meal is included in the process;

Table S18 Inventory sheet of natural grassland.				
Input	Quantity	Unit	Source	Process
CO_2 captured	3.72	t	(Vogtländer et al., 2014; Worrall and Clay, 2014)	
Land occupation	1	ha a	(ecoinvent, 2020)	Occupation, grassland, natural (non-use)
Output				
Emission to air				
N_2O	0.51	kg	(Pehme et al., 2017)	
NO_x	1.28	kg	(Pehme et al., 2017)	
NH_3	0.39	kg	(Pehme et al., 2017)	
NMVOC	3.8	kg	(European Environment Agency, 2019)	
CO_2	3.35	t	(Vogtländer et al., 2014;	

			Worrall and Clay, 2014)	
Emission to water				
Nitrate	31	kg	(Decau et al., 2004; Hussain et al., 2019)	
Emission to soil				
SOC change	0.37	t	(Pehme et al., 2017)	Carbon dioxide, to soil or biomass stock

Table S19 Inventory sheet of woody moorland.				
Input	Quantity	Unit	Source	Process
CO_2 captured	3.72	t	(Vogtländer et al., 2014; Worrall and Clay, 2014)	
Land occupation	1	ha a	(ecoinvent, 2020)	Occupation, grassland, natural (non-use)
Output				
Emission to air				
N_2O	0.51	kg	(Pehme et al., 2017)	
NO_x	1.28	kg	(Pehme et al., 2017)	
NH_3	0.39	kg	(Pehme et al., 2017)	
NMVOC	19.33	kg	(European Environment Agency, 2019)	
CO_2	3.35	t	(Vogtländer et al., 2014; Worrall and Clay, 2014)	
Emission to water				
Nitrate	31	kg	(Hussain et al., 2019)	
Emission to soil				
SOC change	0.37	t	(Pehme et al., 2017)	Carbon dioxide, to soil or biomass stock

Table S20 Indirect land use change (for 1 ha).				
Input	Quantity	Unit	Source	Process
P input	59.14	kg	(Tonini et al., 2016)	Phosphate fertiliser, as P2O5 {GLO}| market for | Conseq, U
N input	21.84	kg	(Tonini et al., 2016)	Nitrogen fertiliser, as N {GLO}| market for | Conseq, U
K input	31.22	kg	(Tonini et al., 2016)	Potassium fertiliser, as K2O {GLO}| market for | Conseq, U
Output				
Emissions to air				

CO_2	0.91	t	(Tonini et al., 2016)	Carbon dioxide, biogenic
CO	25.9	kg	(Tonini et al., 2016)	Carbon monoxide, biogenic
CH_4	1.63	kg	(Tonini et al., 2016)	Methane, biogenic
N_2O	2.34	kg	(Tonini et al., 2016)	Dinitrogen monoxide
NO_x	1.37	kg	(Tonini et al., 2016)	Nitrogen oxides
NH_3	1.58	kg	(Tonini et al., 2016)	Ammonia
Emissions to water				
NO_3^-	29.86	kg	(Tonini et al., 2016)	Nitrate
PO_4^{3-}	0.29	kg	(Tonini et al., 2016)	Phosphate

Table S21 C-vulnerable plantation.				
Input	Quantity	Unit	Source	Process
Marginal land left as marginal, intensive grasslands	-0.53	ha		
Marginal land left as marginal, rapeseed	-0.2	ha		
Marginal land left as marginal, natural grassland	-0.2	ha		
Marginal land left as marginal, woody moorlands	-0.07	ha		

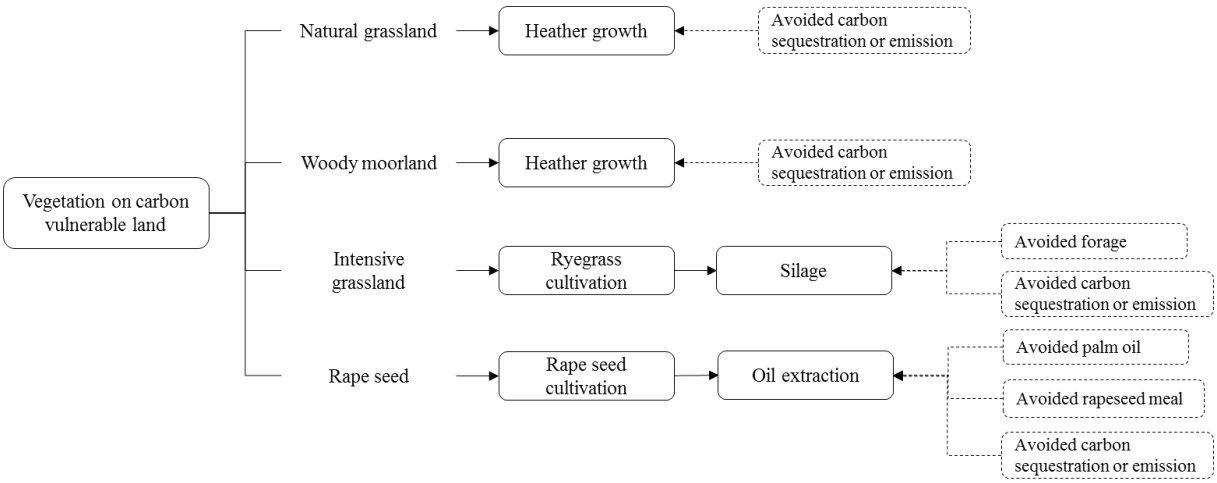

Fig. S3 Diagram of carbon vulnerable land use.

3 Environmental impact in consequential LCA

3.1 Environmental impact categories in consequential LCA

This study chose the Environmental Footprint initiative (EF) methods, which is established and recommended by the European Commission (EC) to assess environmental impacts(Fazio et al., 2018). To track sources of different carbon flows and highlight the function of SOC but avoid double counting, the EF method is slightly adapted as recommended by European Commission(Schau et al., 2013). The following characterization factors are used: biogenic CO_2 =1 kg CO2 eq, biogenic CO= 1.57 kg CO_2 eq, biogenic methane= 34 kg CO_2 eq, CO2 in air= -1 kg CO_2 eq, CO_2 stocked in soil or biomass= 0. Under the EF scheme, 19 environmental impact categories are assessed, including three sub-impacts of climate change (fossil, biogenic, and land transformation). European Commission established three different recommendation levels, satisfactory for categories in level I, needs some improvements for level II, and applied with caution for level III(Fazio et al., 2018).

Table S22 Environmental impacts

Impact category	Unit	Recommendation level
Climate change	kg CO_2 eq	I
Ozone depletion	kg CFC11 eq	I
Ionising radiation, HH	kBq U-235 eq	II
Photochemical ozone formation, HH	kg NMVOC eq	II
Respiratory inorganics	disease inc.	I
Non-cancer human health effects	CTUh	III
Cancer human health effects	CTUh	III
Acidification terrestrial and freshwater	mol H+ eq	II
Eutrophication freshwater	kg P eq	II
Eutrophication marine	kg N eq	II
Eutrophication terrestrial	mol N eq	II
Ecotoxicity freshwater	CTUe	III
Land use	Pt	III
Water scarcity	m3 depriv.	III
Resource use, energy carriers	MJ	III
Resource use, mineral and metals	kg Sb eq	III
Climate change - fossil	kg CO_2 eq	I
Climate change - biogenic	kg CO_2 eq	I
Climate change - land use and transform	kg CO_2 eq	I

3.2 Environmental impact results

Table S23 Abbreviation of substance in contribution analysis.

Substance	Abbreviation	Substance	Abbreviation
Climate change		**Ozone Depletion**	
Carbon dioxide, biogenic	CO_2, bio	Methane, bromochlorodifluoro-, Halon 1211	$CBrClF_2$
Carbon dioxide, fossil	CO_2, fossile	Methane, bromotrifluoro-, Halon 1301	$CBrF_3$
Carbon dioxide, in air	CO_2, air	Ethane, 1,1,2-trichloro-1,2,2-trifluoro-, CFC-113	$C_2Cl_3F_3$
Dinitrogen monoxide	N_2O	Photochemical ozone formation, HH	
Carbon dioxide, land transformation	CO_2, LUC	Nitrogen monoxide	NO
Methane, land transformation	CH_4, LUC	Nitrogen oxides	NO_x
Ionising radiation, HH		NMVOC, non-methane volatile organic compounds, unspecified origin	NMVOC
Carbon-14	C-14	Hexane	C_6H_{14}
Radon-222	Rn-222	Ethene	C_2H_6
Uranium-234	U-234	Formaldehyde	CH_2O
Respiratory inorganics		Propene	C_3H_6
Ammonia	NH3	**Non-cancer human health effects**	
Particulates, < 2.5 um	PM2.5	Zinc, soil	Zn, s
Sulfur dioxide	SO2	Lead	Pb
Cancer human health effects		Mercury	Hg
Chromium, water	Cr, w	Zinc, air	Zn, a
Chromium, air	Cr, a	Arsenic	As
Chromium, soil	Cr, s	**Acidification terrestrial and freshwater**	
Chromium VI	Cr^{6+}	Ammonia	NH_3
Eutrophication freshwater		Nitrogen oxides	NO_x
Phosphorus	PO_4^{3-}	Sulfur dioxide	SO_2
Phosphate	P	Eutrophication marine	
Eutrophication terrestrial		Nitrate	NO^{3-}
Ammonia	NH_3	Nitrogen monoxide	NO
Nitrogen oxides	NO_x	Nitrogen oxides	NO_x
Land use		**Ecotoxicity freshwater**	
Occupation, permanent crop	Lop, per	Chromium	Cr
Occupation, annual crop, non-irrigated, intensive	Lop, no-in	Copper	Cu
Occupation, grassland, natural (non-use)	Lop, nat	Zinc, water	Zn, w
Occupation, annual crop	Lop,an	Zinc, soil	Zn, s
Occupation, annual crop, non-irrigated	Lop, an-non	Zinc, air	Zn, a
Transformation, from annual crop	Ltrans, fa	Acetochlor	Acetochlor
Transformation, to annual crop, non-irrigated, intensive	Ltrans, ta-non	Atrazine	Atrazine
Transformation, to annual crop	Ltrans, ta	Chlorpyrifos	Chlorpyrifos
Resource use, energy carriers		Diflubenzuron	Diflubenzuron
Gas, natural/m3	Natural gas	Antimony, air	Sb, a
Oil, crude	Crude oil	Antimony, water	Sb, w
Coal, brown	Coal, brown	Vanadium	V
Coal, hard	Coal, hard	Arsenic	As
Uranium	U	Nickel	Ni
Resource use, mineral and metals		**Climate change - fossil**	
Cadmium	Cd	Carbon dioxide, fossil	CO_2, fossile
Gold	Au	Dinitrogen monoxide	N_2O

Gold, Au 4.9E-5%, in ore	Au-4,9E	Climate change - biogenic	
Gold, Au 6.7E-4%, in ore	Au-6,7E	Carbon dioxide, in air	CO_2, air
Gold, Au 7.1E-4%, in ore	Au-7,1E	Carbon dioxide, biogenic	CO_2, bio
Climate change - land use and transform			
Carbon dioxide, land transformation	CO_2, LUC		
Methane, land transformation	CH_4, LUC		

Table S24 Abbreviation of process in contribution analysis of scenario SL.

Process	Abbreviation	Sub-process	Abbreviation
C-vulnerable plantation	CV-land	Ryegrass silage	Silage
Hemp cultivation	Cultivation	Induced forage	In-forage
Residue degradation &hemp harvesting	Harvesting	Use of forage	Forage use
Hemp oil, crude | mill operation	Mill	iLUC	iLUC
Hemp seed oil, refinery operation	Refinery	Rape oil, crude rape oil mill operation	Rape mill
Hemp seed market&use	M&Use	CO_2 captured	Photosynthesis
Avoided-palm oil from seed	Av- oil	Nitrogen fertiliser, as N	N-fertilizer
		Emission from residue	Decay
		Tap water	Water
		Palm oil, refined market	Palm oil
		Phosphate fertiliser, as P_2O_5	P-fertilizer
		Combine harvesting	Harvestor
		Avoid meal	Av-Meal
		Marginal land left as marginal, intensive grasslands	C-intensive
		Marginal land left as marginal, rapeseed	C-rapeseed
		Marginal land left as marginal, natural grassland	C-natural grass
		Marginal land left as marginal, woody moorlands	C-moorland
		CO_2 emmision from seed oil	Seed end

Table S25 Abbreviation of process in contribution analysis of scenario IB.

Process	Abbreviation	Sub-process	Abbreviation
C-vulnerable plantation	CV-land	Ryegrass silage	Silage
Hemp cultivation	Cultivation	Induced forage, input- silaged ryegrass	In-feed
Residue degradation &hemp harvesting	Harvesting	Use of forage	Forage use
Hemp oil, crude | mill operation	Mill	iLUC	iLUC
Hemp seed oil, refinery operation	Refinery	Rape oil, crude {FR seed}| rape oil mill operation | Conseq, U	Rape mill
Hemp seed market&use	M&Use	CO2 captured	Photosynthesis
Avoided-palm oil from seed	Av- oil	Hemp cultivation	Cultivation

Retting, input- straw	Retting	Nitrogen fertiliser, as N {GLO}| market for | Conseq, U	N-fertilizer
Baling, input- retted straw	Baling	Phosphate fertiliser, as P2O5 {GLO}| market for | Conseq, U	P-fertilizer
Fiber extraction, input- baled straw	F-extract	Emission from residue	Decay
Concrete manufacture, input- shives	Con-manufacture	Combine harvesting {GLO}| market for | Conseq, U	Harvestor
Concrete use stage, input- hemp concrete	Con-use	Avoid meal, input -seed wet	Av-meal
CO_2 emission from shives in concrete, input- hemp concrete	Con-end	Palm oil, refined market	Mazie
Avoided - gypsum plasterboard	Av-gypsum	Palm oil, refined market	Palm oil
Mixing (insulation), input- fiber	Mixing	Tap water {Europe without Switzerland}| market for | Conseq, U	Water
Insulation manufacture (thermocompression), input- mixed mat	I-manufacture	Electricity, low voltage {FR}| market for | Conseq, U	Electricity {FR}
Avoided-wool thermal insulation	Av-insulation	Lime, hydraulic {RER}| market for lime, hydraulic | Conseq, U	Hydraulic
Landfilling- thermal insulation	Landfilling	Lime, hydrated, packed {RER}| market for lime, hydrated, packed | Conseq, U	Hydrated
		Cement, pozzolana and fly ash 36-55%,non-US {Europe without Switzerland}| market for cement, pozzolana and fly ash 36-55% | Conseq, U	Cement
Sub-process	Abbreviation	CO_2 captured during using	Carbonation
Stone wool factory {GLO}| market for stone wool factory | Conseq, U	Wool	CO_2 emission from shives in concrete, input- hemp concrete	Con-end
Heat, district or industrial, other than natural gas {RER}| market group for | Conseq, U	Heat {RER}	Gypsum plaster (CaSO4 beta hemihydrates) DE S	Gypsum
Kraft paper, bleached {GLO}| market for | Conseq, U	Kraft	Thermoforming, with calendering {RER}| thermoforming, with calendering | Conseq, U	Thermoforming
Steam, in chemical industry {GLO}| market for | Conseq, U	Steam	Core board {GLO}| market for | Conseq, U	Core board
Polyethylene, low density, granulate {GLO}| market for | Conseq, U	Polyethylene	Electricity, medium voltage {RER}| market group for | Conseq, U	Electricity {RER}
Waste plastic, mixture {RER}| market group for waste plastic, mixture | Conseq, U	Waste	Packaging box factory {RER}| construction | Conseq, U	Packaging
Heat {EU}	Heat {EU}	Electricity, medium voltage {RAS}| market group for | Conseq, U	Electricity {RAS}

Silicone	Silicone	Heat, district or industrial, natural gas {RoW}| market for heat, district or industrial, natural gas | Conseq, U	Heat {RAS}
Managanese	Managanese	Glass cullet, sorted {GLO}| market for | Conseq, U	Glass
Urea	Urea	Electricity, medium voltage {RoW}| market for | Conseq, U	Electricity {ROW}
Glass wool	Glass wool	Heat, district or industrial, natural gas {RoW}| market for heat, district or industrial, natural gas | Conseq, U	Heat {ROW}
CO_2-fiber	CO2-fiber	C-rapeseed	C-rapeseed
Fiber	Fiber	C-natural grass	C-natural grass
C-intensive	C-intensive	C-moorland	C-moorland

Table S26 Abbreviation of process in contribution analysis of scenario CP.

Process	Abbreviation	Sub-process	Abbreviation
C-vulnerable plantation	CV-land	Ryegrass silage	Silage
Hemp cultivation	Cultivation	Induced forage, input- silaged ryegrass, method 2	In-forage
Residue degradation &hemp harvesting, straw harvested	Harvesting	Use of forage	Forage use
Hemp oil, crude | mill operation, input -seed wet	Mill	iLUC	iLUC
Hemp seed oil, refinery operation, input- crude oil	Refinery	Rape oil, crude {FR seed}| rape oil mill operation | Conseq, U	Rape mill
Hemp seed market&use, input- refined oil	M&Use	CO_2 captured	Photosynthesis
Avoided-palm oil from seed	Av- oil	Hemp cultivation	Cultivation
Retting, input- straw	Retting	Nitrogen fertiliser, as N {GLO}| market for | Conseq, U	N-fertilizer
Baling, input- retted straw	Baling	Phosphate fertiliser, as P2O5 {GLO}| market for | Conseq, U	P-fertilizer
Fiber extraction, input- baled straw	F-extract	Emission from residue	Decay
Concrete manufacture, input- shives	Con-manufacture	Combine harvesting {GLO}| market for | Conseq, U	Harvestor
Concrete use stage, input- hemp concrete	Con-use	Avoid meal, input -seed wet, method 2	Av-meal
CO_2 emission from shives in concrete, input- hemp concrete	Con-end	Palm oil, refined market	Mazie
Avoided - gypsum plasterboard	Av-gypsum	Palm oil, refined market	Palm oil
Dry (hemp car panel), input- fiber	Dry	Tap water {Europe without Switzerland}| market for | Conseq, U	Water

Matting, input- dry fiber	Matting	Lime, hydraulic {RER}| market for lime, hydraulic | Conseq, U	Hydraulic
Mixing (car panel), input- fiber mat	Mixing	Lime, hydrated, packed {RER}| market for lime, hydrated, packed | Conseq, U	Hydrated
Car panel manufacture, input- reinfored mat	CP-manufacture	Cement, pozzolana and fly ash 36-55%,non-US {Europe without Switzerland}| market for cement, pozzolana and fly ash 36-55% | Conseq, U	Cement
Car panel use, input- car panel	Using	CO2 captured during using	Carbonation
Avoided - glass fiber car panel	Av-CP	CO2 emission from shives in concrete, input- hemp concrete	Con-end
Disposal, input-car panel	Disposal	Gypsum plaster (CaSO4 beta hemihydrates) DE S	Gypsum
		Spinning, bast fibre {IN}| processing | Conseq, U	Spin{IN}
		Spinning, bast fibre {RoW}| processing | Conseq, U	Spin{ROW}

Sub-process	Abbreviation
Ethanol, without water, in 99.7% solution state, from fermentation, at service station {CH}| market for | Conseq, U	Ethanol
Petrol, 5% ethanol by volume from biomass {CH}| production | Conseq, U	Petrol
Core board {GLO}| market for | Conseq, U	Board
EUR-flat pallet {GLO}| market for | Conseq, U	Flat
Packaging box factory {RER}| construction | Conseq, U	Packaging {RER}
Packaging box factory {GLO}| market for | Conseq, U	Packaging {GLO}
Propylene, at plant/kg/RNA	Propene
Polypropylene resin, at plant/RNA	PP resin
Polyethylene, low density, granulate {GLO}| market for | Conseq, U	PE
Kraft paper, bleached {GLO}| market for | Conseq, U	Kraft

Thermoforming, with calendering {RoW}| thermoforming, with calendering | Conseq, U	Thermoforming{RoW}
Thermoforming, with calendering {RER}| thermoforming, with calendering | Conseq, U	Thermoforming{RER}
Waste plastic, mixture {RoW}| market for waste plastic, mixture | Conseq, U	Plastic
Glass fibre {RER}| production | Conseq, U	G-fiber
Compansated CO2 emission in landfilling	CO2-fiber
Fiber in car panel, landfilling	F-Landfilling
Incineration fiber in the car panel	F-Incineration
Incineration PP in the car panel	PP-Incineration
Marginal land left as marginal, intensive grasslands	C-intensive
Marginal land left as marginal, rapeseed	C-rapeseed

Injection moulding {RER}| processing | Conseq, U	Moulding	Marginal land left as marginal, natural grassland	C-natural grass
Heat, district or industrial, other than natural gas {RoW}| market for | Conseq, U	Heat {RoW}	Marginal land left as marginal, woody moorlands	C-moorland
Electricity, high voltage {IN}| market group for electricity, high voltage | Conseq, U	Electricity H {IN}	Electricity, medium voltage {RoW}| market for | Conseq, U	Electricity M {RoW}
Electricity, high voltage {RoW}| market for | Conseq, U	Electricity H {RoW}	Electricity, medium voltage {RAS}| market group for | Conseq, U	Electricity M {RAS}
Electricity, high voltage {RAS}| market group for | Conseq, U	Electricity H {RAS}	Electricity, medium voltage {RER}| market group for | Conseq, U	Electricity M {RER}
		Electricity, low voltage {FR}| market for | Conseq, U	Electricity L {FR}

For each category, processes are divided into two groups according to their positive or negative impact scores, then a contribution analysis was conducted. Processes with scores summed up to represent at least 80% in their groups are selected(Fazio et al., 2018b), then the corresponding sub-processes and substances were identified under the same rules unless processes cannot be divided. It should be noticed that impact scores from processes and substances could be positive or negative, the contribution of one process or substance might exceed 100%, which means there is at least one another substance with scores reversely. To avoid misinterpretation, absolute values are adopted in contribution analysis.

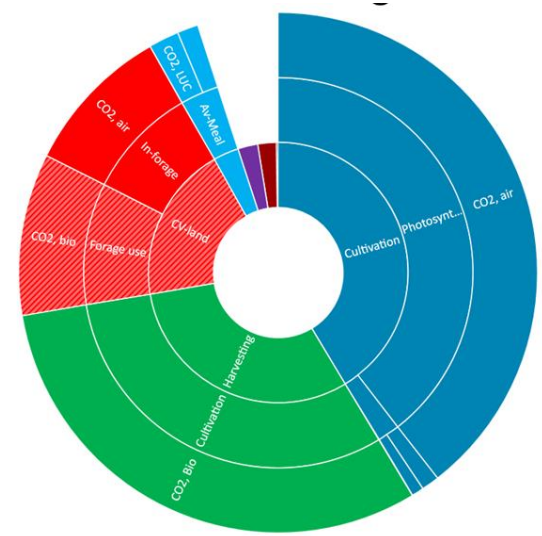

climate change

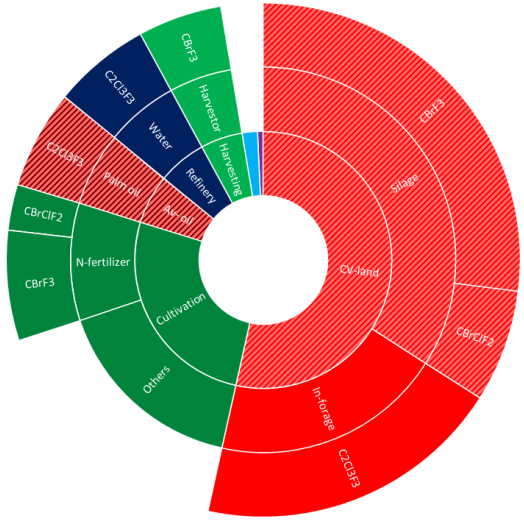

ozone depletion

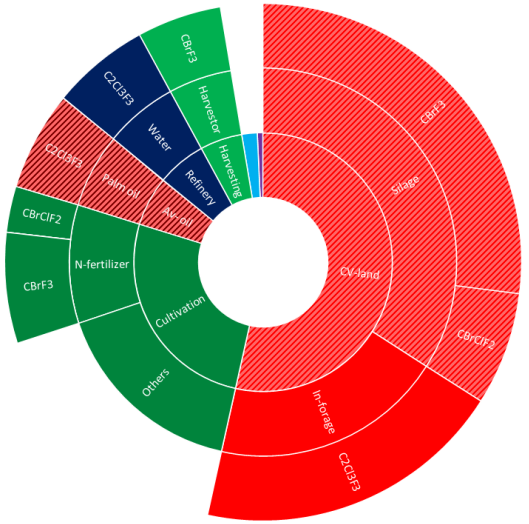

ionizing radiation

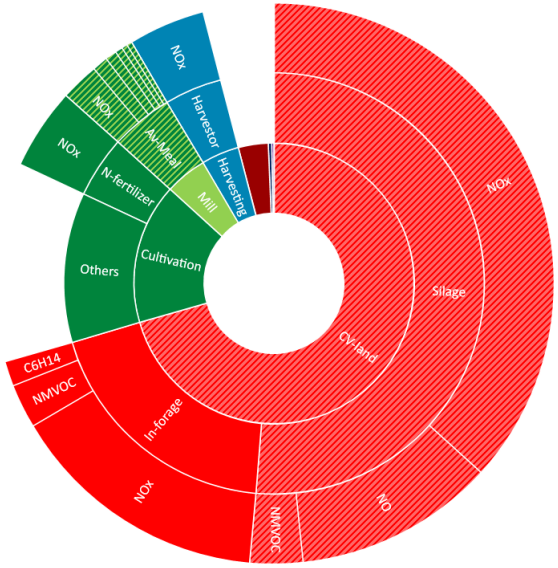

photochemical ozone formation

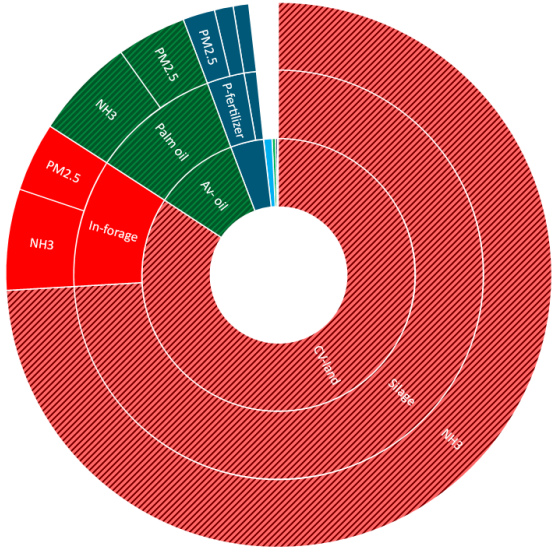

respiratory inorganics

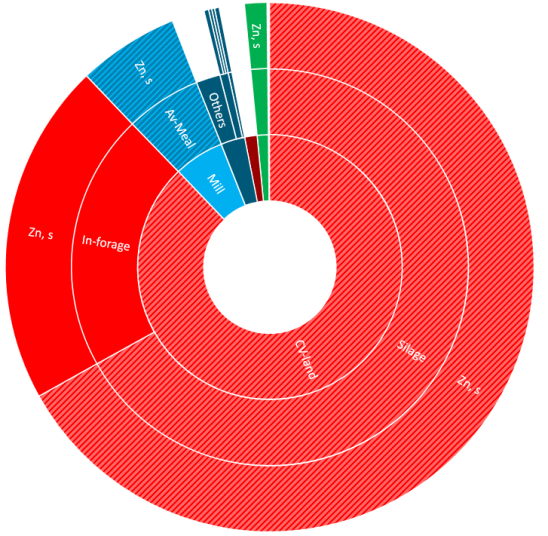

non-cancer human health effects

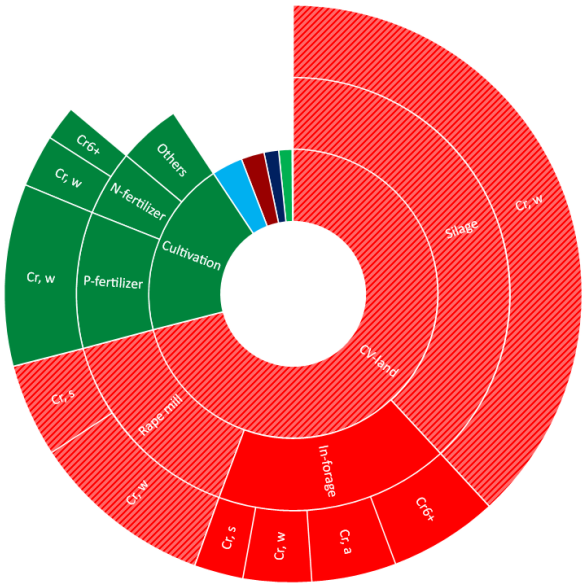

cancer human health

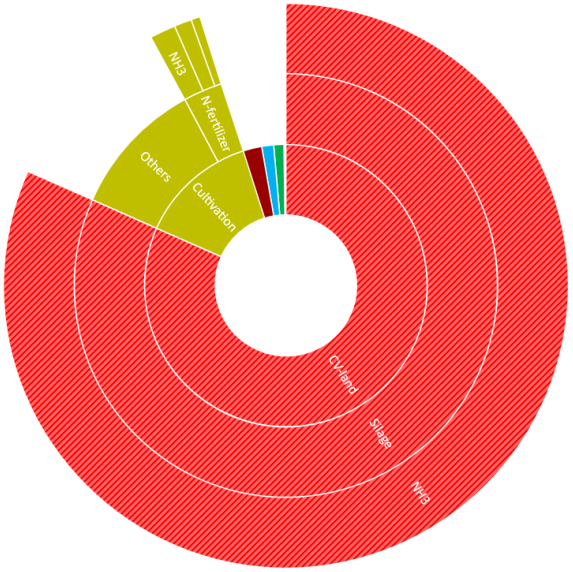

acidification terrestrial and freshwater

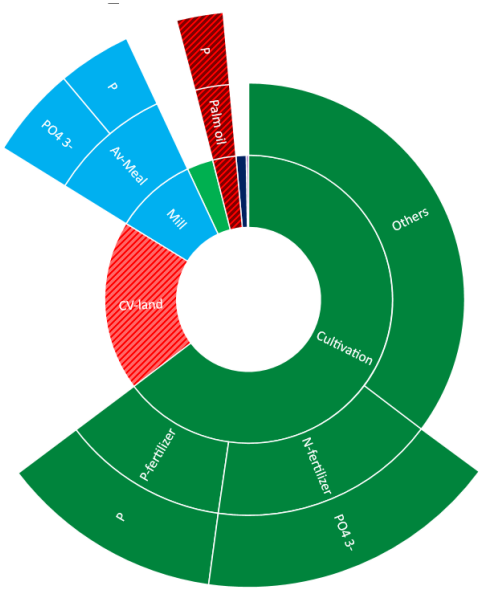

eutrophication freshwater

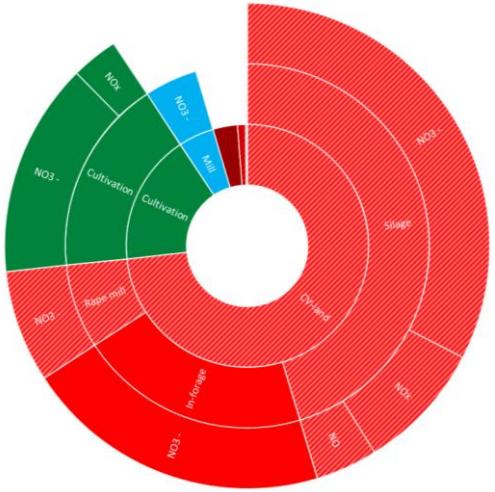

eutrophication marine

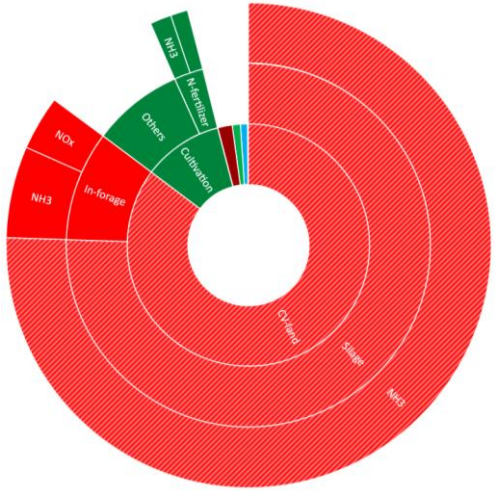

eutrophication terrestrial

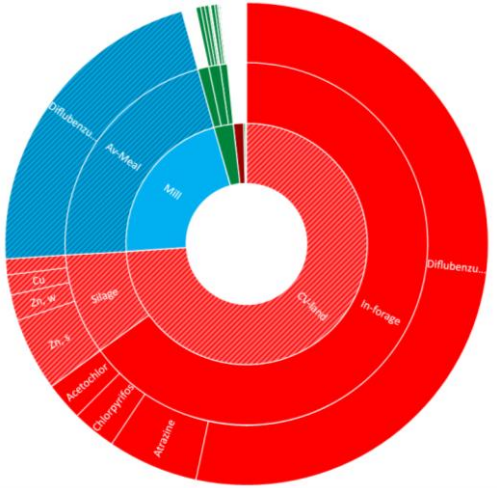

ecotoxicity freshwater

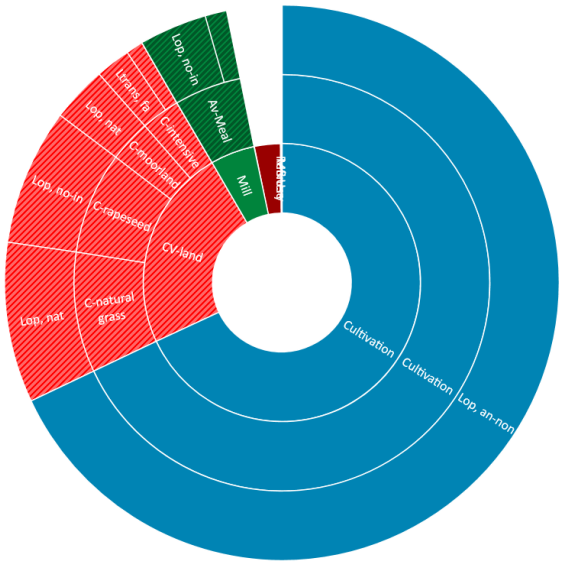

land use

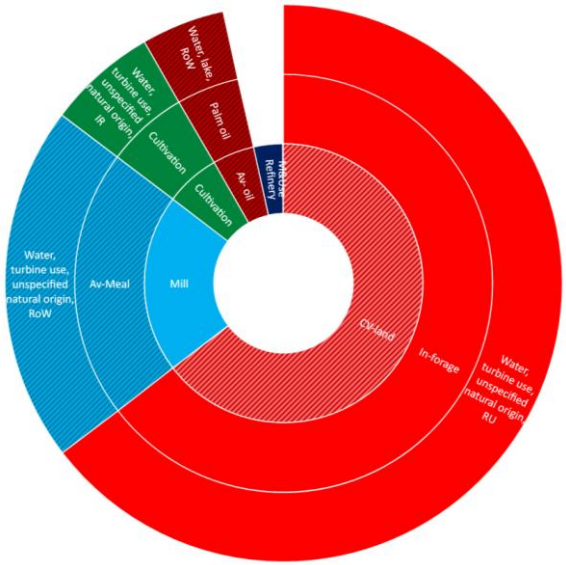

water scarcity

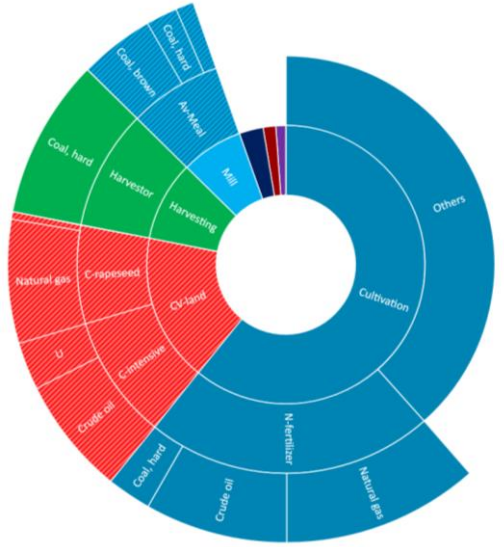

Resource use, energy carriers

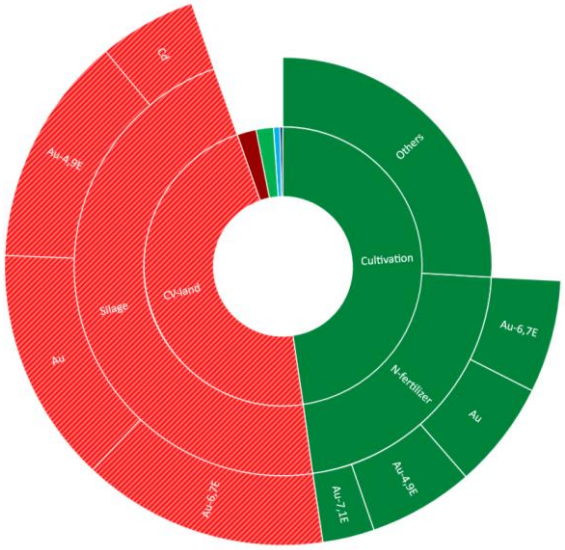

resource use, mineral and metals

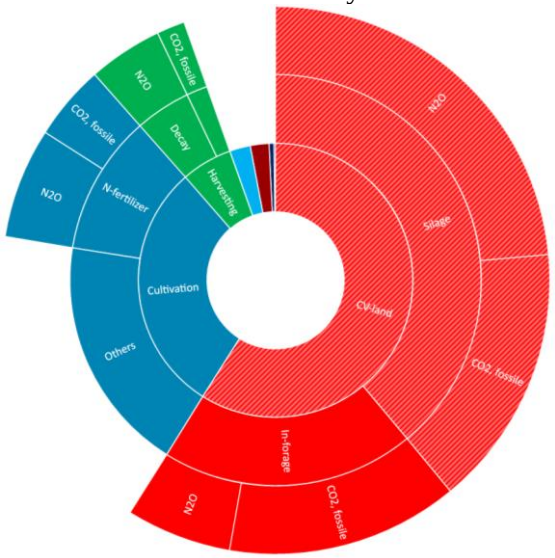

climate change - fossil

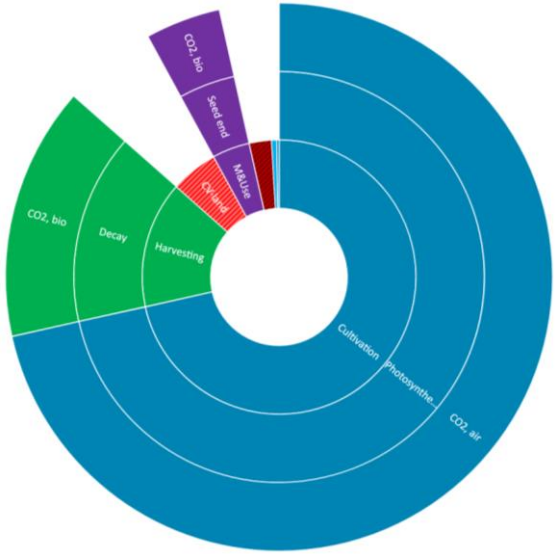

climate change - biogenic

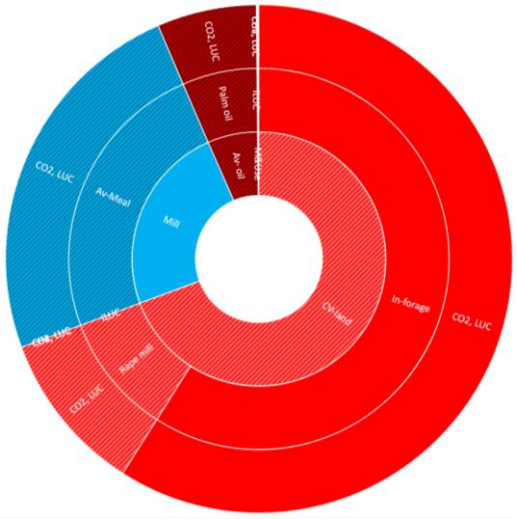

climate change - land use and transform

Fig. S4 LCA results of scenario SL

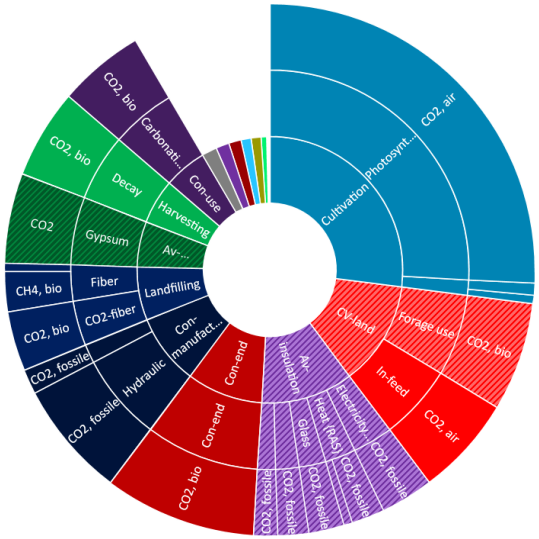

climate change

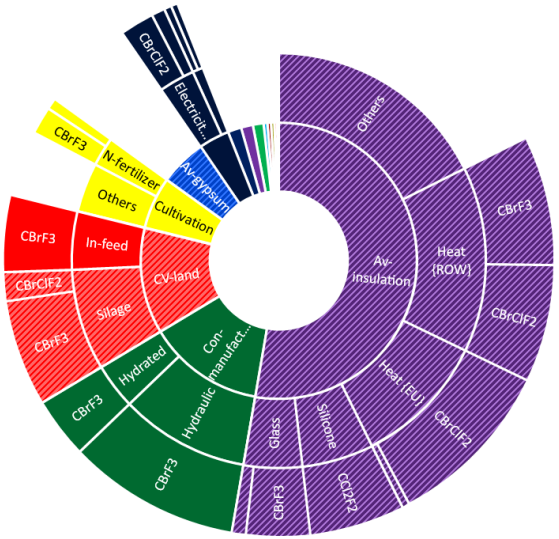

ozone depletion

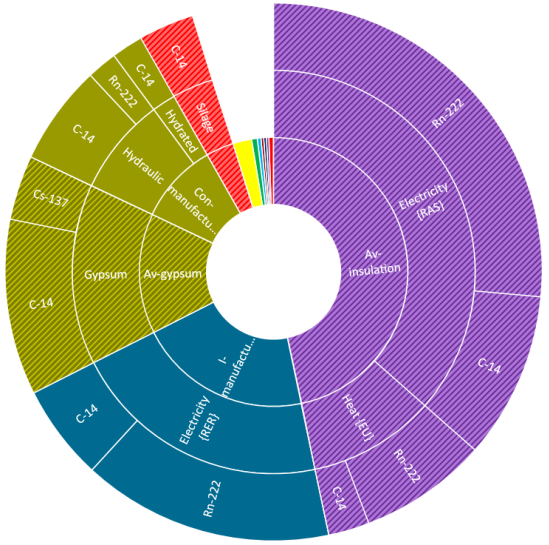

ionizing radiation

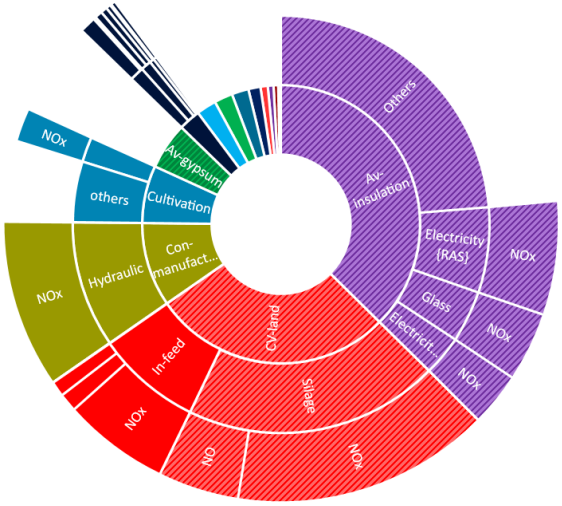

photochemical ozone formation

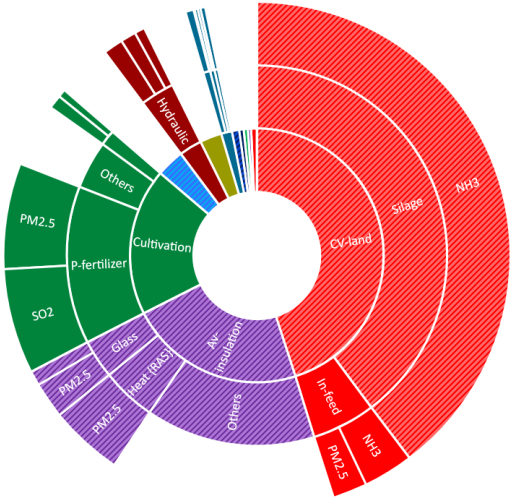

respiratory inorganics

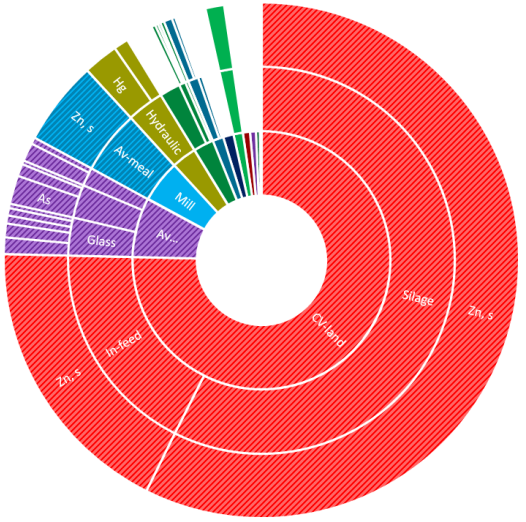

non-cancer human health effects

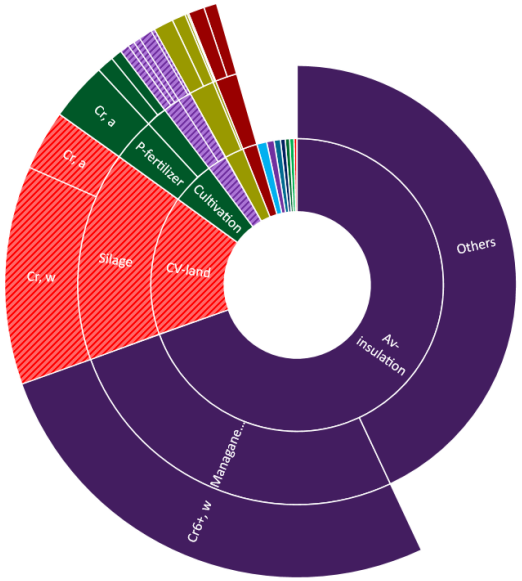

cancer human health

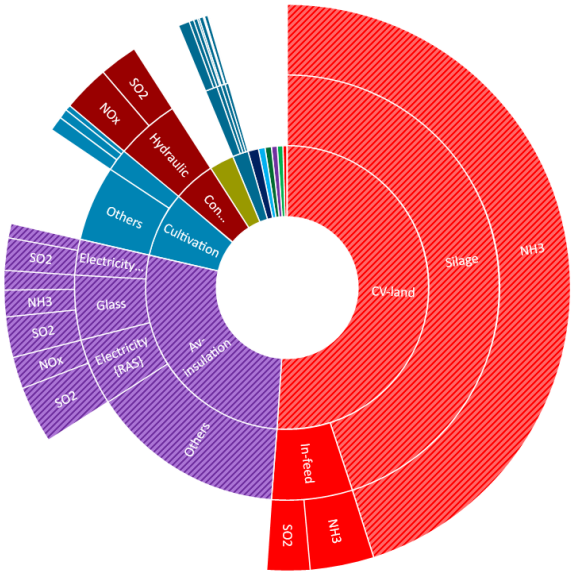

acidification terrestrial and freshwater

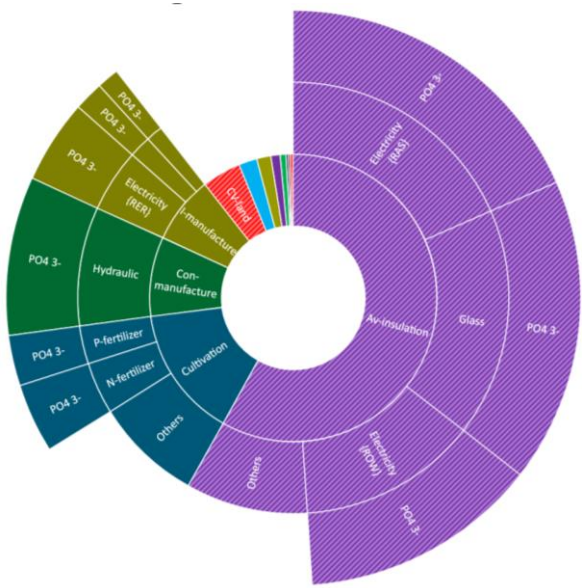

eutrophication freshwater

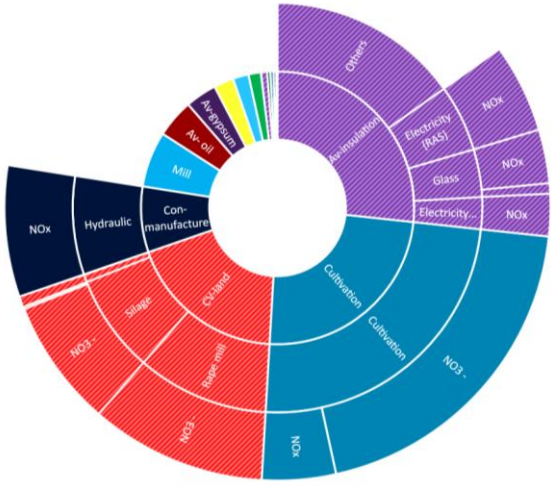

eutrophication marine

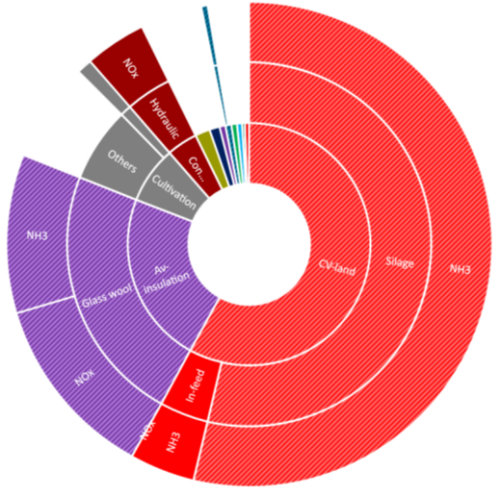

eutrophication terrestrial

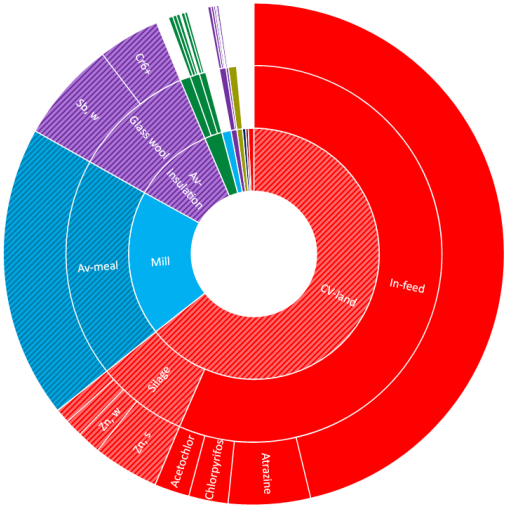

ecotoxicity freshwater

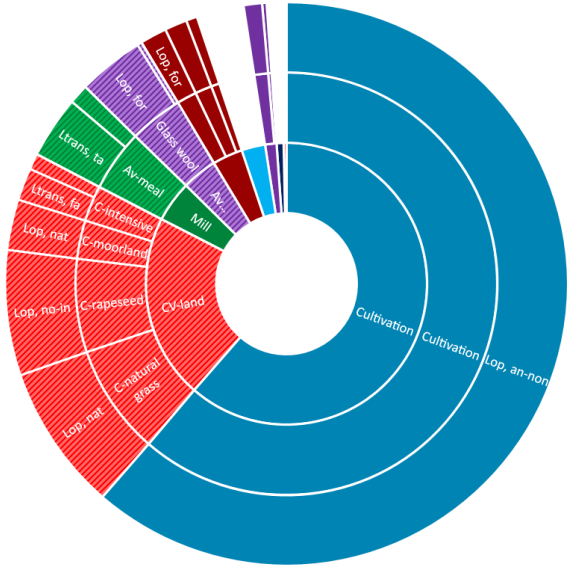

land use

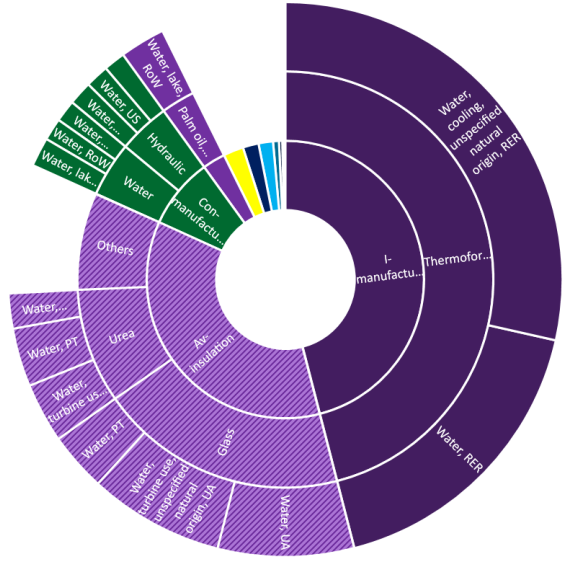

water scarcity

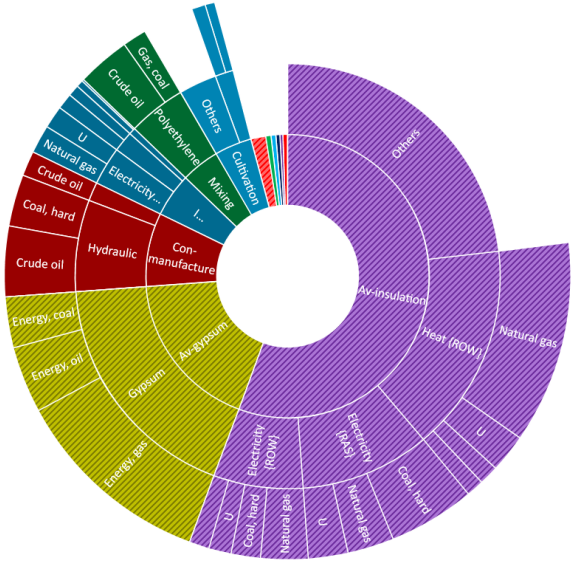

Resource use, energy carriers

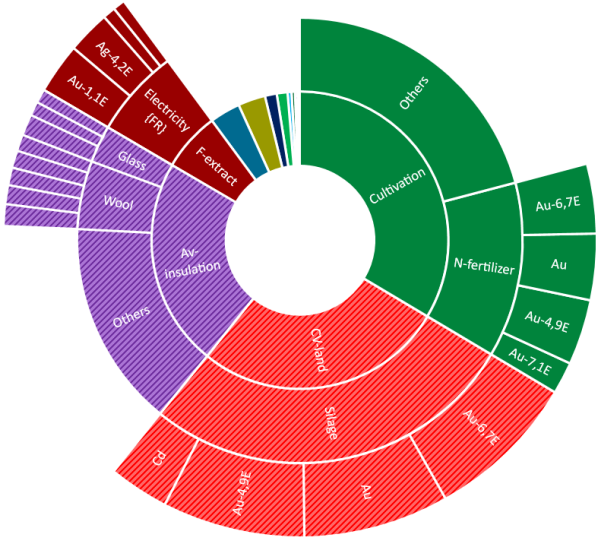

resource use, mineral and metals

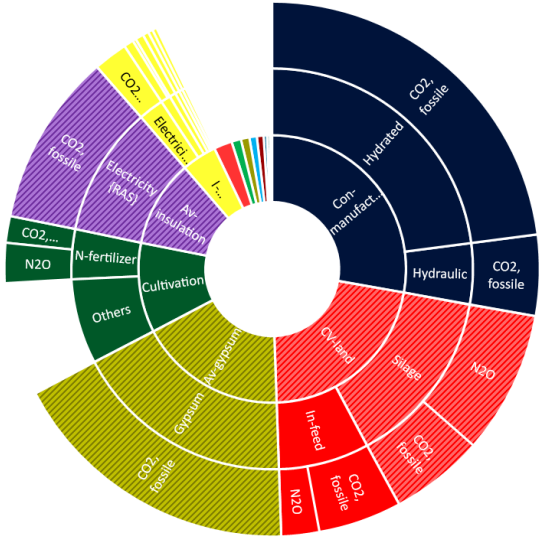

climate change - fossil

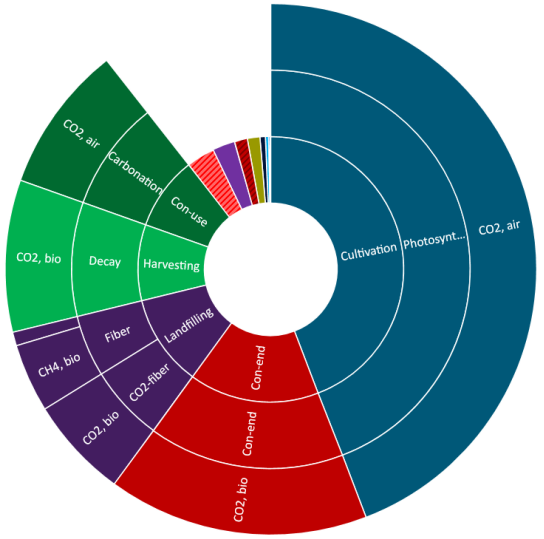

climate change - biogenic

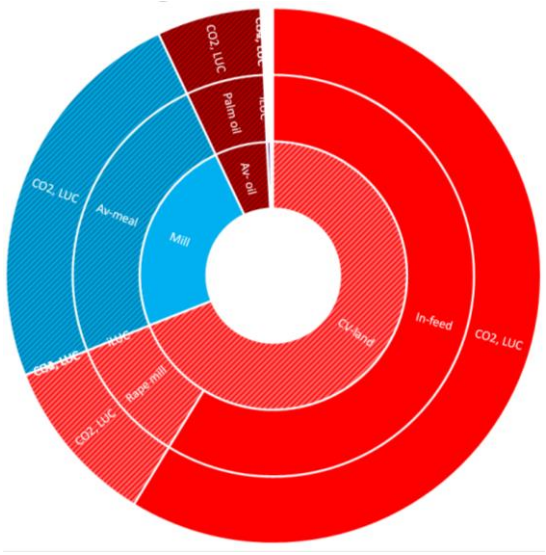

Fig. S5 LCA results of scenario IB

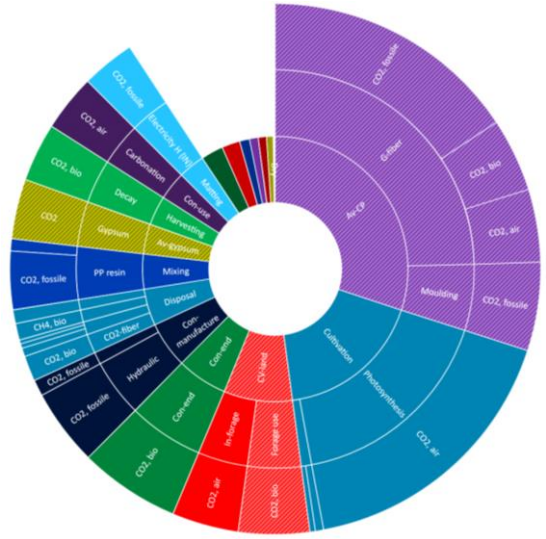

climate change

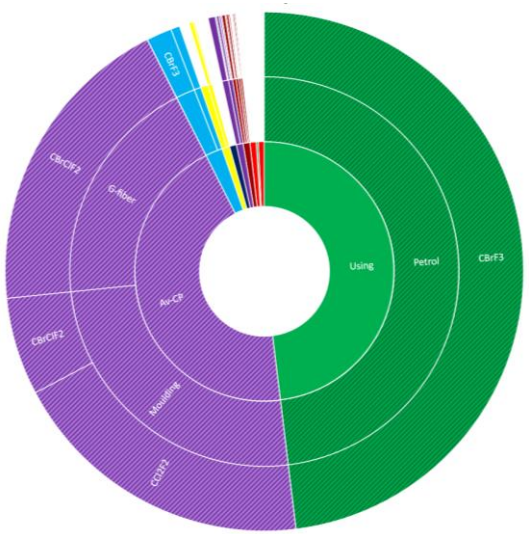

ozone depletion

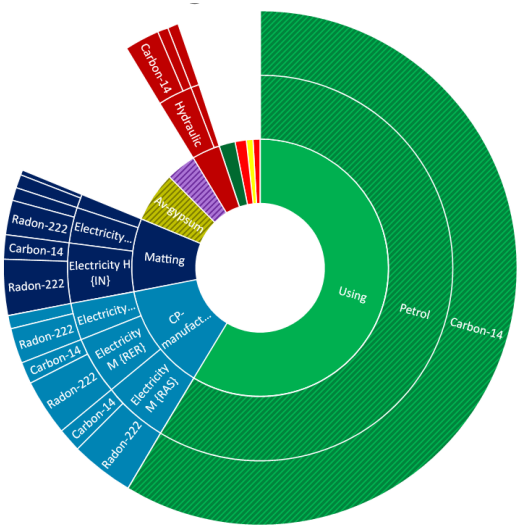

ionizing radiation

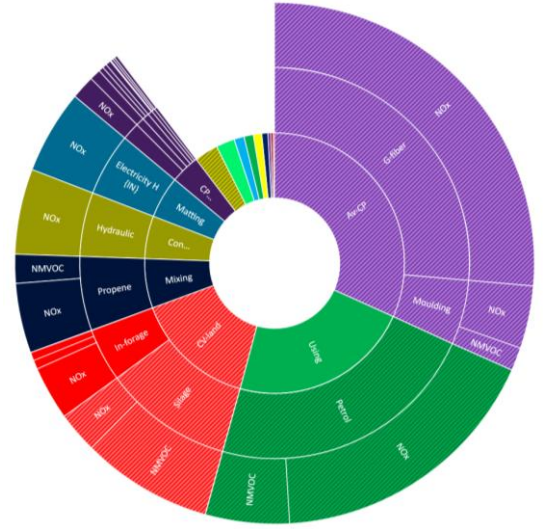

photochemical ozone formation

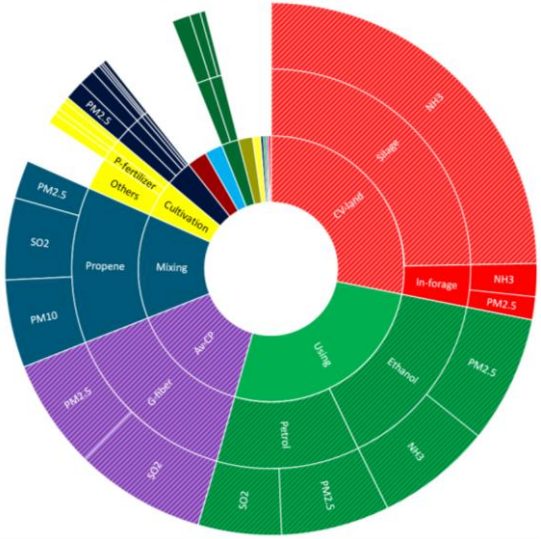

respiratory inorganics

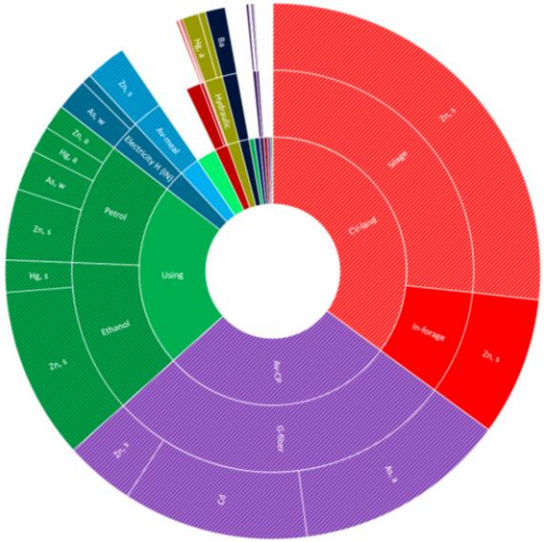

non-cancer human health effects

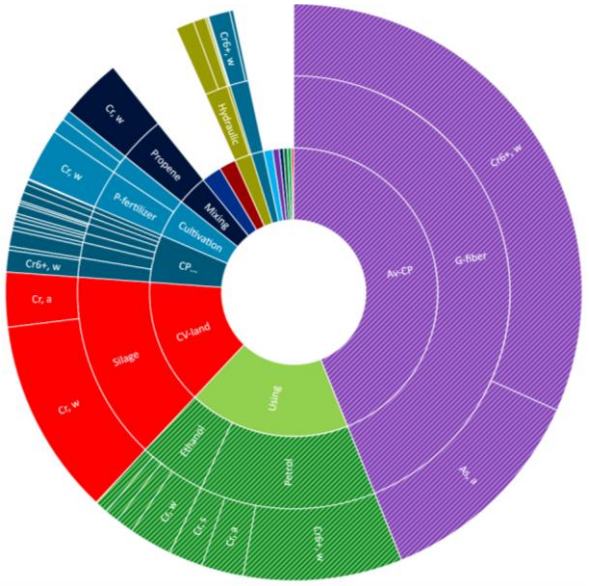

cancer human health

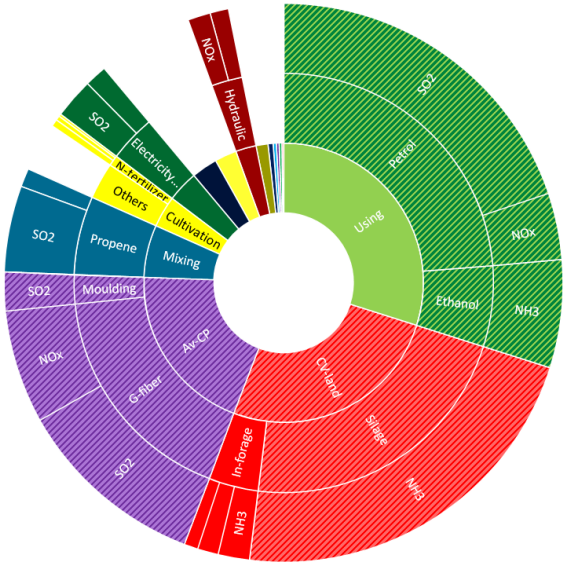

acidification terrestrial and freshwater

eutrophication freshwater

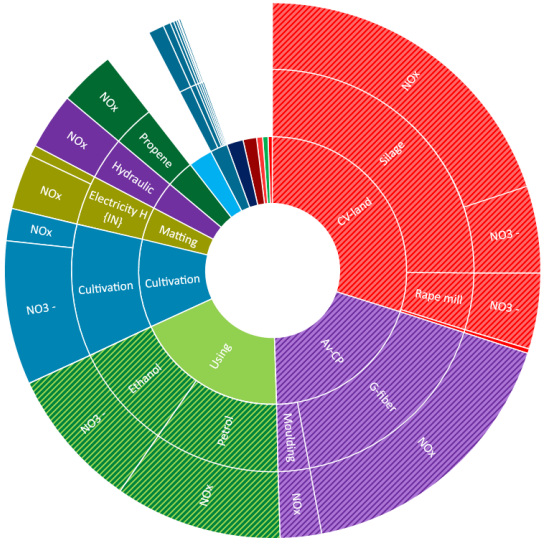

eutrophication marine

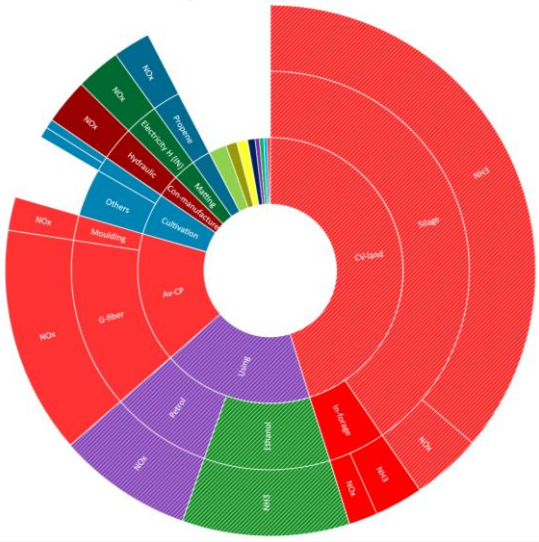

eutrophication terrestrial

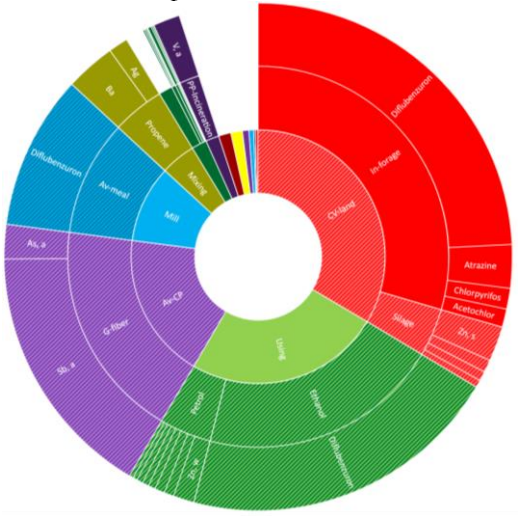

ecotoxicity freshwater

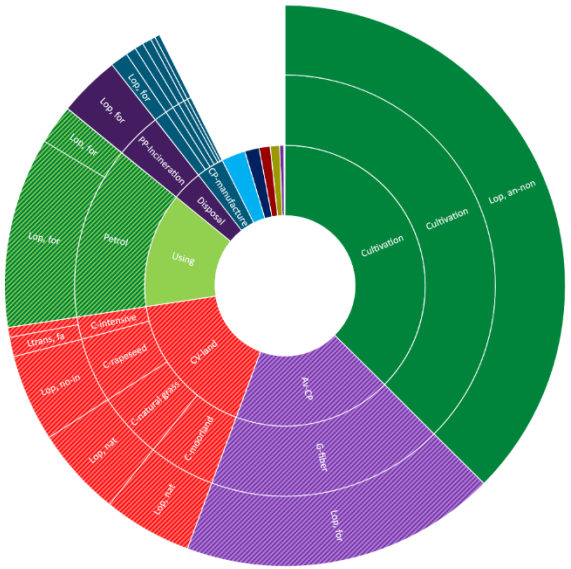

land use

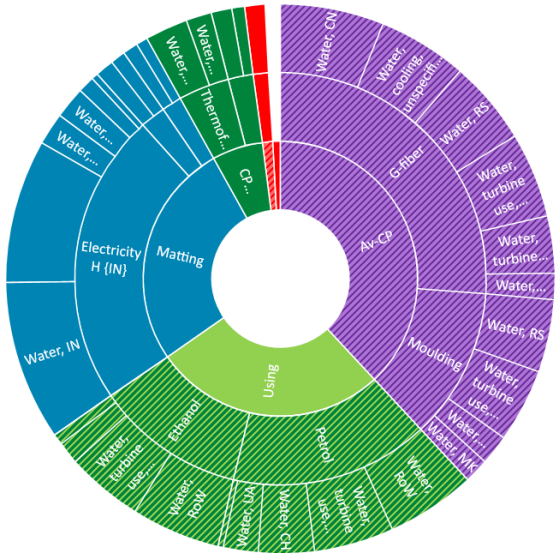

water scarcity

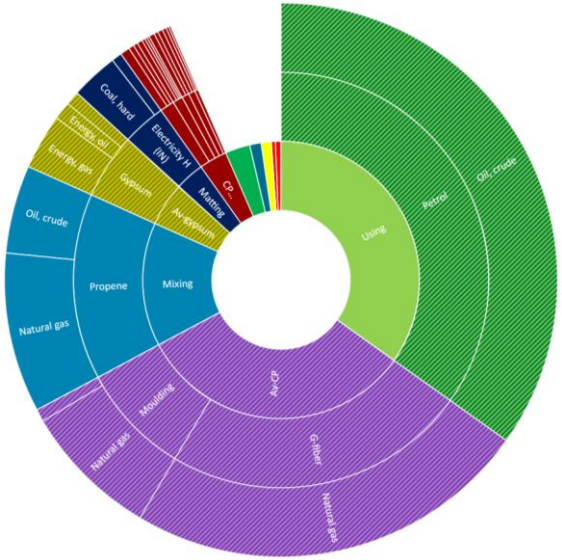

Resource use, energy carriers

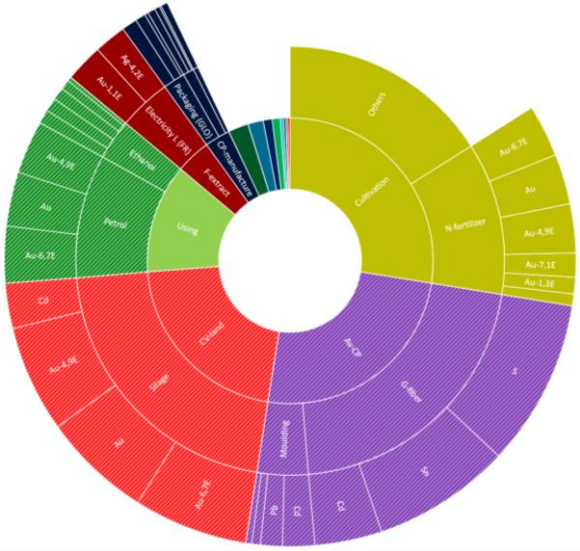

resource use, mineral and metals

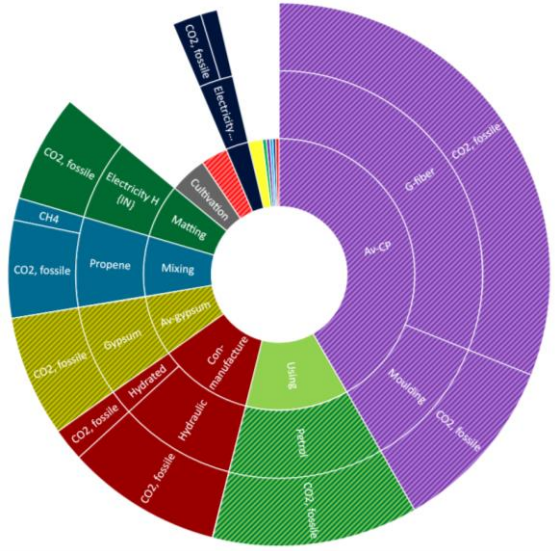

climate change - fossil

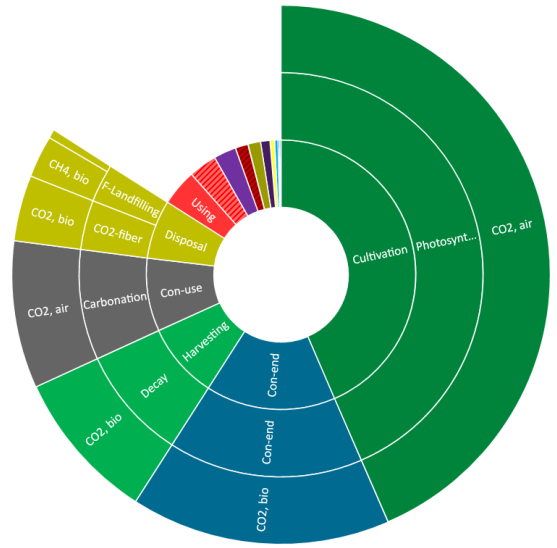

climate change - biogenic

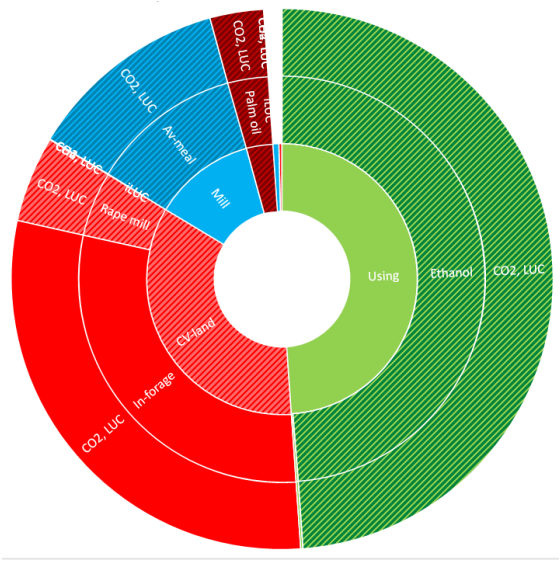

Fig. S6 LCA results of scenario CP

4 GHG considered in dynamic LCA

Table S27 GHG list considered in dynamic LCA.

Hemp-insulation	Hemp-car panel	Hemp, straw left	
Carbon dioxide	Carbon dioxide	Carbon dioxide	C
Carbon dioxide, biogenic	Carbon dioxide, biogenic	Carbon dioxide, biogenic	C
Carbon dioxide, fossil	Carbon dioxide, fossil	Carbon dioxide, fossil	C
Carbon dioxide, in air	Carbon dioxide, in air	Carbon dioxide, in air	C
Carbon dioxide, land transformation	Carbon dioxide, land transformation	Carbon dioxide, land transformation	C
Carbon dioxide, to soil or biomass stock	Carbon dioxide, to soil or biomass stock	Carbon dioxide, to soil or biomass stock	C s
Carbon monoxide	Carbon monoxide	Carbon monoxide	C
Carbon monoxide, biogenic	Carbon monoxide, biogenic	Carbon monoxide, biogenic	C
Carbon monoxide, fossil	Carbon monoxide, fossil	Carbon monoxide, fossil	C
Carbon monoxide, land transformation	Carbon monoxide, land transformation	Carbon monoxide, land transformation	C
Chloroform	Chloroform	Chloroform	I
Dinitrogen monoxide	Dinitrogen monoxide	Dinitrogen monoxide	I
Ethane, 1,1-difluoro-, HFC-152a	Ethane, 1,1-difluoro-, HFC-152a	Ethane, 1,1-difluoro-, HFC-152a	I
Ethane, 1,1,1-trichloro-, HCFC-140	Ethane, 1,1,1-trichloro-, HCFC-140	Ethane, 1,1,1-trichloro-, HCFC-140	I
Ethane, 1,1,1,2-tetrafluoro-, HFC-134a	Ethane, 1,1,1,2-tetrafluoro-, HFC-134a	Ethane, 1,1,1,2-tetrafluoro-, HFC-134a	I C
Ethane, 1,1,2-trichloro-1,2,2-trifluoro-, CFC-113	Ethane, 1,1,2-trichloro-1,2,2-trifluoro-, CFC-113	Ethane, 1,1,2-trichloro-1,2,2-trifluoro-, CFC-113	I
Ethane, 1,1,2-trifluoro-, HFC-143	Ethane, 1,2-dichloro-	Ethane, 1,2-dichloro-	I t
Ethane, 1,2-dichloro-	Ethane, 1,2-dichloro-1,1,2,2-tetrafluoro-, CFC-114	Ethane, 1,2-dichloro-1,1,2,2-tetrafluoro-, CFC-114	I I
Ethane, 1,2-dichloro-1,1,2,2-tetrafluoro-, CFC-114	Ethane, 2-chloro-1,1,1,2-tetrafluoro-, HCFC-124	Ethane, 2-chloro-1,1,1,2-tetrafluoro-, HCFC-124	I
Ethane, 2-chloro-1,1,1,2-tetrafluoro-, HCFC-124	Ethane, hexafluoro-, HFC-116	Ethane, hexafluoro-, HFC-116	I
Ethane, hexafluoro-, HFC-116	Methane	Methane	I
Ethane, pentafluoro-, HFC-125	Methane, biogenic	Methane, biogenic	I
Methane	Methane, bromo-, Halon 1001	Methane, bromo-, Halon 1001	I I
Methane, biogenic	Methane, bromochlorodifluoro-, Halon 1211	Methane, bromochlorodifluoro-, Halon 1211	I
Methane, bromo-, Halon 1001	Methane, bromotrifluoro-, Halon 1301	Methane, bromotrifluoro-, Halon 1301	I
Methane, bromochlorodifluoro-, Halon 1211	Methane, chlorodifluoro-, HCFC-22	Methane, chlorodifluoro-, HCFC-22	I
Methane, bromotrifluoro-, Halon 1301	Methane, chlorotrifluoro-, CFC-13	Methane, chlorotrifluoro-, CFC-13	I
Methane, chlorodifluoro-, HCFC-22	Methane, dichloro-, HCC-30	Methane, dichloro-, HCC-30	I
Methane, chlorotrifluoro-, CFC-13	Methane, dichlorodifluoro-, CFC-12	Methane, dichlorodifluoro-, CFC-12	I
Methane, dichloro-, HCC-30	Methane, dichlorofluoro-, HCFC-21	Methane, dichlorofluoro-, HCFC-21	I
Methane, dichlorodifluoro-, CFC-12	Methane, fossil	Methane, fossil	I
Methane, dichlorofluoro-, HCFC-21	Methane, land transformation	Methane, land transformation	I
Methane, difluoro-, HFC-32	Methane, monochloro-, R-40	Methane, monochloro-, R-40	I

Methane, fossil	Methane, tetrachloro-, CFC-10	Methane, tetrachloro-, CFC-10	
Methane, land transformation	Methane, tetrafluoro-, CFC-14	Methane, tetrafluoro-, CFC-14	
Methane, monochloro-, R-40	Methane, trichlorofluoro-, CFC-11	Methane, trichlorofluoro-, CFC-11	
Methane, tetrachloro-, CFC-10	Methane, trifluoro-, HFC-23	Methane, trifluoro-, HFC-23	
Methane, tetrafluoro-, CFC-14	Nitrogen fluoride	Nitrogen fluoride	
Methane, trichlorofluoro-, CFC-11	Sulfur hexafluoride	Sulfur hexafluoride	
Methane, trifluoro-, HFC-23			
Nitrogen fluoride			
Propane, 1,1,1,3,3-pentafluoro-, HFC-245fa			
Sulfur hexafluoride			

5 Uncertainty analysis

5.1 Method

The method called 'Global sensitivity analysis' is used in this study as it could reduce the temporal and spatial scale significantly compared to traditional uncertainty methods like Monte Carlo, while getting the same results(Bisinella et al., 2016).

First, 11, 12, and 14 parameters are selected for the three scenarios as these parameters influence a lot the climate change results according to the contribution analysis (appendix B). Then, each parameter is increased by 10% in a one-at-a-time (OAT) manner while keeping all other parameters fixed at their value. A sensitivity coefficient (SC) is calculated as follow to represent the sensitivity of each parameter:

$$SC_i = \frac{\Delta \text{score}}{\Delta \text{parameter}} \quad (3)$$

With Δscore and Δparameter are differences before and after OAT of climate change score and parameter respectively, i=1,…n tested parameter. The SC_i calculated here is then used for calculating the analytical variance of the corresponding parameter (V_i), which is shown below:

$$V_i = {SC_i}^2 \cdot V_{input}(i) \quad (4)$$

Where $V_{input}(i)$ is the variance of each parameter, based on their uncertainty and distribution (table A. s21-23). The default distribution of parameters is the normal distribution, while if value data points of parameters are too few or do not follow the normal distribution, but the potential mode is known, then triangle distribution is assumed(Lan et al., 2020). If we only have a maximum and minimum value, then uniform distribution is assumed. The analytical variance of climate change category (V) in each scenario is the sum of V_i, and CV is used to indicate how uncertain the initial climate change score is.

$$V = \sum_{i=1}^{n} V_i \quad (5)$$

$$CV = \sqrt{V} / \text{ initial score} \quad (6)$$

Parameters required to reach 90% of the analytical variance (V) are selected to represent the uncertainty of climate change. So far, the uncertainty of one impact is calculated, the same way is followed by other impacts.

5.2 Parameters in uncertainty analysis

Table S28 Test parameters in global sensitivity analysis, scenario SL

	P1 Hemp Yield	P2 Intensive grassland	P3 Induced maize	P4 Induced soybean	P5 Induced palm oil	P6 N-fertilizer use	P7 Avoided maize	P8 Avoided soybean	P9 Avoided palm oil	P10 Allocmetric of hemp (above residue+belowground)	P11 land expansion area (in iLUC)
μ	12.67	0.53	2946.39	589.25	41.71	106.73	146.80	239.12	25.26	12.06	0.57
Unit	t	ha	kg	kg	kg	kg	kg	t	kg	t ha^{-1}	ha
Uncertainty %	10%	10%	10%	10%	10%	10%	10%	10%	10%	10%	10%
Δ	-1.27	-0.05	-294.64	-58.92	-4.17	-10.67	-14.68	-23.91	-2.53	-1.21	-0.06
Distribution	Normal	Triangle	Normal	Normal	Normal	Normal	Normal	Normal	Normal	Triangle	Triangle
σ^2	0.4011	0.0002	21703.0727	868.0278	4.3488	28.4792	53.8765	142.9443	1.5948	0.0808	0.0002

Table S29 Test parameters in global sensitivity analysis, scenario IB

	P1 Hemp Yield	P2 Intensive grassland	P3 Induced maize	P4 Induced soybean	P5 Induced palm oil	P6 N-fertilizer use	P7 Amount of hydrated lime	P8 landfilling	P9 Density of gypsum	P10 Allocmetric of hemp (above residue+belowground)	P11 CO_2 by lime	P12 Density of avoided insulation
μ	12.67	0.53	2946.39	589.25	41.71	106.73	7.56	0.16	800.00	3.70	4.67	40.00
Unit	t	ha	kg	kg	kg	kg	t	%	kg m^{-3}	t	t	kg m^{-3}
Uncertainty %	10%	10%	10%	10%	10%	10%	10%	10%	10%	10%	10%	10%
Δ	-1.27	-0.05	-294.64	-58.92	-4.17	-10.67	-0.76	-0.02	-80.00	-0.37	-0.47	-4.00
Distribution	Normal	Triangle	Normal	Normal	Normal	Normal	Normal	Triangle	Triangle	Triangle	Triangle	Normal
σ2	0.4011	0.0002	21703.0727	868.0278	4.3488	28.4792	0.1430	1.40E-05	355.5556	0.0076	0.0121	4.0000

Table S30 Test parameters in global sensitivity analysis. scenario CP

	P1 Hemp Yield	P2 Intensive grassland	P3 Induced maize	P4 Induced soybean	P5 Induced palm oil	P6 N-fertilizer use	P7 Amount of hydrated lime	P8 Amount of car panel go into incineration	P9 Density of gypsum	P10 Allocmetric of hemp (above residue+belowground)
μ	12.67	0.53	2946.39	589.25	41.71	106.73	146.80	239.12	25.26	12.06
Unit	t	ha	kg	kg	kg	kg	kg	t	kg m^{-3}	t ha^{-1}
Uncertainty %	10%	10%	10%	10%	10%	10%	10%	10%	10%	10%
Δ	-1.27	-0.05	-294.64	-58.92	-4.17	-10.67	-14.68	-23.91	-2.53	-1.21
Distribution	Normal	Triangle	Normal	Normal	Normal	Normal	Normal	Normal	Normal	Triangle
σ^2	0.4011	0.0002	21703.0727	868.0278	4.3488	28.4792	0.1430	0.0017	355.5556	0.0076

…continued table S30 Test parameters in global sensitivity analysis. scenario CP

	P11 CO_2 by lime	P12 Electricity consumption in matting	P13 PP amount in hemp car panel	P14 Amount of glass in avoided glass car panel
μ	0.57	3864.77	3.35	6.94
Unit	ha	kwh	t	t
Uncertainty %	10%	10%	10%	10%
Δ	-0.06	-386.48	-0.34	-0.69
Distribution	Triangle	Triangle	Normal	Triangle
σ^2	0.0121	8298.0320	0.0281	0.0268

5.3 Uncertainty analysis results

Table S31-S33 show the uncertainty analysis results of three scenarios respectively, the representiveness means the sum of contribution of single-parameter to impact categories. The threshold of representiveness is 90%, which means parameters that are necessary to consist this representiveness have an important influence in this category, could represent the uncertainty of this impact category (CV).

Parameters are shown in codenames here (P1, P2, P3…) due to the space, the detail of parameters (e.g. name) are illustrated in the footnote, consistent with table A. S28-30.

Table S31 Uncertainty analysis of scenario SL

Impact category*	P1	P2	P3	P4	P5	P6	P7	P8	P9	P10	P11	Representiveness	Uncertainty
Climate change	42%	1%	7%	30%	0%	14%	0%	5%	0%	1%	0%	92%	33.76%
Ozone depletion	0%	2%	47%	1%	0%	49%	0%	0%	0%	0%	0%	96%	11.05%
Ionising radiation, HH	1%	28%	15%	15%	0%	37%	0%	2%	0%	0%	0%	96%	-12.20%
Photochemical ozone formation, HH	10%	13%	34%	23%	0%	12%	0%	4%	0%	0%	4%	92%	-7.15%
Respiratory inorganics	4%	80%	8%	0%	0%	7%	0%	0%	0%	0%	0%	95%	-2.71%
Non-cancer human health effects	3%	86%	1%	9%	0%	0%	0%	1%	0%	0%	0%	94%	-2.60%
Cancer human health effects	6%	2%	54%	14%	0%	21%	0%	2%	0%	0%	0%	95%	-4.44%
Acidification terrestrial and freshwater	1%	83%	10%	0%	0%	6%	0%	0%	0%	0%	0%	93%	-2.68%
Eutrophication freshwater	3%	2%	78%	3%	0%	12%	0%	1%	0%	0%	0%	90%	5.00%
Eutrophication marine	15%	9%	50%	20%	0%	1%	0%	3%	0%	0%	2%	94%	-4.77%
Eutrophication terrestrial	1%	88%	5%	0%	0%	5%	0%	0%	0%	0%	0%	94%	-2.54%
Ecotoxicity freshwater	13%	16%	6%	57%	0%	0%	0%	9%	0%	0%	0%	94%	9.54%
Land use	16%	9%	50%	22%	0%	0%	0%	4%	0%	0%	0%	96%	2.66%
Water scarcity	0%	16%	83%	0%	0%	0%	0%	0%	0%	0%	0%	99%	5.97%
Resource use, energy carriers	0%	0%	64%	5%	0%	29%	0%	1%	0%	0%	0%	93%	7.50%
Resource use, mineral and metals	0%	22%	3%	0%	0%	75%	0%	0%	0%	0%	1%	96%	-44.99%

* : Parameters in orange background could represent the uncertainty of impact category in row.

P1 Hemp Yield; P2 Intensive grassland; P3 Induced maize; P4 Induced soybean; P5 Induced palm oi; P6 N-fertilizer use; P7 Avoided maize; P8 Avoided soybean; P9 Avoided palm oil; P10 Allocmetric of hemp (above residue+belowground); P11 land expansion area (in iLUC)

Table S32 Uncertainty analysis of scenario IB

Impact category*	P1	P2	P3	P4	P5	P6	P7	P8	P9	P10	P11	P12	Representiveness	Uncertainty
Climate change	52%	0%	1%	3%	0%	1%	2%	0%	1%	0%	1%	39%	90%	-10.22%
Ozone depletion	30%	0%	0%	0%	0%	0%	0%	0%	0%	0%	0%	69%	99%	-9.37%
Ionising radiation, HH	2%	1%	0%	0%	0%	1%	0%	0%	18%	0%	0%	77%	95%	-26.02%
Photochemical ozone formation, HH	29%	1%	1%	1%	0%	0%	1%	0%	0%	0%	0%	67%	96%	-7.88%
Respiratory inorganics	34%	22%	2%	0%	0%	2%	0%	0%	0%	0%	0%	40%	96%	-3.45%
Non-cancer human health effects	1%	81%	1%	8%	0%	0%	1%	0%	0%	0%	0%	8%	97%	-2.56%
Cancer human health effects	42%	0%	0%	0%	0%	0%	0%	0%	0%	0%	0%	58%	100%	-6.93%
Acidification terrestrial and freshwater	27%	23%	3%	0%	0%	2%	0%	0%	0%	0%	0%	45%	95%	-3.39%
Eutrophication freshwater	30%	0%	4%	0%	0%	1%	1%	0%	0%	0%	0%	64%	94%	-17.06%
Eutrophication marine	33%	4%	19%	7%	0%	0%	1%	0%	0%	0%	0%	36%	95%	-5.02%
Eutrophication terrestrial	23%	38%	2%	0%	0%	2%	0%	0%	0%	0%	0%	35%	95%	-2.90%
Ecotoxicity freshwater	30%	12%	4%	45%	0%	0%	0%	0%	0%	0%	0%	9%	96%	22.30%
Land use	8%	9%	53%	23%	0%	0%	0%	0%	0%	0%	0%	7%	92%	2.45%
Water scarcity	0%	14%	73%	0%	0%	0%	0%	0%	0%	0%	0%	13%	100%	6.20%
Resource use, energy carriers	45%	0%	0%	0%	0%	0%	0%	0%	2%	0%	0%	52%	97%	-7.81%
Resource use, mineral and metals	15%	11%	1%	0%	0%	38%	0%	0%	0%	0%	0%	35%	99%	-11.30%

* : Parameters in orange background could represent the uncertainty of impact category in row.

P1 Hemp Yield; P2 Intensive grassland; P3 Induced maize; P4 Induced soybean; P5 Induced palm oil; P6 N-fertilizer use; P7 Amount of hydrated lime; P8 landfilling;

P9 Density of gypsum; P10 Allocmetric of hemp (above residue+belowground); P11 CO_2 absorbed by lime; P12 Density of avoided insulation.

Table S33 Uncertainty analysis of scenario CP

Impact category*	P1	P2	P3	P4	P5	P6	P7	P8	P9	P10	P11	P12	P13	P14	Representiveness	Uncertainty
Climate change	24%	0%	0%	1%	0%	0%	1%	0%	0%	0%	0%	0%	17%	56%	98%	-13.07%
Ozone depletion	19%	0%	0%	0%	0%	0%	0%	0%	0%	0%	0%	0%	26%	55%	100%	-11.33%
Ionising radiation, HH	5%	0%	0%	0%	0%	0%	0%	0%	0%	0%	0%	0%	44%	52%	95%	-22.85%
Photochemical ozone formation, HH	11%	0%	0%	0%	0%	0%	0%	0%	0%	0%	0%	0%	28%	62%	100%	-14.56%
Respiratory inorganics	4%	1%	0%	0%	0%	0%	0%	0%	0%	0%	0%	0%	42%	53%	95%	-13.21%
Non-cancer human health effects	12%	3%	0%	0%	0%	0%	0%	0%	0%	0%	0%	0%	23%	61%	96%	-6.62%
Cancer human health effects	19%	0%	0%	0%	0%	0%	0%	0%	0%	0%	0%	0%	16%	64%	100%	-10.42%
Acidification terrestrial and freshwater	8%	1%	0%	0%	0%	0%	0%	0%	0%	0%	0%	0%	34%	57%	91%	-11.39%
Eutrophication freshwater	6%	0%	0%	0%	0%	0%	0%	0%	0%	0%	0%	0%	31%	62%	93%	-27.14%
Eutrophication marine	12%	0%	1%	0%	0%	0%	0%	0%	0%	0%	0%	0%	29%	58%	99%	-11.49%
Eutrophication terrestrial	10%	4%	0%	0%	0%	0%	0%	0%	0%	0%	0%	0%	29%	57%	96%	-7.06%
Ecotoxicity freshwater	5%	11%	4%	41%	0%	0%	0%	0%	0%	0%	0%	0%	28%	11%	91%	9.58%
Land use	0%	1%	5%	2%	0%	0%	0%	0%	0%	0%	0%	0%	66%	25%	91%	6.23%
Water scarcity	1%	2%	10%	0%	0%	0%	0%	0%	0%	0%	0%	0%	40%	48%	97%	22.25%
Resource use, energy carriers	9%	0%	0%	0%	0%	0%	0%	0%	0%	0%	0%	0%	36%	55%	91%	-16.93%
Resource use, mineral and metals	19%	12%	1%	0%	0%	40%	0%	0%	0%	0%	0%	0%	1%	27%	98%	-10.31%

* : Parameters in orange background could represent the uncertainty of impact category in row.

P1 Hemp Yield; P2 Intensive grassland; P3 Induced maize; P4 Induced soybean; P5 Induced palm oil; P6 N-fertilizer use; P7 Amount of hydrated lime; P8 Amount of car panel go into incineration; P9 Density of gypsum; P10 Allocmetric of hemp (above residue+belowground); P11 CO_2 absorbed by lime; P12 Electricity consumption in matting; P13 PP amount in hemp car panel; P14 Amount of glass in avoided glass car panel.

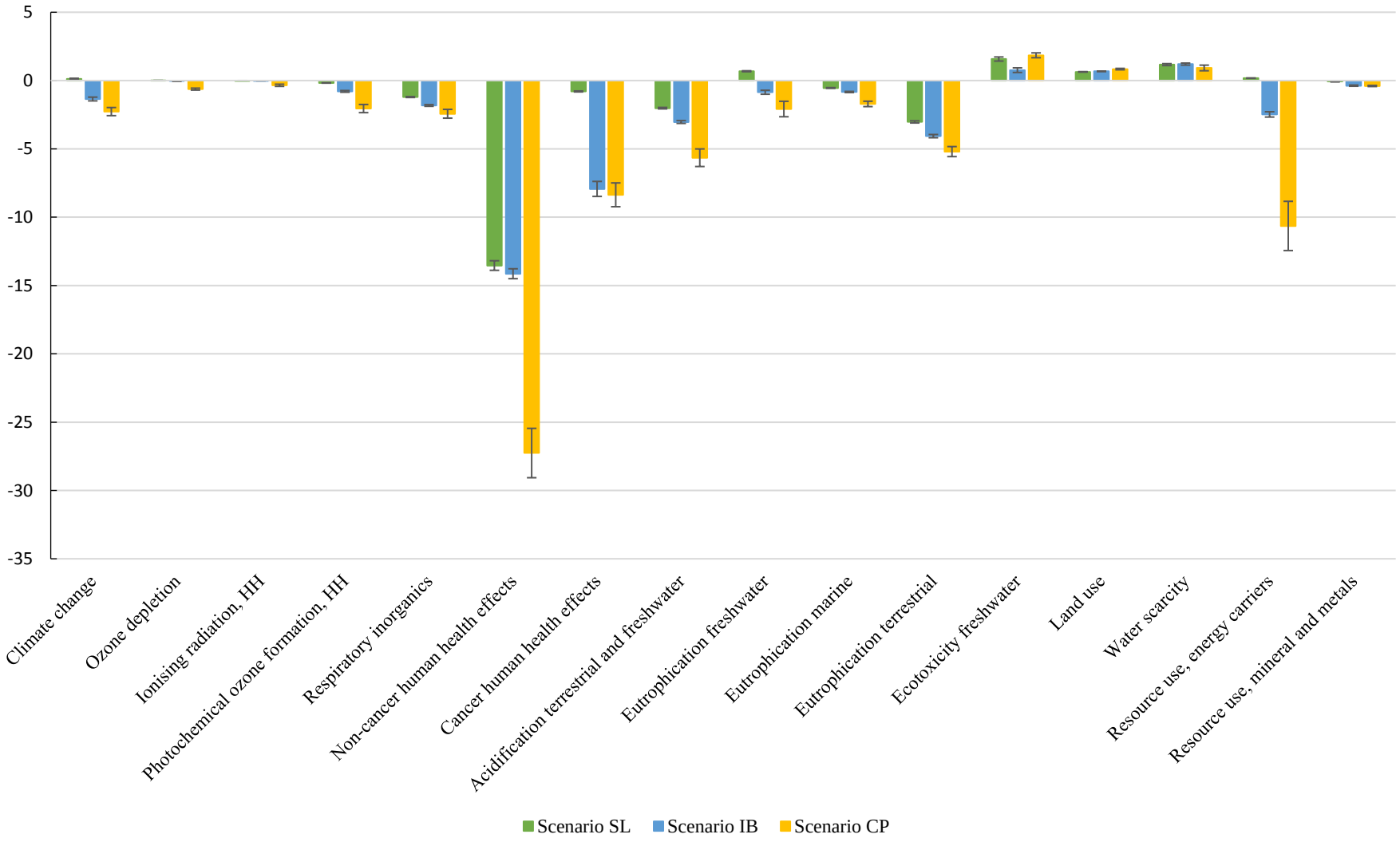

Fig. S7 Uncertainty analysis of all environmental impacts, in normalized impacts scores.

Reference

Akampumuza, O., Wambua, P.M., Ahmed, A., Li, W., Qin, X.H., 2017. Review of the applications of biocomposites in the automotive industry. Polym. Compos. 38, 2553–2569. https://doi.org/10.1002/pc.23847

Aladić, K., Jarni, K., Barbir, T., Vidović, S., Vladić, J., Bilić, M., Jokić, S., 2015. Supercritical CO2 extraction of hemp (Cannabis sativa L.) seed oil. Ind. Crops Prod. 76, 472–478. https://doi.org/10.1016/j.indcrop.2015.07.016

Amaducci, S., Scordia, D., Liu, F.H., Zhang, Q., Guo, H., Testa, G., Cosentino, S.L., 2015. Key cultivation techniques for hemp in Europe and China. Ind. Crops Prod. 68, 2–16. https://doi.org/10.1016/j.indcrop.2014.06.041

Andersson, K., Björhagen, I., 2018. Material Choices for a Fossil-Free Preschool - An Interview Study on How Materials are Chosen, and a Life Cycle Assessment of Hemp Insulation. CHALMERS UNIVERSITY OF TECHNOLOGY.

Bisinella, V., Conradsen, K., Christensen, T.H., Astrup, T.F., 2016. A global approach for sparse representation of uncertainty in Life Cycle Assessments of waste management systems. Int. J. Life Cycle Assess. 21, 378–394. https://doi.org/10.1007/s11367-015-1014-4

Bleuze, L., Chabbert, B., Lashermes, G., Recous, S., 2020. Hemp harvest time impacts on the dynamics of microbial colonization and hemp stems degradation during dew retting. Ind. Crops Prod. 145, 112122. https://doi.org/10.1016/j.indcrop.2020.112122

Bleuze, L., Lashermes, G., Alavoine, G., Recous, S., Chabbert, B., 2018. Tracking the dynamics of hemp dew retting under controlled environmental conditions. Ind. Crops Prod. 123, 55–63. https://doi.org/10.1016/j.indcrop.2018.06.054

Boland, C.S., De Kleine, R., Keoleian, G.A., Lee, E.C., Kim, H.C., Wallington, T.J., 2016. Life Cycle Impacts of Natural Fiber Composites for Automotive Applications: Effects of Renewable Energy Content and Lightweighting. J. Ind. Ecol. 20, 179–189. https://doi.org/10.1111/jiec.12286

Brzyski, P., Barnat-Hunek, D., Suchorab, Z., Lagód, G., 2017. Composite materials based on hemp and flax for low-energy buildings. Materials (Basel). 10, 510. https://doi.org/10.3390/ma10050510

Clivot, H., Mouny, J.C., Duparque, A., Dinh, J.L., Denoroy, P., Houot, S., Vertès, F., Trochard, R., Bouthier, A., Sagot, S., Mary, B., 2019. Modeling soil organic carbon evolution in long-term arable experiments with AMG model. Environ. Model. Softw. 118, 99–113. https://doi.org/10.1016/j.envsoft.2019.04.004

Conen, F., Zimmermann, M., Leifeld, J., Seth, B., Alewell, C., 2008. Relative stability of soil carbon revealed by shifts in δ 15 N and C: N ratio. Biogeosciences 5, 123–128.

COWI A/S and Utrecht University, 2019. Environmental impact assessments of innovative bio-based product - Publications Office of the EU, European Commission. https://doi.org/10.2777/251887

Da Porto, C., Decorti, D., Natolino, A., 2015. Potential Oil Yield, Fatty Acid Composition, and Oxidation Stability of the Hempseed Oil from Four Cannabis sativa L. Cultivars. J. Diet. Suppl. 12, 1–10. https://doi.org/10.3109/19390211.2014.887601

de Bruijn, P.B., Jeppsson, K.H., Sandin, K., Nilsson, C., 2009. Mechanical properties of lime-hemp concrete containing shives and fibres. Biosyst. Eng. 103, 474–479. https://doi.org/10.1016/j.biosystemseng.2009.02.005

Decau, M.L., Simon, J.C., Jacquet, A., 2004. Nitrate Leaching under Grassland as Affected by Mineral Nitrogen Fertilization and Cattle Urine. J. Environ. Qual. 33, 637–644. https://doi.org/10.2134/jeq2004.6370

Delmas, M., Saby, N., Arrouays, D., Dupas, R., Lemercier, B., Pellerin, S., Gascuel-Odoux, C., 2015. Explaining and mapping total phosphorus content in French topsoils. Soil Use Manag. 31, 259–269. https://doi.org/10.1111/sum.12192

Deng, Y., 2014. Life cycle assessment of biobased fibre-reinforced polymer composites. World Scientific. https://doi.org/10.1142/9789814566469_0063

Deng, Y., Acker, K. Van, Dewulf, W., Duflou, J.R., 2011. Glocalized Solutions for Sustainability in Manufacturing. Glocalized Solut. Sustain. Manuf. 3–8. https://doi.org/10.1007/978-3-642-19692-8

DRIAS les futurs du climat, 2014. DRIAS [WWW Document]. URL https://drias-prod.meteo.fr/okapi/accueil/okapiWebDrias/index.jsp

ecoinvent, 2020. Ecoinvent 3.5 database [WWW Document]. URL https://www.ecoinvent.org/database/ecoinvent-37/new-data-in-ecoinvent-37/new-data-in-ecoinvent-37.html

European Environment Agency, 2019. EMEP/EEA air pollutant emission inventory- Other Sources and Sinks: Natural Grassland and Other Vegetation.

Fazio, S., Biganzioli, F., De Laurentiis, V., Zampori, L., Sala, S., Diaconu, E., 2018. Supporting information to the characterisation factors of recommended EF Life Cycle Impact Assessment methods, version 2, from ILCD to EF 3.0, EUR 29600 EN, European Commission, Ispra, 2018, ISBN 978-92-79-98584-3, doi:10.2760/002447, PUBSY No. JRC114822., New Models and Differences with ILCD, EUR. https://doi.org/10.2760/002447

Garcia, A.G.M., 2017. HEMP: A COMPOSITION REVIEW PLUS. Вестник Росздравнадзора 6, 5–9.

Gomez-Campos, A., Vialle, C., Rouilly, A., Sablayrolles, C., Hamelin, L., 2020. Flax Fiber for Technical textile: a life cycle inventory. J. Clean. Prod. 281, 125177. https://doi.org/10.1016/j.jclepro.2020.125177

González-García, S., Hospido, A., Moreira, M.T., Feijoo, G., 2007. Life cycle environmental analysis of hemp production for non-wood pulp. 3rd Int. Conf. Life Cycle Manag. 1–6.

Gueudet, A., 2016a. Analyse Du Cycle De Vie Comparative De Panneaux De Porte Automobiles Biosource (Pp / Fibres De Lin Et De Chanvre) Et Petrosource (Abs).

Gueudet, A., 2016b. 19, Analyse Du Cycle De Vie Comparative De Panneaux De Porte Automobiles Biosource (Pp / Fibres De Lin Et De Chanvre) Et Petrosource (Abs).

Hamelin, L., Jørgensen, U., Petersen, B.M., Olesen, J.E., Wenzel, H., 2012. Modelling the carbon and nitrogen balances of direct land use changes from energy crops in Denmark: A consequential life cycle inventory. GCB Bioenergy 4, 889–907. https://doi.org/10.1111/j.1757-1707.2012.01174.x

Hergoualc'h, K., Akiyama, H., Bernoux, M., Chirinda, N., del Prado, A., Kasimir, Å., MacDonald, J.D., Ogle, S.M., Regina, K., Weerden, T.J. van der, 2019. N2O emissions from managed soils, and CO2 emissions from lime and urea application, in: 2019 Refinement to the 2006 IPCC Guidelines for National Greenhouse Gas Inventories. pp. 1–48.

Hussain, M.Z., Bhardwaj, A.K., Basso, B., Robertson, G.P., Hamilton, S.K., 2019. Nitrate Leaching from Continuous Corn, Perennial Grasses, and Poplar in the US Midwest. J. Environ. Qual. 48, 1849–1855. https://doi.org/10.2134/jeq2019.04.0156

Inglada, J., Vincent, A., Arias, M., Tardy, B., Morin, D., Rodes, I., 2017. Operational High Resolution Land Cover Map Production at the Country Scale Using Satellite Image Time Series. Remote Sens. 9, 95. https://doi.org/10.3390/rs9010095

Ip, K., Miller, A., 2012. Life cycle greenhouse gas emissions of hemp-lime wall constructions in the UK. Resour. Conserv. Recycl. 69, 1–9. https://doi.org/10.1016/j.resconrec.2012.09.001

IPCC, 2019. 2019 Refinement to the 2006 IPCC Guidelines for National Greenhouse Gas Inventories Volume 5 Waste, IPCC Good Practice Guidance and Uncertainty Management in National Greenhouse Gase Inventories.

Islam, M.S., 2008. The Influence of Fibre Processing and Treatments on Hemp Fibre / Epoxy and Hemp Fibre / PLA Composites. Thesis 1994, 1–290.

Jiménez Rivero, A., Sathre, R., García Navarro, J., 2016. Life cycle energy and material flow implications of gypsum plasterboard recycling in the European Union. Resour. Conserv. Recycl. 108, 171–181. https://doi.org/10.1016/j.resconrec.2016.01.014

Kirwan, L., Lüscher, A., Sebastià, M.T., Finn, J.A., Collins, R.P., Porqueddu, C., Helgadottir, A., Baadshaug, O.H., Brophy, C., Coran, C., Dalmannsdóttir, S., Delgado, I., Elgersma, A., Fothergill, M., Frankow-Lindberg, B.E., Golinski, P., Grieu, P., Gustavsson, A.M., Höglind, M., Huguenin-Elie, O., Iliadis, C., Jørgensen, M., Kadziuliene, Z., Karyotis, T., Lunnan, T., Malengier, M., Maltoni, S., Meyer, V., Nyfeler, D., Nykanen-Kurki, P., Parente, J., Smit, H.J., Thumm, U., Connolly, J., 2007. Evenness drives consistent diversity effects in intensive grassland systems across 28 European sites. J. Ecol. 95, 530–539. https://doi.org/10.1111/j.1365-2745.2007.01225.x

Korjenic, A., Petránek, V., Zach, J., Hroudová, J., 2011. Development and performance evaluation of natural thermal-insulation materials composed of renewable resources. Energy Build. 43, 2518–2523. https://doi.org/10.1016/j.enbuild.2011.06.012

La Rosa, A.D., Cozzo, G., Latteri, A., Mancini, G., Recca, A., Cicala, G., 2013. A comparative life cycle assessment of a composite component for automotive. Chem. Eng. Trans. 32, 1723–1728. https://doi.org/10.3303/CET1332288

Lan, K., Kelley, S.S., Nepal, P., Yao, Y., 2020. Dynamic life cycle carbon and energy analysis for cross-laminated timber in the Southeastern United States. Environ. Res. Lett. 15, 124036. https://doi.org/10.1088/1748-9326/abc5e6

Lecompte, T., Levasseur, A., Maxime, D., 2017. Lime and hemp concrete LCA: a dynamic approach of GHG emissions and capture. 2nd Int. Conf. Bio-based Build. Mater. 1st Conf. Ecol. Valoris. Granul. FIbrous Mater. 513–521.

Lee, E.C., Flanigan, C.M., Williams, K.A., Mielewski, D.F., Houston, D.Q., 2016. Hemp Fiber Reinforced Sheet Molding Compounds for Automotive Applications. Ford Mot. Company, Dearborn 1–12.

MARKET STUDY REPORT, 2020. Global Animal Nutrition Market Research Report 2020.

Montserrat-De La Paz, S., Marín-Aguilar, F., García-Giménez, M.D., Fernández-Arche, M.A., 2014. Hemp (Cannabis sativa L.) seed oil: Analytical and phytochemical characterization of the unsaponifiable fraction. J. Agric. Food Chem. 62, 1105–1110. https://doi.org/10.1021/jf404278q

Mustafa, A.F., McKinnon, J.J., Christensen, D.A., 1999. The nutritive value of hemp meal for ruminants. Can. J. Anim. Sci. 79, 91–95. https://doi.org/10.4141/A98-031

Nachtergaele, F., van Velthuizen, H., van Engelen, V., Fischer, G., Jones, A., Montanarella, L., Petri, M., Prieler, S., Teixeira, E., Shi, X., 2012. Harmonized World Soil Database (version 1.2). FAO, Rome, Italy IIASA, Laxenburg, Austria 1–50.

Nemecek, T., Kägi, T., 2007. Life cycle inventories of Agricultural Production Systems. Ecoinvent 1–360.

Nicolardot, B., Recous, S., Mary, B., 2001. Simulation of C and N mineralisation during crop residue decomposition : A simple dynamic model based on the C : N ratio of the residues Author (s): B . Nicolardot , S . Recous and B . Mary Source : Plant and Soil , Vol . 228 , No . 1 , THE 10TH INTERNA. Plant Soil 228, 83–103.

Nicolescu, V.N., Hernea, C., Bakti, B., Keserű, Z., Antal, B., Rédei, K., 2018. Black locust (Robinia pseudoacacia L.) as a multi-purpose tree species in Hungary and Romania: a review. J. For. Res. 29, 1449–1463. https://doi.org/10.1007/s11676-018-0626-5

Norton, A., Alexander, S., Building, F., 2008. Life Cycle Assessments of Natural Fibre Insulation Materials Final Report Study funded by Defra Life Cycle Assessments of Natural Fibre Insulation Materials. Building.

Norton, A.J., 2008. The Life Cycle Assessment and Moisture Sorption Characteristics of Natural Fibre Thermal Insulation Materials. University of Wales, Bangor.

Norton, A.J., Murphy, R., Hill, C.A.S., Newman, G., 2009. the Life Cycle Assessments of Natural Fibre Insulation Materials. Mater. Technol. 6–9.

Novakova, P., Sal, J., 2019. Use of technical hemp for concrete-Hempcrete. IOP Conf. Ser. Mater. Sci. Eng. 603. https://doi.org/10.1088/1757-899X/603/5/052095

Opinion, S., 2011. Scientific Opinion on the safety of hemp (Cannabis genus) for use as animal feed. EFSA J. 9, 1–41. https://doi.org/10.2903/j.efsa.2011.2011

Pehme, S., Veromann, E., Hamelin, L., 2017. Environmental performance of manure co-digestion with natural and cultivated grass – A consequential life cycle assessment. J. Clean. Prod. 162, 1135–1143. https://doi.org/10.1016/j.jclepro.2017.06.067

Pervaiz, M., Sain, M.M., 2003. Carbon storage potential in natural fiber composites. Resour. Conserv. Recycl. 39, 325–340. https://doi.org/10.1016/S0921-3449(02)00173-8

PLANTUREUX, S., PEETERS, A., MCCRACKEN, D., 2005. Biodiversity in intensive grasslands : Effect of management, improvement and challenges. Agron. Res. 3, 417–426.

Pretot, S., Collet, F., Garnier, C., 2014. Life cycle assessment of a hemp concrete wall: Impact of thickness and coating. Build. Environ. 72, 223–231. https://doi.org/10.1016/j.buildenv.2013.11.010

Rapa, M., Ciano, S., Rocchi, A., D'Ascenzo, F., Ruggieri, R., Vinci, G., 2019. Hempseed oil quality parameters: Optimization of sustainable methods by miniaturization. Sustain. 11, 30–35. https://doi.org/10.3390/su11113104

RESEARCH AND MARKET, 2018. Global Hemp Oil Market – Growth, Future Prospects and Competitive Analysis, 2018-2026.

Schau, E.M., Allacker, K., Camillis, C. De, Pant, R., 2013. The development of Product Environmental Footprint (PEF) Category Rules (PEFCR), in: Proceedings of the SETAC Europe 23nd Annual Meeting Glasgow, United Kingdom, 12–16 May 2013. pp. 7–8.

Senga Kiessé, T., Ventura, A., van der Werf, H.M.G., Cazacliu, B., Idir, R., Andrianandraina, 2017. Introducing economic actors and their possibilities for action in LCA using sensitivity analysis: Application to hemp-based insulation products for building applications. J. Clean. Prod. 142, 3905–3916. https://doi.org/10.1016/j.jclepro.2016.10.069

Sepe, R., Bollino, F., Boccarusso, L., Caputo, F., 2018. Influence of chemical treatments on mechanical properties of hemp fiber reinforced composites. Compos. Part B Eng. 133, 210–217. https://doi.org/10.1016/j.compositesb.2017.09.030

Shen Zhou; Ligia Tiruta-Barna Shivesh Kishore Karan; Lorie Hamelin, 2021. Simultaneous Carbon Storage in Arable land and Anthropogenic Products (CSAAP): demonstrating a new concept towards well below 2°C. https://doi.org/10.31224/osf.io/cmvtu

Stapulionienė, R., Tupčiauskas, R., Vaitkus, S., Vėjelis, S., 2016. Development and Investigation of Thermal Insulation From Hemp-Polylactide Fibres. Eng. Struct. Technol. 8, 23–30. https://doi.org/10.3846/2029882x.2016.1158127

TNO innovation for life, 2020. Phyllis2 [WWW Document]. URL https://phyllis.nl/

Tonini, D., Hamelin, L., Astrup, T.F., 2016. Environmental implications of the use of agro-industrial residues for biorefineries: application of a deterministic model for indirect land-use changes. GCB Bioenergy 8, 690–706. https://doi.org/10.1111/gcbb.12290

Turunen, L., van der Werf, H., 2006. Life cycle analysis of hemp textile yarn. INRA, French Natl. Inst. Agron. Res. Fr.

Uihlein, A., Ehrenberger, S., Schebek, L., 2008. Utilisation options of renewable resources: a life cycle assessment of selected products. J. Clean. Prod. 16, 1306–1320. https://doi.org/10.1016/j.jclepro.2007.06.009

Ventura, A., Kiess, T.S., 2015. Sensitivity Analysis of Environmental Process Modeling in a Life Cycle Context: A Case Study of Hemp Crop Production. J. Ind. Ecol. 19, 978–993. https://doi.org/10.1111/jiec.12228

Verchot, L., Lasco, K.T.R., Ogle, S., Raison, J., Li, Y., Martino, D., McConkey, B., Smith, P., 2006. IPCC Guidelines for National Greenhouse Gas Inventories, Chapter 6 Grassland. Intergovernmental Panel on Climate Change, vol. 4: Agriculture, Ipcc. https://doi.org/10.1016/B978-0-12-394807-6.00168-4

Vogtländer, J.G., van der Velden, N.M., van der Lugt, P., 2014. Carbon sequestration in LCA, a proposal for a new approach based on the global carbon cycle; cases on wood and on bamboo. Int. J. Life Cycle Assess. 19, 13–23.

Walker, R., Pavia, S., Mitchell, R., 2014. Mechanical properties and durability of hemp-lime concretes. Constr. Build. Mater. 61, 340–348. https://doi.org/10.1016/j.conbuildmat.2014.02.065

Worrall, F., Clay, G.D., 2014. The potential use of heather, calluna vulgaris, as a bioenergy crop. Biomass and Bioenergy 64, 140–151. https://doi.org/10.1016/j.biombioe.2014.03.007

Yang, T., Adams, J.M., Shi, Y., He, J.S., Jing, X., Chen, L., Tedersoo, L., Chu, H., 2017. Soil fungal diversity in natural grasslands of the Tibetan Plateau: associations with plant diversity and productivity. New Phytol. 215, 756–765. https://doi.org/10.1111/nph.14606

Zah, R., Hischier, R., Leão, A.L., Braun, I., 2007. Curauá fibers in the automobile industry - a sustainability assessment. J. Clean. Prod. 15, 1032–1040. https://doi.org/10.1016/j.jclepro.2006.05.036

Zampori, L., Dotelli, G., Vernelli, V., 2013. Life cycle assessment of hemp cultivation and use of hemp-based thermal insulator materials in buildings. Environ. Sci. Technol. 47, 7413–7420. https://doi.org/10.1021/es401326a

Zhang, X., 2016. Manufacturing of hemp/PP composites and study of its residual stress and aging behavior.

Supplyment Information III. for Chapter V

1 SOC simulation

Based on the rotation of black locust (Robinia pseudoacacia L.), the SOC change in the future 105 years (3 rotations) is investigated in this study. To simulate the SOC change in the future, C-Tool is adopted here. Temperature in the future is obtained from Drias(DRIAS les futurs du climat, 2014), which predicted the temperature from 2022 till 2100, from plots of the whole France, under a moderate scenario, RCP 4.5. The average of the predicted temperature in all plots is used on behalf of that of carbon vulnerable lands(CV-lands). To fulfill the gap after 2100 till the end of the third rotation, the average of temperature of the last ten years (2091-2100) is used. Temperature situation in simulation period is depicted in fig.S1.

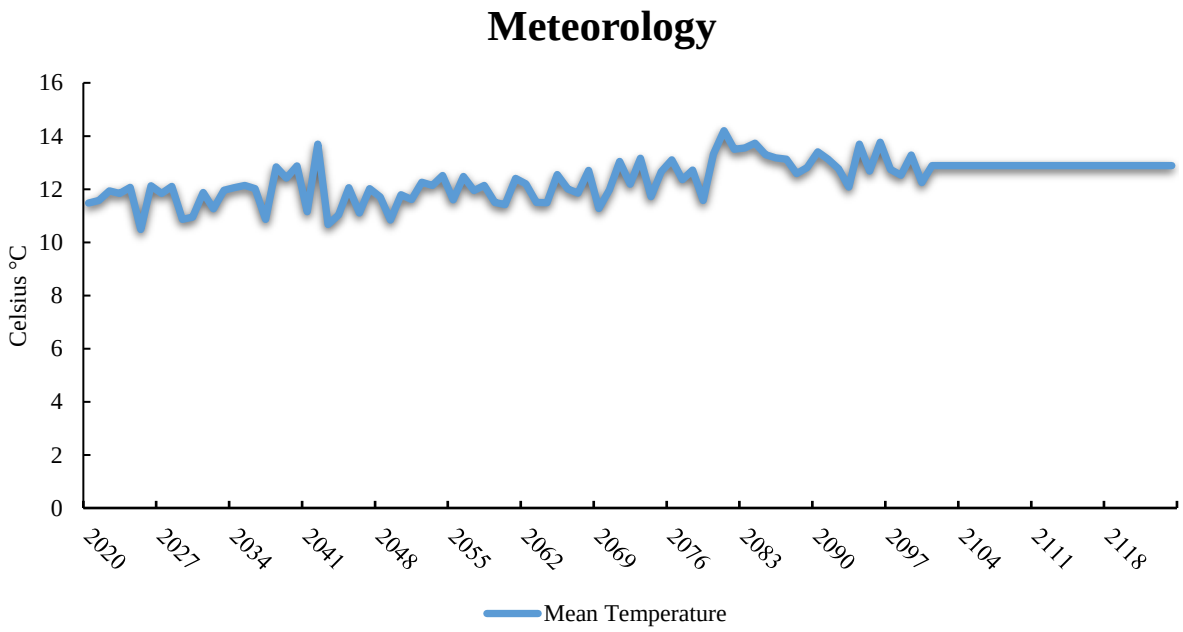

Fig. S1 Predicted temperature as inputs for C-Tool from 2022 to 2126.

Another important setting of C-Tool is the soil characteristics. Initial SOC stock and clay proportion are taken from the Harmonized World Soil Database(Nachtergaele et al., 2012) (FAO) according to the CV-lands range we defined before(Shen et al., 2022a), 42.35 t ha-1 and 0.0216 g kg-1 respectively. While C/N ratio is not included in the FAO database, 11 is used here as it is a general value for France(Dimassi et al., 2018; Launay et al., 2021).

Carbon inputs are calculated in two parts, belowground and aboveground. Aboveground carbon inputs include carbon from aerial biomass, woody dust and grated stump. What is called 'aerial biomass' is the set of foliage, seeds and pods, which are produced annually after the year 6 after cultivation(Nicolescu et al., 2018; Stone, 2009; Warne, 2016). Woody dust is the scrap left on-site during the cutting of trees(Santi et al., 2016). In other studies, stumps and roots were regarded as an integral for belowground(Albers et al., 2019), however, stump would be ground to prevent sprouting in our case(Malcolm et al., 2008), and left on the surface thus the crushed stumps were put as aboveground input, and the coarse root and fine root were the belowground input. Selective thinning and pruning are applied as a management to remove bad growing trees and to ensure the resources like sunshine for the healthy black locust (detailed in section 2.3, chapter V, main paper). In one rotation, there are three cutting periods: first thinning, second thinning, and final logging, and pruning with the second thinning. Aerial biomass would fall down on the ground every year after the year 6, the quantity of aboveground and belowground biomass during the three cutting periods follow their corresponding growth rate (fig.6a,

in the main paper). Aboveground and belowground carbon inputs are shown in table S2, with different dry mass and corresponding carbon percentage (table S1).

Table s2 shows the C input in C-tool for one rotation, and it is assumed to be the same for the other two rotations. In order to include in LCA the effect of residues decomposition after the cultivation period, simulations of SOC were performed for long term. For this simulation, in the year after cultivation (2126), all C input is 0. The results are represented in (fig. s2). In year 2177, the SOC stock is back to the level in 2022 (42.35 Mg ha^{-1}).

Table S1 Characteristics of different parts of black locust.

	Moisture%	Carbon%	Nitrogen%
Aboveground Woody biomass[a]	36.67%(González-García et al., 2011; Manzone, 2015)	48.17%(De Vries et al., 2014; "wood, black locust (Robinia pseudoacacia)," 1998)	0.57%("wood, black locust (Robinia pseudoacacia)," 1998)
Root[b]	36.67%(Rahmonov, 2009)	46.40%(Rahmonov, 2009)	2.19%(Rahmonov, 2009)
Aerial biomass[c]	6.13%(Bhat et al., 2014)	56.00%(Rahmonov, 2009; Rice et al., 2004)	2.13%(Rahmonov, 2009; Rice et al., 2004)

[a]: including branch, woody dust, stem, and stump.
[b]: including coarse root and fine root.
[c]: including foliage, pod, and seed.

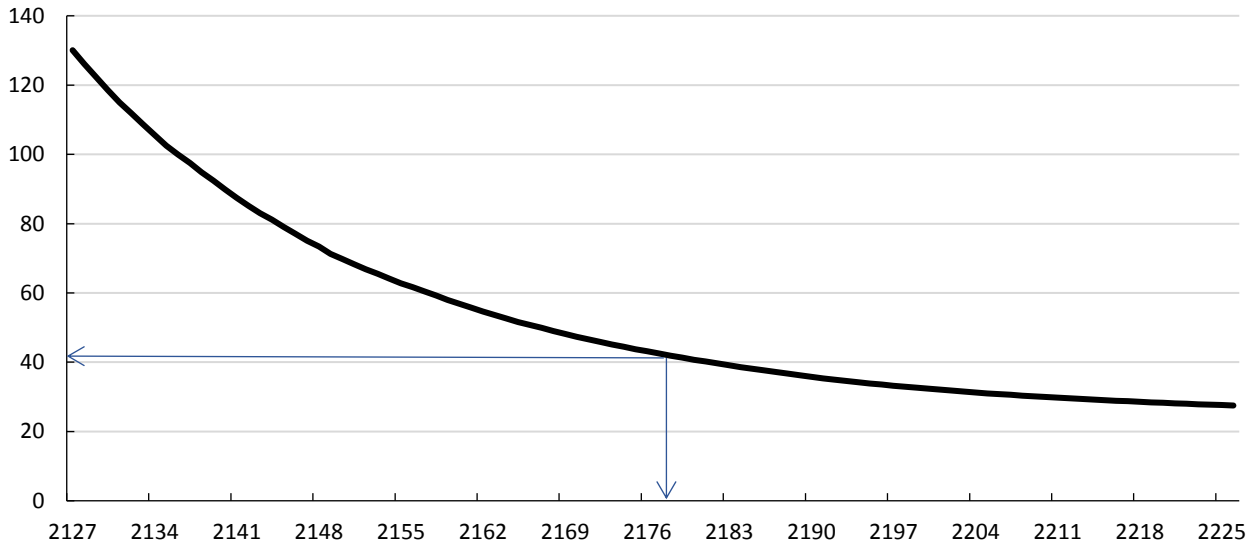

Fig. S2 SOC change in the CV-land after the cultivation period.

Table S2 Carbon input for C-Tool from one black locust cultivating rotation

Year	Aerial biomass residue[a]	Aboveground wood residue	Belowground
1	0.00	0.00	0.00
2	0.00	0.00	0.00
3	0.00	0.00	0.00
4	0.00	0.00	0.00
5	0.00	0.00	0.00
6	0.05	0.00	0.00
7	0.10	0.00	0.00
8	0.16	0.00	0.00
9	0.25	0.00	0.00
10[b]	0.84	0.48	4.65
11	0.25	0.00	0.00
12	0.33	0.00	0.00
13	0.43	0.00	0.00
14	0.54	0.00	0.00
15	0.67	0.00	0.00
16	0.81	0.00	0.00
17	0.96	0.00	0.00
18	1.13	0.00	0.00
19	1.31	0.00	0.00
20[c]	2.68	1.18	19.23
21	0.78	0.00	0.00
22	0.88	0.00	0.00
23	0.98	0.00	0.00
24	1.08	0.00	0.00
25	1.19	0.00	0.00
26	1.29	0.00	0.00
27	1.40	0.00	0.00
28	1.52	0.00	0.00
29	1.63	0.00	0.00
30	1.75	0.00	0.00
31	1.86	0.00	0.00
32	1.98	0.00	0.00
33	2.10	0.00	0.00
34	2.22	0.00	0.00
35[d]	2.34	3.30	65.24

[a]: foliage+seeds+pods.
[b]: first thinning.
[c]: second thinning +pruning;
[d]: harvesting.

2 Life cycle inventory

Inventories of black locust from cultivation till products disposal are presented here, all data are corresponding to the functional unit, which is 1 ha CV-land. To improve the data quality, inventory is built from multi sources, then choosing the average or median value. The main references are listed in the table.

2.1 Black locust cultivation

The principle for cultivating black locust on CV-lands (which are marginal lands) is avoiding agricultural managements unless they are necessary. Following this principle, fertilizer and irrigation are not applied because black locust tolerates dry and is a nitrogen-fix species(captures nitrogen and fix it in the soil) (Nicolescu et al., 2020; Seserman et al., 2018). Moreover, insecticide and herbicide are not needed either since black locust resists to fungal diseases, insect pests(Nicolescu et al., 2020; Seserman et al., 2018) and inhibits the growth of weed(Nicolescu et al., 2020). In this study, the main product is the cross laminated timber (CLT) from stem, thus selective thinning and pruning are necessary to promote valuable trees. Removing defective trees with narrow, full, and symmetrical crowns representing about one third of the height, could help produce high proportion of good quality roundwood.

The land is ploughed first, then black locust is cultivated with seedlings, with a density of 2240 seedlings ha^{-1}, considering the mortality and the defective trees (e.g. forked, badly shaped, wounded, or bent-over)(Keresztesi, 1983; Nicolescu et al., 2018). In fact, seedling planting and sprout are two common methods to cultivate black locust(Nicolescu et al., 2020, 2018). Black locust could sprout from stumps and roots, however, stumps would be crushed as mulch on the ground during logging, and after ploughing, roots are destroyed and then decomposed, thus seedling plantingis adopted to cultivate the new generation here(Mazurek and Bejger, 2014). No fertilization, irrigation and pesticide is applied during the cultivation. First thinning is conducted at the year 10, with 50% of stems are cut(Keresztesi, 1983). After 10 years, 50% of forest would be thinned a second time, following a pruning of branches for the rest of the trees(Keresztesi, 1983; Rédei et al., 2012). Finally, all trees would be logged at the end of rotation, which is at the year 35 after seedling planting(Nicolescu et al., 2018). In addition, the cultivation of black locust occupies the CV-lands on which other plants grown initially, thus other products need to be induced to compensate this lack, leading to the indirect land use change (iLUC); the method of evaluating the iLUC is based on(Tonini et al., 2016), with the updated data used in a previous study(Shen et al., 2022a).

2.2 Black locust growth

Black locust is a long-live species, could live more than 90 years(Lovinska and Sytnyk, 2016), while the growth rate peaks at approximately 20 years of age(Nicolescu et al., 2018), the increment rate slows gradually till 35 years of age(Adamopoulos et al., 2005; Nicolescu et al., 2018; Vítková et al., 2017). Consider the initial target of planting black locust in the CV-lands is to have the maximum CO_2 sequestration, the optimal of rotation is 35 years in this study. After 35 years, black locust could be 22.23 m in height and 30 cm in diameter at breast height (DBH) (Adamopoulos and Voulgaridis, 2002; Keresztesi, 1983; Nicolescu et al., 2018). The growth rate of height and DBH of the stand tree was simulated as following:

$$H(t) = a * \left(1 - e^{-b*t}\right)^{c} \quad (1)$$

$$DBH(t) = (p_1 + p_2 * t) * H(t)/100 \quad (2)$$

where H is the height at year t in meters; a, b, and c are empirical parameters equal to 25.5, 0.07, and 1.5214 respectively. DBH is in cm; $p_1$and p_2 are also empirical parameters equal to 85.9 and 1.4 respectively. To derive these, the known values of $H(35)$ (22 m; Adamopoulos and Voulgaridis, 2002; Nicolescu et al., 2018) and $DBH(35)$ (30 cm; Nicolescu et al., 2018; Vítková et al., 2017) were used. The values of both $p_1$and p_2 fit those that have been used in previous works (Nicolescu et al., 2018; Rédei et al., 2014, 2012).

To determine how much CO_2 would be captured every year and how much GHG would be emitted every year due to the plant growing and logging, especially the emission due to the selective thinning and logging, the growth of tree is modeled. Stem of tree is neither cone nor cylinder. Thus the volume of single stem is calculated as follows (Food and Agriculture Organization of the United Nations, 2005). The result is confirmed by other wood volume estimation equations(Rédei et al., 2014; Tabari and Salehi, 2008), and measurement results(Motta et al., 2009; Nicolescu et al., 2020).

$$V(t) = 0.42 * \pi(DBH(t)/2)^2 * H(t) \quad (3)$$

Where V (m^3) is the estimated volume of wood in the year t. The merchantable height is calculated as the height of the whole tree subtracted the height of stump, as stump is left on the ground. The height of stump ($Stpht$) is estimated by equation 2(Boston and Dysart, 2000):

$$Stpht(t) = 6.77 + 0.0355 * DBH(t) \quad (4)$$

$DBH(t)$ is the diameter at the breast height in the year 35, it should be noticed that the unit in this equation is inch, thus the unit should be converted. To expand the volume of the single tree to the biomass per hectare, the volume of the single tree multiplies the number of tree per hectare, considering the wood density and moisture(Adamopoulos et al., 2007; Manzone, 2015). At the first, second and final logging, amount of black locust per hectare is 2240, 1120, and 560 respectively(Keresztesi, 1983; Motta et al., 2009). After that, the weight of branches and barks are added according to their weight ratio to the stem (25% and 5% respectively) (Laschi et al., 2016; Mirabella et al., 2014; Wilson and Sakimoto, 2005), it is assumed that all woody parts of the tree have the same moisture content(Vangeel et al., 2019).

As aforementioned in section 1, aerial biomass (foliage+pods+seeds) would fall down annually, since the year 6 till the end of the rotation. The moisture and composition differ slightly to the woody part(table S1), the emission from aerial biomass decomposition is accumulated from the year 6 till year 10, the year 11 till 20, and the year 21 till 35, corresponding to the inventory sheet of the first thinning, second thinning, and final logging respectively.

Following the approach described above, there are several assumptions listed for simulating the growth:

1) The whole tree is assumed to grow in the same rate;

2) The proportion of different parts are assumed to be the same during the whole rotation, like the shoot/root ratio. The only exception is branches, after pruning (at the year 20, after second thinning), 25% of branches are cut(Nicolescu et al., 2020).
3) For the harvested woody biomass(DM), 70% of weight is roundwood, 25% of weight is branch(Laschi et al., 2016), and 5% is bark(Wilson and Sakimoto, 2005), and 1.2% is aerial biomass (foliage+seeds+pods)(Addlestone et al., 1998).
4) The residues on the ground are assumed not to influence the existing black locust growing, both trees after thinning and planted for the next rotation;
5) Because sprouting is not considered in this study (reason is explained in the section 2.1), root would not sprout after thinning.

The results of height and diameter are shown in fig. s3. There are several different formulas to describe the height(Nicolescu et al., 2018; Rédei et al., 2014, 2012) and diameter(Nicolescu et al., 2018; Rédei et al., 2014, 2012) change of black locust every year, due to the different rotations and final biomass, the results are slight different, while the growth trends are similar.

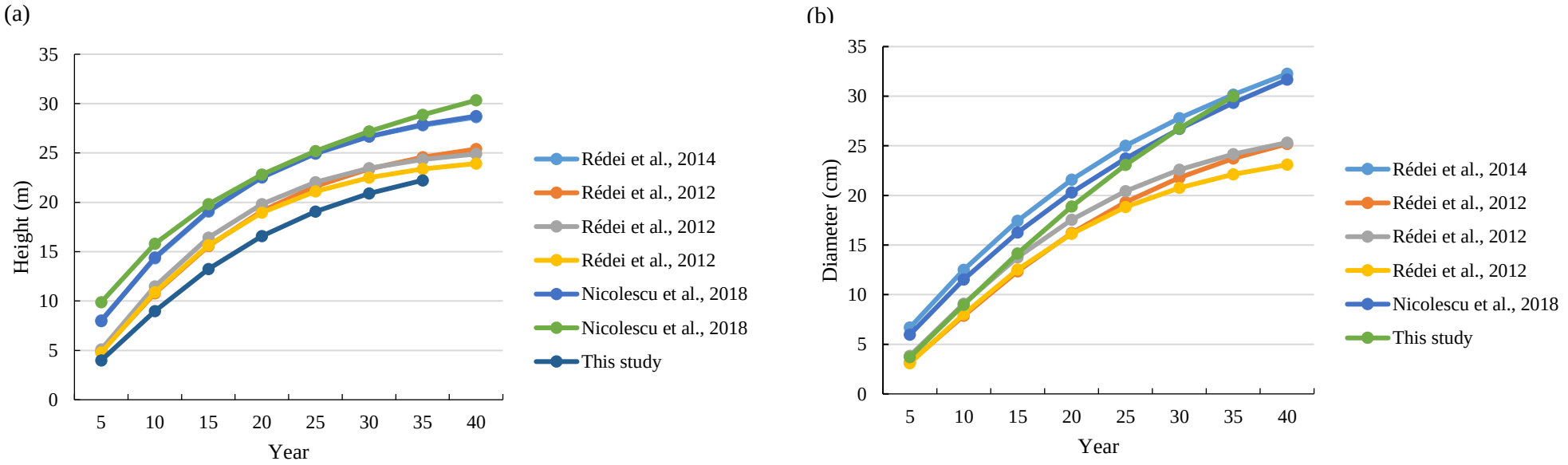

Fig. S3 Black locust growth trend in one rotation (a, height; b, diameter)

2.3 Logging

Black locust logging happens at the year of 10, 20, and 35 after seedling planting, for first thinning, second thinning, and final logging respectively, plus pruning is conducted right after the second thinning. The logging machine and loading process are included, data come from the ecoinvent(ecoinvent, 2020). Biomass from thinning and pruning is considered to be chipped as the ingredient for MDF, since they are not totally mature to be good quality wood. Black locust harvested from the final logging would be delimbed, branches are going to the chipper for MDF producing, and the stem is going to CLT manufacture. In all cases, bark would be incinerated(Silva et al., 2013), emission and avoided heat could be found in table S8. The wood harvesting produces 30 % of biomass loss which are left to decompose in forest, as aboveground carbon input (table S1&2), the rest loses in the air, regarded as PM 10 in the inventory(Wilson, 2010a). After cutting, stumps are left on the ground, would be crushed as mulch over the surface to prevent sprouting, because seedling planting is the only considered way to grow black locust in our case (table S7).

Table S3 Inventory sheet of black locust cultivation				
Cultivation				
Input	**Quantity**	**Unit**	**Source**	**Process**
Seedling	2240	p	(Nicolescu et al., 2018)	Tree seedling, for planting {GLO}| market for tree seedling | Conseq, U
Ploughing	1	ha	(Nicolescu et al., 2018)	Tillage, ploughing {GLO}| market for | Conseq, U
CO_2 total captured from air	1304.69	t		
Land occupation	350000	m2 a	1 rotation=35 years	Occupation, forest, extensive
iLUC	7.87	ha	(Shen et al., 2022a)	
Output				

Table S4 Inventory sheet of first thinning				
First thinning				
Input	**Quantity**	**Unit**	**Source**	**Process**
Harvested biomass	41.24	t		
Logging	2.70	hr	(ecoinvent, 2020)	Loader operation, large
	6.48	hr	(ecoinvent, 2020)	Skidding, skidder {RER}| skidding, skidder | Conseq, U
	6.89	hr	(ecoinvent, 2020)	Wood chipping, chipper, mobile, diesel, at forest road {GLO}| market for | Conseq, U
Stump grinding	1.35	t		
Output				
Emission to air				
CO_2 from residue decomposition	19.95	t		
CH_4 from residue decomposition	0.24	t	(Ros et al., 2013)	
N_2O from residue decomposition	5.03	kg	(Nemecek and Kagi, 2007)	

Dust from logging	0.31	t	(Santi et al., 2016)	

Table S5 Inventory sheet of second thinning				
Second thinning				
Input	**Quantity**	**Unit**	**Source**	**Process**
Harvested biomass	173.00	t		
Logging	11.31	hr		Loader operation, large
	27.16	hr		Skidding, skidder {RER}| skidding, skidder | Conseq, U
	28.89	hr		Wood chipping, chipper, mobile, diesel, at forest road {GLO}| market for | Conseq, U
Stump grinding	3.00	t		
Output				
Emission to air				
CO_2 from residue decomposition	99.18	t		
CH_4 from residue decomposition	1.13	t		
N_2O from residue decomposition	23.60	kg		
Dust from logging	1.29	t		
Table S6 Inventory sheet of final logging				
Final logging				
Input	**Quantity**	**Unit**	**Source**	**Process**
Harvested biomass	551.16	t		
Logging	36.05	hr	(ecoinvent, 2020)	Loader operation, large
	86.53	hr	(ecoinvent, 2020)	Skidding, skidder {RER}| skidding, skidder | Conseq, U
	92.04	hr	(ecoinvent, 2020)	Wood chipping, chipper, mobile, diesel, at forest road {GLO}| market for | Conseq, U
	46.19	hr	(ecoinvent, 2020)	Delimbing/sorting, excavator-based processor {RER}| delimbing, with excavator-based processor | Conseq, U
Stump grinding	7.56	t		
Output				
Emission to air				

CO_2 from residue decomposition	323.18	t		
CH_4 from residue decomposition	3.66	t		
N_2O from residue decomposition	77.01	kg		
Dust from logging	4.82	t		

Table S7 Inventory sheet of grinding stumps				
Grinding stumps				
Input	**Quantity**	**Unit**	**Source**	**Process**
Stumps (total from three cuttings)	11.91	t	(ecoinvent, 2020)	
Grinding	0.001	p	(ecoinvent, 2020)	Chipper, stationary, electric {GLO}| market for | Conseq, U
	377.55	kwh	(ecoinvent, 2020)	Electricity, medium voltage {CH}| market for | Conseq, U
	0.04	kg	(ecoinvent, 2020)	Lubricating oil {RER}| market for lubricating oil | Conseq, U
	0.08	kg	(ecoinvent, 2020)	Steel, low-alloyed, hot rolled {GLO}| market for | Conseq, U
Output				
Emissions from the decomposition of grated stumps are merged in table S4-6				

Table S8 Inventory sheet of bark incineration				
Bark incineration				
Input	**Quantity**	**Unit**	**Source**	**Process**
Bark (total from three cuttings)	37.68	t		
Incineration	1774.06	kwh	(ecoinvent, 2020)	Electricity, low voltage {FR}| market for | Conseq, U
	0.044	p	(ecoinvent, 2020)	Furnace, wood chips, with silo, 50kW {CH}| production | Conseq, U
Output				
Emission to air				
CO_2	30.50	t	(Nielsen et al., 2010)	
Sulphur dioxide (SO_2)	0.92	kg	(Nielsen et al., 2010)	
Nitrogen oxides (NO_X)	39.23	kg	(Nielsen et al., 2010)	
Non-methane volatile organic compounds (NMVOC)	2.47	kg	(Nielsen et al., 2010)	
Methane (CH_4)	1.50	kg	(Nielsen et al., 2010)	
Carbon monoxide (CO)	43.58	kg	(Nielsen et al., 2010)	
Nitrous oxide (N_2O)	387.41	g	(Nielsen et al., 2010)	
TSP	4.84	kg	(Nielsen et al., 2010)	
Cd	0.13	g	(Nielsen et al., 2010)	
Hg	0.19	g	(Nielsen et al., 2010)	
Zn	1.11	g	(Nielsen et al., 2010)	
PCDD/-F	6.78	µg	(Nielsen et al., 2010)	

PAH (BaP)	6.30	mg	(Nielsen et al., 2010)	
∑PAH	321.55	mg	(Nielsen et al., 2010)	
Naphthalene	1.12	g	(Nielsen et al., 2010)	
Ash	954.69	kg	(Nielsen et al., 2010)	
Marginal product				
Avoided heat	363282.94	MJ	(ecoinvent, 2020)	Heat, district or industrial, natural gas {FR}| heat and power co-generation, natural gas, conventional power plant, 100MW electrical | Conseq, U

2.4 CLT manufacture

After debranching and debarking, the roundwood is put on the land to dry in the open air, after several days, the moisture decreases to 15% after open-drying(Żelazna et al., 2019). The rough dried lumber with stickers are then trimmed before sawn into panel in certain size, residues produced during trimming are commonly sold as coproducts, herein would be collected and transported as the ingredients for MDF (section 2.5)(Bergman and Bowe, 2010). Trimmed lumbers are then sawn into the panel, several panels (commonly odd number, e.g. 3/5/7) are compressed together with a little resin according to different strength requirements(Dong et al., 2019). CLT could be used in lots in the construction field. Compare to the conventional construction material like brick, wall build by CLT need extra stone wool to reach the same thermal properties(Takano et al., 2014), which is 0.04 $W\ m^{-1}\ K^{-1}$ and meets the standard of NF EN 15804 and NF EN 16783(Zieger et al., 2020). In the erection phase, building woth CLT is much easier than with bricks, thus the energy consumption by using CLT is less, around 64 MJ/m^2 (100 mm thick). Also, 30% of time could be saved (which cannot be included in the inventory(Jayalath et al., 2020)). The lifespan of CLT is 50 years(Corradini et al., 2019).

Situation is similar for the demolition phase, while the energy consumption is 90% of that in the erection stage. What's more, during the demolition, there is a loss of 10% by mass(Jayalath et al., 2020), this loss is assumed to be collected and sent to the landfilling. Traditional LCA doesn't consider the carbon capture from air and carbon emitted as biogenic, however, we changed the characterization factor of both to track the carbon flow in this study (section 3). Half of the rest demolished CLT would be incinerated with heat recovery, while the other half is recycled (Guo et al., 2017). The common way to recycle CLT is to chop into wood chips (resin part is ignored since it's only 1% of the CLT, table s9). Herein, recycled CLT would go to the chipping process first, same as the harvested branches from the final logging (fig.1, main paper). Similar to recycled CLT, scraps from trimming and final sizing in CLT manufacture are assumed to be collected and then recycled as inputs for MDF manufacture. Because these scraps are already chips, the recycling would begin at the washing process (fig.1, main paper). The inventory for CLT manufacture and till disposal is shown below.

Table S9 Inventory CLT manufacture				
Open-dry				
Input	**Quantity**	**Unit**	**Source**	**Process**
Stem	368.50	t		
Open-dry	3158.05	m2a	(ecoinvent, 2020)	Occupation, industrial area
	1263.96	m2	(ecoinvent, 2020)	Transformation, from unknown
	1263.96	m2	(ecoinvent, 2020)	Transformation, to industrial area
Output				
Emission to air				
Water	92.85	t	(Corradini et al., 2019; Żelazna et al., 2019)	
Trimming				
Input	**Quantity**	**Unit**	**Source**	**Process**
Roundwood after drying	275.65	t		
Trimming	2914.23	kwh	(Corradini et al., 2019; ecoinvent, 2020)	Electricity, medium voltage {FR}| market for | Conseq, U
	0.00023	p	(ecoinvent, 2020)	Planing mill {RER}| production | Conseq, U
Output				
Scrap, collection an transporatation, DM	9.34	t		
Sawing				
Input	**Quantity**	**Unit**	**Source**	**Process**
Trimmed roundwood	264.62	t		
Electricity	4948.42	kwh	(ecoinvent, 2020)	Electricity, medium voltage {FR}| market for | Conseq, U
Diesel	6800.77	MJ	(ecoinvent, 2020)	Diesel, burned in building machine {GLO}| market for | Conseq, U
Lubricant oil	24.80	kg	(ecoinvent, 2020)	Lubricating oil {RER}| market for lubricating oil | Conseq, U

Output				
Scrap, collection an transporatation, DM	18.25	t		
Lubricant waste	3.71	kg		
Glue laminating& cutting/sanding				
Input	**Quantity**	**Unit**	**Source**	**Process**
Sawnwood	243.07	t		
Glue (UF)	2129.30	kg	(Chen et al., 2019; Wood Products Industry, 2002)	Urea formaldehyde resin {RER}| market for urea formaldehyde resin | Conseq, U
Electricity	22897.22	kwh	(ecoinvent, 2020)	Electricity, medium voltage {RER}| market group for | Conseq, U
Diesel	5955.22	MJ	(ecoinvent, 2020)	Diesel, burned in building machine {GLO}| market for | Conseq, U
Heat	393773.86	MJ	(ecoinvent, 2020)	Heat, central or small-scale, other than natural gas {CH}| heat production, hardwood chips from forest, at furnace 50kW | Conseq, U
Factory	0.0000059	p	(ecoinvent, 2020)	Wooden board factory, organic bonded boards {RER}| construction | Conseq, U
Output				
Formaldehyde	2.13	kg	(Basler et al., 2015; Wood Products Industry, 2002)	
Scrap, collection an transporatation, DM	41.16	t	(Bergman and Bowe, 2010)	
Marginal product				
Brick	259.5	t	(Takano et al., 2014)	Light clay brick {GLO}| market for | Conseq, U

Table S10 Inventory of the CLT use				
Erection				
Input	**Quantity**	**Unit**	**Source**	**Process**
CLT	196.59	t		
Nail	0.85	t	(Santi et al., 2016)	Metal working, average for aluminium product manufacturing {GLO}| market for | Conseq, U
Energy saved from construction	-160273.55	MJ	(Corradini et al., 2019; Guo et al., 2017)	Electricity, low voltage {FR}| market for | Conseq, U
Output				
Operation				
Input	**Quantity**	**Unit**	**Source**	**Process**
Extra insulation	28.05	t	(Takano et al., 2014)	Stone wool {GLO}| market for stone wool | Conseq, U
Output				

Table S11 Inventory of end of life of CLT.				
Demolition				
Input	**Quantity**	**Unit**	**Source**	**Process**
Energy saved from demolition	-144246.19	MJ	(Guo et al., 2017)	
Scrap, collection an transporatation, DM	16.64	t	(Jayalath et al., 2020)	
Output				
Disposal				
Input	**Quantity**	**Unit**	**Source**	**Process**
Biomass loss	16.64	t		
CLT going to the incineration	74.08	t		Waste wood, untreated {CH}| treatment of, municipal incineration with fly ash extraction | Conseq, U
	955.37	kg		Waste polyurethane {CH}| treatment of, municipal incineration with fly ash extraction | Conseq, U
Biomass going to the recycling	2538.8	tkm	(ecoinvent, 2020)	Transport, freight, lorry, unspecified {RER}| market for transport, freight, lorry, unspecified | Conseq, U
Disposal of the extra insulation	28.05	t		Waste mineral wool {Europe without Switzerland}| market for waste mineral wool | Conseq, U
Disposal of nails	0.85	t		Scrap aluminium {Europe without Switzerland}| market for scrap aluminium | Conseq, U
Output				
Scrap collection& transporation, 1 t DM				
Input	**Quantity**	**Unit**	**Source**	**Process**
Collection	0.0349	kwh	(ecoinvent, 2020)	Electricity, medium voltage {FR}| market for | Conseq, U
Transportation	0.0287	tkm	(ecoinvent, 2020)	Transport, freight, lorry, unspecified {RER}| market for transport, freight, lorry, unspecified | Conseq, U

2.5 MDF manufacture

MDF is obtained from woody chips mixed with resin. There is no specific requirement for chips, thus lots of stuff could be used to make MDF. In this study, there are five main sources of woody chips, which are biomass from first and second thinning, branches from final logging, scraps from CLT manufacture, and recycled CLT. The logged biomass (including biomass from first thinning, second thinning, and final logging) and recycled CLT, need to be chopped into chips first, while scraps are considered as chips since they come from trimming and sizing. After chopping, chips need to be washed to remove dirt. Although chips from recycled CLT and scraps have went through the open-dry process, thus the moisture content is less than that of fresh logged biomass, after washing process, the moisture of chips from all sources is considered as the same. Clean chips would be refined by steam to soften the fiber. After that, the soften chips are mixed with resin and other additive, like $Al_2(SO_4)_3$ and paraffin, for improving the resistance to water and material strength, respectively. The resinated biomass need to be dried. The dried biomass is matted and compressed in a thermal process, and cut into desired size. Scraps during manufacture are not regarded as recyclable, but collected and treated as landfilling.

MDF is a widely used in construction, like wall or roof or furniture, herein we considered MDF would replace the PVC panel as ceiling materials(Onyeaju et al., 2012; Takano et al., 2014). After 12 years of use(Couret et al., 2017), MDF would be incinerated with heat recovery (ecoinvent, 2020), the lost mass because of demolition or transportation is considered as open-dump as the same in the CLT disposal (biomass loss), and carbon in the woody part is emitted as CH_4 and CO_2 (IPCC, 2019).

Table S12 Inventory of MDF manufacture				
Chipping				
Input	**Quantity**	**Unit**	**Source**	**Process**
Branches	135.94	t		
Demolished CLT	88.46	t		
Biomass from first thinning	38.74	t		
Biomass from second thinning& pruning	162.49	t		
Energy consumption	8695.17	MJ	(Kouchaki-Penchah et al., 2016)	Electricity, medium voltage {CH}| market for | Conseq, U
Lubricating oil	1.40	kg	(ecoinvent, 2020)	Lubricating oil {RER}| market for lubricating oil | Conseq, U
Machine	0.04	p	(ecoinvent, 2020)	Chipper, stationary, electric {GLO}| market for | Conseq, U
	2.80	kg	(ecoinvent, 2020)	Steel, low-alloyed, hot rolled {GLO}| market for | Conseq, U
Scrap, collection	8.37	t		Scrap, collection an transporatation, DM, to in assemble
Output				
Scraps	8.37	t		Waste wood, untreated {GLO}| treatment of waste wood, untreated, open dump, wet infiltration class (500mm) | Conseq, U
Washing				
Input	**Quantity**	**Unit**	**Source**	**Process**
Chipped biomass	417.27	t		
Chips from CLT manufacture	81.19	t		
Water for washing	298.22	m^3	(Rivela et al., 2007)	
Output				
Waste water	241.66	t	(Rivela et al., 2007)	Wastewater from medium density board production {RER}| treatment of wastewater from medium density fibreboard production, capacity 5E9l/year | Conseq, U

Steam refinery				
Input	**Quantity**	**Unit**	**Source**	**Process**
Washed branch	555.02	t		
Steam	872644.87	MJ	(Rivela et al., 2007)	Process steam from natural gas, heat plant, consumption mix, at plant, MJ FR S
Energy consumption	34015.12	MJ	(Kouchaki-Penchah et al., 2016)	Electricity, low voltage {FR}| market for | Conseq, U
Output				
Resinating				
Input	**Quantity**	**Unit**	**Source**	**Process**
Refined biomass	555.02	t		
Ureal formaldehyde resin	42.25	t	(Wilson, 2010a)	Urea formaldehyde resin {RER}| market for urea formaldehyde resin | Conseq, U
Paraffin	1.91	t	(Piekarski et al., 2017)	Paraffin {RER}| production | Conseq, U
Aluminium sulfate	0.38	t	(Wilson, 2010b)	Aluminium sulfate, without water, in 4.33% aluminium solution state {RoW}| production | Conseq, U
Energy consumption	12696.96	MJ	(Kouchaki-Penchah et al., 2016)	Electricity, low voltage {FR}| market for | Conseq, U
Output				
Waste resin	0.38	t		Hazardous waste, for incineration {Europe without Switzerland}| market for hazardous waste, for incineration | Conseq, U
Emission to air				
Formaldehyde	0.06	t		
Drying				
Input	**Quantity**	**Unit**	**Source**	**Process**
Resinated biomass	599.56	t		

Drying	20423.28	m^3	(Rivela et al., 2007)	Drying, natural gas {GLO}| market for | Conseq, U
Output				
Emission to air				
Water	157.17	t		
Methanol	8.40	kg		
Mat forming &thermal compression				
Input	**Quantity**	**Unit**	**Source**	**Process**
Biomass after drying	437.52	t		
Energy consumption, hot oil	418021.27	MJ	(Kouchaki-Penchah et al., 2016)	Heat, district or industrial, natural gas {Europe without Switzerland}| market for heat, district or industrial, natural gas | Conseq, U
Energy consumption, electricity	20601.90	MJ	(Rivela et al., 2006)	Electricity, low voltage {FR}| market for | Conseq, U
Output				
Sizing &sanding, input- Pressed mat				
Input	**Quantity**	**Unit**	**Source**	**Process**
Pressed mat	437.52	t		
Energy consumption, electricity	137159.81	MJ	(Rivela et al., 2006)	Electricity, low voltage {FR}| market for | Conseq, U
Scrap, collection an transportation, DM	1.96	t	(Kouchaki-Penchah et al., 2016)	
Output				
Marginal product				
PVC panel	849.34	t		Polyvinylchloride, bulk polymerised {GLO}| market for | Conseq, U

Table S13 Inventory of MDF disposal				
Chipping				
Input	**Quantity**	**Unit**	**Source**	**Process**
MDF	437.52	t		
Output				
Resin disposal	40.98	t		Waste polyurethane {CH}| treatment of, municipal incineration with fly ash extraction | Conseq, U
Woody part disposal, DM	335.85	t	(ecoinvent, 2020)	Waste wood, untreated {CH}| treatment of, municipal incineration with fly ash extraction | Conseq, U
	0.18	t	(ecoinvent, 2020)	Waste wood, untreated {GLO}| treatment of waste wood, untreated, open burning | Conseq, U
	3.21	t	(ecoinvent, 2020)	Waste wood, untreated {GLO}| treatment of waste wood, untreated, open dump, wet infiltration class (500mm) | Conseq, U

2.6 Carbon vulnerable lands

The cultivation of black locust would replace the original plants on carbon vulnerable lands (CV-lands). Thus, the influence of initial CV-lands is estimated to be a reference scenario to compare to the black locust. The time scale is the same as for the black locust scenario, namely 35 years. As previously stated (Shen et al., 2022), there are four land types identified as CV-lands: intensive grasslands, natural grasslands, rapeseed lands, and woody moorlands.

Intensive grasslands occupies 53% of CV-lands, the dominant plant is perennial ryegrass (*Lolium perenne L.*) (Kirwan et al., 2007; PLANTUREUX et al., 2005). The cultivation of ryegrass and later silage process are considered here. The silage ryegrass is a kind of mixed feed, which could avoid a certain amount of palm, soybean, and maize as marginal products of oil, protein, and, carbohydrate respectively(Gomez-Campos et al., 2020) (method from Tonini et al., 2016).

In case of rapeseed (*Brassica napus L.*), after extracting rapeseed oil as the main product, the seed meal is sold as feed. The proportion of rapeseed in CV-lands is 20%.

For these two kinds of land covers, when they are replaced by black locust, more feeds (the marginal products that we calculated) need to be produced to fill their gaps in the market. These extra demands of marginal feeds would lead to more fertilization and land expansion for corresponding crops. This impact is considered as iLUC (table S3).

Heather (*Calluna vulgaris*) is the representative plant on both natural lands and woody moorlands (20% and 7% of CV-lands)(Inglada et al., 2017). Becauseno specific usage is known, all biomass grown on these two lands are assumed to decay on site. The inventory of CV-lands is built in table S14-18;

Furthermore, the SOC change on CV-lands is estimated by C-Tool, in the same time horizon (2021-2126) as the reference scenario. Soil characteristics and temperature inputs are the same as for black locust (all plants growth in the same conditions). Carbon inputs in C-tool are calculated according to the plant considered in simulation, including aboveground and belowground biomass every year (table S19). After estimating the SOC change for four land covers (fig.s5), an arithmetic mean of SOC is computed based on their proportions in the total area of CV-lands (0.53, 0.2, 0.2, 0.07 for intensive grasslands, rapeseed lands, natural grasslands, and woody moorlands respectivelym table S18), depicted in fig.6b in the main paper.

The biomass residues from the CV-lands with initial vegetation are decomposed totally after the lands conversion to black locust(Verchot et al., 2006), with the tillage applied to cleaning the field before the first black locust seedling planting.

Table S14 Inventory sheet of intensive grassland.

Silage				
Input	**Quantity**	**Unit**	**Source**	**Process**
Silage process[a, b]	8	t	(ecoinvent, 2020)	Ryegrass silage {CH}| catch crop growing, ryegrass, August-April, organic fertiliser 80 kg N, three cuts |

				Conseq, U; 8 t/ha is the amount of ryegrass that would go through the silage.
N fertilizer	222	kg	(Hamelin et al., 2012)	Nitrogen fertiliser, as N {GLO}| market for | Conseq, U
P fertilizer	53.47	kg	(Hamelin et al., 2012)	Phosphate fertiliser, as P2O5 {GLO}| market for | Conseq, U
K fertilizer	18.69	kg	(Hamelin et al., 2012)	Potassium sulfate, as K2O {GLO}| market for | Conseq, U
Lime	542.05	kg	(Hamelin et al., 2012)	Lime, packed {CH}| lime production, milled, packed | Conseq, U
CO_2 in air	12.32	t		CO_2 captured from harvestable part
CO_2 in air	12.58	t		CO_2 captured from above+ belowground residue
Output				
Ryegrass silage	20.6	t	(ecoinvent, 2020)	65% water content
iLUC	-1	ha	(COWI A/S and Utrecht University, 2019)	(Shen et al., 2022a)
Emission to air				
NH_3	69.92	kg	(Hamelin et al., 2012)	From urea
NH_3	4.97	kg	(Hamelin et al., 2012)	From mineral fertilizer like $(NH_4)_2HPO_4$ or $5Ca(NO_3)_2\ NH_4{\cdot}NO_3$
NO	7.64	kg	(Hamelin et al., 2012)	From fertilizer
NO	1.51	kg	(Hamelin et al., 2012)	From residue
NO_x	14	kg	(Hamelin et al., 2012)	
N_2	74.96	kg	(Hamelin et al., 2012)	

N_2O	4.31	kg	(Hamelin et al., 2012)	From fertilizer &residue
N_2O	1.58	kg	(Hamelin et al., 2012)	From N mineralized because of soil carbon loss
CO_2	11.28	t	(Hamelin et al., 2012)	From residue, considered the SOC increased.
CO_2	0.43	t	(Hamelin et al., 2012)	From urea
CO_2	1.23	t	(ecoinvent, 2020)	From carbon loss during the silage
NMVOC	0.36	kg	(Hamelin et al., 2012)	
Emission to water				
Nitrate	149.5	kg	(Hamelin et al., 2012)	N-leaching
Phosphorus	0.032	kg	(Hamelin et al., 2012)	P-leaching
Use of ryegrass silage				
Input	**Quantity**	**Unit**	**Source**	**Process**
Ryegrass silage	20.6	t		
Output				
CO_2, biogenic	11	t		All carbon in the silage would emit back to the atmosphere
Marginal products				
Carbohydrate	-2.4	t	(Tonini et al., 2016)	Maize grain {GLO}| market for | Conseq, U
Protein	-0.49	t	(Tonini et al., 2016)	Soybean meal {GLO}| market for | Conseq, U
Fats	-34.53	kg	(Tonini et al., 2016)	Palm oil, refined {GLO}| market for | Conseq, U

a: plant cultivation and land occupation are included in the process;
b: silage process is modified by using mineral fertilizer, consequential inputs and emissions are shown in the inventory;

Table S15 Inventory sheet of rapeseed.				
Input	**Quantity**	**Unit**	**Source**	**Process**
Oil extraction[a,b]	822	kg	(ecoinvent, 2020)	Rape oil, crude {Europe without Switzerland}| rape oil mill operation | Conseq, U
Output				
Crude rapeseed oil	822	kg	(ecoinvent, 2020)	
SOC change	1.18	t	(Clivot et al., 2019)	Carbon dioxide, to soil or biomass stock
iLUC	-1	ha	(COWI A/S and Utrecht University, 2019)	Indirect land use change (Shen et al., 2022a)
Marginal product				
Crude palm oil	822	kg	(ecoinvent, 2020)	Palm oil, crude {RoW}| palm oil mill operation | Conseq, U
Use of rapeseed				
Input	**Quantity**	**Unit**	**Source**	**Process**
Crude rapeseed oil	822	kg		
Output				
CO_2, biogenic	3814.93	kg		All C in rapeseed oil would emit back to the atmosphere.

a: plant cultivation and land occupation are included in the process;
b: the avoided protein because of the rapeseed meal is included in the process;

Table S16 Inventory sheet of natural grassland.				
Input	**Quantity**	**Unit**	**Source**	**Process**
CO_2 captured	3.72	t	(Vogtländer et al., 2014; Worrall and Clay, 2014)	
Land occupation	1	ha a	(ecoinvent, 2020)	Occupation, grassland, natural (non-use)
Output				
Emission to air				
N_2O	0.51	kg	(Pehme et al., 2017)	
NO_x	1.28	kg	(Pehme et al., 2017)	
NH_3	0.39	kg	(Pehme et al., 2017)	
NMVOC	3.8	kg	(European Environment Agency, 2019)	
CO_2	3.35	t	(Vogtländer et al., 2014; Worrall and Clay, 2014)	
Emission to water				
Nitrate	31	kg	(Decau et al., 2004; Hussain et al., 2019)	
Emission to soil				
SOC change	0.37	t	(Pehme et al., 2017)	Carbon dioxide, to soil or biomass stock

Table S17 Inventory sheet of woody moorland.				
Input	**Quantity**	**Unit**	**Source**	**Process**
CO_2 captured	3.72	t	(Vogtländer et al., 2014; Worrall and Clay, 2014)	
Land occupation	1	ha a	(ecoinvent, 2020)	Occupation, grassland, natural (non-use)
Output				
Emission to air				
N_2O	0.51	kg	(Pehme et al., 2017)	
NO_x	1.28	kg	(Pehme et al., 2017)	
NH_3	0.39	kg	(Pehme et al., 2017)	
NMVOC	19.33	kg	(European Environment Agency, 2019)	
CO_2	3.35	t	(Vogtländer et al., 2014; Worrall and Clay, 2014)	
Emission to water				
Nitrate	31	kg	(Hussain et al., 2019)	
Emission to soil				
SOC change	0.37	t	(Pehme et al., 2017)	Carbon dioxide, to soil or biomass stock

Table S18 C-vulnerable plantation[a].				
Input	**Quantity**	**Unit**	**Source**	**Process**

Marginal land left as marginal, intensive grasslands	-18.55	ha		
Marginal land left as marginal, rapeseed	-7	ha		
Marginal land left as marginal, natural grassland	-7	ha		
Marginal land left as marginal, woody moorlands	-2.45	ha		

[a]: to estimate the marginal lands for 35 years, we ran the CV-lands scenario 35 times in the SimPro, all processes only happen once is adjusted (e.g. land transformation).

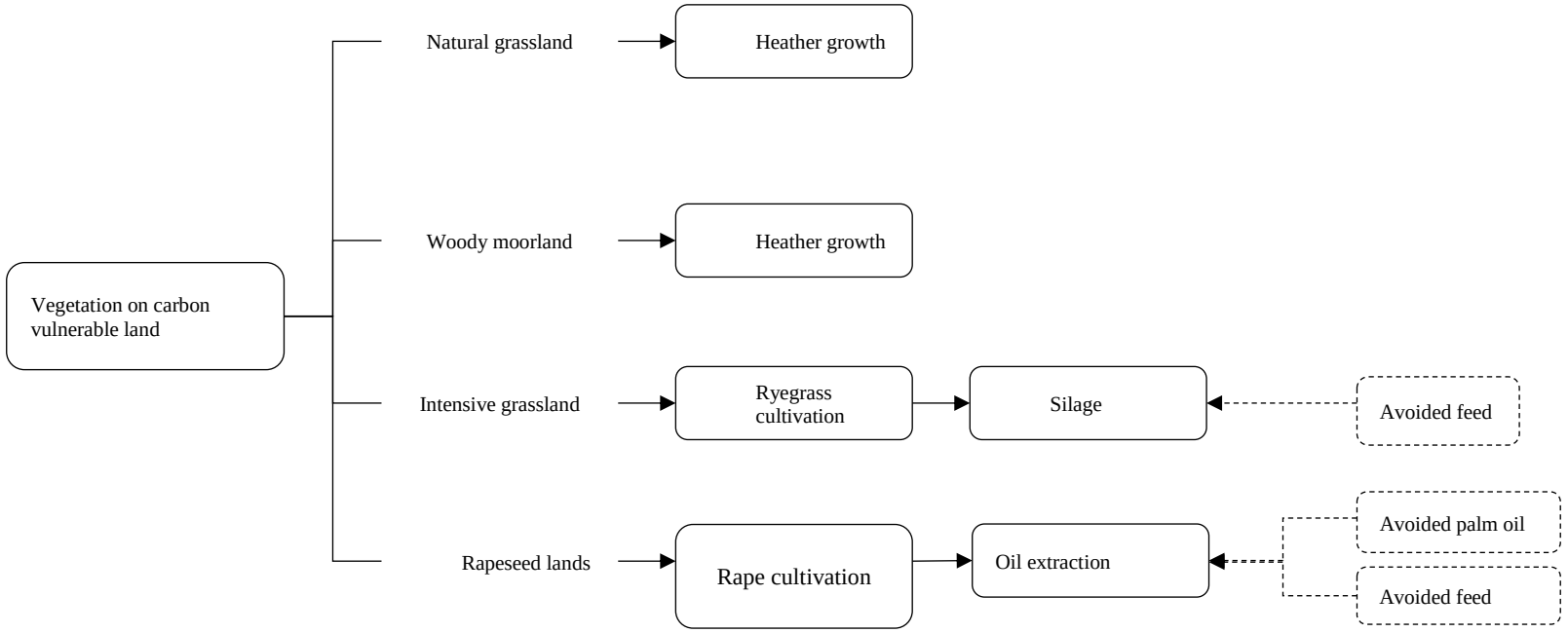

Fig. S4 Diagram of initial vegetation use

Annual C input of four types of the initial vegetation were shown in Table s19, which were assumed to be the same during the whole cultivation.

Table S19 Carbon inputs to C-tool.

	Aboveground carbon input Mg/ ha	Belowground carbon input Mg/ ha
Intensive grasslands	0.68	2.77
Rapeseed lands	3.12	1.17
Natural grasslands	1.07	0.0076
Woody moorlands	1.07	0.0076

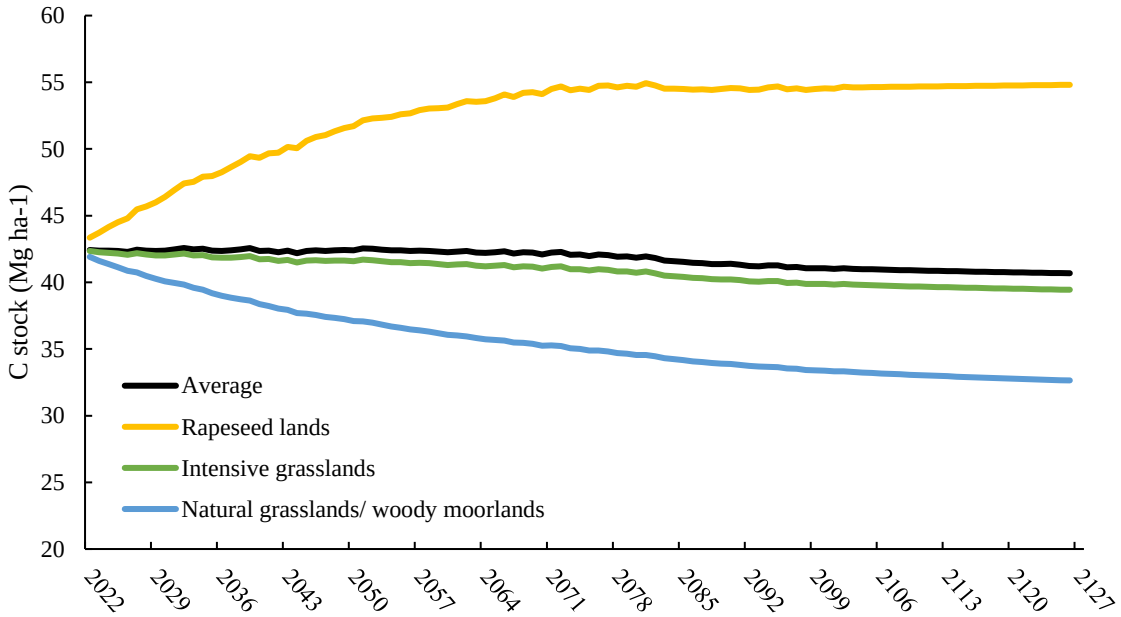

Fig. S5 The SOC simulation results for the four types of initial vegetation on CV-lands.

3 Consequential LCA

3.1 Environmental impact categories in consequential LCA

This study chose the Environmental Footprint initiative (EF) method, which is established and recommended by the European Commission (EC) to assess environmental impacts(Fazio et al., 2018). To track sources of different carbon flows and highlight the function of SOC but avoiding double counting, the EF method is slightly adapted as recommended by European Commission(Schau et al., 2013).

The characterization factors for CO_2 are : biogenic CO_2 =1 kg CO_2 eq, biogenic CO= 1.57 kg CO2 eq, biogenic methane= 34 kg CO_2 eq, CO_2 in air= -1 kg CO_2 eq, CO_2 stocked in soil or biomass= 0.

Under the EF scheme, 19 environmental impact categories are assessed, including three sub-impacts of climate change (fossile, biogenic and land transformation). European Commission gives three recommendation levels: satisfactory for categories in level I, needs some improvements for level II, and applied with caution for level III(Fazio et al., 2018).

Table S20 Environmental impacts.

Impact category	Unit	Recommendation level
Climate change	kg CO2 eq	I
Ozone depletion	kg CFC11 eq	I
Ionising radiation, HH	kBq U-235 eq	II
Photochemical ozone formation, HH	kg NMVOC eq	II
Respiratory inorganics	disease inc.	I
Non-cancer human health effects	CTUh	III
Cancer human health effects	CTUh	III
Acidification terrestrial and freshwater	mol H+ eq	II
Eutrophication freshwater	kg P eq	II
Eutrophication marine	kg N eq	II
Eutrophication terrestrial	mol N eq	II
Ecotoxicity freshwater	CTUe	III
Land use	Pt	III
Water scarcity	m3 depriv.	III
Resource use, energy carriers	MJ	III
Resource use, mineral and metals	kg Sb eq	III
Climate change - fossil	kg CO2 eq	I
Climate change - biogenic	kg CO2 eq	I

Climate change - land use and transform	kg CO2 eq	I	

3.2 Consequential LCA results : Contribution analysis

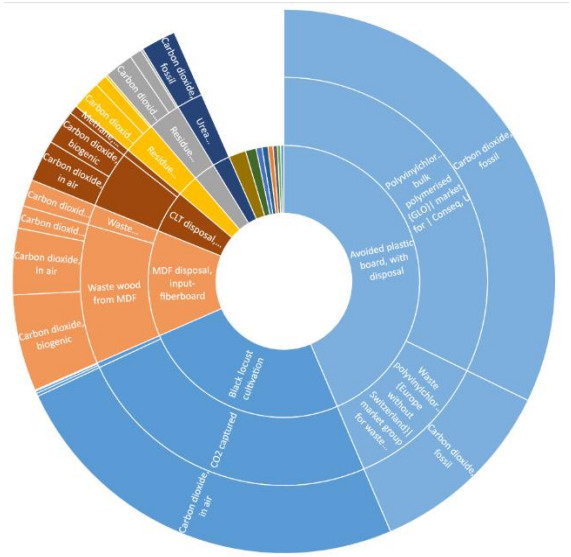

Climate change

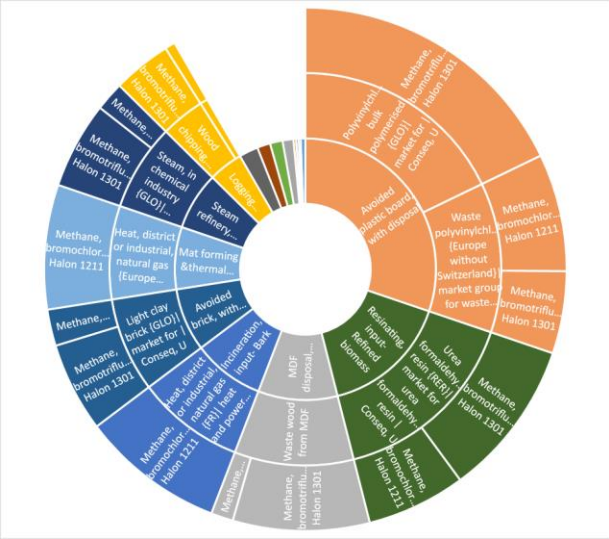

Ozone depletion

Ionizing radiation

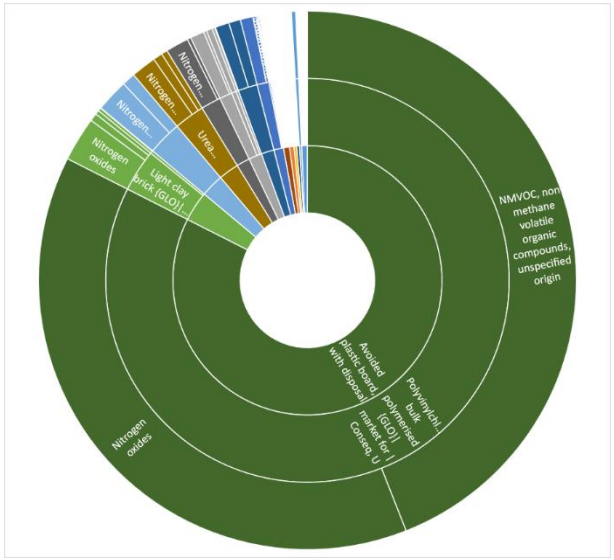

Photochemical ozone formation

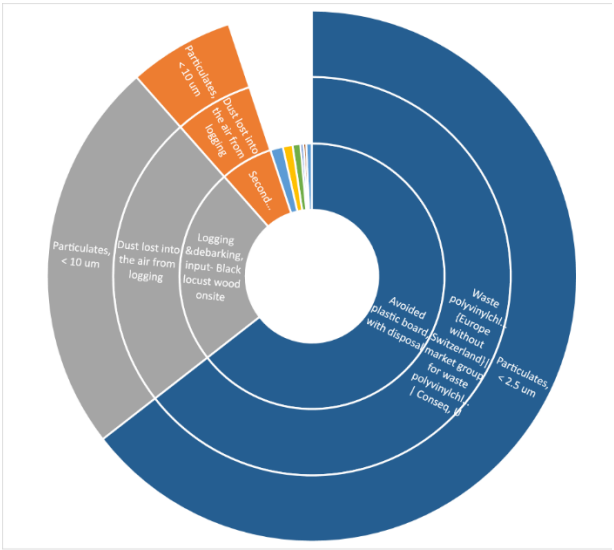

Respiratory inorganics

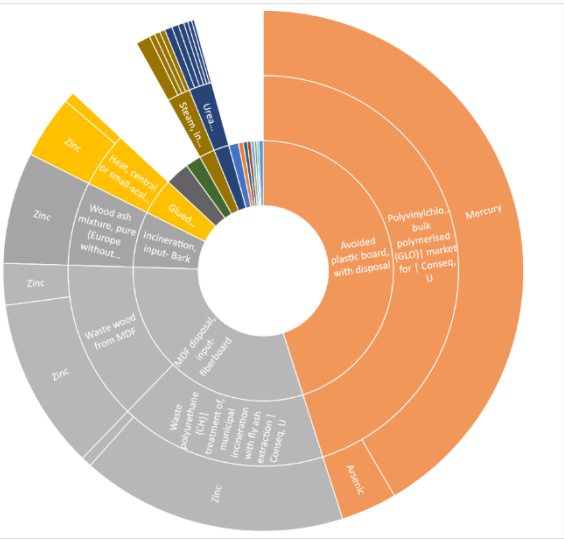

Non- cancer human health

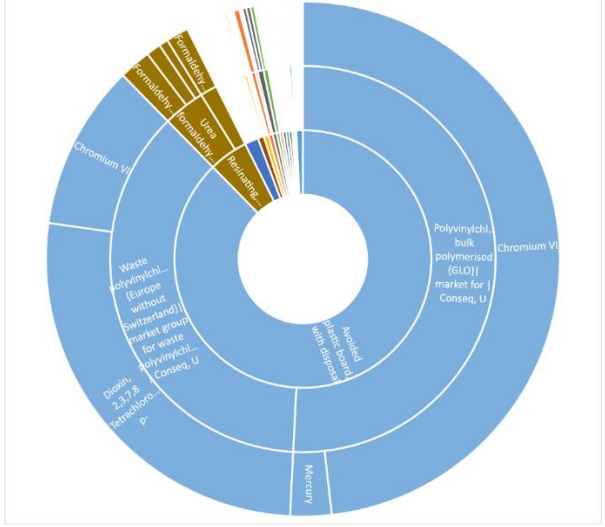

Cancer human health

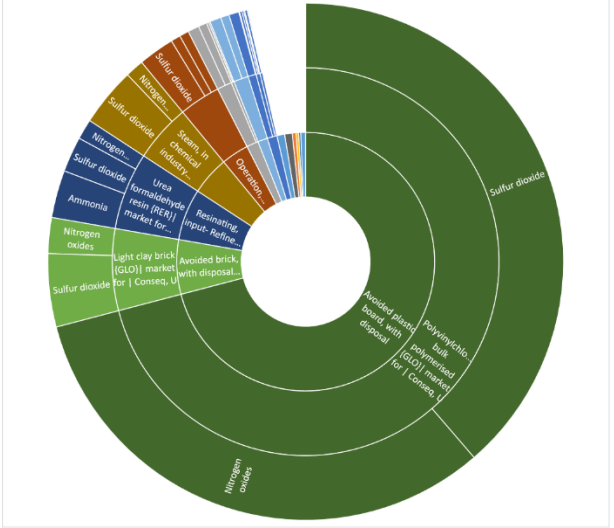

Acidification

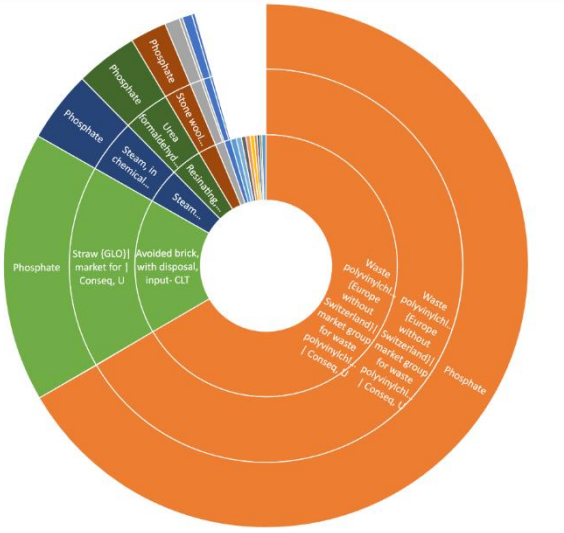

Freshwater eutrophication

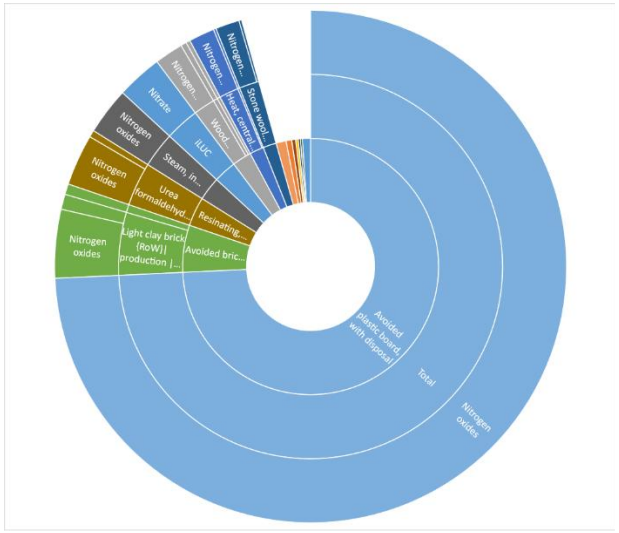

Marine eutrophication

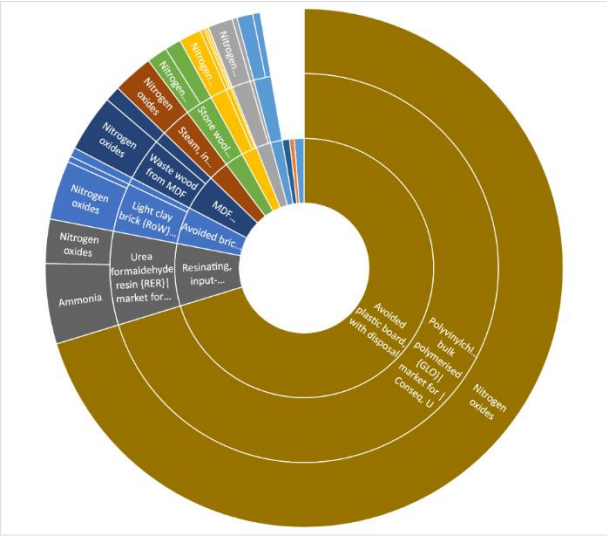

Terrestrial eutrophication

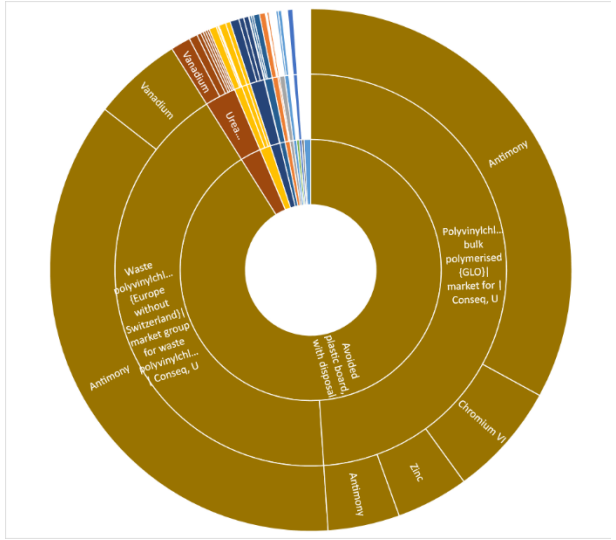

Ecotoxicity freshwater

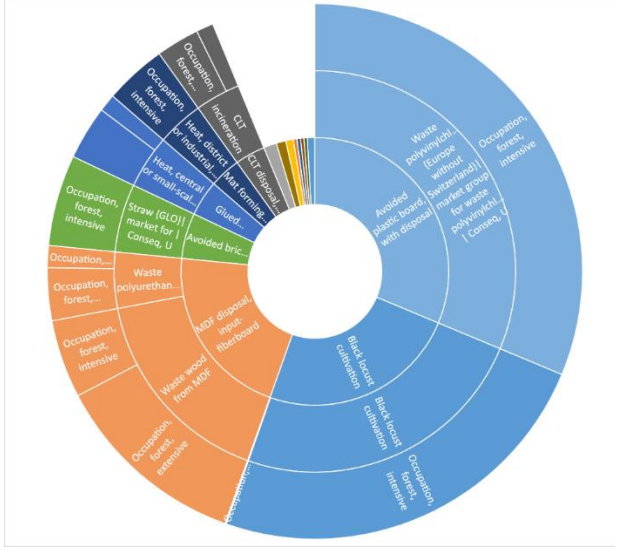

Land use

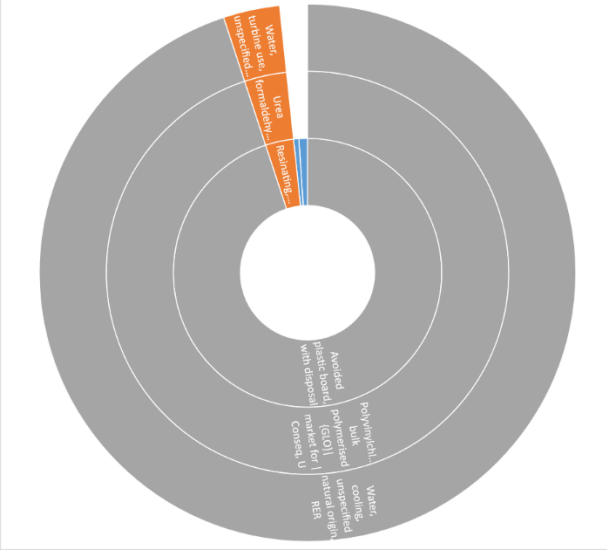

Water scarcity

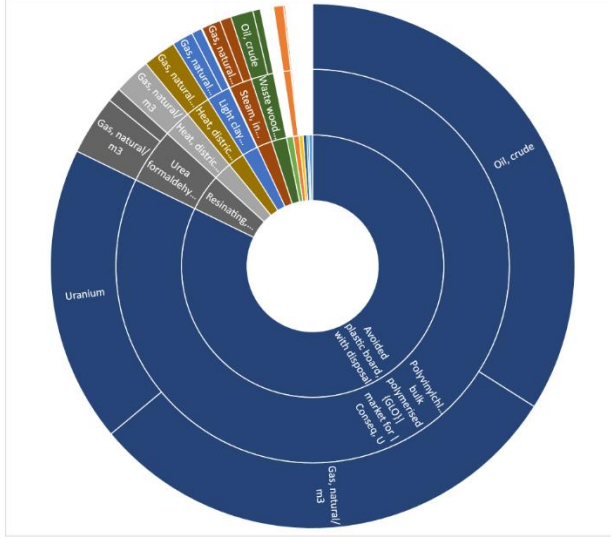

Energy carrier, resource use

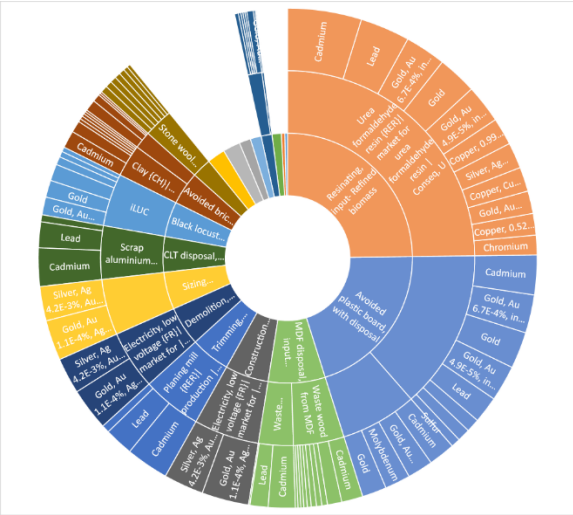

Mineral and mental, resource use

Fig. S6 Contribution analysis of LCA results of the scenario BL

4 Dynamic LCA

4.1 GHG considered in dynamic LCA

GHGs that are considered in dynamic LCA are listed in the table S21.

Table S21 GHG considered in dynamic LCA.

Black locust	CV-lands
Carbon dioxide	Carbon dioxide
Carbon dioxide, biogenic	Carbon dioxide, biogenic
Carbon dioxide, fossil	Carbon dioxide, fossil
Carbon dioxide, in air	Carbon dioxide, in air
Carbon dioxide, land transformation	Carbon dioxide, land transformation
Carbon dioxide, to soil or biomass stock	Carbon dioxide, to soil or biomass stock
Carbon monoxide	Carbon monoxide, biogenic
Carbon monoxide, biogenic	Carbon monoxide, fossil

Carbon monoxide, fossil
Carbon monoxide, land transformation
Chloroform
Dinitrogen monoxide
Ethane, 1,1-difluoro-, HFC-152a
Ethane, 1,1,1-trichloro-, HCFC-140
Ethane, 1,1,1,2-tetrafluoro-, HFC-134a
Ethane, 1,1,2-trichloro-1,2,2-trifluoro-, CFC-113
Ethane, 1,2-dichloro-
Ethane, 1,2-dichloro-1,1,2,2-tetrafluoro-, CFC-114
Ethane, 2-chloro-1,1,1,2-tetrafluoro-, HCFC-124
Ethane, 2,2-dichloro-1,1,1-trifluoro-, HCFC-123
Ethane, hexafluoro-, HFC-116
Methane
Methane, biogenic
Methane, bromo-, Halon 1001
Methane, bromochlorodifluoro-, Halon 1211
Methane, bromotrifluoro-, Halon 1301
Methane, chlorodifluoro-, HCFC-22
Methane, chlorotrifluoro-, CFC-13
Methane, dichloro-, HCC-30
Methane, dichlorodifluoro-, CFC-12
Methane, dichlorofluoro-, HCFC-21
Methane, fossil
Carbon monoxide, land transformation
Chloroform
Dinitrogen monoxide
Ethane, 1,1-difluoro-, HFC-152a
Ethane, 1,1,1-trichloro-, HCFC-140
Ethane, 1,1,1,2-tetrafluoro-, HFC-134a
Ethane, 1,1,2-trichloro-1,2,2-trifluoro-, CFC-113
Ethane, 1,2-dichloro-
Ethane, 1,2-dichloro-1,1,2,2-tetrafluoro-, CFC-114
Ethane, 2-chloro-1,1,1,2-tetrafluoro-, HCFC-124
Ethane, hexafluoro-, HFC-116
Methane
Methane, biogenic
Methane, bromo-, Halon 1001
Methane, bromochlorodifluoro-, Halon 1211
Methane, bromotrifluoro-, Halon 1301
Methane, chlorodifluoro-, HCFC-22
Methane, dichloro-, HCC-30
Methane, dichlorodifluoro-, CFC-12
Methane, dichlorofluoro-, HCFC-21
Methane, fossil
Methane, land transformation
Methane, monochloro-, R-40
Methane, tetrachloro-, CFC-10

Methane, land transformation	Methane, tetrafluoro-, CFC-14
Methane, monochloro-, R-40	Methane, trichlorofluoro-, CFC-11
Methane, tetrachloro-, CFC-10	Methane, trifluoro-, HFC-23
Methane, tetrafluoro-, CFC-14	Nitrogen fluoride
Methane, trichlorofluoro-, CFC-11	Sulfur hexafluoride
Methane, trifluoro-, HFC-23	
Nitrogen fluoride	
Sulfur hexafluoride	

4.2 Electricity and heat mix in the future

Table s22. Electricity mix in the future(Kassara et al., 2019)

Electricity, (TWh)	Gas	Other thermal	Nuclear	Photovoltaic	Onshore wind	Offshore wind	EnR(renewable energy)	Coal	Total
2020	0.6	13.2	422	18	33.5	0	79.5	12.7	579.5
	0.10%	2.28%	72.82%	3.11%	5.78%	0.00%	13.72%	2.19%	100.00%
2030	3.5	13.2	301.2	47	90	27	90	0	571.9
	0.61%	2.31%	52.67%	8.22%	15.74%	4.72%	15.74%	0.00%	100.00%
2040	8.7	6.6	215.5	69.2	149.5	27	116.2	0	592.7
	1.47%	1.11%	36.36%	11.68%	25.22%	4.56%	19.61%	0.00%	100.00%
2050	15.1	0	54.5	115.2	205.8	30.6	127.2	0	548.4
	2.75%	0.00%	9.94%	21.01%	37.53%	5.58%	23.19%	0.00%	100.00%

Table s23. Heat mix in the future(ADEME, 2018)

District heat, (Mtoe)	Others*	Fuelwood (cogeneration)	Fuelwood (heat only)	Gas (cogeneration)	Gas (heat only)	Geothermal	Coal and heating oil	Total
2030	1.3	1.3	1.1	1.2	2.1	0.4	0	7.4
	17.57%	17.57%	14.86%	16.22%	28.38%	5.41%	0.00%	100.00%
2035	1.2	2.1	0.8	1.2	2.1	0.8	0	8.2

	14.63%	25.61%	9.76%	14.63%	25.61%	9.76%	0.00%	100.00%
2040	1.2	2.8	0.5	0.8	1.5	1.1	0	7.9
	15.19%	35.44%	6.33%	10.13%	18.99%	13.92%	0.00%	100.00%
2045	1.2	3.5	0.3	0.4	0.7	1.5	0	7.6
	15.79%	46.05%	3.95%	5.26%	9.21%	19.74%	0.00%	100.00%
2050	1.1	4.2	0	0	0	2	0	7.3
	15.07%	57.53%	0.00%	0.00%	0.00%	27.40%	0.00%	100.00%

*: detailed in table s24.

Table s24. Heat mix of 'others' in the future(ADEME, 2018)

Methanisation	Household waste incineration	Residual heat	Solar thermal energy	Heat pumps
8.33%	50.00%	16.67%	16.67%	8.33%

4.3 Dynamic LCA results

For the whole life cycle of black locust scenario (105 years of cultivation), from biogenic sources, we obtain:

1) Total CO_2 absorption (negative in fig.s7): 3.91E+06 kg

2) Total CO_2 emission: 3.04E+06 kg

3) Total CO emission: 2.11E+02 kg

4) Total CH_4 emission: 1.92E+04 kg

5) Total N_2O emission: 3.08E+02 kg

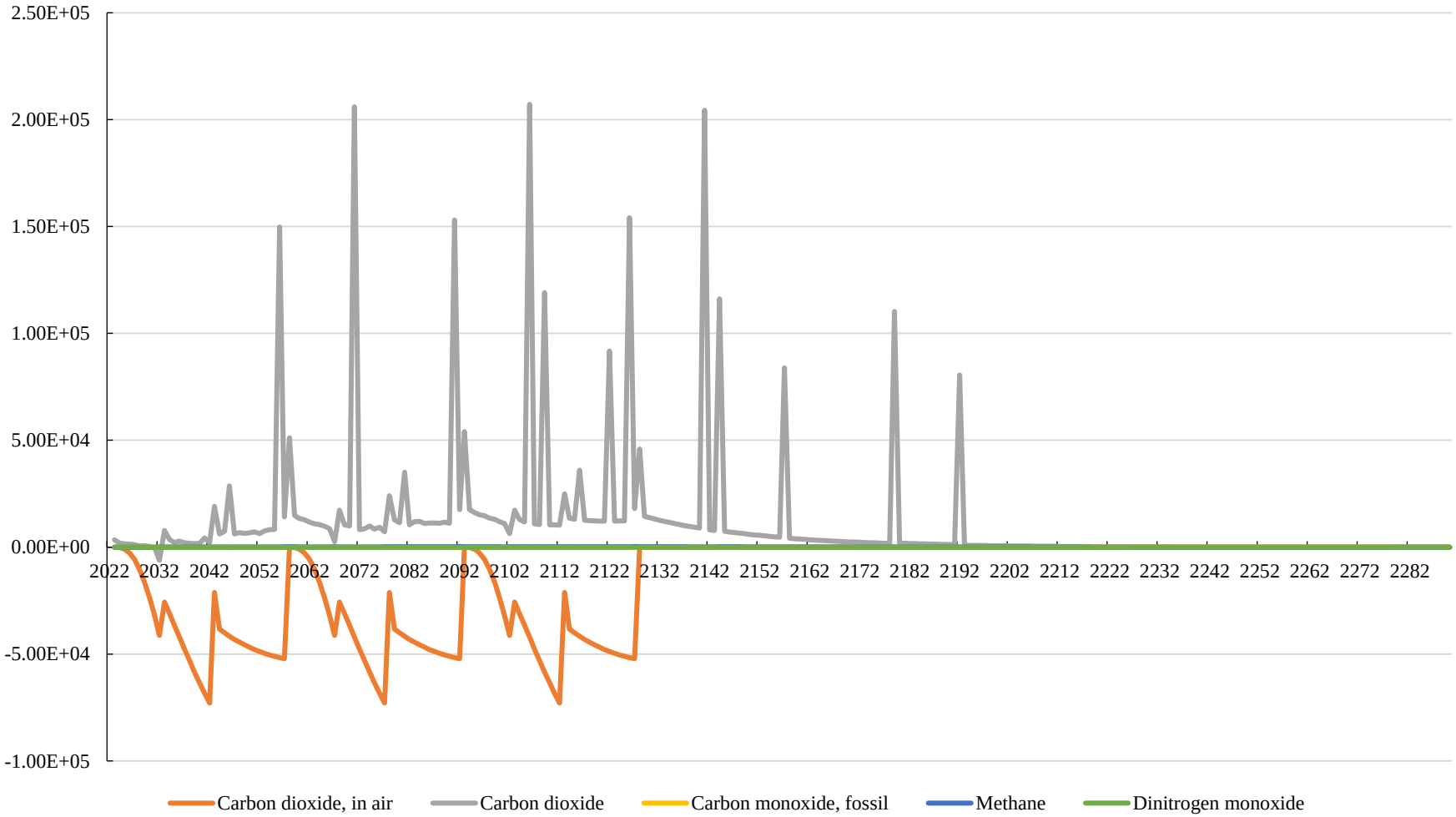

Fig. S7 Biogenic GHG flows (kg year^{-1}) for black locust scenario ('carbon dioxide in air' is the CO_2 captured, all other substances are emitted)

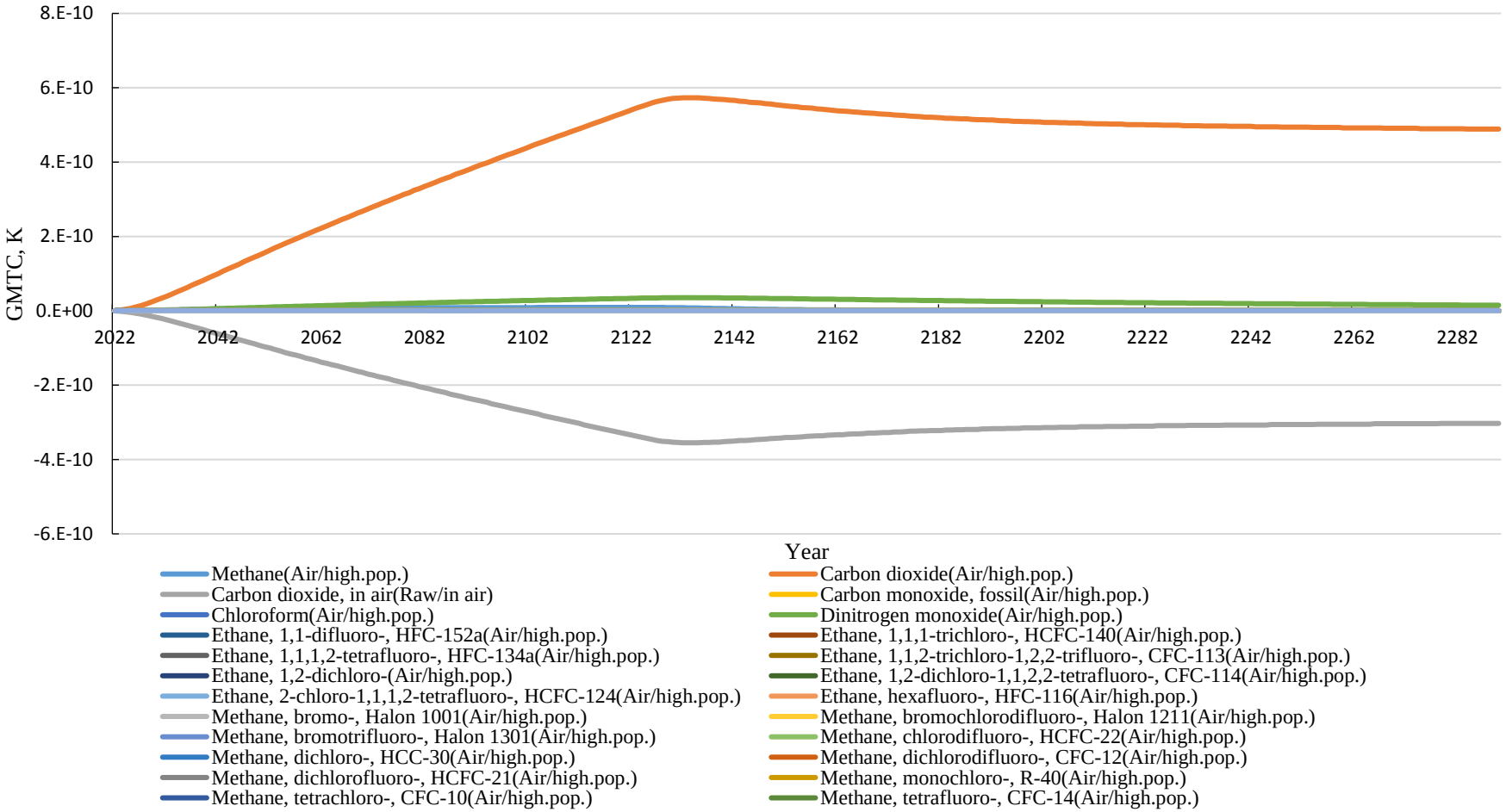

Fig. S8. GMTC of feed production and use in BLa scenario

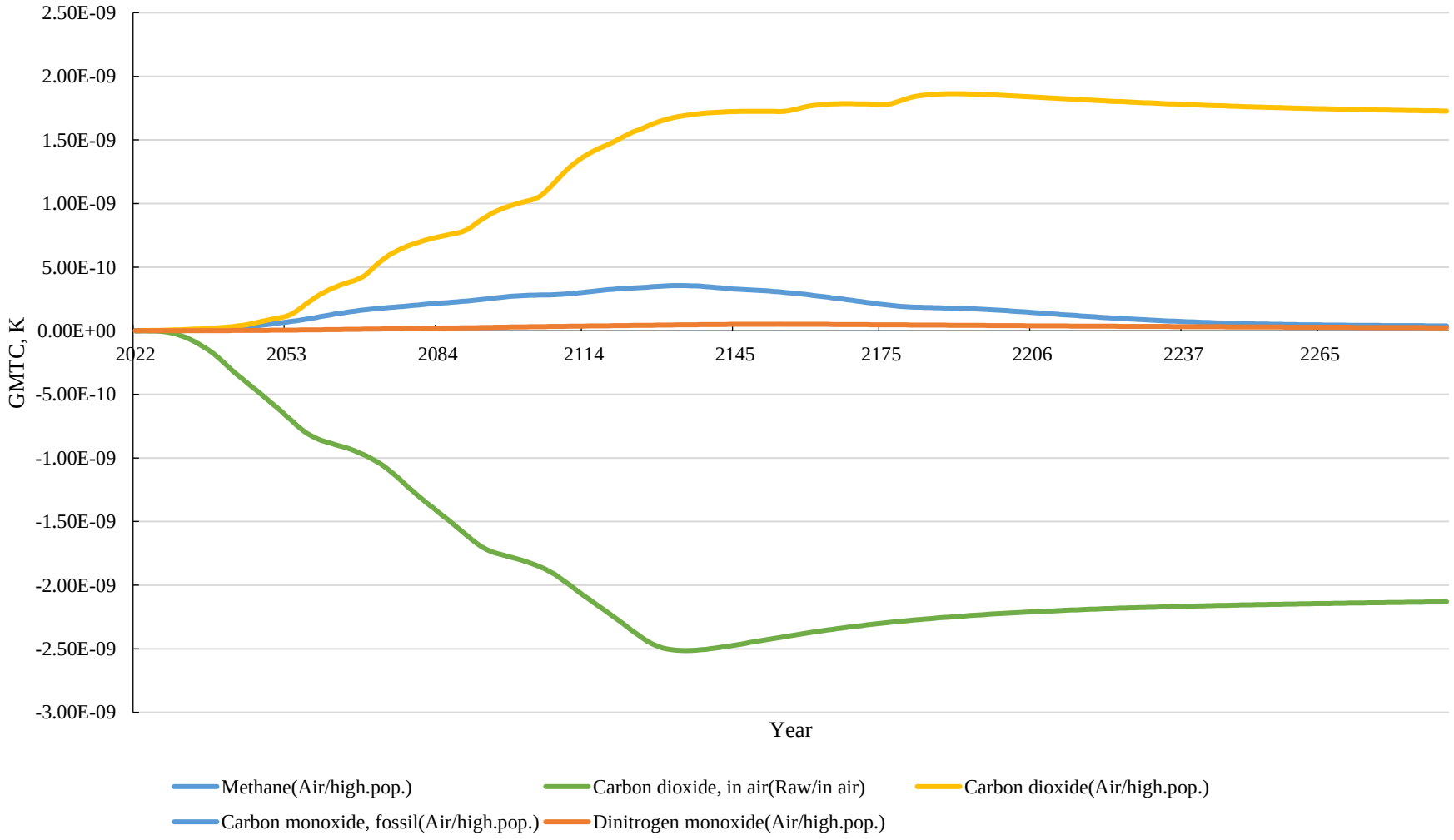

Fig. S9 GMTC of biogenic sources from black locust in BLa and BLc scenario

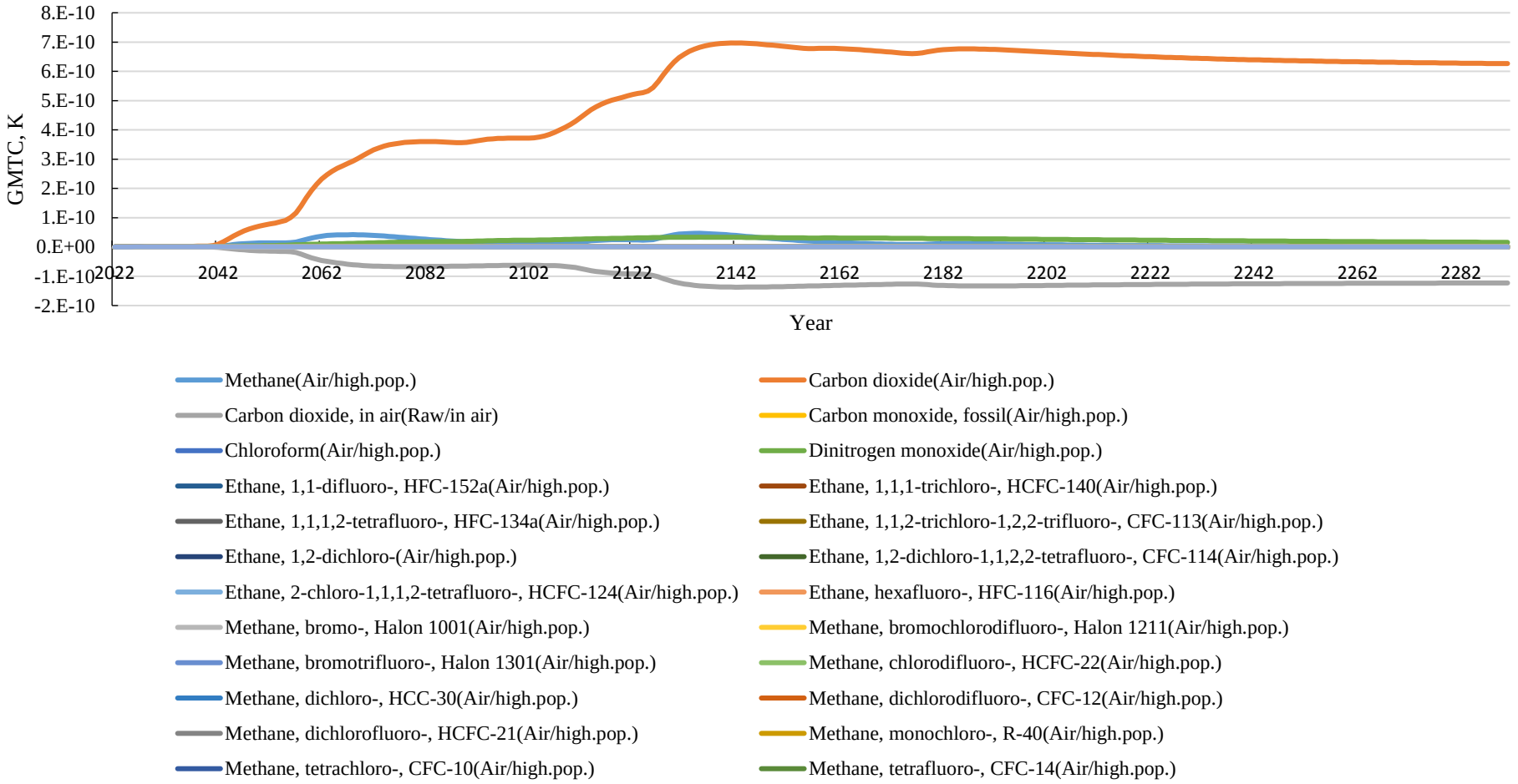

Fig. S10 GMTC of non-biogenic sources from black locust in BLa scenario

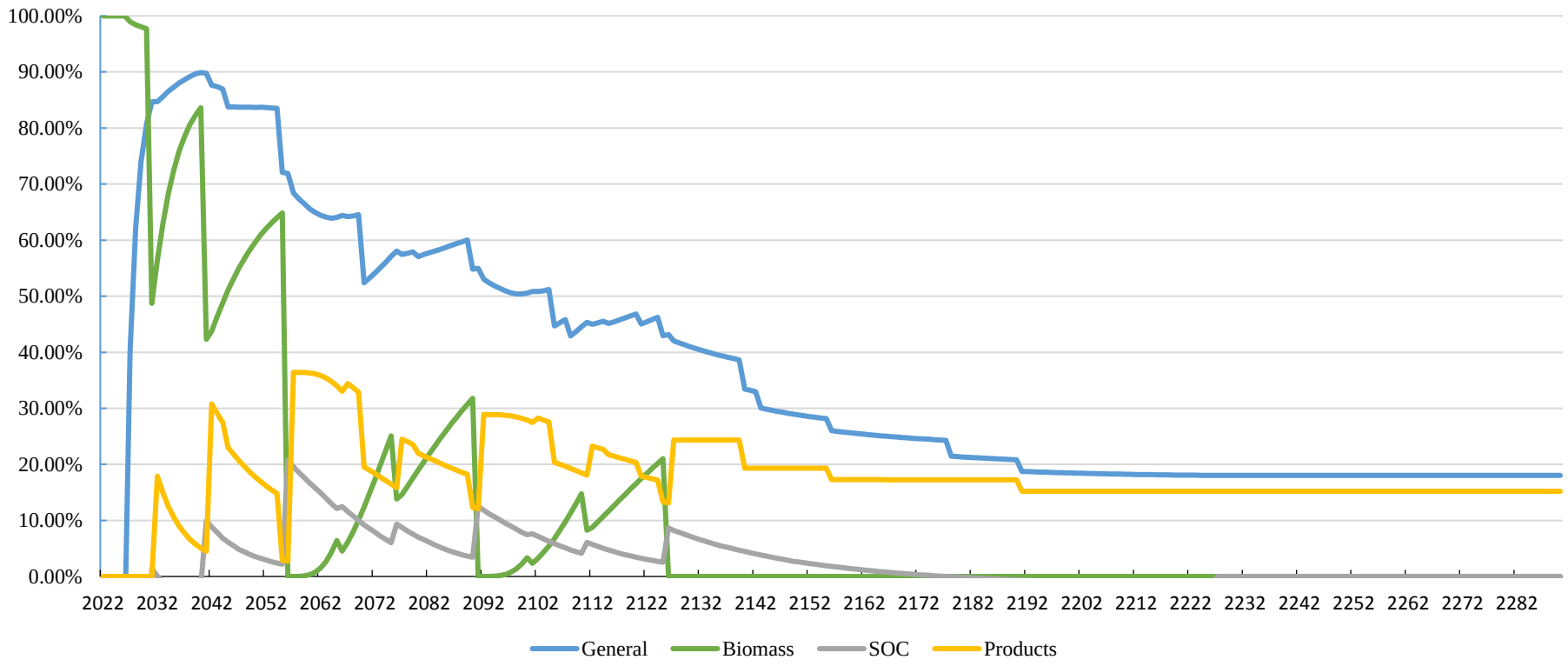

Fig. S11. C stock fraction in different components, with respect to the carbon absorbed (stock in the standing biomass, soil, products and total (general))

5 Uncertainty analysis

5.1 Method

The method called ‘Global sensitivity analysis’ is used in this study as it could reduce the calculation time significantly comparing to traditional Monte Carlo method, while getting similar results(Bisinella et al., 2016).

First, ten parameters are selected for the scenario BL as these parameters influence a lot the climate change impact according to the contribution analysis (fig. s6). Then, each parameter is increased by 10% in a one-at-a-time (OAT) manner while keeping all other parameters fixed at their value. A sensitivity coefficient (SC) is calculated as follow to represent the sensitivity of each parameter:

$$SC_i = \frac{\Delta score}{\Delta \text{parameter}} \tag{5}$$

With $\Delta score$ and Δparameter are differences before and after OAT of climate change score and parameter respectively, i=1,…n tested parameter. The SC_i calculated here is then used for calculating the analytical variance of the corresponding parameter (V_i):

$$V_i = {SC_i}^2 \cdot V_{input}(i) \tag{6}$$

Where $V_{input}(i)$ is the variance of each parameter, based on their uncertainty and distribution (table S25). The analytical variance of climate change category (V) in each scenario is the sum of V_i, and CV is used to indicate how uncertain the initial climate change score is.

$$V = \sum_{i=1}^{n} V_i \tag{7}$$

$$CV = \sqrt{V} / \, initial \; score \tag{8}$$

Parameters reaching 90% of the analytical variance (V) are selected to represent the uncertainty of climate change. In this way, the uncertainty of one impact is calculated; the same is applied to the other impacts.

5.2 Parameters in uncertainty analysis

The factors follow a normal distribution by default. If data for a certain factor are too few or do not follow normal distribution, but the potential mode is known, then triangular distribution is assumed(Lan et al., 2020). If we only have maximum and minimum value, then uniform distribution is assumed.

Table S25 Ten parameters considered for uncertainty analysis in the scenario BLc

	P1Quantity of avoided PVC	P2DM, yield	P3Non-CO2 GHG (CH4+N2O)	P4CH4:CO2 in landfilling	P5Recycling/ incineration in CLT disposal	P6UF resin amount	P7Nuclear/wind in electricity	P8Ash	P9Steam	P10Gas in the heat
μ	1.00	747.06	4936.91	19.18%	88.46	40.98	0.30	36.73	846423.01	31485.80
Unit	m	t	kg	%	t	t	%	t	MJ	m3
Uncertainty %	10%	10%	10%	10%	10%	10%	10%	10%	10%	10%
Δ	0.10	74.71	-493.69	0.02	8.85	4.10	0.03	3.67	84642.30	3148.58
Distribution	Triangle	Normal	Triangular	Triangular	Normal	Normal	Triangular	Triangular	Normal	Triangular
σ^2	5.56E-04	1395.2648	1.35E+04	2.04E-05	19.5629	4.1984	5.00E-05	0.7495	1791079764.5790	550753.0133

Table S26 Nine parameters considered for uncertainty analysis in the scenario REFc

	P1Area of intensive grassland	P2Area of rapeseed lands	P3Area of natural grasslands& woody moorlands	P4Amount of avoided palm oil (by rapeseed oil)	P5Amount of avoided feed (maize)	P6Amount of avoided feed (soybean)	P7Yield of ryegrass	P8Yield of rapeseed	P9N-fertilizer use in ryegrass cultivation
μ	18.55	7.00	9.45	6132.00	103.12	20.62	148.40	6132.00	5090.12
Unit	ha	ha	ha	kg	t	t	t	kg	kg
Uncertainty %	10%	10%	10%	10%	10%	10%	10%	10%	10%
Δ	1.86	0.70	0.95	613.20	10.31	2.06	14.84	613.20	509.01
Distribution	Normal	Normal	Normal	Normal	Normal	Normal	Normal	Normal	Triangle
σ^2	0.8603	0.1225	0.2233	94003.5600	26.5863	1.0633	55.0564	94003.5600	14394.0676

5.3 Uncertainty analysis results

The contribution analysis in section 3.2 identified ten parameters that play a key role in environmental impacts for the uncertainty analysis (table S25). The uncertainty results are presented in (table S27). The parameter column includes parameters representing the uncertainty in this impact, with corresponding uncertainty contributions. The values in the total column mean adding up these parameters together could represent the uncertainty in particular impact in which level (at least >90%). The coefficient of variance (COV) indicates how uncertain the impact result is. Six parameters are of significant contribution (P1, P2, P5, P6, P7, P10). It is concluded that climate mitigation from the plastic boards replacement is the largest negative score contributor in the static LCA. Consistent with this conclusion, most parameters are relative to the amount of avoided

plastic boards (P1, P2, P5). In general, P2 represents the highest uncertainty in most impacts (13 of 16), since the yield of woody biomass influences the entire inventory, e.g. the amount of harvested woody materials would determine the amount of CLT and MDF products, further change the amount of avoided brick and plastic board and the disposal process. P6 links to the UF resin products, representing 73% of uncertainty in mineral resource use, because of the mental use in the production (e.g. cadmium, lead). The uncertainty of P7 is significant in respiratory inorganics only because of the high woody dust lost in the air during the logging.

In general, the uncertainty of all impacts is lower than 10% except in mineral resource use (12%). Combined with the uncertainty of scenario REFc, the vary range of the impact results are shown in table s29. Table s29 shows the maximum and minimum scores in each impact the scenario BLc and REFc could be, it could be stated that there are significant differences between scenario BLc and REFc for the sixteen environmental impacts. Planting black locust on CV-lands is beneficial in thirteen environmental impacts.

Table S27 Uncertainty analysis results of the scenario BLc

Impact category	**Parameter**				**Total**	**COV**
Climate change	P1-50%	P2-28%	P3-21%		99%	±3.86%
Ozone depletion	P1-23%	P2-51%	P6-11%	P10-9%	94%	±7.11%
Ionizing radiation, HH	P2-72%	P5-5%	P6-17%		95%	±5.80%
Photochemical ozone formation, HH	P1-17%	P2-71%	P5-12%		100%	±5.98%
Respiratory inorganics	P1-27%	P2-30%	P5-19%	P7-24%	99%	±9.18%
Non-cancer human health effects	P1-13%	P2-72%	P5-13%		98%	±5.92%
Cancer human health effects	P1-18%	P2-70%	P5-12%		100%	±5.99%
Acidification terrestrial and freshwater	P1-20%	P2-68%	P5-10%		99%	±6.18%
Freshwater eutrophication	P1-17%	P2-66%	P5-16%		98%	±6.10%
Marine eutrophication	P1-19%	P2-70%	P5-11%		100%	±6.27%
Terrestrial eutrophication	P1-20%	P2-68%	P5-11%		100%	±6.22%
Ecotoxicity freshwater	P1-18%	P2-70%	P5-12%		100%	±5.97%
Land use	P1-76%	P5-14%			90%	±3.01%
Water scarcity	P1-17%	P2-71%	P5-12%		100%	±5.94%
Resource use, energy carriers	P1-18%	P2-71%	P5-11%		100%	±5.94%
Resource use, mineral and metals	P1-23%	P6-74%			97%	±12.41%

*P1: Quantity of avoided PVC; P2: woody biomass yield; P5: Recycling/incineration ratio in CLT disposal; P6: used UF resin amount; P7: Dust emitted during logging; P10: the CH_4 use in heat generation (the heat avoided by the heat generated from bark incineration), table S25
COV: coefficient of variation.

Table S28 Uncertainty analysis results of the scenario REFc

Impact category	**Parameter**						**Total**	**COV**
Climate change	P5-14%		P6-64%		P7-6%	P9-6%	90%	±15.35%
Ozone depletion	P1-9%	P3-9%	P5-28%	P7-33%		P9-12%	92%	±6.1%
Ionizing radiation, HH	P1-37%		P3-7%		P7-43%	P9-4%	90%	±7.23%
Photochemical ozone formation, HH	P1-25%		P5-13%		P6-9%	P7-46%	93%	±6.03%
Respiratory inorganics	P1-43%			P7-47%			90%	±7.08%
Non-cancer human health effects	P1-42%		P7-48%				92%	±6.84%
Cancer human health effects	P2-7%		P3-15%	P5-11%	P7-42%	P8-17%	92%	±4.71%
Acidification terrestrial and freshwater	P1-42%		P7-48%				90%	±6.87%
Freshwater eutrophication	P1-7%		P5-78%		P7-5%		90%	±27.33%
Marine eutrophication	P1-17%		P3-6%		P5-16%	P7-50%	90%	±5.15%
Terrestrial eutrophication	P1-42%		P7-48%				90%	±6.89%
Ecotoxicity freshwater	P1-33%		P6-26%		P7-32%		91%	±9.08%
Land use	P1-28%		P3-14%		P5-36	P6-16%	94%	±5.96%
Water scarcity	P1-30%		P5-35%		P7-29%		94%	±9.40%
Resource use, energy carriers	P5-67%		P6-5%		P7-6%	P9-13%	91%	±11.29%
Resource use, mineral and metals	P1-37%		P7-43%		P9-10%		91%	±7.12%

COV: coefficient of variation.

Reference

Adamopoulos, S., Passialis, C., Voulgaridis, E., 2007. Strength properties of juvenile and mature wood in black locust (Robinia pseudoacacia L.). Wood Fiber Sci. 39, 241–249.

Adamopoulos, S., Voulgaridis, E., 2002. WITHIN-TREE VARIATION IN GROWTH RATE AND CELL DIMENSIONS IN THE WOOD OF BLACK LOCUST (ROBINIA PSEUDOACACIA). Iawa J 23, 191–199.

Adamopoulos, S., Voulgaridis, E., Passialis, C., 2005. Variation of certain chemical properties within the stemwood of black locust (Robinia pseudoacacia L.). Holz als Roh - und Werkst. 63, 327–333. https://doi.org/10.1007/s00107-005-0018-3

Addlestone, B.J., Mueller, J.P., Luginbuhl, J.M., 1998. The establishment and early growth of three leguminous tree species for use in silvopastoral systems of the southeastern USA. Agrofor. Syst. 44, 253–265. https://doi.org/10.1023/A:1006254812236

ADEME, 2018. ADEME 2035-2050 Updated Energy-Climate Scenario.

Albers, A., Collet, P., Lorne, D., Benoist, A., Hélias, A., 2019. Coupling partial-equilibrium and dynamic biogenic carbon models to assess future transport scenarios in France. Appl. Energy 239, 316–330. https://doi.org/10.1016/j.apenergy.2019.01.186

Basler, A., Dippold, M., Helfrich, M., Dyckmans, J., 2015. Microbial carbon recycling - an underestimated process controlling soil carbon dynamics - Part 1: A long-term laboratory incubation experiment. Biogeosciences 12, 5929–5940. https://doi.org/10.5194/bg-12-5929-2015

Bergman, R.D., Bowe, S.A., 2010. Environmental impact of manufacturing softwood lumber in northeastern and north central United States. Wood Fiber Sci. 42, 67–78.

Bhat, H.A., Asif, M., Mir, N.A., Aijaz-Un-Nabi, Gatto, A.A., Ahmad, F., Hussain, N., 2014. Maturity indices and dormancy breaking methods of black locust (Rhobinia pseudoacacia) seeds under temperate Kashmir condition. Ecol. Environ. Conserv. 20, 1769–1775.

Bisinella, V., Conradsen, K., Christensen, T.H., Astrup, T.F., 2016. A global approach for sparse representation of uncertainty in Life Cycle Assessments of waste management systems. Int. J. Life Cycle Assess. 21, 378–394. https://doi.org/10.1007/s11367-015-1014-4

Boston, K., Dysart, G., 2000. A Comparison of Felling Techniques on Stump Height and Log Damage with Economic Interpretations. West. J. Appl. For. 15, 59–61. https://doi.org/10.1093/wjaf/15.2.59

Chen, C.X., Pierobon, F., Ganguly, I., 2019. Life Cycle Assessment (LCA) of Cross-Laminated Timber (CLT) produced in Western Washington: The role of logistics and wood species mix. Sustain. 11. https://doi.org/10.3390/su11051278

Clivot, H., Mouny, J.C., Duparque, A., Dinh, J.L., Denoroy, P., Houot, S., Vertès, F., Trochard, R., Bouthier, A., Sagot, S., Mary, B., 2019. Modeling soil organic carbon evolution in long-term arable experiments with AMG model. Environ. Model. Softw. 118, 99–113. https://doi.org/10.1016/j.envsoft.2019.04.004

Corradini, G., Pierobon, F., Zanetti, M., 2019. Product environmental footprint of a cross-laminated timber system: a case study in Italy. Int. J. Life Cycle Assess. 24, 975–988. https://doi.org/10.1007/s11367-018-1541-x

Couret, L., Irle, M., Belloncle, C., Cathala, B., 2017. Extraction and characterization of cellulose nanocrystals from post-consumer wood fiberboard waste. Cellulose 24, 2125–2137. https://doi.org/10.1007/s10570-017-1252-7

COWI A/S and Utrecht University, 2019. Environmental impact assessments of innovative bio-based product - Publications Office of the EU, European Commission. https://doi.org/10.2777/251887

De Vries, S.C., van de Ven, G.W.J., van Ittersum, M.K., 2014. First or second generation biofuel crops in Brandenburg, Germany? A model-based comparison of their production-ecological sustainability. Eur. J. Agron. 52, 166–179. https://doi.org/10.1016/j.eja.2013.09.012

Decau, M.L., Simon, J.C., Jacquet, A., 2004. Nitrate Leaching under Grassland as Affected by Mineral Nitrogen Fertilization and Cattle Urine. J. Environ. Qual. 33, 637–644. https://doi.org/10.2134/jeq2004.6370

Dimassi, B., Guenet, B., Saby, N.P.A., Munoz, F., Bardy, M., Millet, F., Martin, M.P., 2018. The impacts of CENTURY model initialization scenarios on soil organic carbon dynamics simulation in French long-term experiments. Geoderma 311, 25–36. https://doi.org/10.1016/j.geoderma.2017.09.038

Dong, Y., Cui, X., Yin, X., Chen, Y., Guo, H., 2019. Assessment of energy saving potential by replacing conventional materials by cross laminated timber (CLT)-A case study of office buildings in China. Appl. Sci. 9, 1–20. https://doi.org/10.3390/app9050858

DRIAS les futurs du climat, 2014. DRIAS [WWW Document]. URL https://drias-prod.meteo.fr/okapi/accueil/okapiWebDrias/index.jsp

ecoinvent, 2020. Ecoinvent 3.5 database [WWW Document]. URL https://www.ecoinvent.org/database/ecoinvent-37/new-data-in-ecoinvent-37/new-data-in-ecoinvent-37.html

European Environment Agency, 2019. EMEP/EEA air pollutant emission inventory- Other Sources and Sinks: Natural Grassland and Other Vegetation.

Fazio, S., Biganzioli, F., De Laurentiis, V., Zampori, L., Sala, S., Diaconu, E., 2018. Supporting information to the characterisation factors of recommended EF Life Cycle Impact Assessment methods, version 2, from ILCD to EF 3.0, EUR 29600 EN, European Commission, Ispra, 2018, ISBN 978-92-79-98584-3, doi:10.2760/002447, PUBSY No. JRC114822., New Models and Differences with ILCD, EUR. https://doi.org/10.2760/002447

Food and Agriculture Organization of the United Nations, 2005. Knowledge reference for national forest assessments - modeling for estimation and monitoring [WWW Document]. URL http://www.fao.org/forestry/17109/en/

Gomez-Campos, A., Vialle, C., Rouilly, A., Sablayrolles, C., Hamelin, L., 2020. Flax Fiber for Technical textile: a life cycle inventory. J. Clean. Prod. 281, 125177. https://doi.org/10.1016/j.jclepro.2020.125177

González-García, S., Gasol, C.M., Moreira, M.T., Gabarrell, X., Pons, J.R.I., Feijoo, G., 2011. Environmental assessment of black locust (Robinia pseudoacacia L.)-based ethanol as potential transport fuel. Int. J. Life Cycle Assess. 16, 465–477. https://doi.org/10.1007/s11367-011-0272-z

Guo, H., Liu, Y., Meng, Y., Huang, H., Sun, C., Shao, Y., 2017. A Comparison of the energy saving and carbon reduction performance between reinforced concrete and cross-laminated timber structures in residential buildings in the severe cold region of China. Sustain. 9. https://doi.org/10.3390/su9081426

Hamelin, L., Jørgensen, U., Petersen, B.M., Olesen, J.E., Wenzel, H., 2012. Modelling the carbon and nitrogen balances of direct land use changes from energy crops in Denmark: A consequential life cycle inventory. GCB Bioenergy 4, 889–907. https://doi.org/10.1111/j.1757-1707.2012.01174.x

Hussain, M.Z., Bhardwaj, A.K., Basso, B., Robertson, G.P., Hamilton, S.K., 2019. Nitrate Leaching

from Continuous Corn, Perennial Grasses, and Poplar in the US Midwest. J. Environ. Qual. 48, 1849–1855. https://doi.org/10.2134/jeq2019.04.0156

Inglada, J., Vincent, A., Arias, M., Tardy, B., Morin, D., Rodes, I., 2017. Operational High Resolution Land Cover Map Production at the Country Scale Using Satellite Image Time Series. Remote Sens. 9, 95. https://doi.org/10.3390/rs9010095

IPCC, 2019. 2019 Refinement to the 2006 IPCC Guidelines for National Greenhouse Gas Inventories Volume 5 Waste, IPCC Good Practice Guidance and Uncertainty Management in National Greenhouse Gase Inventories.

Jayalath, A., Navaratnam, S., Ngo, T., Mendis, P., Hewson, N., Aye, L., 2020. Life cycle performance of Cross Laminated Timber mid-rise residential buildings in Australia. Energy Build. 223, 110091. https://doi.org/10.1016/j.enbuild.2020.110091

Kassara, G., Pena Verrier, G., Chammas, M., Fournie, L., Mainsant, A., Marchal, D., Parrouffe, J.-M., 2019. Trajectories of evolution of the electricity mix 2020-2060: Additional analyses, FAQs, Report on data.

Keresztesi, B., 1983. Breeding and cultivation of black locust, Robinia pseudoacacia, in Hungary. For. Ecol. Manage. 6, 217–244. https://doi.org/10.1016/S0378-1127(83)80004-8

Kirwan, L., Lüscher, A., Sebastià, M.T., Finn, J.A., Collins, R.P., Porqueddu, C., Helgadottir, A., Baadshaug, O.H., Brophy, C., Coran, C., Dalmannsdóttir, S., Delgado, I., Elgersma, A., Fothergill, M., Frankow-Lindberg, B.E., Golinski, P., Grieu, P., Gustavsson, A.M., Höglind, M., Huguenin-Elie, O., Iliadis, C., Jørgensen, M., Kadziuliene, Z., Karyotis, T., Lunnan, T., Malengier, M., Maltoni, S., Meyer, V., Nyfeler, D., Nykanen-Kurki, P., Parente, J., Smit, H.J., Thumm, U., Connolly, J., 2007. Evenness drives consistent diversity effects in intensive grassland systems across 28 European sites. J. Ecol. 95, 530–539. https://doi.org/10.1111/j.1365-2745.2007.01225.x

Kouchaki-Penchah, H., Sharifi, M., Mousazadeh, H., Zarea-Hosseinabadi, H., 2016. Life cycle assessment of medium-density fiberboard manufacturing process in Islamic Republic of Iran. J. Clean. Prod. 112, 351–358. https://doi.org/10.1016/j.jclepro.2015.07.049

Lan, K., Kelley, S.S., Nepal, P., Yao, Y., 2020. Dynamic life cycle carbon and energy analysis for cross-laminated timber in the Southeastern United States. Environ. Res. Lett. 15, 124036. https://doi.org/10.1088/1748-9326/abc5e6

Laschi, A., Marchi, E., González-García, S., 2016. Forest operations in coppice: Environmental assessment of two different logging methods. Sci. Total Environ. 562, 493–503. https://doi.org/10.1016/j.scitotenv.2016.04.041

Launay, C., Constantin, J., Chlebowski, F., Houot, S., Graux, A.I., Klumpp, K., Martin, R., Mary, B., Pellerin, S., Therond, O., 2021. Estimating the carbon storage potential and greenhouse gas emissions of French arable cropland using high-resolution modeling. Glob. Chang. Biol. 27, 1645–1661. https://doi.org/10.1111/gcb.15512

Lovinska, V., Sytnyk, S., 2016. The structure of Scots pine and Black locust forests in the Northern Steppe of Ukraine. J. For. Sci. 62, 329–336. https://doi.org/10.17221/120/2015-JFS

Malcolm, G.M., Bush, D.S., Rice, S.K., 2008. Soil nitrogen conditions approach preinvasion levels following restoration of nitrogen-fixing black locust (robinia pseudoacacia) stands in a pine-oak Ecosystem. Restor. Ecol. 16, 70–78. https://doi.org/10.1111/j.1526-100X.2007.00263.x

Manzone, M., 2015. Energy and moisture losses during poplar and black locust logwood storage. Fuel Process. Technol. 138, 194–201. https://doi.org/10.1016/j.fuproc.2015.05.026

Mirabella, N., Castellani, V., Sala, S., 2014. Forestry operations in the alpine context. Life cycle assessment to support the integrated assessment of forest wood short supply chain. Int. J. Life Cycle Assess. 19, 1524–1535. https://doi.org/10.1007/s11367-014-0756-8

Motta, R., Nola, P., Berretti, R., 2009. The rise and fall of the black locust (Robinia pseudoacacia L.) in the "Siro Negri" Forest Reserve (Lombardy, Italy): Lessons learned and future uncertainties. Ann. For. Sci. 66, 410–410. https://doi.org/10.1051/forest/2009012

Nachtergaele, F., van Velthuizen, H., van Engelen, V., Fischer, G., Jones, A., Montanarella, L., Petri, M., Prieler, S., Teixeira, E., Shi, X., 2012. Harmonized World Soil Database (version 1.2). FAO, Rome, Italy IIASA, Laxenburg, Austria 1–50.

Nemecek, T., Kagi, T., 2007. Life cycle inventories of Agricultural Production Systems, ecoinvent report No. 15. Final Rep. … 1–360.

Nicolescu, V.N., Hernea, C., Bakti, B., Keserű, Z., Antal, B., Rédei, K., 2018. Black locust (Robinia pseudoacacia L.) as a multi-purpose tree species in Hungary and Romania: a review. J. For. Res. 29, 1449–1463. https://doi.org/10.1007/s11676-018-0626-5

Nicolescu, V.N., Rédei, K., Mason, W.L., Vor, T., Pöetzelsberger, E., Bastien, J.C., Brus, R., Benčať, T., Đodan, M., Cvjetkovic, B., Andrašev, S., La Porta, N., Lavnyy, V., Mandžukovski, D., Petkova, K., Roženbergar, D., Wąsik, R., Mohren, G.M.J., Monteverdi, M.C., Musch, B., Klisz, M., Perić, S., Keça, L., Bartlett, D., Hernea, C., Pástor, M., 2020. Ecology, growth and management of black locust (Robinia pseudoacacia L.), a non-native species integrated into European forests. J. For. Res. 31, 1081–1101. https://doi.org/10.1007/s11676-020-01116-8

Nielsen, M., Nielsen, O.-K., Thomsen, M., 2010. Emissions from decentralised CHP plants 2007 - Energinet.dk Environmental project no. 07/1882. Project report 5 – Emission factors and emission inventory for decentralised CHP production.

Onyeaju, M.C., Osarolube, E., Chukwuocha, E.O., Ekuma, C.E., Omasheye, G.A.J., 2012. Comparison of the Thermal Properties of Asbestos and Polyvinylchloride (PVC) Ceiling Sheets. Mater. Sci. Appl. 03, 240–244. https://doi.org/10.4236/msa.2012.34035

Pehme, S., Veromann, E., Hamelin, L., 2017. Environmental performance of manure co-digestion with natural and cultivated grass – A consequential life cycle assessment. J. Clean. Prod. 162, 1135–1143. https://doi.org/10.1016/j.jclepro.2017.06.067

Piekarski, C.M., de Francisco, A.C., da Luz, L.M., Kovaleski, J.L., Silva, D.A.L., 2017. Life cycle assessment of medium-density fiberboard (MDF) manufacturing process in Brazil. Sci. Total Environ. 575, 103–111. https://doi.org/10.1016/j.scitotenv.2016.10.007

PLANTUREUX, S., PEETERS, A., MCCRACKEN, D., 2005. Biodiversity in intensive grasslands : Effect of management, improvement and challenges. Agron. Res. 3, 417–426.

Rahmonov, O., 2009. The chemical composition of plant litter of black locust (Robinia pseudoacacia L.) and its ecological role in sandy ecosystems. Shengtai Xuebao/ Acta Ecol. Sin. 29, 237–243. https://doi.org/10.1016/j.chnaes.2009.08.006

Rédei, K., Csiha, I., KeserU, Z., Gál, J., 2012. Influence of regeneration method on the yield and stem quality of black locust (Robinia pseudoacacia L.) Stands: A case study. Acta Silv. Lignaria Hungarica 8, 103–112. https://doi.org/10.2478/v10303-012-0008-1

Rédei, K., Csiha, I., Keseru, Z., Rásó, J., Kamandiné Végh, Á., Antal, B., 2014. Growth and Yield of Black Locust (Robinia pseudoacacia L.) Stands in Nyírség Growing Region (North-East Hungary). South-east Eur. For. 5, 13–22. https://doi.org/10.15177/seefor.14-04

Rice, S.K., Westerman, B., Federici, R., 2004. Impacts of the exotic, nitrogen-fixing black locust (Robinia pseudoacacia) on nitrogen-cycling in a pine-oak ecosystem. Plant Ecol. 174, 97–107. https://doi.org/10.1023/B:VEGE.0000046049.21900.5a

Rivela, B., Hospido, A., Moreira, M.T., Feijoo, G., 2006. Life Cycle Inventory of Particleboard: A Case Study in the Wood Sector. Wood Other Renew. Resour. 11, 106–113.

Rivela, B., Moreira, M.T., Feijoo, G., 2007. Life Cycle Inventory of Medium Density Fibreboard. Wood Other Renew. Resour. 12, 143–150.

Ros, J.P.M., Boot, P. a, van Minnen, J.G., Arets, E.J.M.M., 2013. Climate effects of wood used for bioenergy 47.

Santi, S., Pierobon, F., Corradini, G., Cavalli, R., Zanetti, M., 2016. Massive wood material for sustainable building design: the Massiv–Holz–Mauer wall system. J. Wood Sci. 62, 416–428. https://doi.org/10.1007/s10086-016-1570-7

Schau, E.M., Allacker, K., Camillis, C. De, Pant, R., 2013. The development of Product Environmental Footprint (PEF) Category Rules (PEFCR), in: Proceedings of the SETAC Europe 23nd Annual Meeting Glasgow, United Kingdom, 12–16 May 2013. pp. 7–8.

Seserman, D.M., Pohle, I., Veste, M., Freese, D., 2018. Simulating climate change impacts on hybrid-poplar and black locust short rotation coppices. Forests 9, 1–25. https://doi.org/10.3390/f9070419

Shen, Z., Tiruta-Barna, L., Hamelin, L., 2022a. From Hemp Grown on Carbon Vulnerable Lands to Long-Lasting Bio-Based Products: Uncovering Trade-Offs between Overall Environmental Impacts, Sequestration in Soils and Dynamic Influence on Global Temperature. Sequestration Soils Dyn. Influ. Glob. Temp.

Shen, Z., Tiruta-Barna, L., Karan, S.K., Hamelin, L., 2022b. Simultaneous carbon storage in arable land and anthropogenic products (CSAAP): Demonstrating an integrated concept towards well below 2° C. Resour. Conserv. Recycl. 182, 106293.

Silva, D.A.L., Lahr, F.A.R., Garcia, R.P., Freire, F.M.C.S., Ometto, A.R., 2013. Life cycle assessment of medium density particleboard (MDP) produced in Brazil. Int. J. Life Cycle Assess. 18, 1404–1411. https://doi.org/10.1007/s11367-013-0583-3

Stone, K.R., 2009. Robinia pseudoacacia. In: Fire Effects Information System [WWW Document]. U.S. Dep. Agric. For. Serv. Rocky Mt. Res. Station. Fire Sci. Lab. URL https://www.fs.fed.us/database/feis/plants/tree/robpse/all.html

Tabari, M., Salehi, A., 2008. Soil Carbon Sequestration Potential of Eldar Pine and Black Locust Afforestation in a Semi-Arid Zone of Iran. Res. J. Environ. Sci. 2, 483–490.

Takano, A., Hughes, M., Winter, S., 2014. A multidisciplinary approach to sustainable building material selection: A case study in a Finnish context. Build. Environ. 82, 526–535. https://doi.org/10.1016/j.buildenv.2014.09.026

Tonini, D., Hamelin, L., Astrup, T.F., 2016. Environmental implications of the use of agro-industrial residues for biorefineries: application of a deterministic model for indirect land-use changes. GCB Bioenergy 8, 690–706. https://doi.org/10.1111/gcbb.12290

Vangeel, T., Renders, T., Van Aelst, K., Cooreman, E., Van Den Bosch, S., Van Den Bossche, G., Koelewijn, S.F., Courtin, C.M., Sels, B.F., 2019. Reductive catalytic fractionation of black locust bark. Green Chem. 21, 5841–5851. https://doi.org/10.1039/c9gc02139f

Verchot, L., Lasco, K.T.R., Ogle, S., Raison, J., Li, Y., Martino, D., McConkey, B., Smith, P., 2006.

IPCC Guidelines for National Greenhouse Gas Inventories, Chapter 6 Grassland. Intergovernmental Panel on Climate Change, vol. 4: Agriculture, Ipcc. https://doi.org/10.1016/B978-0-12-394807-6.00168-4

Vítková, M., Müllerová, J., Sádlo, J., Pergl, J., Pyšek, P., 2017. Black locust (Robinia pseudoacacia) beloved and despised: A story of an invasive tree in Central Europe. For. Ecol. Manage. 384, 287–302. https://doi.org/10.1016/j.foreco.2016.10.057

Vogtländer, J.G., van der Velden, N.M., van der Lugt, P., 2014. Carbon sequestration in LCA, a proposal for a new approach based on the global carbon cycle; cases on wood and on bamboo. Int. J. Life Cycle Assess. 19, 13–23.

Warne, A., 2016. Black locust (Robinia pseudoacacia L.). Best management practices in Ontario, Ontario invasive plant council, Peterborough.

Wilson, J.B., 2010a. Life-cycle inventory of medium density fiberboard in terms of resources, emissions, energy and carbon. Wood Fiber Sci. 42, 107–124.

Wilson, J.B., 2010b. Life-cycle inventory of particleboard in terms of resources, emissions, energy and carbon. Wood Fiber Sci. 42, 90–106.

Wilson, J.B., Sakimoto, E.T., 2005. Gate-to-gate life-cycle inventory of softwood plywood production. Wood Fiber Sci. 37, 58–73.

wood, black locust (Robinia pseudoacacia) [WWW Document], 1998. . Phyllis2 database. URL https://phyllis.nl/Browse/Standard/ECN-Phyllis#black locust

Wood Products Industry, 2002. Engineered Wood Products Manufacturing.

Worrall, F., Clay, G.D., 2014. The potential use of heather, calluna vulgaris, as a bioenergy crop. Biomass and Bioenergy 64, 140–151. https://doi.org/10.1016/j.biombioe.2014.03.007

Żelazna, A., Kraszkiewicz, A., Przywara, A., Łagód, G., Suchorab, Z., Werle, S., Ballester, J., Nosek, R., 2019. Life cycle assessment of production of black locust logs and straw pellets for energy purposes. Environ. Prog. Sustain. Energy 38, 163–170. https://doi.org/10.1002/ep.13043

Zieger, V., Lecompte, T., Hellouin de Menibus, A., 2020. Impact of GHGs temporal dynamics on the GWP assessment of building materials: A case study on bio-based and non-bio-based walls. Build. Environ. 185, 107210. https://doi.org/10.1016/j.buildenv.2020.107210